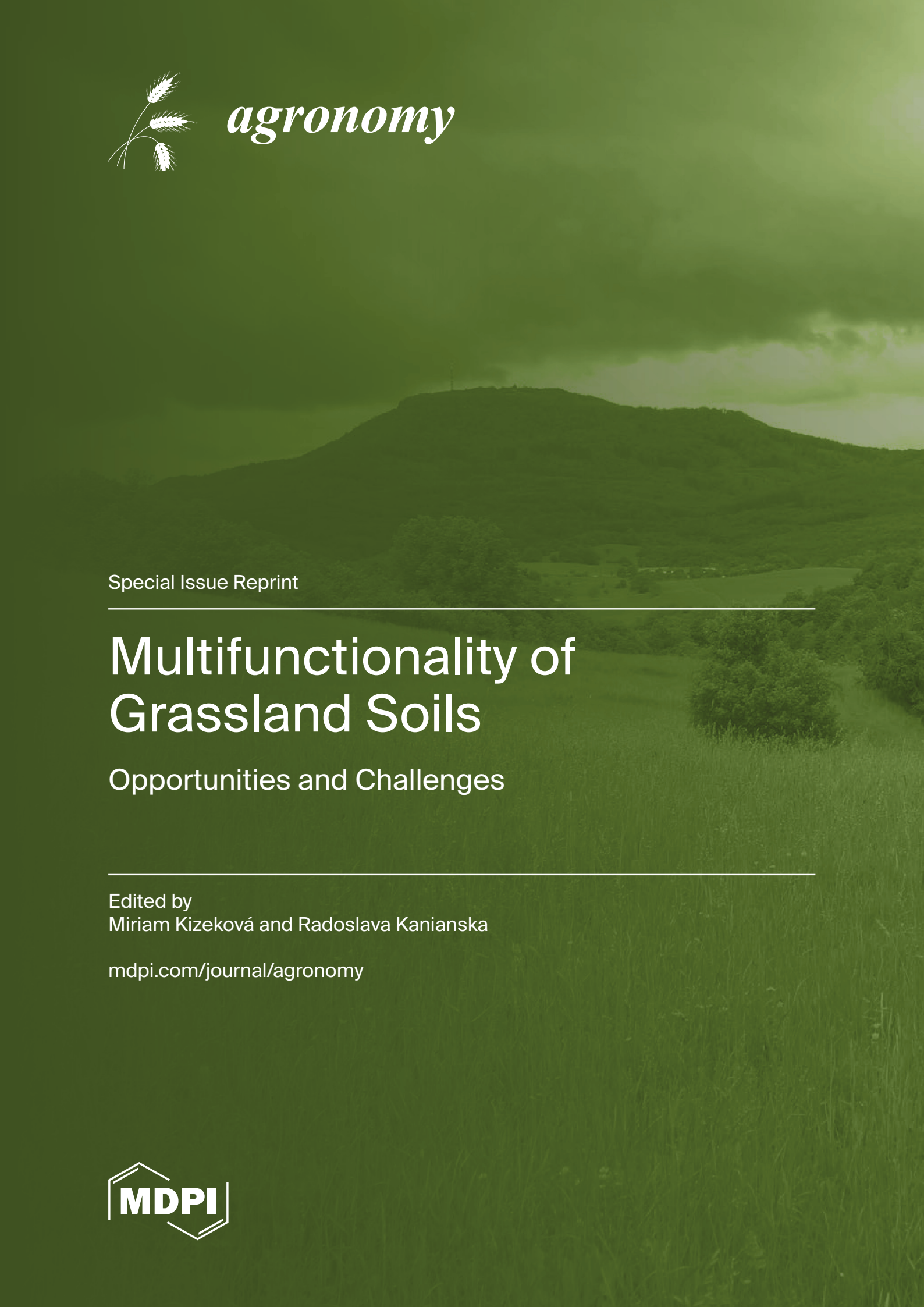


agronomy

Special Issue Reprint

Multifunctionality of Grassland Soils

Opportunities and Challenges

Edited by
Miriam Kizeková and Radoslava Kanianska

mdpi.com/journal/agronomy

MDPI

Multifunctionality of Grassland Soils: Opportunities and Challenges

Multifunctionality of Grassland Soils: Opportunities and Challenges

Guest Editors

Miriam Kizeková
Radoslava Kanianska

MDPI

Basel • Beijing • Wuhan • Barcelona • Belgrade • Novi Sad • Cluj • Manchester

Guest Editors

Miriam Kizeková
Department of Grasslands and Mountain Agriculture
National Agricultural and Food Center
Zvolen
Slovakia

Radoslava Kanianska
Faculty of Natural Sciences
Matej Bel University in Banská Bystrica
Banská Bystrica
Slovakia

Editorial Office

MDPI AG
Grosspeteranlage 5
4052 Basel, Switzerland

This is a reprint of the Special Issue, published open access by the journal *Agronomy* (ISSN 2073-4395), freely accessible at: https://www.mdpi.com/journal/agronomy/special_issues/8088DO0NL4.

For citation purposes, cite each article independently as indicated on the article page online and as indicated below:

Lastname, A.A.; Lastname, B.B. Article Title. *Journal Name* **Year**, *Volume Number*, Page Range.

ISBN 978-3-7258-9145-0 (Hbk)
ISBN 978-3-7258-9146-7 (PDF)
https://doi.org/10.3390/books978-3-7258-9146-7

Cover image courtesy of Kanianska Radoslava

© 2026 by the authors. Articles in this reprint are Open Access and distributed under the Creative Commons Attribution (CC BY) license. The reprint as a whole is distributed by MDPI under the terms and conditions of the Creative Commons Attribution-NonCommercial-NoDerivs (CC BY-NC-ND) license (https://creativecommons.org/licenses/by-nc-nd/4.0/).

Contents

About the Editors . . . . . **vii**

Radoslava Kanianska and Miriam Kizeková
Multifunctionality of Grassland Soils: Opportunities and Challenges
Reprinted from: *Agronomy* **2026**, *16*, 1729, https://doi.org/10.3390/agronomy16171729 . . . . . **1**

Radoslava Kanianska and Miriam Kizeková
Variability of Grassland Soils' Properties in Comparison to Soils of Other Ecosystems
Reprinted from: *Agronomy* **2025**, *15*, 713, https://doi.org/10.3390/agronomy15030713 . . . . . **7**

Xiaowei Wei, Mingyue Sun, Shihan Feng, Ju Zhang, Yidi Gai, Yuheng Yang and Xuechen Yang
Soil Property Alterations and Nitrogen Use Dynamics of *Hemarthria altissima* Under Distinct Nitrogen Forms
Reprinted from: *Agronomy* **2026**, *16*, 155, https://doi.org/10.3390/agronomy16020155 . . . . . **25**

Yuheng Yang, Hao Chen, Guiling Liu, Hang Ruan and Xiaowei Wei
Variation and Trade-Offs in Leaf and Root Traits of Perennial Grasses Under Nitrogen Deposition
Reprinted from: *Agronomy* **2026**, *16*, 739, https://doi.org/10.3390/agronomy16070739 . . . . . **40**

Matej Orešković, Waldemar Spychalski, Barbara Golińska and Piotr Goliński
Effects of Grassland Ley Sward Diversity on Soil Potassium and Magnesium Forms in Two Contrasting Sites
Reprinted from: *Agronomy* **2025**, *15*, 2815, https://doi.org/10.3390/agronomy15122815 . . . . . **58**

Shitong Wei, Chunying Fan, Junqi Zuo, Lingfeng Rui, Jianan Li, Wenjing Tang and Pingting Guan
The Effect of Litter Addition on Soil Organic Carbon Fractions with Intensified Grassland Degradation
Reprinted from: *Agronomy* **2026**, *16*, 835, https://doi.org/10.3390/agronomy16080835 . . . . . **73**

Adrián Jarne, Asunción Usón and Ramón Reiné
Management Practices in Mountain Meadows: Consequences for Soil Nutrient Availability
Reprinted from: *Agronomy* **2024**, *14*, 2419, https://doi.org/10.3390/agronomy14102419 . . . . . **89**

Jie Pan, Feng Yang, Wen Yang, Mingjun Zhang, Shengjiang He and Zhou Li
Fertilizers and Manures Enhance the Bioavailability of Soil Phosphorus Fractions in Karst Grassland
Reprinted from: *Agronomy* **2024**, *14*, 1429, https://doi.org/10.3390/agronomy14071429 . . . . . **105**

Anna Paszkiewicz-Jasińska, Wojciech Stopa, Jerzy Barszczewski, Dorota Gryszkiewicz-Zalega and Barbara Wróbel
Nutrient Balances and Forage Productivity in Permanent Grasslands Under Different Fertilisation Regimes in Western Poland Conditions
Reprinted from: *Agronomy* **2025**, *15*, 2079, https://doi.org/10.3390/agronomy15092079 . . . . . **118**

Yang Shao, Qi Tong, Tsegaye Gemechu Legesse, Changliang Shao and Xiaoguang Zhang
Spring- and Summer Heat Waves Caused Opposite Effects on Soil Respiration in a Eurasian Meadow Steppe
Reprinted from: *Agronomy* **2026**, *16*, 319, https://doi.org/10.3390/agronomy16030319 . . . . . **142**

Igor Bogunovic, Marija Galic, Aleksandra Percin, Sun Geng and Paulo Pereira
The Role of Grassland Land Use in Enhancing Soil Resilience and Climate Adaptation in Periurban Landscapes
Reprinted from: *Agronomy* **2025**, *15*, 1589, https://doi.org/10.3390/agronomy15071589 . . . . . **156**

Cong Chen, Ying Zhang, Zhenbo Cui and Chengyou Cao
Soil Properties and Bacterial Community Responses to Herb Vegetation Succession Beneath Sand-Fixation Plantations in a Sandy Grassland, NE China
Reprinted from: *Agronomy* **2026**, *16*, 342, https://doi.org/10.3390/agronomy16030342 . . . . . **173**

Degyi Yangzom, Shuqin Ma and Xuyang Lu
Quantitative and Qualitative Relationships between Phospholipid Fatty Acid Analysis Biomarkers and Lignin in Soil from the Tibetan Plateau (China) under Laboratory Incubation Conditions
Reprinted from: *Agronomy* **2024**, *14*, 1980, https://doi.org/10.3390/agronomy14091980 . . . . . **191**

About the Editors

Miriam Kizeková

Miriam Kizeková is a scientific researcher at the National Agricultural and Food Center in Slovakia. Her research focuses on grassland ecosystems, with particular emphasis on grassland management, ecosystem services, biodiversity, soil–plant interactions, and sustainable agricultural practices. Her work addresses the multifunctionality of grasslands and their role in supporting sustainable and resilient agricultural systems.

Radoslava Kanianska

Radoslava Kanianska is an associate professor at the Faculty of Natural Sciences of the Matej Bel University in Banská Bystrica, Slovakia, where she teaches Soil and Environmental Sciences and develops her research lines. She is dedicated to comprehensive soil research including physical, chemical and biological properties. She deals with soil degradation processes with emphasis on soil contamination and related ecological and health risk assessments. She also conducts research studies in relationships between abiotic and biotic soil compartments. She asses the impacts of economic sectors (mainly agriculture) and climate change on the soil and environment. She specializes in soil fertility, biomass flows, and sustainable land management. Her primary interests also encompass the soil as a part of ecosystems and its functions and services, including provisioning (biomass provision) and regulating (climatologic, hydrological, filtering, erosion prevention, and biodiversity maintenance).

agronomy

MDPI

Editorial

Multifunctionality of Grassland Soils: Opportunities and Challenges

Radoslava Kanianska [1] and Miriam Kizeková [2,*]

[1] Faculty of Natural Sciences, Matej Bel University in Banská Bystrica, Tajovského 40, 974 01 Banská Bystrica, Slovakia; radoslava.kanianska@umb.sk
[2] Department of Grasslands and Mountain Agriculture, Department of Plant Production, National Agricultural and Food Center, Jozefa Cígera Hronského 1, 960 01 Zvolen, Slovakia
* Correspondence: miriam.kizekova@nppc.sk

1. Introduction

Grasslands are very diverse and their global distribution is determined by the climate, mainly the temperature and precipitation. FAO [1] reported that in 2023, meadows and pastures globally covered 3200 million ha. They are found on all continents except Antarctica, on a wide range of soil types. Temperate grasslands include Eurasian steppes, North American prairies, the pampas lowlands of South America, and Patagonian steppe. Tropical and subtropical savannas occur in Africa and Australia, in the north of South America, in the south of Northern America, and in South Asia and Southeast Asia. These natural grass biomes are under permanent anthropogenic pressure around the world. They are often replaced by intensive agricultural systems [2] and are used as arable land. One of the reasons or this is their high-quality soil, which develops during soil-forming processes thanks to the accumulation of high-quality organic material provided by dead grass bodies. Grasses are generally rich in structural (sugar and starches) and non-structural (cellulose, hemicellulose, pectin, etc.) carbohydrates and contain less protein, minerals, vitamins, and fats in comparison to legumes [3]. They are an excellent prerequisite for high-quality organic matter composition such as that found in the most productive soils on Earth, Chernozems, which only develop in forest–steppe zones [4]. However, grasslands around the world are found on different types of soils, of varying quality, also due to dynamic land use changes. The increased demand for food and fodder results in intensive land utilization. Forests are often being converted into grasslands and pastures, causing significant modifications in soil properties, as reflected in the performance of ecosystem functions and services.

Besides productive functions, grassland soils contribute to a wide range of functions and ecosystem services, including regulating, supporting, and cultural services. They act as carbon sinks [5], contribute to water retention and regulation [6], maintain biogeochemical cycles [7], and are also of major relevance to biodiversity [8].

Despite their importance, grasslands are experiencing widespread and accelerating degradation due to global environmental changes [9], and the percentage of protection for this biome is lower than for all other biomes [10].

Scientists and experts in the field of grasslands are making efforts to increase awareness of the values they offer to humanity, provide new knowledge and improve grasslands' management. They point out their variability, aiming to improve understanding of nutrient cycles and their productivity with the help of sustainable management. They highlight the role of grasslands in dealing with climate change and other environmental risks. Increasing

attention is also dedicated to new, less explored areas, such as the role of grassland soils' microbiome and its contribution to the provision of ecosystem services.

2. An Overview of Published Articles

This Special Issue of *Agronomy* contains 12 research articles focused on the multifunctionality of grassland soils. These original research papers can be grouped into five categories:

(1) Variability of grassland soils' properties (contribution 1).
(2) Grassland soils' nutrients' forms, roots and availability, and factors affecting these (contribution 2, 3, 4).
(3) Grassland soil carbon and nutrients' management(contribution 5, 6, 7, 8).
(4) Grassland soils as buffers against environmental and climate stresses (contribution 9, 10).
(5) Prospective role of microorganisms in grassland soils' processes and functions (contribution 11, 12).

2.1. Variability in Grassland Soils' Properties

Kanianska and Kizeková [1] evaluated the variety of natural conditions and land use patterns (arable land, forest land, and grassland) determining the high variability in soil properties in Central Slovakia. Grasslands situated on alluvial plains were distinguished by the highest biological parameters (earthworm number, biomass and diversity) and a higher capacity for water retention and C and N storage in comparison to other land types, including grasslands situated on slopes.

2.2. Grassland Soil Nutrients' Forms, Roots, Availability and Factors Affecting These

Wei et al. [2] investigated how inorganic nitrogen form regulates nitrogen uptake in *H. altissima* through pot experiments by applying ammonium nitrogen, nitrate nitrogen, mixed nitrogen, and a nitrogen-free control in Songnen grassland ecosystems at the eastern end of Eurasia. Ammonium and nitrate applications reduced soil pH, increased electrical conductivity, and enhanced inorganic nitrogen pools, respectively. Root morphological traits were significantly enhanced under ammonium, nitrate, and mixed nitrogen treatments. Their findings highlight nitrogen form as a key regulator of soil–plant nitrogen coupling.

Yang et al. [3] observed the effect of atmospheric nitrogen on the leaf and root traits of eight perennial grasses in a field experiment, incorporating control and nitrogen addition treatments. Nitrogen addition significantly altered leaf and root trait expression and promoted biomass accumulation in both life forms. Specifically, nitrogen addition increased assimilation rate, leaf nitrogen content, specific root length, and root nitrogen content while markedly reducing the root tissue density of perennial rhizome grass and perennial bunchgrasses. The results indicated a decoupling of above- and belowground resource acquisition strategies at the local scale. Additionally, authors underscored the importance of combining above- and belowground traits to improve predictions of plant performance.

Orešković et al. [4] quantified the soluble, active, and exchangeable forms of K and Mg in two soil types, Cambisols and Luvisols, using grassland ley swards differing in the species composition of their sown mixtures. Thirty-three plant communities were established following a simplex design approach, with sown proportions ranging from 100% (monocultures) to 50%, 33%, 25%, 16.7%, and 0%. Plant diversity only had a slightly negative trend for potassium on Cambisols. Grass-dominated mixtures maintained higher soil K levels as legume-rich swards. Differing effects of the extractants on K regarding indications of the need to use the $CaCl_2$ and NH_4OAc extraction methods were also observed.

https://doi.org/10.3390/agronomy16171729

2.3. Grassland Soil Nutrients Management

Wei et al. [5] observed the effect of litter addition on soil organic carbon fractions with intensified grassland degradation in a 240-day incubation experiment using Leymus chinensis litter incubated on days 0, 23, 60, and 240. Grassland degradation significantly reduced particulate organic carbon (POC) and mineral-associated organic carbon (MAOC) concentrations; moreover, litter addition in degraded grasslands further reduced soil organic carbon (SOC). In the lightly and moderately degraded grasslands, litter addition modulated POC and MAOC via both microbial and physicochemical pathways. In the highly degraded grasslands, litter addition influenced POC and MAOC not only indirectly, through microbial and physicochemical pathways, but also directly, by promoting MAOC formation. Overall, although litter decomposition altered SOC and its fractions, its effects were constrained by the degree of grassland degradation.

Jarne et al. [6] investigated the nitrogen, phosphorus, potassium and carbon balances under three different types of meadows, as follows: intensive meadows (with high livestock load and inorganic fertilization); semi-extensive meadows (with medium livestock load and organic fertilization); and extensive meadows (with low livestock load and low fertilization rates). Nitrogen was more stable in semi-extensive and extensive meadows, due to its organic form. In contrast, intensive meadows showed higher nitrogen variability depending on the climate. Carbon accumulation was more stable in extensive meadows. Potassium showed a strong response to temperature, and phosphorus appeared as a limiting factor.

Phosphorus is one of the major constraints to karst grassland productivity, as observed by Pan et al. [7]. They investigated the effects of fertilizers and manures on soil bioavailability of phosphorus fractions in karst grasslands and explored the relationship between soil properties and soil phosphorus fractions within an experiment with the four fertilizer applications (control; fertilization; manure application; combined fertilization and manure application). The combined application of fertilizer and manure was the most beneficial measure for enhancing soil phosphorus bioavailability.

Paszkiewicz-Jasińska et al. [8] conducted a field experiment at the Experimental Station in Poznań-Strzeszyn, western Poland, under production conditions with different fertilization regimes, varying in both type and dosage. The treatments included an unfertilized control, mineral fertilization (NPK), farmyard manure (FYM), and alternate NPK/FYM fertilizers. The most balanced nutrient budgets were observed under alternate NPK/FYM fertilization, with moderate surpluses of N and P and a smaller K deficit compared to FYM applied alone. In contrast, inorganic and organic fertilization applied separately resulted in greater nutrient surpluses or a pronounced potassium deficit. This study showed how alternating FYM and mineral NPK can maintain productivity and reduce environmental impacts.

2.4. Grassland Soils as Buffers to Environmental and Climate Stresses

Climate changes accompanied by heat ways (HWs) threaten grassland ecosystems. Shao et al. [9] conducted an in situ spring and summer HWs simulation experiment combined with a locally common human disturbance (mowing) to separate soil respiration (Rs) into autotrophic respiration (Ra) and heterotrophic respiration (Rh) on a natural Eurasian meadow steppe. HWs significantly affected grassland Rs, Rh and Ra and also interacted with mowing, but the effect of spring HW and summer HW were different. Rs, Rh and Ra were inhibited by spring HWs but promoted by summer HWs. The results indicated that time changes in HWs have widely divergent influences on the ecosystem, and mowing would decrease the anti-interference ability of the ecosystem.

Bogunovic et al. [10] showed how grassland soils are important components of urban green areas and croplands in the peri-urban area of Zagreb, exhibiting multifunctional

https://doi.org/10.3390/agronomy16171729

benefits, including high organic matter content, improved bulk density and active carbon storage. The presence of permanent vegetation cover contributed to the high capacity for climate and water regulation and carbon sequestration. The results emphasize the importance of protecting and managing grasslands as an important component of urban green areas. Practices such as mulching, minimal disturbance and continuous cover can maximize the resilience to climate change and the ecosystem services of grassland soils.

2.5. Perspective Role of Microorganisms in Grassland Soils Processes and Functions

Chen et al. (contribution 11) found out that shrub plantations on mobile sand dunes are an effective strategy to combat desertification in semi-arid regions. Herbaceous communities developing beneath these plantations enhance ecosystem stability and improve revegetation outcomes. They investigated the structural responses of soil bacterial communities, key functional genes, and plant–soil–microbe interactions across an herbaceous vegetation succession gradient under *Caragana microphylla* sand-fixation plantations in the sandy Horqin Grassland. Plant species richness, diversity, and biomass increased progressively with succession. Concurrent improvements in soil nutrients and enzymatic activities were observed. The most influential factors for soil bacterial community were pH and organic matter. These findings highlight plant–soil–microbe interactions as intrinsic drivers of vegetation succession in desertified ecosystems.

Yangzom et al. (contribution 12) investigated whether lignin is labile or resistant to biological and chemical degradation in soil, particularly in alpine ecosystems. They analyzed the relationship between phospholipid fatty acid biomarkers and the abundance of lignin components in grassland soils from North Tibet, China. Theay collected soil samples and measured the relative abundance of lignin before and after a 210-day incubation period. They found out that the relative abundance of lignin in the alpine grassland soils decreased during the incubation period. Significant relationships were found between the phospholipid fatty acid biomarkers of bacteria, fungi, Gram-positive bacteria, and Gram-negative bacteria and the relative abundance of lignin components. This study contributed to the understanding of soil organic matter degradation and the dynamics of microbial communities in alpine grassland soils in the context of future global warming.

3. Conclusions

Healthy soil, a non-renewable resource, is fundamental to sustaining grassland ecosystem services and ensuring the long-term resilience of agricultural landscapes. This Special Issue demonstrates that grassland soils support a wide range of ecological, environmental, and socio-economic functions that remain insufficiently recognized in both research and policy. The research articles collected here underline the importance of interdisciplinary research for improving our understanding of grassland soil multifunctionality and for developing evidence-based management strategies. We hope that this Special Issue will stimulate further research, strengthen collaboration among scientists and practitioners, and support the integration of soil multifunctionality into sustainable grassland management and policy development.

Author Contributions: Both authors (M.K. and R.K.) contributed equally to the development of this Editorial. All authors have read and agreed to the published version of the manuscript.

Funding: This work was supported by the Ministry of Agriculture and Rural Development of the Slovak Republic under Grant No. 1299/2025/MPRVSR–930.

Acknowledgments: The Editors wish to thank all the authors who invested time and effort in making valuable contributions to this Special Issue.

Conflicts of Interest: The authors declare no conflicts of interest.

https://doi.org/10.3390/agronomy16171729

List of Contributions:

1. Kanianska, R.; Kizeková, M. Variability of grassland soils' properties in comparison to soils of other ecosystems. *Agronomy* **2025**, *15*, 713. https://doi.org/10.3390/agronomy15030713.
2. Wei, X.; Sun, M.; Feng, S.; Zhang, J.; Gai, Y.; Yang, Y.; Yang, X. Soil property alterations and nitrogen use dynamics of *Hemarthria altissima* under distinct nitrogen forms. *Agronomy* **2026**, *16*, 155. https://doi.org/10.3390/agronomy16020155.
3. Yang, Y.; Chen, H.; Liu, G.; Ruan, H.; Wei, X. Variation and trade-offs in leaf and root traits of perennial grasses under nitrogen deposition. *Agronomy* **2026**, *16*, 739. https://doi.org/10.3390/agronomy16070739.
4. Oreškovic, M.; Spychalski, W.; Golinska, B.; Golinski, P. Effects of grassland ley sward diversity on soil potassium and magnesium forms in two contrasting sites. *Agronomy* **2025**, *15*, 2815. https://doi.org/10.3390/agronomy15122815.
5. Wei, S.; Fan, C.; Zuo, J.; Rui, L.; Li, J.; Tang, W.; Guan, P. The effect of litter addition on soil organic carbon fractions with intensified grassland degradation. *Agronomy* **2026**, *16*, 835. https://doi.org/10.3390/agronomy16080835.
6. Jarne, A.; Usón, A.; Reiné, R. Management practices in mountain meadows: Consequences for soil nutrient availability. *Agronomy* **2024**, *14*, 2419. https://doi.org/10.3390/agronomy14102419.
7. Pan, J.; Yang, F.; Yang, W.; Zhang, M.; He, S.; Li, Z. Fertilizers and manures enhance the bioavailability of soil phosphorus fractions in karst grassland. *Agronomy* **2024**, *14*, 1429. https://doi.org/10.3390/agronomy14071429.
8. Paszkiewicz-Jasinska, A.; Stopa, W.; Barszczewski, J.; Gryszkiewicz-Zalega, D.; Wróbel, B. Nutrient balances and forage productivity in permanent grasslands under different fertilisation regimes in western Poland conditions. *Agronomy* **2025**, *15*, 2079. https://doi.org/10.3390/agronomy15092079.
9. Shao, Y.; Tong, Q.; Legesse, T.G.; Shao, C.; Zhang, X. Spring- and summer heat waves caused opposite effects on soil respiration in a Eurasian meadow steppe. *Agronomy* **2026**, *16*, 319. https://doi.org/10.3390/agronomy16030319.
10. Bogunovic, I.; Galic, M.; Percin, A.; Geng, S.; Pereira, P. The role of grassland land use in enhancing soil resilience and climate adaptation in periurban landscapes. *Agronomy* **2025**, *15*, 1589. https://doi.org/10.3390/agronomy15071589.
11. Chen, C.; Zhang, Y.; Cui, Z.; Cao, C. Soil properties and bacterial community responses to herb vegetation succession beneath sand-fixation Plantations in a sandy grassland, NE China. *Agronomy* **2026**, *16*, 342. https://doi.org/10.3390/agronomy16030342.
12. Yangzom, D.; Ma, S.; Lu, X. Quantitative and qualitative relationships between phospholipid fatty acid analysis biomarkers and lignin in soil from the Tibetan Plateau (China) under laboratory incubation conditions. *Agronomy* **2024**, *14*, 1980. https://doi.org/10.3390/agronomy14091980.

References

1. FAO. *Land Statistics 2001–2023—Global, Regional and Country Trends*; FAOSTAT Analytical Briefs, 2025, No. 107; FAO: Rome, Italy, 2025. [CrossRef]
2. French, K.E.; Tkacz, A.; Turnbull, L.A. Conversion of grassland to arable decreases microbial diversity and alters community composition. *Appl. Soil Ecol.* **2017**, *110*, 43–52. [CrossRef]
3. Tambara, A.A.C.; Sippert, M.R.; Jauris, G.C.; Flores, J.L.C.; Henz, É.L.; Velho, J.P. Production and chemical composition of grasses and legumes cultivated in pure form, mixed or in consortium. *Act. Sci. Anim. Sci.* **2017**, *39*, 235–241. [CrossRef]
4. Smirnova, M.A.; Lozbenev, N.I.; Levchenko, E.A.; Fil, P.P.; Kozlov, D.N. Chernozems of Eastern European forest-steppe lowland landscapes: Morphology, classification and spatial distribution. *Geoderma Reg.* **2025**, *41*, e00965. [CrossRef]
5. Bai, Y.; Cotrufo, M.F. Grassland soil carbon sequestration: Current understanding, challenges, and solution. *Science* **2022**, *377*, 603–608. [CrossRef]
6. Liu, H.; Hou, L.; Kang, N.; Nan, Z.; Huang, J. The economic value of grassland ecosystem services: A global meta-analysis. *Grassl. Res.* **2022**, *1*, 63–74. [CrossRef]
7. Rumpel, C.; Cr'eme, A.; Ngo, P.T.; Vel'asquez, G.; Mora, M.L.; Chabbi, A. The impact of grassland management on biogeochemical cycles involving carbon, nitrogen and phosphorus. *J. Soil Sci. Plant Nutr.* **2015**, *15*.. [CrossRef]
8. Thornley, R.H.; Gerard, F.F.; White, K.; Verhoef, A. Prediction of grassland biodiversity using measures of spectral variance: A meta-analytical review. *Remote Sens.* **2023**, *15*, 668. [CrossRef]

9. Bardgett, R.D.; Bullock, J.M.; Lavorel, S.; Manning, P.; Schaffner, U.; Ostle, N.; Chomel, M.; Durigan, G.; Fry, E.L.; Johnson, D.; et al. Combatting global grassland degradation. *Nat. Rev. Earth Environ.* **2021**, *2*, 720–735. [CrossRef]
10. Hoesktra, J.M.; Boucher, T.M.; Ricketts, T.H.; Roberts, C. Confronting a biome crisis: Global disparities of habitat loss and protection. *Ecol. Lett.* **2005**, *8*, 23–29. [CrossRef]

Disclaimer/Publisher's Note: The statements, opinions and data contained in all publications are solely those of the individual author(s) and contributor(s) and not of MDPI and/or the editor(s). MDPI and/or the editor(s) disclaim responsibility for any injury to people or property resulting from any ideas, methods, instructions or products referred to in the content.

agronomy

MDPI

Article

Variability of Grassland Soils' Properties in Comparison to Soils of Other Ecosystems

Radoslava Kanianska [1,*] and Miriam Kizeková [2]

[1] Faculty of Natural Sciences, Matej Bel University in Banská Bystrica, Tajovského 40, 974 01 Banská Bystrica, Slovakia
[2] Grassland and Mountain Agriculture Institute, National Agricultural and Food Centre, Mládežnícka 36, 974 21 Banská Bystrica, Slovakia; miriam.kizekova@nppc.sk
* Correspondence: radoslava.kanianska@umb.sk

Abstract: The variety of natural conditions and land use patterns determine high variability of soil properties. This study focused on the analysis of chemical, physical, and biological properties of grassland (GL) soils (situated on slopes—GLS, and on alluvial plains—GLP) in comparison with soils of other ecosystems (arable land, forest land, riparian zone) in Central Slovakia. We applied an indicator's method combined with models of these properties. The studies showed a large variability, more pronounced in GLS than in GLP. GLP soils were characterized by the highest number, biomass, and diversity of earthworms among all ecosystems. GL soils, in addition to FL soils, also have a relatively high capacity for water retention and C and N storage. However, we found an unfavorable state in available phosphorus, with GLS showing the lowest levels among compared ecosystems.

Keywords: grassland soil; available nutrient; earthworm community; soil water retention; carbon and nitrogen stock

1. Introduction

Grasslands cover about 40% of the Earth's surface, comprising open grassland, grassy shrublands, and savannas, and almost 70% of agricultural lands [1,2]. In the EU, grasslands cover 34% of the land territory [3] and are very diverse, resulting from inherent factors such as climate, soil, and management intensities [4]. They occur commonly where site-specific conditions are less favorable for crop farming [5].

Different types of grasslands exhibit obvious differences in their properties and ecosystem functions, which is also reflected in the fulfilment of their ecosystem services. Therefore, it is of great significance to investigate them [6]. The most important characteristics of grassland soils are their dark, organic matter-rich surface layers and their substantial contents of nutritive elements [7].

Grasslands provide many benefits to humankind including all four categories of ecosystem services, provisioning, regulating, supporting, and cultural [8,9]. They provide feed for livestock, food for people through livestock and its products as meat, milk, and fibre [10]. Grasslands significantly contribute to the regulation of the water cycle [11], nutrient cycle [12], carbon sequestration [13], nitrogen storage [14], or erosion control [15]. Grasslands also play a key role in maintaining biodiversity [16] and provide a buffer against climate variability [17].

Provisioning ecosystem services are particularly emphasized, also having market value (as fodder and livestock production) [18]. Other regulating, supporting, and cultural

services with indirect (such as water and climate regulation) or intangible effect (such as cultural services) are often ignored in land management [19].

It should be emphasized that soil ecosystem services depend on soil properties and their interactions. The definition of the so-called soil-related ecosystem services refers to the frameworks by Dominati et al. [20] and Adhikari and Hartemink [21], emphasizing the link between soil properties and related ecosystem services. However, many studies on the valuation of ecosystem services lack a soil component or soil is poorly defined or too generalized [22]. But soil properties are directly linked to soil functions that ultimately determine the delivery of ecosystem services, which is well documented in many studies [23–25]. For example, the filtration of water is regulated by soil properties such as pore size or bulk density, while the biomass production is determined by nutrient availability or soil moisture.

Similarly, the spatial aspects and dynamics of soil properties to ecosystem services have been studied through mapping or modeling without terrain research as representative, as it is a time- and resource-demanding process. Proxy data are often used, as they are useful in regions where data are scarce [26]. However, due to the possible high spatial variability of soil properties, these models may be questioned. Hence, the results that are the outputs of detailed field research gain importance here.

Despite the importance of grassland, over the past century, changes in land use have led to extensive loss of temperate semi-natural grasslands [27], conversion into agricultural areas, abandonment, or afforestation [28]. Furthermore, high conservation alluvial grasslands historically shaped by river dynamics [29] have seen decline due to river regulations and agricultural intensification [30].

Grassland degradation is widespread and accelerating in many parts of the world, with up to 49% of global grasslands having been degraded to some extent [31]. Grassland degradation thus creates major environmental problems, as grasslands play a critical role in ecosystem services [32].

For effective land management, it is necessary to know and analyze the diverse soils of grasslands, also in comparison with the soils of other ecosystems, and to determine the positive aspects but also the possible negative ones associated with their management. Here, we sampled and measured soil properties and tested the hypothesis that grassland soils are characterized by high diversity conditioned by various factors (e.g., soil type, landscape unit). Our goal was to cover a broad range of soil properties including chemical, physical, and biological. Thus, the main objectives of this study were (1) to characterize different soil types of grasslands developed under different climatic and natural conditions (roughly divided into two groups: slope and plain grasslands) also in comparison to the soils of other different ecosystems (arable land, forest land, riparian zone) by basic chemical, biological, and physical properties, (2) to identify critical properties of grassland soils based on the assessment, (3) to analyze mutual relationships between soil properties, and (4) to examine how land use influences soil properties.

2. Materials and Methods

2.1. Site Description

This study was conducted in Central Slovakia, as a part of the Central and Inner Western Carpathians. The region has a diverse topography that ranges from mountains primarily in the north to rolling hills in the central part, and basins in the south. The elevation varies greatly, with many different landscapes. The climate is temperate but is influenced by elevation and relief. The region is dominated by forests followed by grasslands and arable land [33]. Permanent grasslands are considered the most important

semi-natural habitat in the region for the provision of ecosystem services and for the maintenance of biodiversity.

2.2. Sampling Design

Twenty study sites were selected with 20 permanent grasslands, of which 11 on mountain slopes (slope grasslands—GLSs) and 9 on river alluvial plains (plain grasslands—GLPs), together marked as GLSP. They were situated between 155 m and 930 m of altitude. All 9 GLPs were developed on Fluvisols, and GLSs were developed on 3 different soil types, Cambisols (8), Leptososls (2), Planosol (1), classified according to the World Reference Base for Soil Resources [34]. In order to compare grassland soils with soils of other ecosystems, we selected 18 additional localities within study sites. Within 6 study sites in the plains, we selected a riparian zone in addition to a grassland and within 6 study sites with sloping land, in addition to a grassland, a location with arable land and one with forest land. Thus, at 20 study sites, we selected 38 localities in total, of which 20 were grasslands (11 GLSs and 9 GLPs), 6 arable lands (ALs), 6 forest lands (FLs), and 6 riparian zones (RZs) (Figure 1, Table 1). Grasslands were grazed or mowed. Arable lands were managed intensively, less intensively, or ecologically. Forests were deciduous, mixed, and coniferous. The riparian vegetation consisted mainly of trees such as willows, poplars, shrubs, grasses, and herbs.

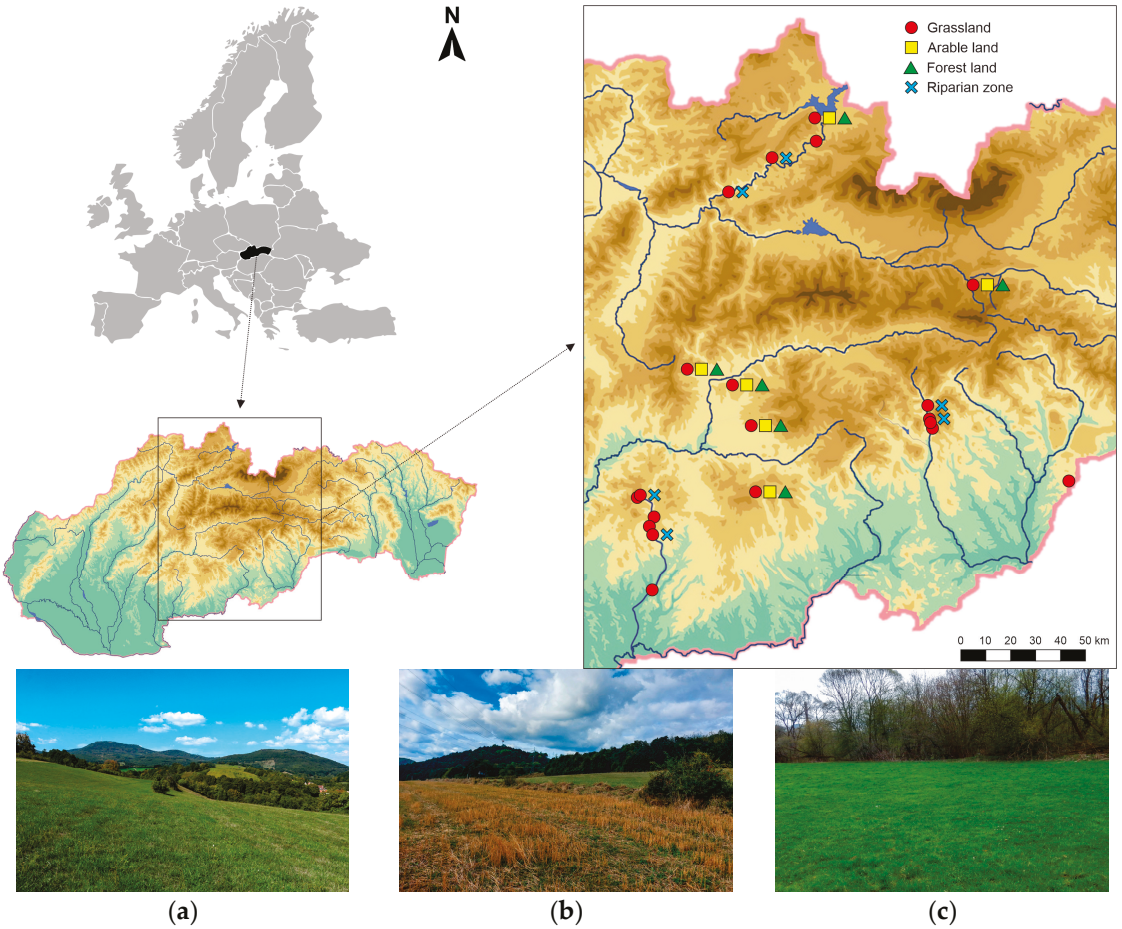


Figure 1. Map of localities in Central Slovakia and photos from selected study sites; (**a**) Grassland on slope; (**b**) Arable land, grassland, and forest land on slope; (**c**) Grassland and riparian zone on plain.

Table 1. Characteristics of the localities.

Cadastre	Locality	Latitude (N)	Longitude (E)	Altitude (A) (m)	Soil Type	Land Use	Landscape Unit
Liptovska Teplicka	GL_S_LP_LT	N48°57.011	E20°06.875	930	LP	GL	S
Stara Huta	GL_S_CM_SH	N48°27.880	E19°17.490	783	CM	GL	S
Banska Stiavnica	GL_S_CM_BS	N48°26.749	E18°53.297	659	CM	GL	S
Oravska Jasenica	GL_S_CM_OJ	N49°24.106	E19°25.976	656	CM	GL	S
Stiavnicke Bane	GL_P_FL_SB	N48°26.136	E18°52.632	648	FL	GL	P
Tajov	GL_S_CM_TA	N48°44.837	E19°03.153	597	CM	GL	S
Nizna	GL_S_CM_NI	N49°18.261	E19°31.029	572	CM	GL	S
Dolna Lehota	GL_S_FL_DL	N49°15.947	E19°21.743	508	FL	GL	P
Horna Micina	GL_S_CM_HM	N48°42.363	E19°13.330	462	LP	GL	S
Zaskov	GL_S_FL_ZA	N49°11.343	E19°12.488	451	FL	GL	P
Ocova	GL_S_PL_OC	N48°36.390	E19°17.122	412	PL	GL	S
Tisovec	GL_P_FL_TI	N48°39.710	E19°56.470	385	FL	GL	P
Svaty Anton	GL_P_FL_SA	N48°22.979	E18°55.854	353	FL	GL	P
Hacava	GL_P_FL_HA	N48°37.257	E19°57.056	351	FL	GL	P
Kecovo	GL_S_CM_KE	N48°28.586	E20°27.858	344	CM	GL	S
Prencov	GL_S_CM_PR	N48°21.675	E18°55.174	335	CM	GL	S
Hnusta	GL_S_CM_HN	N48°36.012	E19°57.588	328	CM	GL	S
Hnusta	GL_P_FL_HN	N48°36.900	E19°57.440	322	FL	GL	P
Prencov	GL_P_FL_PR	N48°20.859	E18°55.871	288	FL	GL	P
Dvorniky	GL_P_FL_DV	N48°12.168	E18°55.733	155	FL	GL	P
Liptovska Teplicka	AL_S_LP_LT	N48°57.009	E20°06.749	920	LP	AL	S
Stara Huta	AL_S_CM_SH	N49°27.897	E19°17.500	781	CM	AL	S
Oravska Jasenica	AL_S_CM_OJ	N49°24.117	E19°25.982	656	CM	AL	S
Tajov	AL_S_CM_TA	N48°44.847	E19°03.117	595	CM	AL	S
Horna Micina	AL_S_LP_HM	N48°42.326	E19°13.320	460	LP	AL	S
Ocova	AL_S_PL_OC	N48°36.383	E19°17.169	410	PL	AL	S
Liptovska Teplicka	FL_S_FL_LT	N48°56.828	E20°06.483	925	LP	FL	S
Stara Huta	FL_S_CM_SH	N49°27.833	E19°17.472	777	CM	FL	S
Oravska Jasenica	FL_S_CM_OJ	N49°24.180	E19°25.737	667	CM	FL	S
Tajov	FL_S_CM_TA	N48°44.791	E19°03.119	580	CM	FL	S
Horna Micina	FL_S_LP_HM	N48°42.385	E19°13.378	465	LP	FL	S
Ocova	FL_S_PL_OC	N48°36.489	E19°17.001	437	PL	FL	S
Stiavnicke Bane	RZ_P_FL_SB	N48°26.113	E18°52.635	648	FL	RZ	P
Dolna Lehota	RZ_P_FL_DL	N49°15.935	E19°21.757	505	FL	RZ	P
Zaskov	RZ_P_FL_ZA	N49°11.367	E19°12.420	451	FL	RZ	P
Tisovec	RZ_P_FL_TI	N48°39.704	E19°56.472	385	FL	RZ	P
Hnusta	RZ_P_FL_HN	N48°36.891	E19°57.465	322	FL	RZ	P
Prencov	RZ_P_FL_PR	N48°20.866	E18°55.900	284	FL	RZ	P

Abbreviations: CM—Cambisol, LP—Leptosol, FL—Fluvisol, PL—Planosol, GL—Grassland, AL—Arable land, FL—Forest land, RZ—Riparian zone, S—Slope, P—Plain.

2.3. Soil Chemical, Physical, and Biological Analysis

At each locality, five sampling points with a Z-shaped pattern were selected. Soil samples were collected at 0–20 cm during spring (March–May) or autumn (September–October) from 2019 to 2023. Field samples consisted of approximately 1 kg of soil; they were mixed, homogenized, air-dried, and sifted through a 2 mm mesh sieve. Soil reaction (pH/H_2O) was measured with a potentiometer in a 1:1 soil-to-water mix, and exchangeable soil reac-

tion (pH/KCl) was determined by the KCl method as a 1:2.5 soil:1M KCl solution mix. Soil organic carbon (SOC) content was determined using an oxidimetric method according to Tjurin (a modification of Nikitin) [35]. Organic matter content (OM) was recalculated from SOC using 1.724 coefficient. Total nitrogen content (NT) was determined by the Kjeldahl method [36]. The available nutrients P, K, and Mg were extracted by Melich III [37]. P was determined calorimetrically on the analyzer Scalar, Mg and K by flame photometry. The carbon and nitrogen stock were calculated for a 20 cm thick upper soil layer according to Tan [38] and Chen [39] (Equation (1)):

$$CS = \sum_{i=1}^{n} SOCi * BDi * Hi * \left(1 - \frac{G}{100}\right) * 10^{-1} \quad (1)$$

where CS is the C stock pool (t.ha^{-1}) of the evaluated soil profile, $SOCi$ is SOC content (g.kg^{-1}), BDi is the bulk density (g.cm^{-3}), Hi is the soil thickness (cm), and G is the volume percent of gravel and stones (particle size > 2 mm) in layer i, respectively.

A similar approach was used to calculate NS (t.ha^{-1}) (Equation (2)):

$$NS = \sum_{i=1}^{n} SNTi * BDi * Hi * \left(1 - \frac{G}{100}\right) * 10^{-1} \quad (2)$$

where NS is the N stock pool (t.ha^{-1}) of the evaluated soil profile, $SNTi$ is the total soil nitrogen content (g.kg^{-1}), BDi is the bulk density (g.cm^{-3}), Hi is the soil thickness (cm), and G is the volume percent of gravel and stones (particle size > 2 mm) in layer i, respectively.

Particle size fractions (clay, silt, sand, and gravel) were determined by the pipette method using soil particle sedimentation and classified according to the United States Department of Agriculture system. Bulk density (BD) was determined using undisturbed soil samples that were hermetically sealed in stainless steel tubes and taken to the laboratory for analyses using the gravimetric method according to Novák [40]. Particle density (PD) was measured by the pycnometer method according to Blake and Hartage [41]. The hydrological soil properties as indicators were calculated according to Gupta and Larson [42] for temperate pedotransfer functions [43] as field water capacity (FWC) (Equation (3)), wilting point (WP) (Equation (4)), available water capacity (AWC) (Equation (5)), and soil water deficit index (SWDI) (Equation (6)):

$$\begin{aligned} FWC = {} & 0.003075 * Sa + 0.005886 * Si + 0.008039 * Cl + 0.002208 * SOM \\ & -0.01434 * BD \end{aligned} \quad (3)$$

$$\begin{aligned} WP = {} & -0.000059 * Sa + 0.001142 * Si + 0.005766 * Cl + 0.002228 * SOM \\ & +0.002671 * BD \end{aligned} \quad (4)$$

where Sa is the percentage of sand, Si is the percentage of silt particles, Cl is the percentage of clay particles, SOM is the percentage of soil organic matter, and BD is the bulk density.

$$AWC = FWC - WP\ (\%) \quad (5)$$

where FWC is the field water capacity in %, WP is the wilting point in %.

The SWDI proposed by Martinez-Fernandez et al. [44] characterizes drought based on soil moisture and calculated hydrological soil properties. This index is capable of adequately identifying the main attributes that define a drought event. For the calculation, the following formula was used:

$$SWDI = \left(\frac{SMa - FWC}{AWC}\right) * 10 \quad (6)$$

where *SMa* is the actual soil moisture in %, *FWC* is the field water capacity in %, and *AWC* is the available water capacity in %.

SWDI positive values mean an excess of water in the soil. When SWDI equals zero, soil is in the field capacity of the water content (that is, without water deficit). Negative values indicate soil drought. The SWDI in the range 0−−2 means mild, −2−−5 moderate, −5−−10 severe, and ≤−10 extreme drought level.

Various chemical, physical, and biological properties were measured directly on the ground at the points from which the samples were collected for chemical and physical analyses. Earthworms were sampled in five 30 cm × 30 cm × 20 cm soil monoliths. The excavated soil monoliths were broken by hand, all earthworms collected, washed, counted, weighed, and thereafter identified to species level [45,46]. Earthworm community was assessed by earthworm number (EN), biomass (EB), and diversity (as Shannon's diversity index H).

Redox potential (Eh) was measured by the Oxygen Diffusion meter (Eijkelkamp Equipment for Soil Research, The Netherlands). Penetrometric resistance (PR in MPa.cm^{-1}) with related depth (DPR in cm) was measured by a penetrologger (Eijkelkamp Equipment for Soil Research, The Netherlands). Actual soil moisture (SM in %) and soil temperature (ST in °C) were measured using a WET sensor (Delta-T Devices Ltd. Cambridge, UK). Soil respiration rates as the net carbon exchange rate (NCER in μmol CO_2.m^{-2}s^{-1}) were measured by the closed-chamber method using an infrared gas analyzer (LC-Pro+, ADC BioScientific Ltd., Hoddesdon, UK).

2.4. Data Analysis

Data were subjected to descriptive statistics such as the mean, Spearman's correlation coefficient, analysis of variance (ANOVA), and hierarchical cluster analysis (HCA). The Shapiro–Wilk test was used to determine whether data come from a normal distribution. Levene's test was used to assess the equality of variances. The Tukey HSD test was used as a post hoc test. Because some data follow non-normal distribution, we used Spearman's correlation coefficient to verify correlation between all variables considering all study sites (n = 38). Subsequently, based on the normality and homogeneity tests, we selected variables tested by ANOVA and HCA considering 30 study sites (n = 30 of 6 GLSs, 6 FLs, 6 ALs, 6 RZs, 6 GLPs). The data were analyzed by using SPSS Statistics 28.

3. Results

3.1. Soil Chemical, Physical, and Biological Properties in Different Ecosystems

The basic statistical characteristics of the chemical, biological, and physical soil properties in GL, AL, FL, and RZ are reported in Tables 2–4.

In the GL soil group, most soil characteristics showed a large variability of selected soil properties, e.g., pH/H_2O ranges from 4.83 to 9.01. Higher variability was more pronounced in GLS compared to GLP soils. When comparing specific properties, the average values of pH and Eh were higher in GLP soils, and on the other hand, properties such as SOC or NT were lower corresponding to a lower supply of organic matter. In addition, the organic matter in GLP soils was of poorer quality, expressed by a higher C/N ratio. In GLSP soils, available Mg (ranging from 220.1 to 4700.4 mg.kg^{-1}) was at a very high level, available K (ranging from 49.1 to 349.3 mg.kg^{-1}) at high level, and available P (ranging from 0.5 to 33.7 mg.kg^{-1}) at a very low level. In GLS soils, Mg reserves were slightly higher, and K and P reserves were found to be lower than those found in GLP soils. Among other ecosystems, GLSP soils were characterized by lower contents of available K and conversely, GLS soils had the highest Mg reserves. Available P reserves in GL and FL soils were the lowest.

Table 2. Soil chemical properties.

Ecosystem	Statistical Characteristics	pH/H_2O	pH/KCl	Eh (mV)	SOC (g kg^{-1})	SOM (g kg^{-1})	NT (g kg^{-1})	C/N	P (mg kg^{-1})	K (mg kg^{-1})	Mg (mg kg^{-1})
GLSP	$\bar{x} \pm SD$	6.37 ± 1.03	5.93 ± 1.17	364 ± 47	28.55 ± 11.64	49.22 ± 20.06	2.70 ± 1.22	10.94 ± 2.98	8.07 ± 9.17	187.8 ± 93.2	818.9 ± 1017.55
	Min	4.84	3.98	291	13.88	23.93	1.42	7.24	0.04	49.1	220.14
	Max	9.01	8.93	451	51.81	89.32	6.09	20.93	33.73	349.3	4700.38
GLS	$\bar{x} \pm SD$	6.20 ± 1.23	5.84 ± 1.43	361 ± 52	33.74 ± 12.73	58.17 ± 21.95	3.27 ± 1.37	10.78 ± 3.47	5.43 ± 6.36	188.50 ± 94.63	1083.24 ± 1286.40
	Min	4.84	3.98	291	15.00	25.86	1.42	7.24	0.04	71.69	220.14
	Max	9.01	8.93	451	51.81	89.32	6.09	20.93	22.83	349.30	4700.38
GLP	$\bar{x} \pm SD$	6.57 ± 0.63	6.06 ± 0.70	368 ± 36	22.21 ± 5.16	38.28 ± 8.89	2.02 ± 0.40	11.15 ± 2.10	11.30 ± 10.33	187.01 ± 86.64	495.90 ± 282.37
	Min	5.36	5.08	317	13.88	23.93	1.42	7.27	2.87	49.11	238.08
	Max	7.44	7.19	448	31.48	54.27	2.72	13.94	33.73	319.35	1078.60
AL	$\bar{x} \pm SD$	6.33 ± 0.59	5.59 ± 0.65	349 ± 29	25.21 ± 14.62	43.96 ± 26.19	2.31 ± 0.94	10.25 ± 1.62	28.45 ± 7.97	409.90 ± 472.49	513.40 ± 270.32
	Min	5.34	4.84	289	10.50	18.10	1.23	8.54	13.88	126.66	127.36
	Max	7.15	6.70	379	53.63	95.46	3.99	13.44	38.23	1461.37	949.12
FL	$\bar{x} \pm SD$	5.88 ± 0.71	5.02 ± 1.11	381 ± 66	74.43 ± 39.18	128.31 ± 67.55	4.62 ± 1.41	15.40 ± 4.32	5.73 ± 4.96	252.97 ± 126.37	640.13 ± 332.46
	Min	5.16	3.84	247	30.00	51.72	3.16	7.13	0.04	106.79	283.41
	Max	7.25	7.12	443	145.44	250.74	7.38	19.71	13.49	437.73	1273.57
RZ	$\bar{x} \pm SD$	7.22 ± 0.46	6.69 ± 0.67	448 ± 220	27.38 ± 3.21	47.19 ± 5.53	2.40 ± 0.53	11.82 ± 2.17	17.58 ± 13.96	244.53 ± 123.54	645.06 ± 351.06
	Min	6.26	5.30	300	23.76	40.96	1.66	8.62	4.63	97.70	266.36
	Max	7.65	7.20	935	33.45	57.67	3.34	14.31	46.67	420.92	1164.62

Abbreviations: GLSP—Grasslands on slope and plain, GLS—Grassland on slope, GLP—Grassland on plain, AL—Arable land, FL—Forest land, RZ—Riparian zone, pH—Soil reaction, Eh—Redox potential, SOC—Soil organic carbon, SOM—Soil organic matter, NT—Nitrogen total, C/N—Carbon to Nitrogen ratio, P—Available P, K—Available K, Mg—Available Mg.

Table 3. Soil physical properties.

Eco-system	Statistical Characteristics	Clay (%)	Silt (%)	Sand (%)	Gravel (%)	BD (g cm^{-3})	PD (g cm^{-3})	ST (°C)	SM (%)	PR (MPa. cm^{-1})	DPR (cm)
GLSP	$\bar{x} \pm SD$	12.2 ± 7.8	46.2 ± 14.7	41.5 ± 16.2	9.3 ± 11.5	1.23 ± 0.13	2.34 ± 0.14	15.1 ± 6.9	26.7 ± 9.2	1.2 ± 0.2	23.1 ± 16.6
	Min	5.3	22.7	12.2	1.1	0.95	2.06	4.3	12.9	0.8	4.4
	Max	38.3	76.0	70.4	50.0	1.47	2.61	28.3	47.6	1.7	62.0
GLS	$\bar{x} \pm SD$	14.4 ± 9.6	50.8 ± 15.6	34.7 ± 15.9	11.1 ± 13.9	1.24 ± 0.12	2.33 ± 0.15	14.2 ± 7.1	25.7 ± 9.1	1.2 ± 0.2	26.5 ± 18.9
	Min	5.3	24.1	12.2	1.1	1.05	2.06	4.3	12.9	0.8	4.4
	Max	38.3	76.0	68.6	50.0	1.43	2.56	24.2	40.4	1.7	62.0
GLP	$\bar{x} \pm SD$	9.5 ± 2.8	40.7 ± 10.6	49.8 ± 11.6	7.0 ± 6.7	1.22 ± 0.13	2.34 ± 0.12	16.1 ± 6.2	27.8 ± 8.7	1.1 ± 0.2	18.9 ± 11.2
	Min	6.3	22.7	33.0	2.0	0.95	2.16	7.4	16.6	0.8	7.4
	Max	15.2	57.9	70.4	20.0	1.47	2.61	28.3	47.6	1.6	38.3
AL	$\bar{x} \pm SD$	14.8 ± 5.8	48.9 ± 10.8	36.4 ± 15.9	5.6 ± 5.3	1.21 ± 0.14	2.48 ± 0.16	17.3 ± 9.0	15.7 ± 6.1	0.9 ± 0.2	31.5 ± 25.2
	Min	8.2	36.1	13.1	0.0	0.97	2.24	4.6	6.1	0.5	6.8
	Max	25.2	67.5	55.8	15.0	1.39	2.68	26.5	22.7	1.2	72.9
FL	$\bar{x} \pm SD$	15.5 ± 10.1	55.7 ± 6.7	28.8 ± 11.6	25.3 ± 16.7	0.98 ± 0.30	2.10 ± 0.29	13.3 ± 6.8	20.8 ± 10.0	1.1 ± 0.4	15.1 ± 7.0
	Min	9.3	48.1	9.2	1.5	0.46	1.58	3.5	7.9	0.5	5.7
	Max	38.0	68.5	41.2	50.0	1.46	2.50	20.9	34.9	1.4	27.4
RZ	$\bar{x} \pm SD$	7.8 ± 1.9	37.3 ± 10.0	54.9 ± 11.0	15.0 ± 9.1	1.07 ± 0.14	2.38 ± 0.13	14.8 ± 4.8	21.7 ± 4.4	0.9 ± 0.3	35.2 ± 26.6
	Min	5.5	16.5	46.8	5.0	0.92	2.18	6.7	16.0	0.4	5.4
	Max	11.3	47.0	78.0	30.0	1.31	2.59	21.8	30.3	1.2	76.8

Abbreviations: GLSP—Grasslands on slope and plain, GLS—Grassland on slope, GLP—Grassland on plain, AL—Arable land, FL—Forest land, RZ—Riparian zone, BD—Bulk density, PD—Particle density, ST—Soil temperature, SM—Soil moisture, PR—Penetrometric resistance, DPR—Depth of penetrometric resistance measurement.

Table 4. Soil biological properties.

Ecosystem	Statistical Characteristics	EN (ind.m^{-2})	EB (g.m^{-2})	H	NCER (μmol CO_2.m^{-2}s^{-1})
GLSP	$\bar{x} \pm$ SD	150.18 ± 132.28	50.81 ± 52.66	0.60 ± 0.45	2.26 ± 1.30
	Min	0.00	0.00	0.00	0.24
	Max	438.40	211.80	1.28	5.26
GLS	$\bar{x} \pm$ SD	87.58 ± 84.64	28.05 ± 22.85	0.36 ± 0.46	2.15 ± 1.22
	Min	0.00	0.00	0.00	0.45
	Max	307.20	67.80	1.28	5.26
GLP	$\bar{x} \pm$ SD	222.68 ± 132.43	78.62 ± 60.87	0.88 ± 0.20	2.40 ± 1.31
	Min	19.60	7.20	0.56	0.24
	Max	438.40	211.80	1.16	4.45
AL	$\bar{x} \pm$ SD	49.63 ± 71.73	17.39 ± 24.32	0.42 ± 0.45	0.93 ± 0.72
	Min	0.00	0.00	0.00	0.18
	Max	204.80	67.50	1.06	2.36
FL	$\bar{x} \pm$ SD	22.33 ± 15.23	6.48 ± 4.46	0.49 ± 0.53	2.44 ± 0.81
	Min	3.30	0.70	0.00	1.34
	Max	51.20	11.80	1.39	3.47
RZ	$\bar{x} \pm$ SD	141.73 ± 121.29	52.75 ± 45.21	0.56 ± 0.44	3.38 ± 1.29
	Min	0.00	0.00	0.00	0.81
	Max	374.40	128.70	1.24	4.77

Abbreviations: GLSP—Grasslands on slope and plain, GLS—Grassland on slope, GLP—Grassland on plain, AL—Arable land, FL—Forest land, RZ—Riparian zone, EN—Earthworm number, EB—Earthworm biomass, H—Shannon's index of biodiversity, NCER—Net carbon exchange rate.

In the case of physical properties, GLP soils were characterized by a lower content of clay and silt particles compared to GLS soils, and conversely, they had a higher content of sand particles. The gravel content was, on average, higher in GLS soils. The average soil temperature and soil moisture were higher in GLP soils, which were also mostly shallower compared to GLS soils in terms of DPR characteristic.

Among all ecosystems, we recorded the most vital characteristics for the presence of earthworm community in GL soils. The highest numbers (438.4 ind.m^{-2}), biomass (211.8 g.m^{-2}), and H (1.2) were present in GLP soils while the lowest ones were found in AL or FL soils. When comparing soils of four different ecosystems (GL, AL, FL, RZ), we recorded the highest maximum or minimum value in GL for some characteristics, such as pH. FL stands out with higher SOC, NT, and Mg reserves. However, the best quality of organic matter was found in AL soils, where we recorded the lowest soil respiration, which was the highest in GL soils. AL stands out with the highest available P and K reserves. Regarding physical properties, FL soils were, on average, characterized by a higher content of clay, silt, and gravel and the lowest BD, which was the highest in GL soils. RZ soils had a higher content of sand. AL soils were characterized by both higher PD and the highest mean soil temperature values. In turn, GL soils had both higher soil moisture and PR.

The FWC, WP, and AWP indicators showed the same trends among ecosystems. We found the highest mean FWC for FL soils (55.5%), followed by GLS soils (54.3%). However, the highest and therefore most favorable SWDI index was calculated for GLP soils.

Among all ecosystems, the highest mean C stock value was found in FL soils (121.5 t.ha^{-1}) followed by GLS soils (76 t.ha^{-1}). However, the median value was higher in GLS soils (82.2 t.ha^{-1}) than in FL soils (72.0 t.ha^{-1}). The mean N stock was higher in GLS soils (8.7 t.ha^{-1}), but again with the highest maximum value found in FL soils (16.9 t.ha^{-1}), for CS (332.4 t.ha^{-1}). Lower stocks were found in other ecosystems (AL, GLP, and RZ).

Figure 2 shows the calculated hydrological indicators and carbon and nitrogen stocks in soils of different ecosystems (GL, AL, FL, and RZ).

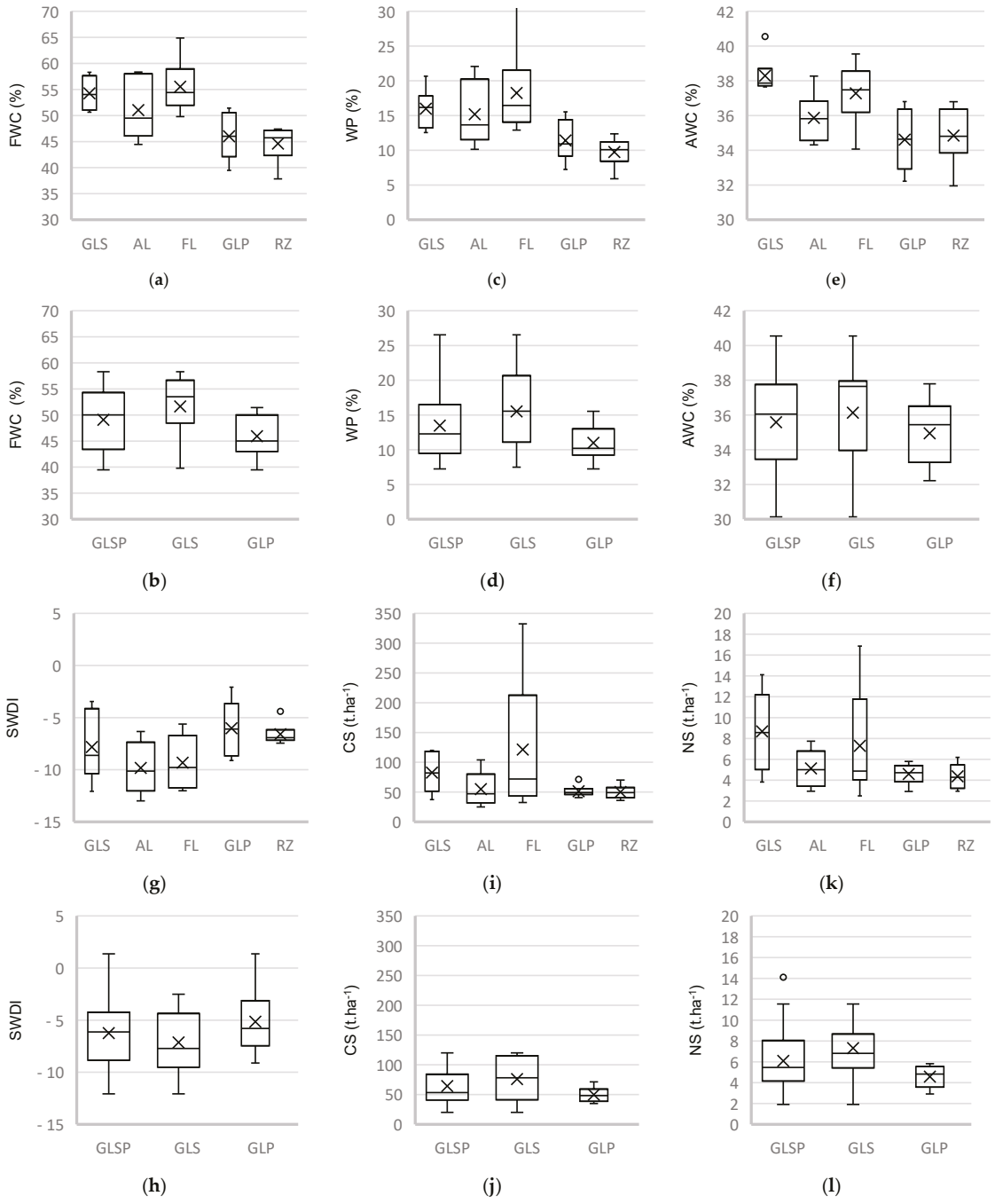


Figure 2. Hydrological indicators and carbon and nitrogen stocks under different land uses; (**a**,**b**) Field water capacity, (**c**,**d**) Wilting point, (**e**,**f**), Available water capacity, (**g**,**h**) Soil water deficit index, (**i**,**j**) Carbon stock, (**k**,**l**) Nitrogen stock. Figures (**a**,**c**,**e**,**g**,**i**,**k**) show indicators within 6 slope and 6 plain study sites with localities of different land uses (GLS, AL, FL at slope study sites; GLP, RZ at plain study sites). Figures (**b**,**d**,**f**,**h**,**j**,**l**) show indicators of all GL localities (GLSP), and separately for slope (GLS) and plain (GLP) localities. Abbreviations: GLSP—Grasslands on slope and plain, GLS—Grassland on slope, GLP—Grassland on plain, AL—Arable land on slope, FL—Forest land on slope, RZ—Riparian zone on plain.

3.2. Relationships Between Soil Properties

The correlations between all soil properties are listed in Table 5.

Table 5. Spearman's correlation coefficients among soil properties.

	A	pH/H_2O	pH/KCl	Eh	SOC	SOM	NT	C/N	NCER	Clay	Silt	Sand	Gravel	BD	PD	ST	SM	PR	DPR	EN	EB	H	P	K	Mg	FWC	WP	AWP	SWDI	CS	NS
A	**1**																														
pH/H_2O	−0.049	**1**																													
pH/KCl	0.004	**0.921 ****	**1**																												
Eh	−0.001	**−0.454 ****	**−0.523 ****	**1**																											
SOC	0.262	−0.171	−0.143	−0.098	**1**																										
SOM	0.262	−0.171	−0.143	−0.098	**1.000 ****	**1**																									
NT	**0.449 ****	−0.252	−0.16	−0.052	**0.858 ****	**0.858 ****	**1**																								
C/N	−0.17	0.04	−0.109	0.06	**0.524 ****	**0.524 ****	0.063	**1**																							
NCER	**−0.342 ***	0.136	0.175	−0.132	0.293	0.293	0.129	**0.366 ***	**1**																						
Clay	0.099	−0.139	−0.16	−0.193	0.09	0.09	0.196	−0.209	−0.281	**1**																					
Silt	**0.323 ***	−0.296	−0.227	−0.174	**0.374 ***	**0.374 ***	**0.338 ***	0.036	−0.213	**0.346 ***	**1**																				
Sand	−0.21	0.312	0.301	0.189	**−0.378 ***	**−0.378 ***	**−0.360 ***	−0.033	0.248	**−0.661 ****	**−0.881 ****	**1**																			
Gravel	0.252	0.222	0.218	0.086	0.077	0.077	0.139	−0.029	0.088	−0.076	−0.125	0.142	**1**																		
BD	−0.248	0.052	0.016	0.28	−0.256	−0.256	−0.215	−0.248	**−0.323 ***	0.254	−0.161	−0.029	−0.154	**1**																	
PD	−0.239	0.127	0.118	−0.056	−0.219	−0.219	−0.193	−0.157	−0.244	0.023	−0.149	0.095	−0.27	**0.353 ****	**1**																
ST	−0.312	−0.036	−0.063	−0.072	0.037	0.037	−0.162	0.177	−0.108	0.162	0.235	−0.21	−0.078	0.07	−0.108	**1**															
SM	−0.13	0.081	0.065	−0.03	0.146	0.146	0.213	−0.03	0.303	−0.204	−0.081	0.046	**−0.320 ***	0.144	0.111	**−0.399 ***	**1**														
PR	−0.003	**−0.438 ****	**−0.352 ****	**0.445 ****	0.143	0.143	0.209	−0.122	−0.161	0.159	0.225	−0.24	0.3	0.283	−0.224	0.231	−0.197	**1**													
DPR	0.058	−0.083	−0.125	0.06	−0.067	−0.067	0.007	−0.063	0.015	0.137	−0.038	−0.092	**−0.445 ****	0.041	−0.029	−0.196	0.267	−0.053	**1**												
EN	−0.097	0.072	0.162	0.021	−0.214	−0.214	−0.058	−0.294	−0.166	0.074	−0.109	0.068	−0.265	0.166	0.038	−0.12	0.257	0.168	**0.447 ****	**1**											
EB	−0.012	0.095	0.156	−0.016	−0.232	−0.232	−0.054	−0.312	−0.091	0.01	−0.095	0.073	−0.265	0.051	0.002	−0.242	**0.337 ***	0.036	**0.515 ****	**0.921 ****	**1**										
H	0.004	0.2	0.206	0.049	−0.028	−0.028	−0.006	0.021	−0.016	0.156	−0.105	0.008	−0.115	0.188	0.274	**−0.335 ***	0.306	0.031	0.313	**0.516 ****	**0.539 ***	**1**									
P	−0.08	**0.341 ***	0.238	−0.204	−0.317	−0.317	−0.256	−0.139	−0.141	0.153	**−0.326 ***	0.205	−0.097	0.038	0.243	−0.137	−0.154	−0.284	0.105	0.093	0.118	0.172	**1**							
K	0.317	−0.166	−0.064	0.214	0.255	0.255	**0.359 ***	0.001	−0.066	0.019	−0.068	0.032	0.157	−0.176	0.009	−0.189	−0.216	0.175	0.049	−0.015	0.077	0.206	0.275	**1**							
Mg	0.122	**0.438 ****	**0.449 ****	**−0.388 ***	**0.370 ***	**0.370 ***	0.262	0.213	0.142	−0.066	0.159	−0.081	0.028	0.017	0.128	0.027	0.129	−0.297	−0.287	−0.197	−0.184	0.022	−0.093	−0.117	**1**						
FWC	0.226	**−0.328 ***	−0.311	−0.188	**0.431 ****	**0.431 ****	**0.435 ****	0.039	−0.216	**0.751 ****	**0.791 ****	**−0.967 ****	−0.121	0.023	−0.118	0.209	−0.098	0.229	0.11	−0.079	−0.083	−0.019	−0.124	0.089	0.048	**1**					
WP	0.207	−0.286	−0.298	−0.19	**0.408 ***	**0.408 ***	**0.438 ****	0.006	−0.23	**0.857 ****	**0.667 ****	**−0.910 ****	−0.138	0.106	−0.082	0.166	−0.1	0.197	0.139	−0.046	−0.064	0.035	−0.026	0.093	0.032	**0.973 ****	**1**				
AWC	**0.390 ***	−0.222	−0.149	−0.199	**0.362 ***	**0.362 ***	0.307	0.099	−0.088	0.119	**0.925 ****	**−0.698 ****	−0.011	**−0.406 ***	−0.249	0.193	−0.117	0.108	−0.096	−0.177	−0.098	−0.159	−0.319	−0.008	0.129	**0.617 ****	**0.469 ****	**1**			
SWDI	−0.174	0.227	0.235	0.041	−0.073	−0.073	−0.031	−0.017	**0.344 ***	**−0.636 ****	**−0.338 ***	**0.483 ****	−0.188	−0.002	0.185	**−0.439 ***	**0.818 ****	−0.241	0.102	0.252	**0.339 ***	0.279	−0.074	−0.172	0.08	**−0.568 ****	**−0.591 ****	−0.238	**1**		
CS	0.111	−0.13	−0.107	−0.092	**0.829 ****	**0.829 ****	**0.694 ****	**0.381 ***	0.074	0.223	**0.358 ***	**−0.437 ***	−0.234	0.155	−0.033	0.132	0.284	0.18	0.124	0.062	0.015	0.171	−0.274	0.154	**0.324 ***	**0.462 ****	**0.469 ****	0.229	0.001	**1**	
NS	0.19	−0.147	−0.075	−0.075	**0.579 ****	**0.579 ****	**0.697 ****	−0.107	−0.116	0.294	0.28	**−0.375 ***	−0.313	0.319	0.089	−0.053	**0.445 ****	0.182	0.212	0.205	0.165	0.231	−0.124	0.155	0.256	**0.395 ****	**0.433 ****	0.095	0.133	**0.837 ****	**1**

pH—Soil reaction, Eh—Redox potential, SOC—Soil organic carbon, SOM—Soil organic matter, NT—Nitrogen total, C/N—Carbon to nitrogen ratio, NCER—Net carbon exchange rate, BD—Bulk density, PD—Particle density, ST—Soil temperature, SM—Soil moisture, PR—Penetrometric resistance, DPR—Depth of penetrometric resistance measurement, EN—Earthworm number, EB—Earthworm biomass, H—Shannon's index of biodiversity, FWC—Field water capacity, WP—Wilting point, AWC—Available water capacity, SWDI—Soil water deficit index, CS—Carbon stock, NS—Nitrogen stock; * r-values shown in bold are significant at $p < 0.05$; ** r-values shown in bold are significant at $p < 0.01$.

Soil pH had a statistically significant negative relationship with Eh, PR, and positive with available P and Mg. SOC, SOM, and NT were positively correlated with silt content and negatively with sand content, which could reflect in a positive correlation with the calculated FWC, WP, AWC, CS, and NS indicators. In addition, SOC and SOM were positively correlated with available Mg, and NT with available K. Soil organic matter quality, expressed by C/N ratio, was positively correlated with NCER and CS. Regarding biological parameters, NCER was negatively correlated with BD and positively with SWDI, EN and EB were negatively correlated with DPR, and EB itself was also positively correlated with SM. As expected, ST was negatively correlated with SWDI while on the contrary, SM was positively correlated. The other correlations only confirm the relationships resulting from the proposed models.

The results of the ANOVA test of normally distributed data assessing the effect of land use are presented in Table 6.

Table 6. Results of ANOVA for the soil properties by land use (n = 30, df = 4).

Soil Characteristic	Land Use	
	F-Value	*p*-Value
pH/H_2O	4.998	**0.004**
pH/KCl	3.214	**0.029**
Silt	6.795	**<0.001**
Sand	5.948	**0.002**
ST	0.311	0.868
SM	1.129	0.365
PR	2.413	0.076
FWC	6.802	**<0.001**
AWC	5.529	**0.002**
SWDI	2.567	**0.063**
NCER	4.362	**0.008**

pH—Soil reaction, ST—Soil temperature, SM—Soil moisture, PR—Penetrometric resistance, FWC—Field water capacity, AWC—Available water capacity, SWDI—Soil water deficit index, NCER—Net carbon exchange rate; *p*-values highlighted in bold are highly statistically significant ($p < 0.001$) and statistically significant ($p < 0.05$).

The statistical analysis showed significant differences between the land uses in case of representative variables of chemical (pH/H_2O, pH/KCl), physical (silt, sand, FWC, AWC, SWDI) and biological (NCER) properties. Significant main effects were explored further using the post hoc Tukey test (Table 7).

The HCA (Figure 3) has highlighted two large clusters (A and B). Cluster A contains three sites on Fluvisol that are situated on plains and used as GL and RZ. Two clusters of lower hierarchical order are recognized in B (B1 and B2). Cluster B1 exclusively includes sites situated on slopes used as GL, FL, and AL. Cluster B2 includes nine sites situated on plains and eight situated on slopes with all land use types.

Table 7. Effect of land use on soil properties.

Land Use	pH/H_2O	pH/KCl	Silt (%)	Sand (%)	ST (°C)	SM (%)	PR (MPa. cm^{-1})	FWC (%)	AWC (%)	SWDI	NCER (µmol CO_2. $m^{-2}s^{-1}$)
GLS	$5.77^{a} \pm 0.87$	$5.56^{ab} \pm 1.00$	$62.72^{c} \pm 6.69$	$24.72^{a} \pm 8.29$	$58.17^{a} \pm 21.95$	$24.27^{a} \pm 10.80$	$1.35^{a} \pm 0.21$	$54.27^{b} \pm 3.15$	$38.22^{b} \pm 1.15$	$-7.82^{a} \pm 3.36$	$1.96^{ab} \pm 0.42$
GLP	$6.85^{ab} \pm 0.53$	$6.31^{ab} \pm 0.76$	$39.38^{ab} \pm 12.27$	$50.25^{bc} \pm 14.12$	$17.47^{a} \pm 7.04$	$25.13^{a} \pm 7.73$	$1.15^{a} \pm 0.31$	$46.02^{a} \pm 4.47$	$34.62^{a} \pm 1.91$	$-6.02^{a} \pm 2.63$	$2.25^{ab} \pm 1.33$
AL	$6.33^{ab} \pm 0.64$	$5.59^{ab} \pm 0.71$	$48.88^{abc} \pm 11.78$	$36.38^{abc} \pm 17.38$	$17.28^{a} \pm 9.83$	$15.70^{a} \pm 6.74$	$0.87^{a} \pm 0.25$	$51.03^{ab} \pm 5.82$	$35.85^{ab} \pm 1.46$	$-9.82^{a} \pm 2.49$	$0.93^{a} \pm 0.79$
FL	$5.88^{a} \pm 0.77$	$5.02^{a} \pm 1.21$	$55.68^{bc} \pm 7.38$	$28.82^{ab} \pm 12.73$	$13.28^{a} \pm 7.40$	$20.82^{a} \pm 10.98$	$1.07^{a} \pm 0.38$	$55.53^{b} \pm 5.26$	$37.28^{ab} \pm 1.80$	$-9.32^{a} \pm 2.55$	$2.44^{ab} \pm 0.88$
RZ	$7.22^{b} \pm 0.50$	$6.69^{b} \pm 0.73$	$37.32^{a} \pm 10.99$	$54.93^{c} \pm 12.01$	$14.77^{a} \pm 5.25$	$21.72^{a} \pm 4.79$	$0.93^{a} \pm 0.32$	$44.58^{a} \pm 3.59$	$34.85^{a} \pm 1.67$	$-6.58^{a} \pm 1.09$	$3.38^{b} \pm 1.42$

Abbreviations: GLS—Grassland on slope, GLP—Grassland on plain, AL—Arable land, FL—Forest land, RZ—Riparian zone, pH—Soil reaction, ST—Soil temperature, SM—Soil moisture, PR—Penetrometric resistance, FWC—Field water capacity, AWC—Available water capacity, SWDI—Soil water deficit index, NCER—Net carbon exchange rate; different letters indicate statistically significant differences according to Tukey's HSD test ($p < 0.05$; mean ± SE; n = 30).

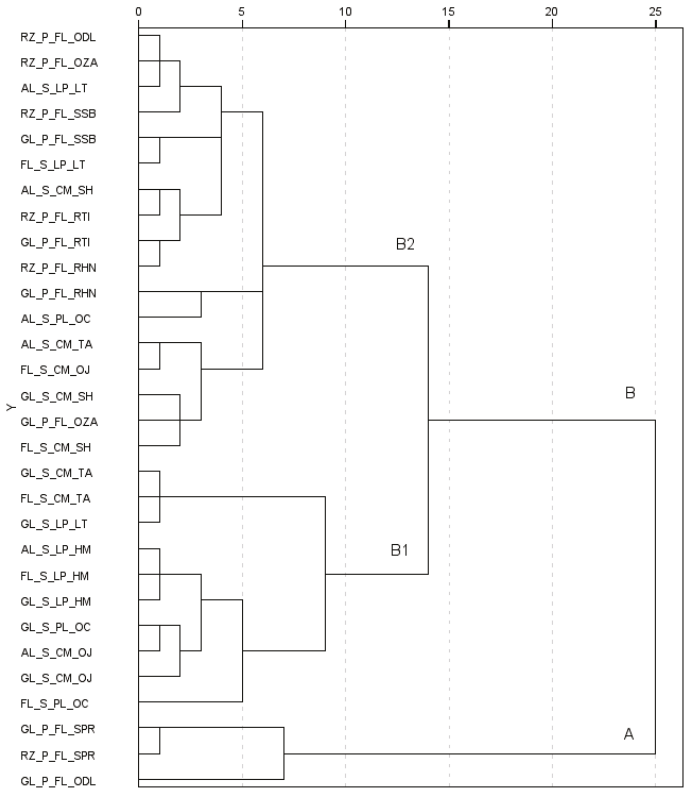


Figure 3. Dendrogram for the hierarchical clustering of sites.

4. Discussion

Soils generally exhibited high variability, which is particularly conditioned by their natural origin. But soil heterogeneity is also affected by ecosystems, land use, and management. Similarly to our study, other authors [47–49] confirmed that spatial variability of soil chemical, biological, and physical properties is significantly affected by both land use and soil type. Usually, long-term intensive land use adversely affects soil properties, having impacts on soil health and provision of ecosystem services [50]. Extensive practices based on ecological principles improve soil properties [51] and subsequently soil supporting and regulating services.

However, this is not generally true. In our study, in the case of earthworms, the positive effect of extensive management forms was confirmed in terms of higher numbers, biomass, and diversity of earthworms in GL soils compared to intensively managed AL soils. This is in line with many studies [52,53]. However, we did not confirm this effect in the case of earthworms in extensively managed FL soils, where earthworm parameters reached similar values to those in intensively managed AL soils. In this case, if the environment is exposed to less pressure, but does not meet the basic requirements of organisms (e.g., soil moisture or temperature), this will affect their presence as well as their management. In addition, Betancur-Corredor et al. [54], based on a global meta-analysis focused on the impact of land use on earthworm communities, concluded that earthworm responses are highly heterogenous and cannot be explained by the individual assessment of climatic, soil-related, or management factors.

Our results showed that ecosystems with different land uses also influence the other chemical soil properties. GLS soils had, among all ecosystems, the highest mean reserve of available Mg, available water capacity, and nitrogen storage. GLP soils excelled in earthworm number, their biomass and diversity, and in SWDI index. On the contrary, GLSs were the worst supplied with available phosphorus.

Phosphorus, as a plant macronutrient, is a key element in photosynthesis, respiration, and frequently limits productivity in both natural and agroecosystems, especially in low-input systems [55]. Although abundant in soils, in both organic and inorganic forms, its availability is restricted [56]. Only a small proportion of the total soil P is available for plant uptake because of fixation. Most P is associated with Al and Fe oxides or hydroxides in acidic soils, and with Ca in calcareous soils [57]. Most P in soil is not readily available to plants. Nutrient limitation to primary productivity is widespread in terrestrial ecosystems, and P is one of the most common limiting elements [58]. Phosphorus availability is often a primary constraint to plant productivity [59]. A solution should be fertilization. A large amount of P geological deposits has been mined to produce fertilizers. Unfortunately, easily mineable P deposits are finite and could be depleted in the next 50–100 years [60]. Therefore, the focus is currently shifting to the use of organic amendments [61]. However, the real problem is that the availability of P from applied sources tends to decrease because of ambiguity and complexity of retention and release mechanisms in soil [62]. Therefore, developing sustainable management strategies to better exploit soil P cycling are urgently needed [63]. This makes phosphorus management a major issue for future nutrients' security for all soils, not just GL soils.

A different situation was observed in the reserves of available Mg, abundant in the soils of all monitored localities and in all ecosystems. Geochemical distribution of Mg in agricultural soils of Europe has shown high Mg concentrations in soil developed over mafic lithologies and in carbonate-rich regions [64], as occurred in our localities. In this case, lithology plays a key role in Mg availability and nutritional status. Available K was measured at a relatively good level in soils at study sites, but the lowest content among ecosystems was registered in GLP. The availability of K can differ substantially between soils. K can become a limiting factor, especially on sandy soils with little clay content [65]. GLP soils of our study, similarly to RZ soils, were developed on river alluvia, characterized by higher sand content (mean sand content in GLP localities was 49.8%; in RZ localities, 54.9%).

Soils comprise a reservoir of biodiversity, providing many benefits for human well-being. Poor land management, including intensification and deforestation, can cause a decline in soil biodiversity and a reduction in these benefits [66]. For the assessment of the earthworm community, we used earthworm abundance and biomass as indicators, since they are indices of soil health and ecosystem services for different ecosystems [67]. The study revealed the highest number, biomass, and diversity of earthworms in GLP soils, followed by FL, GLS, RZ, and AL. These results are consistent with many authors who also found the higher earthworm abundance and biomass at extensively used ecosystems such as grasslands or forests compared to intensively used arable land [68,69]. Spurgeon et al. [70], based on a meta-analysis of 16 studies, reported an average earthworm number of 56.3 ind.m^{-2} under arable land (49.6 ind.m^{-2} in AL in our study) and 229 ind.m^{-2} under grasslands (226.7 ind.m^{-2} in GLP in our study).

As expected, we also found an impact of ecosystem type on the hydrological properties, carbon and nitrogen storage. Soils of extensive ecosystems (FL and GL) had higher water retention capacity and carbon and nitrogen storage than AL soils, as was reported by other researchers [71,72]. However, since the AL on the slopes of the study sites were not very intensively managed (some of them were even organically farmed), the differences between ecosystem types were not found to be very significant. In some cases, these properties were better in AL soils than in GLP and RZP soils. This shows that management intensity can strongly affect soil properties. FL and RZ soils are not disturbed, and GL soils are less disturbed than cultivated ones. In extensive ecosystems, the dense root system of plants provides rich organic matter by influencing the amount of carbon and nitrogen

storages, and also supports greater water storage capacity [73]. GLS and FL excelled in C stock. It is estimated that approximately 10–30% of the global soil organic carbon is stored in grassland soils [74]. In our study, the mean value of SOC stock in GLS soils was lower than in FLS soils, while the opposite was true for the median value. The C stock in soil is highly variable and depends on many environmental conditions and land uses. Canedoli et al. [75], in alpine region, found out that the typologies of habitats have a significant effect on SOC stock. In their study, mixed broadleaf forests store the highest SOC, followed by grasslands, mixed coniferous forests, and spruce forests. Similarly, in the temperate Himalayas, Kumar et al. [76] found the highest total organic carbon pools in the soil under natural forests followed by natural grasslands. However, in addition to land use, the influence of management must also be considered. Many works have shown that organic carbon stocks in soils of grasslands have been largely depleted worldwide due to mismanagement. On the other hand, right management practices could potentially increase soil organic carbon stocks [77]. Grasslands thus play an important role in the global C balance and impact the global climate [78]. High levels of organic carbon can help maintain and improve soil fertility and water availability [79]. In our study, SOC was positively correlated with hydrological indicators such as FWC and WP. Soil water is the most important factor limiting plant growth [80]. Thus, grasslands also play an important role in the water cycle.

5. Conclusions

Understanding how land use and landscape unit influence soil properties can lead to improved soil management, particularly in environments that have undergone changes caused by climate and human activities. We found that similarly to land use patterns, environmental properties and altitude had significant effects on soil.

GL soils are very diverse: most of their characteristics showed large variability, more pronounced in GLS soils than in GLP soils. The properties of GL soils are different from those of other ecosystems and land uses. GL soils provide satisfactory services in addition to many other services that are currently undervalued. Among essential nutrients, we found low availability of phosphorus in all ecosystems, but the lowest in GLS soils. Nutrient deficit should always be considered in soil management. A long-term deficit can negatively disrupt mutual interaction and linkages between properties and, beyond a certain limit, can negatively impact ecosystem services. Therefore, further research should be focused on options for increasing soil phosphorus supply through management measures and adding organic additives to the soil.

Author Contributions: Conceptualization, R.K.; methodology, R.K. and M.K.; formal analysis, R.K.; investigation, R.K. and M.K.; data curation, R.K.; writing—original draft preparation, R.K.; writing—review and editing, M.K.; visualization, R.K.; funding acquisition, M.K. All authors have read and agreed to the published version of the manuscript.

Funding: This research was funded by the Ministry of Environment of the Slovak Republic, grant number 19R01-18-P01-00001, Komponent 19 REPowerEU.

Data Availability Statement: Data are contained within the article or are available from the corresponding author on request.

Conflicts of Interest: The authors declare no conflicts of interest.

References

1. Suttie, J.M.; Reynoslds, S.G.; Batello, C. *Grasslands of the World*, 1st ed.; FAO: Roma, Italy, 2005.
2. Squires, V.R.; Dengler, J.; Hua, L. *Grasslands of the World: Diversity, Management, and Conservation*, 1st ed.; Taylor & Francis: Boca Raton, FL, USA, 2018.

3. Schils, R.L.M.; Bufe, C.; Rhymer, C.M.; Francksen, R.M.; Klaus, V.H.; Abdalla, M.; Milazzo, F.; Lellei-Kovács, E.; Berge, H.T.; Bertora, C.; et al. Permanent grasslands in Europe: Land use change and intensification decrease their multifunctionality. *Agric. Ecosyst. Environ.* **2022**, *330*, 107891. [CrossRef]
4. Blüthgen, N.; Dormann, C.F.; Prati, D.; Klaus, V.H.; Kleinbecker, T.; Hölzel, N.; Alt, F.; Boch, S.; Gockel, S.; Hemp, A.; et al. A quantitative index of land-use intensity in grasslands: Integrating mowing, grazing and fertilization. *Basic Appl. Ecol.* **2012**, *13*, 207–220. [CrossRef]
5. Mayel, S.; Jarrah, M.; Kuka, K. How does grassland management affect physical and biochemical properties of temperate grassland soils? A review study. *Grass Forage Sci.* **2021**, *76*, 215–244. [CrossRef]
6. Wang, X.; Wang, R.; Gao, J. Precipitation and soil nutrient determine the spatial variability of grassland productivity at large scales in China. *Front. Plant Sci.* **2022**, *13*, 996313. [CrossRef] [PubMed]
7. Anderson, D.W. Pedogenesis in the Grassland and Adjacent Forests of the Great Plains. *Adv. Soil Sci.* **1987**, *7*, 53–93. [CrossRef]
8. Paudel, S.; Cobb, A.B.; Boughton, E.H.; Spiegal, S.; Boughton, R.K.; Silveira, M.L.; Swain, H.M.; Reuter, R.; Goodman, L.E.; Steiner, J.L. A framework for sustainable management of ecosystem services and disservices in perennial grassland agroecosystems. *Ecosphere* **2021**, *12*, e03837. [CrossRef]
9. Centeri, C. Effects of grazing on water erosion, compaction and infiltration on grasslands. *Hydrology* **2022**, *9*, 34. [CrossRef]
10. Fraser, M.D.; Vallin, H.E.; Roberts, B.P. Animal board invited review: Grassland-based livestock farming and biodiversity. *Animal* **2022**, *16*, 100371. [CrossRef]
11. Mastalerczuk, G.; Borawska-Jarmulowicz, B. Physiological and morphometric response of forage grass species and their biomass distribution depending on the term and frequency of water deficiency. *Agronomy* **2021**, *11*, 2471. [CrossRef]
12. Richter, F.; Jan, P.; El Benni, N.; Luscher, A.; Buchmann, N.; Klaus, V.H. A guide to assess and value ecosystem services of grasslands. *Ecosyst. Serv.* **2021**, *52*, 101376. [CrossRef]
13. Bai, Y.; Cotrufo, M.F. Grassland soil carbon sequestration: Current understanding, challenges, and solution. *Science* **2022**, *377*, 603–608. [CrossRef]
14. Liu, X.; Wang, Z.; Zheng, K.; Han, C.; Li, L.; Sheng, H.; Ma, Z. Changes in soil carbon and nitrogen stocks following degradation of alpine grasslands on the Qinghai-Tibetan Plateau: A meta-analysis. *Land Degrad. Dev.* **2021**, *32*, 1262–1273. [CrossRef]
15. Lyons, K.G.; Török, P.; Hermann, J.M.; Kiehl, K.; Kirmer, A.; Kollmann, J.; Overbeck, G.E.; Tischew, S.; Allen, E.B.; Bakker, J.D.; et al. Challenges and opportunities for grassland restoration: A global perspective of best practices in the era of climate change. *Glob. Ecol. Conserv.* **2023**, *46*, e02612. [CrossRef]
16. Martins, C.S.C.; Delgado-Baquerizo, M.; Jayaramaiah, R.H.; Tao, D.; Wang, J.T. Aboveground and belowground biodiversity have complementary effects on ecosystem functions across global grasslands. *PLoS Biol.* **2024**, *22*, e3002736. [CrossRef]
17. Pecl, G.T.; Araújo, M.B.; Bell, J.D.; Blanchard, J.; Bonebrake, T.C. Biodiversity redistribution under climate change: Impacts on ecosystems and human well-being. *Science* **2017**, *355*, 987–997. [CrossRef] [PubMed]
18. Bengtsson, J.; Bullock, J.M.; Egoh, B.; Everson, C.; Everson, T.; O'Connor, T.; O'Farrell, P.J.; Smith, H.G.; Lindborg, R. Grasslands-more important for ecosystem services than you might think. *Ecosphere* **2019**, *10*, e02582. [CrossRef]
19. Liu, H.; Hou, L.; Kang, N.; Nan, Z.; Hunag, J. The economic value of grassland ecosystem services: A global meta-analysis. *Grassl. Res.* **2022**, *1*, 63–74. [CrossRef]
20. Dominati, E.; Patterson, M.; Mackay, A. A framework for classifying and quantifying the natural capital and ecosystem services of soils. *Ecol. Econ.* **2010**, *69*, 1858–1868. [CrossRef]
21. Adhikari, K.; Hartemik, A.E. Linking soils to ecosystem services—A global review. *Geoderma* **2016**, *262*, 101–111. [CrossRef]
22. Winkler, R. Valuation of ecosystem goods and services part 1: An integrated dynamic approach. *Ecol. Econ.* **2006**, *59*, 82–93. [CrossRef]
23. Huang, L.; Wang, H.; Liu, H.; A, Z.; Guo, W. Quantitatively linking ecosystem service functions with soil moisture and ecohydrology regimes in watershed. *Sci. Total Environ.* **2024**, *955*, 176866. [CrossRef]
24. Paul, C.; Kuhn, K.; Steinhoff-Knopp, B.; Weishuhn, P.; Helming, K. Towards a standardization of soil-related ecosystem service assessments. *Eur. J. Soil Sci.* **2020**, *72*, 1543–1558. [CrossRef]
25. Williams, A.; Hedlund, K. Indicators of soil ecosystem services in conventional and organic arable fields along a gradient of landscape heterogeneity in southern Sweden. *Appl. Soil. Ecol.* **2013**, *65*, 1–7. [CrossRef]
26. Vrebos, D.; Staes, J.; Vandenbroucke, T.; D'Haeyer, T.; Johnston, R.; Muhumuza, M.; Kasabeke, C.; Meire, P. Mapping ecosystem service flows with land cover scoring maps for data-scarce regions. *Ecosyst. Serv.* **2015**, *13*, 28–40. [CrossRef]
27. Bardgett, R.D.; Bullock, J.M.; Lavorel, S.; Manning, P.; Schaffner, U.; Ostle, N.; Chomel, M.; Durigan, G.; Fry, E.L.; Johnson, D.; et al. Combating global grassland degradation. *Nat. Rev. Earth Environ.* **2021**, *2*, 720–735. [CrossRef]
28. Prangel, E.; Kasari-Toussaint, L.; Neuenkamp, L.; Noreika, N.; Karise, R. Afforestation and abandonment of semi-natural grasslands lead to biodiversity loss and a decline in ecosystem services and functions. *J. Appl. Ecol.* **2023**, *60*, 825–836. [CrossRef]
29. Hejcman, M.; Hejcmanova, P.; Pavlů, V.; Beneš, J. Origin and history of grasslands in Central Europe—A review. *Grass Forage Sci.* **2013**, *68*, 345–363. [CrossRef]

30. Lovász, L.; Korner-Nievergelt, F.; Amrhein, V. Natural grazing by horses and cattle promotes bird diversity in a restored European alluvial grassland. *PeerJ* **2024**, *12*, e17777. [CrossRef]
31. Gibbs, H.K.; Salmon, J.M. Mapping the world's degraded lands. *Appl. Geogr.* **2015**, *57*, 12–21. [CrossRef]
32. O'Mara, F.P. The role of grasslands in food security and climate change. *Ann. Bot.* **2012**, *110*, 1263–1270. [CrossRef]
33. UGKKSR. *Statistical Yearbook on Soil Resources in the Slovak Republic According to Data of Cadastre to 1 January 2024*, 1st ed.; UGKKSR: Bratislava, Slovakia, 2024. (In Slovak)
34. IUSS Working Group WRB. World Reference Base for Soil Resources. In *International Soil Classification System for Naming Soils and Creating Legends for Soil Maps*, 4th ed.; International Union of Soil Sciences (IUSS): Vienna, Austria, 2022; Available online: https://www.isric.org/sites/default/files/WRB_fourth_edition_2022-12-18.pdf (accessed on 20 January 2025).
35. Nikitin, V.; Fishman, V. On the improvement of methods for determination of soil carbon. *Chem. Agric.* **1969**, *3*, 76–77.
36. AOAC. *Official Methods of Analysis*, 17th ed.; AOAC: Washington, DC, USA, 2000.
37. Mehlich, A. Mehlich 3 soil test extractant: A modification of Mehlich 2 extractant. *Commun. Soil Sci. Plant Anal.* **1984**, *15*, 1409–1416. [CrossRef]
38. Tan, Q.; Wang, G.; Liu, X.; Hao, T.; Tan, W. Responses of soil organic carbon turnover to nitrogen deposition are associated with nitrogen input rates: Derived from soil ^{14}C evidence. *Environ. Pollut.* **2018**, *238*, 500–507. [CrossRef]
39. Chen, H.; Li, D.; Gurmesa, G.A.; Yu, G.; Li, L.; Zhang, W.; Fang, H.; Mo, J. Effects of nitrogen deposition on carbon cycle in terrestrial ecosystems of China: A meta-analysis. *Environ. Pollut.* **2015**, *206*, 352–360. [CrossRef] [PubMed]
40. Klika, J.; Novák, A.; Gregor, A. *Practical Lessons in Phytocenology, Ecology, Climatology and Soil Science*; NCSAV: Praha, Czech Republic, 1954. (In Czech)
41. Blake, G.R.; Hartage, K.H. Particle density. In *Methods of Soil Analysis, Part 1, Physical and Mineralogical Methods—Agronomy Monograph No.9*; American Society of Agronomy—Soil Science Society of America: Madison, WI, USA, 1986; pp. 377–382.
42. Gupta, S.C.; Larson, W.E. Estimating soil water retention characteristics from particle size distribution, organic matter percent, and bulk density. *Water Resour. Res.* **1979**, *15*, 1633–1635. [CrossRef]
43. Botula, Y.D.; Cornelis, W.M.; Baert, G.; Van Ranst, E. Evaluation of pedotransfer functions for predicting water retention of soils in Lower Congo (D.R. Congo). *Agric. Water Manag.* **2012**, *111*, 1–10. [CrossRef]
44. Martínez-Fernández, J.; González-Zamora, A.; Sánchez, N.; Gumuzzio, A. A soil water-based index as a suitable agricultural drought indicator. *J. Hydrol.* **2015**, *522*, 265–273. [CrossRef]
45. Zajonc, I. *Earthworms of Slovakia (Oligochaeta: Lumbricidae)*, 1st ed.; VEDA: Bratislava, Slovakia, 1981. (In Slovak)
46. Sherlock, E. *Key to the Earthworms of the UK and Ireland*; FSC and natural History Museum: London, UK, 2012.
47. Behara, S.K.; Mathur, R.K.; Shukla, A.K.; Suresh, K.; Prakash, C. Spatial variability of soil properties and delineation of soil management zones of oil palm plantations grown in a hot and humic tropical region of southern Inda. *Catena* **2018**, *165*, 251–259. [CrossRef]
48. Metwally, M.S.; Shaddad, S.M.; Liu, M.; Yao, R.J.; Abdo, A.I.; Li, P.; Jiao, J.; Chen, X. Soil properties spatial variability and delineation of site-specific management zones based on soil fertility using fuzzy clustering in a hilly field in Jianyang, Sichuan, China. *Sustainability* **2019**, *11*, 7084. [CrossRef]
49. Kosma, C.; Triantafyllidis, V.; Zotos, A.; Pittaras, A.; Kouneli, V. Assessing spatial variability of soil properties in Mediterranean smallholder farming systems. *Land* **2022**, *11*, 557. [CrossRef]
50. Yadav, R.K.; Purakayastha, T.J.; Khan, M.A.; Kaushik, S.C. Long-term impact of manuring and fertilization on enrichment, stability and quality of organic carbon in Inceptisol under two potato-based cropping systems. *Sci. Total Environ.* **2017**, *609*, 1535–1543. [CrossRef] [PubMed]
51. Bommarco, R.; Kleijn, D.; Potts, S.G. Ecological intensification: Harnessing ecosystem services for food security. *Trends Ecol. Evol.* **2013**, *28*, 230–238. [CrossRef]
52. Mazur-Paczka, A.; Paczka, G.; Kostecka, J.; Garcynska, M.; Podolak, A.; Szura, R. Community structure of *Lumbricidae* in permanent grassland and arable land. *J. Ecol. Eng.* **2019**, *20*, 1–6. [CrossRef] [PubMed]
53. Gebremeskel Weldmichael, T.; Szegi, T.; Denish, L.; Kumar Gangwar, R.; Michéli, E.; Simon, B. The patterns of soil microbial respiration and earthworm communities as influenced by soil and land-use type in selected soils of Hungary. *Soil Sci. Annu.* **2020**, *71*, 43–52. [CrossRef]
54. Betancur-Corredor, B.; Zaitsev, A.; Russell, D.J. The impact of multiple agricultural land uses in sustaining earthworm communities in agroecosystems—A global met-analysis. *Sci. Rep.* **2024**, *14*, 30160. [CrossRef] [PubMed]
55. Cong, W.-F.; Suriyagoda, L.D.B.; Lambers, H. Tightening the phosphorus cycle through phosphorus-efficient crop genotypes. *Trends Plant Sci.* **2020**, *25*, 967–975. [CrossRef] [PubMed]
56. Sharma, S.B.; Sayyed, R.; Trivedi, M.H.; Gobi, T.A. Phosphate solubilizing microbes: Sustainable approach for managing phosphorus deficiency in agricultural soils. *SpringerPlus* **2013**, *2*, 587. [CrossRef]
57. Laakso, J.; Uusitalo, R.; Yli-Halla, M. Phosphorus speciation in agricultural catchment soils and in fresh and dried sediments of five constructed wetlands. *Geoderma* **2016**, *271*, 18–26. [CrossRef]

58. Vitousek, P.M.; Porder, S.; Houlton, B.Z.; Chadwick, O.A. Terrestrial phosphorus limitation: Mechanisms, implications, and nitrogen-phosphorus interactions. *Ecol. Appl.* **2010**, *20*, 5–15. [CrossRef]
59. Hou, E.Q.; Luo, Y.; Kuang, Y.; Chen, C.; Lu, X.; Jiang, L.; Luo, X.; Wen, D. Global meta-analysis shows pervasive phosphorus limitation of aboveground plant production in natural terrestrial ecosystems. *Nat. Commun.* **2020**, *11*, 637. [CrossRef]
60. Cordell, D.; Drangert, J.-O.; White, S. The story of phosphorus: Global food security and food for thought. *Glob. Environ. Change* **2009**, *19*, 292–305. [CrossRef]
61. Johan, P.D.; Ahmed, O.H.; Omar, L.; Hasbullah, N.A. Phosphorus transformation in soils following co-application of charcoal and wood ash. *Agronomy* **2021**, *11*, 2010. [CrossRef]
62. Chaparro, J.M.; Sheflin, A.M.; Manter, D.K.; Vivanco, J.M. Manipulating the soil microbiome to increase soil health and plant fertility. *Biol. Fertil. Soils* **2012**, *48*, 489–499. [CrossRef]
63. Chen, X.; Chen, H.Z.H.; Chang, S.X. Meta-analysis shows that plant mixtures increase soil phosphorus availability and plant productivity in diverse ecosystems. *Ecol. Evol.* **2022**, *6*, 1112–1121. [CrossRef] [PubMed]
64. Négrel, P.; Ladenberger, A.; Reimann, C.; Birke, M.; Demetriades, A. GEMAS: Geochemical distribution of Mg in agricultural soil of Europe. *J. Geochem. Explor.* **2021**, *221*, 106706. [CrossRef]
65. Kayser, M.; Isselstein, J. Potassium cycling and losses in grassland systems: A review. *Grass Forage Sci.* **2005**, *60*, 213–224. [CrossRef]
66. Wall, D.H.; Nielsen, U.N.; Six, J. Soil biodiversity and human health. *Nature* **2015**, *528*, 69–76. [CrossRef]
67. Zaghloul, A.; Saber, M.; Gadow, S.; Awad, F. Biological indicators for pollution detection in terrestrial and aquatic ecosystems. *Bull. Natl. Res. Cent.* **2020**, *44*, 127. [CrossRef]
68. Hoeffner, K.; Hotte, H.; Cluzeau, D.; Charrier, X.; Gastal, F.; Pérés, G. Effects of temporary grassland introduction into annual crop rotation and nitrogen fertilization on earthworm communities and forage production. *Appl. Soil Eco.* **2021**, *162*, 103893. [CrossRef]
69. Liu, Q.; Eisenhauer, N.; Scheu, S.; Reitz, T.; Schädler, M. Grasslands support more diverse and resilient earthworm communities to climate change than cropland in Central Europe. *Agric. Ecosyst. Environ.* **2025**, *377*, 109259. [CrossRef]
70. Spurgeon, D.J.; Keith, A.M.; Schmidt, O.; Lammertsma, D.R.; Faber, J.H. Land-use and land-management change: Relationships with earthworm and fungi communities and soil structural properties. *BMC Ecol.* **2013**, *13*, 46. [CrossRef]
71. Antony, D.; Collins, C.D.; Clark, J.M.; Sizmur, T. Soil organic matter storage in temperate lowland arable, grassland and woodland topsoil and subsoil. *Soil Use Manag.* **2022**, *38*, 1532–1546. [CrossRef]
72. Tamburini, G.; Aguilera, G.; öckinger, E. Grasslands enhance ecosystem service multifunctionality above and below-ground in agricultural landscape. *J. Appl. Ecol.* **2022**, *59*, 3061–3071. [CrossRef]
73. Schmidt, M.W.I.; Torn, M.S.; Abiven, S.; Dittmar, T.; Guggenberger, G.; Janssens, I.A.; Kleber, M.; Kögel-Knabner, I.; Lehmann, J.; Manning, D.A.C.; et al. Persistence of soil organic matter as an ecosystem property. *Nature* **2011**, *478*, 49–56. [CrossRef]
74. Zhou, G.; Zhou, X.; He, Y.; Shao, J.; Hu, Z.; Liu, R.; Zhou, H.; Hosseinibai, S. Grazing intensity significantly affects belowground carbon and nitrogen cycling in grassland ecosystems. A meta-analysis. *Glob. Change Biol.* **2017**, *23*, 1167–1179. [CrossRef] [PubMed]
75. Canedoli, C.; Ferre, C.; Abu El Khair, D.; Comolli, R.; Liga, C. Evaluation of ecosystem services in a protected mountain area: Soil organic carbon stock and biodiversity in alpine forests and grasslands. *Ecosyst. Serv.* **2020**, *44*, 101135. [CrossRef]
76. Kumar, S.S.; Wani, O.A.; Mir, S.A.; Babu, S.; Sharma, V.; Chesti, M.U.H.; Baba, Z.A.; Sofi, P.A.; Wani, F.J.; Dar, S.R.; et al. Soil carbon dynamics in the temperate Himalayas: Impact of land use management. *Front. Environ. Sci.* **2022**, *10*, 1009660. [CrossRef]
77. Phukubye, K.; Mutema, M.; Buthelezi, N.; Muchaonyerwa, P.; Cerri, C.; Chaplot, V. On the impact of grassland management on soil carbon socks. A worldwide meta-analysis. *Geoderma Reg.* **2022**, *28*, e00479. [CrossRef]
78. Conant, R.T.; Cerri, E.E.P.; Osborne, B.B.; Paustian, K. Grassland management impacts on soil carbon stocks: A new synthesis. *Ecol. Appl.* **2017**, *27*, 662–668. [CrossRef]
79. Li, J.-P.; Ma, H.-B.; Xie, Y.-Z.; Wang, K.-B.; Qiu, K.-Y. Deep soil C and N pools in long-term fenced and overgrazed temperate grasslands in northwest China. *Sci. Rep.* **2019**, *9*, 16088. [CrossRef]
80. Moreno-de las Heras, M.; Bochet, E.; Monleon, V.; Espigares, T.; Manuel Nicolau, J.; Molina, M.J.; García-Fayos, P. Aridity induces nonlinear effects of human disturbance on precipitation-use efficiency of Iberian woodlands. *Ecosystems* **2018**, *21*, 1295–1305. [CrossRef]

Disclaimer/Publisher's Note: The statements, opinions and data contained in all publications are solely those of the individual author(s) and contributor(s) and not of MDPI and/or the editor(s). MDPI and/or the editor(s) disclaim responsibility for any injury to people or property resulting from any ideas, methods, instructions or products referred to in the content.

agronomy

MDPI

Article

Soil Property Alterations and Nitrogen Use Dynamics of *Hemarthria altissima* Under Distinct Nitrogen Forms

Xiaowei Wei [1], Mingyue Sun [1], Shihan Feng [1], Ju Zhang [1], Yidi Gai [2], Yuheng Yang [3] and Xuechen Yang [4,*]

[1] Jilin Provincial Key Laboratory for Plant Resources Science and Green Production, Jilin Normal University, Siping 136000, China; weixiaowei@jlnu.edu.cn (X.W.); 18543444519@163.com (M.S.); 15604340110@163.com (S.F.); 13894155011@163.com (J.Z.)
[2] College of Life Sciences, Jilin University, Changchun 130000, China; gaiyd1324@mails.jlu.edu.cn
[3] Jilin Provincial Key Laboratory of Tree and Grass Genetics and Breeding, College of Forestry and Grassland Science, Jilin Agricultural University, Changchun 130118, China; yangyh@jlau.edu.cn
[4] State Key Laboratory of Ecological Safety and Sustainable Development in Arid Lands, Xinjiang Institute of Ecology and Geography, Chinese Academy of Sciences, Urumqi 830011, China
* Correspondence: yangxuechen@ms.xjb.ac.cn

Abstract

Atmospheric nitrogen deposition is increasing worldwide, with profound implications for plant nitrogen acquisition and ecosystem nutrient cycling, particularly in nitrogen-limited systems. In this study, we investigated how inorganic nitrogen form regulates nitrogen uptake in *H. altissima* through pot experiments by applying ammonium nitrogen, nitrate nitrogen, mixed nitrogen, and a nitrogen-free control in Songnen grassland ecosystems at the eastern end of Eurasia. Soil abiotic properties, root morphological traits, and nitrogen uptake dynamics were jointly quantified using integrative modeling in combination with ^{15}N stable isotope tracing. Relative to the no-nitrogen control, both ammonium and nitrate nitrogen significantly altered soil physicochemical conditions and stimulated root development, with ammonium consistently exhibiting stronger effects. Ammonium and nitrate applications reduced soil pH by 4.83% and 6.25%, increased electrical conductivity by 2.01% and 1.17%, and enhanced inorganic nitrogen pools by 115.84% and 45.69%, respectively. Root morphological traits were significantly enhanced under ammonium, nitrate, and mixed nitrogen treatments. ^{15}N tracing further demonstrated that ammonium nitrogen significantly increased root ^{15}N uptake compared with the no-nitrogen control ($p < 0.05$) and promoted a 20.10% greater allocation of absorbed nitrogen to aboveground biomass than nitrate nitrogen. Collectively, these findings highlight nitrogen form as a key regulator of soil–plant nitrogen coupling, with ammonium nitrogen more effectively enhancing nitrogen acquisition and internal translocation than nitrate.

Keywords: nitrogen forms; soil property; nitrogen uptake; biomass

1. Introduction

Nitrogen (N) deposition has increased markedly over the past decades as a consequence of intensified anthropogenic activities, including fossil fuel combustion, agricultural fertilization, and industrial emissions [1]. This persistent enhancement of reactive nitrogen input is projected to continue under future global change scenarios, profoundly altering biogeochemical processes and ecosystem function. Grasslands, which constitute nearly one third of the global terrestrial surface, are particularly sensitive to changes in nitrogen availability because of their long-term evolution under nutrient-limited conditions [2]. Thus,

understanding how nitrogen deposition influences soil physicochemical properties, plant nutrient uptake strategies, and ecosystem nutrient cycling has become a central topic in global change ecology. Previous studies have shown that elevated nitrogen deposition can substantially reshape soil chemical environments, including shifts in soil pH, electrical conductivity (EC), mineral nitrogen pools, and ratios reflecting the balance of C, N, and P [3]. In many temperate grasslands, long-term N addition tends to acidify soils and enhance inorganic N availability, which may further alter microbial processes, nutrient turnover, and plant nutrient acquisition [2,4]. However, the response magnitude and pathways are not universal across grassland types. For instance, temperate grasslands often exhibit rapid increases in soil nitrate and declines in pH, semi-arid grasslands display stronger N retention but limited change in soil acidity due to low buffering capacity, whereas alpine grasslands are constrained by low temperature and short growing seasons, resulting in slow N transformation and unique plant adaptation strategies [5,6]. These biome-specific responses highlight the need to investigate nitrogen effects under different chemical forms and ecological contexts, particularly considering the increasing complexity of atmospheric nitrogen composition, which includes ammonium (NH_4^+), nitrate (NO_3^-), and mixed reactive nitrogen [1,7,8].

Different nitrogen forms can markedly alter soil physical and chemical properties in grassland ecosystems, thereby influencing root morphology and biomass accumulation of dominant herbaceous species [8,9]. NH_4^+ inputs often increase soil acidity and modify cation exchange capacity, potentially enhancing the solubility of certain nutrients while affecting soil aggregate stability [10]. In contrast, NO_3^- fertilization tends to increase soil solution mobility and can accelerate leaching processes, shaping soil moisture distribution and nutrient availability in deeper layers [11]. These soil property shifts drive distinct root morphological responses: ammonium frequently promotes denser, more branched root systems concentrated in upper soil horizons, whereas nitrate encourages deeper rooting and greater root elongation due to its vertical mobility [12,13]. As a result, grassland biomass accumulation reflects the interplay between nitrogen form and root foraging strategies, with balanced N inputs enhancing both aboveground productivity and belowground biomass, while excessive or unbalanced nitrogen supply may reduce root-shoot coordination, alter species composition, and ultimately affect grassland ecosystem functioning.

Distinct nitrogen deposition forms exert strong control over soil processes and the pathways through which plants acquire nitrogen [14]. Ammonium usually promotes soil acidification through nitrification, while nitrate is more mobile and easily leached, leading to distinct impacts on soil nitrogen pools and stoichiometric balance. Mixed nitrogen inputs may further generate nonlinear interactions between ammonium and nitrate transformation pathways [8]. Despite extensive research on the effects of nitrogen addition on grassland soils, fewer have simultaneously compared the effects of ammonium nitrogen, nitrate nitrogen, and mixed nitrogen forms under controlled field conditions, limiting our understanding of how nitrogen composition modulates soil–plant feedbacks, especially in dominant grass species such as *Leymus chinensis* and *Hemarthria altissima* [1,8]. *H. altissima*, as a widely distributed perennial grass in temperate and semi-arid regions, plays a critical role in maintaining ecosystem stability, soil conservation, and grassland productivity [15–17]. This species exhibits strong adaptability to nutrient-poor soils, yet its physiological and morphological strategies under differential nitrogen forms remain inadequately understood. Root morphology is a crucial determinant of nitrogen acquisition, while ^{15}N stable isotope tracing offers a powerful means to track nitrogen allocation patterns in plant tissues and soils [18,19]. Integrating root traits, above- and below-ground biomass production, and ^{15}N accumulation provides a comprehensive framework to evaluate plant nitrogen utilization dynamics and to identify preferential uptake of specific nitrogen forms.

https://doi.org/10.3390/agronomy16020155

Previous studies have shown that different nitrogen forms can differentially affect soil acidification, microbial activity, and plant growth [7,17]; however, the mechanisms linking soil biochemical changes with plant nitrogen uptake and allocation remain insufficiently resolved, particularly in perennial grassland species. By integrating soil biochemical responses, root morphological traits, and ^{15}N tracer-based assessments of plant nitrogen uptake and allocation [20], this study aims to clarify how nitrogen form regulates soil nutrient availability, plant nitrogen assimilation, and soil–plant nitrogen coupling. The novelty of this research lies in its process-based comparison of ammonium, nitrate, and mixed nitrogen inputs, explicitly linking changes in soil nitrogen pools and stoichiometry with root-mediated nitrogen acquisition and biomass production. This integrated approach moves beyond assessments of biomass responses alone and provides mechanistic insight into how distinct reactive nitrogen forms drive ecosystem-level nitrogen cycling. Overall, our findings advance the mechanistic understanding of nitrogen form-specific effects on soil–plant interactions in temperate grasslands and provide a theoretical basis for predicting grassland responses to future increases in atmospheric nitrogen deposition, particularly under global change scenarios.

2. Materials and Methods

2.1. Site Description

The experiment was conducted at the Songnen Grassland Ecosystem National Observation and Research Station, Jilin Province, China (44°34′ N, 123°31′ E). The region experiences a typical temperate continental monsoon climate, with warm and humid summers contrasted by long, cold, and dry winters. The surface soil layer (0–20 cm) is characterized as shown in Table 1. The site has a mean annual temperature ranging from 4.6 to 6.5 °C, and annual precipitation varies between 280 and 620 mm, with the majority occurring during the growing season. For the pot experiment, each container was filled with 3.5 kg of wind-deposited sandy soil collected from the grassland. Pots were arranged in a completely randomized block design with six replicates per treatment. The test species was H. altissima, a perennial C_4 grass widely distributed across the Songnen Plain, with six seedlings transplanted into each pot. Four nitrogen treatments were established and applied in two equal installments on May 30 and June 15. These treatments included a no-nitrogen control (N0), ammonium nitrogen supplied as $(NH_4)_2SO_4$ (Sinopharm Chemical Reagent Co., Ltd., Shanghai, China) (AN), nitrate nitrogen supplied as $Ca(NO_3)_2$ (Sinopharm Chemical Reagent Co., Ltd., Shanghai, China) (NN), and a mixed nitrogen treatment consisting of equimolar NH_4^+-N and NO_3^--N (ANN). All nitrogen treatments were applied at a rate equivalent to 10 g N m^{-2}. To suppress nitrification, dicyandiamide (DCD) (Sinopharm Chemical Reagent Co., Ltd., Shanghai, China) was added at 10 mg m^{-2} in the AN treatment and 5 mg m^{-2} in the ANN treatment. To minimize confounding effects unrelated to nitrogen treatments, all pots were maintained under standardized management conditions throughout the experimental period. No chemical pesticides, fungicides, or herbicides were applied at any stage. Weed control was conducted manually at weekly intervals by visual inspection, and any emerging weeds were removed immediately by hand. Plant health status was monitored regularly, and no visible symptoms of pest infestation or disease were observed during the experiment. To avoid potential limitations of other macro- and micronutrients that could interfere with nitrogen uptake and allocation, each pot received 200 mL Hoagland nutrient solution once per month. This solution supplied non-nitrogen nutrients at balanced and non-limiting concentrations, while nitrogen availability was strictly controlled by the experimental nitrogen treatments. The application rate and frequency were identical across all treatments, ensuring that differences in plant responses could be attributed to nitrogen form rather than to other nutrient constraints.

https://doi.org/10.3390/agronomy16020155

Water availability was primarily regulated by natural precipitation. During periods of insufficient rainfall, supplemental irrigation was applied uniformly to all pots to maintain soil moisture near field capacity. Specifically, irrigation was provided when surface soil moisture declined visibly or when prolonged dry periods (>7 consecutive days without precipitation) occurred, with approximately 500 mL per pot per event applied to avoid water stress. No waterlogging was observed during the experiment. Importantly, irrigation frequency and volume were consistent across treatments, thereby minimizing potential interactions between water availability and nitrogen uptake. Plants were harvested on September 15, corresponding to the post-fruiting stage, when biomass accumulation and nitrogen allocation patterns had stabilized. This timing allowed for an integrated assessment of cumulative nitrogen uptake, root morphological development, and soil–plant nitrogen dynamics over the entire growing season.

Table 1. Chemical and physical properties of the basic soil (mean ± SE, *n* = 3).

Soil Properties	Soil pH	Total Nitrogen ($g \cdot kg^{-1}$)	Total Phosphorus ($g \cdot kg^{-1}$)	Total Organic Carbon ($g \cdot kg^{-1}$)	NH_4^+-N ($mg \cdot kg^{-1}$)	NO_3^--N ($mg \cdot kg^{-1}$)	Soil EC ($\mu S \cdot cm^{-1}$)
Content	8.68 ± 0.026	1.02 ± 0.004	0.66 ± 0.002	6.37 ± 1.206	1.23 ± 0.051	1.89 ± 0.063	78.76 ± 1.352

2.2. Determination of Root Morphology and Plant Biomass

Root samples of *H. altissima* were collected for analysis. For each treatment, six pots were selected, with three plants of similar growth vigor chosen from each pot. The root systems were thoroughly washed and then imaged using an Epson 11000 scanner (Epson America, California, Inc., USA). The root characteristics, including root length, surface area, volume, and tip number were quantified using the WinRHIZO 2016b root analysis system (Regent Instrument, Quebec, Canada). The aboveground biomass of the plants was harvested and placed into envelopes. The belowground samples were washed with distilled water, placed in envelopes, and brought to the laboratory. The samples were then blanched at 105 °C for 30 min, followed by drying at 65 °C until a constant weight was achieved. The dry weight of the aboveground tissue was recorded as the aboveground biomass (AGB, g), while the weight of the underground tissue was recorded as the belowground biomass (BGB, g).

2.3. Soil Sample Collection and Physicochemical Property Determination

Soil samples were collected using a composite design, with five random points in each plot. After collection, the samples were sieved through a 100-mesh screen to remove large debris, then further sieved through a 2 mm mesh and divided into two portions. One portion was stored at 4 °C and the other portion was air-dried, ground, and sieved through a 1 mm mesh for subsequent analysis. SWC was calculated as the difference between fresh and dry weights. Soil pH and EC were measured in aqueous extracts [2]. The supernatant was analyzed using a pH meter (PHS-3C, Shanghai Leici Instrument Factory, Shanghai, China) and conductivity meter (DDSJ-318, Shanghai Leici Instrument Factory, Shanghai, China).

Extractable inorganic nitrogen was determined using potassium chloride extraction. NH_4^+-N and NO_3^--N concentrations were quantified using a continuous flow analyzer (Futura, Alliance Flow Analyzer, Frassaillon, France) [1]. Total carbon and nitrogen contents were measured with an elemental analyzer (vario EL cube, Elementar, Langenselbold, Germany). Total phosphorus was quantified by molybdenum–antimony colorimetric detection. The C, N, and P contents and their stoichiometric ratios were calculated from the measured values [8].

https://doi.org/10.3390/agronomy16020155

2.4. ^{15}N Stable-Isotope Labeling

To evaluate the preferential uptake of different nitrogen forms by *H. altissima*, a $\delta^{15}N$-labeling tracer experiment was conducted during the heading stage in late June, following which an analysis was conducted using a modified version of the method proposed by Zhang et al. [21]. Two ^{15}N-labeled nitrogen treatments were applied, $(^{15}NH_4)_2SO_4$ and $Ca(^{15}NO_3)_2$ (Shanghai Chemical Industry Research Institute Co., Ltd., Shanghai, China), with ^{15}N abundances of 9.18% and 9.24%, respectively. Four pots were randomly selected for each treatment to determine the initial ^{15}N abundance before labeling. Subsequently, isotopically labeled nitrogen was supplied by $(^{15}NH_4)_2SO_4$ or $Ca(^{15}NO_3)_2$ to each flask, resulting in equivalent application rates of $^{15}NH_4^+$-N 20 mg N m^{-2} soil and $^{15}NO_3^-$-N 20 mg N m^{-2} soil, respectively. Soil samples (four replicates per ^{15}N treatment) were collected 7d after nitrogen application to determine the concentrations and isotopic compositions of NH_4^+ and NO_3^-. These measurements were then used to assess differences in $\delta^{15}N$ values of plant tissues, soil, and soil-to-plant transfer among the different nitrogen-form treatments. On the 7th day following ^{15}N application, plant samples (leaf, stem and root components) were collected from both labeled and control treatments within each plot. Immediately after harvest, tissues were subjected to enzymatic deactivation at 105 °C for 30 min and subsequently dried at 65 °C for 48 h. Dried materials were weighed and finely homogenized using a ball mill (MM 400; Retsch, Haan, Germany). About 3 mg of finely homogenized sample was sealed in tin capsules and subjected to determination of total nitrogen content and isotopic ratios using an isotope ratio mass spectrometer (Isoprime 100) coupled with an elemental analyzer (vario EL cube; Elementar, Langenselbold, Germany). The $\delta^{15}N$ values were calculated using the following equation [19–21]:

$$\delta^{15}N(‰) \ (\frac{R_{sample}}{R_{standard}} - 1) \ \times \ 1000 \quad (1)$$

where R_{sample} refers to the $^{15}N/^{14}N$ ratio measured in the sample, whereas $R_{standard}$ corresponds to that of atmospheric N_2, which has a fixed ratio of 0.00368.

2.5. Statistical Analysis

Data were processed and analyzed using R software (version 4.5.1). Assumptions of normality and homogeneity of variances were assessed using the Kolmogorov–Smirnov test and Levene's test, respectively. For post hoc comparisons, Tukey's honestly significant difference (HSD) test was applied, with a significance level set at $p < 0.05$. Graphical representations of the data were generated using the ggplot2 package. All analyses were conducted to determine significant treatment effects.

3. Results

3.1. Soil Chemical Properties

Nitrogen addition significantly altered several soil chemical properties, especially pH and EC ($p < 0.05$; Figure 1). Relative to the control, soil pH was markedly reduced under ammonium nitrogen, nitrate nitrogen, and mixed nitrogen treatments, with decreases of 4.81%, 6.25%, and 5.62%, respectively (Figure 1A). Electrical conductivity showed a distinct response to nitrogen form, with the ammonium nitrogen treatment exhibiting significantly higher EC values than control as well as nitrate nitrogen and mixed nitrogen treatments ($p < 0.05$; Figure 1B). In contrast, SWC remained statistically unchanged across all nitrogen treatments (Figure 1C).

https://doi.org/10.3390/agronomy16020155

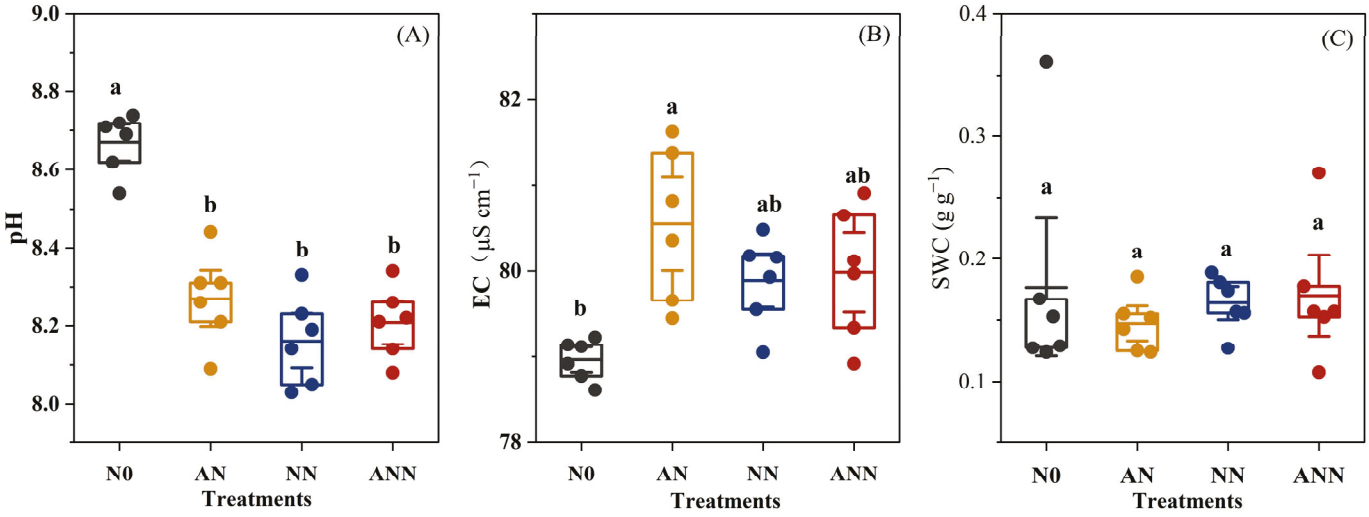


Figure 1. Effects of nitrogen forms on soil pH (**A**), Electrical conductivity (EC) (**B**), and Soil water content (SWC) (**C**) in *H. altissima*. Control(N0), ammonium nitrogen (AN), nitrate nitrogen (NN), mixed nitrogen (ANN). Statistically significant differences between treatments are indicated by different lowercase letters based on the Tukey test ($p < 0.05$; $n = 6$).

3.2. Soil Stoichiometric Characteristics

Soil inorganic nitrogen and total nutrient concentrations varied significantly among the nitrogen-form treatments ($p < 0.05$; Figure 2). NO_3^-–N concentrations were greatest under the ammonium nitrogen treatment, exceeding those in the control, nitrate nitrogen, and mixed nitrogen treatments (Figure 2A). A comparable trend occurred for NH_4^+–N, with the ammonium nitrogen treatment showing substantially higher levels than the other treatments, 167.01%, 73.83%, and 61.88% higher than those of the control, nitrate nitrogen, and mixed nitrogen treatments, respectively (Figure 2B).

Total nitrogen (TN) was highest under the mixed nitrogen treatment, with values significantly surpassing those of the control, ammonium nitrogen, and nitrate nitrogen treatments (Figure 2C). Soil TC also peaked in the mixed nitrogen treatment, increasing by 16.92%, 15.69%, and 15.92% relative to the control, ammonium nitrogen, and nitrate nitrogen treatments, respectively (Figure 2D). In contrast, TP levels showed no significant response to the different nitrogen forms (Figure 2E).

The control, ammonium nitrogen, nitrate nitrogen, and mixed nitrogen treatments exerted statistically significant effects on soil stoichiometric characteristics ($p < 0.05$; Figure 3). Specifically, soils receiving ammonium nitrogen or mixed nitrogen inputs exhibited markedly higher C/N and C/P ratios than those under the control and nitrate-N treatments ($p < 0.05$). Relative to the control, the C/N ratio increased by 11.28% and 9.24% under ammonium nitrogen and mixed nitrogen treatments, respectively (Figure 3A). A comparable pattern was observed for the C/P ratio, which rose by 25.43% in the ammonium nitrogen treatment and by 29.24% in the mixed nitrogen treatment (Figure 3B). In contrast, the N/P ratio remained statistically unchanged across all nitrogen forms, indicating a limited sensitivity of this metric to nitrogen speciation (Figure 3C).

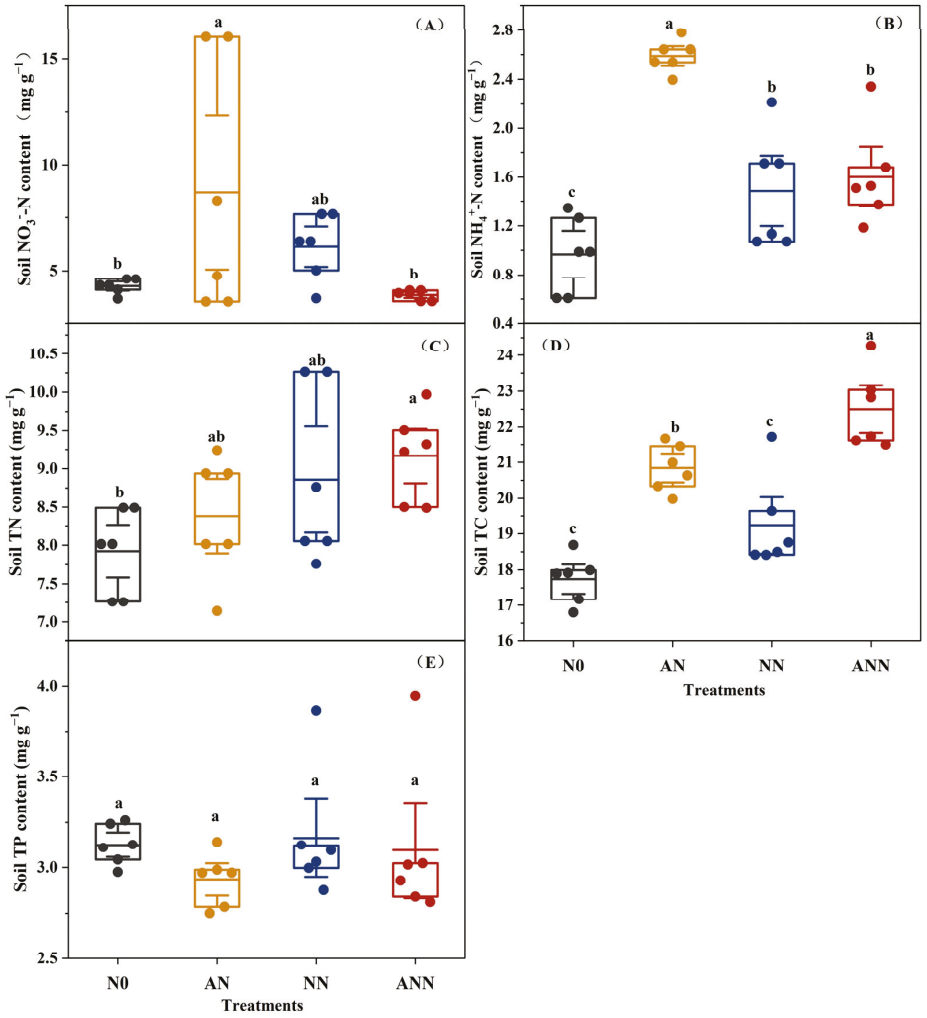


Figure 2. Effects of nitrogen forms on soil NO_3^--N content (**A**), soil NH_4^+-N content (**B**), soil Total nitrogen (TN) content (**C**), soil Total carbon (TC) content (**D**) and soil Total phosphorus (TP) content (**E**) in *H. altissima*. Control(N0), ammonium nitrogen (AN), nitrate nitrogen (NN), mixed nitrogen (ANN). Statistically significant differences between treatments are indicated by different lowercase letters based on the Tukey test ($p < 0.05$; $n = 6$).

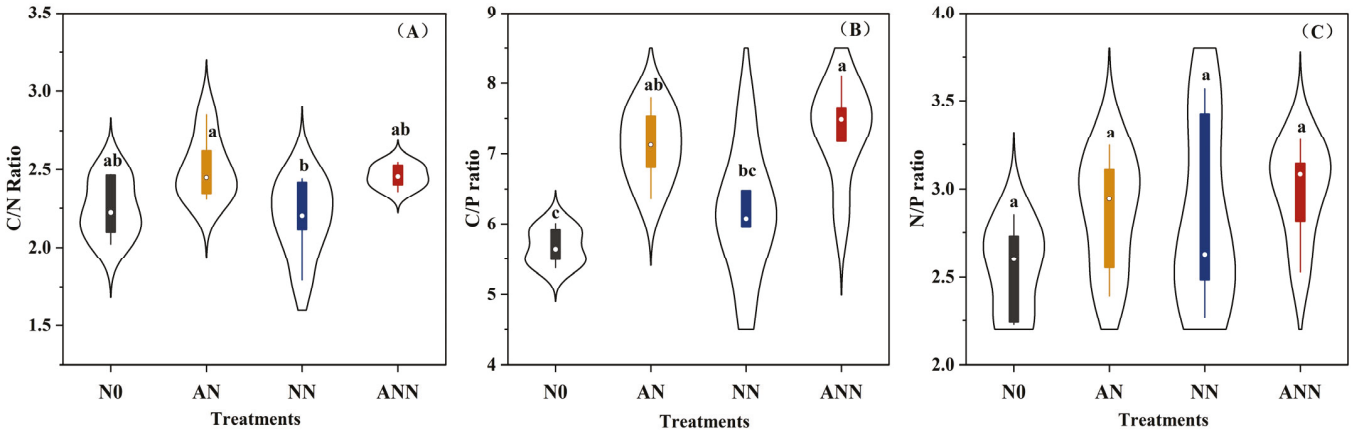


Figure 3. Effects of nitrogen forms on soil C/N ratio (**A**), C/P ratio (**B**) and N/P ratio (**C**) in *H. altissima*. Control(N0), ammonium nitrogen (AN), nitrate nitrogen (NN), mixed nitrogen (ANN). Statistically significant differences between treatments are indicated by different lowercase letters based on the Tukey test ($p < 0.05$; $n = 6$).

https://doi.org/10.3390/agronomy16020155

3.3. Morphological Characteristics of Root Systems

Root morphological characteristics responded distinctly to variations in nitrogen form ($p < 0.05$; Figure 4). Among all treatments, ammonium nitrogen application resulted in the greatest total root length, significantly surpassing those observed under the control, nitrate nitrogen, and mixed nitrogen conditions (Figure 4A). Nitrogen enrichment generally promoted root surface development, as evidenced by the substantially larger root surface area in all nitrogen-supplemented treatments compared with the unfertilized control (Figure 4B). Furthermore, total root volume and the number of root tips were both markedly elevated under ammonium nitrogen treatment relative to the control and nitrate nitrogen treatments (Figure 4C,D), indicating a pronounced stimulatory effect of ammonium nitrogen on root system proliferation.

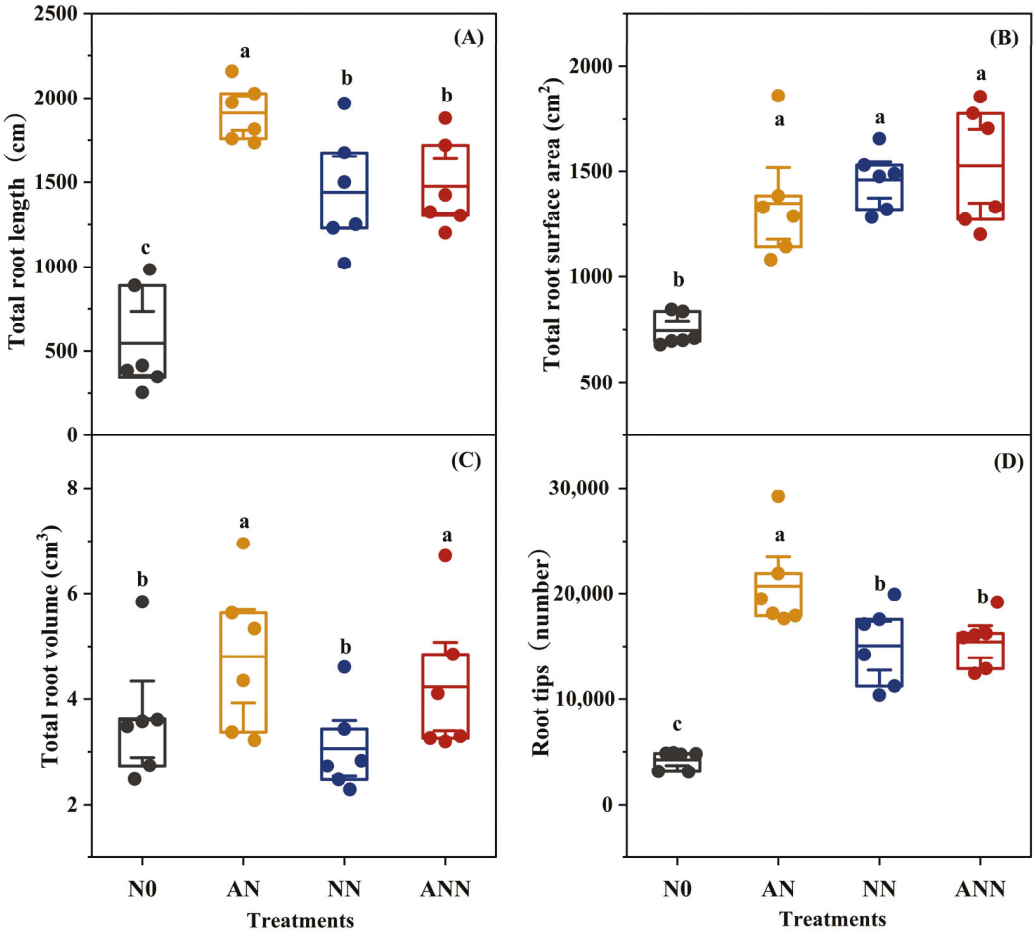


Figure 4. Effects of nitrogen forms on total root length (**A**), total root surface area (**B**), total root volume (**C**) and root tips (**D**) in *H. altissima*. Control(N0), ammonium nitrogen (AN), nitrate nitrogen (NN), mixed nitrogen (ANN). Statistically significant differences between treatments are indicated by different lowercase letters based on the Tukey test ($p < 0.05$; $n = 6$).

3.4. Absorption and Utilization of ^{15}N in Different Forms

Significant differences in $\delta^{15}N$ values of leaves, stems, roots, and soil were observed among the control, ammonium nitrogen, nitrate nitrogen and mixed nitrogen treatments ($p < 0.05$; Table 2). Compared with N0, leaf $\delta^{15}N$ was markedly elevated under ammonium nitrogen, nitrate nitrogen and mixed nitrogen treatments. Stem $\delta^{15}N$ showed higher values in mixed nitrogen and ammonium nitrogen treatments than in control and nitrate nitrogen treatments. Root $\delta^{15}N$ reached its highest level under the ammonium nitrogen treatment and was significantly greater than those of the other treatments. In contrast, soil $\delta^{15}N$

was highest in the nitrate nitrogen treatment, exceeding the values measured in control, ammonium nitrogen and mixed nitrogen treatments.

Table 2. Comparison of the leaf $\delta^{15}N$, stem $\delta^{15}N$, root $\delta^{15}N$ and soil $\delta^{15}N$ in *H.altissima* under different N form treatments (means ± SE, $n = 4$). Control(N0), ammonium nitrogen (AN), nitrate nitrogen (NN), mixed nitrogen (ANN). Statistically significant differences between treatments are indicated by different lowercase letters based on the Tukey test ($p < 0.05$; $n = 6$).

Variable	N0 Control	AN ^{15}N Labeling	NN ^{15}N Labeling	ANN ^{15}N Labeling
Leaf $\delta^{15}N$ (‰)	4.96 ± 0.64 c	14.18 ± 1.52 ab	11.93 ± 0.78 b	17.83 ± 1.05 a
Stem $\delta^{15}N$ (‰)	6.79 ± 0.78 b	26.3 ± 4.28 a	29.1 ± 1.81 a	36.65 ± 3.49 a
Root $\delta^{15}N$ (‰)	143.07 ± 1.35 d	8278.78 ± 59.21 a	6020.23 ± 276.73 c	7212.62 ± 129.14 b
Soil $\delta^{15}N$ (‰)	3.92 ± 0.04 c	145.48 ± 1.32 b	157.40 ± 1.20 a	145.17 ± 0.48 b

3.5. Biomass Accumulation in Different Forms

Aboveground and belowground biomass responded significantly to the different nitrogen form treatments ($p < 0.05$). Compared with the unfertilized control, aboveground biomass was substantially enhanced by nitrogen addition, with increases of 92.09%, 59.94%, and 66.55% under ammonium nitrogen, nitrate nitrogen and mixed nitrogen treatments, respectively (Figure 5A). Similarly, belowground biomass was significantly lower in the control treatment than in all nitrogen-fertilized treatments ($p < 0.05$; Figure 5B).

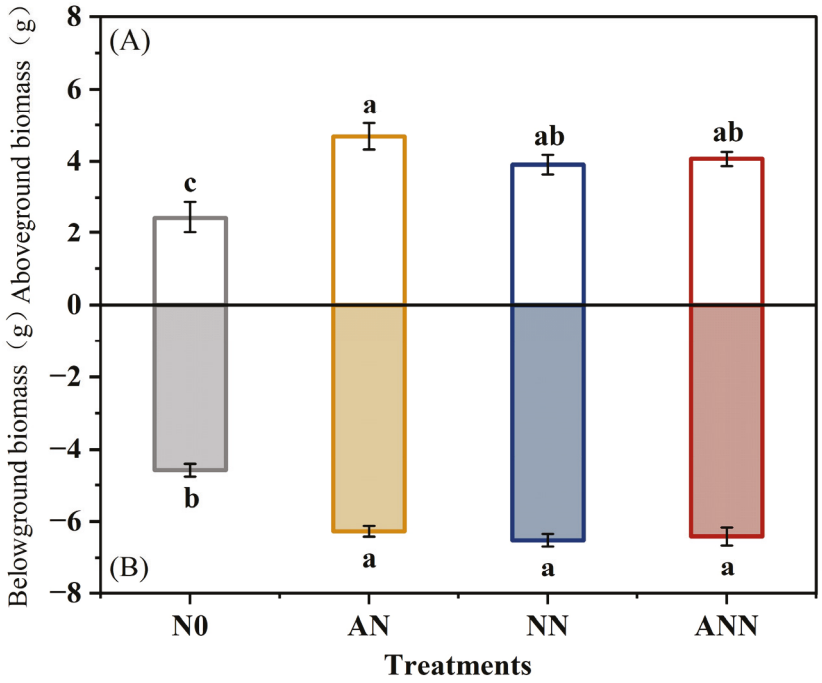


Figure 5. Effects of nitrogen forms on aboveground biomass (**A**) and belowground biomass (**B**) in *H. altissima*. Control(N0), ammonium nitrogen (AN), nitrate nitrogen (NN), mixed nitrogen (ANN). Statistically significant differences between treatments are indicated by different lowercase letters based on the Tukey test ($p < 0.05$; $n = 6$).

Results from the Mantel test revealed that both aboveground and belowground biomass were significantly associated with a broad range of abiotic variables as well as root system traits (Figure 6). Notably, indices related to plant nitrogen acquisition—represented by $\delta^{15}N$ signatures in roots, stems, and leaves—exhibited strong positive correlations with biomass allocation in both plant compartments. In addition, key root morphological attributes, including total root length, root surface area, root volume, and root tip number, were also positively linked to aboveground and belowground biomass of

H. altissima, highlighting the close coupling between nitrogen utilization, root architecture, and plant growth.

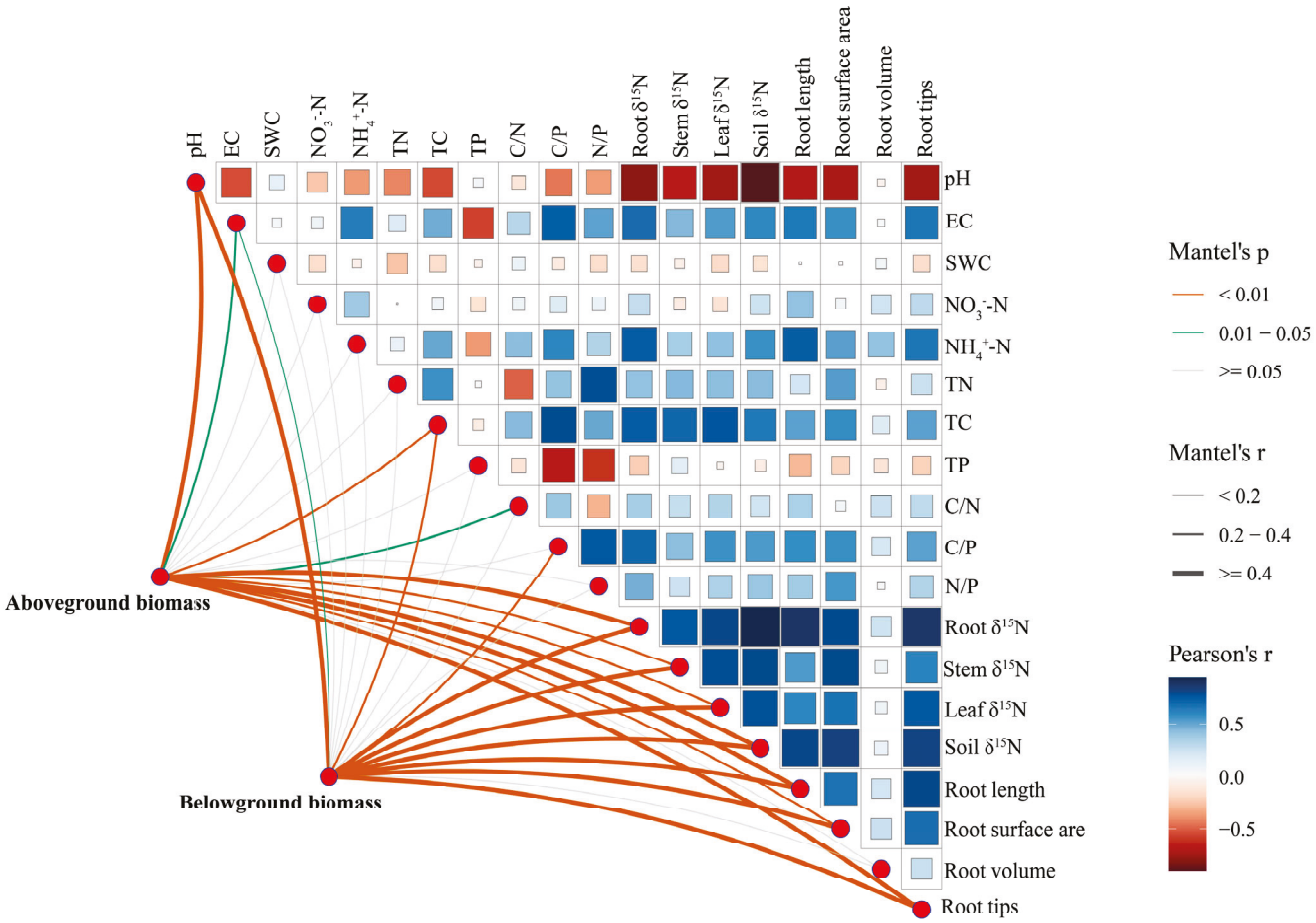


Figure 6. The Mantel test for the relationship between the composition of aboveground biomass and belowground biomass and abiotic factors and plant root characteristics. Abbreviation annotation: Electrical conductivity (EC), Total nitrogen (TN), Total carbon (TC), Total phosphorus (TP), Soil water content (SWC). The edge width and color represent the Mantel's r statistic and statistical significance based on permutations, respectively.

4. Discussion

4.1. Nitrogen Form-Induced Changes in Soil Properties

Soil chemical properties responded sensitively to nitrogen form, with all N additions (ammonium nitrogen, nitrate nitrogen and mixed nitrogen) significantly decreasing soil pH compared with the control. Nitrogen-induced soil acidification is a well-documented phenomenon and is primarily attributed to proton release during nitrification of ammonium and rhizosphere acidification associated with inorganic N uptake [22,23]. Although nitrate is often considered less acidifying than ammonium under field conditions, the observed pH decline under nitrate nitrogen treatment in this study suggests that constrained buffering capacity and limited solute transport in pot systems can amplify acidification responses regardless of N form [11,24]. In contrast to the consistent pH decline, EC increased significantly only under ammonium supply. Soil EC is widely used as an integrative indicator of soluble ion concentration and fertilizer-derived salts in the soil solution [22]. The elevated EC under ammonium nitrogen treatment likely reflects higher ionic strength associated with ammonium fertilizers and enhanced mobilization of exchangeable cations under acidifying conditions. Because soil water content did not differ among treatments, the observed EC increase can be attributed primarily to nitrogen-driven ionic processes rather

than moisture effects. Together, these results indicate that nitrogen form creates distinct belowground chemical environments that may differentially constrain or facilitate root functioning and nutrient acquisition.

Changes in soil nitrogen pools and macronutrient stocks (TC, TN, TP) provide essential context for interpreting plant nitrogen uptake and soil–plant coupling [25]. Nitrogen additions commonly increase soil inorganic nitrogen (NH_4^+-N and NO_3^--N) directly through fertilizer inputs and indirectly by stimulating microbial turnover and N transformations, although the relative dominance of NH_4^+ versus NO_3^- in soil depends strongly on N form supplied and subsequent nitrification/immobilization processes [4,7]. Soil C:N:P stoichiometry offers a mechanistic lens to interpret how N form reshapes nutrient balance and potential limitation [3,26]. Soil C/N, C/P, and N/P ratios are widely used to indicate the relative availability of carbon, nitrogen, and phosphorus, and shifts in these ratios can signal changes in microbial nutrient demand, decomposition processes, and plant nutrient limitation status. In many ecosystems, nitrogen addition tends to increase soil N/P (and sometimes decrease C/N) by enriching N relative to P, which can intensify P limitation over time and reconfigure nutrient cycling pathways [27]. The consistent pH decline across N treatments suggests that N-induced acidification transformations likely occurred concurrently, which can influence the partitioning between NH_4^+-N and NO_3^--N and their persistence in soil.

4.2. Ammonium Enhanced Root Morphological Plasticity as a Mediator of N Acquisition

Root systems of *H. altissima* exhibited strong morphological plasticity in response to nitrogen form, with ammonium supply inducing the greatest increases in total root length, mean root diameter, and root surface area. Root morphological adjustments are widely recognized as an adaptive strategy that allows plants to optimize nutrient foraging under variable soil conditions [28]. Increased root length and surface area enhance the soil–root contact interface and nutrient interception capacity, while greater root diameter may support higher transport capacity and structural investment [29]. The pronounced root development under ammonium supply may reflect a coordinated response to the acidifying and ion-enriched rhizosphere created by ammonium nitrogen treatment. In such environments, expanding the absorptive interface can improve nutrient capture efficiency and buffer plants against localized nutrient depletion or ionic stress [30]. These findings support the view that root traits act as a critical mediator linking nitrogen form-induced soil chemical changes to plant nutrient acquisition strategies.

4.3. ^{15}N Tracer Evidence: Nitrogen Form Regulates Acquisition Magnitude and Within-Plant Partitioning

Stable isotope ^{15}N labeling provided direct mechanistic evidence that nitrogen form regulates both nitrogen acquisition and internal partitioning in *H. altissima*. Compared with the control, all N forms treatments markedly increased $\delta^{15}N$ values in plant organs and soil, confirming effective uptake of applied nitrogen. Across treatments, ^{15}N enrichment consistently followed the hierarchy root > stem > leaf, indicating a pronounced root-centered retention strategy for newly acquired nitrogen.

Nitrogen form strongly influenced the magnitude of ^{15}N enrichment and its distribution among organs. Ammonium treatment resulted in the highest ^{15}N recovery and the greatest allocation of ^{15}N to roots, coinciding with the strongest stimulation of root morphological traits. This convergence between morphological and isotopic responses supports a coherent mechanism whereby ammonium supply enhances root foraging capacity, leading to greater nitrogen capture and preferential retention in belowground tissues [18]. Similar root-centered nitrogen retention patterns under ammonium supply have been reported in other grass species using ^{15}N tracer approaches [21,31].

https://doi.org/10.3390/agronomy16020155

In contrast, nitrate supply tended to promote greater ^{15}N enrichment in stems, suggesting a higher propensity for upward translocation of absorbed nitrogen, consistent with the higher mobility of nitrate within the soil–plant continuum [32]. The mixed nitrogen treatment produced the highest root $\delta^{15}N$ values, indicating potential complementarity between ammonium and nitrate that supports both efficient acquisition and subsequent redistribution of nitrogen within the plant. Such synergistic effects of mixed N supply have been observed in forage grasses and are often interpreted as reflecting reduced physiological constraints compared with single-form supply [15,18,21].

4.4. The Nitrogen Absorption and Utilization Effects of Soil-Root-Aboveground Parts Under Different Nitrogen Forms

Integrating soil chemical responses, root morphological traits, and ^{15}N evidence reveals a clear cascade by which nitrogen form regulates nitrogen use dynamics in *H. altissima*. Nitrogen addition first altered soil chemical conditions, as reflected by universal pH decline and ammonium-specific EC increase. These changes were accompanied by strong root morphological plasticity, particularly under ammonium supply, which expanded the effective absorptive interface. Enhanced root development subsequently translated into higher nitrogen recovery and preferential retention of newly acquired nitrogen in roots [7,28,30].

The nitrogen uptake regulation model emphasizes that nitrogen form affects not only the quantity of nitrogen taken up, but also the transport of that nitrogen within the plant (Figure 7). Root traits emerge as a central mediator linking soil processes to whole-plant nitrogen use efficiency, highlighting the importance of considering soil–root interactions when evaluating nitrogen management strategies. Although pot experiments may limit root expansion and differ from fully natural field conditions, the controlled setting allowed us to disentangle nitrogen form-specific effects on soil properties, root traits, and plant nitrogen uptake by minimizing environmental heterogeneity and uncontrolled nutrient and water variability.

From a forage production perspective, the higher $\delta^{15}N$ recovery and stronger root-centered nitrogen retention under ammonium supply suggest improved short-term nitrogen capture by *H. altissima*, potentially enhancing fertilizer nitrogen retention within the plant–soil system. However, the concurrent soil acidification across all N treatments and the ammonium-induced increase in EC point to potential trade-offs for long-term soil sustainability. Ammonium-based fertilization is widely recognized as a major driver of agricultural soil acidification, with implications for nutrient availability and soil health [7,31,33]. Mixed nitrogen supply may represent a practical compromise by maintaining efficient nitrogen acquisition and redistribution while potentially moderating some adverse soil chemical effects associated with single nitrogen forms. These results underscore the need to balance short-term gains in nitrogen use efficiency with long-term soil chemical stability in intensively managed forage systems.

https://doi.org/10.3390/agronomy16020155

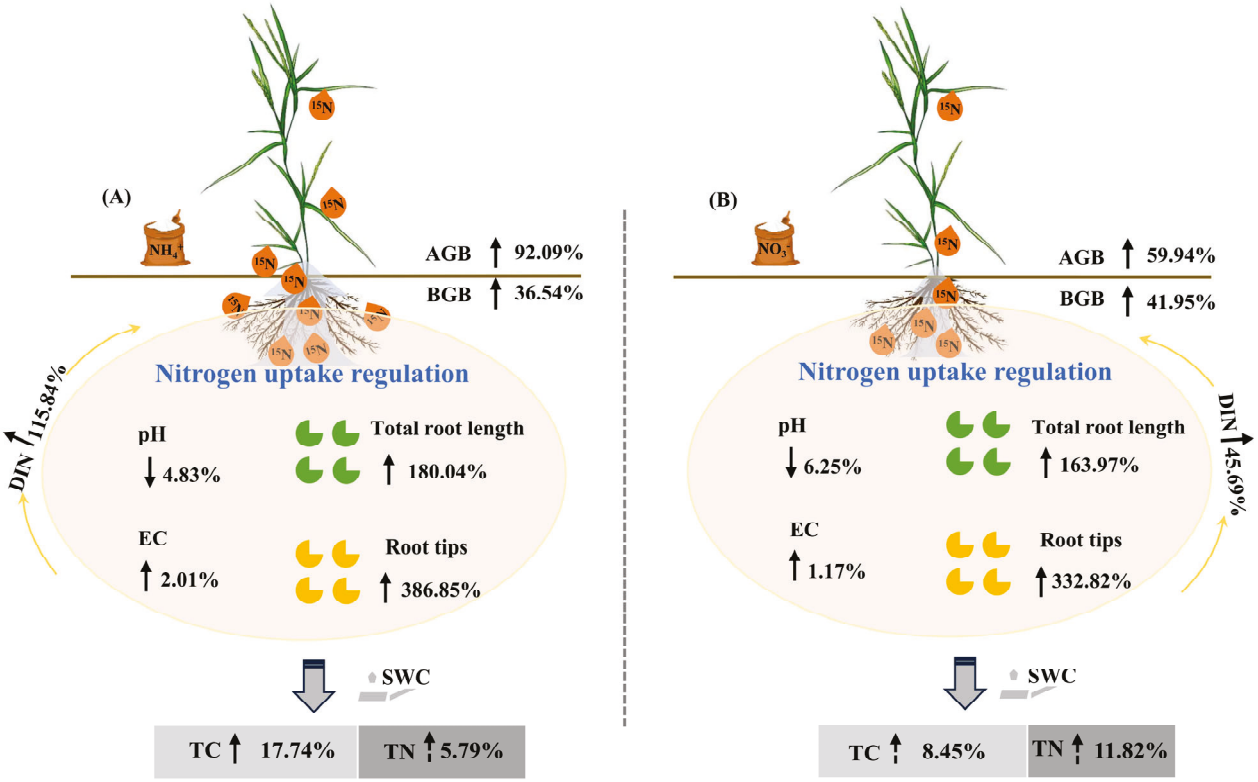


Figure 7. Schematic diagram of nitrogen uptake regulation model. (**A**) Comparison results of nitrogen uptake regulation under ammonium nitrogen treatment and control treatment, (**B**) comparison results of nitrogen uptake regulation under nitrate nitrogen treatment and control treatment. The orange ^{15}N is a marker for the uptake and transport of ^{15}N by the roots, stems and leaves of *H. altissima*. An upward arrow indicates an increase, while a downward arrow indicates a decrease. Abbreviation annotation: Aboveground biomass (AGB), Belowground biomass (BGB), Soil inorganic nitrogen (DIN), Electrical conductivity (EC), Soil water content (SWC), Total carbon (TC) and Total nitrogen (TN).

5. Conclusions

Nitrogen addition exerted strong, form-dependent effects on soil properties, root traits, and plant nitrogen allocation. Compared with the control, all nitrogen treatments reduced soil pH (4.81–6.25%), while ammonium nitrogen caused the greatest increase in electrical conductivity (2.00%), indicating stronger ionic effects. Nitrogen form distinctly reshaped soil nitrogen pools: ammonium nitrogen increased NH_4^+-N and mineral nitrogen availability (167.01%), whereas mixed nitrogen inputs maximized total nitrogen and carbon accumulation (15.8% and 26.83%) and increased C/N and C/P ratios (9.33% and 29.23%). Plant responses closely tracked these soil changes. Biomass production increased by 48.20–55.82% across nitrogen treatments, with ammonium nitrogen inducing the strongest aboveground growth (92.09%). Root morphological traits were consistently enhanced, particularly under ammonium nitrogen, which increased root length, surface area, volume, and tip number by up to 180.04%, 81.12%, 58.71% and 386.85%, thereby strengthening nutrient foraging capacity. ^{15}N tracing revealed divergent nitrogen pathways: ammonium nitrogen promoted plant nitrogen uptake and translocation (root $\delta^{15}N$ 57.86 times), whereas nitrate nitrogen showed greater short-term soil retention (soil $\delta^{15}N$ 40.15 times). Mantel tests confirmed that biomass gains were positively associated with root traits and ^{15}N uptake. Overall, ammonium-dominated nitrogen inputs most strongly promoted root development and nitrogen acquisition, while mixed nitrogen inputs preferentially enhanced soil carbon and total nitrogen accumulation. These findings underscore the critical role of

nitrogen form in regulating soil–plant nitrogen coupling and provide mechanistic insight for predicting grassland responses to future nitrogen enrichment under global change.

Author Contributions: Conceptualization, X.W. and X.Y.; methodology, X.W.; software, Y.G. and J.Z.; validation, X.W., S.F. and M.S.; formal analysis, S.F., J.Z. and Y.G.; investigation, X.Y.; resources, X.Y.; data curation, X.W., J.Z. and Y.G.; writing—original draft preparation, X.W.; writing—review and editing, M.S., S.F. and Y.Y.; visualization, Y.Y.; supervision, M.S.; project administration, X.Y.; funding acquisition, X.W. and X.Y. All authors have read and agreed to the published version of the manuscript.

Funding: This research was funded by the Natural Science Foundation of Jilin Province, China (YDZJ202401456ZYTS).

Data Availability Statement: The datasets generated for this study are available on request to the corresponding author.

Conflicts of Interest: The authors declare no conflicts of interest.

Abbreviations

The following abbreviations are used in this manuscript:

SWC	Soil water content
EC	Electrical conductivity
TN	Total nitrogen
TC	Total carbon
TP	Total phosphorus
DIN	Soil inorganic nitrogen, the total of ammonium nitrogen and nitrate nitrogen
C/N ratio	The ratio of total carbon to total nitrogen
C/P ratio	The ratio of total carbon to total phosphorus
N/P ratio	The ratio of total carbon to total phosphorus

References

1. Wei, X.; Yang, Y.; Yao, J.; Han, J.; Yan, M.; Zhang, J.; Shi, Y.; Wang, J.; Mu, C. Improved Utilization of Nitrate Nitrogen Through Within-Leaf Nitrogen Allocation Trade-Offs in *Leymus chinensis*. *Front. Plant Sci.* **2022**, *13*, 870681. [CrossRef]
2. Li, H.; Li, J.; Han, Z.; Zhu, W.; Liu, Z.; Sun, X.; Fu, C.; Xiao, H.; Qin, L.; Mei, L. Characteristics of Soil Nutrients and Microorganisms at the Grassland–Farmland Interface in the Songnen Agro-Pastoral Ecotone of Northeast China. *Agronomy* **2025**, *15*, 2032. [CrossRef]
3. Blanco, J.A.; Durán, M.; Luquin, J.; San Emeterio, L.; Yeste, A.; Canals, R.M. Soil C/N ratios cause opposing effects in forests compared to grasslands on decomposition rates and stabilization factors in southern European ecosystems. *Sci. Total Environ.* **2023**, *888*, 164118. [CrossRef]
4. Niu, F.; Huo, L.; Wang, Z.; Liu, J.; Gao, Z.; Li, M.; Xu, B. Effects of nitrogen addition and watering on soil seed bank germination in a semiarid grassland on the Loess Plateau of China. *Land Degrad. Dev.* **2023**, *34*, 142–155. [CrossRef]
5. Chen, J.; Li, F.-C.; Jia, B.; Gang, S.; Li, Y.; Mou, X.M.; Kuzyakov, Y.; Li, X.G. Regulation of soil nitrogen cycling by shrubs in grasslands. *Soil Biol. Biochem.* **2024**, *191*, 109327. [CrossRef]
6. Diao, H.; Chen, X.; Zhao, X.; Dong, K.; Wang, C. Effects of nitrogen addition and precipitation alteration on soil respiration and its components in a saline-alkaline grassland. *Geoderma* **2022**, *406*, 115541. [CrossRef]
7. Liu, M.; Xu, X.; Wanek, W.; Sun, J.; Bardgett, R.D.; Tian, Y.; Cui, X.; Jiang, L.; Ma, Z.; Kuzyakov, Y. Nitrogen availability in soil controls uptake of different nitrogen forms by plants. *New Phytol.* **2025**, *245*, 1450–1467. [CrossRef]
8. Xu, N.; Wei, X.; Zhang, J.; Sun, M.; Zhang, J.; Zhao, Z.; Yang, X. Leaf Nitrogen Allocation Trade-Offs Promote Efficient Utilization of Different Nitrogen Forms in *Hemarthria altissima*. *Biology* **2025**, *14*, 1260. [CrossRef]
9. Bai, Y.; Cotrufo, M.F. Grassland soil carbon sequestration: Current understanding, challenges, and solutions. *Science* **2022**, *377*, 603–608. [CrossRef]
10. Mayel, S.; Jarrah, M.; Kuka, K. How does grassland management affect physical and biochemical properties of temperate grassland soils? A review study. *Grass Forage Sci.* **2021**, *76*, 215–244. [CrossRef]
11. Byers, E.; Dörsch, P.; Eich-Greatorex, S.; Bleken, M.A. Deep N acquisition in cultivated grasslands: Uptake of slow-release ^{15}N-labeled ammonium in hemiboreal monospecific leys. *Plant Soil* **2024**, *499*, 393–408. [CrossRef]

12. Feng, H.; Guo, J.; Peng, C.; Kneeshaw, D.; Roberge, G.; Pan, C.; Ma, X.; Zhou, D.; Wang, W. Nitrogen addition promotes terrestrial plants to allocate more biomass to aboveground organs: A global meta-analysis. *Glob. Change Biol.* **2023**, *29*, 3970–3989. [CrossRef] [PubMed]
13. Liu, M.; Zhu, T.; Tian, Y.; Xu, X.; Wang, Y. Plant functional groups shift their nitrogen uptake during restoration of degraded alpine grasslands. *Land Degrad. Dev.* **2022**, *33*, 2898–2910. [CrossRef]
14. Chomel, M.; Lavallee, J.M.; Alvarez-Segura, N.; Baggs, E.M.; Caruso, T.; de Castro, F.; Emmerson, M.C.; Magilton, M.; Rhymes, J.M.; de Vries, F.T. Intensive grassland management disrupts below-ground multi-trophic resource transfer in response to drought. *Nat. Commun.* **2022**, *13*, 6991. [CrossRef]
15. Zhong, S.; Xu, Y.; Meng, B.; Loik, M.E.; Ma, J.-Y.; Sun, W. Nitrogen Addition Increases the Sensitivity of Photosynthesis to Drought and Re-watering Differentially in C_3 Versus C_4 Grass Species. *Front. Plant Sci.* **2019**, *10*, 815. [CrossRef]
16. Zhong, Y.; Yan, W.; Canisares, L.P.; Wang, S.; Brodie, E.L. Alterations in soil pH emerge as a key driver of the impact of global change on soil microbial nitrogen cycling: Evidence from a global meta-analysis. *Glob. Ecol. Biogeogr.* **2023**, *32*, 145–165. [CrossRef]
17. Zhong, S.; Chai, H.; Xu, Y.; Li, Y.; Ma, J.-Y.; Sun, W. Drought Sensitivity of the Carbon Isotope Composition of Leaf Dark-Respired CO_2 in C_3 (*Leymus chinensis*) and C_4 (*Chloris virgata* and *Hemarthria altissima*) Grasses in Northeast China. *Front. Plant Sci.* **2017**, *8*, 1996. [CrossRef]
18. Wang, Y.; Niu, G.; Wang, R.; Rousk, K.; Li, A.; Hasi, M.; Wang, C.; Xue, J.; Yang, G.; Lü, X. Enhanced foliar 15N enrichment with increasing nitrogen addition rates: Role of plant species and nitrogen compounds. *Glob. Change Biol.* **2023**, *29*, 1591–1605. [CrossRef]
19. Guo, J.; Li, H.; Yang, Y. Phenotypic Plasticity in Sexual Reproduction Based on Nutrients Supplied From Vegetative Ramets in a Leymus chinensis Population. *Front. Plant Sci.* **2019**, *10*, 1681. [CrossRef] [PubMed]
20. Barneze, A.S.; Oram, N.J.; Weewer, W.; Abalos, D.; De Deyn, G.B. Optimising grass-legume mixtures based on growth strategies for high N-yield and low N loss in fertilised grasslands. *Plant Soil* **2025**, *516*, 539–557. [CrossRef]
21. Zhang, J.; Wang, L.; Zhao, W.; Hu, H.; Feng, X.; Müller, C.; Cai, Z. Soil gross nitrogen transformations along the Northeast China Transect (NECT) and their response to simulated rainfall events. *Sci. Rep.* **2016**, *6*, 22830. [CrossRef] [PubMed]
22. Fartyal, A.; Bargali, S.S.; Bargali, K.; Negi, B. Changes in soil properties, organic carbon, and nutrient stocks after land-use change from forests to grasslands in *Kumaun Himalaya*, India. *Land Degrad. Dev.* **2025**, *36*, 2438–2457. [CrossRef]
23. Wang, L.; Deng, X.; Zhou, Y.; Geng, X.; Zhang, Z.; Tang, Y. Different nitrogen uptake patterns of plant and soil microorganisms in the forest-grassland transition zone on the Loess Plateau. *Front. Plant Sci.* **2025**, *15*, 1480517. [CrossRef]
24. Cui, X.; Zhang, Y.; Song, X. Asymmetric Response of Grassland Greenhouse Gases to Nitrogen Addition: A Global Meta-Analysis. *Agronomy* **2025**, *15*, 2365. [CrossRef]
25. Francksen, R.M.; Turnbull, S.; Rhymer, C.M.; Hiron, M.; Bufe, C.; Klaus, V.H.; Newell-Price, P.; Stewart, G.; Whittingham, M.J. The effects of nitrogen fertilisation on plant species richness in European permanent grasslands: A systematic review and meta-analysis. *Agronomy* **2022**, *12*, 2928. [CrossRef]
26. Sheng, Z.; Huang, Y.; Duan, L.; He, K.; Xie, D.; Borjigin, N.; Yang, H.; Qi, Y.; Li, E. Effects of simulated nitrogen deposition on N fate in a temperate steppe: Evidence from multi-year ^{15}N isotope study. *J. Environ. Manag.* **2025**, *394*, 127521. [CrossRef]
27. Shi, J.; Gong, J.; Li, X.; Zhang, Z.; Zhang, W.; Li, Y.; Song, L.; Zhang, S.; Dong, J.; Baoyin, T. Phosphorus application promoted the sequestration of orthophosphate within soil microorganisms and regulated the soil solution P supply in a temperate grassland in northern China: A 31P NMR study. *Soil Tillage Res.* **2023**, *227*, 105612. [CrossRef]
28. Liu, P.; Li, X.; Hu, S.; He, W.; Zhou, Y.; Wang, Y. Effects of Nitrogen Forms on Root Morphology and Nitrogen Accumulation in *Pinus tabuliformis* carr. Seedlings under Exponential Fertilization. *Forests* **2024**, *15*, 271. [CrossRef]
29. Jia, Z.; von Wirén, N. Signaling pathways underlying nitrogen-dependent changes in root system architecture: From model to crop species. *J. Exp. Bot.* **2020**, *71*, 4393–4404. [CrossRef]
30. Pandey, A.; Singh, K.; Singh, A.P. Nitrogen forms and their availability-dependent root developmental adaptation in plants. In *Improving Stress Resilience in Plants*; Elsevier: Amsterdam, The Netherlands, 2024; pp. 97–117, ISBN 9780443189272.
31. Loick, N.; Dixon, E.; Matthews, G.P.; Müller, C.; Ciganda, V.S.; López-Aizpún, M.; Repullo, M.A.; Cardenas, L.M. Application of a triple 15N tracing technique to elucidate N transformations in a UK grassland soil. *Geoderma* **2021**, *385*, 114844. [CrossRef]
32. Wu, J.; Song, M.; Ma, W.; Zhang, X.; Shen, Z.; Tarolli, P.; Wurst, S.; Shi, P.; Ratzmann, G.; Feng, Y.; et al. Plant and soil's δ15N are regulated by climate, soil nutrients, and species diversity in alpine grasslands on the northern Tibetan Plateau. *Agric. Ecosyst. Environ.* **2019**, *281*, 111–123. [CrossRef]
33. Li, Z.; Tian, Y.; Song, M.; Yu, M.; Li, X.; Zhang, Y.; Huang, J.; Su, Z.; Sun, S.; Dai, H. Competition between shrubs and grasses in a shrub–encroached temperate grassland: Implications from nitrogen acquisition. *Biol. Fertil. Soils* **2025**, *61*, 1129–1144. [CrossRef]

Disclaimer/Publisher's Note: The statements, opinions and data contained in all publications are solely those of the individual author(s) and contributor(s) and not of MDPI and/or the editor(s). MDPI and/or the editor(s) disclaim responsibility for any injury to people or property resulting from any ideas, methods, instructions or products referred to in the content.

agronomy

MDPI

Article

Variation and Trade-Offs in Leaf and Root Traits of Perennial Grasses Under Nitrogen Deposition

Yuheng Yang [1], Hao Chen [1], Guiling Liu [1], Hang Ruan [1] and Xiaowei Wei [2,*]

[1] Jilin Provincial Key Laboratory of Tree and Grass Genetics and Breeding, College of Forestry and Grassland Science, Jilin Agricultural University, Changchun 130118, China; yangyh@jlau.edu.cn (Y.Y.); chenhao0226@yeah.net (H.C.); 18586488996@163.com (G.L.); ruanh951@nenu.edu.cn (H.R.)

[2] Jilin Provincial Key Laboratory for Plant Resources Science and Green Production, Jilin Normal University, Siping 136000, China

* Correspondence: weixiaowei@jlnu.edu.cn

Abstract

Atmospheric nitrogen deposition is increasing globally, making it essential to understand how leaf and root traits vary and interact to shape plant ecological strategies under changing environmental conditions. We conducted leaf and root traits of eight perennial grasses (rhizomatous and bunchgrass species) in a field experiment conducted in the Songnen grassland, incorporating control and nitrogen addition treatments (10 g m^{-2} yr^{-1}). Nitrogen addition significantly altered leaf and root trait expression and promoted biomass accumulation in both life forms. Specifically, nitrogen addition increased assimilation rate (An; 19.4 and 20.7%), leaf nitrogen content (LNC; 51.5 and 57.8%), specific root length (SRL; 30.1 and 41.1%), and root nitrogen content (RNC; 18.6 and 34.4%), while markedly reducing root tissue density (RTD; 40.2 and 46.6%) of perennial rhizome grass and perennial bunchgrasses. Principal component analysis revealed multiple plant resource strategies reflected by multidimensional variation in leaf and root traits. However, no consistent correlations were detected between leaf and root trait dimensions, and regression relationships differed significantly under nitrogen addition. These results indicate a decoupling of above- and belowground resource acquisition strategies at the local scale. Additionally, we underscore the importance of combining above- and belowground traits to improve predictions of plant performance. Our findings advance understanding of leaf–root trait coordination in perennial grasses and provide insights into plant adaptive strategies in arid and semi-arid regions' grassland ecosystems experiencing increasing nitrogen deposition.

Keywords: leaf economics spectrum; root economics spectrum; leaf-root coordination; nitrogen addition

1. Introduction

Rapid industrialization, agricultural intensification, and urban expansion have made North America, Europe, and East Asia global hotspots of nitrogen deposition [1]. Excess nitrogen inputs can enrich soils beyond optimal levels, alter nitrogen cycling and availability, and reshape ecosystem nitrogen-use strategies, which can influence plant ecological strategies and responses to nitrogen addition in grassland ecosystems [2]. Plant functional traits are measurable characteristics that reflect long-term responses and adaptations to environmental conditions. They provide a powerful framework for linking environmental change to plant performance and community dynamics. Trade-offs among traits capture

fundamental growth, survival strategies, and how plants adjust resource use under changing environments [3]. Examining coordinated variation in leaf and root traits across plant functional types is therefore critical for predicting the consequences of nitrogen deposition for community assembly and ecosystem functioning [4].

Economic theory has been widely applied in plant ecology to quantify relationships among functional traits associated with resource allocation. The leaf economics spectrum (LES) describes coordinated trade-offs among leaf traits along a gradient from fast to slow returns on resource investment [5]. Resource-acquisitive species typically exhibit high leaf nitrogen content and photosynthetic capacity, but low leaf mass per area (LMA; i.e., high specific leaf area, SLA) and short leaf lifespans [6,7]. In contrast, the root economics spectrum (RES) is increasingly recognized as multidimensional and more complex than the LES [8]. One RES dimension reflects a trade-off between resource acquisition and conservation, driven by a negative relationship between RTD and RNC. A second dimension represents a collaboration gradient, characterized by a negative relationship between SRL and RD, reflecting a shift in resource foraging from the root itself, from a "do-it-yourself" strategy to an "outsourcing" strategy with mycorrhizal fungi [9].

The plant economics spectrum (PES) hypothesis further implies that traits across leaves, stems, and roots are coordinated along a common economic strategy, forming an integrated spectrum from acquisitive to conservative strategies at the whole-plant level. Empirical studies have supported this framework, reporting strong coordination between LES and RES [10]. However, growing evidence suggests that leaf–root trait relationships are context dependent and may weaken or decouple under certain environmental conditions [11]. For instance, Delpiano et al. (2020) demonstrated that spatial and temporal variation in soil nutrient availability can decouple leaf and root traits in desert shrub communities [12]. These contrasting findings highlight ongoing uncertainty regarding the mechanisms governing coordinated variation between leaf and root traits, particularly under global change drivers such as nitrogen deposition.

Global atmospheric nitrogen deposition has increased rapidly, profoundly influencing plant growth and resource-use strategies in terrestrial ecosystems. Plant biomass is widely regarded as a key integrative indicator of plant performance and ecosystem functioning, reflecting the cumulative outcomes of resource acquisition, allocation, and growth strategies. Prior research has reported that alterations in nutrient availability, particularly nitrogen enrichment, can substantially alter both aboveground and belowground biomass, thereby reshaping plant competitive hierarchies and community structure [13,14]. Increasing evidence suggests that biomass responses to nitrogen deposition are driven by coordinated shifts in functional traits rather than by individual traits alone. However, how trait-mediated biomass allocation patterns emerge across plant organs under sustained nitrogen deposition remains poorly understood.

Experimental nitrogen addition studies in temperate regions show that increased nitrogen availability enhances plant nitrogen uptake and leaf nitrogen concentration [15]. However, nitrogen enrichment can also exacerbate phosphorus limitation, potentially shifting plants toward more conservative survival strategies [16]. In contrast, other studies report increases in SLA under nitrogen deposition, suggesting a shift toward faster growth and more acquisitive strategies [17]. These contrasting responses indicate that plant functional trait responses to nitrogen deposition are context-dependent and illustrate the trade-offs involved in acquiring and conserving resources. While leaf trait responses to nitrogen deposition have been widely documented, root traits—and their integration with leaf traits—remain comparatively understudied. Existing evidence indicates that root responses to nitrogen enrichment are diverse. A meta-analysis synthesizing 15 root traits showed that nitrogen addition had limited impacts on root morphology but significantly

increased root biomass (RB) and RNC [18]. Similarly, nitrogen addition has been shown to increase SRL and RNC while reducing RTD and root diameter (RD) in temperate grassland species. Other studies suggest that nitrogen deposition may favor species with acquisitive belowground foraging strategies by increasing SRL, RTD, and RD [19]. Because plant functional traits do not vary independently but covary through allocation trade-offs among competing demands, understanding how leaf and root traits jointly respond to nitrogen deposition is essential for predicting shifts in whole-plant ecological strategies. However, it remains unclear whether increasing nitrogen deposition promotes coordinated variation between leaf and root traits.

The northern grasslands of China constitute the country's second-largest grassland region and provide multiple essential ecosystem services. Within this region, the Songnen grassland, a typical agropastoral ecotone and representative meadow steppe, is highly productive despite harsh soil and climatic conditions, making it particularly sensitive to global environmental change. Perennial grasses dominate the Songnen grassland at the eastern edge of the Eurasian continent and contribute disproportionately to ecosystem productivity. Here, we focus on eight perennial grass species representing two life forms (perennial rhizome grass and perennial bunchgrasses) to examine how nitrogen deposition influences coordinated variation between leaf and root functional traits. Specifically, this study addresses two key questions: (1) how leaf and root traits of different perennial grasses respond to nitrogen deposition; and (2) whether nitrogen enrichment alters the degree of coupling between leaf and root traits. By integrating responses of both above- and belowground traits, this work enhances our understanding of plant strategy trade-offs and offers new perspectives on plant adaptation and ecosystem functioning under increasing nitrogen inputs.

2. Materials and Methods

2.1. Site Description

The study was conducted at the Jilin Songnen Grassland Ecosystem National Field Scientific Observation and Research Station in Changling County, Jilin Province (44°30′–44°45′ N, 123°31′–123°56′ E), on the eastern margin of the Eurasian steppe. The area experiences a temperate monsoon climate, ranging from semi-arid to semi-humid, at elevations of 140–160 m. Mean annual temperature is 4.6–6.4 °C, and annual precipitation averages ~470 mm. Soils are primarily chernozem and meadow types, with surface layer (0–20 cm) characteristics summarized in Table 1.

Table 1. Chemical and physical properties of the basic soil.

Soil Properties	Soil pH	Total Nitrogen ($g \cdot kg^{-1}$)	Total Carbon ($g \cdot kg^{-1}$)	Total Phosphorus ($g \cdot kg^{-1}$)	Soil EC ($\mu S \cdot cm^{-1}$)
Content	8.12	0.08	0.89	0.47	136.13

Meadow steppe is the predominant grassland type in the Songnen Grassland, mainly composed of meso-xerophytic perennial rhizome grass and perennial bunchgrasses. *Leymus chinensis* is the dominant and constructive species. Other associated plant species include *Phragmites australis*, *Puccinellia tenuiflora*, *Kalimeris integrifolia*, *Artemisia anethifolia*, and *Kochia sieversiana*.

In this study, eight perennial grass species from the Songnen Grassland were selected, including four perennial rhizome grasses and four perennial bunchgrasses, representing a total of six genera. Detailed information on each plant species is provided in Table 2.

https://doi.org/10.3390/agronomy16070739

Table 2. Information on the grasses in this study.

Life Form	Genera	Plant Species
PR	Agropyron	*Agropyron michnoi* Roshev. (Gramineae)
	Leymus	*Leymus chinensis* (Trin.) Tzvel.
	Leymus	*Leymus secalinus* (Georgi) Tzvel.
	Phragmites	*Phragmites australis* (Cav.) Trin. ex Steud.
PB	Achnatherum	*Achnatherum splendens* (Trin.) Nevski
	Elymus	*Elymus dahuricus* Turcz.
	Puccinellia	*Puccinellia chinampoensis* Ohwi
	Puccinellia	*Puccinellia tenuiflora* (Griseb.) Scribn. et Merr.

Note: perennial rhizome grass (PR), perennial bunchgrasses (PB).

According to earlier research findings, in the northern temperate grassland ecosystem, the rate of nitrogen deposition is approximately 10.5 g m^{-2} yr^{-1}. Therefore, a completely randomized design was employed with two nitrogen addition levels (N0: 0 g m^{-2} yr^{-1} and N10: 10 g m^{-2} yr^{-1}), each replicated three times. Each plot contained only one species, resulting in a total of 48 plots (8 species × 2 nitrogen addition levels × 3 replicates). Each plot measured 2.5 m × 2.5 m, with a spacing of 0.5 m between adjacent plots and 1 m between blocks. Nitrogen was applied in the form of ammonium nitrate (NH_4NO_3) (Sinopharm Chemical Reagent Co., Ltd., Shanghai, China). Nitrogen addition was carried out once each month in mid-month from May to September. At each application, nitrogen (2 g N m^{-2}) was dissolved in 20 L of water and applied uniformly.

Seeds of the study species were collected from untreated natural meadows within the study area. Germination tests were conducted in a climate-controlled growth chamber to ensure good seed quality. The seeding rate for each plot was determined based on the germination percentage of grass seeds. After sowing, plots were irrigated once a week to ensure seedling emergence. Following emergence, weeds were regularly removed. Plant growth relied primarily on natural precipitation, with supplemental watering provided during periods of low rainfall to ensure normal plant growth.

2.2. Sample Collection and Determination

At the peak of the growing season, five individuals were randomly selected from each plot. An was measured on the second and third fully expanded leaves from the apex using a CIRAS-3 portable photosynthesis system. (PP Systems, Amesbury, MA, USA). Conditions were controlled at a leaf chamber temperature of 25 °C. The concentration of CO_2 was the same as the CO_2 concentration in the atmosphere under natural conditions and a 500 μmol s^{-1} flow rate. Photosynthetic photon flux density (PPFD) was set to 1600 μmol m^{-2} s^{-1} (90% red, 5% blue, 5% white), with relative humidity maintained at 65%. After measurement, leaves were immediately sealed in plastic bags containing moist filter paper and transported to the laboratory at 4 °C. Surface moisture was removed prior to recording fresh mass (FM). Leaf area (LA) was determined using a portable scanner (AM-350, ADC Bioscientific Ltd., London, UK), followed by oven-drying at 65 °C for 48 h to obtain dry mass (DM).

At the end of the growing season, a 0.5 m × 0.5 m quadrat was randomly placed within each plot, and all aboveground plants within the quadrat were harvested. Following oven-drying at 65 °C (~48 h) to constant mass, samples were ground (MM 400, Retsch, Haan, Germany) and screened through a 100-mesh sieve. Leaf carbon content (LCC) and leaf nitrogen content (LNC) were determined using a stable isotope analyzer (vario EL

https://doi.org/10.3390/agronomy16070739

cube, Elementar, Langenselbold, Germany). Specific leaf area (SLA, $m^2\ g^{-1}$) and leaf dry matter content (LDMC, %) were calculated using standard formulas:

$$\text{SLA} = \frac{\text{Leaf area}}{\text{Leaf dry mass}} \quad (1)$$

$$\text{LDMC} = \frac{\text{Leaf dry mass}}{\text{Leaf fresh mass}} \times 100\% \quad (2)$$

At the end of the growing season, belowground plant parts were sampled using the diagonal sampling method. In each plot, soil cores (0–30 cm depth) were obtained with an 11 cm diameter root auger. The collected material consisted of fine roots. For perennial rhizomatous grasses, both roots and rhizomes were present; however, rhizomes were excluded from subsequent analyses. Samples were rinsed with water using mesh bags and transported to the laboratory under refrigerated conditions (4 °C). In the laboratory, roots were gently washed, spread evenly in a root scanning tray, and analyzed using an Epson Perfection scanner coupled with WinRHIZO Pro 2012 software to determine root length (RL), root diameter (RD), and root volume (RV). Following scanning, root samples were oven-dried at 65 °C for approximately 48 h to a constant mass and weighed to obtain dry mass (DM). Root carbon (RCC) and nitrogen content (RNC) were measured following the same procedure used for leaf samples. Specific root length (SRL, $m\ g^{-1}$) and root tissue density (RTD, $g\ cm^{-3}$) were calculated using standard formulas:

$$\text{SRL} = \frac{\text{Root length}}{\text{Root dry mass}} \quad (3)$$

$$\text{RTD} = \frac{\text{Root dry mass}}{\text{Root volume}} \quad (4)$$

During the peak of the growing season, plant biomass was also sampled. A 0.25 m^2 (0.5 m × 0.5 m) quadrat was randomly placed within each plot. Aboveground biomass within the quadrat was collected by clipping, while belowground biomass was sampled using the root auger method. All harvested plant materials were transported to the laboratory. Above- and belowground components were separated, oven-dried at 65 °C (~48 h) to constant mass, and weighed. Total biomass was calculated as the sum of both fractions for each treatment.

2.3. Statistical Analysis

Data processing and statistical analyses were performed using the R software (R version 4.5.2). First, the normality of all variables was tested using the Kolmogorov–Smirnov test, followed by a test for homogeneity of variances. Two-way analysis of variance (ANOVA) was performed to test the effects of nitrogen addition, life form, and their interaction on leaf traits, root traits, and biomass. Independent-samples t-tests were applied to analyze the effects of nitrogen addition on leaf traits, root traits, and biomass under perennial rhizome grass and perennial bunchgrasses. Principal component analysis (PCA) was conducted to evaluate leaf and root traits of different grass species under the two treatments. Standardized major axis (SMA) regression was used to analyze the relationships between leaf and root traits.

3. Results

3.1. Influence of Nitrogen Addition on Leaf Traits

Two-way ANOVA demonstrated that nitrogen addition had highly significant impacts on An and LNC, while life form had a strong influence on LA. No significant interaction

https://doi.org/10.3390/agronomy16070739

between nitrogen addition and life form was detected for any leaf functional trait (Table 3). Nitrogen addition significantly increased An and LNC in both perennial rhizome grass and perennial bunchgrasses, 19.4–20.7% and 51.5–57.8% higher than the control treatment, respectively (Figure 1d,e; $p < 0.05$). By contrast, nitrogen addition did not produce a statistically significant impact on the remaining leaf functional traits, although an overall increasing trend was observed (Figure 1a–c,f; $p > 0.05$).

Table 3. Results (F-values) of two-way ANOVAs on the effects of nitrogen addition (N) and life form (L) on leaf traits.

Leaf Traits	N	L	N × L
LA	0.248	**15.424** ***	0.178
SLA	0.869	2.821	1.327
LDMC	0.077	1.208	1.004
An	**29.353** ***	1.245	0.003
LNC	**42.500** ***	1.839	0.000
LCC	0.612	1.655	1.132

Note: * denotes significant difference at $p < 0.05$; ** denotes significant difference at $p < 0.01$; *** denotes significant difference at $p < 0.001$.

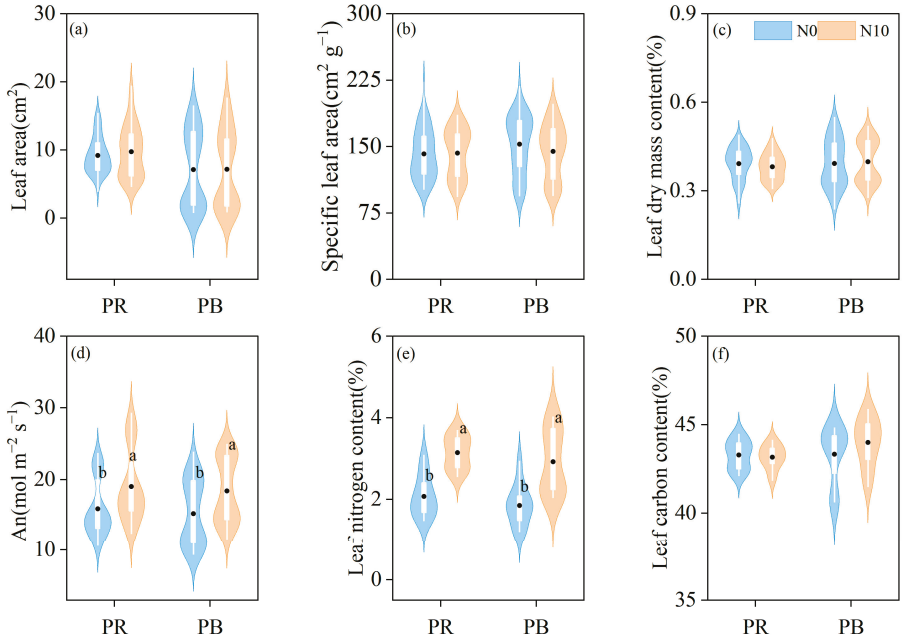


Figure 1. Effect of nitrogen addition on leaf traits. PR: perennial rhizome grass; PB: perennial bunchgrasses. The violin plot where the black pot, white box and white lines display the median, interquartile range, whiskers (upper/lower limits), respectively (**a**–**f**). Statistically significant differences between treatments are indicated by different lowercase letters ($p < 0.05$; $n = 12$).

3.2. Influence of Nitrogen Addition on Root Traits

Nitrogen addition exerted significant impacts on RL, SRL, RTD, and RNC. Life form significantly influenced RL, RNC, and RCC, whereas a significant interaction between nitrogen addition and life form was observed only for RCC (Table 4). Nitrogen addition significantly reduced RL and RTD in perennial rhizome grass, with decreases of 31.7% and 40.2%, respectively (Figure 2a,d; $p < 0.05$). In perennial bunchgrasses, RTD was also markedly lower under nitrogen treatment, showing a 46.6% decline compared with the control (Figure 2d; $p < 0.05$). By contrast, SRL and RNC increased significantly under nitrogen addition in both life forms, with values 30.1–41.1% and 18.6–34.4% higher than those of the control, respectively (Figure 2b,e; $p < 0.05$). Additionally, RCC was significantly

enhanced in perennial bunchgrasses (Figure 2f; $p < 0.05$). No significant effect of nitrogen addition on RD was detected in either perennial rhizome grass or perennial bunchgrasses (Figure 2c; $p > 0.05$).

Table 4. Results (F-values) of two-way ANOVAs on the effects of nitrogen addition (N) and life form (L) on root traits.

Leaf Traits	N	L	N × L
RL	**7.717** **	**4.239** *	0.383
SRL	**20.593** ***	0.211	0.444
RD	1.395	1.626	0.132
RTD	**36.063** ***	0.240	1.104
RNC	**29.580** ***	**34.569** ***	0.706
RCC	0.974	**4.144** *	**9.996** **

Note: * denotes significant difference at $p < 0.05$; ** denotes significant difference at $p < 0.01$; *** denotes significant difference at $p < 0.001$.

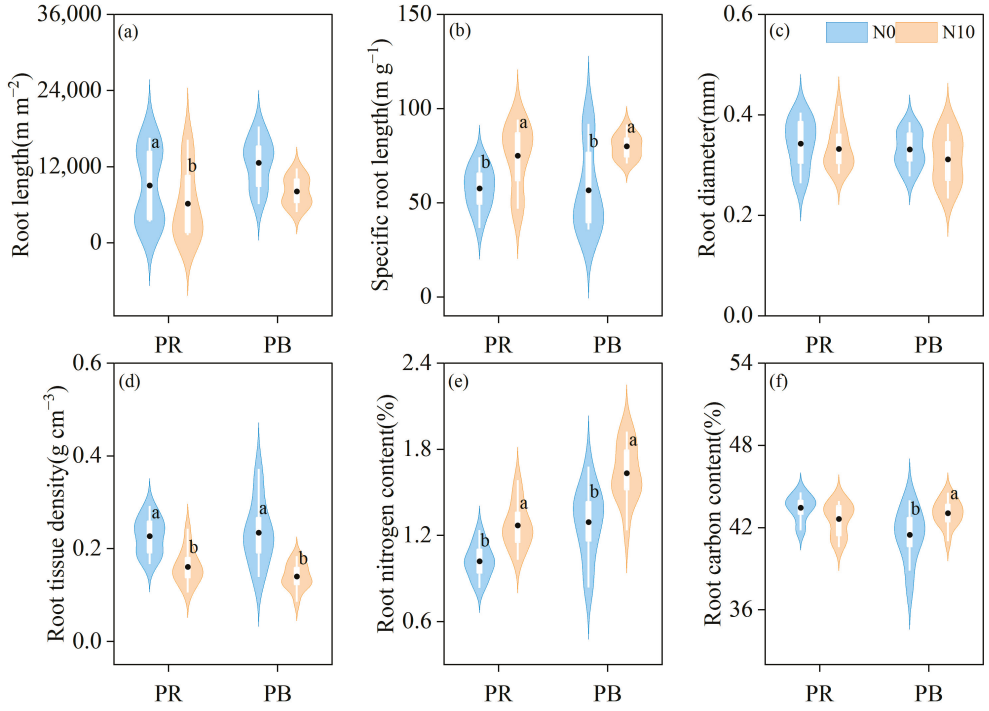


Figure 2. Effect of nitrogen addition on root traits. PR: perennial rhizome grass, PB: perennial bunchgrasses. The violin plot where the black pot, white box and white lines display the median, interquartile range, whiskers (upper/lower limits), respectively (**a**–**f**). Statistically significant differences between treatments are indicated by different lowercase letters ($p < 0.05$; $n = 12$).

3.3. Influence of Nitrogen Addition on Biomass

Nitrogen addition and life form both had highly significant impacts on aboveground, belowground, and total biomass, while the interaction between the two significantly affected only BGB (Table 5). Nitrogen addition significantly increased aboveground and total biomass in both perennial rhizome grass and perennial bunchgrasses, 44.6–48.4% and 26.4–44.2% higher than the control treatment, respectively (Figure 3a,c; $p < 0.05$). Relative to the control, the BGB increased by 43.7% only in perennial rhizome grass under nitrogen treatment (Figure 3b; $p < 0.05$).

Table 5. Results (F-values) of two-way ANOVAs on the effects of nitrogen addition (N) and life form (L) on biomass.

Leaf Traits	N	L	N × L
AGB	**12.079** **	**42.334** ***	1.228
BGB	**9.395** **	**45.158** ***	**6.377** *
TB	**13.954** **	**55.039** ***	3.468

Note: * denotes significant difference at $p < 0.05$; ** denotes significant difference at $p < 0.01$; *** denotes significant difference at $p < 0.001$.

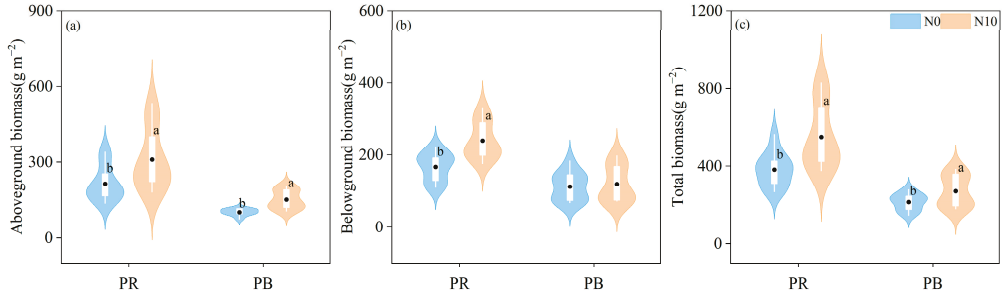


Figure 3. Effect of nitrogen addition on biomass. PR: perennial rhizome grass; PB: perennial bunchgrasses. The violin plot where the black pot, white box and white lines display the median, interquartile range, whiskers (upper/lower limits), respectively (**a**–**c**). Statistically significant differences between treatments are indicated by different lowercase letters ($p < 0.05$; $n = 12$).

3.4. The Relationship Between Leaf and Root Traits Responses to Nitrogen Addition

Principal component analysis revealed the resource acquisition strategies of different grass species under nitrogen addition (Figure 4). LPC1 is primarily determined by LA, An, and LNC, explaining 43.4% and 49.3% of the variation under control and nitrogen treatments, respectively (Figure 4a,b, Table S1). LPC2 is mainly determined by leaf coordination traits (SLA, LDMC), explaining 28.0% and 23.8% of the variation under control and nitrogen treatments, respectively (Figure 4a,b, Table S1). These results suggest that LPC1 represents the gradient of leaf resource acquisition, while LPC2 primarily reflects the gradient of leaf resource conservation.

In contrast to leaf traits, root traits exhibited more complex and multidimensional characteristics. RPC1 is determined by RD, SRL, and RL (Figure 4c,d, Table S1), representing a cooperative gradient of resource acquisition. It reflects as an axis associated with variation in root morphological traits related to potential resource acquisition strategies, explaining 36.1% and 43.5% of the variation under control and nitrogen treatments, respectively (Figure 4c,d). RPC2 is determined by RL, RTD, and RNC (Figure 4c,d, Table S1) and represents the root conservation gradient. It explains 25.3% and 23.5% of the variation under control and nitrogen treatments, respectively (Figure 4c,d).

The analysis of the relationship between leaf and root trait dimensions revealed no general significant correlations. However, nitrogen addition induced a directional shift in these associations (Figure 5, Table S3). Under control treatment, RPC1 was significantly correlated with LPC1 (Figure 5a, Table S2). Under nitrogen addition, only LPC1 showed significant correlations with RPC2 (Figure 5b, Table S2). These findings suggest that leaf and root trait dimensions are not significantly correlated, indicating a decoupling between above- and belowground resource acquisition strategies. Furthermore, nitrogen addition may lead to variations in this decoupling pattern.

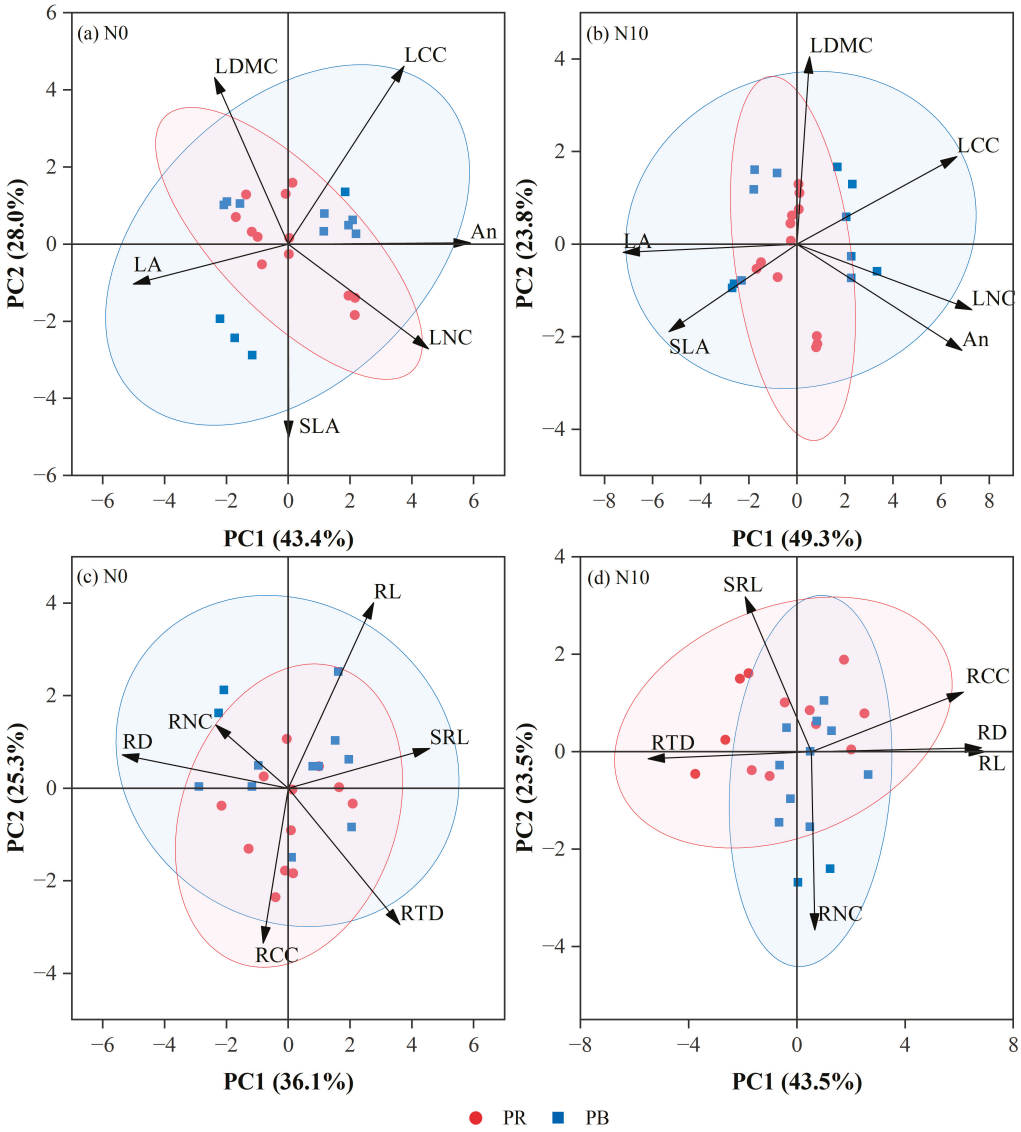


Figure 4. Principal component analysis (PCA) of leaf and root functional traits. In the (**a**–**d**), the red circles and blue squares represent different sample points, which indicate the positions of the samples in the principal component space. Leaf traits: leaf area (LA), specific leaf area (SLA), assimilation ability (An), leaf nitrogen content (LNC), leaf carbon content (LCC). Root traits: root length (RL), specific leaf area (SRL), root diameter (RD), root tissue density (RTD), root nitrogen content (RNC), root carbon content (RCC).

3.5. The Relationship Between Leaf and Root Traits and Biomass Responses to Nitrogen Addition

The Mantel test results showed significant correlations between aboveground, belowground, and total biomass with leaf and root traits (Figure 6). Notably, root traits related to plant growth, such as RL, were significantly correlated with AGB, while leaf traits associated with carbon acquisition strategy and growth rate, such as LDMC and LLNC, were significantly correlated with BGB. Additionally, root traits related to resource acquisition, such as RD, were significantly correlated with aboveground, belowground, and total biomass.

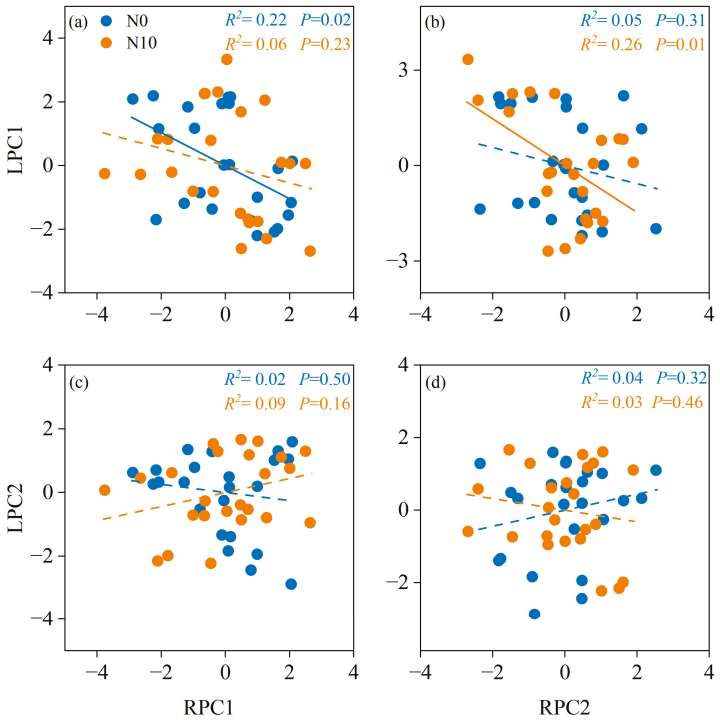


Figure 5. Correlations between multiple leaf and root trait dimensions under nitrogen treatment. The blue and orange circles respectively represent N0 (control) and N10 (nitrogen addition). Solid lines show linear relationships when $p < 0.05$. LPC1 and LPC2, the scores of the first two axes from LPCA (PCA axis for leaf traits), represent the leaf conservation and acquisitive gradient, respectively (**a**–**d**); RPC1 and RPC2, the scores of the first two axes from RPCA (PCA axis for root traits), represent the root collaboration and conservation gradients, respectively.

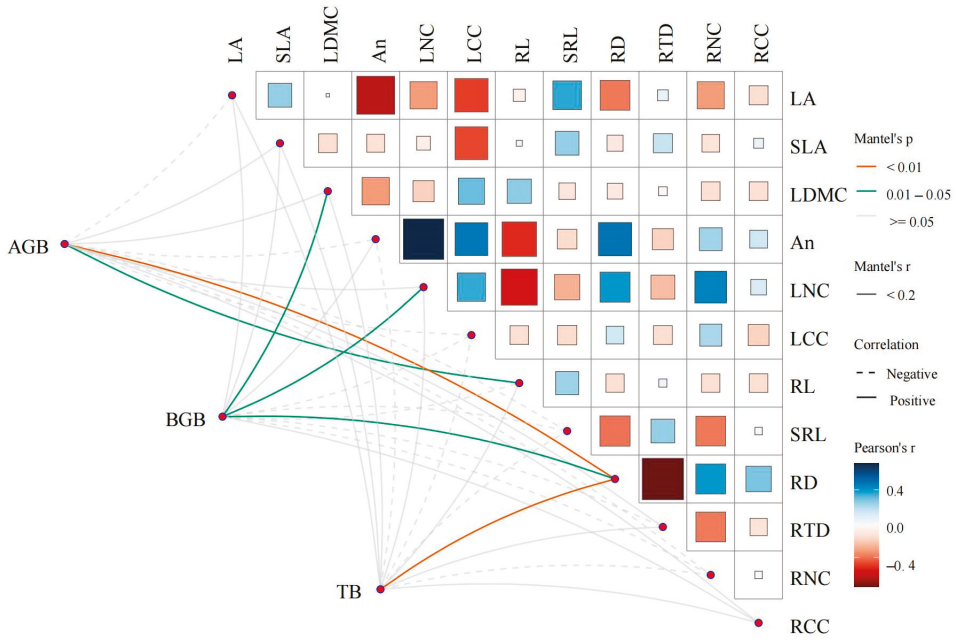


Figure 6. The Mantel test for the relationship between the composition of AGB (aboveground biomass), BGB (belowground biomass), TB (total biomass), and leaf, root traits. Leaf traits: leaf area (LA), specific leaf area (SLA), assimilation ability (An), leaf nitrogen content (LNC), leaf carbon content (LCC). Root traits: root length (RL), specific leaf area (SRL), root diameter (RD), root tissue density (RTD), root nitrogen content (RNC), root carbon content (RCC). The edge width and color represent Mantel's r statistic and statistical significance based on permutations, respectively.

https://doi.org/10.3390/agronomy16070739

4. Discussion

4.1. The Variation in Leaf and Root Traits Under Nitrogen Addition

Plants respond to environmental disturbances by modifying their functional traits, allowing them to adjust to shifting conditions. Leaves, as the primary organs of photosynthesis, are also among the most environmentally sensitive plant organs. Leaf traits are closely linked to resource acquisition and plant adaptation strategies, representing key trade-offs between carbon gain and its subsequent use, which contribute to overall functional optimization. Our results showed that nitrogen addition significantly increased An and LNC in both perennial grass species, whereas other leaf traits remained largely unchanged (Figure 1). These findings are consistent with previous studies [20,21], which have demonstrated that nitrogen inputs enhance assimilation ability and leaf nitrogen content. This response is largely attributed to increased aboveground productivity and enhanced light interception resulting from greater canopy cover under nitrogen enrichment [22]. The absence of significant changes in other leaf traits may be explained by several underlying factors. As soil nitrogen availability increases, nitrogen is no longer a limiting factor for plant growth [23–25]. Under such conditions, nitrogen addition is more likely to promote plant growth by enhancing carbon assimilation capacity rather than inducing changes in leaf morphological plasticity.

Roots are the primary organs responsible for water and nutrient uptake, and root traits are key determinants of the ability to acquire soil resources. In this study, nitrogen addition significantly reduced RL in perennial rhizome grass (Figure 2a), while significantly increasing SRL in both perennial grass (Figure 2b). This pattern suggests a lower construction cost per unit root length, thereby enabling more efficient nutrient uptake from the soil [26]. Perennial grasses exhibit two distinct clonal growth strategies. Perennial rhizome grass mainly relies on rhizomes for vegetative reproduction; under nitrogen addition, sufficient nitrogen can be acquired with a shorter root system, thereby reducing carbon investment in roots and allowing greater allocation of carbon to rhizome spatial expansion. In contrast, perennial bunchgrasses also reproduce vegetatively but tend to allocate more carbon to sustain plant growth, resulting in increased SRL. Root tissue density, defined as the ratio of root dry mass to root volume, reflects biomass investment per unit root length and is closely associated with plant growth, defense capacity, and lifespan. Species with higher RTD typically possess a greater proportion of thick-walled tissues, enabling slower growth under stressful environmental conditions. RTD is generally higher in nutrient-poor soils, and previous studies have shown that it decreases with increasing nutrient availability [27]. Our results support this pattern, as nitrogen addition significantly reduced root tissue density (Figure 2d). RNC is an important indicator of fine-root physiological activity. In this study, nitrogen addition significantly increased RNC in both perennial grass species (Figure 2e), indicating enhanced nitrogen uptake and greater allocation of nitrogen to belowground tissues, thereby promoting root growth.

In summary, nitrogen addition primarily enhanced plant growth by increasing carbon assimilation efficiency, as evidenced by higher assimilation ability and leaf nitrogen content, rather than altering leaf morphological traits. For root traits, nitrogen enrichment reduced root construction costs and increased root physiological activity, reflected by higher SRL, lower RTD, and elevated RNC, thereby improving nutrient uptake efficiency. These leaf and root trait responses indicate that nitrogen addition shifts plant strategies toward more efficient resource acquisition and utilization, with life-form-specific adjustments in carbon allocation and growth pathways.

https://doi.org/10.3390/agronomy16070739

4.2. The Trait Dimensions and Correlations Under Nitrogen Addition

Identifying the principal dimensions of variation in leaf and root traits is essential for evaluating above- and belowground processes and plant functioning. Our results show that under nitrogen addition, the first leaf principal component (LPC1) was primarily determined by LA, An, and LNC, whereas LPC2 was mainly driven by leaf coordination traits, including SLA and LDMC. This pattern corresponds to the leaf economics spectrum, with one end representing a resource-acquisitive strategy and the other representing a resource-conservative strategy. Notably, the axis distinguishing conservative traits from economic trait variation is consistent with patterns previously reported at global [28,29], regional scales [30], and interspecific [28–30].

For root traits, RD and SRL defined PC1, whereas PC2 was mainly driven by RTD, RL, and RNC, indicating a two-dimensional structure of the RES. Within the broader RES framework [9], the first axis represents a trade-off between SRL and RD, corresponding to a collaboration gradient that ranges from "do-it-yourself" strategies (characterized by high SRL and low RD) to "outsourcing" strategies (low SRL and high RD). Our findings are consistent with findings reported across both regional [31,32] and global studies [9,33,34]. The second dimension captures a trade-off between fast and slow resource returns, commonly referred to as the root conservation gradient [9]. RNC as an indicator of nutrient concentration and metabolic activity, whereas RTD reflects carbon investment per unit volume. Along this gradient, acquisitive roots typically exhibit high RNC and low RTD, while conservative roots display the opposite pattern, with higher RTD and lower RNC. Overall, the multidimensional variation observed in both leaf and root traits underscores the diversity of plant ecological strategies and suggests that such trait combinations enable plants to flexibly respond to complex and heterogeneous environmental conditions [11].

Understanding the coordination between leaf and root traits is critical for elucidating whole-plant ecological strategies. Growing evidence suggests that there are broadly coordinated economics between plant above- and belowground organs at the interspecies level [34–36]. However, in contrast to previous studies, our study found that these relationships are not always apparent (Figure 5). This discrepancy may be explained by at least two factors. First, environmental drivers may exert differential influences on leaf versus root traits. Our results fully support this view that the magnitude of trait variation between corresponding leaf and root traits is not consistent under N addition. Plant organs may exhibit contrasting responses to the same environmental pressures, potentially resulting in a decoupling of resource-use strategies between leaves and roots [37]. In addition, belowground organs operate in more complex environments, as soil conditions with biotic (e.g., microbial communities) and abiotic (e.g., physicochemical properties) may differ fundamentally from those aboveground [38]. These differences can drive divergence in resource acquisition strategies between roots and leaves [9,37]. Second, the degree of leaf–root trait coordination may depend on spatial scale. Previous studies have shown that the strength of correlations between leaf and root traits can vary with spatial scale and even disappear at smaller scales [39]. For example, Liu found that leaf and root economics were coordinated at the regional scale [40]; however, such coordination was absent at the local scale [39,41], likely due to the relatively low environmental heterogeneity at smaller spatial extents. Overall, these two factors may explain the decoupling of intraspecific leaf and root traits. Lastly, we also considered an early-stage response to nitrogen addition. Leaves, which generally respond more rapidly to nutrient addition, exhibited increased An and LNC, whereas root traits showed more complex and sometimes delayed responses. This difference in response timing could lead to decoupling in a short-term N addition. Future multi-year experiments would help determine whether these decoupling patterns persist, diminish, or shift under prolonged nitrogen addition.

https://doi.org/10.3390/agronomy16070739

Although the relationship between leaf and root trait dimensions revealed no general significant correlations, nitrogen addition induced a directional shift in these associations (Figure 5, Table S3). In our study, nitrogen addition significantly increased An and LNC, and root traits also showed substantial changes, including increased SRL and reduced RTD (Figures 1 and 2). This suggests that leaf traits were mainly associated with photosynthetic capacity and nutrient acquisition, whereas root traits reflected soil resource foraging and structural investment. In addition, leaf and root traits may be organized along different multidimensional axes. Leaf traits were primarily structured along resource acquisition and conservation gradients, whereas root traits exhibited more complex and multidimensional variation. Such differences may alter the direction of the relationship between leaf root traits, highlighting the dynamic nature of plant resource-use strategies under nitrogen addition.

4.3. The Trait–Performance Relationships Under Nitrogen Addition

Nitrogen addition significantly promoted both aboveground and belowground biomass accumulation in perennial rhizome grass (Figure 3a,b), resulting in a marked increase in total biomass (Figure 3c). In this life form, biomass accumulation in above- and belowground organs is governed by trade-offs between carbon assimilation and nutrient uptake [42]. Perennial rhizome grass primarily relies on aboveground tissues for carbohydrate synthesis and energy conversion, while belowground tissues function in mineral nutrient and water absorption as well as vegetative reproduction. Consequently, nitrogen addition provides sufficient nutrients for perennial rhizome grass, thereby stimulating biomass accumulation across plant organs. Nitrogen addition significantly increased aboveground and total biomass in perennial bunchgrasses, but had no significant effect on belowground biomass (Figure 3). This pattern suggests that perennial bunchgrasses are no longer limited by nutrient availability under nitrogen-enriched conditions; instead, their growth is primarily constrained by photosynthetic capacity. As a result, these species enhance leaf biomass investment to enhance light acquisition and photosynthetic performance, thereby increasing overall biomass production.

Plant functional traits are widely recognized as expressions of ecological strategies, and accumulating evidence indicates that variation in plant biomass is closely linked to adaptive shifts in these traits [43]. Our results show significant coupling across plant organs, indicating that variation in aboveground, belowground, and total biomass is structured by coordinated leaf and root strategies. Notably, traits traditionally associated with belowground foraging and growth (e.g., RL) were most strongly linked to aboveground biomass, whereas leaf economic traits associated with carbon acquisition strategy and growth rates (e.g., LDMC and LNC) were most strongly linked to belowground biomass. In addition, root diameter—often interpreted as a key axis of belowground resource acquisition and transport—was significantly correlated with aboveground, belowground, and total biomass, suggesting whole-plant integration in which belowground structural investment covaries with overall plant size or performance (Figure 6).

Leaf traits associated with acquisitive strategies (higher leaf N and lower LDMC) were most strongly correlated with belowground biomass. One explanation is that higher photosynthetic capacity associated with leaf N increases carbon availability, permitting greater construction and maintenance of root systems [44,45]. Meanwhile, we consider increasing nitrogen availability, as acquisition of leaf traits may not only stimulate carbon assimilation but also elevate plant demand for other limiting nutrients, particularly phosphorus (P). This shift may progressively drive ecosystems from N limitation toward P limitation, thereby reinforcing belowground investment in nutrient acquisition [46,47]. A complementary explanation is that nutrient-rich leaves have higher nutrient requirements, potentially selecting for greater belowground investment to sustain N uptake (via roots and

associated symbionts) [29,48]. The positive association between root growth-related traits and aboveground biomass is consistent with the idea that shoot production is frequently constrained by belowground acquisition. Greater root length can increase the volume of soil explored and the rate at which plants encounter mobile resources and water, thereby reducing belowground limitation and allowing greater investment in leaves and stems [49]. In addition, root diameter was correlated with biomass across compartments, pointing to an integrated axis linking belowground structure with whole-plant biomass. Recent studies have revealed that with regard to root system functioning within a two-dimensional root economics spectrum, RD has been identified as a key trait, which is usually associated with mycorrhizal fungi symbiosis and metabolic activity [36,50]. Thicker roots may enhance transport capacity and persistence, and may be associated with mycorrhizal collaboration, both of which could promote sustained resource acquisition and growth across organs [51]. Overall, our findings indicate that predicting plant biomass allocation requires consideration of coordinated trait syndromes spanning leaves and roots. Therefore, the linkage between plant functional traits and biomass allocation may be inherently context-dependent, varying with background nutrient availability and soil development. Although phosphorus was not explicitly manipulated in this study, future work incorporating coupled N and P dynamics would help to further resolve these interactions.

5. Conclusions

To explore how plant functional traits and resource-use strategies respond to nitrogen deposition, we conducted a nitrogen addition experiment focusing on changes in leaf and root traits and their associated acquisition strategies. Our results demonstrate that nitrogen enrichment significantly reshaped trait expression and resource-use patterns in perennial grasses. In particular, nitrogen inputs shifted both leaf and root traits toward more acquisitive strategies, while also influencing patterns of biomass allocation. Principal component analysis revealed multiple plant resource strategies reflected by multidimensional variation in leaf and root traits. Our results indicate this pattern corresponds to the leaf economics spectrum, with one end representing a resource-acquisitive strategy and the other a resource-conservative strategy. Similarly, root traits were structured along a two-dimensional RES, characterized by conservation and collaboration gradients, consistent with previous studies. However, we observed no coordination between leaf and root trait dimensions (Figure 7). The Mantel test revealed significant associations between leaf and root traits and aboveground, belowground, and total biomass. These results indicate that variation in biomass is correlated with multidimensional leaf and root trait patterns. These findings support a multidimensional view of plant functional traits in the studied perennial grasses and provide insights into plant adaptive responses under nitrogen enrichment in the Songnen grassland. The implications of these results need to be explored through longer-term nitrogen addition experiments, along with the integration of environmental factors and larger-scale studies, in order to determine whether the observed phenomena are stable or temporary.

https://doi.org/10.3390/agronomy16070739

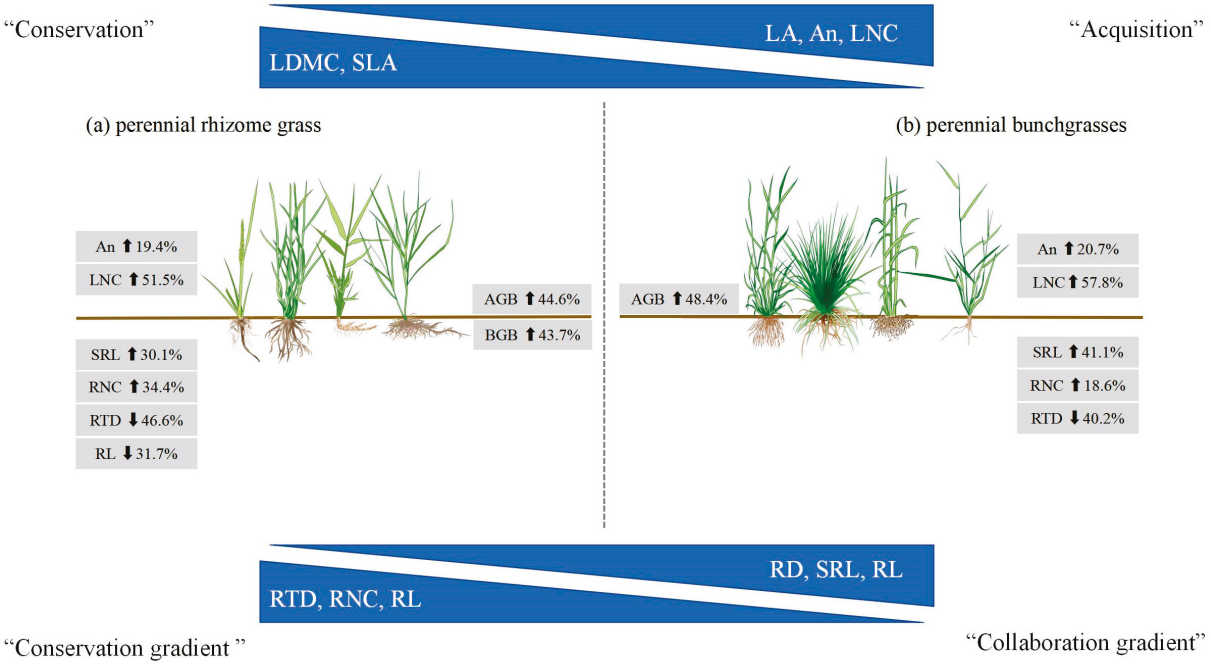


Figure 7. Conceptual framework illustrating the contrasting coordination of economics spectrums in leaves and roots. (**a**) Comparison results of trait variations in perennial rhizome grass under nitrogen treatment, (**b**) comparison results of trait variations in perennial bunchgrasses under nitrogen treatment. An upward arrow indicates an increase, while a downward arrow indicates a decrease. Abbreviation annotation: aboveground biomass (AGB), belowground biomass (BGB), assimilation ability (An), leaf nitrogen content (LNC), root length (RL), specific leaf area (SRL), root tissue density (RTD), root nitrogen content (RNC), root carbon content (RCC).

Supplementary Materials: The following supporting information can be downloaded at https://www.mdpi.com/article/10.3390/agronomy16070739/s1, Table S1. PCA loadings of the leaf, root traits. Table S2. Standardized major axis regression (SMA) analyses of the leaf traits principal component axis 1 (LPC1) and the root traits principal component axis 1 (RPC1), leaf traits principal component axis 1 (LPC1) and root traits principal component axis 2 (RPC2), leaf traits principal component axis 2 (LPC2) and root traits principal component axis 1 (RPC1), leaf traits principal component axis 2 (LPC2) and root traits principal component axis 2 (RPC2) under nitrogen addition treatments. Table S3. Standardized major axis regression (SMA) analyses of the leaf, root principal component axis (LPC1, LPC2, RPC1, RPC2, PPC1, PPC2) between N0 vs N10 treatments.

Author Contributions: Conceptualization, Y.Y. and X.W.; methodology, Y.Y.; software, H.C. and G.L.; validation, Y.Y. and H.C.; formal analysis, G.L. and H.R.; investigation, X.W.; resources, X.W.; data curation, Y.Y. and G.L.; writing—original draft preparation, Y.Y.; writing—review and editing, H.C., G.L. and H.R.; visualization, H.R.; supervision, H.C.; project administration, X.W.; funding acquisition, Y.Y., and X.W. All authors have read and agreed to the published version of the manuscript.

Funding: This research was funded by the Fundamental Research Funds for the Science and Technology Project of the Jilin Provincial Education Department (JJKH20250599KJ).

Data Availability Statement: The original contributions presented in this study are included in the article/Supplementary Materials. Further inquiries can be directed to the corresponding author.

Acknowledgments: During the preparation of this manuscript, the author used DeepSeek, v3.2, for the purposes of checking the grammar of the manuscript. The authors have reviewed and edited the output and take full responsibility for the contents of this publication.

Conflicts of Interest: The authors declare no conflicts of interest.

Abbreviations

The following abbreviations are used in this manuscript:

LA	leaf area
SLA	specific leaf area
An	assimilation ability
LNC	leaf nitrogen content
LCC	leaf carbon content
RL	root length
SRL	specific leaf area
RD	root diameter
RTD	root tissue density
RNC	root nitrogen content
RCC	root carbon content
AGB	aboveground biomass
BGB	belowground biomass
TB	total biomass

References

1. Zhu, J.; Jia, Y.; Yu, G.; Wang, Q.; He, N.; Chen, Z.; He, H.; Zhu, X.; Li, P.; Zhang, F.; et al. Changing patterns of global nitrogen deposition driven by socio-economic development. *Nat. Commun.* **2025**, *16*, 46. [CrossRef]
2. Wang, F.; Zhang, J.; Zeng, Y.; Wang, H.; Zhao, X.; Chen, Y.; Deng, H.; Ge, L.; Dahlgren, R.A.; Gao, H.; et al. Arsenic mobilization and nitrous oxide emission modulation by different nitrogen management strategies in a flooded ammonia-enriched paddy soil. *Pedosphere* **2024**, *34*, 1051–1065. [CrossRef]
3. Blumstein, M.; Sala, A.; Weston, D.J.; Holbrook, N.M.; Hopkins, R. Plant carbohydrate storage: Intra- and inter-specific trade-offs reveal a major life history trait. *New Phytol.* **2022**, *235*, 2211–2222. [CrossRef] [PubMed]
4. Peng, J.; Ma, F.; Tian, D.; Quan, Q.; Chen, C.; Liao, J.; Zhou, Q.; Niu, S. Plant C:N ratio predicts community composition changes under N addition in an alpine meadow. *J. Ecol.* **2023**, *111*, 589–600. [CrossRef]
5. Wright, I.J.; Reich, P.B.; Westoby, M.; Ackerly, D.D.; Baruch, Z.; Bongers, F.; Cavender-Bares, J.; Chapin, T.; Cornelissen, J.H.C.; Diemer, M.; et al. The worldwide leaf economics spectrum. *Nature* **2004**, *428*, 821–827. [CrossRef]
6. Zhang, P.; Ding, J.; Wang, Q.; McDowell, N.G.; Kong, D.; Tong, Y.; Yin, H. Contrasting coordination of non-structural carbohydrates with leaf and root economic strategies of alpine coniferous forests. *New Phytol.* **2024**, *243*, 580–590. [CrossRef]
7. Wang, Z.; Townsend, P.A.; Kruger, E.L. Leaf spectroscopy reveals divergent inter- and intra-species foliar trait covariation and trait-environment relationships across NEON domains. *New Phytol.* **2022**, *235*, 923–938. [CrossRef]
8. Weemstra, M.; Mommer, L.; Visser, E.J.W.; van Ruijven, J.; Kuyper, T.W.; Mohren, G.M.J.; Sterck, F.J. Towards a multidimensional root trait framework: A tree root review. *New Phytol.* **2016**, *211*, 1159–1169. [CrossRef]
9. Bergmann, J.; Weigelt, A.; van der Plas, F.; Laughlin, D.C.; Kuyper, T.W.; Guerrero-Ramirez, N.; Valverde-Barrantes, O.J.; Bruelheide, H.; Freschet, G.T.; Iversen, C.M.; et al. The fungal collaboration gradient dominates the root economics space in plants. *Sci. Adv.* **2020**, *6*, eaba3756. [CrossRef] [PubMed]
10. de La Riva, E.G.; Tosto, A.; Pérez-Ramos, I.M.; Navarro-Fernández, C.M.; Olmo, M.; Anten, N.P.; Marañón, T.; Villar, R. A plant economics spectrum in Mediterranean forests along environmental gradients: Is there coordination among leaf, stem and root traits? *J. Veg. Sci.* **2016**, *27*, 187–199. [CrossRef]
11. Sun, K.; Sun, R.; Liu, L.; Li, Y.; Zhou, G.; Xu, Z. Global coordination and trade-off of grassland species traits and climatic drivers. *J. Ecol.* **2025**, *113*, 3210–3224. [CrossRef]
12. Delpiano, C.A.; Prieto, I.; Loayza, A.P.; Carvajal, D.E.; Squeo, F.A. Different responses of leaf and root traits to changes in soil nutrient availability do not converge into a community-level plant economics spectrum. *Plant Soil* **2020**, *450*, 463–478. [CrossRef]
13. Wang, Y.; Tian, X.; Yang, C.; Guo, C.; Li, Y.; Lyu, X.; Li, N.; Guo, H. Adaptive Plasticity of Phragmites australis in Aboveground and Belowground Productivity Under Salinization and Nitrogen Enrichment. *Agronomy* **2025**, *15*, 2031. [CrossRef]
14. Yang, Z.; Minggagud, H.; Wang, Q.; Pan, H. Interacting Effects of Nitrogen Addition and Mowing on Plant Diversity and Biomass of a Typical Grassland in Inner Mongolia. *Agronomy* **2023**, *13*, 2125. [CrossRef]
15. Zhang, H.; Li, W.; Adams, H.D.; Wang, A.; Wu, J.; Jin, C.; Guan, D.; Yuan, F. Responses of Woody Plant Functional Traits to Nitrogen Addition: A Meta-Analysis of Leaf Economics, Gas Exchange, and Hydraulic Traits. *Front. Plant Sci.* **2018**, *9*, 683. [CrossRef]

16. Su, Y.; Tang, Y.; Hu, Y.; Liu, M.; Lu, X.; Duan, B. Exploring plant adaptation strategies to phosphorus limitation induced by nitrogen addition: Foliar phosphorus allocation and root functional traits analysis in two dominant subalpine tree species. *J. Plant Ecol.* **2024**, *17*, rtae060. [CrossRef]
17. Hai, X.; Shangguan, Z.; Peng, C.; Deng, L. Leaf trait responses to global change factors in terrestrial ecosystems. *Sci. Total Environ.* **2023**, *898*, 165572. [CrossRef] [PubMed]
18. Li, W.; Jin, C.; Guan, D.; Wang, Q.; Wang, A.; Yuan, F.; Wu, J. The effects of simulated nitrogen deposition on plant root traits: A meta-analysis. *Soil Biol. Biochem.* **2015**, *82*, 112–118. [CrossRef]
19. Caplan, J.S.; Stone, B.W.G.; Faillace, C.A.; Lafond, J.J.; Baumgarten, J.M.; Mozdzer, T.J.; Dighton, J.; Meiners, S.J.; Grabosky, J.C.; Ehrenfeld, J.G. Nutrient foraging strategies are associated with productivity and population growth in forest shrubs. *Ann. Bot.* **2017**, *119*, 977–988. [CrossRef] [PubMed]
20. Yu, J.; Song, Z.; Hou, J. Life form-dependent nitrogen–phosphorous allocation strategies of leaf and fine root in a temperate natural forest under long-term nitrogen addition. *J. Plant Ecol.* **2023**, *16*, rtad013. [CrossRef]
21. Shi, X.-M.; Qi, J.-H.; Liu, A.-X.; Zakari, S.; Song, L. Leaf phenotypic plasticity coupled with integration facilitates the adaptation of plants to enhanced N deposition. *Environ. Pollut.* **2023**, *327*, 121570. [CrossRef] [PubMed]
22. Ye, X.; Bu, W.; Hu, X.; Wang, F.; Sun, R.; He, P.; Liang, X.; Chen, F. Are small trees more responsive to nutrient addition than large trees in an evergreen broadleaved forest? *For. Ecol. Manag.* **2023**, *543*, 121129. [CrossRef]
23. Yu, G.; Chen, J.; Li, A.; Wang, S.; Song, L.; Shi, X.; Yan, J.; Xu, M.; Xue, Y.; Lu, X.; et al. Plant morphological and physiological traits are stable in a nitrogen-saturated tropical forest after 18-year nitrogen additions. *Plant Soil* **2025**, *514*, 1703–1716. [CrossRef]
24. Lu, X.; Vitousek, P.M.; Mao, Q.; Gilliam, F.S.; Luo, Y.; Zhou, G.; Zou, X.; Bai, E.; Scanlon, T.M.; Hou, E.; et al. Plant acclimation to long-term high nitrogen deposition in an N-rich tropical forest. *Proc. Natl. Acad. Sci. USA* **2018**, *115*, 5187–5192. [CrossRef]
25. Tian, J.; Dungait, J.A.J.; Lu, X.; Yang, Y.; Hartley, I.P.; Zhang, W.; Mo, J.; Yu, G.; Zhou, J.; Kuzyakov, Y. Long-term nitrogen addition modifies microbial composition and functions for slow carbon cycling and increased sequestration in tropical forest soil. *Glob. Change Biol.* **2019**, *25*, 3267–3281. [CrossRef]
26. Wen, Z.; Pang, J.; Tueux, G.; Liu, Y.; Shen, J.; Ryan, M.H.; Lambers, H.; Siddique, K.H.M. Contrasting patterns in biomass allocation, root morphology and mycorrhizal symbiosis for phosphorus acquisition among 20 chickpea genotypes with different amounts of rhizosheath carboxylates. *Funct. Ecol.* **2020**, *34*, 1311–1324. [CrossRef]
27. Gao, W.; Chen, D.; Hu, X.; Fang, X.; Li, Q.; Huang, Q.; Sun, F.; Zhou, J.; Bai, Y.; Zhang, J.; et al. Nitrogen deposition drives the intricate changes of fine root traits. *Glob. Ecol. Conserv.* **2023**, *43*, e02443. [CrossRef]
28. Díaz, S.; Kattge, J.; Cornelissen, J.H.C.; Wright, I.J.; Lavorel, S.; Dray, S.; Reu, B.; Kleyer, M.; Wirth, C.; Prentice, I.C.; et al. The global spectrum of plant form and function. *Nature* **2016**, *529*, 167–171. [CrossRef]
29. Joswig, J.S.; Wirth, C.; Schuman, M.C.; Kattge, J.; Reu, B.; Wright, I.J.; Sippel, S.D.; Rüger, N.; Richter, R.; Schaepman, M.E.; et al. Climatic and soil factors explain the two-dimensional spectrum of global plant trait variation. *Nat. Ecol. Evol.* **2022**, *6*, 36–50. [CrossRef]
30. Puglielli, G.; Bricca, A.; Chelli, S.; Petruzzellis, F.; Acosta, A.T.R.; Bacaro, G.; Beccari, E.; Bernardo, L.; Bonari, G.; Bolpagni, R.; et al. Intraspecific variability of leaf form and function across habitat types. *Ecol. Lett.* **2024**, *27*, e14396. [CrossRef]
31. de La Riva, E.G.; Prieto, I.; Marañón, T.; Pérez-Ramos, I.M.; Olmo, M.; Villar, R. Root economics spectrum and construction costs in Mediterranean woody plants: The role of symbiotic associations and the environment. *J. Ecol.* **2021**, *109*, 1873–1885. [CrossRef]
32. Ding, J.; Kong, D.; Zhang, Z.; Cai, Q.; Xiao, J.; Liu, Q.; Yin, H. Climate and soil nutrients differentially drive multidimensional fine root traits in ectomycorrhizal-dominated alpine coniferous forests. *J. Ecol.* **2020**, *108*, 2544–2556. [CrossRef]
33. Weigelt, A.; Mommer, L.; Andraczek, K.; Iversen, C.M.; Bergmann, J.; Bruelheide, H.; Fan, Y.; Freschet, G.T.; Guerrero-Ramírez, N.R.; Kattge, J.; et al. An integrated framework of plant form and function: The belowground perspective. *New Phytol.* **2021**, *232*, 42–59. [CrossRef]
34. Carmona, C.P.; Bueno, C.G.; Toussaint, A.; Träger, S.; Díaz, S.; Moora, M.; Munson, A.D.; Pärtel, M.; Zobel, M.; Tamme, R. Fine-root traits in the global spectrum of plant form and function. *Nature* **2021**, *597*, 683–687. [CrossRef]
35. Sanaei, A.; Andraczek, K.; Kretz, L.; Schnabel, F.; Richter, R.; Kahl, A.; Nabel, N.; von Sivers, L.; Künne, T.; van Braak, J.L.; et al. Above- and below-ground trait coordination across 90 angiosperm and gymnosperm tree species in a common garden experiment. *J. Ecol.* **2026**, *114*, e70220. [CrossRef]
36. Fan, A.; Wang, X.; Yan, X.; Chen, T.; Jiang, Q.; Jia, L.; Wang, W.; Xiong, D.; Huang, J.; Chen, G. Does a whole plant conservation gradient exist within a subtropical broadleaved evergreen forest? *Front. Plant Sci.* **2024**, *15*, 1481323. [CrossRef]
37. Laughlin, D.C.; Lusk, C.H.; Bellingham, P.J.; Burslem, D.F.R.P.; Simpson, A.H.; Kramer-Walter, K.R. Intraspecific trait variation can weaken interspecific trait correlations when assessing the whole-plant economic spectrum. *Ecol. Evol.* **2017**, *7*, 8936–8949. [CrossRef] [PubMed]
38. Mommer, L.; Weemstra, M. The role of roots in the resource economics spectrum. *New Phytol.* **2012**, *195*, 725–727. [CrossRef]
39. Fraterrigo, J.M.; Chen, W.; Loyal, J.; Euskirchen, E.S. Soil microenvironmental variation drives below-ground trait variation and interacts with macroclimate to structure above-ground trait variation of arctic shrubs. *J. Ecol.* **2024**, *112*, 901–916. [CrossRef]

40. Liu, R.; Yang, X.; Gao, R.; Huang, Z.; Cornelissen, J.H.C. Coordination of economics spectra in leaf, stem and root within the genus *Artemisia* along a large environmental gradient in China. *Glob. Ecol. Biogeogr.* **2023**, *32*, 324–338. [CrossRef]
41. Da, R.; He, H.; Zhang, Z.; Zhao, X.; von Gadow, K.; Zhang, C. Leaf and root economics space in *Fraxinus mandshurica*: A test of the multidimensional trait framework within species. *J. Ecol.* **2025**, *113*, 1004–1017. [CrossRef]
42. Zou, Y.; Li, B.; Peñuelas, J.; Sardans, J.; Yu, H.; Chen, X.; Deng, X.; Cheng, D.; Zhong, Q. Response of functional traits in *Machilus pauhoi* to nitrogen addition is influenced by differences of provenances. *For. Ecol. Manag.* **2022**, *513*, 120207. [CrossRef]
43. Li, Y.; Jiang, Y.; Zhao, K.; Chen, Y.; Wei, W.; Shipley, B.; Chu, C. Exploring trait-performance relationships of tree seedlings along experimentally manipulated light and water gradients. *Ecology* **2022**, *103*, e3703. [CrossRef]
44. Blumenthal, D.M.; Mueller, K.E.; Kray, J.A.; Ocheltree, T.W.; Augustine, D.J.; Wilcox, K.R. Traits link drought resistance with herbivore defence and plant economics in semi-arid grasslands: The central roles of phenology and leaf dry matter content. *J. Ecol.* **2020**, *108*, 2336–2351. [CrossRef]
45. Polley, H.W.; Collins, H.P.; Fay, P.A. Community leaf dry matter content predicts plant production in simple and diverse grassland. *Ecosphere* **2022**, *13*, e4076. [CrossRef]
46. Li, C.; Lu, X.; Chen, J.; Tan, Q.; Luo, G.; Wu, L.; Chen, F.; Ran, C.; Zhang, S.; Xiong, L.; et al. Silicate chemical weathering disrupts the global patterns of phosphorus limitation. *Nat. Commun.* **2025**, *16*, 10742. [CrossRef]
47. Zhao, Y.; Wang, H.; Song, B.; Xue, P.; Zhang, W.; Peth, S.; Lee Hill, R.; Horn, R. Characterizing uncertainty in process-based hydraulic modeling, exemplified in a semiarid Inner Mongolia steppe. *Geoderma* **2023**, *440*, 116713. [CrossRef]
48. Goud, E.M.; Agrawal, A.A.; Sparks, J.P. A direct comparison of ecological theories for predicting the relationship between plant traits and growth. *Ecology* **2023**, *104*, e3986. [CrossRef] [PubMed]
49. Freschet, G.T.; Pagès, L.; Iversen, C.M.; Comas, L.H.; Rewald, B.; Roumet, C.; Klimešová, J.; Zadworny, M.; Poorter, H.; Postma, J.A.; et al. A starting guide to root ecology: Strengthening ecological concepts and stand-ardising root classification, sampling, processing and trait measurements. *New Phytol.* **2021**, *232*, 973–1122. [CrossRef] [PubMed]
50. de La Riva, E.G.; Querejeta, J.I.; Villar, R.; Pérez-Ramos, I.M.; Marañón, T.; Galán Díaz, J.; de Tomás Marín, S.; Prieto, I. The Economics Spectrum Drives Root Trait Strategies in Mediterranean Vegetation. *Front. Plant Sci.* **2021**, *12*, 773118. [CrossRef]
51. Weemstra, M.; Kiorapostolou, N.; van Ruijven, J.; Mommer, L.; de Vries, J.; Sterck, F. The role of fine-root mass, specific root length and life span in tree performance: A whole-tree exploration. *Funct. Ecol.* **2020**, *34*, 575–585. [CrossRef]

Disclaimer/Publisher's Note: The statements, opinions and data contained in all publications are solely those of the individual author(s) and contributor(s) and not of MDPI and/or the editor(s). MDPI and/or the editor(s) disclaim responsibility for any injury to people or property resulting from any ideas, methods, instructions or products referred to in the content.

agronomy

MDPI

Article

Effects of Grassland Ley Sward Diversity on Soil Potassium and Magnesium Forms in Two Contrasting Sites

Matej Orešković [1,*], Waldemar Spychalski [2], Barbara Golińska [1] and Piotr Goliński [1]

[1] Department of Grassland and Natural Landscape Sciences, Poznań University of Life Sciences (PULS), Wojska Polskiego 28, 60-637 Poznań, Poland; barbara.golinska@up.poznan.pl (B.G.); piotr.golinski1@up.poznan.pl (P.G.)
[2] Department of Soil and Microbiology Sciences, Poznań University of Life Sciences (PULS), Wojska Polskiego 28, 60-637 Poznań, Poland; waldemar.spychalski@up.poznan.pl
* Correspondence: matej.oreskovic@up.poznan.pl

Abstract: Although multispecies grassland leys are known to influence nutrient dynamics in soils, little is known about the soil potassium (K) and magnesium (Mg) quantities in such systems. In this study, we quantified soluble, active, and exchangeable forms of K and Mg in two contrasting sites differing in soil types: Cambisols and Luvisols. These measurements were conducted in grassland ley swards differing in the species composition of their sown mixtures. The grassland ley experiment included six species belonging to three functional groups: grasses (G1: *Lolium perenne*, G2: *Phleum pratense*), legumes (L1: *Trifolium repens*, L2: *Trifolium pratense*), and herbs (H1: *Cichorium intybus*, H2: *Plantago lanceolata*). Thirty-three plant communities were established following a simplex design approach, with sown proportions ranging from 100% (monocultures) to 50%, 33%, 25%, 16.7%, and 0% across the different mixture combinations. Plant diversity only had a slightly negative trend for potassium on Cambisols. Grass-dominated mixtures maintained higher soil K levels, while legume-rich swards exhibited lower concentrations, consistent with legumes' greater K demand. Notably, the different effects of extractants on K were most evident in Cambisols, indicating stronger cation retention. This indicates the need to use the $CaCl_2$ and NH_4OAc extraction methods to determine the potassium content in this type of soil, and that these methods should be considered for evaluation of soil fertility.

Keywords: grassland ley; sward diversity; potassium; magnesium; cation forms; Cambisols; Luvisols

1. Introduction

Grasslands cover roughly 26% of the Earth's terrestrial surface and about 70% of agricultural utilized area [1]; as such, they are ecologically and economically significant habitats. For intensively managed forage production systems, perennial ryegrass monoculture with high nitrogen fertilization is still a common practice [2]. Over the years, with a rise in input costs and EU incentives, farmers have adopted grass-clover and, to a lesser extent, multispecies swards as a sustainable practice. To date, extensive research has been conducted on various ecosystem functions of the multispecies swards, including plant biomass [2]; plant C:N ratio [3]; N leaching [4]; soil microbial C [5]; soil microbial C:N ratio [5]; root biomass [6]; plant N and P uptake [7] and decomposition of the litter [8]; drought resilience [9]; pollinators and nematode abundance [10,11]; and yield of the follow-on crop [12]. Species diversity is a significant factor across a multitude of ecosystem

functions, including productivity, stability, weed invasion, and drought resilience [13–15], with a generally positive but saturating relationship [8].

Soil is an irreplaceable and vital resource that is increasingly under threat worldwide. The European Council has indicated that about 60–70% of soils in the EU are currently in an unhealthy state [16]. Unsustainable bad management practices following the premise that high input equals high yield without long-term consideration leads to loss of soil structure and SOC, soil compaction, erosion, contamination, and decline of biodiversity [16,17]. Potassium (K^+) is the seventh most abundant element on Earth's crust, and its quantity depends on the content of clay minerals [18]. The overall content of potassium in soil ranges between 0.4 and 30 $g \cdot kg^{-1}$, with a median of approximately 10 $g \cdot kg^{-1}$, and is derived from the origin parent material [19]. We can divide soil K into four forms, in terms of its availability to plants: mineral K (mostly unavailable), fixed K (slowly available), exchangeable K (available), and soil solution K (available) with quantities of 90–98%, 1–10%, 1–2%, and 0.1–0.2% of total soil K, respectively [20,21]. "Fixed K" is slowly released into the soil solution but contributes to the potassium reserve, while "mineral K" is structurally bound with soil minerals. Cation exchange is a reversible process associated with mineral nutrient balance, and the depletion of soil solution cations will result in the release of cations from the clay surface [22]. Cations are held at negatively charged sites on soil particles and humus, and are readily available to plants [23]. The uptake of potassium by plants is surpassed only by nitrogen, and the quantities of K removed through the harvesting of plant biomass in intensive agricultural systems may even surpass those of nitrogen [24].

Potassium is fundamentally linked to nitrogen (N) nutrition in plants, playing a critical role in processes such as nitrate (NO^-_3-N) uptake [25]. It is involved in protein synthesis by enhancing the activities of key enzymes like leaf carbonic anhydrase and nitrate reductase, both of which are essential for photosynthesis and amino acid formation. As a result, potassium significantly influences how effectively plants utilize N. As N fertilization enhances growth, it consequently increases the demand for K [26], and optimal K fertilization in grass swards may increase N uptake in grass DM [27]. Potassium is considered the most important cation because of its key role in assimilation, phloem loading, assimilate transport, N metabolism, and storage processes [26].

Magnesium (Mg^{2+}) is the eighth most abundant element on the Earth's crust [28], although the majority of soil Mg (90–98%) is part of the soil's structural minerals and is not immediately available for plant uptake [29]. Magnesium plays a crucial role in plant physiology, such as chlorophyll and protein synthesis, enzyme activation, phosphorylation, photosynthesis, and carbohydrate partitioning [30]. An imbalance between magnesium results from losses through leaching and biomass removal, and the relatively infrequent inputs from dung or fertilizer often leads to a general shortage of plant-available magnesium in grasslands [29].

Nutrient cycling in the soil is a complex process, with plants, animals, and abiotic factors all influencing one another. Unavailable nutrient forms are transformed into available forms within the soil, subsequently absorbed by root systems, translocated, and utilized by plants, which are eaten by animals and—via urine (mostly K), and dung (mostly Mg)—returned to the ecosystem in concentrated clusters commonly known as urine patches. Physical, chemical, and biological properties of the soil can favor the growth of specific functional groups and/or species. Due to their atmospheric nitrogen fixation ability (symbiosis with *Rhizobium* bacteria), legumes do not depend on soil N when plant available N decreases in the soil; on the other hand, they rely heavily on the potassium in the soil, which is needed to maintain this symbiotic relationship. Problems especially arise in organic and leaching-prone sandy soils, which are generally poor in K- and Mg-bearing

minerals, thus making them completely dependent on K input [25,31]. On the other hand, a high input of K can displace Mg from exchangers, which is why Mg is considered the major cation leached [32]. The soil equilibrium of these elements is important as they have impacts on plant, animal, and human nutrition. Grass tetany and milk fever in lactating cows are caused by high K and low Mg content in herbage, inhibition of plant growth caused by a lack of plant-available Mg, and human Mg deficiencies are only some problems along the food chain caused by imbalances of these cations [33–35].

Although numerous studies have investigated nitrogen (N) and phosphorus (P) dynamics in grassland systems, far fewer have examined the behavior of both potassium (K) and magnesium (Mg). Previous research in permanent meadows and pastures has addressed K dynamics [27,36–38] and Mg dynamics [37–39], but these studies typically relied on a single extraction method. Only one study [31] has compared different extraction procedures for assessing K and Mg availability, or across different species richness gradients [27]. To our understanding, no work has examined the soil status of K and Mg in highly productive grassland leys using three extraction methods.

The aim of this study was to assess how the species richness of grassland leys influences the forms of soluble, active, and exchangeable potassium (K) and magnesium (Mg), using separate models for different soil types and chemical extractants (H_2O, $CaCl_2$, and NH_4OAc).

2. Materials and Methods

2.1. Site Description

A grassland ley experiment was established within the LegumeLegacy project in September 2022 in Szelejewo (PL1) in the Division of Plant Breeding, Danko Ltd. (Szelejewo, Poland), (51°51′44″ N; 17°09′13″ E; 127 m a.s.l.); and in April 2023 in Brody (PL2) in the Experimental Station of the Department of Grassland and Natural Landscape Sciences of PULS (Brody, Poland) (52°26′11″ N; 16°17′47″ E; 94 m a.s.l.). In order to classify the soil at both sites, granulometric analysis was conducted to determine the soil particle size distribution. Both sites are located on mineral soils, with PL1 according to the IUSS Working Group WRB taxonomy [40] classified as Eutric Cambisols (Loamic, Aric), in which the soil texture of the top horizon is sandy loam and the fraction content is as follows: sand 76%, silt 16%, and clay 8%. The soils located on the PL2 site were classified as Albic Abruptic Luvisols (Anoarenic, Aric, Cutanic, Endoloamic, Ochric). The soil texture of the top horizon was classified as loamy sand and the content of granulometric fractions was as follows: sand 76%, silt 19%, and clay 3%.

2.2. Basic Chemical Soil Properties

Before establishment of the experiment, soil samples were taken randomly from the PL1 and PL2 sites to measure chemical properties of the soils via methods commonly used in Poland. Available forms of potassium and phosphorus were determined according to the Egner–Riehm method (DL test) and available forms of magnesium were assessed using the Schachtschabel method (0.0125 mol·dm^{-3} $CaCl_2$ in a 1:10 solution). The basic chemical properties are given in Table 1. The Cambisols soil (PL1) indicated higher pH value and P content, while higher N and C contents were determined in the Luvisols soil (PL2).

The same soil investigations were conducted after termination of the experiment in September 2024 (Table 2). The soils at both sites were characterized by lower pH and higher N and C contents, as well as increased phosphorus content. In the case of potassium and magnesium—which are the subject of our study—changes in their content in the soils before establishment of the grassland ley experiment and after its termination are presented in Table 3. The amounts of these macronutrients in the soils varied after the grassland ley

phase (18 and 24 months for PL2 and PL1, respectively): the content of K decreased at both sites, but Mg decreased in PL1 and increased in PL2.

Table 1. Basic chemical properties of the soils before establishment of the grassland ley experiment (mean values).

Soil Chemical Properties	Unit	PL1 Cambisols Soil	PL2 Luvisols Soil
pH_{H_2O}	-	6.45	5.92
pH_{KCl}	-	5.55	5.17
Exchangeable H^+ (H_e^+)	cmol(+) kg^{-1}	1.85	2.15
Total exchangeable base (TEB)	cmol(+) kg^{-1}	7.08	6.03
Cation-exchange capacity (CEC)	cmol(+) kg^{-1}	8.93	8.18
Total nitrogen content (N)	%	0.06	0.07
Total carbon content (C)	%	0.59	0.68
Phosphorus content (P)	mg·kg^{-1}	57.41	32.26
Class of abundance	-	medium	low

Table 2. Basic chemical properties of the soils after termination of the grassland ley experiment (mean values).

Soil Chemical Properties	Unit	PL1 Cambisols Soil	PL2 Luvisols Soil
pH_{H_2O}	-	6.34	5.67
pH_{KCl}	-	5.37	4.85
Exchangeable H^+ (H_e^+)	cmol(+) kg^{-1}	2.09	2.79
Total exchangeable base (TEB)	cmol(+) kg^{-1}	6.05	4.08
Cation-exchange capacity (CEC)	cmol(+) kg^{-1}	8.14	6.87
Total nitrogen content (N)	%	0.07	0.09
Total carbon content (C)	%	0.76	1.04
Phosphorus content (P)	mg·kg^{-1}	66.01	47.47
Class of abundance	-	high	medium

Table 3. Potassium and magnesium in the soils of the grassland ley experiment (mean values).

Experiment Stage	Cation	PL1 Cambisols Soil	PL2 Luvisols Soil
Before establishment	Potassium content (K) (mg·kg^{-1})	99.88	107.62
	Class of abundance	medium	medium
	Magnesium content (Mg) (mg·kg^{-1})	14.60	14.00
	Class of abundance	very low	very low
After termination	Potassium content (K) (mg·kg^{-1})	91.31	84.60
	Class of abundance	low	low
	Magnesium content (Mg) (mg·kg^{-1})	13.96	14.70
	Class of abundance	very low	very low

2.3. Experimental Design

The grassland ley experiment included six forage species belonging to three functional groups: grasses (G1: *Lolium perenne*, G2: *Phleum pratense*), legumes (L1: *Trifolium repens*, L2: *Trifolium pratense*), and herbs (H1: *Cichorium intybus*, H2: *Plantago lanceolata*). Thirty-three plant communities were established following a simplex design approach [41], with sown proportions ranging from 100% (monocultures) to 50%, 33%, 25%, 16.7%, and 0% across the different mixture combinations. This resulted in a gradient of diversity that ranged from monocultures to a equi-proportional six-species mixture.

In total, 47 plots (3 × 7 m)—comprising 18 monoculture plots and 29 mixture plots—were established, with proportions randomly assigned within each site. All 47 plots were managed at the same level of nitrogen (N) fertilizer (based on local practice, 120 kg ha^{-1} and

150 kg ha^{-1} y^{-1} for PL1 and PL2, respectively), with no additional potassium (K) or magnesium (Mg) fertilization applied. As a reference for conventional grassland ley management, five replicates of a *Lolium perenne* monoculture were sown on each site (3 × 7 m), which received double the recommended nitrogen rate (HighN). In the grassland phase, plots were harvested by mowing 4 and 3 times a year at sites PL1 and PL2, respectively. The difference in mowing frequency was due to the higher soil fertility in PL1 compared to PL2, as well as the greater resistance of Cambisols soil to short-term water deficits; which, in the case of Luvisols soil, reduced plant growth. According to the adopted methodology, mowing of the sward on both sites was carried out when the perennial ryegrass reached the stage of suitability for silage harvesting.

2.4. Sampling

Aggregated soil samples (homogenized) for potassium and magnesium analyses were collected from each plot using a soil sampler (Eijkelkamp Soil & Water company, Giesbeek, The Netherlands) after the termination of the grassland ley experiment in September 2024, resulting in a total of 104 samples. The average sample consisted of 15–20 individual punctures from a depth of 0–20 cm. In the laboratory, the samples were air-dried at room temperature, crushed in a porcelain mortar, and sieved through a 2 mm sieve. Laboratory analyses were conducted on air-dried soil samples using the following methods: soil texture was determined with the hydrometer method. Soil reaction (pH) was measured potentiometrically in distilled H_2O extractant and 1 mol·dm^{-3} KCl (Polish Chemical Reagents Avantor, Zawroty, Poland) (soil-to-solution ratio 1:2.5). Organic C and total N were quantified via elemental analysis using an Elementar Vario Max analyzer (Elementar Analysensysteme GmbH, Langenselbold, Germany). The content of exchangeable forms of base cations were extracted with 1 mol·dm^{-3} ammonium acetate (Polish Chemical Reagents Avantor, Zawroty, Poland) at pH 7.0, and their concentrations were measured using a Spectra AA 220 FS atomic absorption spectrometer (Varian Australia Pty Ltd., Sydney, Australia). Exchangeable hydrogen was determined using 1 mol·dm^{-3} sodium acetate (Polish Chemical Reagents Avantor, Zawroty, Poland) at pH 8.2 [42], and the contents of potassium and magnesium forms were assessed using the procedure described in detail in Table 4.

Table 4. Analytical procedures for determining K and Mg forms using a Varian FS 220 (Varian Australia Pty Ltd., Sydney, Australia) [43].

K and Mg Forms	Extractant	Denotation	Description of the Extraction Method
H_2O-soluble	H_2O	K-H_2O Mg-H_2O	100 g soil + 100 cm^3 H_2O (1:1) → shake 1.5 h → filter
Active	0.01 mol·dm^{-3} $CaCl_2$	K-$CaCl_2$ Mg-$CaCl_2$	2 g soil + 100 cm^3 0.01 mol·dm^{-3} $CaCl_2$ (1:50) → shake 1.5 h → filter
Exchangeable	1 mol·dm^{-3} NH_4OAc by pH 7.0	K-CH_3COONH_4 Mg-CH_3COONH_4	2 g soil + 100 cm^3 CH_3COONH_4 (1:50) → shake 1.5 h → filter

2.5. Data Analysis

Data analysis was conducted in R (version 4.5.1) [44] using the DImodels package (version 1.3.3) [45]. The response variables were potassium (K) and magnesium (Mg) concentrations, assessed across different soil types and extractants. For each combination of site, cation, and extractant, a separate Diversity–Interaction (DI) model was fitted, giving a total of 12 models (2 sites × 2 cations × 3 extractants). Model comparison was performed based on the corrected Akaike Information Criterion (AICc) [46]. DI models are multiple regression models in which the predictors are species proportions constrained to sum to

one, accompanied by interaction terms and model residuals. Although several interaction structures are available in DImodels, we retained only the identity-effects (ID) and average-interaction (AV) models, as these received the best AICc values. The ID model assumes that species contribute independently to the ecosystem function (mixture performance can be predicted directly from monoculture values), while the AV model assumes that all pairwise interspecific interactions share a common interaction coefficient (single average interaction term across species combinations) [47]. Cation contents for potassium (K^+) at the PL2 site in water and ammonium, as well as magnesium (Mg^{2+}) at the PL1 site, were log-transformed prior to analysis to meet the assumptions of normality and homoscedasticity. Model predictions were back-transformed from the logarithmic scale using the parametric bias correction [48] by multiplying each prediction with $e^{0.5\sigma 2}$, where s^2 is the residual variance determined from the fitted model.

3. Results

3.1. Diversity Interaction Models

Separate Diversity–Interaction models were fitted for each site, cation, and extractant combination, resulting in 12 models in total (2 sites × 2 cations × 3 extractants). Among these, only potassium (K) extracted with water at the PL1 site showed an antagonistic effect of increasing species richness, reflected in a significant negative average interaction effect (-4.59 ± 2.04, $p = 0.03$). For all other site–cation–extractant combinations, no evidence of synergistic or antagonistic interactions between species composition and cation content in the soil was detected. The raw data in Figure 1 illustrate the observed pattern. Consequently—and supported by AICc-based model selection—the final models for these cases included only species identity terms (ID models).

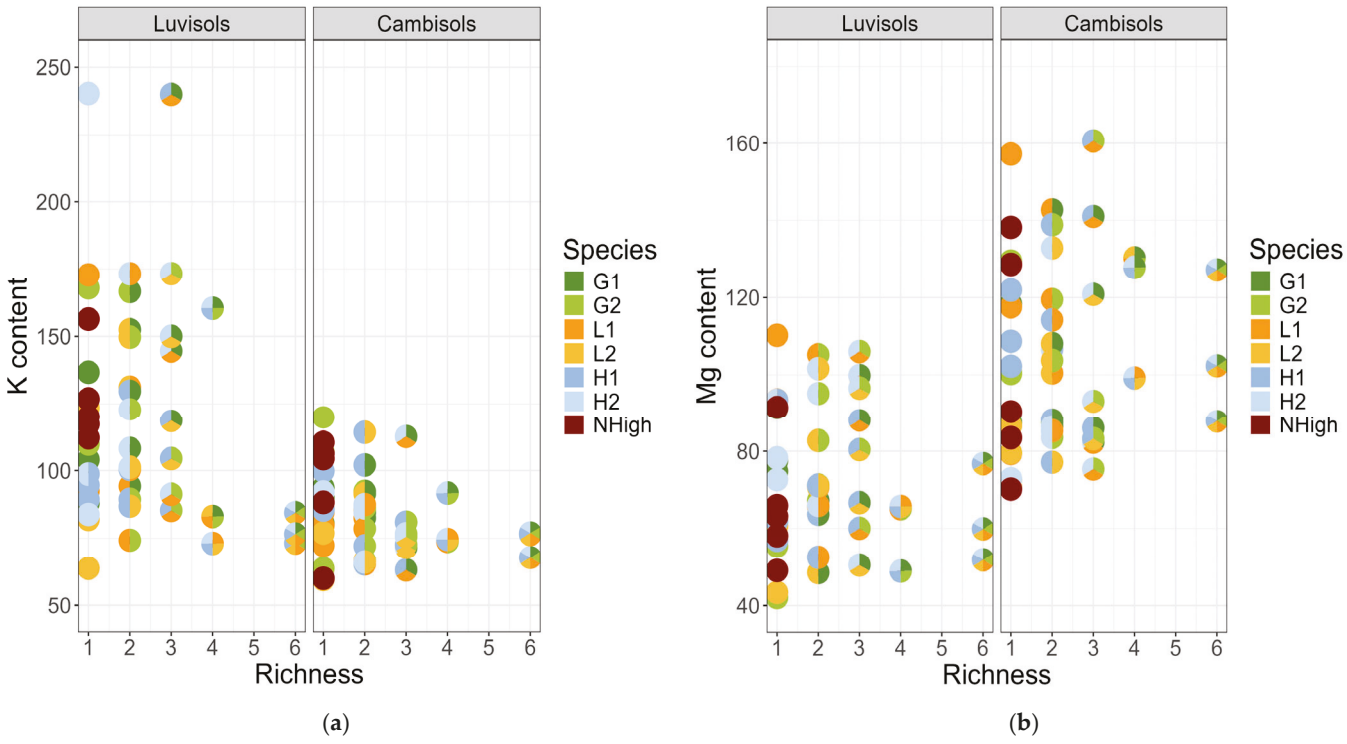


Figure 1. Scatterplots with pie-glyphs showing (**a**) potassium content and (**b**) magnesium content at both sites, measured via $CaCl_2$ extraction (raw data). Pie-glyphs represent species composition (1—monoculture; 2–6—mixtures).

3.2. Identity Effects

Across all ID models, the identity effects of species were consistently significant ($p < 0.001$), except for magnesium (Mg) extracted with water at the PL2 site, where a smaller but significant effect was observed ($p < 0.01$) for G1 identity. The PL2 site showed higher baseline values for all cation-extractant combinations except for Mg dissolved in $CaCl_2$ and NH_4OAc, compared to PL1. On average, potassium values (across the diversity gradient from the raw data) were 1.39, 1.42, and 2.86 times higher at PL2 compared to PL1, with NH_4OAc, $CaCl_2$, and H_2O, respectively. Conversely, magnesium contents in the soil were 1.38 and 1.48 times higher at PL1 with NH_4OAc and $CaCl_2$, while PL2 had a 1.58-fold higher magnesium value in H_2O. When averaging soil cation contents across sites, potassium levels exceeded those of magnesium in all extractants, with the greatest fold increase observed in H_2O (8.07), followed by NH_4OAc (1.21) and $CaCl_2$ (1.14). Regardless of the cation, water extraction consistently produced the lowest contents for both cations in the soil, whereas $CaCl_2$ and NH_4OAc extractions yielded higher values (Table 5).

Table 5. Mean values and standard error (SE) of soil potassium and magnesium contents (raw data), depending on site and extraction method ($mg \cdot kg^{-1}$).

Cation	Site No.	Soil Type	Extractant					
			H_2O		$CaCl_2$		NH_4OAc	
			Mean	SE	Mean	SE	Mean	SE
K	PL1	Cambisols	13.26	0.33	83.90	2.07	99.96	1.72
	PL2	Luvisols	37.90	3.00	119.13	5.79	138.56	5.50
Mg	PL1	Cambisols	2.45	0.08	104.19	3.38	113.24	3.40
	PL2	Luvisols	3.86	0.23	71.90	2.58	82.15	3.27

3.3. Pairwise Linear Contrasts

To explore differences in species contributions and cation-specific responses across models, pairwise linear hypothesis tests were conducted between identity effects, the high-nitrogen G1 treatment, and the six-species equi-proportional mixture (Table S1). Overall, 50 significant ($p < 0.05$) and 25 marginally significant ($p < 0.1$) contrasts were identified across all models. Most significant contrasts were associated with magnesium (37), followed by extractants in H_2O (21) and NH_4OAc (20). The results were nearly balanced between sites PL2 (24) and PL1 (26), while potassium extracted with NH_4OAc from PL2 soil was the only model without any significant pairwise differences.

At the PL1 site, G1 exhibited higher potassium content than G2, L1, and L2 in water (marginally significant for L1, $p < 0.1$; and, for G2 and L2, $p < 0.1$), as well as higher content than L1, L2, and the six-species mixture in NH_4OAc (marginally for the six-species mixture, $p < 0.1$; L1, $p < 0.05$; L2, $p < 0.01$), and higher content than L2 in $CaCl_2$ (marginally, $p < 0.1$).

Across both sites and nearly all extractants (except water in PL2), L1 consistently showed higher magnesium contents compared to the other treatments. On PL2, L1 had higher Mg than G1, G2, L2, H1, the six-species mixture, and HighN in $CaCl_2$ (marginally for G1 and G2, $p < 0.1$; L2, $p < 0.01$; H1, the six-species mixture, and HighN, $p < 0.05$), and similar contrasts were found in NH_4OAc (marginally for G2 and the six-species mixture, $p < 0.1$; G1, L2, H1, and HighN, $p < 0.05$). On PL1, L1 followed the same trend, showing higher Mg values than L2, H2, and the six-species mixture in $CaCl_2$ (marginally for six-species mixture, $p < 0.1$; L2 and H2, $p < 0.05$); higher than L2, H2, six-species mixture, and HighN in water (L2 and H2, $p < 0.01$; the six-species mixture and HighN, $p < 0.05$); and higher than L2, H2, and the six-species mixture in NH_4OAc (all $p < 0.05$).

3.4. Model Predictions

Ternary diagrams from the 12 models showed consistent changes in predicted cation values along gradients of grasses, legumes, and herbs. On both sites, potassium values were highest in grass-dominated swards and lowest in legume-dominated ones (Figure 2). In contrast, magnesium patterns varied between sites and extractants: on PL2, Mg peaked in legume-rich communities and was lowest in grass-dominated swards; except for NH_4OAc, where the highest values occurred in herb-dominated ones, while the lowest remained in grass-dominated swards (Figure 3). On PL1, Mg was highest in grass-dominated communities for all extractants, while the herb-dominated swards consistently had the lowest Mg values.

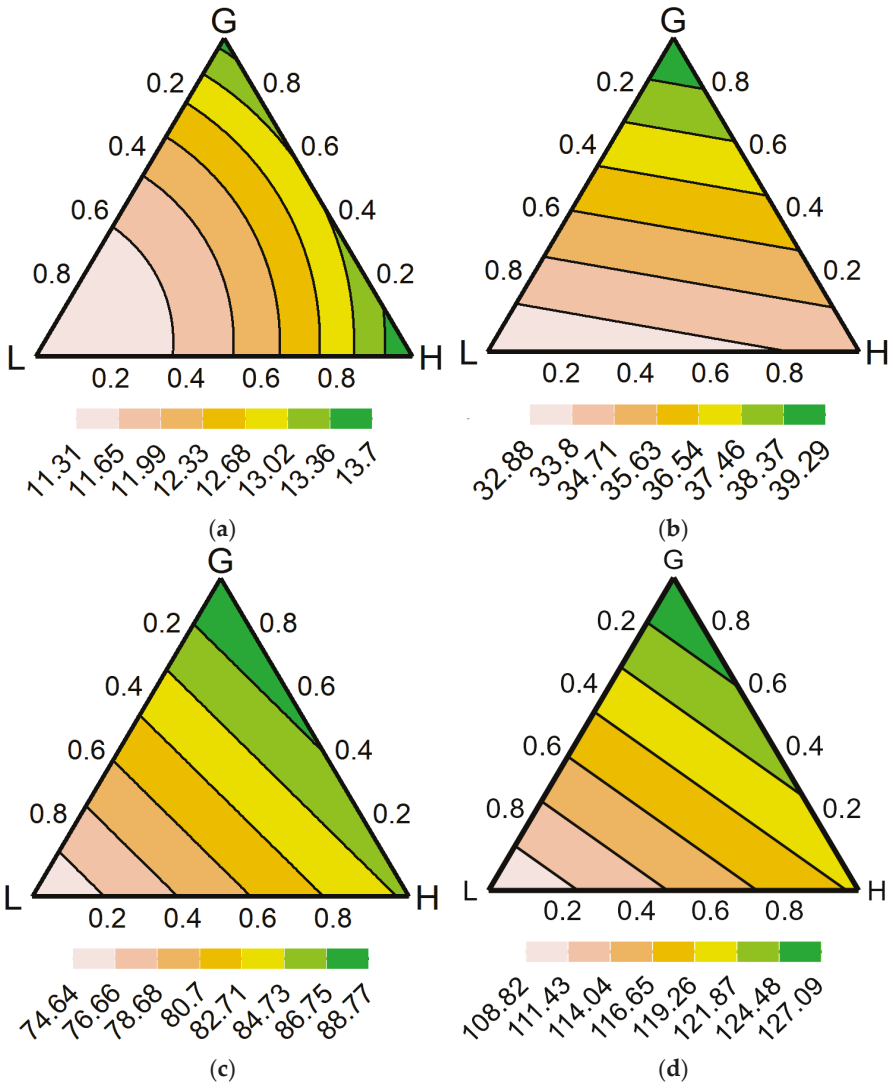
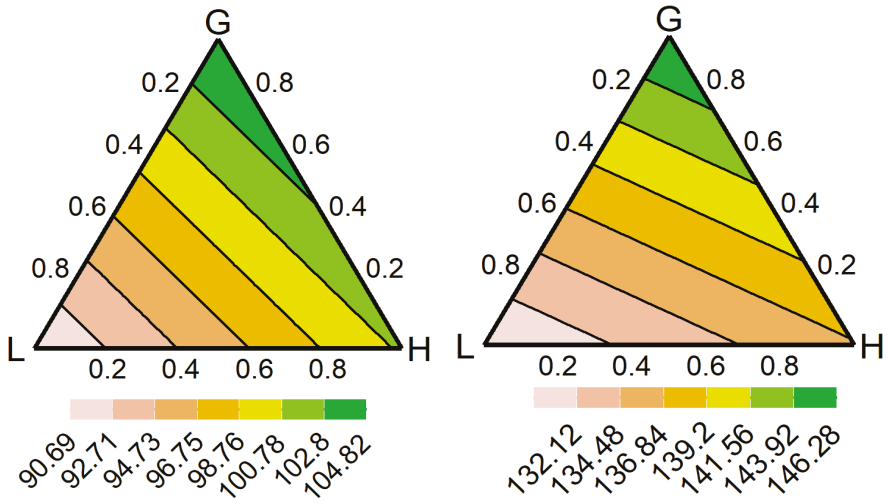
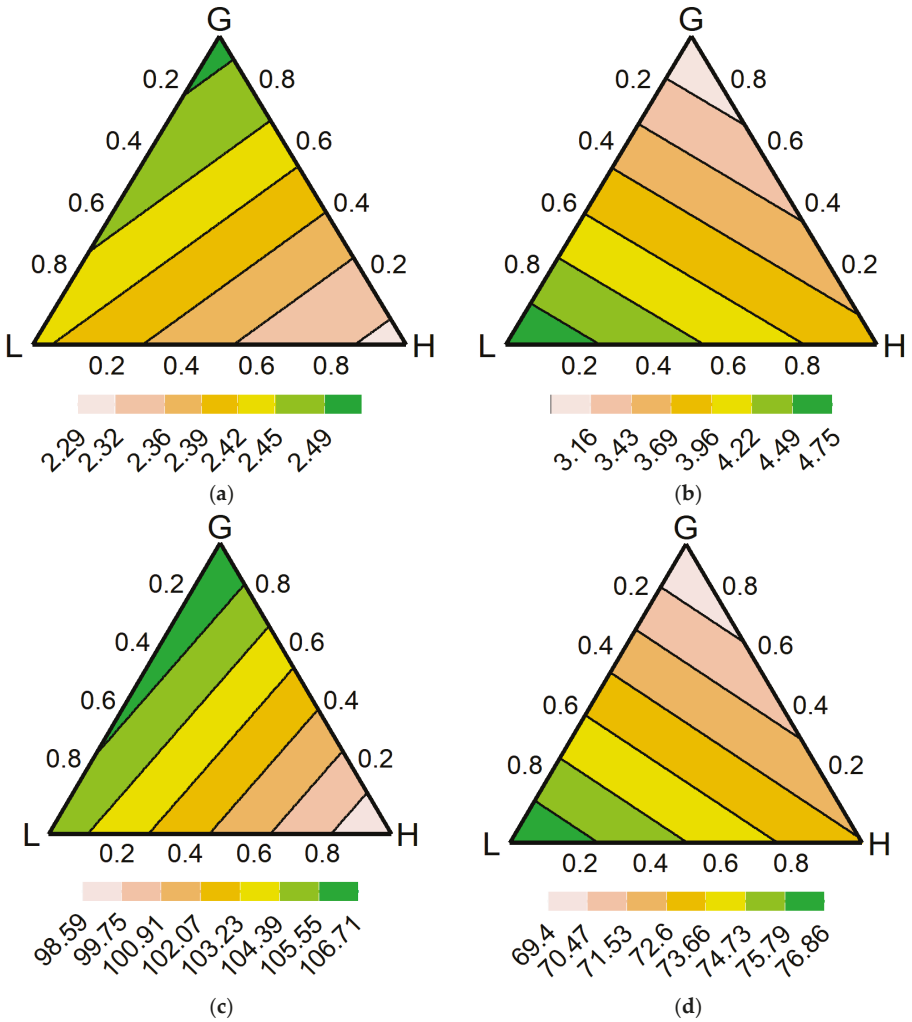


Figure 2. *Cont.*



(**e**) (**f**)

Figure 2. Ternary diagrams illustrating predicted soil potassium (K) contents across all grassland ley sown mixtures. Functional groups are merged at the vertices: grasses G (G1 + G2), legumes L (L1 + L2, and herbs H (H1 + H2). Panels in the first row (**a**,**b**) display predictions for the water extractant, the second row (**c**,**d**) for the $CaCl_2$ extractant, and the third row (**e**,**f**) for the NH_4OAc extractant. The left-hand panels (**a**,**c**,**e**) correspond to site PL1, while the right-hand panels (**b**,**d**,**f**) correspond to site PL2.



(**a**) (**b**)

(**c**) (**d**)

Figure 3. *Cont*.

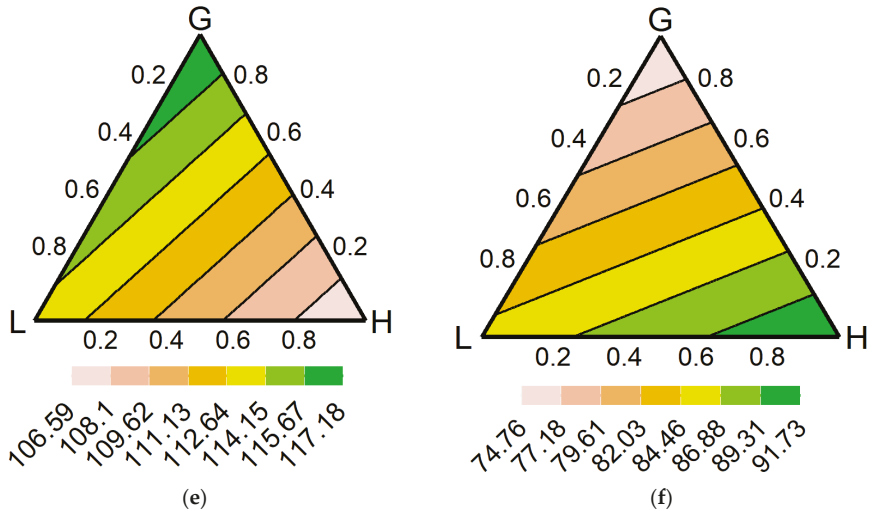


Figure 3. Ternary diagrams illustrating predicted soil magnesium (Mg) contents across all grassland ley sown mixtures. Functional groups are merged at the vertices: grasses G (G1 + G2), legumes L (L1 + L2), and herbs H (H1 + H2). Panels in the first row (**a**,**b**) display predictions for the water extractant, the second row (**c**,**d**) for the $CaCl_2$ extractant, and the third row (**e**,**f**) for the NH_4OAc extractant. The left-hand panels (**a**,**c**,**e**) correspond to site PL1, while the right-hand panels (**b**,**d**,**f**) correspond to site PL2.

4. Discussion

Our research contributes to evaluation of the benefits of grassland leys in crop rotation as an agronomic element that improves soil fertility. Previous studies have assessed the impacts of grasses and legumes—grown either in monocultures or in grass–legume mixtures forming grassland leys—on the accumulation of nitrogen, carbon, and organic matter in the soil, which serve as nutrient sources for the follow-on crops in the rotation, such as cereals. In this study, we focused on two mineral macronutrients which are important for the growth of follow-on crops: potassium and magnesium. We evaluated the effects of sward diversity in grassland leys at two contrasting sites differing in soil type (Cambisols and Luvisols) on the contents of various forms of potassium and magnesium available for plants: soluble, active, and exchangeable. This represents a novel approach that substantially advances current knowledge, going beyond what is reported in the available literature. Analyzing potassium and magnesium contents using three extractants enabled more accurate quantification of the relationships among cation forms under the two soil types and with different levels of diversity of grassland leys, allowing for rational decision-making regarding plant nutrition of the follow-on crop, particularly during early growth and development.

4.1. Species Richness Effect

Overall, no significant species interactions were detected in most models (a feature of the ID model). This suggests that the mixture response is a linear combination of the component monoculture responses. Similar findings were reported by Dietrich et al. [49], who also observed limited effects of species diversity on plant-available soil potassium. Only the PL1 site located on Cambisols soil showed a significant negative average interaction effect (-4.59 ± 2.04, $p < 0.05$). This pattern likely reflects overyielding effects, as often reported in biodiversity–ecosystem functioning (BEF) studies, where higher species richness enhances biomass productivity [50]. Higher biomass production can intensify nutrient depletion from the soil—a mechanism well documented in previous work [51]—as potassium is second only to nitrogen in terms of plant uptake [24].

4.2. Differences Between Soil Types

Higher baseline cation levels at the Luvisols site can likely be attributed to fertilization history [38], which resulted in a 7.7% higher potassium and a 4.0% lower magnesium content compared to the Cambisols site at the start of the experiment. Lower magnesium availability in acidic and sandy soils is commonly linked to reduced clay and silt content [39]. The higher magnesium content in the Cambisols soil compared with Luvisols when using the $CaCl_2$ extractant aligns with findings from the large-scale FRIBO experiment conducted across more than 250 sites in Switzerland [39]. However, the higher NH_4OAc and lower water-extractable values in Cambisols observed in our study showed the opposite trend. This discrepancy may stem from differences in extractant pH or land-use history (cropland vs. permanent pasture), as noted in the FRIBO dataset.

4.3. Differences Among Extractants

Exchangeable magnesium is not always strongly correlated with organic carbon; only about 45% of its variation can be explained by soil pH and clay content [52]. Similarly, plant-available potassium is not always reliably represented by exchangeable K alone. Although the contribution of non-exchangeable cations depends on weathering and environmental conditions, these pools can substantially supplement plant nutrition [22,53]. Therefore, measuring multiple forms of available cations should be standard practice to ensure accurate fertilization recommendations and maintain long-term nutrient balance. In this study, regardless of the element, water extraction consistently produced the lowest contents, whereas $CaCl_2$ and NH_4OAc extractions yielded considerably higher values, consistent with previous research [31,39]. In our study, the magnesium contents extracted in water were 46.22 and 21.28 times lower than in NH_4OAc, and 42.53 and 18.63 times lower in $CaCl_2$ for Cambisols and Luvisols soils, respectively. These results emphasize the role of the soil colloidal fraction in replenishing soluble cations and the importance of clay content and cation-binding capacity, both of which were higher in Cambisols than in Luvisols soil.

4.4. Optimal Range of Communities

Across both sites, predicted potassium values were highest in grass-dominated communities and lowest in legume-dominated ones. This supports the view that legumes require large amounts of potassium for proper development and symbiotic nitrogen fixation [38]. Although grasses produce large amounts of biomass, they also return potassium-rich residues to the soil, which may explain the consistently higher K contents determined with different extractants over the two growing seasons [49]. The exchangeable potassium values in our study are comparable to those from similar experiments [22,38]. The magnesium patterns in our study, on the other hand, varied with soil type and extractant, similar to the findings of Frau et al. [39]. In Luvisols soil, legumes had the highest magnesium contents, followed by herbs and grasses, in both water and $CaCl_2$ extractions, consistent with the observations of Grzegorczyk et al. [37]; in contrast, for the NH_4OAc extraction, herbs surpassed legumes. Notably, magnesium levels were highest in grass-dominated communities and lowest in herb-dominated ones on Cambisols soil. This pattern may be linked to the weaker performance of grass mixtures G1 and G2 on Cambisols soil, where the annual DM yields in 2024 were 2.42 and 1.13 times lower, respectively, than those on Luvisols (unpublished data).

4.5. Nutrient Cycling Complexity

Nutrient cycling in soil is a highly dynamic process, where insoluble nutrient forms are continuously transformed into plant-available ones through biological and physico-chemical interactions. By applying three extractants that target the water-soluble, active,

and exchangeable cation pools, this study provides a detailed picture of how soil type and sward diversity of grassland ley sown mixtures jointly influence the contents of potassium and magnesium in soil. The combined use of the three extractants provided a more precise quantification of the relationships among cation forms, and could be adopted as a standard method in routine soil testing for fertilization recommendations. Importantly, the ternary diagrams developed here offered a practical visual framework to identify the range of plant sward compositions associated with the lowest and highest cation values across both soil types. To further strengthen future research, incorporating mineralogical characterization of coarser soil fractions and increasing the number of replicates would help to better elucidate the mechanisms controlling nutrient transformation and mobility.

5. Conclusions

Overall, increasing sward diversity did not bring a significant change to soil potassium and magnesium values, except on Cambisols soil, where a negative interaction was observed. The potassium content in the soil, regardless of the soil type and extractant, was highest for grass-dominated swards, while legume-dominated communities showed lower values. This relationship confirms the greater potassium requirement of legumes compared to herbs and grasses and, at the same time, the depletion of potassium in the soil following the use of grassland leys for fodder purposes. Magnesium values varied across sites and extractants, which suggests that grassland ley sward diversity has a lower effect on soil magnesium content than in the case of potassium. The difference in potassium content between the water-soluble and exchangeable forms extracted with NH_4OAc in Cambisols soil was substantially higher than that in Luvisols soil (7.5 and 3.7, respectively). A similar relation was found between the forms of potassium in the soil (i.e., water-soluble and active) extracted with $CaCl_2$. This difference results from the larger sorption complex of soil colloids in Cambisols and the higher retention of potassium cations in soil. These results indicate the need to use both the $CaCl_2$ and NH_4OAc extraction methods when determining the potassium content in this type of soil; this approach should be considered for soil fertility evaluation, particularly after termination of legume-dominated grassland ley swards.

Supplementary Materials: The following supporting information can be downloaded at: https://www.mdpi.com/article/10.3390/agronomy15122815/s1, Table S1. Pairwise linear contrasts (from the fitted DI models) comparing predicted cation concentrations among monocultures (n = 6), the six-species mixture, and the HighN reference treatment.

Author Contributions: Conceptualization: P.G., B.G. and W.S.; methodology: P.G., B.G. and W.S.; software: M.O.; validation: M.O.; formal analysis: M.O.; investigation: M.O.; resources: P.G. and B.G.; data curation: M.O.; writing—original draft preparation: M.O.; writing—review and editing, P.G., B.G., W.S. and M.O.; visualization: M.O.; supervision: P.G., B.G. and W.S.; project administration: P.G. and B.G.; funding acquisition: P.G. and B.G. All authors have read and agreed to the published version of the manuscript.

Funding: This study was supported by European Union's Horizon 2021 doctoral network programme under the Marie Skłodowska–Curie grant agreement No. 101072579 (Legume Legacy).

Data Availability Statement: The raw data supporting the conclusions of this article will be made available by the authors upon request.

Conflicts of Interest: The authors declare no conflicts of interest.

References

1. FAO, Food and Agriculture Organization of the United Nations. Available online: https://www.fao.org/faostat/en/#data/LC (accessed on 22 October 2025).
2. Golińska, B.; Vishwakarma, R.; Brophy, C.; Goliński, P. Positive effects of plant diversity on dry matter yield while maintaining a high level of forage digestibility in intensively managed grasslands across two contrasting environments. *Grass Forage Sci.* **2023**, *78*, 438–461. [CrossRef]
3. Schaub, S.; Finger, R.; Leiber, F.; Probst, S.; Kreuzer, M.; Weigelt, A.; Buchmann, N.; Scherer-Lorenzen, M. Plant diversity effects on forage quality, yield and revenues of semi-natural grasslands. *Nat. Commun.* **2020**, *11*, 768. [CrossRef]
4. Suter, M.; Huguenin-Elie, O.; Lüscher, A. Multispecies for multifunctions: Combining four complementary species enhances multifunctionality of sown grassland. *Sci. Rep.* **2021**, *11*, 3835. [CrossRef]
5. Lama, S.; Velescu, A.; Leimer, S.; Weigelt, A.; Chen, H.; Eisenhauer, N.; Scheu, S.; Oelmann, Y.; Wilcke, W. Plant diversity influenced gross nitrogen mineralization, microbial ammonium consumption and gross inorganic N immobilization in a grassland experiment. *Oecologia* **2020**, *193*, 731–748. [CrossRef]
6. Eriksen, J.; Mortensen, T.; Søegaard, K. Root biomass and carbon storage in differently managed multispecies temporary grasslands. *Grass Forage Sci. Eur.* **2012**, *17*, 610–612.
7. Obasoro, O.; Shackleton, J.; Grace, C.; Kennedy, J.; Oram, N.J.; Sheridan, H.; Schmidt, O.; De Goede, R.; Hoffland, E.; Obasoro, O.; et al. Multispecies swards improve nitrogen use efficiency and reduce nitrogen surplus in agricultural grasslands. *Plant Soil* **2025**, 1–15. [CrossRef]
8. Cardinale, B.J.; Duffy, J.E.; Gonzalez, A.; Hooper, D.U.; Perrings, C.; Venail, P.; Narwani, A.; MacE, G.M.; Tilman, D.; Wardle, D.A.; et al. Biodiversity loss and its impact on humanity. *Nature* **2012**, *486*, 59–67. [CrossRef] [PubMed]
9. Lüscher, A.; Barkaoui, K.; Finn, J.A.; Suter, D.; Suter, M.; Volaire, F. Using plant diversity to reduce vulnerability and increase drought resilience of permanent and sown productive grasslands. *Grass Forage Sci.* **2022**, *77*, 235–246. [CrossRef]
10. Cong, W.; Dupont, Y.L.; Søegaard, K.; Eriksen, J. Optimizing yield and flower resources for pollinators in intensively managed multi-species grasslands. *Agric. Ecosyst. Environ.* **2020**, *302*, 107062. [CrossRef]
11. Ikoyi, I.; Grange, G.; Finn, J.A.; Brennan, F.P. Plant diversity enhanced nematode-based soil quality indices and changed soil nematode community structure in intensively-managed agricultural grasslands. *Eur. J. Soil Biol.* **2023**, *118*, 103542. [CrossRef]
12. Komainda, M.; Muto, P.; Isselstein, J. Interaction of multispecies sward composition and harvesting management on herbage yield and quality from establishment phase to the subsequent crop. *Grass Forage Sci.* **2022**, *77*, 89–99. [CrossRef]
13. Brophy, C.; Finn, J.A.; Lüscher, A.; Suter, M.; Kirwan, L.; Sebastià, M.T.; Helgadóttir, Á.; Baadshaug, O.H.; Bélanger, G.; Black, A.; et al. Major shifts in species' relative abundance in grassland mixtures alongside positive effects of species diversity in yield: A continental-scale experiment. *J. Ecol.* **2017**, *105*, 1210–1222. [CrossRef]
14. Finn, J.A.; Kirwan, L.; Connolly, J.; Sebastià, M.T.; Helgadottir, A.; Baadshaug, O.H.; Bélanger, G.; Black, A.; Brophy, C.; Collins, R.P.; et al. Ecosystem function enhanced by combining four functional types of plant species in intensively managed grassland mixtures: A 3-year continental-scale field experiment. *J. Appl. Ecol.* **2013**, *50*, 365–375. [CrossRef]
15. Grange, G.; Brophy, C.; Vishwakarma, R.; Finn, J.A. Effects of experimental drought and plant diversity on multifunctionality of a model system for crop rotation. *Sci. Rep.* **2024**, *14*, 10265. [CrossRef]
16. EU. *Proposal for a Directive of the European Parliament and of the Council on Soil Monitoring and Resilience (Soil Monitoring Law)*; European Commission: Brussels, Belgium, 2023.
17. Weninger, T.; Ramler, D.; Bondi, G.; Asins, S.; O'Sullivan, L.; Assennato, F.; Astover, A.; Bispo, A.; Borůvka, L.; Buttafuoco, G.; et al. Do we speak one language on the way to sustainable soil management in Europe? A terminology check via an EU-wide survey. *Eur. J. Soil Sci.* **2024**, *75*, e13476. [CrossRef]
18. Schroeder, D. Structure and weathering of potassium containing minerals. In Proceedings of the 11th Congress of the International Potash Institute, Tokyo, Japan, 27–28 August 1978; International Potash Institute: Bern, Switzerland, 1978; pp. 43–63.
19. Sparks, D.L. Potassium Dynamics in Soils. In *Proceedings of the Advances in Soil Science*; Stewart, B.A., Ed.; Springer: New York, NY, USA, 1987; pp. 1–63. [CrossRef]
20. Carey, P.L.; Curtin, D.; Scott, C.L. An improved procedure for routine determination of reserve-K in pastoral soils. *Plant Soil* **2011**, *341*, 461–472. [CrossRef]
21. Sumner, M.E. *Handbook of Soil Science*; CRC Press: Boca Raton, FL, USA, 2000; p. 2148.
22. Andrist-Rangel, Y.; Edwards, A.C.; Hillier, S.; Öborn, I. Long-term K dynamics in organic and conventional mixed cropping systems as related to management and soil properties. *Agric. Ecosyst. Environ.* **2007**, *122*, 413–426. [CrossRef]
23. Sparks, D.L.; Huang, P.M. Physical chemistry of soil potassium. In *Potassium in Agriculture*; Munson, R.D., Ed.; American Society of Agronomy: Madison, WI, USA, 1985; pp. 201–276.
24. Kayser, M.; Isselstein, J. Potassium cycling and losses in grassland systems: A review. *Grass Forage Sci.* **2005**, *60*, 213–244. [CrossRef]

25. Hylton, L.O.; Ulrich, A.; Cornelius, D.R. Potassium and Sodium Interrelations in Growth and Mineral Content of Italian Ryegrass. *Agron. J.* **1967**, *59*, 311–314. [CrossRef]
26. Zhang, F.; Niu, J.; Zhang, W.; Chen, X.; Li, C.; Yuan, L.; Xie, J. Potassium nutrition of crops under varied regimes of nitrogen supply. *Plant Soil* **2010**, *335*, 21–34. [CrossRef]
27. McCarthy, T.; Wall, D.P.; Casey, I.A.; Humphreys, J.; Forrestal, P.J. Integrating Soil Potassium Status and Fertilisation Strategies to Increase Grassland Production and Mitigate Potassium Management Induced Metabolic Disorders in Grazing Livestock. *Soil Use Manag.* **2025**, *41*, e70074. [CrossRef]
28. Maguire, M.E.; Cowan, J.A. Magnesium chemistry and biochemistry. *Biometals* **2002**, *15*, 203–210. [CrossRef] [PubMed]
29. Senbayram, M.; Gransee, A.; Wahle, V.; Thiel, H. Role of magnesium fertilisers in agriculture: Plant-soil continuum. *Crop Pasture Sci.* **2015**, *66*, 1219–1229. [CrossRef]
30. Cakmak, I.; Yazici, A.M. Magnesium: A forgotten element in crop production. *Better Crops* **2010**, *94*, 23–25.
31. Staugaitis, G.; Rutkauskienė, R. Comparison of magnesium determination methods as influenced by soil properties. *Agriculture* **2010**, *97*, 105–116.
32. Mikkelsen, R. Soil and fertilizer magnesium. *Better Crops* **2010**, *94*, 26–28.
33. Guo, W.; Nazim, H.; Liang, Z.; Yang, D. Magnesium deficiency in plants: An urgent problem. *Crop J.* **2016**, *4*, 83–91. [CrossRef]
34. Hawkesford, M.; Horst, W.; Kichey, T.; Lambers, H.; Schjoerring, J.; Møller, I.S.; White, P. Functions of Macronutrients. In *Marschner's Mineral Nutrition of Higher Plants*, 3rd ed.; Marschner, P., Ed.; Pergamon Press: Pergamon, UK, 2011; pp. 135–189. [CrossRef]
35. Schonewille, J.T. Magnesium in dairy cow nutrition: An overview. *Plant Soil* **2013**, *368*, 167–178. [CrossRef]
36. Cooledge, E.C.; Sturrock, C.J.; Atkinson, B.S.; Mooney, S.J.; Brailsford, F.L.; Murphy, D.V.; Leake, J.R.; Chadwick, D.R.; Jones, D.L. Herbal leys have no effect on soil porosity, earthworm abundance, and microbial community composition compared to a grass-clover ley in a sheep grazed grassland after 2-years. *Agric. Ecosyst. Environ.* **2024**, *365*, 108928. [CrossRef]
37. Grzegorczyk, S.; Alberski, J.; Olszewska, M. Accumulation of potassium, calcium and magnesium by selected species of grassland legumes and herbs. *J. Elem.* **2013**, *18*, 69–78. [CrossRef]
38. Moir, J.; Seidel, M.; Kayser, M. Potassium dynamics of four grassland soils contrasting in soil K management history. *Grassl. Sci.* **2013**, *59*, 1–10. [CrossRef]
39. Frau, L.J.; Libohova, Z.; Joost, S.; Levasseur, C.; Jeangros, B.; Bragazza, L.; Sinaj, S. Regional investigation of spatial-temporal variability of soil magnesium—A case study from Switzerland. *Geoderma Reg.* **2020**, *21*, e00278. [CrossRef]
40. IUSS Working Group WRB, World Reference Base for Soil Resources. *International Soil Classification System for Naming Soils and Creating Legends for Soil Maps*, 4th ed.; International Union of Soil Sciences: Rome, Italy, 2022.
41. Cornell, J.A. *Experiments with Mixtures: Designs, Models, and the Analysis of Mixture Data*, 3rd ed.; John Wiley & Sons Inc.: Hoboken, NJ, USA, 2011.
42. Van Reeuwijk, L.P. *Procedures for Soil Analysis*, 6th ed.; Technical Paper No. 9; FAO/ISRIC: Wageningen, The Netherlands, 2002; p. 120.
43. R Core Team. R: A Language and Environment for Statistical Computing. R Foundation for Statistical Computing. 2020. Available online: https://www.R-project.org/ (accessed on 22 October 2025).
44. Moral, R.A.; Vishwakarma, R.; Connolly, J.; Byrne, L.; Hurley, C.; Finn, J.A.; Brophy, C. Going beyond richness: Modelling the BEF relationship using species identity, evenness, richness and species interactions via the DImodels R package. *Methods Ecol. Evol.* **2023**, *14*, 2250–2258. [CrossRef]
45. Burnham, K.P.; Anderson, D.R. *Model Selection and Multimodel Inference: A Practical Information-Theoretic Approach*, 2nd ed.; Springer: New York, NY, USA, 2002; p. 408. [CrossRef]
46. Kirwan, L.; Connolly, J.; Finn, J.A.; Brophy, C.; Nyfeler, D. Diversity-interaction modeling: Estimating contributions of species identities and interactions to ecosystem function. *Ecology* **2009**, *90*, 2032–2038. [CrossRef] [PubMed]
47. Miller, D.M. Reducing transformation bias in curve fitting. *American Statistician* **1984**, *38*, 124–126. [CrossRef]
48. Spychalski, W.; Kosiada, T.; Otremba, K. Content of potassium forms in an anthropogenic soil formed from post-mining lands under diversified agricultural practices. *Acta Sci. Pol.—Agric.* **2007**, *6*, 53–64.
49. Dietrich, P.; Eisenhauer, N.; Roscher, C. Linking plant diversity–productivity relationships to plant functional traits of dominant species and changes in soil properties in 15-year-old experimental grasslands. *Ecol. Evol.* **2023**, *13*, e9883. [CrossRef]
50. Nyfeler, D.; Huguenin-Elie, O.; Suter, M.; Frossard, E.; Connolly, J.; Lüscher, A. Strong mixture effects among four species in fertilized agricultural grassland led to persistent and consistent transgressive overyielding. *J. Appl. Ecol.* **2009**, *46*, 683–691. [CrossRef]
51. Öborn, I.; Edwards, A.C.; Hillier, S. Quantifying uptake rate of potassium from soil in a long-term grass rotation experiment. *Plant Soil* **2010**, *335*, 3–19. [CrossRef]

52. Hailes, K.J.; Aitken, R.L.; Menzies, N.W. Magnesium in tropical and subtropical soils from north-eastern Australia. I. Magnesium fractions and interrelationships with soil properties. *Aust. J. Soil Res.* **1997**, *35*, 615–627. [CrossRef]
53. Simonsson, M.; Andersson, S.; Andrist-Rangel, Y.; Hillier, S.; Mattsson, L.; Öborn, I. Potassium release and fixation as a function of fertilizer application rate and soil parent material. *Geoderma* **2007**, *198*, 140–188. [CrossRef]

Disclaimer/Publisher's Note: The statements, opinions and data contained in all publications are solely those of the individual author(s) and contributor(s) and not of MDPI and/or the editor(s). MDPI and/or the editor(s) disclaim responsibility for any injury to people or property resulting from any ideas, methods, instructions or products referred to in the content.

agronomy

MDPI

Article

The Effect of Litter Addition on Soil Organic Carbon Fractions with Intensified Grassland Degradation

Shitong Wei [1], Chunying Fan [1], Junqi Zuo [1], Lingfeng Rui [1], Jianan Li [1], Wenjing Tang [1] and Pingting Guan [1,2,3,*]

[1] Key Laboratory of Wetland Ecology and Vegetation Restoration, Ministry of Ecology and Environment, Northeast Normal University, Changchun 130117, China; weist377@nenu.edu.cn (S.W.); fancy693@nenu.edu.cn (C.F.); zuojq957@nenu.edu.cn (J.Z.); ruilf@nenu.edu.cn (L.R.); lijn691@nenu.edu.cn (J.L.); tangwenjing318@nenu.edu.cn (W.T.)
[2] Key Laboratory of Vegetation Ecology, Ministry of Education, Northeast Normal University, Changchun 130024, China
[3] Jilin Provincial Key Laboratory of Animal Resource and Ecological Security, Northeast Normal University, Changchun 130117, China
* Correspondence: guanpt994@nenu.edu.cn; Tel.: +86-13039324607

Abstract

Litter decomposition plays a critical role in the formation and turnover of soil organic carbon (SOC) and its fractions. However, the effects of litter on SOC dynamics across grassland degradation remain poorly understood. The objectives of this study were to investigate the responses of SOC and its fractions, including particulate organic carbon (POC) and mineral-associated organic carbon (MAOC), to litter decomposition in lightly, moderately, and highly degraded grasslands. A 240-day incubation experiment using Leymus chinensis litter incubated on day 0, 23, 60, and 240 was conducted to investigate the biotic and abiotic factors regulating SOC stability. Grassland degradation significantly reduced POC and MAOC concentrations; moreover, litter addition in degraded grasslands further reduced SOC. In the lightly and moderately degraded grasslands, litter addition modulated POC and MAOC via both microbial and physicochemical pathways. In the highly degraded grasslands, litter addition influenced POC and MAOC not only indirectly through microbial and physicochemical pathways but also directly by promoting MAOC formation. Overall, although litter decomposition altered SOC and its fractions, its effects were constrained by the degree of grassland degradation. These findings indicate that restoration strategies should prioritize enhancing microbial biomass and activity in lightly and moderately degraded grasslands while increasing litter inputs in highly degraded grasslands to improve soil carbon sequestration.

Keywords: litter decomposition; degradation gradient; SOC fractions; POC; MAOC

1. Introduction

Grasslands cover approximately 40.5% of the Earth's land area and store about one-third of the global terrestrial carbon [1]. However, grassland degradation has led to a 33% to 90% reduction in soil organic carbon (SOC) [1,2]. SOC is a complex organic material composed of plant, animal, and microbial residues with varying degrees of decomposition [3,4]. It can be divided into particulate organic carbon (POC) and mineral-associated organic carbon (MAOC) fractions, with only a minor portion (1 to 2%) present as dissolved organic matter [5]. POC and MAOC differ in their formation, physical and chemical properties, and mean residence times in soil [6,7]. POC primarily consists of plant-derived polymers and

is less decomposed within large soil aggregates [1]. In contrast, MAOC is predominantly microbial-derived and characterized by stable associations with mineral surfaces through physicochemical interactions [6]. Compared with POC, MAOC is more effectively protected against decomposition because of its association with soil minerals [8,9]. The POC to MAOC ratio therefore reflects the relative stability of SOC fractions [10]. This distinction is particularly important in degraded grasslands, where disruption of soil structure and weakening of mineral protection may limit MAOC preservation and alter the balance between labile and stable carbon pools [11]. Previous studies have shown that grassland degradation decreases SOC storage and alters the distribution of SOC fractions by reducing plant carbon inputs, weakening soil aggregation, and changing microbial processing of organic matter [1,7,12,13]. Consequently, POC usually declines rapidly because it is more labile and closely linked to fresh plant inputs, whereas MAOC often responds more slowly or variably depending on mineral protection and microbial transformation capacity [12–14]. Degradation-induced changes in vegetation composition, soil salinity/alkalinity, and nutrient availability may further shift the balance between labile and stable carbon pools [7,12]. Therefore, distinguishing between POC and MAOC is essential for understanding SOC dynamics in degraded grasslands, where disrupted soil structure and reduced mineral protection may limit MAOC preservation and compromise overall soil carbon stability [13]. Accordingly, investigating the responses of soil organic carbon and its fractions to grassland degradation is crucial for understanding carbon dynamics and informing effective restoration strategies.

Litter serves as a crucial source of SOC and its fractions in grassland ecosystems [15,16]. Research has shown that litter addition can increase SOC accumulation by increasing carbon inputs, stimulating microbial activity, and promoting the formation of both POC and MAOC [15,17,18]. For example, litter inputs may directly increase coarse organic matter pools and indirectly contribute to MAOC formation through microbial transformation and subsequent mineral association [15,18]. However, the magnitude and direction of these effects vary among ecosystems and degradation stages because litter decomposition is strongly regulated by soil physicochemical conditions, microbial communities, and nutrient availability. In degraded grasslands, litter addition has been shown to increase SOC fractions, whereas in other cases its effects are offset by adverse soil conditions or accelerated decomposition losses [17,18]. Therefore, litter addition emerges as a key driver that regulates soil carbon pool composition and sequestration through direct addition and indirect modulation in grassland ecosystems [18].

Leymus chinensis, a perennial rhizomatous bunchgrass, is widely distributed in the grasslands of East Asia [19,20]. It has strong tolerance to drought, high soil pH, and low soil fertility [21,22]. These characteristics make it a dominant species in grasslands and a pioneer species in grassland restoration [21]. *Leymus chinensis* contributes significantly to SOC through inputs of aboveground and belowground biomass [23]. Furthermore, its exudates serve as a labile carbon source for soil microorganisms, stimulating their growth and activity. This microbial response subsequently modulates the formation and stabilization of SOC through biochemical transformation and mineral association processes. At the same time, *Leymus chinensis* plays a critical role in regulating carbon input, influencing soil carbon steady-state dynamics, and shaping carbon sink potential under grassland degradation scenarios [21]. Although previous studies have documented the importance of litter inputs and degradation status for SOC dynamics, less is known about how *Leymus chinensis* litter decomposition affects POC and MAOC across different degradation levels, particularly through linked biotic and abiotic pathways. Therefore, *Leymus chinensis* was selected as the experimental material to examine the effects of litter addition on the grassland carbon pool. We hypothesized that POC and MAOC exhibited distinct responses to litter addition with

https://doi.org/10.3390/agronomy16080835

increasing degradation levels. In order to explore the effects of litter decomposition on SOC fractions in degraded grasslands, we conducted a 240-day decomposition experiment using *Leymus chinensis* litter. This study aimed to (1) determine the effects of litter decomposition on SOC and its fractions (POC and MAOC) across grassland degradation gradients and (2) elucidate the mechanisms governing the cycling of SOC and its fractions across different degradation stages.

2. Materials and Methods

2.1. Study Sites and Sampling Collection

The study was conducted in the meadow steppe of the Grassland Ecological Research Station of Northeast Normal University, Jilin province, China (44°45′ N, 123°45′ E). This region is characterized by a semi-arid continental monsoon climate, with cold, dry winters and warm, rainy summers. The mean annual temperature is 4.6–6.4 °C, and the mean annual precipitation is 282–400 mm, mostly falling between June and August [24]. The soil type is saline–alkaline meadow soil with a high degree of heterogeneity. Soil pH in the study area ranges from 8.5 to 10.0 [25]. Based on soil pH, soil properties, plant cover, and the actual conditions of the study area, there are three levels of degradation in this region: lightly, moderately, and highly degraded grasslands [26–28]. Specifically, the degradation levels are distinguished according to the cover of *Leymus chinensis*, with approximately 70%, 50%, and 30% cover representing lightly, moderately, and highly degraded grasslands, respectively [29]. Plant community composition varies among degradation levels. The lightly degraded grassland is still dominated by *Leymus chinensis*, whereas the moderately degraded grassland is characterized by a greater abundance of *Chloris virgata*. In the highly degraded grassland, the plant community shifts further toward salt-tolerant species, with *Suaeda heteroptera* becoming dominant. The plant communities gradually change from *Leymus* chinensis to more salt-/degradation-tolerant species under increasing degradation [30].

Soil samples were collected from the three levels of degraded grasslands on 13 October 2019. In each degradation level, five plots (25 m × 25 m) were randomly selected as replicates. After the removal of surface impurities, 25 soil cores (0–10 cm depth, 5 cm diameter) were randomly collected from each plot using a soil auger and homogenized to form a composite sample. A total of about 6 kg of soil was collected as one soil sample from each plot. We collected the aboveground biomass of *Leymus chinensis* from *Leymus chinensis*-dominated communities for the subsequent decomposition experiment. All samples were transported to the laboratory and stored at 4 °C. The physicochemical properties of both the soil and the litter were measured and are listed in Table S1.

The *Leymus chinensis* was used as the litter material. After drying at 60 °C in an oven for 48 h, the *Leymus chinensis* litter was cut into 1 cm pieces. A total of 3.00 g litter was placed into each plastic litter bag (1 mm mesh). This amount was selected to provide a standardized litter input representative of the dominant species in the local *Leymus chinensis* grassland, where *Leymus chinensis* contributes most of the aboveground biomass, and to maintain consistency with previous decomposition microcosm studies conducted in the Songnen meadow steppe/saline–alkali grassland [31]. The soil samples were passed through an 8 mm sieve to remove stones and roots. A total of 400 g of field-moist soil was weighed into a PVC tube (9 cm inner diameter and 15 cm height). This amount was consistent with a comparable decomposition experiment previously conducted using soils from the same region [32]. All PVC tubes were pre-incubated in an incubator under standardized conditions (25 °C, 60% water-holding capacity) for 7 days to balance water and nutrients [33]. The litter bag was then placed on the soil surface of each PVC tube for the litter treatment, whereas the control treatment received no litter addition. The

https://doi.org/10.3390/agronomy16080835

experiment began on 21 October 2019. PVC tubes were placed in an incubator under the same standardized conditions as the pre-incubation. All tubes were weighed and rehydrated every 2 days to maintain 60% water-holding capacity during the experimental period [34]. Destructive sampling was performed on days 0, 23, 60, and 240 using separate PVC tubes assigned to each sampling date. Each PVC tube was sampled only once, and soil and litter were collected only at its designated sampling time. Thus, observations from different sampling dates were derived from different independently incubated PVC tubes rather than from repeated measurements of the same experimental unit. There were 60 experimental units in total. A total of 60 experimental units were included. The no-litter control represented day 0 of litter decomposition and was established across the three degradation levels with five replicates per level (15 units in total). The litter treatment was sampled after 23, 60, and 240 days across the same three degradation levels, with five replicates for each treatment combination (45 units in total). Litter was gently sieved through a 2 mm sieve to remove any adhering soil particles and then oven-dried at 60 °C for 48 h to reach a constant weight. Soil samples were stored in plastic bags and maintained at 4 °C and analyzed within one week of sampling.

2.2. Soil Organic Carbon and Physicochemical Property Analysis

The SOC content was determined using the dichromate oxidation method by Walkley and Black [35]. The 53 μm cutoff is a widely used operational threshold in soil organic matter fractionation in which the coarse fraction (>53 μm) is considered particulate organic carbon whereas the fine fraction (<53 μm) is considered mineral-associated organic carbon because it is more closely associated with silt- and clay-sized minerals [36,37]. Therefore, the POC fraction (>53 μm) and the MAOC fraction (<53 μm) were separated using the sodium hexametaphosphate method [31]. Soil dissolved organic carbon (DOC) was extracted with deionized water, filtered through a 0.45 μm membrane, and then quantified using a total C analyzer (TOC VCPH, Shimadzu, Kyoto, Japan) [38]. Soil microbial biomass carbon (MBC) was extracted using the fumigation–extraction method and measured with a fully automated chemical analyzer (Multi C/N 2100S, Analytik Jena, Jena, Germany). Soil pH was measured using a pH meter (Orion 868, Thermo Fisher Scientific, Waltham, MA, USA) in a 1:5 soil–deionized water suspension. The contents of total carbon and total nitrogen in the litter (LitterC and LitterN) and soil (SoilC and SoilN) were determined using an automatic elemental analyzer (Flash EA 1112, Thermo Fisher Scientific, Milan, Italy). The contents of total phosphorus in the litter (LitterP) and soil (SoilP) were detected using a continuous flow analyzer (Skalar, Breda, The Netherlands).

2.3. Phospholipid Fatty Acid Analysis (PLFA)

The soil microbial communities were characterized by using phospholipid fatty acid analysis (PLFA) as described and modified by Bossio et al. [39] with further slight modifications as described by Certini et al. [40]. Lipids were extracted from 8 g of freeze-dried soil using a chloroform–methanol–citrate buffer mixture (1:2:0.8) (Sinopharm Chemical Reagent Co., Ltd., Shanghai, China). PLFA biomarkers were used to characterize bacteria, fungi, and arbuscular mycorrhizal fungi (AMF), and the specific biomarkers assigned to each microbial group are listed in Table S2 [41–44]. All of the PLFAs indicated above were considered to be representative of the total PLFAs of soil microbial communities. The PLFA richness was calculated as the number of different PLFAs in each sample, and the PLFA abundance was expressed in nmol g^{-1} dry soil [45–47].

https://doi.org/10.3390/agronomy16080835

2.4. Analysis of Enzyme Activity

The activities of soil extracellular enzymes, including C-acquiring enzyme (β-1,4-glucosidase (BG) and cellobiose (CB)), N-acquiring enzyme (β-1,4-N-acetyl glucosaminidase (NAG) and 1-leucine aminopeptidase (LAP), and P-acquiring enzyme (alkaline phosphatase (AP)), were assayed using a microplate protocol [48]. The enzyme activity was expressed as nmol g^{-1} soil h^{-1}.

Microbial nutrient limitation was assessed using extracellular enzyme stoichiometric vector analysis following DeForest and Moorhead [49]. A greater vector length indicates stronger microbial C limitation. A vector angle of <45° indicates microbial N limitation, whereas a vector angle of >45° indicates microbial P limitation [44]. The *x*-axis was defined as (BG + CB)/AP, and the *y*-axis was defined as (BG + CB)/(LAP + NAG) [50,51]. Vector length (unitless) and vector angle (degree) were calculated as follows:

$$\text{Vector length} = \sqrt{\left[\frac{\ln(\text{BG} + \text{CB})}{\ln(\text{NAG} + \text{LAP})}\right]^2 + \left[\frac{\ln(\text{BG} + \text{CB})}{\ln\text{AP}}\right]^2} \quad (1)$$

$$\text{Vector angle} = \text{Degrees}\left\{\text{ATAN2}\left[\frac{\ln(\text{BG}+\text{CB})}{\ln \text{AP}}, \frac{\ln(\text{BG} + \text{CB})}{\ln(\text{NAG} + \text{LAP})}\right]\right\} \quad (2)$$

2.5. Statistical Analyses

A three-way ANOVA was first performed to examine the effects of degradation level, litter decomposition treatment, decomposition time, and their interactions on SOC, POC, and MAOC. Because decomposition time had no significant effect on these indicators, subsequent analyses were conducted using two-way ANOVA to evaluate the effects of degradation level, litter decomposition treatment, and their interaction. The two-way ANOVA approach was also used to assess soil physicochemical properties, microbial PLFA biomass, and enzyme activities. Duncan's post hoc test was used for multiple comparisons when significant effects were detected ($p < 0.05$). Mantel tests were used to evaluate the relationships of POC and MAOC with litter, soil physicochemical properties, and microbial indices. Structural equation modeling (SEM) was used to test the conceptual hypothesis that litter decomposition influences POC and MAOC both directly and indirectly through changes in soil physicochemical properties and microbial attributes. The detailed conceptual logic of the SEM is presented in Supplementary Table S3. The SEM was fitted using the lavaan package based on independent observations, as samples collected at each incubation time were destructively harvested and therefore treated as independent rather than repeated measures. Model fit was assessed based on the chi-square statistic (χ^2) and *p*-value, along with the standardized root mean square residual (SRMR), comparative fit index (CFI), and goodness-of-fit index (GFI). All SEM analyses were performed using the lavaan and piecewiseSEM packages in R 4.3.2 (R Foundation for Statistical Computing, Vienna, Austria). All statistical analyses were conducted using R 4.3.2. Final data visualization was performed using Origin 2024 (OriginLab Corporation, Northampton, MA, USA).

3. Results

3.1. Impact of Litter Addition on SOC and Its Fractions at Different Degradation Levels

Grassland degradation significantly reduced POC and MAOC ($p < 0.05$) but had no significant effect on SOC ($p > 0.05$) (Figure 1). Litter decomposition significantly decreased SOC in degraded grasslands. In the highly degraded grassland, litter decomposition significantly increased MAOC ($p < 0.05$). The POC/MAOC ratio reflects the stability of SOC. A lower ratio indicates a shift of carbon from the more labile POC pool to the more

https://doi.org/10.3390/agronomy16080835

stable MAOC pool. Degradation level had no significant effect on the POC/MAOC ratio ($p > 0.05$) (Figure 1). However, in the highly degraded grassland, litter decomposition significantly decreased the POC/MAOC ratio ($p < 0.05$).

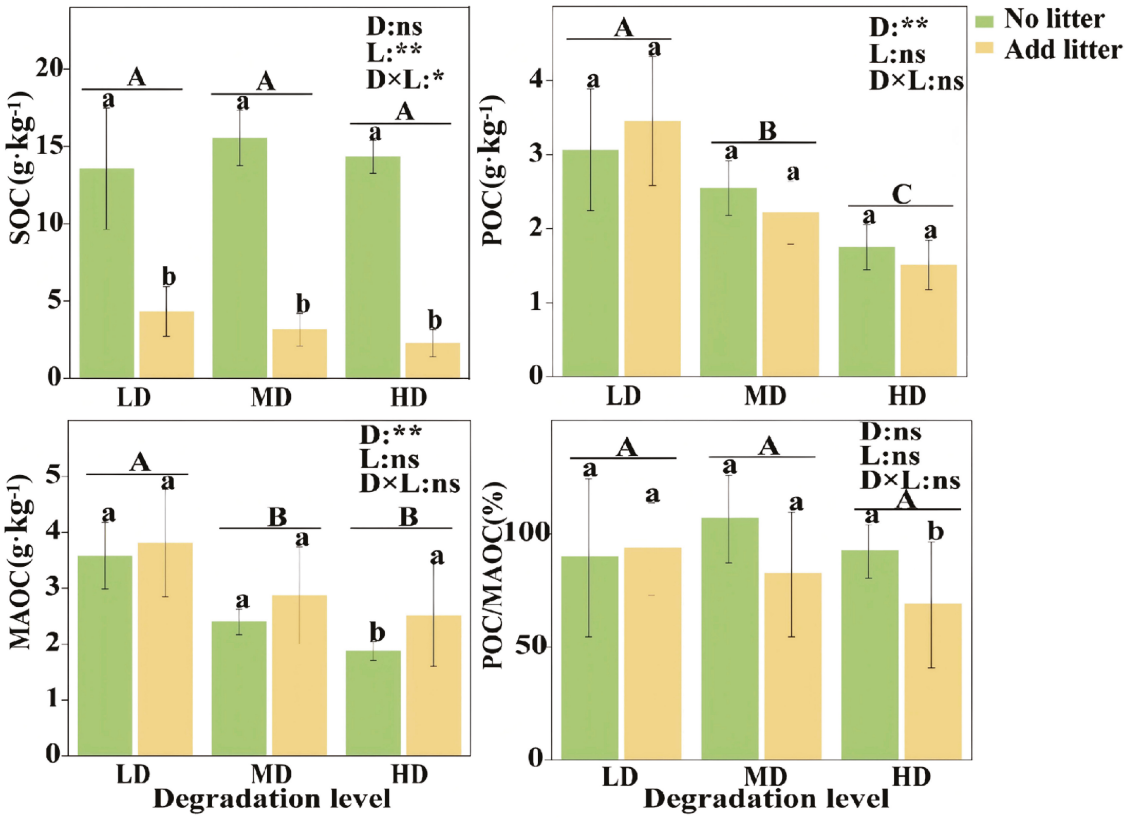


Figure 1. Effects of litter addition on SOC and its fractions in grasslands with different degradation levels. Different uppercase letters indicate significant differences among degradation-level treatments at $p < 0.05$; different lowercase letters indicate significant differences among litter addition treatments within the same degradation level at $p < 0.05$. D represents the degradation level; L represents litter decomposition; D × L represents the interaction between degradation level and litter decomposition; ns indicates no significant difference at the 0.05 level; * indicates significance at the 0.05 level; ** indicates significance at the 0.01 level.

3.2. Impact of Litter Addition on Soil Microbial Communities at Different Degradation Levels

Based on absolute PLFA biomass values, grassland degradation had a significant effect on bacteria, AMF, and the fungi/bacteria ratio ($p < 0.05$). Bacteria biomass were higher in the moderately degraded grasslands than in the highly degraded ones. The fungi/bacteria ratio significantly increased ($p < 0.05$), while AMF declined as degradation intensified ($p < 0.05$). In the lightly degraded grassland, litter addition led to significant reductions in the absolute PLFA biomass of fungi, bacteria, and the fungi/bacteria ratio ($p < 0.05$). In the moderately degraded grassland, litter addition caused a significant decrease in bacteria biomass and a significant increase in the fungi/bacteria ratio ($p < 0.05$). In the highly degraded grasslands, litter addition significantly decreased the absolute PLFA biomass of bacteria and AMF while increasing the fungi/bacteria ratio ($p < 0.05$) (Figure 2).

https://doi.org/10.3390/agronomy16080835

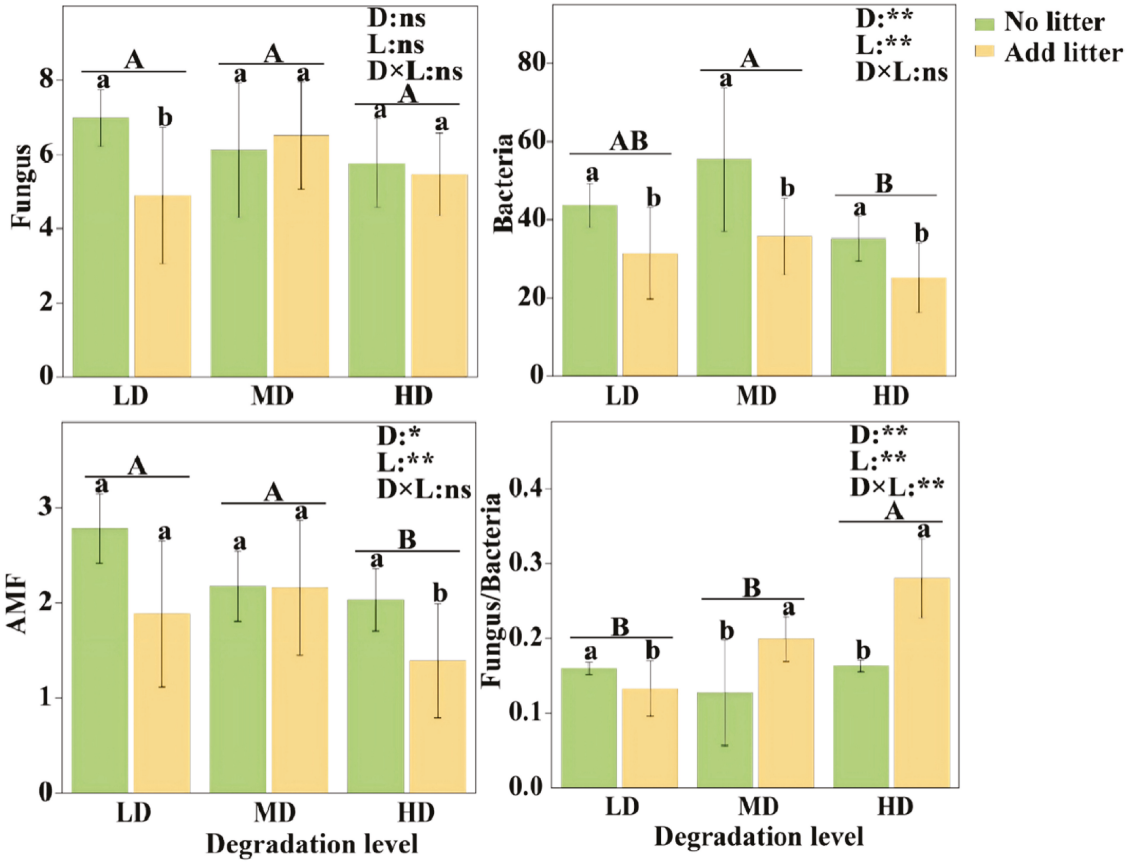


Figure 2. Effects of litter addition on PLFA in grasslands with different degradation levels. Different uppercase letters indicate significant differences among degradation-level treatments at $p < 0.05$; different lowercase letters indicate significant differences among litter addition treatments within the same degradation level at $p < 0.05$. D represents the degradation level; L represents litter decomposition; D × L represents the interaction between degradation level and litter decomposition; ns indicates no significant difference at the 0.05 level; * indicates significance at the 0.05 level; ** indicates significance at the 0.01 level.

3.3. Impact of Litter Addition on Soil Enzyme Activity at Different Degradation Levels

Grassland degradation significantly suppressed the C-enzyme, N-enzyme, and P-enzyme activity, vector length, and vector angle ($p < 0.05$). In the lightly and moderately degraded grasslands, litter addition significantly decreased N-enzyme activity and increased P-enzyme activity ($p < 0.05$). In the highly degraded grasslands, litter addition significantly suppressed the activities of C-enzyme and N-enzyme, vector length, and vector angle, whereas it significantly enhanced P-enzyme activity ($p < 0.05$). Across all three degradation levels, the vector angle remained below 45 degrees, indicating that soil microbial communities are predominantly in N-limited conditions (Figure 3).

3.4. Influence of Litter, Soil Physiochemistry, and Soil Microbes on POC and MAOC

In the lightly degraded grasslands, POC significantly correlated with soil pH, litter carbon, litter phosphorus, C-enzyme, vector length, and the fungi/bacteria ratio, whereas MAOC was primarily related to microbial biomass and community composition ($p < 0.05$) (Figure 4A,B). In the moderately degraded grasslands, POC was mainly correlated with labile carbon and litter nutrient variables, while MAOC was significantly correlated with soil pH and microbial attributes ($p < 0.05$) (Figure 4C,D). In the highly degraded grasslands, POC was significantly correlated with soil pH, DOC, litter phosphorus, and C-enzyme,

https://doi.org/10.3390/agronomy16080835

whereas MAOC was significantly associated with MBC, litter phosphorus, AMF, vector angle, and fungi/bacteria ratio ($p < 0.05$) (Figure 4E,F).

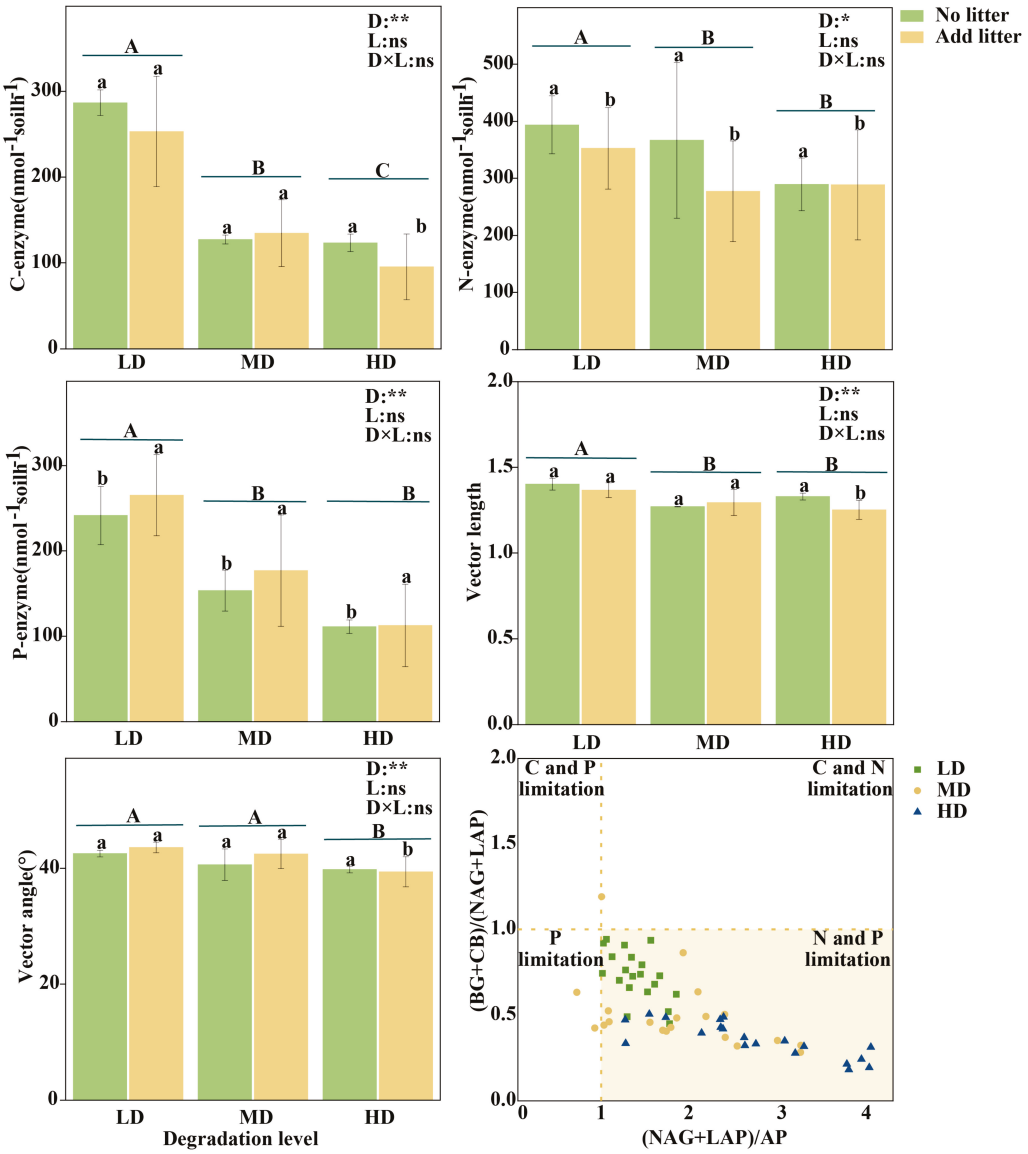


Figure 3. Effects of litter addition on soil extracellular enzyme activities, vector length, and angle in grasslands with different degradation levels. Different uppercase letters indicate significant differences among degradation-level treatments at $p < 0.05$; different lowercase letters indicate significant differences among litter addition treatments within the same degradation level at $p < 0.05$. D represents the degradation level; L represents litter decomposition; D × L represents the interaction between degradation level and litter decomposition; ns indicates no significant difference at the 0.05 level; * indicates significance at the 0.05 level; ** indicates significance at the 0.01 level.

The SEM in the lightly degraded level provided a good fit to the data ($p = 0.67$, $\chi^2 = 4.961$, df = 7, SRMR = 0.05, CFI = 1.00, GFI = 0.91). Litter addition indirectly affected both POC and MAOC by influencing soil physicochemical properties and microbial and enzyme activity. The SEM in the moderately degraded level provided a good fit to the data ($p = 0.68$, $\chi^2 = 4.00$, df = 6, SRMR = 0.07, CFI = 1.00, GFI = 0.94). Litter addition was associated with soil physicochemical properties and enzyme activity, and litter addition can directly affect POC and MAOC. The SEM in the highly degraded level provided a good fit to the data ($p = 0.70$, $\chi^2 = 2.19$, df = 4, SRMR = 0.04, CFI = 1.00, GFI = 0.98). Litter addition indirectly regulated both POC and MAOC through modifications in soil physicochemical

properties. Furthermore, litter addition directly enhanced MAOC and indirectly enhanced POC through enzyme activity. The SEM that examined the effects of degradation level and litter addition on POC and MAOC provided a good fit to the data (p = 0.58, χ^2 = 3.80, df = 5, SRMR = 0.03, CFI = 1.00, GFI = 1.00). Degraded grassland affected POC by altering soil physicochemical properties and interacting with microorganisms. It influenced MAOC through modifications in enzyme activities. Litter addition showed no significant influence on POC or MAOC (Figure 5).

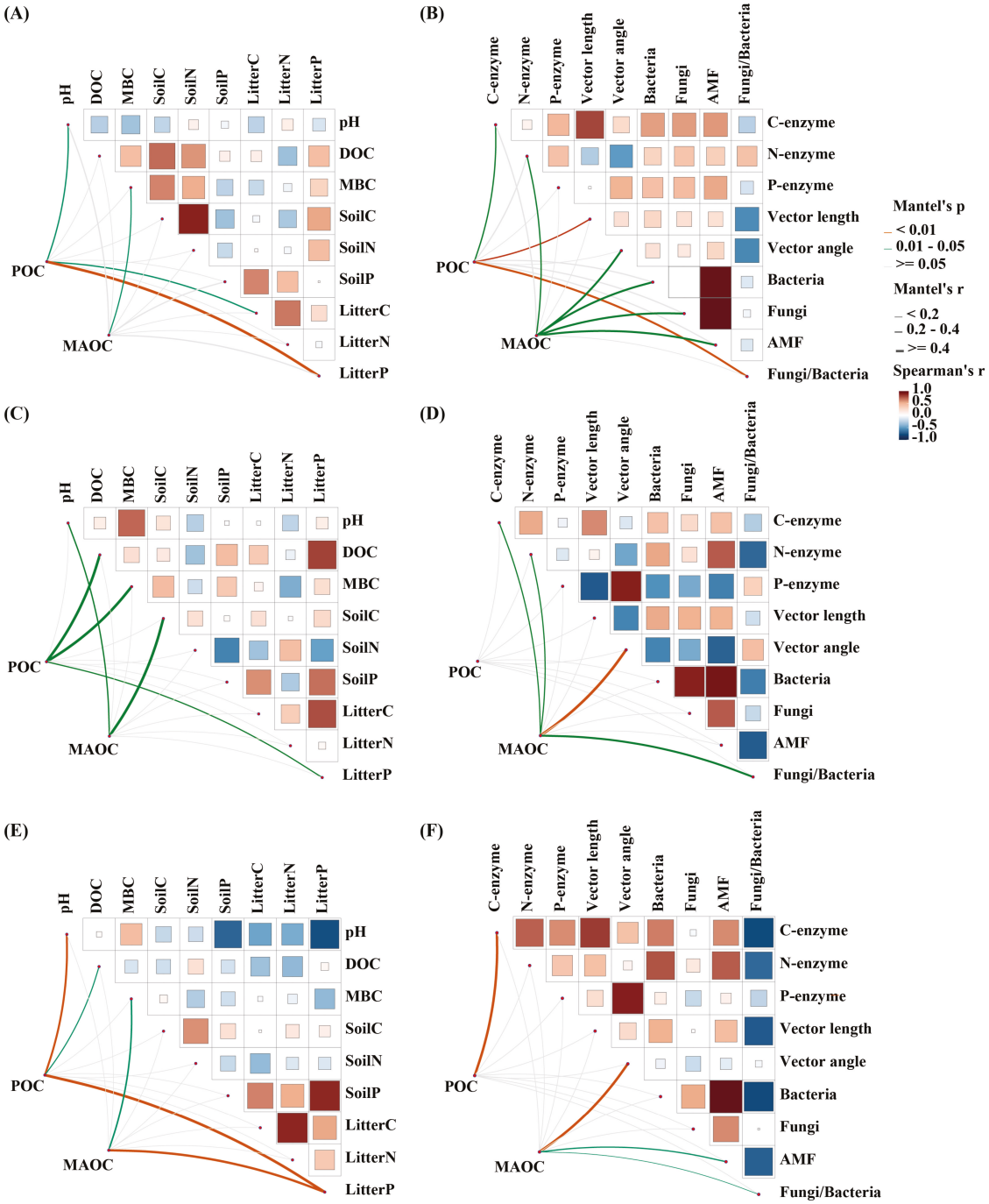


Figure 4. Correlation of litter, soil physicochemical properties, and microorganisms with POC and MAOC in grasslands with different degradation levels: (**A**,**B**) lightly degraded level; (**C**,**D**) moderately degraded level; (**E**,**F**) highly degraded level.

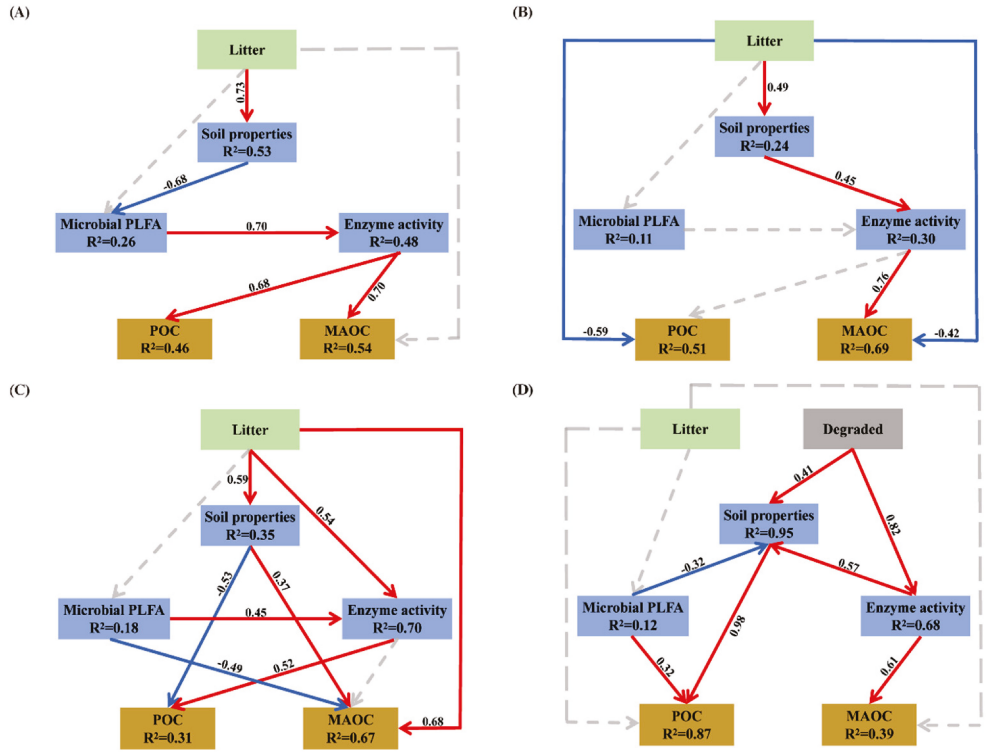


Figure 5. Path model of the effects of litter addition on POC and MAOC in grasslands with different degradation levels: (**A**) lightly degraded level; (**B**) moderately degraded level; (**C**) highly degraded level; (**D**) an overall model including litter addition and degradation level as exogenous drivers. The red and blue solid arrows indicate significant positive and negative effects, respectively.

4. Discussion

4.1. Effects of Grassland Degradation and Litter Addition on SOC and Its Fractions Contents

Our study demonstrated that grassland degradation significantly reduced POC and MAOC. This may be attributed to the fact that degradation deteriorates both above- and belowground environmental conditions, ultimately decreasing carbon inputs to the soil [2,52]. As plant-derived carbon constitutes the primary source of POC, a degradation-induced reduction in litter input may directly decrease POC concentrations [53]. The decline in MAOC with degradation may be attributed to a decrease in microbial biomass, which slows the formation of MAOC from microbial residues [54,55]. This result is consistent with previous studies that degradation significantly reduced both POC and MAOC, with POC often exhibiting a greater decline than MAOC [12,56]. The POC/MAOC ratio was used as an indicator reflecting the relative distribution of SOC between the more labile POC pool and the more stable MAOC pool and thus as a proxy for SOC stability within the degraded grasslands. Degradation had no significant effect on the POC/MAOC ratio, which may indicate that grassland degradation did not significantly alter the overall distribution of SOC between POC and MAOC and therefore did not significantly change SOC stability in Songnen grassland [57,58]. However, it is, unlike previous reports, showing a decline in the POC/MAOC ratio under degradation. Such differences may reflect the relatively greater persistence of MAOC than POC, which may allow MAOC to decline more slowly during degradation [53–55]. This interpretation is also supported by previous studies emphasizing the relatively persistent nature of mineral-associated organic carbon in soils [59].

In the lightly and moderately degraded grasslands, POC, MAOC, and their ratio were unchanged by litter addition. This likely indicates that litter addition did not significantly change the contents of these carbon fractions in the degraded grasslands under the incubation conditions used in this study [60]. In the highly degraded grasslands, litter addition

significantly increased MAOC. Compared to lightly and moderately degraded grasslands, highly degraded grasslands may have more fragile soil conditions and ecosystem instability, making them more responsive to microbial activation [61]. Thus, litter addition may stimulate microbial utilization of labile carbon components. Microorganisms may promote the association of labile carbon components with soil minerals, thereby facilitating the formation of MAOC [62]. Under the fragile habitat conditions of highly degraded grasslands, litter addition may therefore be more favorable for MAOC accumulation. Therefore, the effect of litter addition on SOC fractions became more evident as degradation intensified.

4.2. Mechanisms of SOC Fractions Following Litter Addition Across Grassland Degradation

In this study, the effects of litter addition on POC and MAOC varied with grassland degradation levels. The SEM results mainly reflected how litter addition influenced POC and MAOC through different pathways rather than whether litter addition significantly changed their final contents. In the lightly degraded grasslands, litter addition may have altered soil physicochemical properties, thereby influencing microbial enzyme activities and affecting POC and MAOC. One possible explanation is that changes in soil pH influenced microbial activity and organic carbon turnover [63]. However, according to the SOC fraction content results of this study, these pathway effects were not expressed as significant changes in POC or MAOC contents under light degradation. This suggests that in lightly degraded grasslands, litter addition may have modified the processes related to SOC fractions without producing sufficiently strong effects to alter their measured contents. In the moderately degraded grassland, the soil physicochemical and enzyme activities also contributed to POC and MAOC, but the mechanism was different from lightly degraded grassland. Similar patterns have also been reported in previous studies where microbial and environmental factors influenced the pathways related to SOC fractions even though no significant changes were observed in POC or MAOC contents [56,64]. Nevertheless, in the present study, litter addition did not significantly affect POC or MAOC contents under moderate degradation. Therefore, although litter addition influenced the pathways related to these two fractions, these effects were not strong enough to cause significant changes in their contents [65]. In the highly degraded grassland, biotic and abiotic factors exerted substantial effects on POC and MAOC. This may have been due to a combination of altering carbon availability and increasing environmental stress in the highly degraded grasslands. Under these conditions, fresh litter inputs may have been used more efficiently by microorganisms, thereby promoting microbial turnover and facilitating the incorporation of litter-derived carbon into POC and MAOC fractions [8,66,67]. This interpretation is consistent with previous studies on degraded grasslands showing that changes in carbon input and microbial carbon transformation can strongly affect the formation and stabilization of SOC fractions [54,68]. In our study, this interpretation is also consistent with the significant increase in MAOC under litter addition in the highly degraded grasslands.

Taken together, the following interpretation is intended as a conceptual framework for understanding the responses of SOC fractions along the degradation gradient, rather than as a direct result derived from this study. As degradation increased, litter addition appeared to influence POC and MAOC through an increasing variety of pathways. Within this conceptual context, the lightly degraded grasslands may approximate a relatively stable state close to a healthy ecosystem, the moderately degraded grasslands may be regarded as a transitional state with restoration potential, and the highly degraded grasslands may represent a more severely degraded condition with limited recovery potential [69]. This interpretation is also consistent with current conceptual frameworks of SOC formation, which emphasize that the balance among litter inputs, microbial transformation, and mineral stabilization governs the partitioning of carbon between POC and MAOC [70,71].

https://doi.org/10.3390/agronomy16080835

Accordingly, as ecosystems became increasingly vulnerable along the degradation gradient, biotic and abiotic constraints may have exerted progressively stronger effects on SOC fractions and their distribution in the degraded Songnen grasslands under the litter decomposition conditions examined in this study.

5. Conclusions

This study investigated the influence of litter addition on soil carbon through distinct transformation mechanisms in degraded grasslands. Grassland degradation led to an overall decline in SOC and its components, and litter addition exerted varying effects on MAOC across different degradation gradients. Litter addition in lightly degraded grasslands mainly acted through soil physicochemical and enzymatic pathways; in moderately degraded grasslands, it altered related pathways without significantly changing SOC fraction contents; and in highly degraded grasslands, stronger biotic and abiotic interactions were associated with clearer MAOC formation. As degradation increases, litter addition modulates SOC and its fractions through increasingly complex drivers involving a combination of biotic and abiotic factors. This suggests that the degraded soil ecosystem becomes more vulnerable, amplifying the effects of these factors on the SOC pool. Collectively, the positive effect of limited litter addition was insufficient to counteract degradation-induced carbon losses. The SEM results showed that increasing degradation was associated with more complex biotic and abiotic controls over POC and MAOC, indicating that degradation affected not only the magnitude of SOC decline but also the pathways regulating SOC fraction dynamics. Therefore, we recommend adopting restoration strategies that improve soil conditions conducive to MAOC formation (e.g., maintaining soil pH to facilitate microbial recovery) while implementing litter addition in degraded grasslands with sufficient duration and intensity to offset degradation-induced carbon losses and promote ecosystem recovery.

Supplementary Materials: The following supporting information can be downloaded at https://www.mdpi.com/article/10.3390/agronomy16080835/s1, Table S1: Effects of adding litter in degraded grasslands on litter and soil physicochemical properties. Table S2: Soil microbial phospholipid fatty acids (PLFA). Table S3: Ecological hypotheses to each pathway of the structural equation model [32,62,67,72–85].

Author Contributions: P.G. contributed to the study's conception and design. S.W., C.F., J.L. and J.Z. performed material preparation and data collection. S.W., L.R. and W.T. performed data analyses. S.W. wrote the manuscript. P.G. revised the manuscript. All authors have read and agreed to the published version of the manuscript.

Funding: This research was funded by the National Key R&D Program of China (2024YFD1501305), the National Science and Technology Fundamental Resources Investigation Program of China (2024FY100400), and the National Nature Science Foundation of China (41807046).

Data Availability Statement: The original contributions presented in the study are included in the article/Supplementary Material. Further inquiries can be directed to the corresponding author.

Acknowledgments: We thank Yunga Wu, Chao Hao and Peng Zhang for helping with field work.

Conflicts of Interest: The authors declare no conflicts of interest.

Abbreviations

The following abbreviations are used in this manuscript:

LD	Lightly degraded level
MD	Moderately degraded level
HD	Highly degraded level

Soil C	Soil total carbon
Soil N	Soil total nitrogen
Soil P	Soil total phosphorus
Litter C	Litter carbon
Litter N	Litter nitrogen
Litter P	Litter phosphorus

References

1. Bai, Y.; Cotrufo, M.F. Grassland soil carbon sequestration: Current understanding, challenges, and solutions. *Science* **2022**, *377*, 603–608. [CrossRef]
2. Dlamini, P.; Chivenge, P.; Manson, A.; Chaplot, V. Land degradation impact on soil organic carbon and nitrogen stocks of sub-tropical humid grasslands in South Africa. *Geoderma* **2014**, *235–236*, 372–381. [CrossRef]
3. Wu, Y.; He, J.; Liu, W.; Cheng, W.; Shaaban, M.; Jiang, Y. The effects of continuous straw returning strategies on SOC balance upon fresh straw incorporation. *Environ. Res.* **2023**, *232*, 116225. [CrossRef] [PubMed]
4. Neubauer, T.A.; Hauffe, T.; Silvestro, D.; Schauer, J.; Kadolsky, D.; Wesselingh, F.P.; Harzhauser, M.; Wilke, T. Current extinction rate in European freshwater gastropods greatly exceeds that of the late Cretaceous mass extinction. *Commun. Earth Environ.* **2021**, *2*, 97. [CrossRef]
5. Hu, Y.; Ao, G.; Fu, L.; Ji, C.; Zeng, H.; Zhu, B. Linking plant traits, soil nutrients, climate and soil microbes in temperate grasslands. *Plant Soil* 2025, *in press*. [CrossRef]
6. Lavallee, J.M.; Soong, J.L.; Cotrufo, M.F. Conceptualizing soil organic matter into particulate and mineral-associated forms to address global change in the 21st century. *Glob. Change Biol.* **2020**, *26*, 261–273. [CrossRef] [PubMed]
7. Zhang, S.; Zhou, X.; Chen, Y.; Du, F.; Zhu, B. Soil organic carbon fractions in China: Spatial distribution, drivers, and future changes. *Sci. Total Environ.* **2024**, *919*, 170890. [CrossRef]
8. Wu, J.; Zhang, H.; Pan, Y.; Cheng, X.; Zhang, K.; Liu, G. Particulate organic carbon is more sensitive to nitrogen addition than mineral-associated organic carbon: A meta-analysis. *Soil Tillage Res.* **2023**, *232*, 105770. [CrossRef]
9. Zhu, Y.; Hu, M.; Hui, D.; Niu, G.; Li, J.; Yao, X.; Hu, Y.; Huang, X.; Li, Y.; Zhang, D.; et al. Plants and microorganisms both contribute to soil organic matter formation through mineral interactions: Evidence from a subtropical forest succession. *Geoderma* **2024**, *452*, 117099. [CrossRef]
10. Zhang, Y.; Ge, X.; Li, Q.; Zhuang, S.; Shi, M.; Huang, X.; Qian, Z. Continuous organic mulching enhances the stability of soil organic carbon in *Phyllostachys praecox*: A 5-year in situ experiment. *Soil Ecol. Lett.* **2025**, *7*, 240290. [CrossRef]
11. Zhang, X.; Chang, F.; Zhang, H.; Wang, X.; Li, H.; Song, J.; Kan, Z.; Du, Z.; Zhou, J.; Chen, J.; et al. Divergent responses of particulate and mineral-associated organic carbon with soil depth under straw interlayer in saline-alkali soil. *Agric. Ecosys. Environ.* **2024**, *371*, 109073. [CrossRef]
12. Zhang, H.; Liu, G.; Wu, J. The Effect of Land Degradation and Restoration on Particulate and Mineral-Associated Organic Carbon. *Appl. Soil Ecol.* **2024**, *196*, 105322. [CrossRef]
13. Macheroum, A.; Chenchouni, H. Short-term land degradation driven by livestock grazing does not affect soil properties in semiarid steppe rangelands. *Front. Environ. Sci.* **2022**, *10*, 846045. [CrossRef]
14. Yang, N.; Zhang, M.; Pan, X.; Dang, P.; Wang, S.; Han, X.; Wang, X.; Zhang, C.; Meng, M.; Wang, W.; et al. Characteristics of changes to POC and MAOC after straw returning in China: A meta-analysis. *Land Degrad. Dev.* **2025**, *36*, 5199–5211. [CrossRef]
15. Feng, J.; He, K.; Zhang, Q.; Han, M.; Zhu, B. Changes in plant inputs alter soil carbon and microbial communities in forest ecosystems. *Glob. Change Biol.* **2022**, *28*, 3426–3440. [CrossRef]
16. Sokol, N.W.; Bradford, M.A. Microbial formation of stable soil carbon is more efficient from belowground than aboveground input. *Nat. Geosci.* **2019**, *12*, 46–53. [CrossRef]
17. Su, T.; Jiang, Y.; Chen, H.; Wang, Y.; Yang, Q.; Li, J.; Lu, J.-L.; Ran, H.; Yang, H.; Liu, W.; et al. Short-term nutrient addition increases soil organic carbon accumulation in tropical forest. *Plant Soil* **2025**, *514*, 3013–3029. [CrossRef]
18. Zeng, J.; Li, X.; Song, R.; Xie, H.; Li, X.; Liu, W.; Liu, H.; Du, Y.; Xu, M.; Ren, C.; et al. Mechanisms of litter input changes on soil organic carbon dynamics: A microbial carbon use efficiency-based perspective. *Sci. Total Environ.* **2024**, *949*, 175092.
19. Zhang, X.; You, Y.; Wang, D.; Zhu, L. Quality evaluation of the soil-root composites layer of Leymus chinensis grassland based on different degradation degrees. *Catena* **2022**, *215*, 106330. [CrossRef]
20. Liu, L.; Zuo, S.; Ma, M.; Li, J.; Guo, L.; Huang, D. Appropriate nitrogen addition regulates reproductive strategies of Leymus chinensis. *Glob. Ecol. Conserv.* **2021**, *27*, e01599. [CrossRef]
21. Wang, R.Z. Responses of Leymus chinensis (Poaceae) to long-term grazing disturbance in the Songnen grasslands of north-eastern China. *Grass Forage Sci.* **2004**, *59*, 191–195. [CrossRef]

22. Renzhong, W.; Ripley, E.A. Effects of grazing on a Leymus chinensis grassland on the Songnen plain of north-eastern China. *J. Arid Environ.* **1997**, *36*, 307–318. [CrossRef]
23. He, N.; Yu, Q.; Wu, L.; Wang, Y.; Han, X. Carbon and nitrogen store and storage potential as affected by land-use in a Leymus chinensis grassland of northern China. *Soil Biol. Biochem.* **2008**, *40*, 2952–2959. [CrossRef]
24. Wang, D.; Du, J.; Zhang, B.; Ba, L.; Hodgkinson, K.C. Grazing intensity and phenotypic plasticity in the clonal grass Leymus chinensis. *Rangel. Ecol. Manag.* **2017**, *70*, 740–747. [CrossRef]
25. Li, X.; Liu, J.; Fan, J.; Ma, Y.; Ding, S.; Zhong, Z.; Wang, D. Combined effects of nitrogen addition and litter manipulation on nutrient resorption of Leymus chinensis in a semi-arid grassland of northern China. *Plant Biol.* **2015**, *17*, 9–15. [CrossRef]
26. Pan, C.; Liu, C.; Zhao, H.; Wang, Y. Changes of soil physico-chemical properties and enzyme activities in relation to grassland salinization. *Eur. J. Soil Biol.* **2013**, *55*, 13–19. [CrossRef]
27. Wu, X.; Yang, J.; Ruan, H.; Wang, S.; Yang, Y.; Naeem, I.; Wang, L.; Liu, L.; Wang, D. The diversity and co-occurrence network of soil bacterial and fungal communities and their implications for a new indicator of grassland degradation. *Ecol. Indic.* **2021**, *129*, 107989. [CrossRef]
28. Yang, T.; Chen, J.; Zhong, X.; Yang, X.; Wang, G.; Yao, Y.; Sternberg, M.; Sun, W. Divergent responses of plant biomass and its allocation to the altered precipitation regimes among different degraded grasslands in China. *Plant Soil* **2022**, *473*, 149–166. [CrossRef]
29. Liu, H.; Yin, Y.; Tian, Y.; Ren, J.; Wang, H. Climatic and anthropogenic controls of topsoil features in the semi-arid East Asian steppe. *Geophys. Res. Lett.* **2008**, *35*, L04401. [CrossRef]
30. Liu, Y.; Zhou, Y.; Fang, L.; Yang, C. Arbuscular mycorrhizal fungal colonization at different succession stages in Songnen saline-alkali grassland. *Phyton* **2023**, *92*, 297. [CrossRef]
31. Zhao, C.; Li, Q.; Cheng, L.; Zhong, R. Effects of mowing regimes on forage yield and crude protein of *Leymus chinensis* (Trin.) Tzvel in Songnen grassland. *Grassl. Sci.* **2021**, *67*, 275–284. [CrossRef]
32. Li, J.; Niu, X.; Wang, P.; Yang, J.; Liu, J.; Wu, D.; Guan, P. Soil degradation regulates the effects of litter decomposition on soil microbial nutrient limitation: Evidence from soil enzymatic activity and stoichiometry. *Front. Plant Sci.* **2022**, *13*, 1090954. [CrossRef]
33. Maggiotto, G.; Sabatté, L.; Marina, T.I.; Fueyo-Sánchez, L.; Ramírez Londoño, A.M.; Díaz Porres, M.; Rionda, M.; Domínguez, M.; Perelli, R.; Momo, F.R. Soil fauna community and ecosystem's resilience: A food web approach. *Acta Oecol.* **2019**, *99*, 103445. [CrossRef]
34. Creamer, C.A.; Macdonald, L.M.; Baldock, J.A.; Sanderman, J.; Farrell, M. Divergent responses of organic matter composition to incubation temperature. *Geoderma* **2015**, *259–260*, 279–287. [CrossRef]
35. Cambardella, C.A.; Elliott, E.T. Particulate soil organic-matter changes across a grassland cultivation sequence. *Soil Sci. Soc. Am. J.* **1992**, *56*, 777–783. [CrossRef]
36. Six, J.; Conant, R.T.; Paul, E.A.; Paustian, K. Stabilization mechanisms of soil organic matter: Implications for C-saturation of soils. *Plant Soil* **2002**, *241*, 155–176. [CrossRef]
37. Castellano, M.J.; Mueller, K.E.; Olk, D.C.; Sawyer, J.E.; Six, J. Mechanisms of soil organic carbon and nitrogen stabilization in mineral-associated organic matter: Insights from modeling in phase space. *Glob. Change Biol.* **2015**, *21*, 4544–4559.
38. Wu, H.; Lu, X.; Tong, S.; Batzer, D.P. Soil engineering ants increase CO_2 and N_2O emissions by affecting mound soil physicochemical characteristics from a marsh soil: A laboratory study. *Appl. Soil Ecol.* **2015**, *87*, 19–26. [CrossRef]
39. Bossio, D.A.; Scow, K.M.; Gunapala, N.; Graham, K.J. Determinants of soil microbial communities: Effects of agricultural management, season, and soil type on phospholipid fatty acid profiles. *Microb. Ecol.* **1998**, *36*, 1–12. [CrossRef]
40. Certini, G.; Campbell, C.D.; Edwards, A.C. Rock fragments in soil support a different microbial community from the fine earth. *Soil Biol. Biochem.* **2004**, *36*, 1119–1128. [CrossRef]
41. Dempsey, M.A.; Fisk, M.C.; Yavitt, J.B.; Fahey, T.J.; Balser, T.C. Exotic earthworms alter soil microbial community composition and function. *Soil Biol. Biochem.* **2013**, *67*, 263–270. [CrossRef]
42. Briar, S.S.; Fonte, S.J.; Park, I.; Six, J.; Scow, K.; Ferris, H. The distribution of nematodes and soil microbial communities across soil aggregate fractions and farm management systems. *Soil Biol. Biochem.* **2011**, *43*, 905–914. [CrossRef]
43. Bach, E.M.; Baer, S.G.; Meyer, C.K.; Six, J. Soil texture affects soil microbial and structural recovery during grassland restoration. *Soil Biol. Biochem.* **2010**, *42*, 2182–2191. [CrossRef]
44. McKinley, V.L.; Peacock, A.D.; White, D.C. Microbial community PLFA and PHB responses to ecosystem restoration in tallgrass prairie soils. *Soil Biol. Biochem.* **2005**, *37*, 1946–1958. [CrossRef]
45. de Vries, F.T.; Thébault, E.; Liiri, M.; Birkhofer, K.; Tsiafouli, M.A.; Bjørnlund, L.; Jørgensen, H.B.; Brady, M.V.; Christensen, S.; de Ruiter, P.C.; et al. Soil food web properties explain ecosystem services across European land use systems. *Proc. Natl. Acad. Sci. USA* **2013**, *110*, 14296–14301. [CrossRef]
46. Klamer, M. Estimation of conversion factors for fungal biomass determination in compost using ergosterol and PLFA 18:2ω6,9. *Soil Biol. Biochem.* **2004**, *36*, 57–65. [CrossRef]

47. Olsson, P.A.; Bååth, E.; Jakobsen, I.; Söderström, B. The use of phospholipid and neutral lipid fatty acids to estimate biomass of arbuscular mycorrhizal fungi in soil. *Mycol. Res.* **1995**, *99*, 623–629. [CrossRef]
48. Sinsabaugh, R.L.; Lauber, C.L.; Weintraub, M.N.; Ahmed, B.; Allison, S.D.; Crenshaw, C.; Contosta, A.R.; Cusack, D.; Frey, S.; Gallo, M.E.; et al. Stoichiometry of soil enzyme activity at global scale. *Ecol. Lett.* **2008**, *11*, 1252–1264. [CrossRef]
49. DeForest, J.L.; Moorhead, D.L. Effects of elevated pH and phosphorus fertilizer on soil C, N and P enzyme stoichiometry in an acidic mixed mesophytic deciduous forest. *Soil Biol. Biochem.* **2020**, *150*, 107996. [CrossRef]
50. Bai, X.; Dippold, M.A.; An, S.; Wang, B.; Zhang, H.; Loeppmann, S. Extracellular enzyme activity and stoichiometry: The effect of soil microbial element limitation during leaf litter decomposition. *Ecol. Indic.* **2021**, *121*, 107200. [CrossRef]
51. Moorhead, D.L.; Rinkes, Z.L.; Sinsabaugh, R.L.; Weintraub, M.N. Dynamic relationships between microbial biomass, respiration, inorganic nutrients and enzyme activities: Informing enzyme-based decomposition models. *Front. Microbiol.* **2013**, *4*, 223. [CrossRef]
52. Peng, F.; Xue, X.; You, Q.; Huang, C.; Dong, S.; Liao, J.; Duan, H.; Tsunekawa, A.; Wang, T. Changes of soil properties regulate the soil organic carbon loss with grassland degradation on the Qinghai-Tibet Plateau. *Ecol. Indic.* **2018**, *93*, 572–580. [CrossRef]
53. Chen, J.; Xiao, W.; Zheng, C.; Zhu, B. Nitrogen addition has contrasting effects on particulate and mineral-associated soil organic carbon in a subtropical forest. *Soil Biol. Biochem.* **2020**, *142*, 107708. [CrossRef]
54. Pereira, A.P.D.A.; Mendes, L.W.; Oliveira, F.A.S.; Antunes, J.E.L.; Melo, V.M.M.; Araujo, A.S.F. Land degradation affects the microbial communities in the Brazilian Caatinga biome. *Catebna* **2022**, *211*, 105961. [CrossRef]
55. Liang, C.; Schimel, J.P.; Jastrow, J.D. The importance of anabolism in microbial control over soil carbon storage. *Nat. Microbiol.* **2017**, *2*, 17105. [CrossRef]
56. Song, M.; Pang, R.; Tian, Y.; Li, Y.; Wang, G.; Xu, X. Functional shift in soil microbiome with decline in photosynthetic carbon input signifies rapid decrease of soil organic carbon during alpine grassland degradation. *Biol. Fertil. Soils* **2025**, *61*, 893–908. [CrossRef]
57. Jiang, R.; Liu, S.; Jiang, F.; Guo, Z.; Adingo, S.; Chen, Z.; Gao, L.; Peng, X. Soil organic carbon trade-offs under conservation tillage: Carbon stock versus stability mediated by particulate and mineral-associated fractions. *Soil Tillage Res.* **2025**, *254*, 106704. [CrossRef]
58. Kong, W.; Xiao, J.; Liu, J.; Yao, Y.; Qiu, L.; Shao, M.; Wei, X. Spatiotemporal variability in divergent accrual of particulate and mineral-associated organic carbon by vegetation restoration on the Loess Plateau. *Agric. Ecosyst. Environ.* **2025**, *393*, 109856. [CrossRef]
59. Lavallee, J.M.; Soong, J.L.; Cotrufo, M.F. Soil carbon storage informed by particulate and mineral-associated organic matter. *Nat. Geosci.* **2020**, *13*, 794–804.
60. Georgiou, K.; Angers, D.; Champiny, R.E.; Cotrufo, M.F.; Craig, M.E.; Doetterl, S.; Grandy, A.S.; Lavallee, J.M.; Lin, Y.; Lugato, E.; et al. Soil carbon saturation: What do we really know? *Glob. Change Biol.* **2025**, *31*, e70197. [CrossRef]
61. Liao, C.; Chang, K.; Wu, B.; Zhang, D.; Wang, C.; Cheng, X. Divergence in soil particulate and mineral-associated organic carbon reshapes carbon stabilization along an elevational gradient. *Catena* **2024**, *235*, 107682. [CrossRef]
62. Wang, K.; Ma, Z.; Qin, W.; Li, X.; Shi, H.; Hasi, B.; Liu, X. Soil nutrients and pH modulate carbon dynamics in particulate and mineral-associated organic matter during restoration of a tibetan alpine grassland. *Ecol. Eng.* **2025**, *212*, 107522. [CrossRef]
63. Xu, S.; Sayer, E.J.; Eisenhauer, N.; Lu, X.; Wang, J.; Liu, C. Aboveground litter inputs determine carbon storage across soil profiles: A meta-analysis. *Plant Soil* **2021**, *462*, 429–444. [CrossRef]
64. Kotroczó, Z.; Veres, Z.; Fekete, I.; Krakomperger, Z.; Tóth, J.A.; Lajtha, K.; Tóthmérész, B. Soil enzyme activity in response to long-term organic matter manipulation. *Soil Biol. Biochem.* **2014**, *70*, 237–243. [CrossRef]
65. Kleber, M.; Eusterhues, K.; Keiluweit, M.; Mikutta, C.; Mikutta, R.; Nico, P.S. Mineral–organic associations: Formation, properties, and relevance in soil environments. In *Advances in Agronomy*; Sparks, D.L., Ed.; Academic Press: San Diego, CA, USA, 2015; Volume 130, pp. 1–140.
66. Yang, Y.; Dou, Y.; Wang, B.; Wang, Y.; Liang, C.; An, S.; Soromotin, A.; Kuzyakov, Y. Increasing contribution of microbial residues to soil organic carbon in grassland restoration chronosequence. *Soil Biol. Biochem.* **2022**, *170*, 108688. [CrossRef]
67. Hansen, P.M.; Zhang, Y.; Guseva, K.; Kaiser, C.; Cotrufo, M.F. Microbial community regulation of extracellular enzyme production can mediate patterns of particulate and mineral-associated organic matter accumulation in undersaturated soils. *Soil Biol. Biochem.* **2026**, *214*, 110056. [CrossRef]
68. Bastida, F.; García, C.; Fierer, N.; Eldridge, D.J.; Bowker, M.A.; Abades, S.; Alfaro, F.D.; Berhe, A.A.; Cutler, N.A.; Gallardo, A.; et al. Global ecological predictors of the soil priming effect. *Nat. Commun.* **2019**, *10*, 3481. [CrossRef] [PubMed]
69. Wu, M.; Chen, L.; Chen, S.; Chen, Y.; Ma, J.; Zhang, Y.; Pang, D.; Li, X. Soil microbial carbon and nitrogen limitation constraints soil organic carbon stability in arid and semi-arid grasslands. *J. Environ. Manag.* **2025**, *373*, 123675. [CrossRef]
70. Kramer, C.; Gleixner, G. Variable use of plant- and soil-derived carbon by microorganisms in agricultural soils. *Soil Biol. Biochem.* **2006**, *38*, 3267–3278. [CrossRef]

71. Liu, M.; Liu, S.; Xu, X.; Soromotin, A.V.; Kuzyakov, Y. Does restoration of degraded grasslands follow the theory of multiple stable states? *Agric. Ecosyst. Environ.* **2025**, *383*, 109508. [CrossRef]
72. Chen, R.; Yin, L.; Wang, X.; Chen, T.; Jia, L.; Jiang, Q.; Lyu, M.; Yao, X.; Chen, G. Mineral-associated organic carbon predicts the variations in microbial biomass and specific enzyme activities in a subtropical forest. *Geoderma* **2023**, *439*, 116671. [CrossRef]
73. Gao, H.; Zhang, S.; Yang, Z.; Xu, H.; Huang, H.; Wang, C.; Zhang, L. Effects of Litter Input on Soil Enzyme Activities and Their Stoichiometric Ratios in Sandy Soil. *Agronomy* **2025**, *15*, 1152. [CrossRef]
74. Heijboer, A.; de Ruiter, P.C.; Bodelier, P.L.E.; Kowalchuk, G.A. Modulation of litter decomposition by the soil microbial food web under influence of land use change. *Front. Microbiol.* **2018**, *9*, 2860. [CrossRef] [PubMed]
75. King, A.E.; Amsili, J.P.; Córdova, S.C.; Culman, S.; Fonte, S.J.; Kotcon, J.; Liebig, M.; Masters, M.D.; McVay, K.; Olk, D.C.; et al. A soil matrix capacity index to predict mineral-associated but not particulate organic carbon across a range of climate and soil pH. *Biogeochemistry* **2023**, *165*, 1–14. [CrossRef]
76. Li, Y.; Zhao, L.; Hilal, M.G.; Guo, L.; Zhang, Y.; Ji, Y.; Jiang, X.; Hao, L.; Lin, K. Effects of grassland degradation on soil ecological stoichiometry and soil microbial community on the South of the Greater Khingan Mountains. *Front. Microbiol.* **2024**, *15*, 1438787. [CrossRef]
77. Liang, Y.; Leifheit, E.F.; Lehmann, A.; Rillig, M.C. Soil organic carbon stabilization is influenced by microbial diversity and temperature. *Sci. Rep.* **2025**, *15*, 13990. [CrossRef]
78. Norris, C.E.; Swallow, M.J.B.; Liptzin, D.; Cope, M.; Mac Bean, G.; Cappellazzi, S.B.; Greub, K.L.H.; Rieke, E.L.; Tracy, P.W.; Morgan, C.L.S.; et al. Use of phospholipid fatty acid analysis as phenotypic biomarkers for soil health and the influence of management practices. *Appl. Soil Ecol.* **2023**, *185*, 104793. [CrossRef]
79. She, Y.; Zhang, Z.; Ma, L.; Xu, W.; Huang, X.; Zhou, H. Vegetation attributes and soil properties of alpine grassland in different degradation stages on the Qinghai-Tibet Plateau, China: A meta-analysis. *Arab. J. Geosci.* **2022**, *15*, 193. [CrossRef]
80. Si, Q.; Chen, K.; Wei, B.; Zhang, Y.; Sun, X.; Liang, J. Dissolved carbon flow to particulate organic carbon enhances soil carbon sequestration. *Soil* **2024**, *10*, 441–450. [CrossRef]
81. Taggart, M.G.; Baah, D.S.; Allen, S.; Khan, Z.; Arnscheidt, J.; Jordan, P.; O'Hagan, B.M.G.; Ibrahim, A.D.; Rao, J.R.; Ternan, N.G. Fitting soil extracellular enzyme activity into the complex network of abiotic and biotic soil properties often associated with soil health. *Front. Microbiol.* **2025**, *16*, 1638267. [CrossRef]
82. Wang, S.; Abalori, T.A.; Wang, W.; Deng, X.; Liu, W.; Wang, J.; Cao, W. Response of soil microbial compositional and functional heterogeneity to grazing exclusion in alpine shrub and meadows in the Qinghai–Tibet Plateau. *Front. Microbiol.* **2022**, *13*, 1038805. [CrossRef] [PubMed]
83. Yan, S.; Shang, Z.; Deng, A.; Zhang, W. Spatiotemporal Characteristics and Reduction Approaches of Farmland N_2O Emission in China. *Crops* **2022**, *38*, 1–8.
84. Zeng, P.; Zuo, H.; Sun, Q.; Wen, Y.; Zhang, Z.; Luo, Q.; Wang, X.; Zhu, J.; Wang, Q. Active restoration of degraded alpine grassland weakens mineral-associated soil organic carbon retention. *J. Appl. Ecol.* **2025**, *62*, 1282–1295. [CrossRef]
85. Zheng, T.; Liang, C.; Xie, H.; Zhao, J.; Yan, E.; Zhou, X.; Bao, X. Rhizosphere effects on soil microbial community structure and enzyme activity in a successional subtropical forest. *FEMS Microbiol. Ecol.* **2019**, *95*, fiz043. [CrossRef] [PubMed]

Disclaimer/Publisher's Note: The statements, opinions and data contained in all publications are solely those of the individual author(s) and contributor(s) and not of MDPI and/or the editor(s). MDPI and/or the editor(s) disclaim responsibility for any injury to people or property resulting from any ideas, methods, instructions or products referred to in the content.

agronomy

MDPI

Article

Management Practices in Mountain Meadows: Consequences for Soil Nutrient Availability

Adrián Jarne, Asunción Usón and Ramón Reiné *

Departamento de Ciencias Agrarias y del Medio Natural, Escuela Politécnica Superior, Universidad de Zaragoza, Ctra Cuarte s/n, 22071 Huesca, Spain; ajarne@unizar.es (A.J.); mauson@unizar.es (A.U.)
* Correspondence: rreine@unizar.es

Abstract: Soil nutrient availability in meadows has been poorly studied from the management point of view, despite its great impact. In this study, three different types of meadows have been analysed, as follows: intensive meadows, with high livestock load and inorganic fertilization; semi-extensive meadows, with medium livestock load and organic fertilization; and extensive meadows, with low livestock load and low fertilization rates. We looked at the nitrogen, phosphorus, potassium and carbon balances of each meadow type during two different years. Nitrogen was more stable in semi-extensive and extensive meadows, due to its organic form. In contrast, intensive meadows showed higher nitrogen variability depending on climate. Phosphorus is seen as the limiting nutrient, and it accumulates less in the soil than what is estimated in the crop balance, being more balanced in extensive meadows. Potassium has a strong response to temperature, being more available in June than in February, but crop balance was always negative for extensive meadows, and its soil concentration decreases each year, which could cause long-term potassium deficiency. Carbon accumulation was more stable in extensive meadows, where there was accumulation regardless of the year, whereas intensive and semi-extensive meadows become carbon emitters during the drought year.

Keywords: grassland; nitrate; phosphorus; potassium; carbon; nutrient balance

1. Introduction

Soil nutrient availability has been largely studied in many different crops and grasslands. It has been shown that many different factors affect it, ranging from climate to soil microorganisms. In the specific case of mountain meadows, there is not much information about nutrient availability, and even less from the management point of view [1,2].

Mountain meadows of the Spanish central Pyrenees are grazed during the spring and autumn; there is also mowing at the end of spring or the start of the summer to obtain hay for the winter [3,4]. In some cases, and depending on the climate, it is possible to have a second cut. Fertilization can vary according to location and farm management dynamics. Usually, meadows are fertilized using the manure from the farm, or they are not fertilized. We can also find meadows where inorganic fertilizers are applied to increase their productivity [5]. Typically, because of mountain orography, meadows are in small plots, with steep slopes that complicate their management. Also, their soils are usually shallow and have low fertility, with a climate that makes the growing season short, resulting in low productivity. As farms are getting larger and more mechanized, some meadows have been abandoned, and others have been intensified. In some valleys, up to 40% of meadow areas have been lost [6,7].

Meadows are composed of various species from different botanical families, making them important reservoirs of biodiversity [8]. Although plant diversity makes them more adaptable to a various range of conditions, it makes them more complex to study, as each meadow will behave differently, according to its floristic composition [9].

Management has an impact on different aspects of meadow dynamics. Mowing frequency, fertilization and livestock load can change floristic composition and nutrient availability [10,11]:

- Increasing the livestock load will increase the amount of nutrient input as excrements, but on the other hand can put excessive pressure on plants and provoke changes in meadow composition [12].
- Fertilization has been shown to be one of the major drivers of floristic composition changes, especially when there is inorganic nitrogen fertilization, which can lead to an increase in grass species and a decline in legumes [10,13,14]. Nutrient availability is also affected by changes in management. For example, when too much nitrogen is applied, it could lead to depletion of the phosphorus and potassium soil reservoir and therefore reduce yield [15,16].
- Even the fertilizer type can have an impact. Organic fertilizers are usually applied in high volumes and have much organic matter, enhancing nutrient availability and enrichment of soil, whereas inorganic fertilizers can also enrich the soil, but nutrients could remain immobilized [17,18].

The nutrient balance of meadows has been poorly analysed compared to other crops, even though it determines meadows' long-term sustainability. Nitrogen, phosphorus and potassium are the most important nutrients; if the balance becomes negative year on year, it will cause nutrient depletion and consequently yield decrease [19]. On the other hand, when the balance is positive year on year, especially in the case of nitrogen, it could lead to environmental issues like water eutrophication. In addition, a positive balance of any nutrient implies that the farmer is investing more resources than needed to get the same yield, making their business less efficient and affecting their profitability [15,20].

There are many environmental ecosystemic services that are provided by meadows, such as serving as biodiversity reservoirs, decreasing fire risks, and reducing erosion [21]. Carbon storage is also an important ecosystemic service, as meadows act as carbon sinks through the accumulation of organic matter. As there is no ploughing, organic matter accumulates in the soil, although it has been observed that during heat and drought stress, meadows can swift from carbon sinks into carbon sources during the stress [22–25].

In this study, we are going to analyse the nitrogen, phosphorus, potassium and carbon balances of three different meadow types, which have three different levels of intensification practices. Our hypothesis is that meadow intensification could increase nitrogen soil concentration, which could cause environmental problems such as water eutrophication due to nitrogen lixiviation. On the other hand, we expect phosphorus and potassium soil concentration to decrease as intensification increases, because of fertilization imbalance. We also expect to find higher carbon accumulation in extensive meadows.

2. Materials and Methods

The study is in the central area of the Spanish Pyrenees, in the valleys of the Gállego, Cinca and Ésera rivers. Along the three valleys, we sampled a total of 12 meadows corresponding to 3 different types: intensive, semi-extensive, and extensive [26,27]:

- Intensive meadows: located in the bottom of the valley, usually close to the barn, where the animals stay many days, resulting in high livestock loads. To be able to deal with the livestock load and increase their productivity, the meadows are usually fertilized with inorganic fertilizer.
- Semi-extensive meadows: located in the middle of the valley, also close to the barn and usually in deep soils with high fertility. Due to their location close to the barn, they are fertilized with manure from the farm, which increases their productivity and soil fertility. But as the climate is colder than in the bottom of the valley, there are fewer available days for grazing, resulting in lower livestock loads.
- Extensive meadows: located in the high areas of the valley and surrounded by forest, they are the fields farthest from the farm. They are rarely fertilized, mainly due to the

distance from the farm, and as a result they have lower productivity. Also, the colder climate limits the number of days where they can be grazed, which in combination with their lower productivity leads to lower livestock load capacity.

We can observe in Figure 1 that intensive meadows are in the lower parts of the valleys, and as a result they are at lower altitudes. In Table 1, we found the highest altitudes in extensive meadows. All meadows except extensive meadows are fertilized yearly. The fertilizer type is organic, except in intensive meadows, where it is inorganic. Slopes are higher in semi-extensive and extensive meadows. Legume cover is similar in all cases, being more variable in intensive meadows. All meadows are in Haplic Regosol soils. Intensive meadows have more clay content, whereas extensive meadows have more sand. pH is higher in intensive meadows. Conductivity is higher in semi-extensive meadows. Organic matter in extensive and semi-extensive meadows is more than double that of intensive meadows.

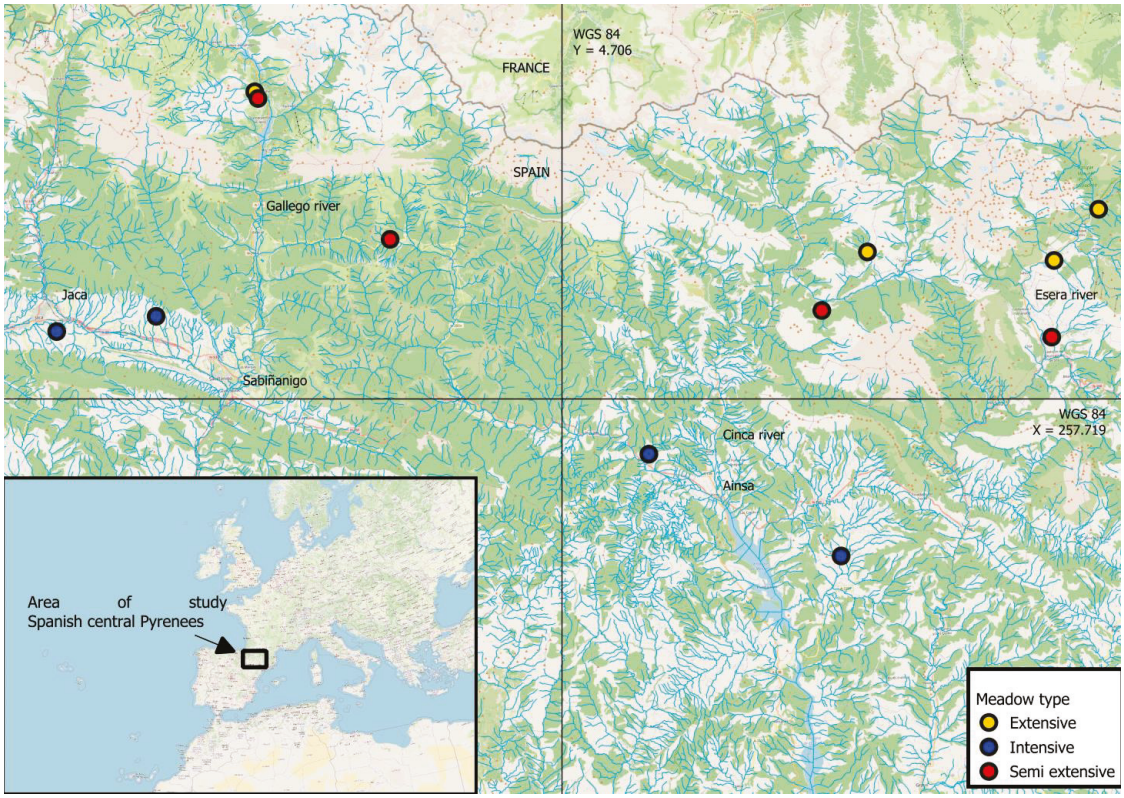


Figure 1. Map of studied meadows.

Table 1. Meadow characteristics [3].

	Intensive Meadow	Semi-Extensive Meadow	Extensive Meadow
Altitude (m)	602–890	902–1290	1100–1612
Fertilization type	Inorganic	Organic	Organic/None
Fertilization frequency	Yearly	Yearly	Rarely
Slope (%)	9.63 ± 4.13	18.6 ± 4.99	16.1 ± 5.35
Legume cover (%)	26.25 ± 21.99	24.3 ± 5.95	23.3 ± 5.33
Soil type (WRB)	Haplic Regosol	Haplic Phaeozem	Haplic Phaeozem
Clay (%)	30.47 ± 4.87	23.62 ± 4.26	16.29 ± 5.04
Sand (%)	21.01 ± 7.92	40.50 ± 9.49	51.61 ± 9.88
pH	7.71 ± 0.3	6.94 ± 0.29	6.82 ± 0.41
Electric conductivity (dS/m)	0.23 ± 0.05	0.28 ± 0.06	0.21 ± 0.06
Organic matter (%)	3.78 ± 2.12	9.93 ± 3.58	9.25 ± 3.18

Hay samples were taken from 6 plot enclosures (40 cm × 60 cm), half of them being mowed as the same time as the farmer and the other half earlier, when the crop reached its optimal protein content. Production (kg DM/ha) was calculated by weighing the oven-dried biomass (65 °C for 48 h).

For nutrient extraction, protein and fibre content, samples were taken to the laboratory, where the determinations were performed as follows: laboratory dry matter at 105 °C for 4 h; nitrogen content (N) was determined using the Kjeldahl method, and crude protein (CP) concentrations were calculated from it by multiplying N × 6.25. Ash-free neutral detergent fibre (NDF) and acid detergent fibre (ADF) were quantified using an Ankom 200 fibre analyser (Ankom Technol. Corp., Fairport, NY, USA), according to Van Soest et al. [28].

Relative feed value (RFV) is an index that combines important nutritional factors (potential intake and digestibility) into a single number, providing a quick and effective method for evaluating feed value or quality. The RFV was calculated using the estimates of digestible dry matter (DDM%) and potential dry matter intake (DMI% of body weight) of the forage, based on the ADF and the NDF fractions [29].

Soil samples of 1 kg were taken at random from 3 different places in the meadows using an Eijkelkamp hand auger and homogenized into a single sample. They were taken at two times: at the beginning of the year, during February, before fertilizer was applied, and the last one in June, right after hay harvest.

Soil analysis covered nitrogen in its nitrate fraction by spectrophotometry analysis, phosphorus by the Olsen method, potassium by ammonic acetate extraction, and organic matter by spectrophotometry.

The Braun-Blanquet method [30] was used to carried out flora inventories in the central 100 m^2 of each meadow. From them, the Shannon index was used to calculate plant biodiversity (35).

The climatic parameters were obtained from the climatic stations 9446, 9789A, 9784P, 9814X, 9838A, 9838B, and 9843A of the network of the Agencia Estatal de Meteorología [31]. The accumulated rainfall and the accumulated evapotranspiration (ETO) were calculated daily from March 1st using the Penman-Monteith method. Evapotranspiration was calculated from temperature data according to CROPWAT 8.0 procedures [32]. The growing degree days were calculated 1 February 1st by the sum of the daily average temperatures when they were between 0 and 18 °C. If the averages were negative, we limited them to 0 °C, and to 18 °C when they were > 18 °C [33,34]. All climate parameters were calculated until the mowing day.

Farm information was obtained from interviews with the farmers where they were asked how much time the meadow is grazed, the number of animals, how much fertilizer is applied and what type, and what is the average production of the meadow. Stocking rate was expressed as livestock units (LU) per ha.

As was shown in [27], spring grazing corresponds to 15% of the hay production, whereas autumn grazing is 25% of the hay production. In order to get the nutrient extraction by grazing, we use the following equation:

$$G = (K_a \cdot 0.25 \cdot M) + (K_s \cdot 0.15 \cdot M) \quad (1)$$

where G is nutrient extraction by grazing, M is nutrient extraction by mowing, K_a is a coefficient that indicates if the meadow was grazed in autumn (1 if grazed, 0 if not) and K_s is a coefficient that indicates if the meadow was grazed in spring (1 if grazed, 0 if not).

Nutrient input via excrements were estimated using stocking load, and data from previous studies were nutrient concentrations of livestock excrements were determined [35], as shown in the following equation:

$$E = N \cdot C \quad (2)$$

where E is nutrient input by excrements, N is the number of days spent by the animal in the meadow per hectare, and C is the daily nutrient input according to the literature, as it can be summarized in Table 2:

Table 2. Estimation of nutrient content in excrements [35].

	N (kg day^{-1})	P (kg day^{-1})	K (kg day^{-1})
Cow	0.2192	0.0767	0.2685
Sheep	0.0246	0.0086	0.0302

Nitrogen fixation was estimated according to meadow legume cover and using data from previous studies, which calculated 160 kg ha^{-1} for Pyrenees meadow legumes [27]. The following equation was used:

$$NX = 160 \cdot LC \tag{3}$$

where NX is nitrogen fixation by legumes in kg ha^{-1}, and LC is legume cover in m^2 of legume surface per m^{-2} of crop surface.

Nutrient crop balance was calculated by adding the values of nitrogen fertilization and nitrogen content estimated in animal droppings and subtracting nutrient extraction by mowing and estimated nutrient extraction by grazing, as shown in the following equations:

$$NB = NF + NE + NX - NM - NG \tag{4}$$

where NB is nitrogen balance, NF is nitrogen fertilization, NE is nitrogen in excrements, NX is nitrogen fixation, NE is nitrogen extracted by mowing, and NG is nitrogen extracted by grazing.

$$PB = PF + PE - PM - PG \tag{5}$$

where PB is phosphorus balance, PF is phosphorus fertilization, PE is phosphorus in excrements, PM is phosphorus extracted by mowing, and PG is phosphorus extracted by grazing.

$$KB = KF + KE - KM - KG \tag{6}$$

where KB is potassium balance, KF is potassium fertilization, KE is potassium in excrements, KM is potassium extracted by mowing, and KG is potassium extracted by grazing.

Soil organic carbon (SOC) was calculated using the following formula:

$$SOC\left[Mg\ ha^{-1}\right] = OC \cdot LT \cdot BD \cdot (1 - RF) \cdot 10^4 \tag{7}$$

where OC is the organic concentration (%), LT is the layer thickness (in our case 0.3 m), BD is the bulk density (Mg m^{-3}), and RF is the rock fragment concentration [36].

To calculate soil balance, nutrient soil concentration in June was subtracted by nutrient concentration in February, as shown in the following equation:

$$SB = N_j - N_f \tag{8}$$

where SB is soil nutrient balance, N_j is soil nutrient content in June, and N_f is soil nutrient content in February.

All data were checked by the Shapiro–Wilk normality test, and as the data were nonparametric, the Wilcoxon test was used to compare differences among meadow type and year. Additionally, the post hoc Wilcoxon test was carried out to check between which group were the differences.

We have considered the differences to be statistically significant when $p < 0.05$. All statistical analyses were carried out using R version 4.4.0 [37].

3. Results

3.1. General Characterization

The following table shows the general parameters of the farms during each year of study.

As shown in Table 3, intensive meadows had the lowest Shannon Index, whereas extensive meadows had the highest. On the other hand, livestock load had the opposite effect pattern, being higher in intensive meadows and the lowest in extensive meadows. Looking at climate variables, extensive and semi-extensive meadows had similar precipitation and evapotranspiration, being significantly higher than in intensive meadows. Degree days showed no significant difference between each meadow type.

Table 3. General parameters of 2022. Shannon biodiversity index, stocking rate expressed in livestock units per hectare, production expressed in kilograms of dry matter per hectare, precipitation expressed in millimetres of rainfall from March 1st to mowing date, degree days from February 1st to mowing date expressed in degrees Celsius, evapotranspiration (ETO) expressed in millimetres from March 1st to mowing date, crude protein (CP) expressed in percentage from dry matter and relative feed value (RFV). Mean and standard deviation. Sig: significance differences for $p < 0.05$; different letters in the same row indicate differences (Wilcoxon test).

	Intensive Meadow	Semi-Extensive Meadow	Extensive Meadow
Shannon index	1.79 ± 0.18^{c}	2.84 ± 0.31^{b}	3.23 ± 0.14^{a}
Stocking rate (LU/ha)	0.56 ± 0.08^{a}	0.33 ± 0.29^{b}	0.20 ± 0.10^{c}
Production (kgDM/ha)	6097.23 ± 1367.54^{a}	5273.94 ± 1583.28^{a}	3544.45 ± 915.09^{b}
Precipitation (mm)	193.05 ± 29.35^{b}	345.53 ± 64.75^{a}	322.05 ± 54.74^{a}
Degree days (°C)	1182.99 ± 67.38^{a}	1227.19 ± 259.81^{a}	1022.17 ± 235.97^{a}
ETO (mm)	310.28 ± 8.95^{b}	366.28 ± 69.84^{a}	357.69 ± 37.91^{a}
CP (% DM)	10.01 ± 2.24^{a}	11.71 ± 3.65^{a}	11.56 ± 2.19^{a}
RFV	100.97 ± 7.31^{b}	114.24 ± 23.51^{ab}	119.83 ± 16.72^{a}

There were no significant differences in protein content, but RFV was higher in extensive meadows and lower in intensive meadows.

Table 4 shows fewer differences than Table 3. Although we can find significant differences in biodiversity from each meadow type, we cannot find significant differences in livestock load between extensive and semi-extensive meadows.

Table 4. General parameters of 2023. Shannon biodiversity index, stocking rate expressed in livestock units per hectare, production expressed in kilograms of dry matter per hectare, precipitation expressed in millimetres of rainfall from March 1st to mowing date, degree days from February 1st to mowing date expressed in degrees Celsius, evapotranspiration (ETO) expressed in millimetres from March 1st to mowing date, crude protein (CP) expressed in percentage from dry matter and relative feed value (RFV). Mean and standard deviation. Sig: significance differences for $p < 0.05$; different letters in the same row indicate differences (Wilcoxon test).

	Intensive Meadow	Semi-Extensive Meadow	Extensive Meadow
Shannon index	1.82 ± 0.15^{c}	2.76 ± 0.33^{b}	3.23 ± 0.14^{a}
Stocking rate (LU/ha)	0.59 ± 0.10^{a}	0.16 ± 0.04^{b}	0.20 ± 0.10^{b}
Production (kgDM/ha)	2329.28 ± 1332.86^{b}	3665.58 ± 1207.28^{a}	2443.73 ± 1285.41^{ab}
Precipitation (mm)	180.40 ± 44.79^{b}	289.97 ± 83.85^{a}	298.40 ± 128.66^{a}
Degree days (°C)	1142.18 ± 185.32^{a}	1084.02 ± 270.86^{ab}	919.66 ± 286.82^{b}
ETO (mm)	320.15 ± 38.26^{a}	331.27 ± 61.98^{a}	337.06 ± 81.73^{a}
CP (% DM)	14.56 ± 4.98^{a}	13.09 ± 2.10^{a}	14.56 ± 3.08^{a}
RFV	111.04 ± 16.38^{b}	124.66 ± 15.20^{a}	147.11 ± 56.59^{a}

In Table 5 we observed that production showed fewer differences than in the previous year and they were considerably lower. Precipitation was also lower in 2023 than in 2022, but it showed the same tendency, being higher in semi-extensive and extensive meadows.

Differences in degree days showed a similar pattern, being higher in extensive meadows and lower in intensive meadows. On the other hand, evapotranspiration showed no significant differences.

Table 5. General parameters comparison between 2022 and 2023. Production expressed in kilograms of dry matter per hectare, precipitation expressed in millimetres of rainfall from March 1st to mowing date, degree days from February 1st to mowing date expressed in degrees Celsius, evapotranspiration (ETO) expressed in millimetres from March 1st to mowing date, crude protein (CP) expressed in percentage from dry matter and relative feed value (RFV). Mean and standard deviation. Sig: significance differences for $p < 0.05$; different letters in the same row indicate differences (Wilcoxon test).

	2022	2023
Production (kgDM/ha)	4746.80 + 1663.08 [a]	2735.34 + 1404.00 [b]
Precipitation (mm)	305.64 + 79.54 [a]	253.19 + 108.19 [b]
Degree days (°C)	1136.34 + 243.17 [a]	1045.40 + 268.28 [a]
ETO (mm)	351.64 + 54.63 [a]	329.33 + 63.74 [b]
CP (% DM)	11.31 + 2.94 [b]	14.16 + 3.75 [a]
RFV	113.82 + 19.78 [b]	127.87 + 39.56 [a]

In contrast with the previous year, we found significant differences in protein content, it being higher in intensive and extensive meadows than in semi-extensive meadows. RFV also had the same behaviour.

As shown in Figure 2, temperature had similar patterns in both years, the climate being warmer in 2022 than 2023, whereas spring was warmer in 2023 than 2022. It should be noted that those higher temperatures in spring matched lower rainfall in March and April, a critical period for meadow growth. Indeed, this drought period lasted until the end of May, when there began to appear heavy rains. In contrast, autumn showed huge rainfall in 2023, when there were flooding events.

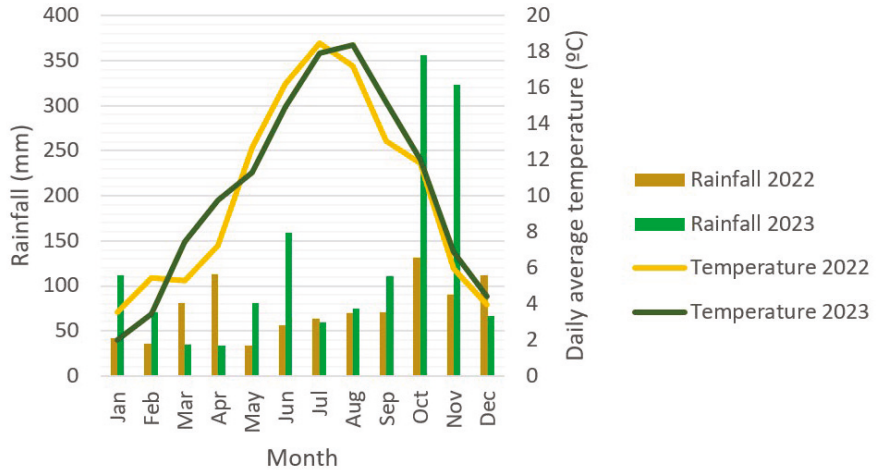


Figure 2. Average daily temperature and monthly rainfall in 2022 and 2023.

3.2. Nitrogen

Crop balance and soil balance in nitrogen during each year:

In both cases (Tables 6 and 7), there are significant differences in nitrogen fertilization for each meadow type. There are fewer differences in grazing, excrements, fixation and mowing. Crop balances are significantly different for each meadow type, and soil balance has no significant differences between semi-extensive and extensive meadows.

Table 6. Nitrogen balance of 2022 expressed in kg NO_3^- ha^{-1}. Mean and standard deviation. Sig: significance differences for $p < 0.05$; different letters in the same row indicate differences (Wilcoxon test).

		Intensive Meadow	Semi-Extensive Meadow	Extensive Meadow
Input	Fertilization	58.20 ± 44.20 [b]	219.22 ± 131.30 [a]	6.17 ± 10.69 [c]
	Excrements	55.13 ± 7.49 [a]	26.06 ± 17.24 [b]	19.70 ± 9.25 [b]
	Fixation	64.02 ± 45.78 [a]	38.88 ± 10.65 [a]	37.32 ± 9.54 [a]
Output	Mowing	96.39 ± 27.99 [a]	92.83 ± 25.28 [a]	66.02 ± 22.32 [b]
	Grazing	24.10 ± 7.00 [a]	25.98 ± 6.18 [a]	19.93 ± 10.79 [a]
	Crop balance	56.88 ± 33.40 [b]	165.35 ± 106.36 [a]	−22.76 ± 31.41 [c]
Soil	February	62.40 ± 3.90 [c]	195.00 ± 94.37 [a]	83.17 ± 26.70 [b]
	June	62.40 ± 35.10 [c]	341.25 ± 203.67 [a]	208.65 ± 149.13 [b]
	Soil balance	0.00 ± 31.20 [a]	146.25 ± 225.64 [b]	125.48 ± 131.26 [b]

Table 7. Nitrogen balance of 2023 expressed in kg NO_3^- ha^{-1}. Mean and standard deviation. Sig: significance differences for $p < 0.05$; different letters in the same row indicate differences (Wilcoxon test).

		Intensive Meadow	Semi-Extensive Meadow	Extensive Meadow
Input	Fertilization	67.16 ± 37.45 [b]	251.90 ± 136.80 [a]	6.17 ± 10.69 [c]
	Excrements	54.77 ± 7.70 [a]	16.33 ± 4.22 [b]	19.70 ± 9.25 [b]
	Fixation	41.99 ± 39.34 [a]	40.41 ± 11.91 [a]	37.32 ± 9.54 [a]
Output	Mowing	47.24 ± 21.08 [b]	75.49 ± 26.11 [a]	53.14 ± 23.24 [b]
	Grazing	11.81 ± 5.27 [b]	18.87 ± 6.53 [a]	15.92 ± 9.92 [ab]
	Crop balance	104.88 ± 17.79 [b]	214.29 ± 123.08 [a]	−5.87 ± 32.33 [c]
Soil	February	29.25 ± 19.60 [b]	93.60 ± 40.65 [a]	31.20 ± 19.69 [b]
	June	246.68 ± 73.14 [c]	390.00 ± 0.00 [a]	288.60 ± 145.82 [b]
	Soil balance	217.42 ± 58.98 [a]	296.40 ± 40.65 [b]	257.40 ± 132.05 [b]

3.3. Phosphorous

Crop balance and soil balance in phosphorous during each year.

As was shown in the case of nitrogen, phosphorus shows the same differences in fertilization and in grazing and excrements. However, in mowing we found more significant differences in the year 2022 (Table 8) than in 2023 (Table 9).

Table 8. Phosphorous balance of 2022 expressed in kg $P_2O_5^{2-}$ ha^{-1}. Mean and standard deviation. Sig: significance differences for $p < 0.05$; different letters in the same row indicate differences (Wilcoxon test).

		Intensive Meadow	Semi-Extensive Meadow	Extensive Meadow
Input	Fertilization	37.82 ± 15.42 [b]	309.30 ± 275.90 [a]	11.57 ± 20.05 [c]
	Excrements	19.29 ± 2.62 [a]	9.12 ± 6.03 [b]	6.89 ± 3.24 [b]
Output	Mowing	31.38 ± 7.86 [a]	25.99 ± 10.92 [b]	15.50 ± 7.02 [c]
	Grazing	7.84 ± 1.97 [a]	7.37 ± 3.02 [a]	4.54 ± 2.37 [b]
	Crop balance	17.90 ± 13.77 [b]	285.05 ± 264.68 [a]	−1.58 ± 14.11 [c]
Soil	February	540.33 ± 477.81 [a]	468.88 ± 423.85 [a]	122.80 ± 51.45 [a]
	June	611.77 ± 486.74 [a]	482.27 ± 502.01 [a]	109.40 ± 44.38 [b]
	Soil balance	71.45 ± 8.93 [a]	13.40 ± 211.39 [a]	−13.40 ± 34.30 [b]

Table 9. Phosphorous balance of 2023 expressed in kg $P_2O_5^{2-}$ ha^{-1}. Mean and standard deviation. Sig: significance differences for $p < 0.05$; different letters in the same row indicate differences (Wilcoxon test).

		Intensive Meadow	Semi-Extensive Meadow	Extensive Meadow
Input	Fertilization	47.48 ± 14.83 [b]	365.52 ± 298.08 [a]	11.57 ± 20.05 [c]
	Excrements	19.17 ± 2.69 [a]	5.72 ± 1.48 [b]	6.89 ± 3.24 [b]
Output	Mowing	12.19 ± 6.19 [b]	18.60 ± 8.75 [a]	11.91 ± 8.64 [b]
	Grazing	3.05 ± 1.55 [b]	4.65 ± 2.19 [a]	3.45 ± 2.54 [ab]
	Crop balance	51.41 ± 19.10 [b]	347.98 ± 293.41 [a]	3.11 ± 15.00 [c]
Soil	February	551.49 ± 785.76 [a]	628.15 ± 664.24 [a]	229.97 ± 200.44 [a]
	June	424.22 ± 401.67 [ab]	503.11 ± 461.73 [a]	174.15 ± 128.26 [b]
	Soil balance	−127.27 ± 410.02 [a]	−125.03 ± 202.61 [a]	−55.82 ± 85.52 [a]

Crop balance had significant differences between each meadow type in both years, but soil balance lacks significant differences; only in 2022 was phosphorus soil balance significantly lower in extensive meadows.

Even though crop and soil balance are notoriously different in every case, in year 2022 (Table 8) they have the same tendency. In year 2023 (Table 9), they had the opposite tendency.

3.4. Potassium

Crop balance and soil balance in potassium during each year:

Fertilization, grazing, and excrements show the same differences as in the case of nitrogen and phosphorus. Mowing is lower in extensive meadows, but in 2023 was like that in intensive meadows.

Crop balance is similar in 2022 (Table 10), but it was significantly lower in extensive meadows in 2023 (Table 11). In soil balance, we find differences in 2022 (Table 10), but in 2023 (Table 11) the differences were less significant.

Table 10. Potassium balance of 2022 expressed in kg K_2O ha^{-1}. Mean and standard deviation. Sig: significance differences for $p < 0.05$; different letters in the same row indicate differences (Wilcoxon test).

		Intensive Meadow	Semi-Extensive Meadow	Extensive Meadow
Input	Fertilization	79.20 ± 23.20 [a]	143.32 ± 142.46 [a]	11.57 ± 20.05 [b]
	Excrements	67.54 ± 9.17 [a]	31.92 ± 21.11 [b]	24.13 ± 11.33 [b]
Output	Mowing	167.77 ± 27.27 [a]	155.23 ± 71.52 [a]	74.42 ± 27.79 [b]
	Grazing	41.94 ± 6.82 [b]	43.80 ± 18.80 [a]	22.52 ± 13.03 [c]
	Crop balance	−62.97 ± 41.37 [a]	−23.79 ± 79.66 [a]	−61.24 ± 36.85 [a]
Soil	February	2676.96 ± 1890.72 [a]	1701.18 ± 1538.35 [b]	844.74 ± 406.94 [b]
	June	6144.84 ± 4984.20 [a]	2098.98 ± 1662.64 [b]	1067.04 ± 640.94 [b]
	Soil balance	3467.88 ± 3093.48 [a]	397.80 ± 246.36 [b]	222.30 ± 850.10 [c]

Table 11. Potassium balance of 2023 expressed in kg K_2O ha^{-1}. Mean and standard deviation. Sig: significance differences for $p < 0.05$; different letters in the same row indicate differences (Wilcoxon test).

		Intensive Meadow	Semi-Extensive Meadow	Extensive Meadow
Input	Fertilization	69.56 ± 35.56 [a]	166.20 ± 158.00 [a]	11.57 ± 20.05 [b]
	Excrements	67.09 ± 9.43 [a]	20.01 ± 5.17 [b]	24.13 ± 11.33 [b]
Output	Mowing	53.66 ± 28.62 [b]	94.60 ± 42.24 [a]	57.65 ± 32.15 [b]
	Grazing	13.41 ± 7.15 [b]	23.65 ± 10.56 [a]	17.45 ± 12.71 [b]
	Crop balance	69.58 ± 36.03 [a]	67.96 ± 140.52 [a]	−39.40 ± 41.14 [b]
Soil	February	2024.10 ± 2150.68 [a]	2165.28 ± 1605.97 [a]	788.58 ± 530.16 [b]
	June	2665.26 ± 3084.64 [a]	2458.56 ± 1714.44 [a]	835.38 ± 347.48 [b]
	Soil balance	641.16 ± 943.33 [a]	293.28 ± 115.99 [a]	46.80 ± 307.24 [b]

3.5. Carbon

Soil balance in carbon during each year (Table 12):

Table 12. Carbon balance of 2022 and 2023 in Mg SOC ha^{-1}. Mean and standard deviation. Sig: significance differences for $p < 0.05$; different letters in the same row indicate differences (Wilcoxon test).

		Intensive Meadow	Semi-Extensive Meadow	Extensive Meadow
2022	February	73.52 ± 20.13 [b]	192.85 ± 53.17 [a]	222.49 ± 59.27 [a]
	June	86.64 ± 23.30 [b]	225.65 ± 47.44 [a]	225.99 ± 44.56 [a]
	Soil balance	13.12 ± 3.17 [a]	32.80 ± 58.44 [a]	3.51 ± 51.46 [a]
2023	February	91.73 ± 56.04 [b]	267.09 ± 91.65 [a]	196.24 ± 80.85 [a]
	June	79.52 ± 25.26 [b]	214.38 ± 8.06 [a]	224.07 ± 28.60 [a]
	Soil balance	−12.22 ± 35.19 [a]	−52.71 ± 84.13 [a]	27.82 ± 79.99 [a]

Intensive meadows have lower carbon content than semi-extensive and extensive meadows. Carbon balance was always positive in year 2022, but in 2023 it was positive only in extensive meadows.

4. Discussion

We analyze the results according to type and year.

4.1. Year Variability

This study was carried out in two years with different climate behaviour. If we look just at the global numbers, we see not many differences, but if we look at precipitation distribution, those differences appear to be clear. Looking at Figure 2, we can observe that in 2023 there was less precipitation from March to the end of May, a critical period in crop development, and temperatures were higher, causing drought stress in may crops. In the lowest parts of the valley, where the cycle is faster, the plants started flowering at low height and yielded markedly low yields. Indeed, due to the spring drought, the local government had to implement special aid to the farmers to help them to buy feed for their animals, because there was very little pasture available [38]. The same pattern has been observed in other studies [8].

As was shown in other papers, when yield falls, quality, in terms of protein and RFV, rises [3,12]. Consequently, in 2023 we found higher protein and RFV values than in 2022.

It is quite interesting to note that extensive meadows showed the lowest yield fall in the drought year (2023). It has been shown that a higher diversity index is correlated with lower yields, but also with higher resilience to stresses [21,39].

Looking at nitrogen, we found higher nitrogen extractions in 2022 than in 2023, due to its higher yield, similar to other cases [40]. Crop balance was positive in semi-extensive and intensive meadows both years, whereas in extensive meadows a negative balance occurred in both years. Considering that extensive meadows had almost no nitrogen applied in fertilization, this seems like a logical consequence. In 2023, we had higher nitrogen accumulation in the crop balance, due to lower production with similar fertilization. In order to simplify calculations, we have considered nitrogen fixation as a constant, regardless of climate, but considering drought stress during 2023 that limited legume development, nitrogen fixation could be lower than what we have considered, as has been shown in other studies [41,42].

Crop balance and soil balance differ from each other in most cases. Those differences are higher in 2023, most likely being due to climate. Looking at February soil nitrogen content in Tables 6 and 7, we observe that 2023 had half of the nitrogen soil content of 2022, and if we look at Figure 2, winter temperatures were lower in 2023. On the other hand,

nitrogen soil content in June was higher in 2023 than in 2022, and spring temperatures contrasted with winter temperatures, being higher in 2023 than in 2022. Some studies have shown that temperature can alter nitrogen soil content [43,44], which could be one of the driving factors that lead to differences between crop and soil balance.

In phosphorus, we also had higher extraction in mowing in 2022 than in 2023, due to the higher yield. Crop balance was always positive except for extensive meadows in 2022, which had a small phosphorus deficit, caused by the higher yield this year and the same fertilization. Soil balance was positive in 2022 for intensive and semi-extensive meadows, whereas in extensive meadows and all meadows in 2023 it was negative. That is especially noted in intensive meadows, where the crop balance indicates phosphorus accumulation and soil balance shows phosphorus deficit; it has been shown that, in some meadows, phosphorus is most limiting nutrient [19,45]. As phosphorus availability is highly dependent on microbial dynamics, drought conditions and higher temperatures during the spring could have led to higher phosphorus blockage, as well as increasing phosphorus intake by the plant due to the increasing temperatures [46].

As was the case for nitrogen and phosphorus, potassium also had higher extraction values in mowing in 2022 due to the higher yield. Caused by the higher yield, 2022 showed a potassium deficit in every meadow type, in contrast to 2023 where only extensive meadows had a potassium deficit. Other studies have seen potassium deficits in meadows [5]. However, the soil balance was positive in both years for all meadow types. Indeed, it was higher in 2022 when the potassium crop balance was lower; in some cases, potassium accumulation has been related to lower-than-average yields [47].

Carbon balance varied by year and meadow type. In 2022, there was carbon accumulation, when meadows acted as carbon sinks. In contrast, in 2023 only extensive meadows had positive carbon balances, making semi-extensive and intensive meadows carbon emitters during that year. It has been shown that, in drought conditions, the carbon balance can be negative in meadows [23,48].

4.2. Meadow Type

As intensification increases, by increasing livestock load and fertilization, biodiversity decreases, as has been reflected in many papers [49]. Semi-extensive meadows had the higher fertilization rate, but given its organic nature, it had a lower impact in biodiversity than the inorganic fertilizers used in intensive meadows. It should be noted that intensive meadows are considered by farmers as the least productive fields, as they also have fields with higher production with cereals and forage crops such as alfalfa, where they use their manure. In semi-extensive meadows, however, due to their higher slopes and smaller plots, cereals and forage crops are rarely grown, so all the manure is applied on them.

Precipitation varies according to meadow location. Intensive meadows' locations in the bottoms of the valleys explain why they have lower precipitation, which increases by around 100 mm of rainfall for each 100 m of altitude gain [50]. Water losses due to runoff are small, thanks to terracing that reduces slopes [51]. On the other hand, degree days have been identified as one of the major drivers in meadow development; when the meadow reaches 900 °C, it starts flowering; then, depending on climate, the farmer will mow, leading to differences depending on when the weather is favourable to mowing.

From the quality point of view, protein content does not depend on meadow type but is mostly driven by yield. As yield increases, protein content decreases [3,12]. On the other hand, RFV increases as biodiversity increases, although yield seems to have a similar effect, as was seen in protein content.

Nitrogen inputs are higher in semi-extensive meadows, because of the use of manure from the farms. Some of the nitrogen will not be available to the crop, as it will be used by microbes to degrade organic matter. Also, the nitrogen in manure is more stable than in inorganic fertilizer, which can have more losses in lixiviation [52].

Intensive and semi-extensive meadows had the highest nitrogen extraction values in mowing in 2022, whereas in 2023 semi-extensive meadows had the highest values.

Probably, increasing nitrogen availability increases nitrogen extraction by the plant, which will be coherent with other studies [1,53].

Extensive meadows always show a nitrogen deficit in crops; since no fertilizer is applied, that result is logical. In the soil balance, semi-extensive meadows have fewer differences between crop and soil balance. In both years, semi-extensive and extensive meadows had the highest nitrogen accumulation, proving that inorganic fertilization could have poorer results than organic or no fertilization in meadows. Organic fertilization has more complex dynamics, which leads to bigger changes during the year, but if we compare nitrogen soil content in the same period of both years, we find that nitrogen content increases [20]. Intensive meadows have the lowest deficits in both years, as most of the nitrogen is applied by inorganic fertilizer, and most of the nitrogen that is not consumed by the plant is lixiviated [1,54].

There are clear differences in the phosphorus crop balance between each meadow type, the lowest being in the extensive meadows, where they are close to being balanced. On the other hand, semi-extensive meadows show the highest phosphorus accumulation in the crop balance. Nonetheless, both intensive and semi-extensive meadows show lower soil phosphorus accumulation than in the crop balance; when phosphorus is limited, it could cause a decrease in legumes, which could explain the lower Shannon index [55]. In both cases, fertilization could have led to an increase in blocked phosphorus, which was higher in the drought year. In contrast, extensive meadows show lower differences, as no fertilizer was applied. The absence of fertilization has been related to higher soil biological dynamics, which could lead to the higher stability of phosphorus that we have observed in extensive meadows [56,57]. Soil phosphorus balance in intensive meadows had the opposite trend, showing the biggest variability between each year. As inorganic fertilization has a negative effect in soil biological dynamics, there is a greater variation in phosphorus soil accumulation [58].

Potassium seems to have a different behaviour from nitrogen and phosphorus. Extensive meadows had potassium deficit both years, while intensive and semi-extensive meadows showed a deficit in 2022, the year with higher production, and accumulation in 2023, when yield was lower. Those results were expected according to their circumstances, but in soil, regardless of the crop balance trend, in all cases there is potassium accumulation. Temperature could be the biggest driver of this phenomena, as has been shown in many papers; as temperature decreases, potassium availability also decreases [54,59–61]. As soil balance is calculated as the difference between potassium content in June minus potassium content in February, there are important temperature differences between both sample dates [62,63]. In any case, it seems difficult to find potassium deficiency in meadows; it could only appear in high-yielding meadows with low potassium fertilization [64].

Intensification has been correlated with lower carbon storage, by increasing cut frequency or by increasing fertilization [65]. However, as shown in Table 12, although intensive meadows have significantly lower SOC, extensive and semi-extensive meadows have no significant differences, which leads us to argue that some degree of meadow intensification can be achieved without decreasing SOC. Meadows have remarkable carbon storage capacity, especially semi-extensive and extensive meadows, where we found carbon content above 200 Mg ha^{-1}, high values even for meadows [66].

According to our study, organic fertilization and no fertilization are the best nutritional practices for mountain meadows. The use of inorganic fertilizers can increase yield when there is a favourable climate, but it lowers resilience. Further research is needed to evaluate if those results are consistent in the long term, as our study was carried out during only two years.

5. Conclusions

Meadows are complex systems where management practices have implications for soil nutrient availability.

Nitrogen availability depends both on management and climate. Inorganic fertilization is the least stable source, decreasing fast in the soil when there are more rainfall events; on the other hand, semi-extensive meadows have higher soil nitrogen stability even though it is applied in higher doses. Extensive meadows, despite lacking nitrogen fertilization, are more stable, relying less on climate.

Usually, phosphorus is the nutrient that limits yield, as is clearly shown in extensive meadows, which have reached an equilibrium between input and output. In intensive and semi-extensive meadows, we found lower phosphorus accumulation than the crop balance estimates, probably due to its blockage.

Potassium is clearly influenced by temperature, as we have found high differences between its concentration in June versus its concentration in February, even when the crop balance shows negative values. Only in extensive meadows is there always a potassium deficit, which could eventually cause potassium deficiency.

Carbon accumulation is also highly influenced by climate. Our results showed that when there is drought stress, meadows shift from a carbon sink into a carbon source. Extensive meadows were the only type that was able to accumulate carbon even in the drought year.

Further research will be needed to assess the long-term consequences of management, as this study is based on only two specific years.

Author Contributions: Conceptualization, A.J., A.U. and R.R.; methodology, A.J. and R.R.; formal analysis, A.J., A.U. and R.R.; investigation, A.J. and R.R.; resources R.R.; writing—original draft preparation A.J., A.U. and R.R.; writing—review and editing, A.J., A.U. and R.R.; project administration, R.R.; funding acquisition, R.R. All authors have read and agreed to the published version of the manuscript.

Funding: This research was funded by Gobierno de Aragón, Project number GCP2021000100 (Programa de Desarrollo Rural para Aragón 2014–2020, Departamento de Desarrollo Rural y Sostenibilidad del Gobierno de Aragón, and the European Agricultural Fund for Rural Development, European Union).

Data Availability Statement: Dataset available on request from the authors. The raw data supporting the conclusions of this article will be made available by the authors on request.

Acknowledgments: The authors wish to express their gratitude to Jesús Betrán and Antonio López, responsible for the Laboratorio Agroambiental of the Gobierno de Aragón, for the analytical determinations, as well as to the farmers who have lent their meadows for the trials. To Victor Antín and Luis Buetas, technicians from the Agropecuaria del Sobrarbe Cooperative, and to Félix Salanova, an agronomy student, for his participation in the sampling work in the meadows.

Conflicts of Interest: The authors declare no conflicts of interest.

References

1. Hrevusova, Z.; Hejcman, M.; Hakl, J.; Mrkvicka, J. Soil Chemical Properties, Plant Species Composition, Herbage Quality, Production and Nutrient Uptake of an Alluvial Meadow after 45 Years of N, P and K Application. *Grass Forage Sci.* **2015**, *70*, 205–218. [CrossRef]
2. Boob, M.; Truckses, B.; Seither, M.; Elsäßer, M.; Thumm, U.; Lewandowski, I. Management Effects on Botanical Composition of Species-Rich Meadows within the Natura 2000 Network. *Biodivers. Conserv.* **2019**, *28*, 729–750. [CrossRef]
3. Ascaso, J.; Reiné, R. Temporal Variations in the Production—Quality and Optimal Cutting Date of Hay Meadows in the Central Pyrenees (Spain). *Agronomy* **2022**, *12*, 918. [CrossRef]
4. Humbert, J.-Y.; Pellet, J.; Buri, P.; Arlettaz, R. Does Delaying the First Mowing Date Benefit Biodiversity in Meadowland? *Environ. Evid.* **2012**, *1*, 9. [CrossRef]
5. Álvarez, J.; Afif, E.; Díaz, T.E.; García, L.; Oliveira, J.A. Effects of Management Practices on Soil Properties and Plant Nutrition in Hay Meadows in Picos de Europa. *Environments* **2021**, *8*, 38. [CrossRef]
6. Ascaso, J.; Reiné, R.; Barrantes, O. Evolution of Hay Meadows between 1956, 1986, and 2016 and Its Relation to the Characteristics and Location of the Parcels in the Valley of the River Esera (Pyrenees, Spain). *Agronomy* **2020**, *10*, 329. [CrossRef]
7. Cortijos-López, M.; Sánchez-Navarrete, P.; de la Parra-Muñoz, I.; Lasanta, T.; Nadal-Romero, E. A Strategy to Enhance Soil Quality and Soil Organic Carbon Stock in Abandoned Lands: Pasture Regeneration through Shrub Clearing. *Land Degrad. Dev.* **2024**, *35*, 3392–3406. [CrossRef]

8. Reiné, R.; Barrantes, O.; Chocarro, C.; Juárez-Escario, A.; Broca, A.; Maestro, M.; Ferrer, C. Pyrenean Meadows in Natura 2000 Network: Grass Production and Plant Biodiversity Conservation. *Span. J. Agric. Res.* **2014**, *12*, 61–77. [CrossRef]
9. Chocarro, C.; Reiné, R.J. El cultivo de los prados en el Pirineo. In *Pastos del Pirineo*; Consejo Superior de Investigaciones Científicas, CSIC: Madrid, Spain, 2008; pp. 141–158. ISBN 978-84-00-08614-5.
10. Dolezal, J.; Lanta, V.; Mudrak, O.; Leps, J. Seasonality Promotes Grassland Diversity: Interactions with Mowing, Fertilization and Removal of Dominant Species. *J. Ecol.* **2019**, *107*, 203–215. [CrossRef]
11. Chmolowska, D.; Kozak, M.; Laskowski, R. Soil Physicochemical Properties and Floristic Composition of Two Ecosystems Differing in Plant Diversity: Fallows and Meadows. *Plant Soil* **2016**, *402*, 317–329. [CrossRef]
12. Kotas, P.; Choma, M.; Santruckova, H.; Leps, J.; Triska, J.; Kastovska, E. Linking Above- and Belowground Responses to 16 Years of Fertilization, Mowing, and Removal of the Dominant Species in a Temperate Grassland. *Ecosystems* **2017**, *20*, 354–367. [CrossRef]
13. Kocięcka, J.; Liberacki, D.; Kupiec, J.M.; Stróżecki, M.; Dłużewski, P. Effects of Silicon Application and Groundwater Level in a Subirrigation System on Yield of a Three-Cut Meadow. *Water* **2023**, *15*, 2103. [CrossRef]
14. Reiné, R.; Ascaso, J.; Barrantes, O. Nutritional Quality of Plant Species in Pyrenean Hay Meadows of High Diversity. *Agronomy* **2020**, *10*, 883. [CrossRef]
15. Raus, J.; Knot, P.; Hrabě, F. Effect of Fertilization and Harvest Frequency on Floristic Composition and Yields of Meadow Stand. *Acta Univ. Agric. Silvic. Mendel. Brun.* **2012**, *60*, 181–186. [CrossRef]
16. Müller, I.B.; Buhk, C.; Lange, D.; Entling, M.H.; Schirmel, J. Contrasting Effects of Irrigation and Fertilization on Plant Diversity in Hay Meadows. *Basic Appl. Ecol.* **2016**, *17*, 576–585. [CrossRef]
17. Pauli, D.; Peintinger, M.; Schmid, B. Nutrient Enrichment in Calcareous Fens: Effects on Plant Species and Community Structure. *Basic Appl. Ecol.* **2002**, *3*, 255–266. [CrossRef]
18. Follett, R.H.; Westfall, D.G.; Shanahan, J.F.; Lybecker, D.W. Nitrogen Fertilization of Mountain Meadows. *J. Prod. Agric.* **1995**, *8*, 239–243. [CrossRef]
19. Scotton, M.; Ziliotto, U. Long-Term Patterns of Grassland Vegetation and Species Richness in a Full-Factorial NPK Fertilization Experiment. *Sci. Total Environ.* **2024**, *906*, 167555. [CrossRef] [PubMed]
20. Samutenko, L.V.; Slavkina, V.P.; Fedorova, L.V. Results of the Study of Long-Term Dynamics of Microbiological and Agro-Chemical Indexes of the Fertility of the Meadow-Sod Soils with the Use of Fertilization Systems of Different Intensity (Sakhalin Island). *IOP Conf. Ser. Earth Environ. Sci.* **2020**, *613*, 012129. [CrossRef]
21. van der Hoek, D.; van Mierlo, A.; van Groenendael, J.M. Nutrient Limitation and Nutrient-Driven Shifts in Plant Species Composition in a Species-Rich Fen Meadow. *J. Veg. Sci.* **2004**, *15*, 389–396. [CrossRef]
22. Schellberg, J.; Möseler, B.M.; Kühbauch; Rademacher. Long-Term Effects of Fertilizer on Soil Nutrient Concentration, Yield, Forage Quality and Floristic Composition of a Hay Meadow in the Eifel Mountains, Germany. *Grass Forage Sci.* **1999**, *54*, 195–207. [CrossRef]
23. Wezel, A.; Stöckli, S.; Tasser, E.; Nitsch, H.; Vincent, A. Good Pastures, Good Meadows: Mountain Farmers' Assessment, Perceptions on Ecosystem Services, and Proposals for Biodiversity Management. *Sustainability* **2021**, *13*, 5609. [CrossRef]
24. Blackburn, D.A.; Oliphant, A.J.; Davis, J.D. Carbon and Water Exchanges in a Mountain Meadow Ecosystem, Sierra Nevada, California. *Wetlands* **2021**, *41*, 39. [CrossRef]
25. Reed, C.C.; Merrill, A.G.; Drew, W.M.; Christman, B.; Hutchinson, R.A.; Keszey, L.; Odell, M.; Swanson, S.; Verburg, P.S.J.; Wilcox, J.; et al. Montane Meadows: A Soil Carbon Sink or Source? *Ecosystems* **2021**, *24*, 1125–1141. [CrossRef]
26. Reed, C.C.; Berhe, A.A.; Moreland, K.C.; Wilcox, J.; Sullivan, B.W. Restoring Function: Positive Responses of Carbon and Nitrogen to 20 Years of Hydrologic Restoration in Montane Meadows. *Ecol. Appl.* **2022**, *32*, e2677. [CrossRef]
27. Bagcilar, S.H.; Reed, C.C.; Poulson, S.R.; Verburg, P.S.J.; Sullivan, B.W. Does Montane Meadow Restoration Influence the Mineral Association and Stability of Soil Carbon? *Biogeochemistry* **2024**, *167*, 1089–1105. [CrossRef]
28. Van Soest, P.J.; Robertson, J.B.; Lewis, B.A. Methods for Dietary Fiber, Neutral Detergent Fiber, and Nonstarch Polysaccharides in Relation to Animal Nutrition. *J. Dairy Sci.* **1991**, *74*, 3583–3597. [CrossRef] [PubMed]
29. INRA. Alimentation des Ruminants: Apports Nutritionnels—Besoins et Réponses des Animaux—Rationnement—Tables des Valeurs des Aliments. Available online: https://abiodoc.docressources.fr/index.php?lvl=notice_display&id=39834 (accessed on 22 May 2023).
30. Braun-Blanquet, J. *Plant Sociology—The Study of Plant Communities*; Hafner Publishing Company: New York, NY, USA, 1965; ISBN 978-3-87429-208-5.
31. AEMET. Sede Electronica de la Agencia Estatal de Meteorología. Available online: https://sede.aemet.gob.es/AEMET/es/GestionPeticiones/home (accessed on 20 July 2024).
32. FAO. Cropwat v8.0 A Computer Program for Irrigation Plannning and Management. Water Resources Development and Management Service. Land and Water Development Division. Food and Agriculture Organization of the UN. Available online: https://www.fao.org/land-water/databases-and-software/cropwat/es/ (accessed on 20 July 2024).
33. Theau, J.P.; Zerourou, A. Herb'âge, Une Méthode de Calcul Des Sommes de Températures Pour La Gestion Des Prairies. In *Outil Pour La Gestion Des Prairies Permanentes*; HAL: Castanet-Tolosan, France, 2008; pp. 91–102.
34. Ansquer, P.; Al Haj Khaled, R.; Cruz, P.; Theau, J.-P.; Therond, O.; Duru, M. Characterizing and Predicting Plant Phenology in Species-Rich Grasslands. *Grass Forage Sci.* **2009**, *64*, 57–70. [CrossRef]

35. Ziegler, D.; Heduit, M. *Engrais de Ferme: Valeur Fertilisante Gestion, Environnement*; Institut Technique du Porc: Paris, France; Institut Technique des Céréales et des Fourrages: Paris, France; Institut Technique de l'Elevage Bo: Paris, France, 1991.
36. Tadiello, T.; Perego, A.; Valkama, E.; Schillaci, C.; Acutis, M. Computation of Total Soil Organic Carbon Stock and Its Standard Deviation from Layered Soils. *MethodsX* **2022**, *9*, 101662. [CrossRef]
37. R Core Team. *R: A Language and Environment for Statistical Computing*; R Core Team: Vienna, Austria, 2024.
38. *Cuantías, Zonas y Cultivos Afectados Relativos a Las Ayudas Directas a Los Sectores Agrícolas*; Ministerio de Agricultura: Pesca y Alimentación, España, 2023; pp. 109089–109098.
39. Klein, N.; Theux, C.; Arlettaz, R.; Jacot, A.; Pradervand, J.-N. Modeling the Effects of Grassland Management Intensity on Biodiversity. *Ecol. Evol.* **2020**, *10*, 13518–13529. [CrossRef] [PubMed]
40. Cudlin, O.; Hakl, J.; Hejcman, M.; Cudlin, P. The Use of Compressed Height to Estimate the Yield of a Differently Fertilized Meadow. *Plant Soil Environ.* **2018**, *64*, 76–81. [CrossRef]
41. Makarov, M.I.; Onipchenko, V.G.; Malysheva, T.I.; Zuev, A.G.; Tiunov, A.V. Symbiotic Nitrogen Fixation by Legumes in Alpine Ecosystems: A Vegetation Experiment. *Russ. J. Ecol.* **2021**, *52*, 9–17. [CrossRef]
42. Lonati, M.; Probo, M.; Gorlier, A.; Lombardi, G. Nitrogen Fixation Assessment in a Legume-Dominant Alpine Community: Comparison of Different Reference Species Using the 15N Isotope Dilution Technique. *Alp. Bot.* **2015**, *125*, 51–58. [CrossRef]
43. Wang, S.; Duan, J.; Xu, G.; Wang, Y.; Zhang, Z.; Rui, Y.; Luo, C.; Xu, B.; Zhu, X.; Chang, X.; et al. Effects of Warming and Grazing on Soil N Availability, Species Composition, and ANPP in an Alpine Meadow. *Ecology* **2012**, *93*, 2365–2376. [CrossRef]
44. Gong, S.; Guo, R.; Zhang, T.; Guo, J. Warming and Nitrogen Addition Increase Litter Decomposition in a Temperate Meadow Ecosystem. *PLoS ONE* **2015**, *10*, e0116013. [CrossRef]
45. Seastedt, T.R.; White, C.T.; Tucker, C.; Beaury, E.M.; Concilio, A.L.; Gasarch, E.; Haggans, V.J.; Smith, J.G. Decadal Dynamics of Dry Alpine Meadows under Nitrogen and Phosphorus Additions. *Plant Ecol.* **2020**, *221*, 647–658. [CrossRef]
46. Gasarch, E.I.; Seastedt, T.R. Plant Community Response to Nitrogen and Phosphorus Enrichment Varies across an Alpine Tundra Moisture Gradient. *Plant Ecol. Divers.* **2015**, *8*, 739–749. [CrossRef]
47. Pavlu, L.; Poetsch, E.M.; Pavlu, V.V.; Titera, J.; Hejcman, M.; Gaisler, J.; Hopkins, A. The Admont Grassland Experiment: 70 Years of Fertilizer Application and Its Effects on Soil and Vegetation Properties in an Alluvial Meadow Managed under a Three-Cut Regime. *Sci. Total Environ.* **2022**, *808*, 152081. [CrossRef]
48. Guasconi, D. The Hidden Half of the Meadow: Interactions between Drought, Soil Carbon, Roots and Soil Microbial Communities. Ph.D. Thesis, Department of Physical Geography, Stockholm University, Stockholm, Sweden, 2024.
49. Chytry, M.; Hejcman, M.; Hennekens, S.M.; Schellberg, J. Changes in Vegetation Types and Ellenberg Indicator Values after 65 Years of Fertilizer Application in the Rengen Grassland Experiment, Germany. *Appl. Veg. Sci.* **2009**, *12*, 167–176. [CrossRef]
50. Lemus-Canovas, M.; Lopez-Bustins, J.A.; Martín-Vide, J.; Halifa-Marin, A.; Insua-Costa, D.; Martinez-Artigas, J.; Trapero, L.; Serrano-Notivoli, R.; Cuadrat, J.M. Characterisation of Extreme Precipitation Events in the Pyrenees: From the Local to the Synoptic Scale. *Atmosphere* **2021**, *12*, 665. [CrossRef]
51. Buisan, S.T.; Saz, M.A.; López-Moreno, J.I. Spatial and Temporal Variability of Winter Snow and Precipitation Days in the Western and Central Spanish Pyrenees. *Int. J. Climatol.* **2015**, *35*, 259–274. [CrossRef]
52. Ortikov, T.; Shoniyozov, B.; Makhmatmurodov, A.; Mashrabov, M. Influence of Mineral and Organic Fertilizers on the Properties of Serozem-Meadow Soils, Nutritional Dynamics and Productivity of Amaranth. *E3S Web Conf.* **2023**, *462*, 02017. [CrossRef]
53. Comakli, B.; Mentese, O.; Koc, A. Nitrogen Fertilizing and Pre-Anthesis Cutting Stage Improve Dry Matter Production, Protein Content and Botanical Composition in Meadows. *Acta Agric. Scand. Sect. B Soil Plant Sci.* **2005**, *55*, 125–130. [CrossRef]
54. Best, E.P.H.; Jacobs, F.H.H. Production, Nutrient Availability, and Elemental Balances of Two Meadows Affected by Different Fertilization and Water Table Regimes in The Netherlands. *Plant Ecol.* **2001**, *155*, 61–73. [CrossRef]
55. Zarzycki, J.; Kopec, M. The Scheme of Nutrient Addition Affects Vegetation Composition and Plant Species Richness in Different Ways: Results from a Long-Term Grasslands Experiment. *Agric. Ecosyst. Environ.* **2020**, *291*, 106789. [CrossRef]
56. Onipchenko, V.G.; Makarov, M.I.; Akhmetzhanova, A.A.; Soudzilovskaia, N.A.; Aibazova, F.U.; Elkanova, M.K.; Stogova, A.V.; Cornelissen, J.H.C. Alpine Plant Functional Group Responses to Fertiliser Addition Depend on Abiotic Regime and Community Composition. *Plant Soil* **2012**, *357*, 103–115. [CrossRef]
57. Campdelacreu Rocabruna, P.; Domene, X.; Matteazzi, A.; Figl, U.; Fundneider, A.; Fernández-Martínez, M.; Venir, E.; Robatscher, P.; Preece, C.; Peñuelas, J.; et al. Effect of Organic Fertilisation on Soil Phosphatase Activity, Phosphorus Availability and Forage Yield in Mountain Permanent Meadows. *Agric. Ecosyst. Environ.* **2024**, *368*, 109006. [CrossRef]
58. Ye, L.F.; Liu, H.Y.; Dan Deng, H.; Zheng, Y.P.; Han, Y.W.; Gao, X.T.; Abbott, L.K.; Zhao, C.M.; Li, J.H. Effects of Decadal Nitrogen and Phosphorus Fertilization on Microbial Taxonomic and Functional Attributes Associated with Soil Organic Carbon Decomposition and Concentration in an Alpine Meadow. *Ecol. Indic.* **2023**, *146*, 109790. [CrossRef]
59. Oosterhuis, D.M.; Loka, D.A.; Kawakami, E.M.; Pettigrew, W.T. Chapter Three—The Physiology of Potassium in Crop Production. In *Advances in Agronomy*; Sparks, D.L., Ed.; Academic Press: Cambridge, MA, USA, 2014; Volume 126, pp. 203–233.
60. Managing Potassium for Organic Crop Production in: HortTechnology Volume 17 Issue 4. 2007. Available online: https://journals.ashs.org/horttech/view/journals/horttech/17/4/article-p455.xml (accessed on 21 August 2024).
61. Critical Aspects of Potassium Management in Agricultural Systems—Öborn—2005—Soil Use and Management—Wiley Online Library. Available online: https://bsssjournals.onlinelibrary.wiley.com/doi/abs/10.1111/j.1475-2743.2005.tb00114.x (accessed on 21 August 2024).

62. Khati, P.; Mishra, P.K.; Parihar, M.; Kumari, A.; Joshi, S.; Bisht, J.K.; Pattanayak, A. Potassium Solubilization and Mobilization: Functional Impact on Plant Growth for Sustainable Agriculture. In *Advances in Plant Microbiome and Sustainable Agriculture: Functional Annotation and Future Challenges*; Yadav, A.N., Rastegari, A.A., Yadav, N., Kour, D., Eds.; Springer: Singapore, 2020; pp. 21–39. ISBN 9789811532047.
63. Rosolem, C.A.; Mallarino, A.P.; Nogueira, T.A.R. Considerations for Unharvested Plant Potassium. In *Improving Potassium Recommendations for Agricultural Crops*; Murrell, T.S., Mikkelsen, R.L., Sulewski, G., Norton, R., Thompson, M.L., Eds.; Springer International Publishing: Cham, Switzerland, 2021; pp. 147–162.
64. Venterink, H.O.; van der Vliet, R.E.; Wassen, M.J. Nutrient Limitation along a Productivity Gradient in Wet Meadows. *Plant Soil* **2001**, *234*, 171–179. [CrossRef]
65. Duffkova, R.; Kvívtek, T. Effect of Cutting Regime on Soil Physical Properties of Wet Thistle Meadows. *Soil Water Res.* **2009**, *4*, 104–115. [CrossRef]
66. Rodríguez, A.; Canals, R.M.; Sebastià, M.-T. Positive Effects of Legumes on Soil Organic Carbon Stocks Disappear at High Legume Proportions Across Natural Grasslands in the Pyrenees. *Ecosystems* **2022**, *25*, 960–975. [CrossRef]

Disclaimer/Publisher's Note: The statements, opinions and data contained in all publications are solely those of the individual author(s) and contributor(s) and not of MDPI and/or the editor(s). MDPI and/or the editor(s) disclaim responsibility for any injury to people or property resulting from any ideas, methods, instructions or products referred to in the content.

agronomy

MDPI

Article

Fertilizers and Manures Enhance the Bioavailability of Soil Phosphorus Fractions in Karst Grassland

Jie Pan [1], Feng Yang [2], Wen Yang [3], Mingjun Zhang [4], Shengjiang He [1] and Zhou Li [1,*]

[1] Key Laboratory of Animal Genetics, Breeding and Reproduction in the Plateau Mountainous Region, Ministry of Education, College of Animal Science, Guizhou University, Guiyang 550025, China
[2] Guizhou Grassland Technology Experiment and Extension Station, Guiyang 550025, China
[3] Yunnan Forage and Fodder Workstation, Kunming 650225, China
[4] Livestock and Poultry Genetic Resources Management Station of Guizhou Province, Guiyang 550025, China
* Correspondence: zli8@gzu.edu.cn

Abstract: Phosphorus is one of the major constraints to karst grassland productivity. Understanding the effects of different fertilization practices on soil phosphorus dynamics is essential for enhancing phosphorus bioavailability and rational management of soil phosphorus in karst grasslands. Here, we investigated the effects of fertilizers and manures on soil bioavailability of phosphorus fractions and explored the relationship between soil properties and soil phosphorus fractions. The four fertilizer application designs were as follows: control (CK; no fertilizer or manure); fertilization (F); manure application (M); fertilization and manure application (FM). The results showed that total phosphorus (TP) concentration was elevated by 23%, 1%, and 42% in F, M, and FM treatments, respectively, compared with CK. F and FM treatments enhanced the total inorganic phosphorus (Pi) concentration by 65% and 66%, respectively, while M and FM treatments enhanced the total organo-phosphorus (Po) concentration by 21% and 35%, respectively. FM treatment elevated bioavailable P, active Po, secondary mineral P, primary mineral P, and occluded P by 69%, 39%, 50%, 31%, and 41%, respectively. Fertilizers inhibited soil acid phosphatase activity, whereas alkaline phosphatase did not respond significantly to fertilizer management in low-latitude karst regions. SOM, TN, AP, and MBP are the key factors affecting the bioavailability of phosphorus fractions. The combined application of fertilizer and manure is the most beneficial measure for enhancing soil phosphorus bioavailability. This research helps deepen our understanding of soil phosphorus dynamics in the karst areas and provides a basis for further enhancement of nutrient availability and vegetation productivity of grassland ecosystems.

Keywords: fertilizer; manure; soil bioavailability of phosphorus fractions; karst area; grassland

1. Introduction

Phosphorus (P) is an essential macro-nutrient for plant growth and is involved in many important nutritional and physiological processes in plants, as well as many key microbial and biochemical functions of soil ecosystems [1,2]. Thus, phosphorus limitation often constrains the maintenance of plant productivity and soil microbial structure and community health. Soil phosphorus is always limiting as it is highly susceptible to immobilization by reactive metal ions or microorganisms, and phosphate is readily adsorbed on positively charged soil minerals. The phosphorus concentration of the soil solution is also controlled by a continuous process of adsorption, precipitation, desorption, and dissolution [3]. The uptake and utilization of soil phosphorus fractions by plants and microorganisms often depend on their solubility and bioavailability [4]. The chemical fractionation method proposed by Hedley et al. [5]. provides researchers with an efficient way to separate and characterize different forms of phosphorus, which play different roles in soil phosphorus transformations. Tiessen et al. [6]. developed an empirical pathway

model for inferring whether one soil phosphorus fraction can be converted to another. Hou et al. [7]. optimized and validated this model based on previous work to make it more accurate for assessing the importance of different soil phosphorus fractions or phosphorus pools in determining soil phosphorus availability. Redefining the bioavailability phosphorus fractionation methods based on this model may open new pathways for soil phosphorus availability studies in the future [8].

Fertilization is widely used by humans to enhance the productivity of agricultural systems, which typically involves using organic matter or inorganic fertilizers to enhance the amount of plant-available phosphorus in the soil [9–11]. With the rapid increase in food demand by the global population, the consumption of phosphorus fertilizer has also increased significantly [12]. Soil phosphorus management is of greater importance in low-latitude areas, where phosphorus limitation is more prominent. This is particularly true for the karst areas featuring precipitation abundance, severe water runoff, and shallow soil profile [13,14]. The chemical form of phosphorus in a fertilizer or manure is one of the key factors determining its potential bioavailability. After the fertilizer enters the soil, part of the phosphate directly affects the soil's inorganic phosphorus content, and part of it may stimulate the decomposition of organic matter or be associated with changing the soil Pi content by improving soil properties [15]. Manure enters the soil and stimulates organic phosphorus mineralization or affects the turnover of soil phosphorus fractions [16,17]. Understanding the chemical form of phosphorus in the soil after fertilizer application is critical to understanding soil phosphorus dynamics. Although the beneficial effects of the combined application of manure and mineral fertilizers on the maintenance of soil phosphorus fertility have been tentatively demonstrated in parts of the subtropics [16], similar information in the Karst areas is extremely limited. For example, a previous study has shown that fertilization is beneficial in increasing total phosphorus in grassland soils [18] and promoting inter-root phosphorus turnover in legumes [19]. However, information is still lacking regarding the bioavailability of phosphorus and the effects of fertilizer practices on soil phosphorus dynamics within pasture ecosystems in subtropical karst regions.

Therefore, this study was designed based on a three-year field experiment to investigate the effects of fertilizer and manure application on soil phosphorus dynamics in karst grassland. We aimed to evaluate (i) the effect of mineral fertilizers and manure on the soil bioavailability of phosphorus fractions and (ii) the relationship between soil properties and soil bioavailability of phosphorus fractions. We hypothesized that mineral fertilizers and manure would enhance soil phosphorus bioavailability, and bioavailable phosphorus fractions are closely related to phosphatase and microbial biomass phosphorus.

2. Materials and Method

2.1. Site Description

The study was carried out in the research base of grassland ecology at the Oil fir River pasture (27°23′ N, 105°52′ E), in Bijie City, Guizhou province. During the experimental period (2012–2015), the average annual temperature was 11.3 °C, and the average annual precipitation was 1014 mm. Locally, fertilization and grazing are the main factors. The pasture was originally established as a natural grassland dominated by shrubs and warm-season grasses in the fall of 2012. The whole research area was enclosed by cattle fences. The initial establishment of forages included red clover (*Trifolium pratense*), white clover (*Trifolium repens*), duck grass (*Dactylis glomerata*), and perennial ryegrass (*Lolium perenne*), at a seeding rate of 4.5, 7.5, 9.0, and 18.0 kg ha^{-1}, respectively. Within the whole pasture area, 0.05 ha was fenced out and selected as the test area. Plots were set up starting at 5 m from the fence with 2 m between plots. Each plot was set up as 40 m^2 (5 × 8 m). The experiment was set up as a randomized, complete block design with three blocks with repeated measures. This area is protected from livestock grazing and other human disturbance by fencing systems. Soil phosphorus fractions prior to implementation of management are shown in Table 1.

Table 1. The mean of soil total P (TP), bioavailable P, active Po, secondary mineral P, primary mineral P, and occluded P at different layers in the unused land (UL), abandoned grazing pastureland (APL), grazing pastureland (GPL), and fertilized grazing pastureland (FGPL) treatments in 2012.

Layer (cm)	Bioavailable P (mg kg^{-1})	Active Po (mg kg^{-1})	Secondary Mineral P (mg kg^{-1})	Primary Mineral P (mg kg^{-1})	Occluded P (mg kg^{-1})	TP (g kg^{-1})
0–10	15.65	270.94	51.33	42.57	39.44	0.43
10–30	6.24	256.07	29.60	33.04	38.28	0.37

2.2. Study Design

The experiment consisted of four different types of treatment: (i) control (CK): no fertilizer or manure inputs; (ii) fertilization (F): use of NPK fertilization; (iii) manure application (M): using a mixture of cattle manure and urine; (iv) fertilization and manure application (FM): application of the mixture of manure, urine, and NPK fertilizer. Grazing was simulated using mechanical mowing based on typical grazing management practices from local livestock producers in all treatments. Specifically speaking, once the average canopy height reaches 20 cm, the entire area is mowed using machinery, leaving a stubble height of 5 cm. The herd species grazed on the ranch are Angus and Simmental cattle. According to the digestive and excretory characteristics of the two types of cattle [20], under the stocking rate of 1.5 head ha^{-1}, the amount of manure applied was maintained at 5400 kg ha^{-1} of feces–urine mixture [21]. Manures with an average phosphorus content of 0.36% were applied each month to the plots corresponding to the treatments. Fertilizers were applied in accordance with a total amount of 300 kg ha^{-1} per year, of which 15% each of N, $P_2O_{5,}$ and K_2O elements. Fertilizer is applied during the annual pasture return season (March), the summer season, when the pasture is actively growing (June), and the compensatory growing season after fall utilization (September). The FM treatment application consisted of 2730 kg of manure and 150 kg of compound fertilizer was also applied at the same time as described above.

2.3. Soil Sample and Analysis

In August of 2012 and 2015, soil sampling was carried out using a 5 cm corer and "S-sampling" method. The sampling depths include both the 0–10 (topsoil) cm and 10–30 (subsoil) cm layers. The samples from the same plot with the same soil layer were mixed to form a composite sample, and stones and roots were removed before any laboratory analysis.

Soil total P (TP) and available P (AP) were measured using the Mo-Sb colorimetric method [22]. Microbial biomass P (MBP) was determined by chloroform fumigation method [23]. Soil P fractions were analyzed according to the Hedley sequential extraction procedure [5,24]. Briefly, P fractions were extracted using the following solvents: deionized water, 0.5 M $NaHCO_3$, 0.1 M NaOH, 1M HCl, concentrated HCl, and concentrated H_2SO_4. The organic P (Po) concentration of the different extracts was calculated by total P and inorganic P (Pi). Residue P was calculated by TP and the sum of the P fractions above. Total Pi was calculated as the sum of the different Pi fractions above, and total Po was calculated as the sum of the different Po fractions. Phosphorus fractions were classified into five types according to their bioavailability based on the model developed by Hou et al. [7]. Bioavailability P included resin-P and $NaHCO_3$-Pi. Active Po included $NaHCO_3$-Po and NaOH-Po. NaOH-Pi was defined as secondary mineral P. Primary mineral P includes 1M HCl-Pi, conc. HCl-Pi, and total conc. HCl-P. Residual P was defined as occluded P [8].

Soil pH was determined by a pH meter (Mettler-Toledo Seven Compact S210, Switzerland) with a soil–water ratio of 1:5 (w/v) [25]. Bulk density (BD) was measured using the metal ring [26]. Total nitrogen (TN) was determined by the Kjeldahl method (Hanon-K1100, Hyene Future Technology Group Co., Ltd., Jinan, Shandong, China) [27]. Soil organic matter (SOM) was calculated by soil organic carbon (SOC), and SOC was determined via

the SKALAR carbon analyzer (Primacs ATC 100-IC-E, Skalar Analytical B.V., Breda, Netherlands) [28]. The soil alkaline phosphatase (AKP) and acid phosphatase (ACP) activity was analyzed using the methods described by Acosta-Martínez and Ali Tabatabai [29].

2.4. Statistical Analysis

We used univariate analysis of variance (ANOVA, $p < 0.05$) to test the effects of different treatments, soil depth on soil P fractions, and soil enzyme activities. Duncan's multiple range test was used for mean separation. Two-way ANOVA was used to compare the effect of fertilizers and manures and their interaction at $p < 0.05$ level. Principal component analysis (PCA) was used to identify the relationship between environmental factors and different soil bioavailability of phosphorus fractions (R software, version 4.3.2). Structural equation modeling was performed using the "plspm" package.

3. Results

3.1. Soil Total Phosphorus

In the topsoil, the TP and total Pi concentration of FM treatment were greater than CK and M treatments (Figure 1; $p < 0.05$). The TP of the F treatment was greater than the CK treatment ($p < 0.05$). The total Pi of the F treatment was greater than that of the CK and M treatments. The total Po of the FM treatment was greater than that of the CK and F treatments. Compared with CK treatment, the total Po concentration of F treatment was increased by 9.62%. The total Po concentration of M treatment was increased by 21.84%, and the total Po concentration of FM treatment was increased by 35.06%. In the subsoil, there were no significant differences between the four treatments in TP, total Pi, and total Po. Both F and M had a significant effect on TP.

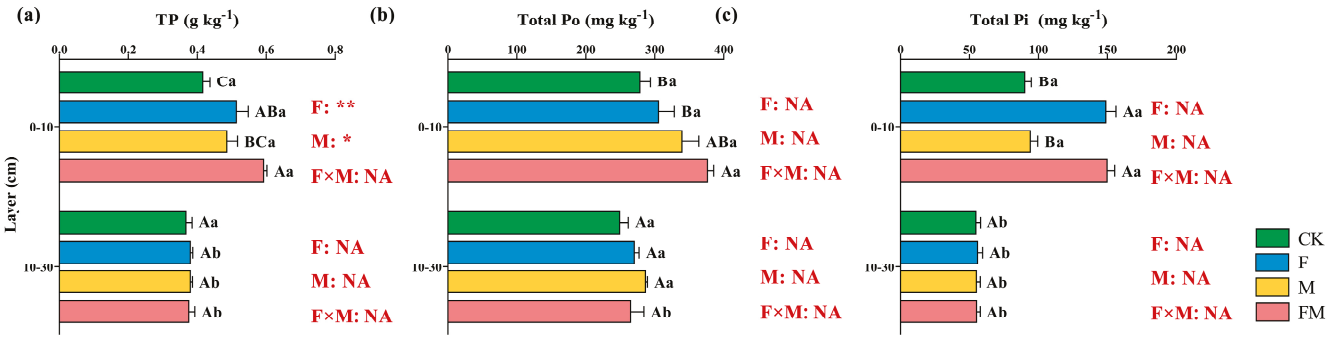


Figure 1. The concentration of (**a**) total P (TP), (**b**) total organic P (TPo), and (**c**) total inorganic P (TPi) at 0–10 and 10–30 cm in the control (CK), mow and fertilize (F), mow and manure (M), and mow fertilize and manure (FM) treatments in 2015. Mean ± standard error of three blocks. Different capital letters indicate significant differences between different treatments in the same soil layer, and different lowercase letters indicate significant differences between different soil layers in the same treatment. Two-way ANOVA results are shown in red. ** $p \leq 0.01$, and * $p \leq 0.05$. NA indicates no significant effect. F is for fertilizers, M is for manures, and F × M is for the interaction of fertilizers and manures.

3.2. Soil Bioavailability of Phosphorus Fractions

In the topsoil, the bioavailable P concentration of FM treatment was greater than other treatments (Figure 2; $p < 0.05$), and the bioavailable P concentration of F treatment was greater than that of CK and M treatments ($p < 0.05$). The active Po concentration of FM and F treatments was greater than the CK treatment. The secondary mineral P concentration of FM treatment was greater than other treatments. The secondary mineral P concentration of the M treatment was greater than the CK treatment. The primary mineral P concentration of the FM treatment was greater than that of the CK and F treatments. The occluded P concentration of FM treatment was greater than other treatments. In the subsoil, there

were no significant differences between the four treatments in bioavailable P, active Po, secondary mineral P, primary mineral P, and occluded P. Both F and M had a significant effect on bioavailable P. F has a significant effect on active Po; significant interaction effects of F and M on secondary mineral P. Both F and M had a significant effect on secondary mineral P. M has a significant effect on primary mineral P. Both F and M had a significant effect on occluded P.

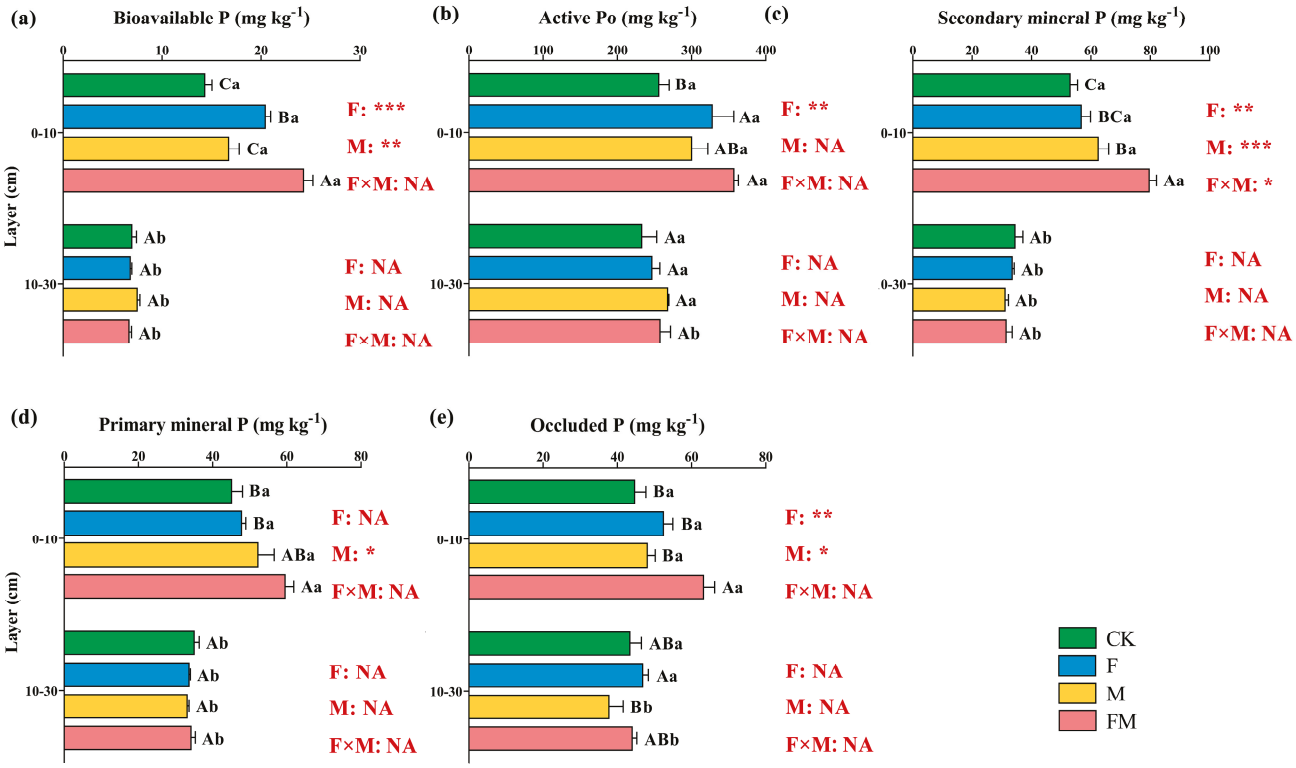


Figure 2. The concentration of (**a**) bioavailable P, (**b**) active Po, (**c**) secondary mineral P, (**d**) primary mineral P, and (**e**) occluded P at 0–10 and 10–30 cm in the control (CK), mow and fertilize (F), mow and manure (M), and mow fertilize and manure (FM) treatments in 2015. Mean ± standard error of three blocks. Different capital letters indicate significant differences between different treatments in the same soil layer, and different lowercase letters indicate significant differences between different soil layers in the same treatment. Two-way ANOVA results are shown in red. *** $p \leq 0.001$, ** $p \leq 0.01$, and * $p \leq 0.05$. NA indicates no significant effect. F is for fertilizers, M is for manures, and F × M is for the interaction of fertilizers and manures.

Active Po dominates the TP with about 61.16–64.70% in topsoil (Figure 3). The percentage of bioavailable P in TP was 3.47–4.16%. The percentage of secondary mineral P in TP was 11.27–13.64%. The percentage of primary mineral P in TP was 9.53–10.91%. The percentage of occluded P in TP was 10.05–10.83%. In the subsoil, active Po dominates the TP with about 64.21–71.57%. The percentage of bioavailable P in TP was 1.79–2.00%. The percentage of secondary mineral P in TP was 8.33–9.57%. The percentage of primary mineral P in TP was 8.87–9.72%. The percentage of occluded P in TP was 9.20–14.56%.

3.3. Soil Biological Activity

In the topsoil, the ACP activity of the F treatment was lower than the CK and M treatments, and the ACP activity of the FM treatment was lower than the CK treatment (Figure 4; $p < 0.05$). The concentrations of MBP in the FM treatment were greater than in other treatments, and those in the CK treatment were lower than in other treatments.

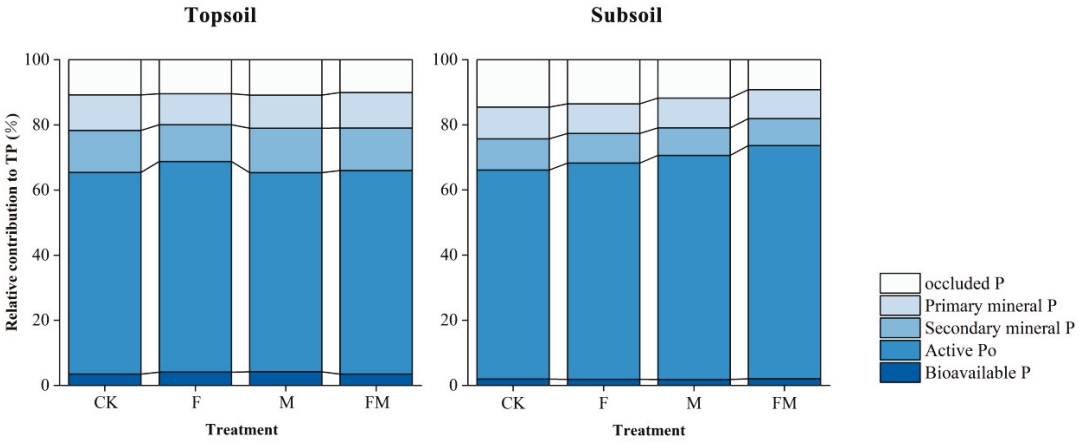


Figure 3. The proportion of bioavailable P, active Po, secondary mineral P, primary mineral P, and occluded P at 0–10 (topsoil) and 10–30 (subsoil) cm in the control (CK), mow and fertilize (F), mow and manure (M), and mow fertilize and manure (FM) treatments in 2015.

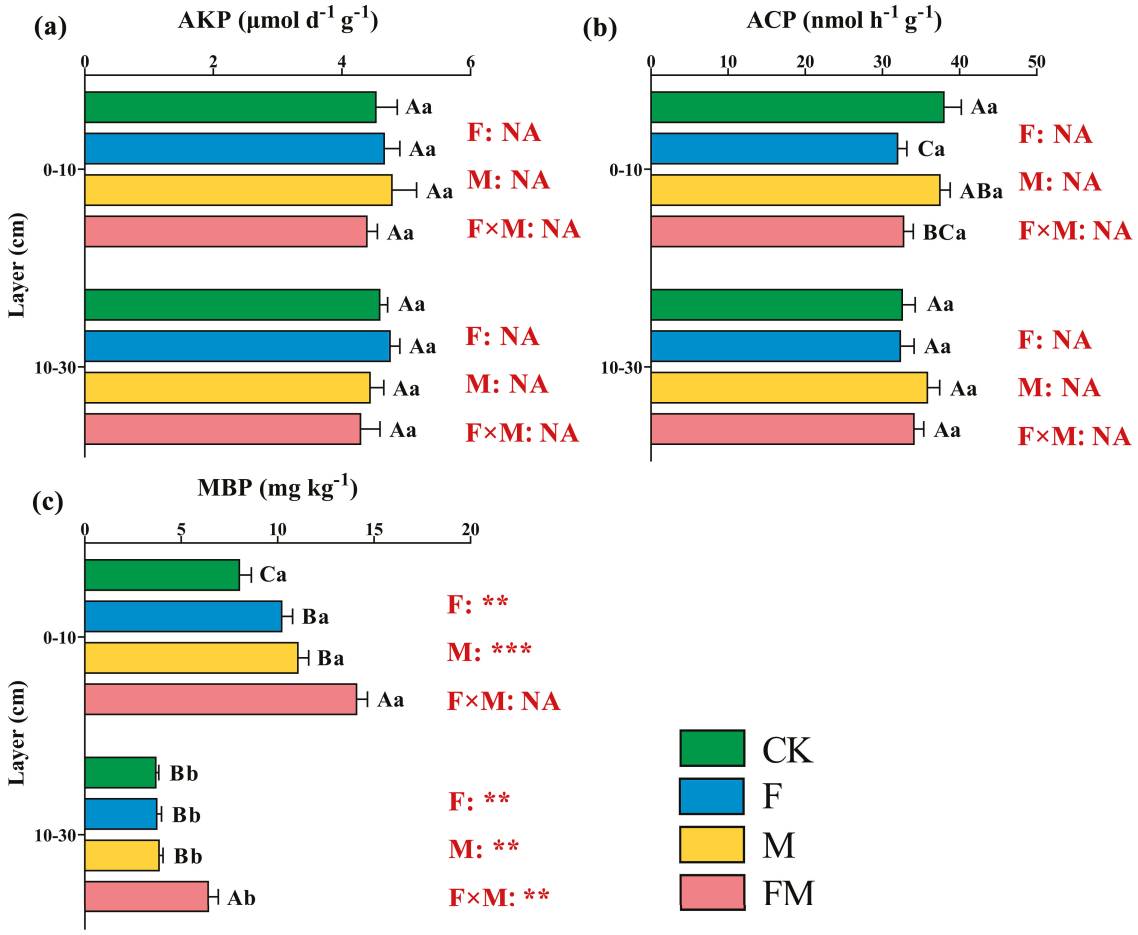


Figure 4. The concentration of (**a**) the activity of alkaline phosphatase (AKP), (**b**) acid phosphatase (ACP) and (**c**) microbial biomass phosphorus (MBP) treatments in 2015. Mean ± standard error of three blocks. Different capital letters indicate significant differences between different treatments in the same soil layer, and different lowercase letters indicate significant differences between different soil layers in the same treatment. Two-way ANOVA results are shown in red. *** $p \leq 0.001$, ** $p \leq 0.01$. NA indicates no significant effect. F is for fertilizers, M is for manures, and F × M is for the interaction of fertilizers and manures.

In the subsoil, the concentration of MBP in the FM treatment was greater than other treatments. There was no significant difference between the four treatments in AKP and ACP activity. Both in the topsoil and subsoil, there were no significant differences between the four treatments in AKP activity.

3.4. The Relationship of Environmental Factors and Soil Bioavailability of Phosphorus Fractions

At the 0–10 cm layer, the pH values of M and FM were greater than F and CK (Table 2). The SOM of FM was greater than other treatments. The SOM of F was greater than CK. At the 0–10 cm and 10–30 cm layers, the TN of FM was greater than CK and M.

Table 2. Mean of the soil properties in different treatments.

Treatment	Layer	pH	BD	SOM	TN
CK	0–10	4.79 Ba	0.99 Aa	88.13 Ca	2.59 Ba
MF	0–10	4.75 Ba	0.99 Aa	101.13 Ba	2.85 ABa
MM	0–10	4.94 Aa	1 Aa	92.49 BCa	2.72 Ba
MFM	0–10	5.06 Aa	0.96 Aa	123.36 Aa	3.12 Aa
CK	10–30	4.84 Aa	1.04 Aa	51.45 Ab	1.76 Bb
MF	10–30	4.89 Aa	1.03 Ba	51.17 Ab	1.77 ABb
MM	10–30	4.96 Aa	1.09 ABa	47.99 Ab	1.75 Bb
MFM	10–30	5.01 Aa	1.01 Ba	49.86 Ab	1.85 Ab
Two-way ANOVA					
F	0–10	NA	NA	***	*
M	0–10	**	NA	**	NA
F × M	0–10	NA	NA	*	NA
F	10–30	NA	NA	NA	NA
M	10–30	NA	NA	NA	NA
F × M	10–30	NA	NA	NA	NA

Notes: Mean of three blocks. Capital letters indicate significant differences between different treatments in the same soil layer, and lowercase letters indicate significant differences between different soil layers in the same treatment. *** $p \leq 0.001$, ** $p \leq 0.01$, and * $p \leq 0.05$. NA indicates no significant effect. F is for fertilizers, M is for manures, and F × M is for the interaction of fertilizers and manures.

In the CK treatment (Figure 5), principal component 1 (PC1) explained 59.4% of the total variation, and principal component 2 (PC2) explained 19.8% of the total variation. SOM, TN, MBP, and AP are the key factors influencing the variation in bioavailable P, active Po, secondary mineral P, and primary mineral P. In the F treatment, PC1 explained 63.7% of the total variation and PC2 explained 15.6% of the total variation. SOM, TN, MBP, AP, and MBP are the key factors influencing the variation in soil phosphorus fractions. In the M treatment, PC1 explained 69.8% of the total variation, and PC2 explained 12.9% of the total variation. SOM, TN, MBP, AP, AKP, and ACP had a strong correlation with soil phosphorus fractions. In the FM treatment, PC1 explained 69.8% of the total variation and PC2 explained 12.9% of the total variation. SOM, TN, MBP, AP, and pH had a strong correlation with soil phosphorus fractions. On PC2, pH and BD are critical factors for AKP and ACP.

BD had a significant positive effect on AKP (Figure 6). SOM had a significant negative effect on ACP. pH has a strong negative effect on ACP. TN has a strong negative effect on MBP. pH and BD each had strong positive effects on the soil bioavailability of phosphorus fractions. BD had a strong positive effect on MBP and ACP.

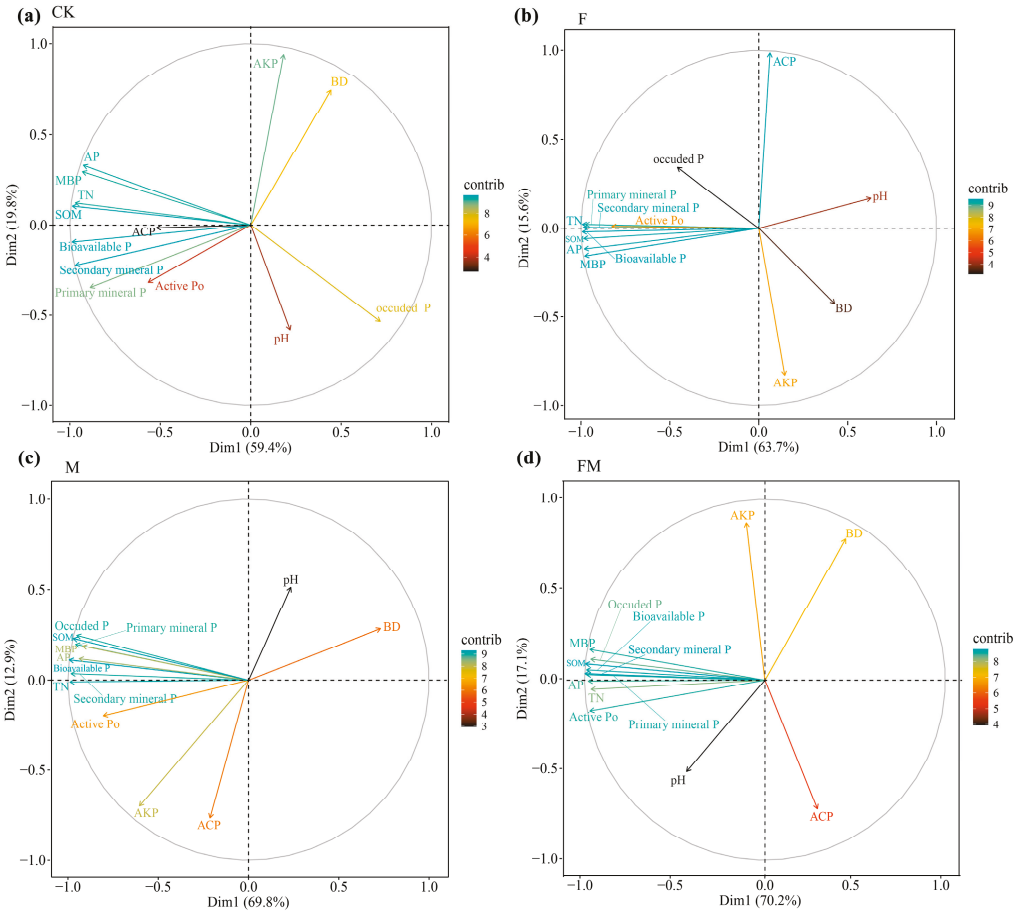


Figure 5. The PCA between environmental factors and soil bioavailability of phosphorus fractions in (**a**) the control (CK), (**b**) mow and fertilize (F), (**c**) mow and manure (M), and (**d**) mow fertilize and manure (FM) treatments different treatments.

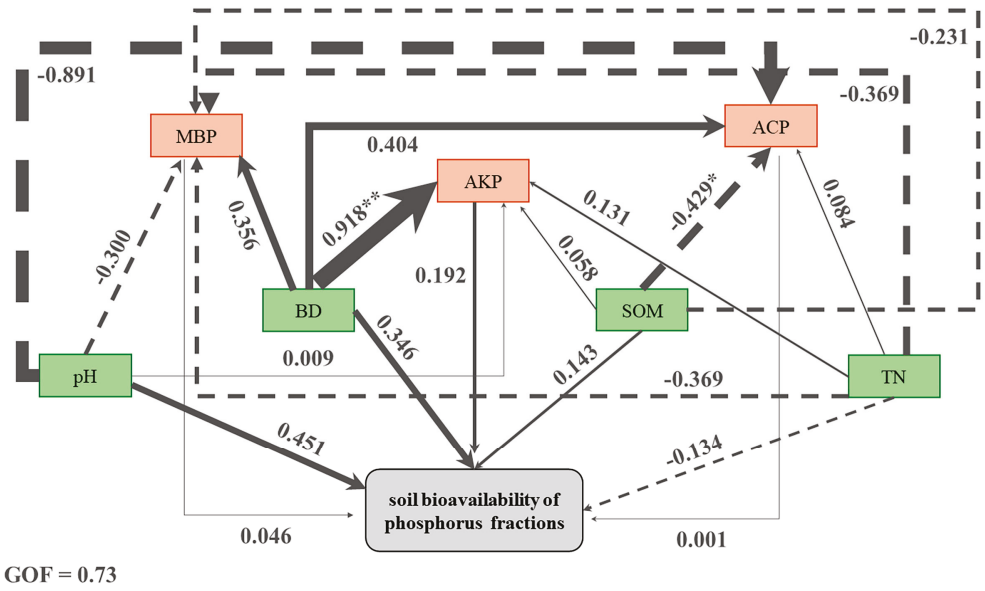


Figure 6. Conceptual model depicting the hypothesized relationship between environmental factors and soil bioavailability of phosphorus fractions. The numbers represent the path coefficient. Solid and dash arrows indicate positive and negative effects, respectively. Goodness of fit (GOF) is used to assess the overall fit of the model. Significance levels of each symbol are ** $p \leq 0.01$, and * $p \leq 0.05$.

4. Discussion

4.1. Effect of Different Fertilizers on Soil Total Phosphorus

Compared to CK, the application of manure alone did not significantly elevate TP, but it showed an increasing trend in total Po. The fecal composition of animals varies greatly due to genetics, food sources, and nutritional requirements [30]. The manure in this study was obtained from cattle excreta, and its high organic phosphorus content resulted in an upward trend in soil organic phosphorus [31]. Application of mineral fertilizers alone significantly increased soil TP as well as total Pi, which is consistent with the results reported by Wang et al. [32] in the Loess Plateau. It is noteworthy that the application of manure and mineral fertilizers significantly increased the TP, total Pi, and total Po content of the soil, which is consistent with the results reported by Anthonio et al. [33] and Wang et al. [17]. Agricultural soils can receive phosphorus through resource inputs from both organic and inorganic sources [34]. However, information relating to the comparison between inorganic and organic sources on soil phosphorus status, particularly under the equal P amount level, remains scanty. As indicated in our study and previous research work, manure and mineral fertilizers applied in combination can significantly enhance phosphorus recovery [35]. It is also possible that the incorporation of manure reduces the precipitation rate of Ca^{2+}, etc. when combined with the phosphate from fertilizers [36]. We therefore concluded that mineral fertilizers combined with manure had the highest capacity for phosphorus nutrient enrichment.

At the same time, we need to be concerned that solely increases in a single aspect of soil inorganic or organic phosphorus fraction may lead to alterations/interferences in the soil phosphorus cycle or phosphorus turnover. These changes are more likely to result from changes in microbial communities, such as elevating the abundance of bacteria with the potential for organophosphorus mineralization or altering the composition of bacterial communities with the potential for phosphate solubilization [37]. In contrast, FM treatment increased soil phosphorus in both inorganic and organic forms in a balanced manner, thereby promoting healthy maintenance of soil microbial activity (MBP) and community structure [16]. The interaction of fertilizer and manure was significant in elevating secondary mineralized phosphorus. This is beneficial for the long-term supply of bioavailable phosphorus and also benefits from the rapid turnover of phosphorus under strong microbial activity [7].

4.2. Effect of Different Fertilizers on the Soil Bioavailability of Phosphorus Fractions

The results of this study showed that the combination of mineral fertilizers and manure significantly enhanced soil bioavailable P compared to CK. Additionally, the application of mineral fertilizers alone also significantly enhanced soil bioavailable P, but the application of manure alone did not. This suggests that the rapid release of fast-acting nutrients from mineral fertilizers dominates in increasing soil-effective phosphorus during short-term fertilizer management [15]. Although not evaluated in this study, other nutrient/microbial beneficial impacts caused by manure should not be ignored. We also found significantly higher bioavailable P concentrations in FM than in F. This may be due to the fact that manure reduces the fixation of phosphorus by soil particles and promotes the conversion of low bioavailable phosphorus fractions to high bioavailable phosphorus fractions [17]. Compared to mineral fertilizers, animal manure has a more complex composition, containing organic substances such as organic acids, humus, and lignin, which can improve soil phosphorus bioavailability by increasing the decomposition of organic matter [38]. This is also reflected in the significantly higher MBP concentrations in FM. Similarly, the present study found that mineral fertilizers in combination with manure application significantly enhanced active Po. This is in agreement with the results reported by Khan et al. [15], stating that fertilizer management can significantly enhance the soil's active phosphorus pools including NaOH-Po and $NaHCO_3$-Po. These reactive organic phosphorus are also the components with the highest percentage in TP. This is consistent with the average percentage of organic phosphorus in most soils [39]. It has

been shown that fertilizer application alters soil phosphorus dynamics in karst regions [19]. In our environment, the higher protonation of minerals at lower pH might increase the ability of iron or aluminum ions to adsorb phosphorus, represented in the form of more active Po and secondary mineral P [3]. This fraction of phosphorus, although not as directly and rapidly available as bioavailable phosphorus to provide nutrients to plants and microorganisms, can still be activated and utilized by plants or microorganisms through certain access strategies [40].

In this study, manure alone did not significantly increase soil primary mineral P and occluded P, but both phosphorus fractions increased significantly when applied in combination with mineral fertilizers. After mineral fertilizers are added, a portion of the orthophosphate is rapidly converted to recalcitrant phosphorus in the soil solution [41]. Khan et al. [15] suggested that under conditions of sufficient effective phosphorus, newly added phosphorus may increase binding to colloidal or organic compounds in the soil, which promotes the transport of phosphorus in the soil. Although this fraction of phosphorus is not active enough relative to the bioavailable P and active Po fractions, it may also become available under conditions of long-term active root activity [42]. The present study also found that AKP was generally unresponsive to treatment, which may be due to the fact that alkaline phosphatase does not play a dominant role in areas of lower pH [43]. Whereas, compared to manure, mineral fertilizers containing phosphorus significantly inhibited the activity of ACP, which is consistent with the results of Touhami et al. [44]. Another possible explanation is that the increase in acid phosphatase activity is induced when phosphorus limitation is exacerbated, and there is an increase in organophosphorus substrates [45].

In addition, the combination of mineral fertilizers and manure in this study can additionally provide effective nutrients to support phosphorus uptake by plants or microorganisms. For example, an increase in soil SOM, MBP, and TN concentrations through favorable environmental conditions can play a dominant role in the mineralization of soil organic phosphorus [15]. The results of PCA analysis in this study showed that soil properties (SOM, TN, AP, and MBP) were the key factors influencing the individual bioavailable phosphorus fractions. Meanwhile, the conceptual modeling results indicated that pH and BD not only have direct positive effects on phosphorus fractions but also indirectly affect phosphorus fractions by influencing ACP, AKP, and MBP. This was also reported in the findings of Bhupenchandra et al. [46]. Fertilizer application may also affect the effectiveness of soil phosphorus nutrients, soil solution flow, and storage by improving soil physical properties, such as the formation and stability of soil macroaggregates [47]. This study investigated the effects of mineral fertilizers and manure on phosphorus fractions from the perspective of bioavailability and emphasized the enhancement effect of soil phosphorus nutrient enrichment capacity and bioavailability by the application of mineral fertilizers in conjunction with manure. Further research is warranted to better delineate the linkage between soil phosphorous status and microbial community structure and/or enrichment of functional genes, such as *phoD*, *phn*, and *phoU* [48].

5. Conclusions

This study revealed that mineral fertilizers combined with manure had the highest capacity for phosphorus nutrient enrichment. Rapid release of mineral fertilizer nutrients played a dominant role in enhancing soil bioavailable phosphorus. In contrast, manure also enhances soil bioavailable phosphorus in terms of both reduced phosphorus fixation and increased organic matter decomposition. The combination of the two directly enhances the individual bioavailable phosphorus fractions of soil and supports better plant or microbial phosphorus uptake by providing favorable environmental conditions or additional effective nutrients (SOM, TN, etc.). The application of mineral fertilizers alone inhibits soil acid-phosphatase activity. To our knowledge, there is very little prior research considering the effects of chemical fertilizers, manure, and the mixture of the two on soil phosphorus fractions from the perspective of bioavailability in the karst areas. Thus, the findings from this study could provide foundational knowledge for future research directions.

Author Contributions: Conceptualization, S.H. and Z.L.; data curation, J.P. and Z.L.; formal analysis, J.P. and Z.L.; funding acquisition, Z.L.; investigation, S.H.; methodology, F.Y. and Z.L.; project administration, M.Z.; resources, F.Y., W.Y. and M.Z.; supervision, F.Y. and Z.L.; validation, W.Y. and Z.L.; writing—original draft, J.P.; writing—review and editing, J.P. and Z.L. All authors have read and agreed to the published version of the manuscript.

Funding: This research was financed by the National Natural Science Foundation of China (32160337), the Guizhou Provincial Science and Technology Projects (Qian Ke He Zhi Cheng [2022] Yi Ban 106; Qian Ke He Zhi Cheng [2023] Yi Ban 473; QKHPTRC-CXTD [2022]011).

Data Availability Statement: The data presented in this study are available on request from the corresponding author.

Conflicts of Interest: The authors declare no conflicts of interest.

References

1. Elser, J.J.; Bracken, M.E.S.; Cleland, E.E.; Gruner, D.S.; Harpole, W.S.; Hillebrand, H.; Ngai, J.T.; Seabloom, E.W.; Shurin, J.B.; Smith, J.E. Global analysis of nitrogen and phosphorus limitation of primary producers in freshwater, marine and terrestrial ecosystems. *Ecol. Lett.* **2007**, *10*, 1135–1142. [CrossRef]
2. Fu, D.; Wu, X.; Duan, C.; Zhao, L.; Li, B. Different life-form plants exert different rhizosphere effects on phosphorus biogeochemistry in subtropical mountainous soils with low and high phosphorus content. *Soil Tillage Res.* **2020**, *199*, 104516. [CrossRef]
3. Hinsinger, P. Bioavailability of soil inorganic P in the rhizosphere as affected by root-induced chemical changes: A review. *Plant Soil* **2001**, *237*, 173–195. [CrossRef]
4. Cross, A.F.; Schlesinger, W.H. A literature review and evaluation of the. Hedley fractionation: Applications to the biogeochemical cycle of soil phosphorus in natural ecosystems. *Geoderma* **1995**, *64*, 197–214. [CrossRef]
5. Hedley, M.J.; Stewart, J.W.B.; Chauhan, B.S. Changes in Inorganic and Organic Soil Phosphorus Fractions Induced by Cultivation Practices and by Laboratory Incubations. *Soil Sci. Soc. Am. J.* **1982**, *46*, 970–976. [CrossRef]
6. Tiessen, H.; Stewart, J.W.B.; Cole, C.V. Pathways of Phosphorus Transformations in Soils of Differing Pedogenesis. *Soil Sci. Soc. Am. J.* **1984**, *48*, 853–858. [CrossRef]
7. Hou, E.; Chen, C.; Kuang, Y.; Zhang, Y.; Heenan, M.; Wen, D. A structural equation model analysis of phosphorus transformations in global unfertilized and uncultivated soils. *Glob. Biogeochem. Cycles* **2016**, *30*, 1300–1309. [CrossRef]
8. Tian, X.; Bing, H.; Wu, Y.; Zhu, H.; Zhao, W.; He, Q.; Xiong, D. Farmland abandonment decreases soil bioavailable phosphorus but increases organic phosphorus in the mid-hills of Nepal. *Catena* **2022**, *211*, 106000. [CrossRef]
9. MacDonald, G.K.; Bennett, E.M.; Potter, P.A.; Ramankutty, N. Agronomic phosphorus imbalances across the world's croplands. *Proc. Natl. Acad. Sci. USA* **2011**, *108*, 3086–3091. [CrossRef]
10. Li, Z.; Cui, S.; Zhang, Q.; Xu, G.; Feng, Q.; Chen, C.; Li, Y. Optimizing Wheat Yield, Water, and Nitrogen Use Efficiency with Water and Nitrogen Inputs in China: A Synthesis and Life Cycle Assessment. *Front. Plant Sci.* **2022**, *13*, 930484. [CrossRef]
11. Li, Y.; Li, Y.; Zhang, Q.; Xu, G.; Liang, G.; Kim, D.-G.; Carmona, C.R.; Yang, M.; Xue, J.; Xiang, Y.; et al. Enhancing soil carbon and nitrogen through grassland conversion from degraded croplands in China: Assessing magnitudes and identifying key drivers of phosphorus reduction. *Soil Tillage Res.* **2024**, *236*, 105943. [CrossRef]
12. Tian, X.; Engel, B.A.; Qian, H.; Hua, E.; Sun, S.; Wang, Y. Will reaching the maximum achievable yield potential meet future global food demand? *J. Clean. Prod.* **2021**, *294*, 126285. [CrossRef]
13. Ford, D.; Williams, P. Introduction to Karst. In *Karst Hydrogeology and Geomorphology*; Ford, D., Williams, P., Eds.; Wiley: Hoboken, NJ, USA, 2007; pp. 1–8. [CrossRef]
14. Du, E.; Terrer, C.; Pellegrini, A.F.A.; Ahlström, A.; van Lissa, C.J.; Zhao, X.; Xia, N.; Wu, X.; Jackson, R.B. Global patterns of terrestrial nitrogen and phosphorus limitation. *Nat. Geosci.* **2020**, *13*, 221–226. [CrossRef]
15. Khan, A.; Zhang, G.; Li, T.; He, B. Fertilization and cultivation management promotes soil phosphorus availability by enhancing soil P-cycling enzymes and the phosphatase encoding genes in bulk and rhizosphere soil of a maize crop in sloping cropland. *Ecotoxicol. Environ. Saf.* **2023**, *264*, 115441. [CrossRef]
16. Qaswar, M.; Ahmed, W.; Huang, J.; Liu, K.-L.; Zhang, L.; Han, T.-F.; DU, J.-X.; Ali, S.; Ur-Rahim, H.; Huang, Q.-H.; et al. Interaction of soil microbial communities and phosphorus fractions under long-term fertilization in paddy soil. *J. Integr. Agric.* **2022**, *21*, 2134–2144. [CrossRef]
17. Wang, Q.; Qin, Z.-H.; Zhang, W.-W.; Chen, Y.-H.; Zhu, P.; Peng, C.; Wang, L.; Zhang, S.-X.; Colinet, G. Effect of long-term fertilization on phosphorus fractions in different soil layers and their quantitative relationships with soil properties. *J. Integr. Agric.* **2022**, *21*, 2720–2733. [CrossRef]
18. Qin, W.; Zhao, X.; Yang, F.; Chen, J.; Mo, Q.; Cui, S.; Chen, C.; He, S.; Li, Z. Impact of fertilization and grazing on soil N and enzyme activities in a karst pasture ecosystem. *Geoderma* **2023**, *437*, 116578. [CrossRef]
19. Tian, J.; Lu, X.; Chen, Q.; Kuang, X.; Liang, C.; Deng, L.; Lin, D.; Cai, K.; Tian, J. Phosphorus fertilization affects soybean rhizosphere phosphorus dynamics and the bacterial community in karst soils. *Plant Soil* **2022**, *475*, 137–152. [CrossRef]

20. Gooneratne, S.; Laarveld, B.; Pathirana, K.; Christensen, D. Effects of dietary Cu, Mo and S on urinary Cu and Zn excretion in Simmental and Angus cattle. *Res. Veter Sci.* **2011**, *91*, e116–e120. [CrossRef]
21. Salim, H.; Wood, K.M.; Abo-Ismail, M.K.; McEwen, P.L.; Mandell, I.B.; Miller, S.P.; Cant, J.P.; Swanson, K.C. Influence of feeding increasing levels of dry corn distillers grains plus solubles in whole corn grain-based finishing diets on total tract digestion, nutrient balance, and excretion in beef steers1,2. *J. Anim. Sci.* **2012**, *90*, 4441–4448. [CrossRef]
22. Kuo, S. Phosphorus. In *Methods of Soil Analysis: Part 3 Chemical Methods, 5.3*; Sparks, D.L., Page, A.L., Helmke, P.A., Loeppert, R.H., Soltanpour, P.N., Tabatabai, M.A., Johnston, C.T., Sumner, M.E., Eds.; Wiley: Hoboken, NJ, USA, 1996; pp. 869–919. [CrossRef]
23. Brookes, P.C.; Powlson, D.S.; Jenkinson, D.S. Measurement of microbial biomass phosphorus in soil. *Soil Biol. Biochem.* **1982**, *14*, 319–329. [CrossRef]
24. Tiessen, H.; Moir, J.O. Characterization of Available P by Sequential Extraction. In *Soil Sampling and Methods of Analysis*; Carter, M.R., Ed.; Lewis Publishers: Boca Raton, FL, USA, 1993; pp. 75–86.
25. Thomas, G.W. Soil pH and Soil Acidity. In *Methods of Soil Analysis: Part 3 Chemical Methods, 5.3*; Sparks, D.L., Page, A.L., Helmke, P.A., Loeppert, R.H., Soltanpour, P.N., Tabatabai, M.A., Johnston, C.T., Sumner, M.E., Eds.; Wiley: Hoboken, NJ, USA, 1996; pp. 475–490. [CrossRef]
26. Blake, G.R.; Hartge, K.H. Bulk Density. In *Methods of Soil Analysis*; Klute, A., Ed.; Wiley: Hoboken, NJ, USA, 1986; pp. 363–375. [CrossRef]
27. Bremner, J.M.; Tabatabai, M.A. Use of an ammonia electrode for determination of ammonium in Kjeldahl analysis of soils. *Commun. Soil Sci. Plant Anal.* **1972**, *3*, 159–165. [CrossRef]
28. Brady, N.; Weil, R. *The Nature and Properties of Soils*, 7th ed.; Prentice Hall: Upper Saddle River, NJ, USA, 1996.
29. Acosta-Martínez, V.; Ali Tabatabai, M. Phosphorus Cycle Enzymes. In *Methods of Soil Enzymology*; Dick, R.P., Ed.; Wiley: Hoboken, NJ, USA, 2011; pp. 161–183. [CrossRef]
30. Shafqat, M.N.; Pierzynski, G.M.; Xia, K. Phosphorus Source Effects on Soil Organic Phosphorus: $A^{31}P$ NMR Study. *Commun. Soil Sci. Plant Anal.* **2009**, *40*, 1722–1746. [CrossRef]
31. Chen, G.; Yuan, J.; Chen, H.; Zhao, X.; Wang, S.; Zhu, Y.; Wang, Y. Animal manures promoted soil phosphorus transformation via affecting soil microbial community in paddy soil. *Sci. Total. Environ.* **2022**, *831*, 154917. [CrossRef] [PubMed]
32. Wang, J.; Liu, W.-Z.; Mu, H.-F.; Dang, T.-H. Inorganic Phosphorus Fractions and Phosphorus Availability in a Calcareous Soil Receiving 21-Year Superphosphate Application. *Pedosphere* **2010**, *20*, 304–310. [CrossRef]
33. Anthonio, C.K.; Jing, H.; Jin, C.; Khan, M.N.; Jiangxue, D.; Garba, H.N.; Dongchu, L.; Guangrong, L.; Shujun, L.; Lisheng, L.; et al. Impact of long-term fertilization on phosphorus fractions and manganese oxide with their interactions in paddy soil aggregates. *J. Environ. Manag.* **2023**, *333*, 117440. [CrossRef] [PubMed]
34. Bhat, N.A.; Riar, A.; Ramesh, A.; Iqbal, S.; Sharma, M.P.; Sharma, S.K.; Bhullar, G.S. Soil Biological Activity Contributing to Phosphorus Availability in Vertisols under Long-Term Organic and Conventional Agricultural Management. *Front. Plant Sci.* **2017**, *8*, 1523. [CrossRef] [PubMed]
35. Halajnia, A.; Haghnia, G.; Fotovat, A.; Khorasani, R. Phosphorus fractions in calcareous soils amended with P fertilizer and cattle manure. *Geoderma* **2009**, *150*, 209–213. [CrossRef]
36. Delgado, A.; Madrid, A.; Kassem, S.; Andreu, L.; del Carmen del Campillo, M. Phosphorus fertilizer recovery from calcareous soils amended with humic and fulvic acids. *Plant Soil* **2002**, *245*, 277–286. [CrossRef]
37. Bi, Q.-F.; Li, K.-J.; Zheng, B.-X.; Liu, X.-P.; Li, H.-Z.; Jin, B.-J.; Ding, K.; Yang, X.-R.; Lin, X.-Y.; Zhu, Y.-G. Partial replacement of inorganic phosphorus (P) by organic manure reshapes phosphate mobilizing bacterial community and promotes P bioavailability in a paddy soil. *Sci. Total. Environ.* **2020**, *703*, 134977. [CrossRef]
38. Chen, G.-L.; Xiao, L.; Xia, Q.-L.; Wang, Y.; Yuan, J.-H.; Chen, H.; Wang, S.-Q.; Zhu, Y.-Y. Characterization of Different Phosphorus Forms in Flooded and Upland Paddy Soils Incubated with Various Manures. *ACS Omega* **2021**, *6*, 3259–3266. [CrossRef] [PubMed]
39. Condron, L.M.; Turner, B.L.; Cade-Menun, B.J. Chemistry and Dynamics of Soil Organic Phosphorus. In *Phosphorus: Agriculture and the Environment*; Sims, T., Sharpley, A.N., Eds.; Wiley: Hoboken, NJ, USA, 2005; pp. 87–121. [CrossRef]
40. Guan, Z.-H.; Cao, Z.; Li, X.G.; Kühn, P.; Hu, G.; Scholten, T.; Zhu, J.; He, J.-S. Effects of winter grazing and N addition on soil phosphorus fractions in an alpine grassland on the Qinghai-Tibet Plateau. *Agric. Ecosyst. Environ.* **2023**, *357*, 108700. [CrossRef]
41. Chtouki, M.; Naciri, R.; Garré, S.; Nguyen, F.; Zeroual, Y.; Oukarroum, A. Phosphorus fertilizer form and application frequency affect soil P availability, chickpea yield, and P use efficiency under drip fertigation. *J. Plant Nutr. Soil Sci.* **2022**, *185*, 603–611. [CrossRef]
42. Gu, Y.; Ros, G.H.; Zhu, Q.; Zheng, D.; Shen, J.; Cai, Z.; Xu, M.; de Vries, W. Responses of total, reactive and dissolved phosphorus pools and crop yields to long-term fertilization. *Agric. Ecosyst. Environ.* **2023**, *357*, 108658. [CrossRef]
43. Wang, Y.; Luo, D.; Xiong, Z.; Wang, Z.; Gao, M. Changes in rhizosphere phosphorus fractions and phosphate-mineralizing microbial populations in acid soil as influenced by organic acid exudation. *Soil Tillage Res.* **2023**, *225*, 105543. [CrossRef]
44. Touhami, D.; Condron, L.M.; McDowell, R.W.; Moss, R. Effects of long-term phosphorus fertilizer inputs and seasonal conditions on organic soil phosphorus cycling under grazed pasture. *Soil Use Manag.* **2023**, *39*, 385–401. [CrossRef]
45. Peng, S.; Kuang, X.; Cheng, H.; Wei, K.; Cai, K.; Tian, J. Post-agricultural succession affects the accumulation and enzymatic transformation of organic phosphorus in a karst area, southwest China. *Plant Soil* **2023**, *498*, 5–20. [CrossRef]

46. Bhupenchandra, I.; Basumatary, A.; Dutta, S.; Das, A.; Choudhary, A.K.; Lal, R.; Sharma, A.D.; Sen, A.; Prabhabati, Y.; Sahoo, M.R. Repercussions of fertilization with boron and enriched organic manure on soil chemical characteristics, boron and phosphorus fractions, and French bean productivity in an acidic Inceptisol of eastern Himalaya. *Sci. Hortic.* **2024**, *324*, 112589. [CrossRef]
47. Guo, Z.; Zhang, L.; Yang, W.; Hua, L.; Cai, C. Aggregate Stability under Long-Term Fertilization Practices: The Case of Eroded Ultisols of South-Central China. *Sustainability* **2019**, *11*, 1169. [CrossRef]
48. Dai, Z.; Liu, G.; Chen, H.; Chen, C.; Wang, J.; Ai, S.; Wei, D.; Li, D.; Ma, B.; Tang, C.; et al. Long-term nutrient inputs shift soil microbial functional profiles of phosphorus cycling in diverse agroecosystems. *ISME J.* **2020**, *14*, 757–770. [CrossRef]

Disclaimer/Publisher's Note: The statements, opinions and data contained in all publications are solely those of the individual author(s) and contributor(s) and not of MDPI and/or the editor(s). MDPI and/or the editor(s) disclaim responsibility for any injury to people or property resulting from any ideas, methods, instructions or products referred to in the content.

agronomy

MDPI

Article

Nutrient Balances and Forage Productivity in Permanent Grasslands Under Different Fertilisation Regimes in Western Poland Conditions

Anna Paszkiewicz-Jasińska, Wojciech Stopa, Jerzy Barszczewski, Dorota Gryszkiewicz-Zalega and Barbara Wróbel *

Institute of Technology and Life Sciences—National Research Institute, 3 Hrabska Avenue, 05-090 Raszyn, Poland; a.paszkiewicz@itp.edu.pl (A.P.-J.); w.stopa@itp.edu.pl (W.S.); j.barszczewski@itp.edu.pl (J.B.); d.gryszkiewicz-zalega@itp.edu.pl (D.G.-Z.)
* Correspondence: b.wrobel@itp.edu.pl

Abstract: Effective nutrient management in grassland ecosystems is essential for maintaining soil nutrient balance and ensuring high forage productivity. A field experiment was conducted between 2022 and 2024 on a permanent dry meadow at the Experimental Station in Poznań-Strzeszyn, western Poland. The trial, established in autumn 2021, was carried out under production conditions on large plots (140 m^2 each). Plots were assigned to different fertilisation regimes, varying in both type and dosage. The treatments included an unfertilised control, three levels of annual mineral NPK fertilisation (NPK1, NPK2, NPK3), three levels of annually applied farmyard manure (FYM1, FYM2, FYM3), and three levels of mineral and organic fertilisers applied every two years (NPK1/FYM1, NPK2/FYM2, NPK3/FYM3). Throughout the study, botanical composition, annual dry matter yield (DMY), nitrogen (N), phosphorus (P), and potassium (K) content in the plant biomass were assessed. A simplified nutrient balance was calculated based on nutrient input from fertilisers and nutrient output with harvested yield. The average N balance across three years ranged from −12.17 kg N ha^{-1} in control to +20.6 kg N ha^{-1} in FYM3. For phosphorus, average balances ranged from −7.2 kg P ha^{-1} in the control to +9.8 kg P ha^{-1} in FYM3. In contrast, potassium balances were mostly negative: from −51.7 kg K ha^{-1} in FYM1 to −7.4 kg K ha^{-1} in NPK1. The most balanced nutrient budgets were observed under alternate NPK/FYM fertilisation, with moderate surpluses of N and P and a smaller K deficit compared to FYM applied alone. In contrast, inorganic and organic fertilisation applied separately resulted in greater nutrient surpluses or a pronounced potassium deficit. This study emphasises the importance of balanced nutrient management in permanent meadows, showing that moderate fertilisation strategies, such as alternating FYM and mineral NPK, can maintain productivity, and reduce environmental impacts. These findings provide a practical basis for developing sustainable grassland management practices under variable climatic conditions.

Keywords: permanent meadow; nitrogen balance; phosphorus balance; potassium balance; mineral fertilisation; farmyard manure fertilisation; yield

1. Introduction

Permanent grasslands are a key component of the European agricultural landscape, covering nearly 38% of agricultural land [1]. Globally, they make up around 67% of all arable land [2]. These areas are used for forage production and are covered with grasses or

other fodder crops that are not included in crop rotation for at least five years [3]. Beyond their productive role, permanent grasslands also contribute significantly to environmental protection by reducing soil erosion, supporting biodiversity, and providing a range of ecosystem services [4–7].

Fertilisation is one of the key factors determining yield and forage quality [8]. In practice, inorganic fertilisers and various forms of organic fertilisers, including manure and slurry, are used on grasslands [9,10]. Both types of fertilisation contribute to increased biomass production from grassland [8]. Organic fertilisation, especially with manure, also promotes the development of leguminous plants such as clover (*Trifolium* spp.) [11–13] improves feed quality and has a positive effect on protein content and fibre digestibility [10,11,14,15]. However, these effects are not always clear. Some studies have not found significant differences in feed quality [16].

Organic fertilisers provide not only major nutrients but also micronutrients, thereby supporting growth and the nutritional value of feed. In addition, the use of organic fertilisers has a positive effect on soil fertility, increases humus content, improves nutrient availability, and mitigates acidification [17]. It can also increase the humic substance content and improve the quality of organic matter [18].

Mineral fertilisers in contrast, offer faster nutrient release and more precise dosing, which allows for closer alignment with plant needs. However, long-term reliance on mineral fertilisers can degrade soil structure and reduce biological activity [19]. Nitrogen-based mineral fertilisers may acidify the soil (pH < 4.5) and negatively impact soil organic carbon accumulation [17]. Their use has also been linked to reduced species diversity, especially among dicotyledonous and leguminous plants.

To address these challenges, integrated fertilisation strategies that combine mineral and organic sources are increasingly adopted. Such approaches help to optimize yield and forage quality while maintaining or even improving soil fertility [20]. They also support soil microbial activity, improve microbial community structure, increase enzymatic processes, and facilitate more efficient nutrient cycling [21].

Nevertheless, excessive fertiliser application can result in economic losses and environmental harm [22]. This makes monitoring fertiliser efficiency, particularly through nutrient balance calculations using simplified net methods, an important management tool. These assessments help fine-tune fertilisation practices and limit nutrient losses or overaccumulation in the soil [23,24]. Nitrogen balance is especially critical, as surpluses can lead to greenhouse gas emissions and nitrate leaching [25], while deficits may impair soil fertility over time.

This study aimed to evaluate how various levels and types of manure and mineral fertilisers affect the nitrogen (N), phosphorus (P), and potassium (K) balance and the productivity of permanent grasslands on mineral soils. The working hypothesis was that alternating between organic and mineral fertilisation would improve nutrient efficiency and lead to more balanced nutrient budgets than relying on either source alone.

2. Materials and Methods

2.1. Experimental Site

The experiment was set up on a three-cut production meadow located at the Experimental Station in Poznań-Strzeszyn (52°28′29″ N, 16°50′59″ E), in western Poland. The area belongs to the Institute of Technology and Life Sciences—PIB (Figure 1).

A field-scale experiment was established in autumn 2021 on a permanent meadow situated on mineral soil. According to the World Soil Classification System [26], this soil is classified as Phaeozem.

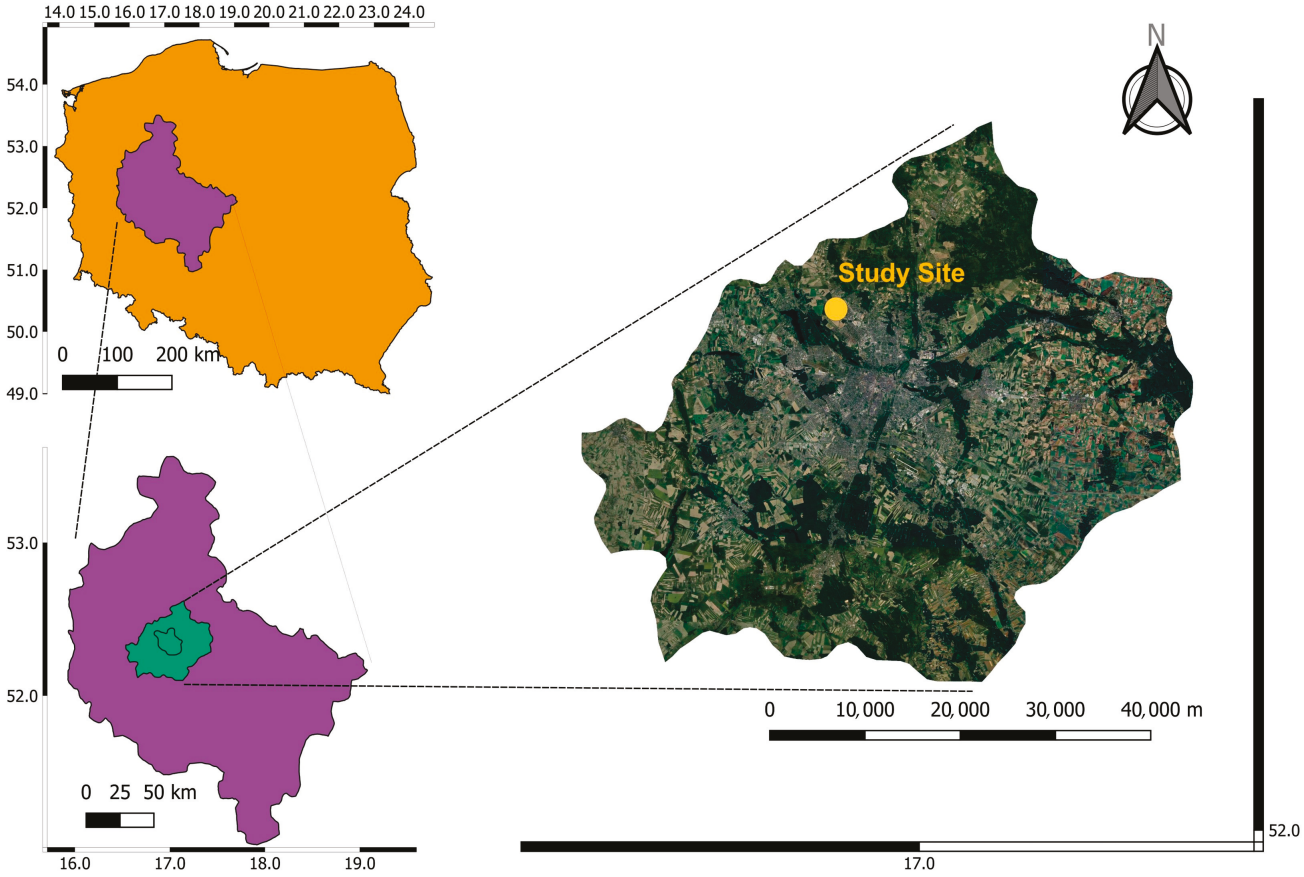


Figure 1. Location of the study site.

2.2. Fertilisation Treatments

Ten experimental plots, each measuring 10 × 14 m (140 m^2), were designated as follows: Control, NPK1, NPK2, NPK3, FYM1, FYM2, FYM3, NPK1/FYM1, NPK2/FYM2, and NPK3/FYM3. Nine plots received annual fertilisation using either mineral fertilisers (NPK1–3), farmyard manure (FYM1–3), or alternating applications of mineral fertiliser and manure (NPK/FYM combinations). Each treatment involved one of three fixed rates of nitrogen (N), phosphorus (P), and potassium (K), which remained constant throughout the experiment. The Control plot received no fertilisation. The experimental setup is shown in Figure 2.

The fertilisation levels used were adopted on the basis of previous work on the fertilisation of permanent grassland [27,28], taking into account the need for recommendations on low-input production methods. In addition, when determining manure doses, the nitrogen, phosphorus, and potassium content of the manure was taken into account, adopting the following equivalents for the use of these components from Barszczewski and Szatyłowicz [29] as follows: nitrogen—0.5, phosphorus—0.9, and potassium—0.7.

The macronutrient application rates used in each treatment are shown in Table 1.

On plots fertilised only with mineral fertilisers (NPK1, NPK2, NPK3), fertilisation was applied annually in 2022, 2023, and 2024. In spring, the full annual dose of phosphorus (P) and one-third of the nitrogen (N) and potassium (K) doses were applied. The remaining two-thirds of N and K were applied after the first and second harvest, respectively. The mineral fertilisers used included ammonium nitrate (34% N), potassium salt (60% K_2O), and granulated triple superphosphate (46% P_2O_5). For treatments fertilised with organic matter (FYM1, FYM2, FYM3), farmyard manure was applied each autumn (2021, 2022, and 2023) in three dosage levels corresponding to those of the mineral fertiliser treatments.

Farmyard cattle manure with an average nutrient content of 3.0% N, 0.70% P, and 3.18% K (based on dry matter) and an average dry matter content of 34% was used for both organic and alternating treatments. The solid manure applied in the experiment was obtained from dairy cows kept in a livestock housing facility. Prior to application, the manure was aged in a heap for approximately six months. Chemical analyses of this manure were carried out before application to the plots. For this purpose, manure samples were taken from the heap in triplicate. On the alternately fertilised plots (NPK1/FYM1, NPK2/FYM2, NPK3/FYM3), manure was applied in the autumn of 2021 and 2023, while mineral fertilisers were used in 2022. The mineral fertilisers were applied at the same time and according to the same application scheme as in the NPK treatments.



Figure 2. Schematic diagram of the experimental setup. Treatments: Control—0 kg N ha^{-1}, 0 kg P ha^{-1}, 0 kg K ha^{-1}; NPK1—30 kg N ha^{-1}, 10 kg P ha^{-1}, 27 kg K ha^{-1}; NPK2—45 kg N ha^{-1}, 15 kg P ha^{-1}, 41 kg K ha^{-1}; NPK3—60 kg N ha^{-1}, 20 kg P ha^{-1}, 54 kg K ha^{-1}; FYM1—32 kg N ha^{-1}, 11 kg P ha^{-1}, 32 kg K ha^{-1}; FYM2—46 kg N ha^{-1}, 16.5 kg P ha^{-1}, 48 kg K ha^{-1}; FYM3—62 kg N ha^{-1}, 22 kg P ha^{-1}, 64 kg K ha^{-1}; NPK1/FYM1−30/32 kg N ha^{-1}, 10/11 kg P ha^{-1}, 27/32 kg K ha^{-1}; NPK2/FYM2—45/46 kg N ha^{-1}, 15/16.5 kg P ha^{-1}, 41/48 kg K ha^{-1}; NPK3/FYM3—60/62 kg N ha^{-1}, 20/22 kg P ha^{-1}, 54/64 kg K ha^{-1}. NPK1, NPK2, NPK3—mineral fertilisation, FYM1, FYM2, FYM3—farmyard manure, NPK1/FYM1, NPK2/FYM2, NPK3/FYM3—alternate fertilisation.

Table 1. Fertilisation treatments and nutrient application rates.

Macronutrient	Control	Nutrient Application Rates (kg ha^{-1})								
		Mineral Fertilisation			Farmyard Manure			Alternate Fertilisation		
		NPK1	NPK2	NPK3	FYM1	FYM2	FYM3	NPK1/FYM1	NPK2/FYM2	NPK3/FYM3
Nitrogen	0	30	45	60	32	46	62	30/32	45	60/62
Phosphorus	0	10	15	20	11	16.5	22	10	15	20
Potassium	0	27	41	54	32	48	64	27/32	41/48	54/64

2.3. Soil and Plant Sampling

In autumn 2021, prior to the application of manure, soil samples were collected from the experimental plots using an Egner stick at two depths: 0–10 cm and 10–20 cm. In each plot, 13 punctures (primary samples) were taken, separately for both layers. From these primary samples, two bulk samples were prepared for each plot, giving a total of 20 samples. The samples were analysed to determine soil pH as well as phosphorus (P), potassium (K), magnesium (Mg), and calcium (Ca) content. The characteristics of soil conditions at each test site are shown in Table 2.

Table 2. Characteristics of soil conditions on individual experimental plots.

Soil Reaction/ Soil Layer	Control	Mineral Fertilisation			Farmyard Manure			Alternate Fertilisation		
		NPK1	NPK2	NPK3	FYM1	FYM2	FYM3	NPK1/FYM1	NPK2/FYM2	NPK3/FYM3
pH										
0–10 cm	4.9	5.2	5.2	5.1	4.9	4.9	4.9	4.8	4.6	4.7
10–20 cm	4.5	5.2	5.2	4.6	4.8	4.4	4.5	4.6	4.6	4.7
Nitrogen g 100^{-1} soil										
0–10 cm	0.12	0.12	0.13	0.14	0.15	0.14	0.15	0.14	0.17	0.18
10–20 cm	0.08	0.07	0.09	0.08	0.14	0.11	0.11	0.10	0.12	0.12
Phosphorus g 100^{-1} soil										
0–10 cm	0.01	0.01	0.01	0.01	0.02	0.01	0.01	0.01	0.01	0.00
10–20 cm	0.01	0.01	0.01	0.01	0.02	0.01	0.01	0.01	0.01	0.00
Potassium g 100^{-1} soil										
0–10 cm	0.01	0.01	0.02	0.02	0.02	0.02	0.01	0.02	0.02	0.02
10–20 cm	0.01	0.01	0.01	0.01	0.02	0.01	0.02	0.02	0.02	0.01
Magnesium g 100^{-1} soil										
0–10 cm	0.01	0.01	0.01	0.01	0.01	0.01	0.01	0.01	0.01	0.01
10–20 cm	0.00	0.01	0.01	0.01	0.00	0.00	0.00	0.00	0.01	0.00
Calcium g 100^{-1} soil										
0–10 cm	0.03	0.06	0.06	0.04	0.07	0.06	0.04	0.04	0.01	0.07
10–20 cm	0.01	0.03	0.03	0.03	0.03	0.03	0.02	0.03	0.00	0.04

Treatments: Control—0 kg N ha^{-1}, 0 kg P ha^{-1}, 0 kg K ha^{-1}; NPK1—30 kg N ha^{-1}, 10 kg P ha^{-1}, 27 kg K ha^{-1}; NPK2—45 kg N ha^{-1}, 15 kg P ha^{-1}, 41 kg K ha^{-1}; NPK3—60 kg N ha^{-1}, 20 kg P ha^{-1}, 54 kg K ha^{-1}; FYM1—32 kg N ha^{-1}, 11 kg P ha^{-1}, 32 kg K ha^{-1}; FYM2—46 kg N ha^{-1}, 16.5 kg P ha^{-1}, 48 kg K ha^{-1}; FYM3—62 kg N ha^{-1}, 22 kg P ha^{-1}, 64 kg K ha^{-1}; NPK1/FYM1—30/32 kg N ha^{-1}, 10/11 kg P ha^{-1}, 27/32 kg K ha^{-1}; NPK2/FYM2—45/46 kg N ha^{-1}, 15/16.5 kg P ha^{-1}, 41/48 kg K ha^{-1}; NPK3/FYM3—60/62 kg N ha^{-1}, 20/22 kg P ha^{-1}, 54/64 kg K ha^{-1}. NPK1, NPK2, NPK3—mineral fertilisation, FYM1, FYM2, FYM3—farmyard manure, NPK1/FYM1, NPK2/FYM2, NPK3/FYM3—alternate fertilisation.

Each year, prior to the first harvest (in May), the botanical composition of the sward was assessed on all plots using the Klapp estimation method [30]. In each plot, a square

with an area of 25 m^2 (5 m × 5 m) was randomly designated. In each square, all species were recorded in the order of grasses, legumes, and others (herbs and weeds). According to the adopted method, the percentage share of individual species in each group was estimated, with an accuracy of 1%, starting from the most numerous species. For all plots, the functional group structure was also determined, expressed as the percentage share of grasses, legumes, herbs, and weeds, along with the number of species in each group.

During the period (2022–2024), plant material samples were collected from each treatment plot during successive harvests to determine dry matter yield (DMY) and analyse chemical composition. Plant green mass samples were collected from each plot in four replicates. For this purpose, four equal areas were designated on each plot. On each of these areas, a random location for plant material sampling was selected using a 1 m^2 (1 m × 1 m) frame. The plants were cut manually with scissors to a height of 5 cm. The collected biomass samples were weighed and combined into an averaged sample for each treatment (10 samples in total). They were then left to dry to obtain air-dry weight.

2.4. Dry Matter Yield and Chemical Analyses

Dry matter yield (DMY) was calculated based on the fresh weight of plant material harvested from an area of 1 m^2. Dry matter content was determined by drying 100 g of plant material in a laboratory oven at 105 °C for 4 h. The results were expressed in tonnes of dry matter per hectare. The remaining plant material was used for chemical analysis. After drying and grinding, nitrogen (N), phosphorus (P), and potassium (K) content were determined for all samples.

Chemical analyses were conducted at the ITP–PIB laboratory. Soil pH was measured using the potentiometric method in a 1 mol dm^{-3} KCl solution [31]. Nitrogen (N) content was determined using the Kjeldahl method. Total phosphorus (P) was analysed colorimetrically using ammonium molybdate and sodium metabisulfite. Potassium (K) content was measured using flame emission spectrometry. Magnesium (Mg) and calcium (Ca) contents were determined by atomic absorption spectrometry (S series AA spectrometer, Thermo Fisher Scientific, Waltham, MA, USA).

2.5. Nutrient Balance Calculation

Based on the results obtained, simplified nutrient balances were calculated. Annual balances of nitrogen, phosphorus, and potassium were determined for each treatment by calculating the difference between inputs and outputs.

On the input side, nutrient loads from fertilisers and atmospheric deposition were included. The average nutrient input from precipitation was adopted from previous research on permanent grasslands in Poland conducted by Barszczewski and Burs [32] and amounted to 17.3 kg N ha^{-1}, 0.4 kg P ha^{-1}, and 4.4 kg K ha^{-1} per year.

The nitrogen balance also accounted for biological nitrogen input from soil microorganisms and symbiotic nitrogen fixation by leguminous species. The microbial contribution to nitrogen input was assumed to be 10 kg N ha^{-1}, based on data from Pietrzak [33]. Nitrogen fixation by legumes was estimated according to their percentage share in the sward composition. A 1% share of leguminous species was assumed to correspond to 3 kg of fertiliser-equivalent nitrogen, in line with national agricultural recommendations [34], which include practices for protecting water resources against nitrate pollution from agricultural sources. On the output side, nutrient removal was calculated based on the nutrient content of the harvested plant biomass.

2.6. Meteorological Data

Meteorological data, including temperature and precipitation, were recorded throughout the study to evaluate their influence on nutrient uptake, sward yield, and nutrient

balances, key objectives of this experiment. The data were obtained from the nearest weather station located in Poznań and sourced from a publicly accessible online database maintained by the Institute of Meteorology and Water Management—National Research Institute [35]. The dataset covered the growing season in Polish conditions, defined as the period from April to September, for the years 2022–2024. These data were used to calculate average monthly temperatures and total precipitation for each month of the growing season.

Based on the obtained data, the Sielianinov hydrothermal coefficient (HTC) was also calculated [36]. This index was used to characterise the pluviothermal conditions during the study period in more detail. The HTC takes into account both temperature and precipitation and it is flexible enough to be applied on a monthly or 10-day basis. It is sensitive to dry conditions, making it a useful tool for monitoring agricultural drought. The HTC was calculated using the following formula:

$$HTC = (P\ 10)/\Sigma t \quad (1)$$

P—the total monthly rainfall (mm), t—the monthly total of average daily air temperatures > 0 °C.

The following classes were used to assess pluviothermal conditions: extremely wet HTC > 3.0; very wet 2.5 < HTC $\leq$ 3.0; wet 2.0 < HTC $\leq$ 2.5; fairly wet 1.6 < HTC $\leq$ 2.0; optimal 1.3 < HTC $\leq$ 1.6; fairly dry 1.0 < HTC $\leq$ 1.3; dry 0.7 < HTC $\leq$ 1.0; very dry 0.4 < HTC $\leq$ 0.7; extremely dry HTC $\leq$ 0.4.

2.7. Statistical Analysis

Due to the field-based nature of the study, the experiment did not include replications within a single year. Therefore, the statistical model treated fertilisation and year (as a blocking factor) as sources of variation. The effect of fertilisation treatment was assessed using two-way ANOVA, followed by Tukey's post hoc test to compare means at a significance level of $\alpha = 0.05$. All statistical analyses were performed using Statgraphics 18 software.

3. Results

3.1. Meteorological Conditions

The meteorological conditions in April–September in 2022–2024 are presented in Table 3.

Table 3. Average monthly temperatures and precipitation in 2022–2024 at the meteorological station in Poznań [32].

Month	Temperature [°C]	Precipitation [mm]	Temperature [°C]	Precipitation [mm]	Temperature [°C]	Precipitation [mm]
	2022		2023		2024	
April	13	36	13.2	37	16.5	50
May	20.8	23	19.4	30	23.4	52
June	26.4	63	25.7	39	24.4	93
July	26.4	23	26.8	62	26.6	75
August	27.8	53	24.6	156	27.2	39
September	18.5	32	25.0	3	22.9	56

In the first year of the study (2022), average temperatures during the growing season ranged from 13.0 °C in April to 27.8 °C in August. In 2023, temperatures varied between

13.2 °C in April and 26.8 °C in July, while in 2024 they ranged from 16.4 °C in April to 27.2 °C in August. The smallest temperature variation occurred in 2024. That year, the start of the growing season was noticeably warmer than in the previous years, but temperatures remained relatively stable throughout the following months. The warmest final month of the growing season was recorded in 2023, with an average temperature of 25.0 °C in September, while the coolest was in 2022, with 18.5 °C. Total precipitation across the study period amounted to 229 mm in 2022 (the driest year), 326 mm in 2023, and 365 mm in 2024 (the wettest year). The highest variation in monthly rainfall occurred in 2023, with a record 156 mm in August followed by just 3 mm in September. In the other years, the highest monthly rainfall was recorded in June. The driest months were May and July 2022 (23 mm each) and August 2024 (39 mm). Interestingly, August 2023, despite exceptionally high rainfall, was also the coldest August of the three-year period. Table 4 shows the values of the HTC.

Table 4. Monthly values of the HTC for selected months in the years 2022–2024.

Year	Month					
	April	**May**	**June**	**July**	**August**	**September**
2022	1.5	0.5	1.1	0.4	0.8	0.8
2023	1.5	0.7	0.7	1.0	2.5	0.1
2024	0.9	0.7	1.3	0.9	0.5	0.8

Extremely wet HTC > 3.0; very wet 2.5 < HTC $\leq$ 3.0; wet 2.0 < HTC $\leq$ 2.5; fairly wet 1.6 < HTC $\leq$ 2.0; optimal 1.3 < HTC $\leq$ 1.6; fairly dry 1.0 < HTC $\leq$ 1.3; dry 0.7 < HTC $\leq$ 1.0; very dry 0.4 < HTC $\leq$ 0.7; extremely dry HTC $\leq$ 0.4.

Throughout the experiment, HTC ranged from 0.1 to 1.5, indicating mostly very dry or dry conditions, with occasional months classified as optimal. The only exception was August 2023, which, due to total rainfall of 156 mm, was classified as wet. The beginning of the growing season was optimal in both 2022 and 2023, while in 2024 it was already dry. May conditions were consistently very dry across all three years. June was particularly dry in 2023, with an HTC of 0.7. The greatest variation between years was observed during the final three months of the growing season. July was very dry in 2022, and dry in both 2023 and 2024. August showed the sharpest contrast: it was very dry in 2024 but wet in 2023. September 2022 and 2024 were classified as dry, while 2023 experienced extremely dry conditions. When considering the growing season, 2024 was the driest year on average, and 2023 was the wettest. However, taking the entire study period into account, all three years can generally be classified as dry.

3.2. Species Richness and Botanical Composition of the Sward

The number of plant species in the botanical composition of the meadow sward across individual treatments over the three-year study period is presented in Figure 3. Overall, the average number of species recorded per treatment showed little variation and did not exhibit any clear relationship with the type or dose of fertilisation. On the control plots, the number of species ranged from 15 to 17. Similar patterns were observed on fertilised plots, with only slight differences: 14–19 species under mineral fertilisation, 14–21 under manure fertilisation, and 14–20 under alternating fertilisation. No distinct year-to-year trends were identified. In the first year, species counts ranged from 14 to 19 across all treatments. In the second year, the range increased slightly to 16–21 species, while in the third year it narrowed to 15–18. These findings suggest that species richness remained relatively stable regardless of the fertilisation strategy applied.

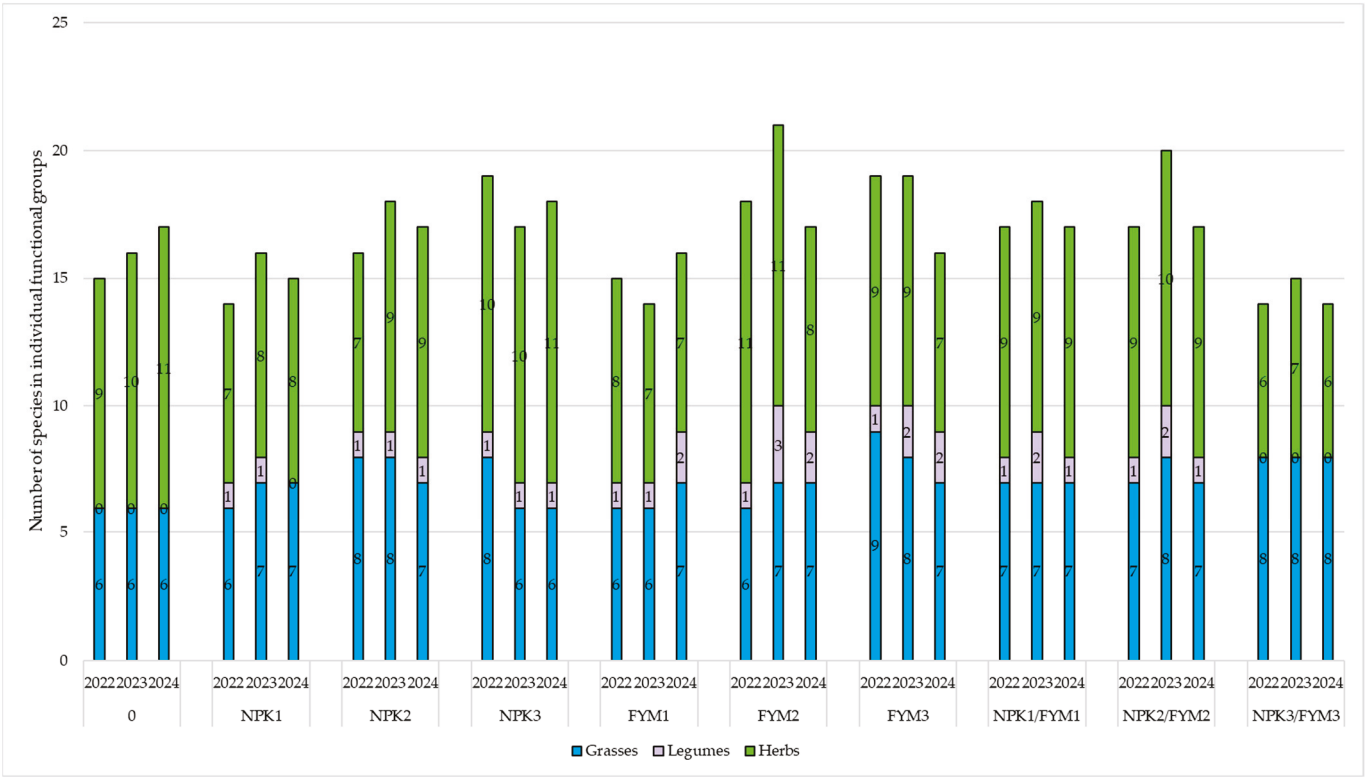


Figure 3. Number of species in individual functional groups. Treatments: Control—0 kg N ha^{-1}, 0 kg P ha^{-1}, 0 kg K ha^{-1}; NPK1—30 kg N ha^{-1}, 10 kg P ha^{-1}, 27 kg K ha^{-1}; NPK2—45 kg N ha^{-1}, 15 kg P ha^{-1}, 41 kg K ha^{-1}; NPK3—60 kg N ha^{-1}, 20 kg P ha^{-1}, 54 kg K ha^{-1}; FYM1—32 kg N ha^{-1}, 11 kg P ha^{-1}, 32 kg K ha^{-1}; FYM2—46 kg N ha^{-1}, 16.5 kg P ha^{-1}, 48 kg K ha^{-1}; FYM3—62 kg N ha^{-1}, 22 kg P ha^{-1}, 64 kg K ha^{-1}; NPK1/FYM1—30/32 kg N ha^{-1}, 10/11 kg P ha^{-1}, 27/32 kg K ha^{-1}; NPK2/FYM2—45/46 kg N ha^{-1}, 15/16.5 kg P ha^{-1}, 41/48 kg K ha^{-1}; NPK3/FYM3—60/62 kg N ha^{-1}, 20/22 kg P ha^{-1}, 54/64 kg K ha^{-1}. NPK1, NPK2, NPK3—mineral fertilisation, FYM1, FYM2, FYM3—farmyard manure, NPK1/FYM1, NPK2/FYM2, NPK3/FYM3—alternate fertilisation.

The proportions of different plant groups in the meadow sward across treatments and study years are shown in Figure 4. Grasses consistently formed the dominant group in all treatments and played a key role in determining yield. Their average share in the sward was 83% in the first year, 81% in the second, and 80% in the third year. The most common species within this group included *Arrhenatherum elatius* (L.) P. Beauv. ex J. Presl & C. Presl, *Poa pratensis* L., *Festuca rubra* L., *Holcus lanatus* L., *Dactylis glomerata* L., *Alopecurus pratensis* L., and *Festuca pratensis* Huds.

The second largest functional group comprised broad-leaved dicotyledonous species, mainly classified as herbs and weeds. This group included, among others, *Plantago lanceolata* L., *Taraxacum officinale* F.H. Wigg., *Achillea millefolium* L., and *Rumex acetosa* L. Their average share in the sward was 16% in 2022 and 18% in both 2023 and 2024. A slightly higher proportion of these species was observed on plots receiving higher doses of mineral fertilisers (NPK2 and NPK3).

Legumes (Fabaceae) made up the smallest group, contributing only 1–3% to the sward composition. This group consisted mainly of *Vicia cracca* L., *Vicia sepium* L., *Lotus corniculatus* L., and occasionally *Vicia angustifolia* L. The average proportion of legumes was 1% in the first year, increasing slightly to 2% in the second and third years. A modest increase in Fabaceae presence (by 1–2%) was noted on all plots fertilised with farmyard manure (FYM1, FYM2, FYM3), as well as on those receiving alternating fertilisation. An

exception was the NPK3/FYM3 treatment, where legumes were absent throughout the entire study period. On plots fertilised solely with mineral fertilisers, the share of legumes remained low and stable, with a decline observed in the third year on the NPK1 plot.

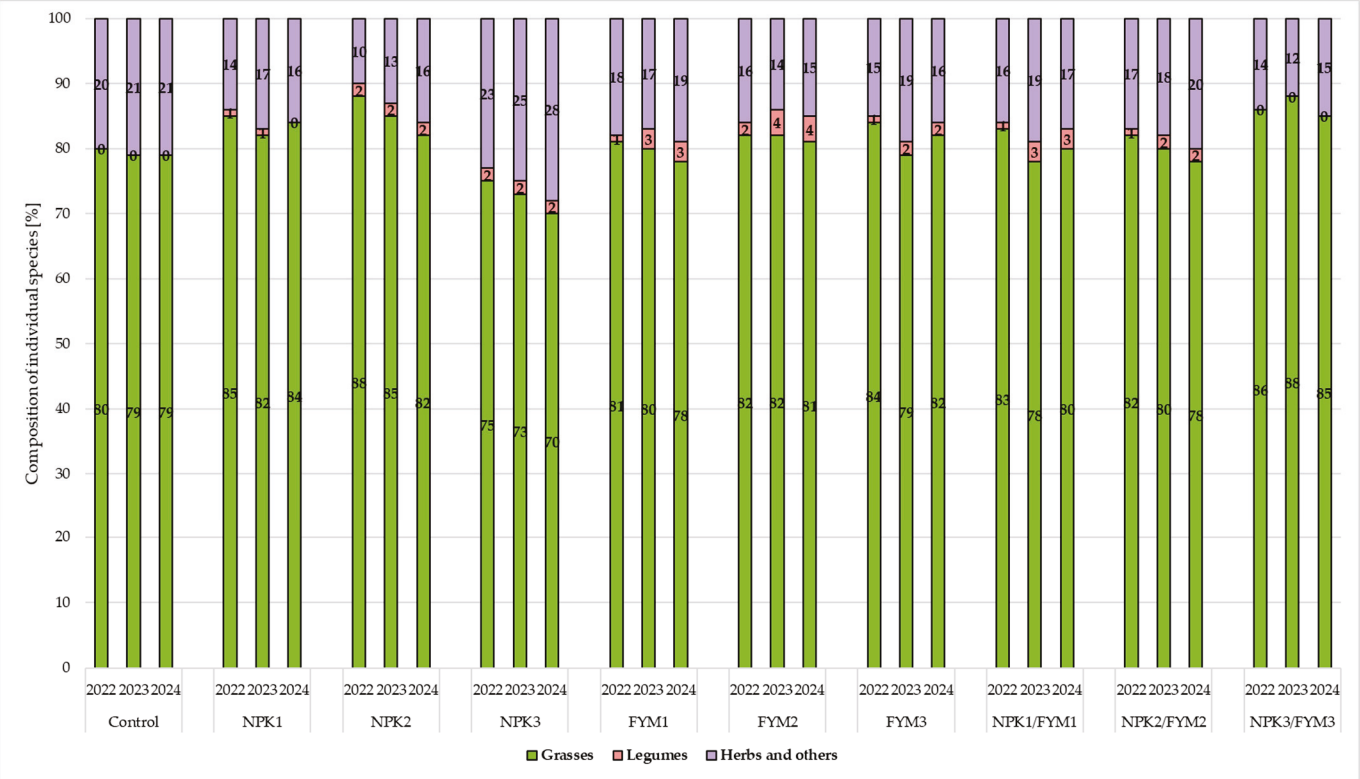


Figure 4. Share of species in individual functional groups. Treatments: Control—0 kg N ha^{-1}, 0 kg P ha^{-1}, 0 kg K ha^{-1}; NPK1—30 kg N ha^{-1}, 10 kg P ha^{-1}, 27 kg K ha^{-1}; NPK2—45 kg N ha^{-1}, 15 kg P ha^{-1}, 41 kg K ha^{-1}; NPK3—60 kg N ha^{-1}, 20 kg P ha^{-1}, 54 kg K ha^{-1}; FYM1—32 kg N ha^{-1}, 11 kg P ha^{-1}, 32 kg K ha^{-1}; FYM2—46 kg N ha^{-1}, 16.5 kg P ha^{-1}, 48 kg K ha^{-1}; FYM3—62 kg N ha^{-1}, 22 kg P ha^{-1}, 64 kg K ha^{-1}; NPK1/FYM1 − 30/32 kg N ha^{-1}, 10/11 kg P ha^{-1}, 27/32 kg K ha^{-1}; NPK2/FYM2—45/46 kg N ha^{-1}, 15/16.5 kg P ha^{-1}, 41/48 kg K ha^{-1}; NPK3/FYM3—60/62 kg N ha^{-1}, 20/22 kg P ha^{-1}, 54/64 kg K ha^{-1}. NPK1, NPK2, NPK3—mineral fertilisation, FYM1, FYM2, FYM3—farmyard manure, NPK1/FYM1, NPK2/FYM2, NPK3/FYM3—alternate fertilisation.

3.3. Meadow Sward Yield

The DMY of the meadow sward across individual treatments over the three-year study period are presented in Table 5 and Figure 5. In the first year of the study (2022), the average DMY was 4.31 Mg ha^{-1}. The highest yields (4.52 Mg ha^{-1} on average) were obtained on plots fertilised solely with mineral fertilisers (NPK1, NPK2, NPK3). Slightly lower yields were recorded on plots fertilised with farmyard manure applied in autumn 2021 (FYM1, FYM2, FYM3), where the average yield was 4.49 Mg ha^{-1}. For plots receiving alternating fertilisation (NPK1/FYM1, NPK2/FYM2, NPK3/FYM3), the average DMY amounted to 4.42 Mg ha^{-1}, which was only 2.3% lower than for mineral-fertilised plots and 1.6% lower than for those fertilised with manure.

The highest average DMY across the entire study were recorded in the second year (2023), reaching 4.40 Mg ha^{-1}. This was 2% higher than in 2022 and 32% higher than in 2024. A major contribution to this result came from the third cut. In August 2023, heavy rainfall occurred following the second cut in July, which significantly improved regrowth and boosted the final yield, as shown in Figure 5. In that year, the highest average

DMY (4.96 Mg ha^{-1}) were achieved on plots with alternating fertilisation, followed by plots fertilised with manure (4.81 Mg ha^{-1}), while the lowest DMY (4.09 Mg ha^{-1}) were observed on plots fertilised with mineral fertilisers. It is worth noting that plots with alternate fertilisation in 2023 were fertilised with mineral fertilisers only, yet the high DMY may have been influenced by the residual effect of manure applied two years earlier (autumn 2021).

Table 5. Effect of analysed factors on DMY [Mg ha^{-1}].

Factor	Control	NPK1	NPK2	NPK3	FYM1	FYM2	FYM3	NPK1/FYM1	NPK2/FYM2	NPK3/FYM3
Count	3	3	3	3	3	3	3	3	3	3
LS Mean	2.58	3.29	4.26	4.47	3.87	4.52	4.29	3.89	4.19	4.72
Homogeneous Groups	a	ab	bc	bc	bc	bc	bc	bc	bc	c

Means within columns followed by the same letter are not significantly different from each other, according to Tukey's test at $p < 0.05$. Treatments: Control—0 kg N ha^{-1}, 0 kg P ha^{-1}, 0 kg K ha^{-1}; NPK1—30 kg N ha^{-1}, 10 kg P ha^{-1}, 27 kg K ha^{-1}; NPK2—45 kg N ha^{-1}, 15 kg P ha^{-1}, 41 kg K ha^{-1}; NPK3—60 kg N ha^{-1}, 20 kg P ha^{-1}, 54 kg K ha^{-1}; FYM1—32 kg N ha^{-1}, 11 kg P ha^{-1}, 32 kg K ha^{-1}; FYM2—46 kg N ha^{-1}, 16.5 kg P ha^{-1}, 48 kg K ha^{-1}; FYM3—62 kg N ha^{-1}, 22 kg P ha^{-1}, 64 kg K ha^{-1}; NPK1/FYM1—30/32 kg N ha^{-1}, 10/11 kg P ha^{-1}, 27/32 kg K ha^{-1}; NPK2/FYM2—45/46 kg N ha^{-1}, 15/16.5 kg P ha^{-1}, 41/48 kg K ha^{-1}; NPK3/FYM3—60/62 kg N ha^{-1}, 20/22 kg P ha^{-1}, 54/64 kg K ha^{-1}. NPK1, NPK2, NPK3—mineral fertilisation, FYM1, FYM2, FYM3—farmyard manure, NPK1/FYM1, NPK2/FYM2, NPK3/FYM3—alternate fertilisation.

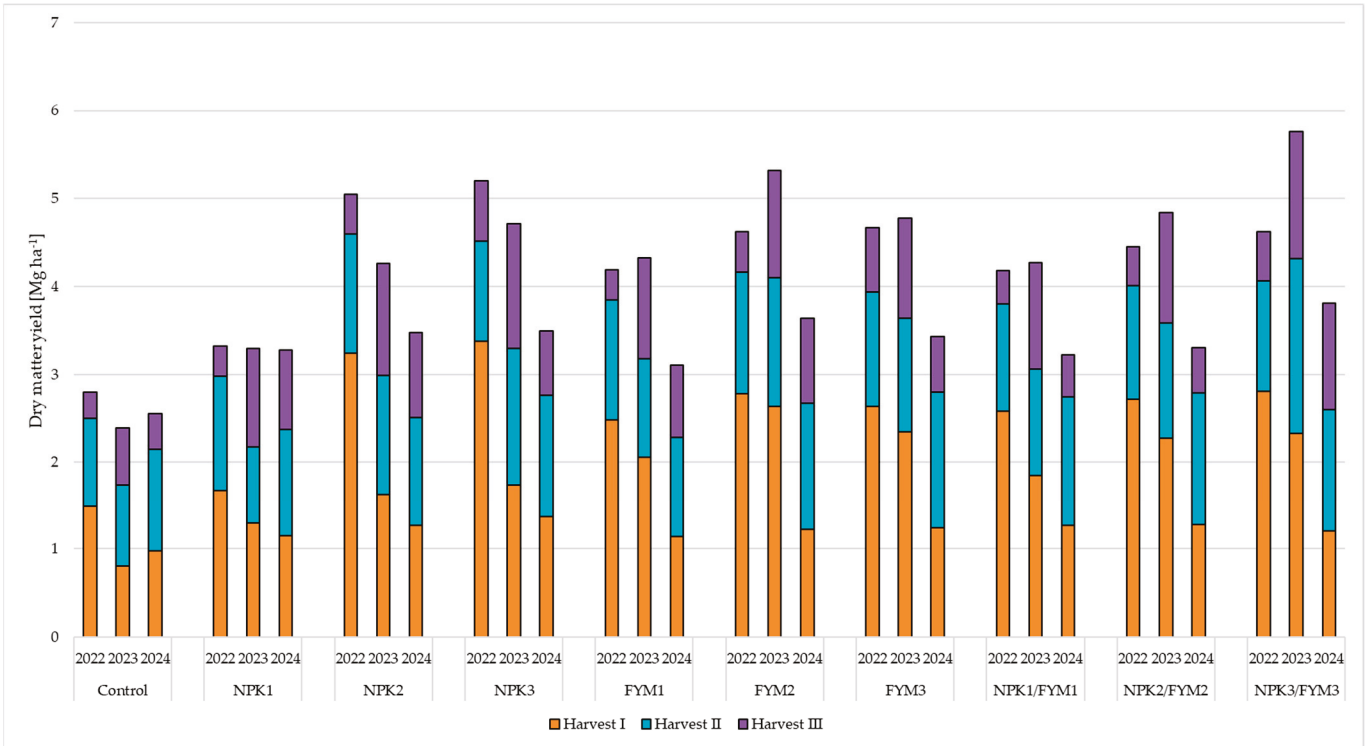


Figure 5. Effect of fertilisation treatments on DMY in following years of experiment. Treatments: Control—0 kg N ha^{-1}, 0 kg P ha^{-1}, 0 kg K ha^{-1}; NPK1—30 kg N ha^{-1}, 10 kg P ha^{-1}, 27 kg K ha^{-1}; NPK2—45 kg N ha^{-1}, 15 kg P ha^{-1}, 41 kg K ha^{-1}; NPK3—60 kg N ha^{-1}, 20 kg P ha^{-1}, 54 kg K ha^{-1}; FYM1—32 kg N ha^{-1}, 11 kg P ha^{-1}, 32 kg K ha^{-1}; FYM2—46 kg N ha^{-1}, 16.5 kg P ha^{-1}, 48 kg K ha^{-1}; FYM3—62 kg N ha^{-1}, 22 kg P ha^{-1}, 64 kg K ha^{-1}; NPK1/FYM1—30/32 kg N ha^{-1}, 10/11 kg P ha^{-1}, 27/32 kg K ha^{-1}; NPK2/FYM2—45/46 kg N ha^{-1}, 15/16.5 kg P ha^{-1}, 41/48 kg K ha^{-1}; NPK3/FYM3—60/62 kg N ha^{-1}, 20/22 kg P ha^{-1}, 54/64 kg K ha^{-1}. NPK1, NPK2, NPK3—mineral fertilisation, FYM1, FYM2, FYM3—farmyard manure, NPK1/FYM1, NPK2/FYM2, NPK3/FYM3—alternate fertilisation.

The lowest yields were recorded in the final year of the study (2024), averaging 3.33 Mg ha^{-1}. Average yields for this year were as follows: 3.42 Mg ha^{-1} on plots with mineral fertilisation, 3.39 Mg ha^{-1} on manure fertilised plots, and 3.44 Mg ha^{-1} on plots receiving alternating fertilisation. These results were, on average, 1.52 Mg ha^{-1} lower than in the previous year.

When considering the full three-year period, the lowest average DMY (2.58 Mg ha^{-1}) was recorded on the unfertilised control plot. This plot yielded 2.80 Mg ha^{-1} in 2022, 2.39 Mg ha^{-1} in 2023, and 2.56 Mg ha^{-1} in 2024. The control plot significantly underperformed compared to the fertilised plots, with the exception of the NPK1 treatment, where the difference was not statistically significant (Table 5). The three-year average DMY for the fertilised plots were: 4.01 Mg ha^{-1} for mineral fertilisation, 4.23 Mg ha^{-1} for manure fertilisation, and 4.27 Mg ha^{-1} for alternating fertilisation. No significant differences were observed among most of the fertilised treatments, except between NPK1 and NPK3/FYM3.

3.4. Nutrient Balance

3.4.1. Nitrogen Balance

Nitrogen balance values varied depending on the type of fertilisation and the year of the study (Figure 6). In the unfertilised treatment (Control), a negative nitrogen balance was recorded throughout the study period. The values ranged from −14.7 kg N·ha^{-1} in 2022 to −8.9 kg N·ha^{-1} in 2024.

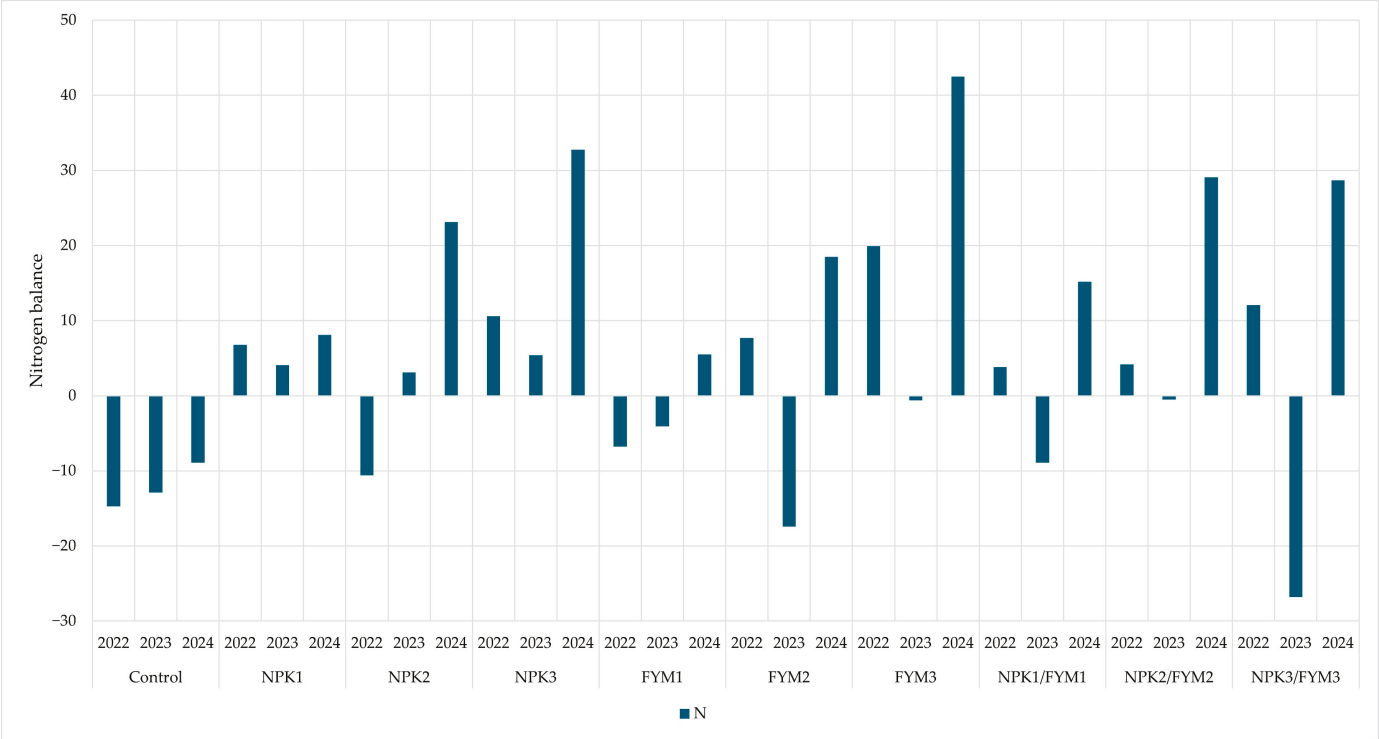


Figure 6. Effect of fertilisation treatments on nitrogen balance. Treatments: Control—0 kg N ha^{-1}, 0 kg P ha^{-1}, 0 kg K ha^{-1}; NPK1—30 kg N ha^{-1}, 10 kg P ha^{-1}, 27 kg K ha^{-1}; NPK2—45 kg N ha^{-1}, 15 kg P ha^{-1}, 41 kg K ha^{-1}; NPK3—60 kg N ha^{-1}, 20 kg P ha^{-1}, 54 kg K ha^{-1}; FYM1—32 kg N ha^{-1}, 11 kg P ha^{-1}, 32 kg K ha^{-1}; FYM2—46 kg N ha^{-1}, 16.5 kg P ha^{-1}, 48 kg K ha^{-1}; FYM3—62 kg N ha^{-1}, 22 kg P ha^{-1}, 64 kg K ha^{-1}; NPK1/FYM1−30/32 kg N ha^{-1}, 10/11 kg P ha^{-1}, 27/32 kg K ha^{-1}; NPK2/FYM2—45/46 kg N ha^{-1}, 15/16.5 kg P ha^{-1}, 41/48 kg K ha^{-1}; NPK3/FYM3—60/62 kg N ha^{-1}, 20/22 kg P ha^{-1}, 54/64 kg K ha^{-1}. NPK1, NPK2, NPK3—mineral fertilisation, FYM1, FYM2, FYM3—farmyard manure, NPK1/FYM1, NPK2/FYM2, NPK3/FYM3—alternate fertilisation.

In treatments fertilised only with mineral fertilisers, the nitrogen balance was mostly positive, except for NPK2 in 2022, where a negative value of −10.6 kg N·ha^{-1} was recorded. In the first two years, nitrogen balances were relatively low and similar between treatments. The highest nitrogen balances were observed in the third year (2024), especially in the NPK3 treatment, where the balance reached +32.8 kg N·ha^{-1}.

In treatments fertilised each year with manure only, nitrogen balance values varied depending on the year and fertiliser dose. In the FYM1 treatment, the nitrogen balance was slightly negative in the first two years (−6.8 kg N·ha^{-1} in 2022 and −4.1 kg N·ha^{-1} in 2023) and became positive in 2024 (+5.5 kg N·ha^{-1}). The FYM2 treatment showed greater variability: the balance was strongly negative in 2023 (−17.4 kg N·ha^{-1}) and positive in 2024 (+18.5 kg N·ha^{-1}). The highest nitrogen balance values, especially in 2024 (+42.5 kg N·ha^{-1}), were recorded in the FYM3 treatment.

A similar pattern was observed in the alternating fertilisation treatments. In 2022, the balances were positive, reaching up to +12.1 kg N·ha^{-1} in NPK3/FYM3. In 2023, all alternating treatments showed negative balances, with the lowest value of −26.8 kg N·ha^{-1} also in NPK3/FYM3. In 2024, nitrogen balances were positive again, reaching up to +29.1 kg N·ha^{-1} in the NPK2/FYM2 treatment.

Regardless of fertiliser type and dose, the year of the study had a clear effect on nitrogen balance values. In 2022, balances ranged from −14.7 kg N·ha^{-1} (Control) to +19.9 kg N·ha^{-1} (FYM3), and the differences between fertilised treatments were relatively small. In 2023, the results varied widely, from −26.8 kg N·ha^{-1} (NPK3/FYM3) to +5.4 kg N·ha^{-1} (NPK3). Negative balances were recorded in all manure and alternating treatments, as well as in the unfertilised control. In 2024, all fertilised treatments showed a positive nitrogen balance, ranging from +5.5 kg N·ha^{-1} (FYM1) to +42.5 kg N·ha^{-1} (FYM3), which was the highest value in the entire study period. The analysis of variance did not reveal a statistically significant effect of the treatments on nitrogen balance (p = 0.0513) (Table 6). Although the differences were not statistically significant, a clear trend was evident. The most favourable nitrogen balance was recorded in the FYM3 treatment (mean = 20.6), while the lowest was observed in the Control (mean = −12.2).

Table 6. Effect of analysed factors on nitrogen balance.

Factor	Control	NPK1	NPK2	NPK3	FYM1	FYM2	FYM3	NPK1/FYM1	NPK2/FYM2	NPK3/FYM3
Count	3	3	3	3	3	3	3	3	3	3
LS Mean	−12.2	6.3	5.2	16.3	−1.8	2.9	20.6	3.4	10.9	4.7

Since the differences between means were only marginally significant (p = 0.0513, ANOVA), no Tukey's post hoc test was conducted.

3.4.2. Phosphorus Balances

Phosphorus balances were positive in most fertilisation treatments and showed little change between years (Figure 7). Negative balances occurred only in the unfertilised treatment (Control), where there were steady phosphorus losses throughout the study period, ranging from −6.6 kg P ha^{-1} in 2022 to −8.3 kg P ha^{-1} in 2024, indicating that soil phosphorus reserves were being depleted.

In mineral fertilisation, phosphorus balances were stable and increased with higher doses: from about +0.6 kg P ha^{-1} and −0.6 kg P ha^{-1} (NPK1) to just over 9.0 kg P ha^{-1} (NPK3) in the last two years. The highest value was recorded in 2024 at the NPK3 site (9.8 kg P ha^{-1}). Positive phosphorus balances were also recorded in the first year, ranging from 2.1 to 11 kg P ha^{-1}.

Treatments with manure also showed positive phosphorus balances, especially at the highest dose (FYM3), reaching +11.2 kg P ha^{-1} in 2022 and +10.2 kg P ha^{-1} in 2024, although these values varied more between years compared to mineral fertilisation.

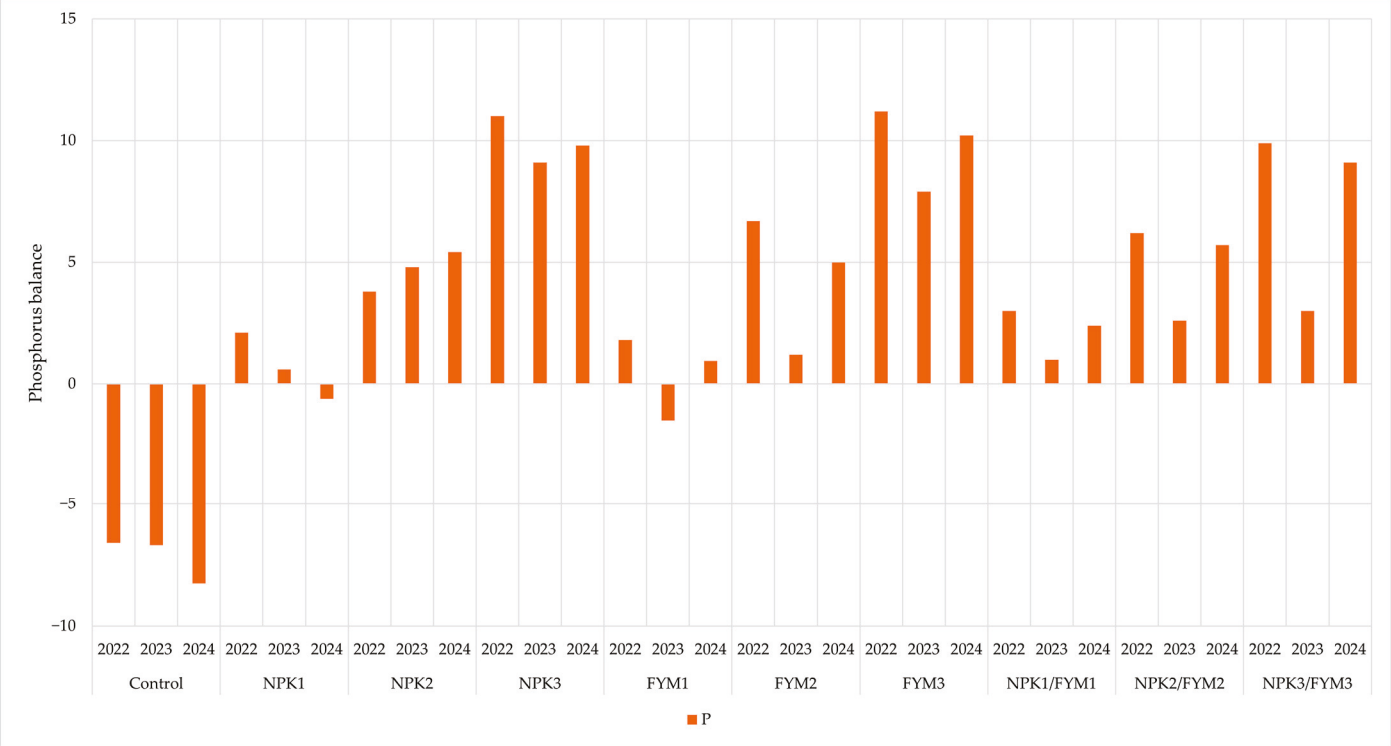


Figure 7. Effect of fertilisation treatments on phosphorus balance. Treatments: Control—0 kg N ha^{-1}, 0 kg P ha^{-1}, 0 kg K ha^{-1}; NPK1—30 kg N ha^{-1}, 10 kg P ha^{-1}, 27 kg K ha^{-1}; NPK2—45 kg N ha^{-1}, 15 kg P ha^{-1}, 41 kg K ha^{-1}; NPK3—60 kg N ha^{-1}, 20 kg P ha^{-1}, 54 kg K ha^{-1}; FYM1—32 kg N ha^{-1}, 11 kg P ha^{-1}, 32 kg K ha^{-1}; FYM2—46 kg N ha^{-1}, 16.5 kg P ha^{-1}, 48 kg K ha^{-1}; FYM3—62 kg N ha^{-1}, 22 kg P ha^{-1}, 64 kg K ha^{-1}; NPK1/FYM1—30/32 kg N ha^{-1}, 10/11 kg P ha^{-1}, 27/32 kg K ha^{-1}; NPK2/FYM2—45/46 kg N ha^{-1}, 15/16.5 kg P ha^{-1}, 41/48 kg K ha^{-1}; NPK3/FYM3—60/62 kg N ha^{-1}, 20/22 kg P ha^{-1}, 54/64 kg K ha^{-1}. NPK1, NPK2, NPK3—mineral fertilisation, FYM1, FYM2, FYM3—farmyard manure, NPK1/FYM1, NPK2/FYM2, NPK3/FYM3—alternate fertilisation.

Alternating treatments (NPK/FYM) gave similar results to the organic and mineral fertilisers. Phosphorus balances increased with the dose, from 1 to 3 kg P ha^{-1} at the lowest dose, up to over 9 kg P ha^{-1} at the highest dose.

Like with nitrogen balance, phosphorus balance values changed depending on the year. In the first year, phosphorus balances ranged from −6.6 kg P ha^{-1} (Control) to +11.0 kg P ha^{-1} (NPK3) and +11.2 kg P ha^{-1} (FYM3). The second year showed slightly better values, from −6.7 kg P ha^{-1} (Control) to +9.1 kg P ha^{-1} (NPK3). In the last year, phosphorus balances ranged from −8.3 kg P ha^{-1} (Control) to +10.2 kg P ha^{-1} (FYM3).

As observed for nitrogen, phosphorus balances also varied depending on the year of the study. In 2022, balances ranged from −6.6 kg P ha^{-1} in the control to +11.0 kg P ha^{-1} in NPK3 and +11.2 kg P ha^{-1} in FYM3. In 2023, the values were slightly more favourable, spanning from −6.7 kg P ha^{-1} (control) to +9.1 kg P ha^{-1} (NPK3). The final year (2024) showed the widest range, from −8.3 kg P ha^{-1} in the control to +10.2 kg P ha^{-1} in FYM3.

The applied fertiliser regimes had a significant effect on the phosphorus balance. The Control recorded the lowest and significantly negative P balance, indicating the strongest negative impact on phosphorus content. All fertilised treatments resulted in significantly

higher phosphorus balances compared to the Control (Table 7). The highest, statistically similar positive P balances were observed in the treatments with the highest fertiliser doses: NPK3 and FYM3. The NPK3/FYM3 treatment did not differ significantly from either the FYM3 and NPK3 group or the group receiving FYM2, NPK2, and NPK2/FYM2 application rates.

Table 7. Effect of analysed factors on phosphorus balance.

Factor	Control	NPK1	NPK2	NPK3	FYM1	FYM2	FYM3	NPK1/FYM1	NPK2/FYM2	NPK3/FYM3
Count	3	3	3	3	3	3	3	3	3	3
LS Mean	−7.2	0.7	4.7	10.0	0.4	4.3	9.8	2.1	4.8	7.3
Homogeneous Groups	a	bc	cd	e	b	bcd	e	bc	cd	de

Means within columns followed by the same letter are not significantly different from each other, according to Tukey's test at $p < 0.05$. Treatments: Control—0 kg N ha^{-1}, 0 kg P ha^{-1}, 0 kg K ha^{-1}; NPK1—30 kg N ha^{-1}, 10 kg P ha^{-1}, 27 kg K ha^{-1}; NPK2—45 kg N ha^{-1}, 15 kg P ha^{-1}, 41 kg K ha^{-1}; NPK3—60 kg N ha^{-1}, 20 kg P ha^{-1}, 54 kg K ha^{-1}; FYM1—32 kg N ha^{-1}, 11 kg P ha^{-1}, 32 kg K ha^{-1}; FYM2—46 kg N ha^{-1}, 16.5 kg P ha^{-1}, 48 kg K ha^{-1}; FYM3—62 kg N ha^{-1}, 22 kg P ha^{-1}, 64 kg K ha^{-1}; NPK1/FYM1—30/32 kg N ha^{-1}, 10/11 kg P ha^{-1}, 27/32 kg K ha^{-1}; NPK2/FYM2—45/46 kg N ha^{-1}, 15/16.5 kg P ha^{-1}, 41/48 kg K ha^{-1}; NPK3/FYM3—60/62 kg N ha^{-1}, 20/22 kg P ha^{-1}, 54/64 kg K ha^{-1}. NPK1, NPK2, NPK3—mineral fertilisation, FYM1, FYM2, FYM3—farmyard manure, NPK1/FYM1, NPK2/FYM2, NPK3/FYM3—alternate fertilisation.

3.4.3. Potassium Balances

Potassium balances are shown in Figure 8. The data show that, for most fertilisation treatments, the potassium balance was negative, and the values varied greatly both between treatments and between years of the study. Positive potassium balances were recorded only in 2024, and only in treatments fertilised with higher doses (NPK2, NPK3, NPK2/FYM2, NPK3/FYM3). Treatments fertilised with both mineral fertilisers and manure had varying balance values, but generally, the negative potassium balance was greater in treatments with manure.

In the first year of the study (2022), potassium balances ranged from −8.4 kg K ha^{-1} (NPK1) to −58.6 kg K ha^{-1} (FYM1). Less favourable balances were found in treatments fertilised with manure and in alternating treatments. In the second year (2023), the range was even wider, from −11.0 kg K ha^{-1} (NPK1) to −78.6 kg K ha^{-1} (FYM2). This was also the year with the highest average dry matter yield, which suggests that potassium fertilisation was not enough to meet the plants' needs, especially when manure was used.

In 2024, potassium balances were more favourable than in the previous two years, ranging from +7.9 kg K ha^{-1} (NPK2/FYM2) to −22.7 kg K ha^{-1} (FYM1). This was also the year with the lowest sward yield throughout the study, which resulted in lower potassium uptake and, consequently, more positive balance values.

As shown in Table 8, the most advantageous treatments were those grouped under the homogeneous letters "bc" and "c", corresponding to NPK1, NPK2, and NPK3. Across all years, most treatments exhibited a negative potassium balance, indicating that the applied fertiliser doses did not fully meet the potassium requirements of the plants. Less negative balances were observed only in the year with the lowest yields, suggesting reduced potassium uptake due to lower biomass production.

Table 8. Effect of analysed factors on potassium balance.

Factor	Control	NPK1	NPK2	NPK3	FYM1	FYM2	FYM3	NPK1/FYM1	NPK2/FYM2	NPK3/FYM3
Count	3	3	3	3	3	3	3	3	3	3
LS Mean	−26.4	−7.4	−10.6	−13.6	−51.7	−45.0	−22.8	−22.5	−21.2	−26.4
Homogeneous Groups	abc	c	bc	bc	a	ab	abc	abc	abc	abc

Means within columns followed by the same letter are not significantly different from each other, according to Tukey's test at $p < 0.05$. Treatments: Control—0 kg N ha^{-1}, 0 kg P ha^{-1}, 0 kg K ha^{-1}; NPK1—30 kg N ha^{-1}, 10 kg P ha^{-1}, 27 kg K ha^{-1}; NPK2—45 kg N ha^{-1}, 15 kg P ha^{-1}, 41 kg K ha^{-1}; NPK3—60 kg N ha^{-1}, 20 kg P ha^{-1}, 54 kg K ha^{-1}; FYM1—32 kg N ha^{-1}, 11 kg P ha^{-1}, 32 kg K ha^{-1}; FYM2—46 kg N ha^{-1}, 16.5 kg P ha^{-1}, 48 kg K ha^{-1}; FYM3—62 kg N ha^{-1}, 22 kg P ha^{-1}, 64 kg K ha^{-1}; NPK1/FYM1—30/32 kg N ha^{-1}, 10/11 kg P ha^{-1}, 27/32 kg K ha^{-1}; NPK2/FYM2—45/46 kg N ha^{-1}, 15/16.5 kg P ha^{-1}, 41/48 kg K ha^{-1}; NPK3/FYM3—60/62 kg N ha^{-1}, 20/22 kg P ha^{-1}, 54/64 kg K ha^{-1}. NPK1, NPK2, NPK3—mineral fertilisation, FYM1, FYM2, FYM3—farmyard manure, NPK1/FYM1, NPK2/FYM2, NPK3/FYM3—alternate fertilisation.

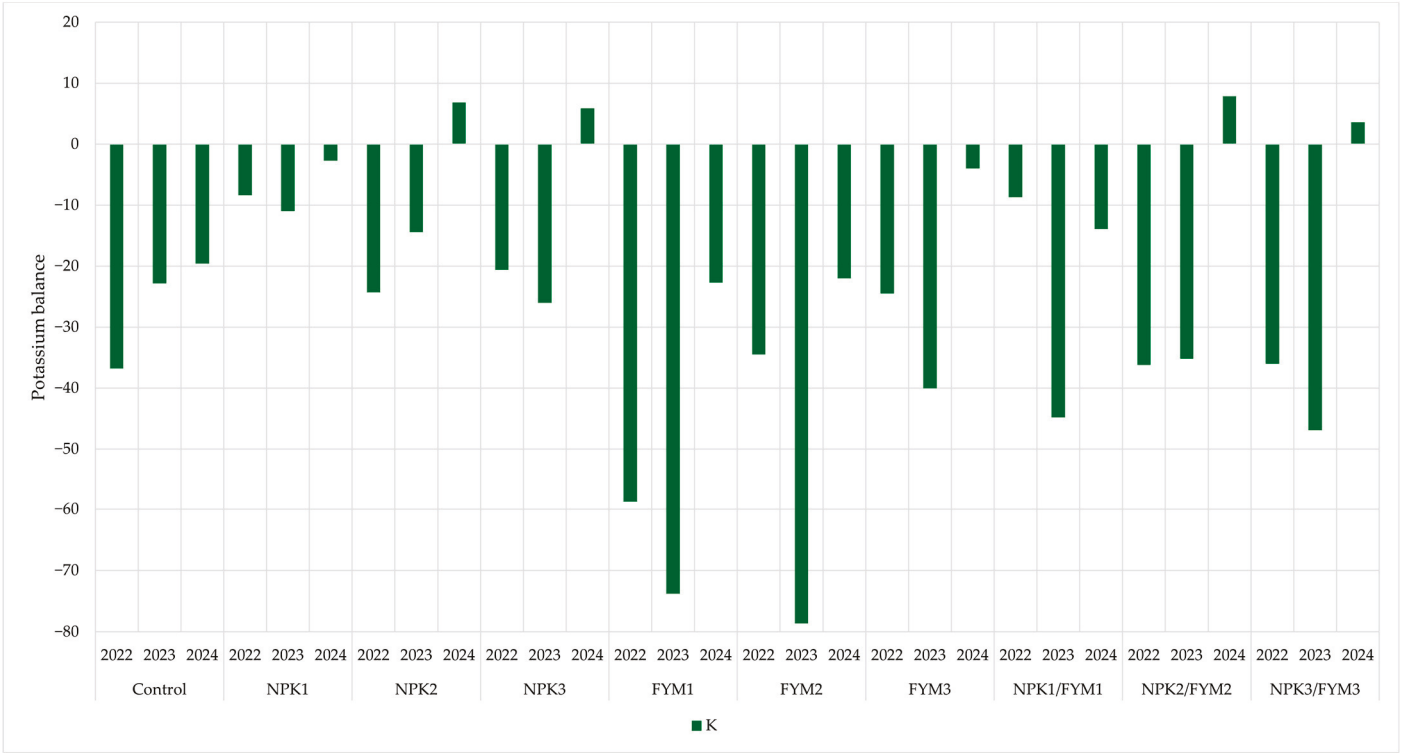


Figure 8. Effect of fertilisation treatments on potassium balance. Treatments: Control—0 kg N ha^{-1}, 0 kg P ha^{-1}, 0 kg K ha^{-1}; NPK1—30 kg N ha^{-1}, 10 kg P ha^{-1}, 27 kg K ha^{-1}; NPK2—45 kg N ha^{-1}, 15 kg P ha^{-1}, 41 kg K ha^{-1}; NPK3—60 kg N ha^{-1}, 20 kg P ha^{-1}, 54 kg K ha^{-1}; FYM1—32 kg N ha^{-1}, 11 kg P ha^{-1}, 32 kg K ha^{-1}; FYM2—46 kg N ha^{-1}, 16.5 kg P ha^{-1}, 48 kg K ha^{-1}; FYM3—62 kg N ha^{-1}, 22 kg P ha^{-1}, 64 kg K ha^{-1}; NPK1/FYM1—30/32 kg N ha^{-1}, 10/11 kg P ha^{-1}, 27/32 kg K ha^{-1}; NPK2/FYM2—45/46 kg N ha^{-1}, 15/16.5 kg P ha^{-1}, 41/48 kg K ha^{-1}; NPK3/FYM3—60/62 kg N ha^{-1}, 20/22 kg P ha^{-1}, 54/64 kg K ha^{-1}. NPK1, NPK2, NPK3—mineral fertilisation, FYM1, FYM2, FYM3—farmyard manure, NPK1/FYM1, NPK2/FYM2, NPK3/FYM3—alternate fertilisation.

4. Discussion

4.1. Effect of Fertiliser Type and Dose on the Botanical Composition of the Sward

The use of fertilisers often leads to a decline in plant species richness and changes in vegetation structure and functional composition [17,37,38]. This is important because species composition, both the number of species and their share in the sward, determines the productivity and practical value of permanent grassland [39].

As shown by a meta-analysis conducted by Shi et al. [8], mineral fertilisation, although it increases biomass production, caused an average reduction in species richness of 18%. Organic fertilisers, by improving soil structure, increasing sorption capacity, and supporting the soil microbiome, can promote the development of specific functional groups, including legumes. For example, Stybnarova et al. [10] reported that fertilisation with cattle manure and slurry, combined with moderate or intensive grassland use, increased the share of legumes in the sward.

Shi et al. [8] also report that both nitrogen and phosphorus fertilisation contributed to a decline in species richness. In the case of nitrogen, this is due to stronger, more competitive species outcompeting weaker ones [40,41]. In contrast, in our study, the number of species remained relatively stable throughout the observation period. No clear decline in species richness was observed in the mineral-fertilised treatments, nor was there a significant improvement in botanical composition due to organic fertilisation.

Apart from the fertiliser type, the applied dose also plays an important role. On intensively fertilised grasslands, increased light competition eliminates smaller and less competitive plants [42]. A meta-analysis by Francksen et al. [43] showed a negative correlation between nitrogen input and the number of species, estimating a loss of about 1.5 species per 100 kg N·ha^{-1}·yr^{-1}. Legumes are particularly sensitive to high nitrogen levels [44]. Kacorzyk et al. [45] observed that applying sheep manure at nitrogen rates below 69 kg N·ha^{-1} increased the share of legumes, while higher rates (69–103 kg N·ha^{-1}) favoured grasses at their expense. In addition, some studies suggest that mineral phosphorus fertilisation can also significantly reduce species richness [46].

However, the impact of high mineral and organic fertiliser doses on species diversity may vary. For instance, Shi et al. [8] did not find a significant effect of organic fertiliser rate on total species number. This could be because nutrients in organic fertilisers become available only after the decomposition of organic matter, which delays their uptake and reduces competitive pressure.

In our study, the applied fertiliser dose also had no effect on the botanical composition of the sward. Overall, the lack of a clear effect in our experiment may be due to the moderate fertiliser doses used (up to 60 kg N·ha^{-1} and 20 kg P·ha^{-1}) and the relatively short duration of the study (three years). Habitat-specific conditions should also be taken into account. The response of the sward to fertilisation depends not only on the fertiliser type and rate, but also on soil and climatic conditions, as well as the initial composition of the plant community, which may explain why our findings differ in some respects from studies conducted under more intensive or long-term fertilisation regimes.

4.2. Effect of Fertiliser Type and Dose on DMY

The DMY obtained on the control plots (i.e., without fertilisation) averaged 2.58 Mg·ha^{-1}, reflecting the natural production potential of dry meadows under temperate climate conditions. The application of different fertilisation types had a significant impact on yield compared to the control. On average, DMY increased by 55.3% with mineral fertilisation (NPK), by 63.9% with organic fertilisation (FYM), and by 65.45% with alternating NPK and FYM fertilisation (NPK/FYM). These results are broadly consistent with findings from previous studies. For instance, Shi et al. [8] reported that organic fertilisers increased biomass production more than mineral ones (on average by 56% ± 5% vs. 42% ± 2%), while Stybnarova et al. [10] found that fertilisation with manure and slurry fertilisation significantly increased DMY, by 51.9% and 56%, respectively, compared to the control (4.81 t·ha^{-1}). Our observed increases, particularly in the combined NPK/FYM treatments, slightly exceed these reported values, suggesting a potential synergistic effect under our experimental conditions.

In our study, the greatest biomass increase was observed in the treatment with the highest alternating NPK and FYM fertilisation rate (NPK3/FYM3), where yield rose by more than 83% compared to the control. This supports literature reports suggesting that the combined application of mineral and organic fertilisers produces a synergistic effect: it improves soil fertility, which in turn enables higher yields than when each type of fertiliser is applied separately [20,21,47].

Organic fertilisers supply numerous macro- and micronutrients. By gradually releasing nutrients, they increase soil humus content, improve soil structure, and support microbial development [48], contributing to sustained productivity over time. Mineral fertilisers, in contrast, provide nutrients more rapidly, supporting intensive plant growth and development [49]. Combining both fertiliser types helps reduce nutrient losses typical of mineral fertilisers, supplies carbon as an energy source for the soil microbiome, and compensates for the slower nutrient release from organic fertilisers [50], which can explain the higher yields in NPK/FYM treatments.

In our study, significant differences in yield were also observed between years, primarily due to variations in weather conditions. The lowest average DMY (3.33 Mg·ha^{-1}) was recorded in the final year of the study (2024). In contrast, the highest average DMY across all treatments occurred in the second year (2023), reaching 4.40 Mg·ha^{-1}. This was 2% higher than in 2022 and as much as 32% higher than in 2024. The high DMY in 2023 was largely due to the abundant third cut. In August, during the regrowth period following the second cut (in July), heavy rainfall created highly favourable conditions for plant regrowth, leading to a substantial increase in total annual yield.

The smallest differences between years and harvests were observed in the Control and NPK1 treatments. Analysis of the first harvest showed the maximum yield in 2022, likely due to optimal early-season conditions and a delayed harvest date (15 June). In contrast, the first harvest in 2023 occurred much earlier (22 May), a 24-day difference, contributing to lower relative yields. In 2024, the first cut was similar to 2023 (13 May), while lower yields were likely due to less favourable early-season weather. Differences in the second harvests were smaller between treatments and years. The third harvest in 2023, performed the latest (2 October), reached the highest yields, whereas in 2022 and 2024 the final cut took place at the beginning of September (Figure 4).

4.3. Effect of Fertiliser Type and Dose on Nitrogen, Phosphorus, and Potassium Balances

Nutrient balances calculated for different fertilisation types and doses are a useful tool for evaluating whether nutrient inputs match plant requirements under specific environmental conditions (soil, precipitation, temperature), which ultimately determine yield levels [51]. Small balance values, whether positive (+) or negative (−), indicate that the fertilisation applied is well aligned with actual crop needs and sustainable nutrient management.

The analysis of nitrogen, phosphorus, and potassium balances confirmed that both the type and dose of fertilisation significantly influenced nutrient surpluses or deficits. The control treatment showed consistent nutrient shortages in all years, with average negative balances of −12.2 kg N·ha^{-1}, −7.2 kg P·ha^{-1}, and −26.4 kg K·ha^{-1}. These results indicate ongoing soil nutrient depletion in the absence of external inputs.

In mineral fertilisation treatments, nitrogen balances were positive at all doses, especially at 30 kg N·ha^{-1} (average +6.3 kg N·ha^{-1}). The highest N dose (60 kg N·ha^{-1}) led to a nitrogen surplus of +16.3 kg N·ha^{-1}, suggesting excess nitrogen relative to plant demand. Phosphorus balances also increased with dose, ranging from +0.7 kg P·ha^{-1} at the lowest rate to +10.0 kg P·ha^{-1} at the highest. Potassium balances, however, remained negative at all NPK levels (from −7.4 to −13.6 kg K·ha^{-1}), likely due to high plant uptake or leaching losses, a pattern observed in other studies of mineral fertilisation on light-textured soils [52].

Manure fertilisation also led to positive nitrogen and phosphorus balances, with the highest values being +20.6 kg N·ha^{-1} and +9.8 kg P·ha^{-1}. Nevertheless, potassium balances were strongly negative across all FYM treatments (from −51.7 to −22.8 kg K·ha^{-1}), reflecting both the relatively low K content of FYM and the high mobility of potassium in soils, especially under leaching-prone conditions. Kayser and Isselstein [49] noted that potassium in grassland systems is poorly retained in the soil and is easily lost due to uptake by plants and export with harvested biomass, even under moderate fertilisation.

Interestingly, our results differ from Barszczewski and Ducka [53], who reported negative nitrogen and potassium balances and near-zero phosphorus balances at comparable fertiliser rates (60 kg N·ha^{-1}) in a permanent meadow on degraded black soil. This highlights how soil type and initial nutrient status can strongly influence nutrient balance outcomes.

The alternating application of NPK and FYM (NPK/FYM) had a positive effect on nutrient balances for all three elements. For nitrogen, it improved the balance compared to FYM alone, without causing the large surpluses typical of continuous NPK application. For phosphorus, it helped reduce the risk of accumulation observed under exclusive NPK fertilisation. Regarding potassium, alternating fertilisation reduced the deficit typical of FYM treatments and improved potassium availability to plants.

4.4. Impact of Weather Conditions on Nitrogen, Phosphorus, and Potassium Balances

The results, regardless of the type of fertilisation used, confirm that weather conditions in each year had a strong influence on nitrogen, phosphorus and potassium balances. In 2022, moderate spring temperatures combined with rainfall promoted efficient nutrient uptake by the plants. As a result, nitrogen and phosphorus balances were positive across all fertilisation variants. Despite the favourable conditions, potassium balances remained clearly negative, especially in the FYM treatments (e.g., FYM1: −58.6 kg K·ha^{-1}), indicating that manure alone may not fully satisfy the potassium demands of the plants.

In 2023, although temperatures were close to the long-term average, there was a large variation in rainfall, with water shortages in spring and heavy rains in August (156 mm). This contributed to the highest yield of the entire study period (average 4.40 Mg·ha^{-1}), which in term strongly influenced the nutrient balances. Negative nitrogen balances were recorded in most FYM and NPK/FYM variants. Only the highest NPK treatment showed a positive balance (+5.4 kg N·ha^{-1}). Phosphorus balances were also lower than in the previous year but remained positive in the NPK/FYM2 variant (+2.6 kg P·ha^{-1}). Potassium balances dropped to their lowest levels during the study, for example FYM2: −78.6 kg K·ha^{-1}, likely due to high leaching losses caused by intense rainfall in the second half of the growing season.

In 2024, spring was unusually hot (April: 16.5 °C, May: 23.4 °C) and rainfall was highly variable. Due to reduced yields (average 3.33 Mg·ha^{-1}), all fertilised variants showed positive nitrogen balances, with the highest in FYM3 (+42.5 kg N·ha^{-1}) and NPK3 (+32.8 kg N·ha^{-1}). These results suggest that plant nitrogen uptake was limited under heat stress and lower biomass production. Similarly, high phosphorus balances in the intensively fertilised variants (FYM3: +10.2 kg P·ha^{-1}, NPK3/FYM3: +9.1 kg P·ha^{-1}) also point to reduced nutrient uptake. Potassium balances improved slightly, especially in NPK3/FYM3 (+3.6 kg K·ha^{-1}) and NPK3 (+5.9 kg K·ha^{-1}), but remained negative in the FYM-only treatments, highlighting persistent K deficiency despite organic inputs.

4.5. Assessment of Nutrient Balances in the Context of Environmental Guidelines

For environmental reasons, nutrient balances should ideally be balanced. This is generally true in closed natural ecosystems where no plant biomass is harvested. However,

under field conditions, perfectly balanced nutrient levels are rarely achieved, as confirmed by both the literature and our own research. As noted by Fotyma et al. [54], achieving completely neutral nutrient balances in agricultural practice is difficult, especially while maintaining profitable production. Some surplus, particularly nitrogen in intensive fertilisation, is inevitable, but its magnitude should be managed to reduce environmental pollution risks [55].

OECD experts consider nutrient balances between 20 and 30 kg ha^{-1} per year to be within safe limits for fertiliser management and water protection. According to Toczyński [55], optimal nitrogen balance values in Polish conditions should range from 38.6 to 47.2 kg N ha^{-1}, phosphorus between −1.0 and +4.0 kg P ha^{-1}, and potassium between 8.7 and 13.7 kg K ha^{-1}.

In most of the fertilisation treatments, nitrogen balances were within safe or optimal ranges. Even the highest nitrogen balance (+42.5 kg N ha^{-1}), observed with the highest manure dose (FYM3), did not exceed Toczyński's upper recommended limit [56].

A three-level water quality risk scale was also developed for phosphorus: balances below 20 kg P ha^{-1} are considered safe; 20–30 kg P ha^{-1} represent medium risk; and above 30 kg P ha^{-1} indicate a high risk of phosphorus accumulation in soil and leaching into surface waters. Most phosphorus balances in our study fell into the low or moderate risk categories (below 20 kg P ha^{-1}). None exceeded the 30 kg P ha^{-1} threshold, which marks the risk limit for accumulation and leaching. Moreover, many variants, especially in 2023 and 2024 under moderate fertilisation, had phosphorus balances close to the recommended range for Poland (−1.0 to +4.0 kg P ha^{-1}) [55]. This suggests that the applied phosphorus doses fully met plant nutritional needs without excessive accumulation [57].

The largest deviations from reference values were seen with potassium. In most variants and years, potassium balances were clearly negative, especially in manure-fertilised treatments, where a balance of −73.8 kg K ha^{-1} was recorded in 2023. Only a few cases, mainly in 2024, showed a positive potassium balance. Considering the optimal potassium balance range in Poland is +8.7 to +13.7 kg K ha^{-1} [56], these deficits likely resulted from both high plant uptake and losses through leaching, especially during wet seasons such as 2023. Such large negative potassium balances can reduce soil potassium reserves, lower yields in subsequent years, and degrade yield quality. Excessive potassium depletion can lead to soil degradation through damage to clay mineral structure, which is rich in potassium [58,59].

While this study provides valuable insights into nitrogen, phosphorus, and potassium balances depending on fertilisation type in permanent meadows, it has certain limitations. The experiment was conducted on mineral soils, limiting direct application of results to other soil types (e.g., organic soils) or climates. Also, balance calculations used a simplified method that did not account for all nutrient loss pathways, such as losses during fertiliser application. Another limitation is the relatively short three-year study period (2022–2024), which, although covering variable weather (Tables 3 and 4), cannot fully reflect long-term effects of fertilisation on permanent grasslands seen in longer-term experiments, e.g., the 120-year study by Kidd et al. [17]. In addition, the absence of experimental replicates reduces the statistical robustness of the results and should be considered when interpreting the findings. Therefore, future research should extend observation periods and, if possible, include replicated plots to better capture changes in nutrient balances over the long term and refine practical fertilisation recommendations for permanent grasslands

The results of this study highlight several important considerations for fertiliser management in permanent meadows. Monitoring nutrient balances can help adjust fertiliser doses to better match plant requirements, improving nutrient use efficiency and maintaining yield stability. Careful nitrogen management is essential to prevent environmental

pollution while ensuring adequate plant nutrition, particularly under variable weather conditions. Phosphorus fertilisation appears adequate in the studied systems, but persistent negative potassium balances indicate the need for supplementary potassium inputs to avoid soil depletion and maintain long-term productivity. Implementing combined fertilisation strategies, such as alternating FYM and mineral NPK, offers a promising approach to balance plant nutrition, support environmental protection, and enhance sustainable grassland management.

5. Conclusions

The type and dose of fertilisation clearly influenced both sward yield and nutrient balances. The highest positive nitrogen and phosphorus balances were observed in the intensively fertilised organic treatment (FYM3) and in the alternate fertilisation treatment (NPK3/FYM3). In contrast, potassium balances were mostly negative, particularly in manure-fertilised plots.

Weather conditions strongly affected N, P, and K balances. In years with favourable rainfall, nutrient uptake was more efficient, resulting in improved and more balanced nutrient budgets. Conversely, periods of water shortage reduced nutrient availability, leading to greater imbalances despite consistent fertilisation practices.

Nitrogen balances remained below levels considered environmentally risky. However, in most cases, they were also below the recommended range for Polish conditions, indicating limited nitrogen uptake under stressful weather.

Phosphorus balances were positive but remained within safe environmental limits, reflecting efficient use of this nutrient.

Potassium balances, especially in FYM-fertilised treatments, were negative. Persistent negative potassium balances may gradually deplete soil reserves unless supplemented by additional mineral potassium inputs.

Among the fertilisation treatments studied, alternate fertilisation—combining FYM and mineral NPK, emerged as a promising approach for improving nutrient use efficiency, increasing dry matter yield, and maintaining more balanced nutrient budgets.

The study emphasises the importance of balanced nutrient management in permanent meadows, showing that moderate fertilisation strategies, such as alternating FYM and mineral NPK, can maintain productivity while reducing environmental impacts. Future research should focus on long-term monitoring to better understand nutrient dynamics and optimize fertilisation practices for sustainable grassland management.

Author Contributions: Conceptualization, J.B., A.P.-J. and B.W.; methodology, J.B. and A.P.-J.; validation, W.S., B.W. and A.P.-J.; formal analysis, W.S.; investigation, D.G.-Z., A.P.-J., W.S. and B.W.; resources, D.G.-Z., A.P.-J., W.S. and B.W.; data curation, A.P.-J., W.S. and B.W.; writing—original draft preparation, B.W., A.P.-J. and W.S.; writing—review and editing, B.W.; visualization, W.S.; supervision, A.P.-J.; project administration, J.B. and A.P.-J.; funding acquisition, J.B. All authors have read and agreed to the published version of the manuscript.

Funding: The research was funded by the Ministry of Agriculture and Rural Development in Poland in 2022 (DIW.ib.070.1.2022) and in 2023 (DIW.ib.070.1.2023). In 2024, the research was not externally funded.

Data Availability Statement: The original contributions presented in this study are included in the article. Further inquiries can be directed to the corresponding author.

Conflicts of Interest: The authors declare no conflicts of interest.

References

1. FAOSTAT. *Agri-Environmental Indicators, Land Use*; FAO: Rome, Italy, 2019; ISBN 978-3-9525031-4-0. Available online: http://www.fao.org/faostat/en/#data/EL (accessed on 5 May 2024).
2. Statistics Poland. Statistical Yearbook of Agriculture 2024. Available online: https://stat.gov.pl/obszary-tematyczne/roczniki-statystyczne/roczniki-statystyczne/rocznik-statystyczny-rolnictwa-2024,6,18.html (accessed on 5 May 2025).
3. European Union. Regulation (EU) No 1307/2013 of the European Parliament and of the Council of 17 December 2013 Establishing Rules for Direct Payments to Farmers Under Support Schemes Within the Framework of the Common Agricultural Policy and Repealing Council Regulation (EC) No 637/2008 and Council Regulation (EC) No 73/2009. *Off. J. Eur. Union* **2013**, *347*, 608.
4. Huyghe, C.; De Vliegher, A.; Golinski, P. European grasslands overview: Temperate region. In *Grassland Science in Europe*; European Grassland Federation: Aberystwyth, UK, 2014; Volume 19, pp. 29–40.
5. Milazzo, F.; Francksen, R.M.; Zavattaro, L.; Abdalla, M.; Hejduk, S.; Enri, S.R.; Pittarello, M.; Price, P.N.; Schils, R.L.M.; Smith, P.; et al. The role of grassland for erosion and flood mitigation in Europe: A meta-analysis. *Agric. Ecosyst. Environ.* **2023**, *348*, 108443. [CrossRef]
6. Isselstein, J.; Kayser, M. Functions of grassland and their potential in delivering ecosystem services. *Grassl. Sci. Eur.* **2014**, *19*, 199–214.
7. Schils, R.L.M.; Bufe, C.; Rhymer, C.M.; Francksen, R.M.; Klaus, V.H.; Abdalla, M.; Milazzo, F.; Lellei-Kovács, E.; ten Berge, H.; Bertora, C.; et al. Permanent Grasslands in Europe: Land Use Change and Intensification Decrease Their Multifunctionality. *Agric. Ecosyst. Environ.* **2022**, *330*, 107891. [CrossRef]
8. Shi, T.S.; Collins, S.L.; Yu, K.; Peñuelas, J.; Sardans, J.; Li, H.; Ye, J.-S. A global meta-analysis on the effects of organic and inorganic fertilization on grasslands and croplands. *Nat. Commun.* **2024**, *15*, 3411. [CrossRef] [PubMed]
9. Brummerloh, A.; Kuka, K. The Effects of Manure Application and Herbivore Excreta on Plant and Soil Properties of Temperate Grasslands—A Review. *Agronomy* **2023**, *13*, 3010. [CrossRef]
10. Štýbnarová, M.; Mičová, P.; Fiala, K.; Karabcová, H.; Látal, O.; Pozdíšek, J. Effect of organic fertilizers on botanical composition of grassland, herbage yield and quality. *Agriculture* **2014**, *60*, 87–97. [CrossRef]
11. Vîntu, V.; Samuil, C.; Trofin, A.; Popovici, I.C. The influence of organic and mineral fertilizers on fodder quality in NE Romania. *Grassl. Sci. Eur.* **2008**, *13*, 637–639.
12. Simić, A.; Marković, J.; Vučković, S.; Stojanović, B.; Bijelić, Z.; Mandić, V.; Dželetović, Ž. The Use of Different N Sources for the Treatment of Permanent Grassland and Effect on Forage Quality. *Emir. J. Food Agric.* **2019**, *31*, 180–187. [CrossRef]
13. Walie, M.; Amogne, F.T.; Mekuriaw, Y.; Tsunekawa, A.; Kobayashi, N.; Ichinohe, T.; Haregeweyn, N.; Wolde, A.; Mekuriaw, S.; Masunaga, T.; et al. Biomass Yield, Quality, and Soil Nutrients of Pasture Influenced by Farmyard Manure and Enrichment Planting. *Rangel. Ecol. Manag.* **2023**, *88*, 174–181. [CrossRef]
14. Simić, A.; Stojanović, B.; Vučković, S.; Marković, J.; Božičković, A.; Bijelić, Z.; Mandić, V. Application of farmyard manure in grassland production. *AGROFOR Int. J.* **2016**, *1*, 20–27. [CrossRef]
15. Szewczyk, W.; Kasperczyk, M.; Kacorzyk, P. Role of farmyard manure on upland meadows. *Grassl. Sci. Eur.* **2004**, *9*, 714–716.
16. Cherney, J.H.; Cherney, D.J.R. Impact of Fertilization on Forage Production and Animal Performance. In Proceedings of the Colloque sur les Plantes Fourrageres, Drummondville, QC, Canada, 9 December 2015; pp. 1–7. Available online: https://www.craaq.qc.ca/documents/files/EPLF1501/Cherney_resume_va.pdf (accessed on 21 April 2025).
17. Kidd, J.; Manning, P.; Simkin, J.; Peacock, S.; Stockdale, E. Impacts of 120 years of fertilizer addition on a temperate grassland ecosystem. *PLoS ONE* **2017**, *12*, e0174632. [CrossRef]
18. Plisková, J.; Pospíšilová, L.; Nerušil, P.; Šimon, T.; Menšík, L. Effect of Grasslands Fertilisation on Soil Organic Matter Quality and Nutrients Status. *Agriculture* **2024**, *69*, 129–139. [CrossRef]
19. Zhang, Z.; Chen, R.; Blagodatskaya, E.; Blagodatsky, S.; Liu, D.; Yu, Y.; Feng, Y. Long-Term Application of Mineral Fertilizer Weakens the Stability of Microbial N-Transforming Functions via the Decrease of Soil Microbial Diversity. *J. Sustain. Agric. Environ.* **2024**, *3*, 1–11. [CrossRef]
20. Genç Lermi, A.; Erkovan, H.İ.; Koç, A. Determination of Combined Effects of Organic and Mineral Fertilizer on Forage Yield and Quality of Annual Ryegrass. *Agronomy* **2023**, *13*, 2935. [CrossRef]
21. Xing, Y.; Xie, Y.; Wang, X. Enhancing soil health through balanced fertilization: A pathway to sustainable agriculture and food security. *Front. Microbiol.* **2025**, *16*, 1536524. [CrossRef]
22. Phohlo, M.P.; Swanepoel, P.A.; Hinck, S. Excessive Nitrogen Fertilization Is a Limitation to Herbage Yield and Nitrogen Use Efficiency of Dairy Pastures in South Africa. *Sustainability* **2022**, *14*, 4322. [CrossRef]
23. Kupiec, J. Przegląd metod bilansowania makroskładników NPK w produkcji rolnej. *Inżynieria Ochr. Sr.* **2015**, *18*, 323–342. (In Polish)
24. Dalgaard, T.; Bienkowski, J.F.; Bleeker, A.; Dragosits, U.; Drouet, J.L.; Durand, P.; Frumau, A.; Hutchings, N.J.; Kedziora, A.; Magliulo, V.; et al. Farm nitrogen balances in six European landscapes as an indicator for nitrogen losses and basis for improved management. *Biogeosciences* **2012**, *9*, 5303–5321. [CrossRef]

25. Fraters, D.; van Leeuwen, T.; Boumans, L.; Reijs, J. Use of long-term monitoring data to derive a relationship between nitrogen surplus and nitrate leaching for grassland and arable land on well-drained sandy soils in the Netherlands. *Acta Agric. Scand. Sect. B—Soil Plant Sci.* **2015**, *65* (Suppl. S2), 144–154. [CrossRef]
26. IUSS Working Group WRB. World Reference Base for Soil Resources 2014, update 2015. In *International Soil Classification System for Naming Soils and Creating Legends for Soil Maps*; Schad, P., van Huyssteen, C., Micheli, E., Eds.; World Soil Resources Reports No. 106; FAO: Rome, Italy, 2015; 192p. Available online: https://www.researchgate.net/publication/301340673_World_Reference_Base_for_Soil_Resources_2014_update_2015 (accessed on 10 May 2025).
27. Barszczewski, J.; Wesołowski, P. Użytkowanie kośne oraz nawożenie łąk. In *Racjonalne Wykorzystanie Potencjału Produkcyjnego Trwałych Użytków Zielonych w Polsce w Różnych Warunkach Glebowych i Systemach Gospodarowania*, 1st ed.; Barszczewski, J., Ed.; Wydawnictwo ITP: Falenty, Poland, 2015; pp. 57–79. (In Polish)
28. Barszczewski, J.; Wróbel, B.; Szatylowicz, M. Wpływ różnych sposobów nawożenia na skład runi łąki trwałej oraz jej jakość. *Zesz. Probl. Post. Nauk Rol.* **2011**, *565*, 15–23. (In Polish)
29. Barszczewski, J.; Szatyłowicz, M. Gospodarka azotem w warunkach zróżnicowanego nawożenia łąki na glebie torfowo-murszowej. *Woda-Sr.-Obsz. Wiej.* **2011**, *11*, 7–19. (In Polish)
30. Klapp, R. *Łąki i Pastwiska*; PWRiL: Warszawa, Poland, 1962. (In Polish)
31. *PN-EN ISO 10390:2022-09*; Soil, Treated Biowaste and Sludge–Determination of pH. Polish Committee for Standardizations: Warsaw, Poland, 2022.
32. Barszczewski, J.; Burs, W. Polowe bilanse azotu, fosforu i potasu w gospodarstwie na przykładzie Zakładu Doświadczalnego w Falentach. *Woda-Sr.-Obsz. Wiej.* **2003**, *3*, 25–37. (In Polish)
33. Pietrzak, S. Metoda uproszczonego bilansowania azotu w gospodarstwie rolnym. *Mater. Instr.* **1997**, *108*, 22. (In Polish)
34. Ministerstwo Rolnictwa i Rozwoju Wsi. *Zbiór Zaleceń Dobrej Praktyki Rolniczej Mający na Celu Ochronę Wód Przed Zanieczyszczeniem Azotanami Pochodzącymi ze Źródeł Rolniczych*; MRiRW: Warszawa, Poland, 2024. Available online: https://www.gov.pl/attachment/86ce2b76-3c7c-450d-b4bd-207ccad05bf8 (accessed on 15 June 2025). (In Polish)
35. Institute of Meteorology and Water Management—National Research Institute. Available online: https://imgw.pl/ (accessed on 8 May 2025).
36. Selyaninov, G.T. Methods of Agricultural Climatology. *Agric. Meteorol.* **1930**, *22L*, 4–20.
37. Allan, E.; Manning, P.; Alt, F.; Binkenstein, J.; Blaser, S.; Bluthgen, N.; Böhm, S.; Grassein, F.; Hölzel, N.; Klaus, V.H.; et al. Landuse intensification alters ecosystem multifunctionality via loss of biodiversity and changes to functional composition. *Ecol. Lett.* **2015**, *18*, 83443. [CrossRef] [PubMed]
38. Seabloom, E.W.; Adler, P.B.; Alberti, J.; Biederman, L.; Buckley, Y.M.; Cadotte, M.W.; Collins, S.L.; Dee, L.; Fay, P.A.; Firn, J.; et al. Increasing effects of chronic nutrient enrichment on plant diversity loss and ecosystem productivity over time. *Ecology* **2021**, *102*, e03218. [CrossRef]
39. Wróbel, B.; Zielewicz, W.; Paszkiewicz-Jasińska, A. Improving Forage Quality from Permanent Grasslands to Enhance Ruminant Productivity. *Agriculture* **2025**, *15*, 1438. [CrossRef]
40. Harpole, W.S.; Sullivan, L.L.; Lind, E.M.; Firn, J.; Adler, P.B.; Borer, E.T.; Chase, J.; Fay, P.A.; Hautier, Y.; Hillebrand, H.; et al. Addition of Multiple Limiting Resources Reduces Grassland Diversity. *Nature* **2016**, *537*, 93–96. [CrossRef]
41. Ladouceur, E.; Blowes, S.A.; Chase, J.M.; Clark, A.T.; Garbowski, M.; Alberti, J.; Arnillas, C.A.; Bakker, J.D.; Barrio, I.C.; Bharath, S.; et al. Linking Changes in Species Composition and Biomass in a Globally Distributed Grassland Experiment. *Ecol. Lett.* **2022**, *25*, 2699–2712. [CrossRef]
42. Hautier, Y.; Niklaus, P.A.; Hector, A. Competition for Light Causes Plant Biodiversity Loss After Eutrophication. *Science* **2009**, *324*, 636–638. [CrossRef]
43. Francksen, R.M.; Turnbull, S.; Rhymer, C.M.; Hiron, M.; Bufe, C.; Klaus, V.H.; Newell-Price, P.; Stewart, G.; Whittingham, M.J. The Effects of Nitrogen Fertilisation on Plant Species Richness in European Permanent Grasslands: A Systematic Review and Meta-Analysis. *Agronomy* **2022**, *12*, 2928. [CrossRef]
44. Tang, J.; Li, W.; Wei, T.; Huang, R.; Zeng, Z. Patterns and Mechanisms of Legume Responses to Nitrogen Enrichment: A Global Meta-Analysis. *Plants* **2024**, *13*, 3244. [CrossRef]
45. Kacorzyk, P.; Głąb, T. Effect of Ten Years of Mineral and Organic Fertilization on the Herbage Production of a Mountain Meadow. *J. Elem.* **2012**, *22*, 219–233. [CrossRef]
46. Wassen, M.J.; Venterink, H.O.; Lapshina, E.D.; Tanneberger, F. Endangered plants persist under phosphorus limitation. *Nature* **2005**, *437*, 547–550. [CrossRef] [PubMed]
47. Liu, M.; Li, Y.; Che, Y.; Deng, S.; Xiao, Y. Effects of different fertilizers on growth and nutrient uptake of Lolium multiflorum grown in Cd-contaminated soils. *Environ. Sci. Pollut. Res.* **2017**, *24*, 23363–23370. [CrossRef] [PubMed]
48. Tian, J.; Lou, Y.; Gao, Y.; Fang, H.; Liu, S.; Xu, M.; Blagodatskaya, E.; Kuzyakov, Y. Response of soil organic matter fractions and composition of microbial community to long-term organic and mineral fertilization. *Biol. Fertil. Soils* **2017**, *53*, 523–532. [CrossRef]
49. Timsina, J. Can organic sources of nutrients increase crop yields to meet global food demand? *Agronomy* **2018**, *8*, 214. [CrossRef]

50. Dincă, L.C.; Grenni, P.; Onet, C.; Onet, A. Fertilization and soil microbial community: A review. *Appl. Sci.* **2022**, *12*, 1198. [CrossRef]
51. Kopiński, J. Bilans azotu brutto jako agrośrodowiskowy wskaźnik zmian intensywności produkcji rolniczej w Polsce. *Zesz. Probl. Post. Nauk Rol.* **2010**, *547*, 185–191. (In Polish)
52. Kayser, M.; Isselstein, J. Potassium cycling and losses in grassland systems: A review. *Grass Forage Sci.* **2005**, *60*, 213–224. [CrossRef]
53. Barszczewski, J.; Ducka, M. Bilans wybranych makroskładników łąki trwałej nawożonej nawozami mineralnymi i naturalnymi. *Woda-Sr.-Obsz. Wiej.* **2012**, *12*, 7–23. (In Polish)
54. Fotyma, M.; Jadczyszyn, T.; Pietruch, C. System wspierania decyzji w zakresie zrównoważonej gospodarki składnikami mineralnymi-MACROBIL. *Pamiętnik Puławski* **2001**, *124*, 81–89. (In Polish)
55. Jadczyszyn, T.; Kopiński, J. Nawożenie azotem w Polsce–aspekt produkcyjny i środowiskowy (Nitrogen fertilization in Poland–production and environmental aspec). *Stud. Rap. IUNG-PIB* **2013**, *34*, 125–143. (In Polish)
56. Toczyński, T.; Wrzaszcz, W.; Zegar, J.S. *Zrównoważenie Polskiego Rolnictwa, Powszechny Spis Rolny 2010, Warszawa*; Instytut Ekonomiki Rolnictwa i Gospodarki Żywnościowej–Państwowy Instytut Badawczy: Warszawa, Poland, 2013; p. 219. (In Polish)
57. Sapek, B. Nagromadzanie i uwalnianie fosforu w glebach–źródła, procesy, przyczyny. *Woda-Sr.-Obsz. Wiej.* **2014**, *14*, 77–100. (In Polish)
58. Phocharoen, Y.; Aramrak, S.; Chittamart, N.; Wisawapipat, W. Potassium influence on soil aggregate stability. *Commun. Soil Sci. Plant Anal.* **2018**, *49*, 2162–2174. [CrossRef]
59. Sapek, A. Azot, fosfor i potas w glebie oraz plonowanie trwałego użytku zielonego na długoletnich doświadczeniach łąkowych. Przedmowa. *Woda-Sr.-Obsz. Wiej.* **2006**, *6*, 5–13. (In Polish)

Disclaimer/Publisher's Note: The statements, opinions and data contained in all publications are solely those of the individual author(s) and contributor(s) and not of MDPI and/or the editor(s). MDPI and/or the editor(s) disclaim responsibility for any injury to people or property resulting from any ideas, methods, instructions or products referred to in the content.

agronomy

MDPI

Article

Spring- and Summer Heat Waves Caused Opposite Effects on Soil Respiration in a Eurasian Meadow Steppe

Yang Shao [1,†], Qi Tong [2,†], Tsegaye Gemechu Legesse [2], Changliang Shao [2,*] and Xiaoguang Zhang [1,*]

[1] School of Resources and Environment, Qingdao Agricultural University, Qingdao 266109, China; heysyyy@163.com
[2] State Key Laboratory of Efficient Utilization of Arid and Semi-Arid Arable Land in Northern China, Institute of Agricultural Resources and Regional Planning, Chinese Academy of Agricultural Sciences, Beijing 100081, China; tongqi120465@foxmail.com (Q.T.); tsegaye@caas.cn (T.G.L.)
* Correspondence: shaochangliang@caas.cn (C.S.); zhangxg_66@sina.com (X.Z.)
† These authors contributed equally to this work.

Abstract

Heat waves (HWs), characterized by periods of unusually high temperature, would inevitably affect the soil microenvironment and then soil respiration (Rs), which is considered to be the most active part of the global carbon cycle. An in situ spring and summer HWs simulation experiment combined with a locally common human disturbance (mowing) was conducted to separate Rs into autotrophic respiration (Ra) and heterotrophic respiration (Rh) on a natural Eurasian meadow steppe in 2018 and 2019. HWs significantly affected grassland Rs, Rh and Ra ($p < 0.01$) and also interacted with mowing, but the effect of spring HW and summer HW were different. During the summer HWs, daily Rs of the non-mowed plots increased by 1.07 μmol m^{-2} s^{-1} (11.71%) and increased in the mowed plots by 2.15 μmol m^{-2} s^{-1} (23.81%). During the spring HWs, daily Rs of the non-mowed plots decreased by 0.13 μmol m^{-2} s^{-1} (2.36%) and decreased by 0.52 μmol m^{-2} s^{-1} (9.02%) in the mowed plots. Rs, Rh and Ra were inhibited by spring HWs, but promoted by summer HWs. Our results indicated that the occurring time change in HWs would cause widely divergent influences on the ecosystem, and mowing would decrease the anti-interference ability of the ecosystem, which acted as an enhancement on both the positive and negative effects of HWs. These findings have important implications for accurate model prediction and carbon budget assessment.

Keywords: heat stress; mowing; autotrophic respiration; heterotrophic respiration; carbon budget

1. Introduction

Under the continuous influence of natural processes and human activities, the frequency and intensity of heat waves (HWs) were increased, and the duration of HWs promoted. As a typical extreme climate against the background of global warming, HWs have attracted more and more attention from the scientific community [1–3]. The main reason is that although HWs occur for a short time, its effects are not temporary; it exerts a significant impact on the natural ecosystem, regional economy and human health [4–7]. For example, a 10-day long HW in Europe reduced the net primary productivity of the ecosystem by 30%, and there was a 5-year legacy effect [8]. Studies on typical grasslands have also shown that HWs significantly decreased the net ecosystem exchange (NEE) of CO_2, ecosystem respiration (ER) and gross ecosystem productivity (GEP) by 31%, 5% and

16%, respectively [6]. The impact of HWs on NEE was much greater than that on ER, with a gap of up to six times; the hypothesis was that (1) ER had multiple sources, such as plant respiration and soil respiration (Rs) [9]; (2) the increase in litter in areas where HWs occurred might promote Rs in the ecosystem [10,11], but this hypothesis still lacks direct evidence.

It is also necessary to consider time when the HWs occurred [3,12]. Historical data of different Inner Mongolia grasslands showed the increasing frequency of HWs and also indicated an advancing trend in which the HW occurrence time changed from July to June [6]. HWs occurring at different times and their impact intensity and mechanisms would be different due to the different hydrothermal conditions and plant growth stages [4]. In addition to the different effects of the HW periods, compared with the common HWs at a later time, the HWs affected the plants for a longer time in the year, and the medium- and long-term effects (i.e., the legacy effect of the HWs) would be coupled to the subsequent environment conditions, which had a more profound impact on vegetation [13]. Studies on HWs found that spring HWs were beneficial to alleviate the damage of summer drought to plants. The carbon budget was that the increased carbon absorption of spring HWs offset the decrease in carbon absorption caused by summer droughts, and the ecosystem still acted as a carbon sink in the drought year [3]. However, such a conclusion was controversial; if the spring HWs could offset part of the destructive effects of the summer drought and increase the carbon absorption of the ecosystem, it indicated that the spring HWs were beneficial to plant growth. But more plants also carried a higher consumption of soil water resources to the increasing of evapotranspiration, thereby magnifying the damage of the summer drought [14]. Moreover, the earlier HWs would increase carbon absorption, and such results were contrary to most previous conclusions that HWs led to a decline in carbon absorption. Previous studies proved that the long-term legacy of a heat wave one year after the occurrence reduced carbon absorption capacity by 38% [6]. Therefore, in this study, we simulated different HWs occurring at different times to verify and explore such contradictory conclusions and their potential mechanism.

Rs refers to all the metabolic processes that produce CO_2 in the undisturbed soil. It includes three biological processes: soil microbial respiration, root respiration, and soil animal respiration; and one non-biological process, which is the chemical oxidation of carbonaceous minerals: the contribution of this process to Rs was very small, usually negligible, of which roots and microorganisms had the greatest impact on Rs [15]. As the second-largest carbon flux, Rs was the most active part of the global carbon cycle. Very small changes in the frequency or severity of HWs might also greatly increase Rs, thereby reducing carbon sinks, and might have huge implications on global warming [16,17]. It was found that HWs on wetlands, when combined with drought, had almost no effect on Rs [18]. Against the background of frequent HWs caused by global warming, the increase in frequency of HWs (currently common summer HWs in the middle and late summer, and spring HWs in spring and early summer) would undoubtedly affect the changes in soil carbon pools. At present, the degree and mechanism of influence on Rs and its components (i.e., autotrophic respiration (Ra) and heterotrophic respiration (Rh)) are still unclear. A comparative study on the transition and sustained effects of spring and summer HWs in autotrophic and heterotrophic respiration is needed.

The Inner Mongolia grassland was an important part of the Eurasian grassland. The region has been affected by climate change and human activities for decades, which has caused great changes in land use patterns and vegetation coverage. These changes were bound to have a huge impact on the regional carbon cycle, and as an important driving process of climate change, they had an effect on the structure and function of the grassland ecosystem [6,19,20]. In the past 20 years, with the implementation of the national "returning

grazing to grass" project, the traditional free grazing was replaced by shed-raising and half-living livestock raising methods, and mowing became the most important way of using grassland and carrying out human activities in Inner Mongolia. In addition to its impact on the biological processes of grassland ecosystems, mowing had a particularly significant impact on vegetation structure and coverage patterns and might reduce the ability to cope with extreme climates. A study on the effects of HWs combined with mowing on the typical steppe ecosystem carried out in Inner Mongolia in 2012–2014 showed that HWs had a significant impact on reducing the stability of the ecosystem and the tolerance to climate change [21].

An in situ HW simulation experiment was conducted on a natural meadow grassland in Inner Mongolia, combined with a local human disturbance (mowing) to systematically study the occurrence of HWs in different periods (spring HWs, summer HWs) and the short-, medium-, and long-term effects of mowing and its interaction on Rs. The aims are (1) assess the impact of HWs (spring and summer HWs) on meadow grassland Rs and partitioning (Rh and Ra); (2) assess the effect of mowing on Rs and the interaction with HWs; (3) quantify the short-, medium-, and long-term effects of the advancement of HWs on Rs (i.e., instantaneous, post-mortem and residual effects). We hypothesized that spring HWs have a greater impact on meadow grassland Rs than summer HWs, and their effects are significantly different when combined with mowing.

2. Materials and Methods

2.1. Experimental Site

This research work was carried out in the experimental plot of the Hulunbuir National Research Station of the Chinese Academy of Agricultural Sciences (49°23′13″ N, 120°02′47″ E). It is the most concentrated and most representative of temperate meadow grasslands in China. The region belongs to a mid-temperate semi-arid continental climate, with an altitude of 627~635 m, an average annual temperature of 2.4 °C, an annual accumulated temperature of 1580~1800 °C, and a frost-free period of 110 days. The long-term average annual precipitation is around 380–400 mm, mostly in July to September. The vegetation type is a meadow grassland *Leymus chinensis* community. The subdominant species include *Stipa baicalensis*, *Thalictrum squarrosum*, *Carex duriuscula*, etc. The soil type is dark chestnut soil. The 0–10 cm soil pH value is 6.41 ± 0.36, soil organic carbon 3.39 ± 0.57 g kg^{-1}, total nitrogen 3.52 ± 0.55 g kg^{-1}, and total phosphorus 0.40 ± 0.14 g kg^{-1}. The daily maximum temperature data of the Hulunbuir League Hailar Meteorological Station in the past 40 years (1978–2017, data source: China Meteorological Data Network http://data.cma.cn/site/index.html, accessed on 10 January 2019) is used to determine the time of the HWs and occurrence intensity.

2.2. Experimental Design

The specific experimental design included two factors: HWs and mowing. HWs were divided into three levels: heat wave in advance of occurrence time (spring HWs), heat wave did not occur in advance (summer HWs), and no HWs. There were 2 levels: mowing and without mowing; in total, 6 treatments were included, namely, spring heat wave mowing (HWsp × M), summer heat wave mowing (HWsu × M), spring heat wave without mowing (HWsp), summer heat wave without mowing (HWsu), no heat wave mowing (M), and no heat wave and no mowing (Control). Each treatment was repeated 4 times, for a total of 24 plots. Each plot area was 2 m × 2 m with a buffer zone of 2 m between any two adjacent plots (Figure 1).

https://doi.org/10.3390/agronomy16030319

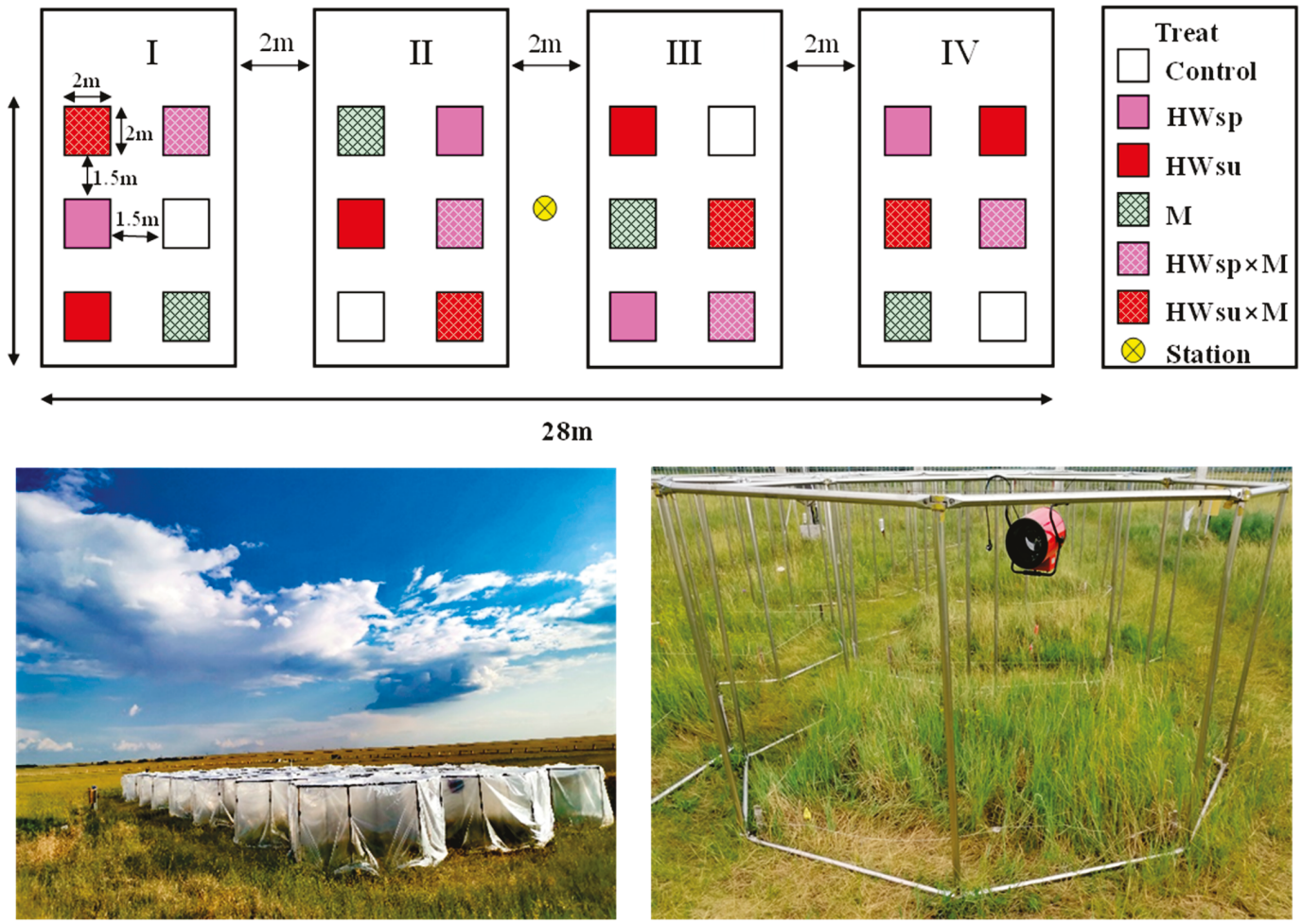


Figure 1. Field layout of interactive experiments on HWs with mowing and warming devices for HWs experiment (6 treatments, namely, spring heat wave mowing (HWsp × M), summer heat wave mowing (HWsu × M), spring heat wave without mowing (HWsp), summer heat wave without mowing (HWsu), no heat wave mowing (M), and no heat wave and no mowing (Control); each treatment was repeated 4 times).

2.3. HWs and Mowing Treatment

In order to simulate the HWs effect, that is, asymmetric day and night temperature increase, an OTC (open-top chamber) with a heater was set up to simulate the HWs event (Figure 1). The test box was composed of 24 hollow steel pipes, each with a 2 m diameter and a 1.5 m height [6]. During the experiment, it was covered with transparent plastic cloth and a heater was hung in the heating box to increase the temperature. The plastic cloth was made of highly transparent polyvinyl chloride (PVC) plastic cloth, with the film light transmittance > 90%. The air temperature could be raised to ~10 °C during the day and ~4 °C at night. The heating period was selected in fully sunny days [22]. After calculation (Table 1), the summer HWs experiment started from 10 to 14 August 2018, and the spring HWs experiment started from 8 to 13 July 2019, with continuous heating over five days, and the second summer HWs experiment started from 2 to 5 August of the same year.

A light lawn mower (Yard-man 160CC, USA) was used for mowing to simulate the local mowing or grazing treatment. The height of mowing stubble was 5~8 cm, which is commonly used in management. In 2018, the mowing process was carried out on 30 July. In 2019, the mowing process was carried out on 20 August.

Table 1. Statistics of 40-year heat waves in the Hailar steppe on the Mongolian Plateau from 1978 to 2017 (10-year interval).

	HWs (Time/10 yr)	Mean HWs Length (Day)	Max HWs Length (Day)	Times Per Month		
				June	July	August
1978–1987	4	8	10	2	2	-
1988–1997	6	6	9	1	4	1
1998–2007	15	7	10	3	8	4
2008–2017	15	7	12	6	5	4
Mean	10	7	10	3.0	4.8	2.3
Total	40			12	19	9

2.4. Rs, Ts and SWC Measurement

In order to distinguish between Ra and Rh, two Rs ring bases were arranged in the middle of each plot half a month in advance, for a total of 48 bases. The base was a polypropylene ring with a diameter of 10.5 cm. The heights of the two bases were 5 cm and 20 cm, and the ground was 3 cm. At the same time, the plants in the base were evenly mowed.

Measuring Rs used the LI-8100A soil carbon flux automatic measurement system (Li-Cor Inc., Lincoln, NE, USA). The temperature and humidity sensors (10 cm in length) were connected through the auxiliary sensor port on the LI-8100A soil carbon flux automatic measurement system. A LI-8100-102 soil breathing chamber with an inner diameter of 10.3 cm was buckled on the base to measure Rs. At the same time, the temperature and humidity sensor measured Ts and SWC. Rs, Ts and SWC were measured once before heating, each day during heating, and at 1, 2, 3, 4, 5, 6, 7, 8, and 15 days after heating, fixed at 9:00–11:00 in the morning or 2:00–4:00 in the afternoon.

2.5. Biomass Measurement (Above and Underground)

Before mowing in 2018 and 2019, we used a 0.5 m × 0.5 m sample box to sample in a clockwise order at the same site in each plot, separated the green leaves from the dead stand, dried them at 65 °C (more than 48 h) until constant, and weighed them to estimate the peak value of ANPP. After the end of the HWs experiment in 2018 and 2019, a root drill was used to collect the underground soil samples of each plot, divided into five layers (0–10 cm, 10–20 cm, 20–30 cm, 30–40 cm, 40–50 cm), and the roots were washed. After drying to constant weight, it was weighed to estimate the peak BNPP.

2.6. Statistical Analysis

We used SPSS 23.0 for statistical analysis (repeated-measures ANOVA, post hoc tests), and SigmaPlot 12.5 for drawing analysis. And we analyzed the correlations between Ts, SWC and Rs, Rh, Ra, and analyzed the correlations between ANPP, BNPP and Ra.

3. Results

3.1. Changes in HWs on Rs and Its Components

The differences in Rs, Rh and Ra between the six different treatments were significant ($p < 0.01$), showing that summer HWs increased Rs while spring HWs decreased Rs. During the summer HWs, the Rs of the mowed and non-mowed plots increased overall, and the Rs of the non-mowed plots increased by 1.07 μmol m^{-2} s^{-1} (11.71%) per day on average. The Rs of the mowed plots increased 2.15 μmol m^{-2} s^{-1} (23.81%), which was 1.03 times higher than that of non-mowed plots. During the spring HWs, the Rs of the mowed and non-mowed plots decreased, and the Rs of the non-mowed plots

https://doi.org/10.3390/agronomy16030319

decreased by 0.13 μmol m^{-2} s^{-1} (2.36%) on average. The Rs of the mowed plots decreased to 0.52 μmol m^{-2} s^{-1} (9.02%), which was 2.83 times that of the non-mowed plots.

HWs had different effects on the Ra of mowed and non-mowed plots, with the summer HWs increasing non-mowed Ra, while spring HWs decreased both mowed and non-mowed Ra. The first summer HWs reduced the Ra of the mowed and non-mowed plots, and the Ra of the non-mowed plots decreased by 0.75 μmol m^{-2} s^{-1} (16.03%) on average, but the Ra of the mowed plots increased by 0.59 μmol m^{-2} s^{-1} (16.48%). Different from the first summer HWs, the second summer HWs increased the Ra of the mowed and non-mowed plots, and the Ra of the non-mowed plot increased by 1.34 μmol m^{-2} s^{-1} (38.84%) on average, but the Ra of the mowed plot increased by 2.53 μmol m^{-2} s^{-1} (79.98%), which was an increase of 1.06 times compared with that of the non-mowed plot. The spring HWs reduced the Ra of the mowed and non-mowed plots. The Ra of the non-mowed plots decreased by 0.22 μmol m^{-2} s^{-1} (12.28%) on average, but the Ra of the mowed plots decreased by 0.50 μmol m^{-2} s^{-1} (23.87%), which was 0.94 times that of the non-mowed plots.

The first summer HWs increased while the second one decreased the Rh at both the mowed and non-mowed plots, while the spring HWs showed a convergent response to the mowed and non-mowed plots. The Rh of the non-mowed plots increased by 1.71 μmol m^{-2} s^{-1} (30.92%) on average, and the Rh of the mowed plots increased by 1.00 μmol m^{-2} s^{-1} (16.05%). On the contrary, the second summer HWs reduced the Rh at both the mowed and non-mowed plots. The Rh of the non-mowed plots decreased by 0.17 μmol m^{-2} s^{-1} (3.45%) on average, but the Rh of the mowed plots increased by 0.18 μmol m^{-2} s^{-1} (3.26%), and the result was completely different than that of the mowed plots. The spring HWs made the Rh of the mowed and non-mowed plots increase and decrease, and the Rh of the non-mowed plots increased by 0.09 μmol m^{-2} s^{-1} (2.20%) on average, but the Rh of the mowed plots only decreased 0.02 μmol m^{-2} s^{-1} (0.52%); the difference was not obvious (Figures 2 and 3).

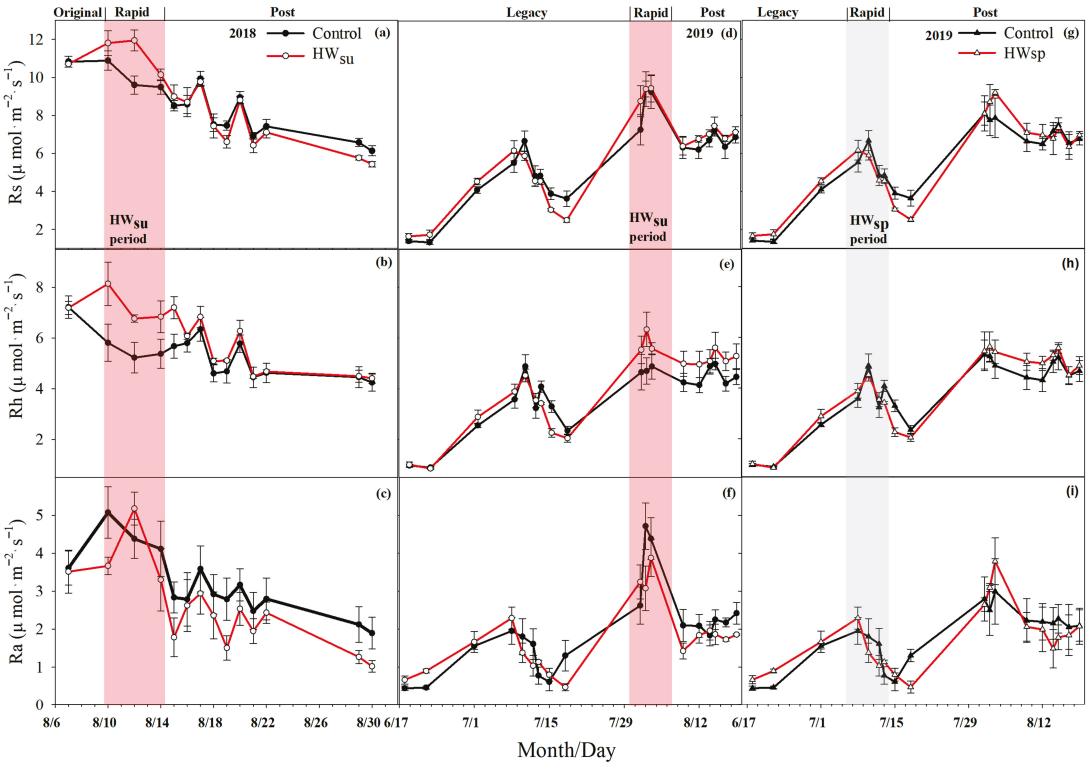


Figure 2. Changes in soil respiration (Rs), heterotrophic respiration (Rh) and autotrophic respiration (Ra) under different heat wave treatments (without mowing). (**a**–**c**), summer heat wave in 2018, (**d**–**f**), summer heat wave in 2019, (**g**–**i**), spring heat wave in 2019.

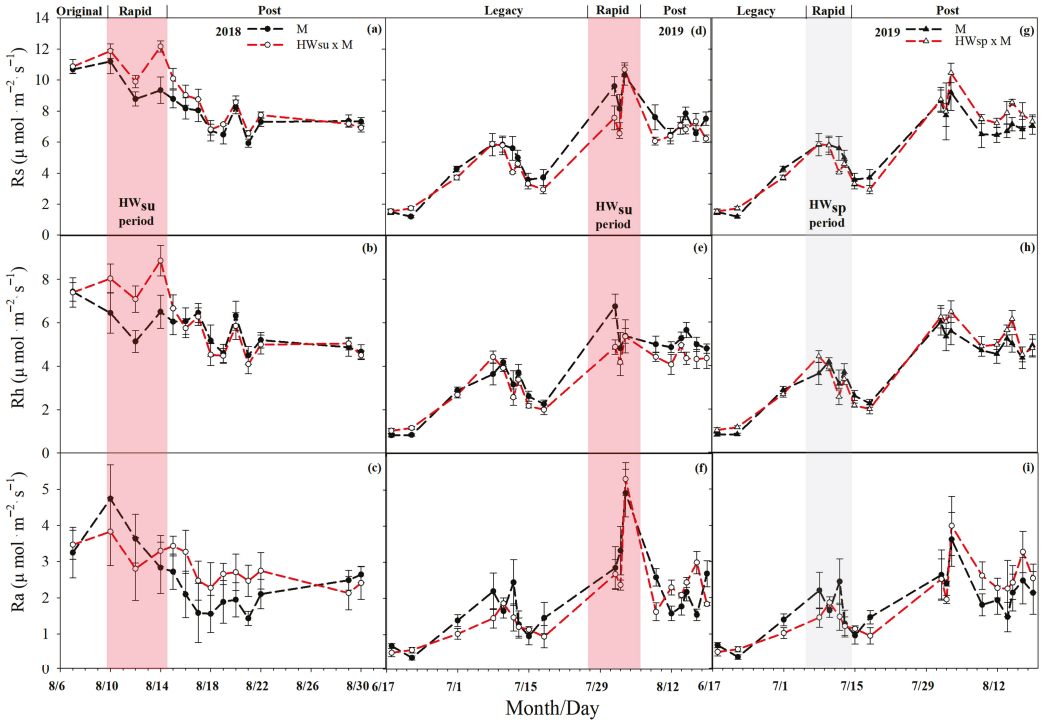


Figure 3. Changes in soil respiration (Rs), heterotrophic respiration (Rh) and autotrophic respiration (Ra) under different heat wave treatments (with mowing). (**a**–**c**), summer heat wave in 2018, (**d**–**f**), summer heat wave in 2019, (**g**–**i**), spring heat wave in 2019.

3.2. Rs Composition Changes Under Different HWs Treatment Conditions

During the heating period, the proportion of Rh in the mowed and non-mowed plots would increase with the extension of the heating time. Among them, the proportion of Rh in the mowed plots increased more significantly than that of the non-mowed plots; on the contrary, the proportion of Ra decreased with the extension of heating time in both the mowed and non-mowed plots, and the decrease in the mowed plots was more obvious; after a period of time, the proportions of Rh and Ra were basically stable. During the heating period, the proportion of Rh in the control plots were between 45% and 75%, the proportion of Rh in the M plots were between 55% and 70%, the proportion of Rh in the HWsp plots were between 60% and 80%, the proportion of Rh in the HWsp × M plots were between 60% and 75%, the proportion of Rh in the HWsu plots were between 55% and 70%, and the proportion of Rh in the HWsu × M plots were between 45% and 75% (Tables 2 and 3, Figures 4–6).

Table 2. The ratio and percentage of Ra and Rh in different treatments in 2019 (spring HWs).

Treatment	Control			M			HWsp			HWsp × M		
□	Rh/Rs	Ra/Rs	Rh/Ra	Rh/Rs	Ra/Rs	Rh/Ra	Rh/Rs	Ra/Rs	Rh/Ra	Rh/Rs	Ra/Rs	Rh/Ra
Before HWs SE	65.38 ± 1.51	34.62 ± 1.51	1.90 ± 0.13	63.9 ± 3.95	36.0 ± 3.95	1.86 ± 0.28	57.26 ± 3.67	42.74 ± 3.67	1.39 ± 0.19	68.92 ± 1.45	31.08 ± 1.45	2.24 ± 0.16
During HWs SE	68.13 ± 2.04	31.87 ± 2.04	2.18 ± 0.22	63.48 ± 3.65	36.52 ± 3.65	1.83 ± 0.30	72.27 ± 3.84	27.73 ± 3.84	2.79 ± 0.45	68.89 ± 2.79	31.11 ± 2.79	2.30 ± 0.32
After HWs SE	77.45 ± 0.10	22.55 ± 0.10	4.12 ± 0.04	69.46 ± 3.56	30.54 ± 3.56	2.40 ± 0.34	76.65 ± 1.85	23.35 ± 1.85	3.37 ± 0.38	69.08 ± 1.95	30.92 ± 1.95	2.28 ± 0.22

Table 3. The ratio and percentage of Ra and Rh in different treatments in 2018 and 2019 (summer HWs).

Treatment	Control			M			HWsu			HWsu × M		
□	Rh/Rs	Ra/Rs	Rh/Ra	Rh/Rs	Ra/Rs	Rh/Ra	Rh/Rs	Ra/Rs	Rh/Ra	Rh/Rs	Ra/Rs	Rh/Ra
Before HWs, 2018 SE	70.17 ± 4.08	29.83 ± 4.08	2.35 ± 0.34	84.75 ± 3.94	15.25 ± 3.94	5.56 ± 0.27	73.12 ± 5.77	26.88 ± 5.77	2.72 ± 0.48	73.63 ± 5.56	26.37 ± 5.56	2.10 ± 0.45
During HWs, 2018 SE	54.66 ± 2.07	45.34 ± 2.07	1.22 ± 0.09	64.07 ± 2.47	35.93 ± 2.47	1.84 ± 0.19	65.28 ± 3.07	34.72 ± 3.07	1.96 ± 0.23	62.65 ± 5.51	37.35 ± 5.51	1.90 ± 0.37
After HWs, 2018 SE	64.52 ± 1.27	35.48 ± 1.27	1.83 ± 0.10	73.47 ± 2.10	26.53 ± 2.10	2.87 ± 0.31	69.43 ± 3.68	30.57 ± 3.68	2.48 ± 0.45	67.37 ± 2.16	32.63 ± 2.16	2.12 ± 0.23
Before HWs, 2019 SE	66.63 ± 0.62	33.37 ± 0.62	2.00 ± 0.06	67.91 ± 0.84	32.09 ± 0.84	2.13 ± 0.08	72.65 ± 2.66	27.35 ± 2.66	2.80 ± 0.37	70.80 ± 0.24	29.20 ± 0.24	2.43 ± 0.03
During HWs, 2019 SE	54.79 ± 4.15	45.21 ± 4.15	1.27 ± 0.21	57.24 ± 1.77	42.76 ± 1.77	1.35 ± 0.09	61.69 ± 1.41	38.31 ± 1.41	1.62 ± 0.10	68.72 ± 3.41	31.28 ± 3.41	2.36 ± 0.37
After HWs, 2019 SE	68.32 ± 0.85	31.68 ± 0.85	2.16 ± 0.08	70.73 ± 2.11	29.27 ± 2.11	2.49 ± 0.27	72.89 ± 1.47	27.11 ± 1.47	2.74 ± 0.22	66.76 ± 2.35	33.24 ± 2.35	2.01 ± 0.17

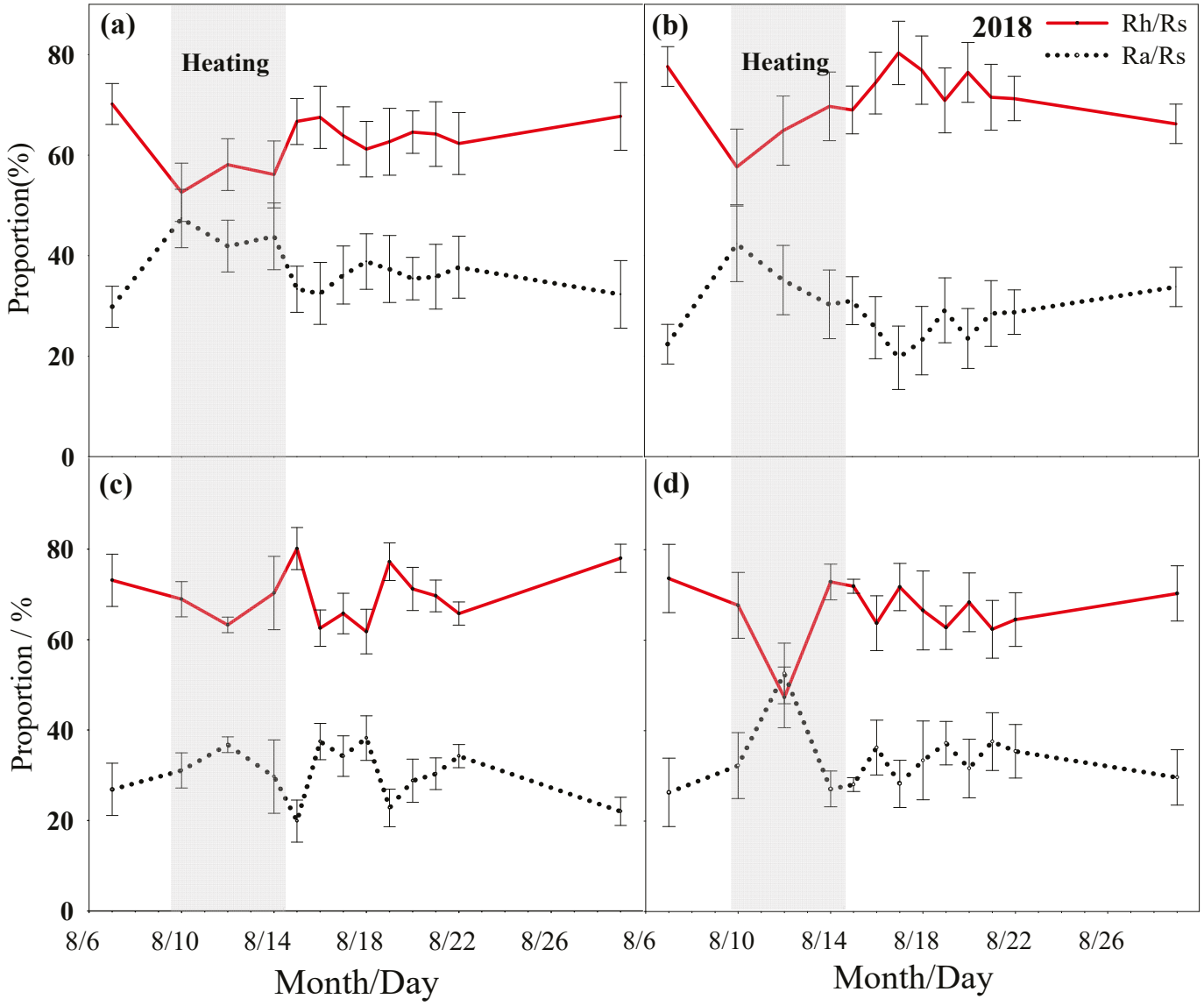


Figure 4. Rs ratio changes under different summer HWs treatment conditions in 2018 ((**a**) no heat wave no mowing, (**b**) no heat wave mowing, (**c**) summer heat wave without mowing, (**d**) summer heat wave mowing).

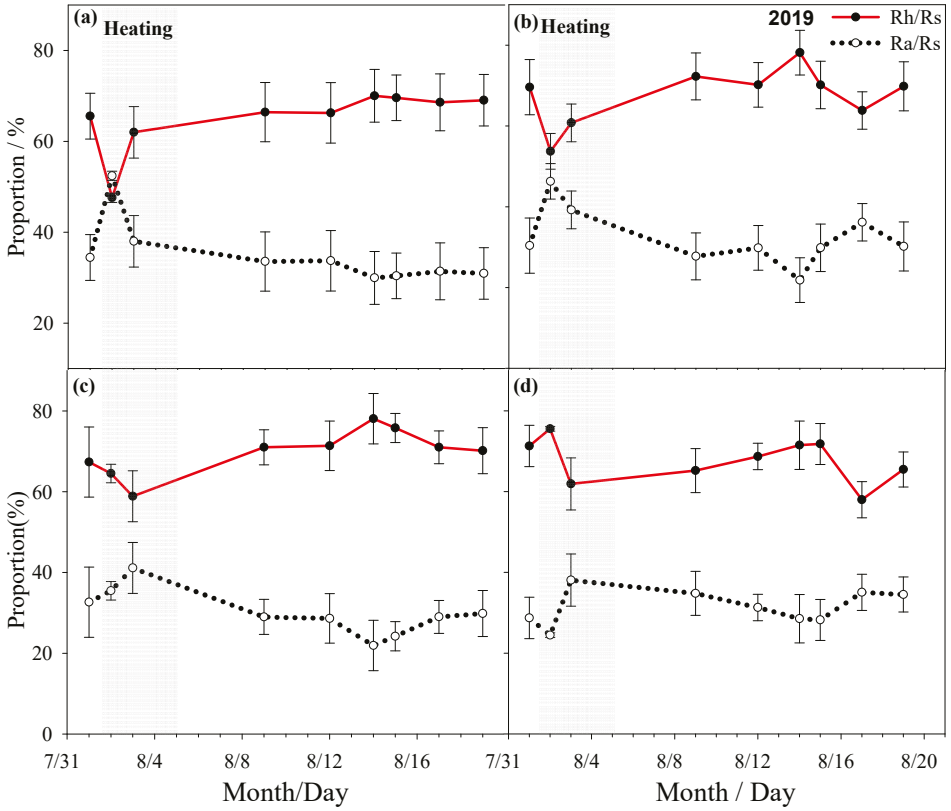


Figure 5. Rs ratio changes under different summer HWs treatment conditions in 2019 ((**a**) no heat wave no mowing, (**b**) no heat wave mowing, (**c**) summer heat wave without mowing, (**d**) summer heat wave mowing).

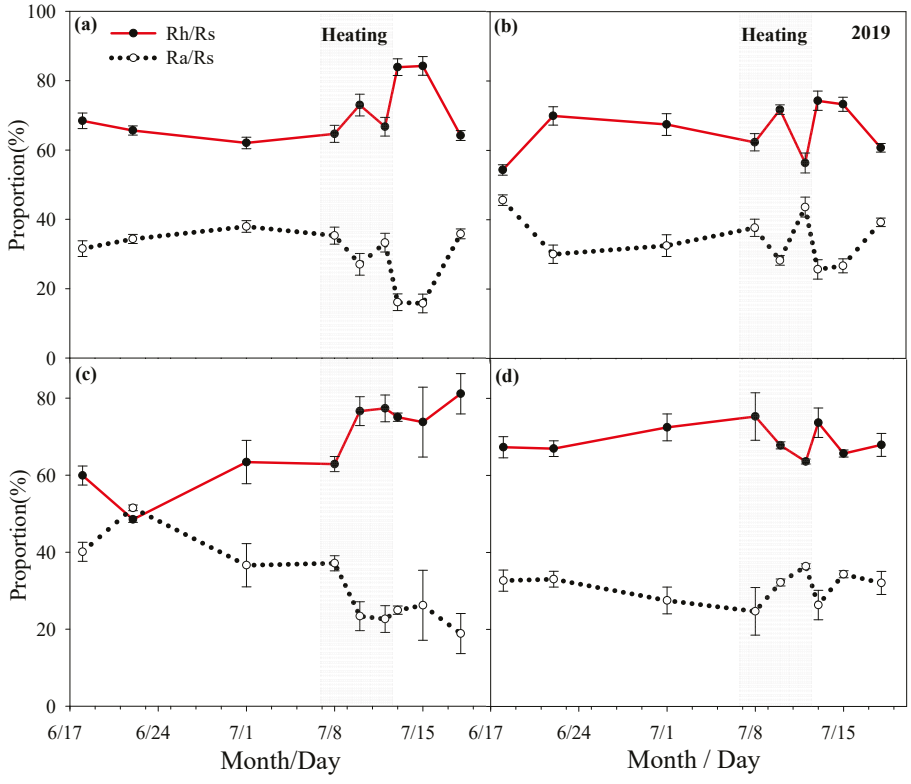


Figure 6. Rs ratio changes under different spring HWs treatment conditions in 2019 ((**a**) no heat wave no mowing, (**b**) no heat wave mowing, (**c**) spring heat wave without mowing, (**d**) spring heat wave mowing).

3.3. Correlation of Rs, Rh, Ra with Ts and SWC Under Different HWs Treatments

Under summer HWs conditions, the Rs, Rh and Ra of the different treatment plots all had a high correlation with Ts. Under the condition of spring HWs, the Rs, Rh and Ra of the different treatment plots all had a high correlation with SWC (Table 4).

Table 4. Correlation of Rs, Rh, Ra with Ts and SWC. ** indicates that the difference is significant at level $p < 0.01$; * at $p < 0.05$.

Rs	Related Index (R^2)		Rh	Related Index (R^2)		Ra	Related Index (R^2)	
	Ts	SWC		Ts	SWC		Ts	SWC
Control	0.487 *	0.228	Control	0.260	0.115	Control	0.556 **	0.267
M	0.613 **	0.215	M	0.422 *	0.109	M	0.559 **	0.237
HWsu	0.629 **	0.231	HWsu	0.575 **	0.173	HWsu	0.564 **	0.249
HWsu × M	0.771 **	0.252	HWsu × M	0.770 **	0.146	HWsu × M	0.526 **	0.408
HWsp	0.159	0.957 **	HWsp	0.308	0.909 **	HWsp	0.221	0.816 **
HWsp × M	0.305	0.820 **	HWsp × M	0.250	0.838 **	HWsp × M	0.420	0.692 *

3.4. Effects of Different Treatments of Biomass on Ra

Under the condition of spring HWs, the Ra of mowed plots had a high correlation with BNPP. Under the summer HWs condition, the Ra of the non-mowed plots had a high correlation with the ANPP and BNPP. The Ra of the mowed plots had a high correlation with the BNPP (Table 5).

Table 5. Correlation between ANPP or BNPP and Ra. ** indicates that the difference is significant at level $p < 0.01$; * at $p < 0.05$.

Ra	Related Index (R^2)					
Treatment Biomass	Control	M	HWsu	HWsu × M	HWsp	HWsp × M
ANPP	0.716 **	0.521	0.906 *	0.403	0.489	0.408
BNPP	0.918 *	0.795	0.995 **	0.822 *	0.698	0.989 **

4. Discussion

4.1. Response of Rs, Rh and Ra to HWs

The response of Rs, Rh and Ra to HWs was mainly because HWs could change Ts and SWC [18,23]. By studying the effects of HWs on Rs, we found that HWs could increase Ts but decrease SWC. Our results showed that in the meadow grasslands, summer HWs could promote Rs, Rh and Ra, which was especially obvious in mowed plots. On the contrary, spring HWs could inhibit Rs, Rh and Ra, which was especially obvious at mowed plots. Both were interesting phenomena.

The most similar experimental results showed that Rs increases with the increase in Ts, and the relationship between Rh and Ts satisfied an exponential regression relationship, and a linear regression relationship with SWC [24–26]. Although there was no related literature directly describing how HWs affect Rh, many studies found that increasing Ts could directly or indirectly affect Rh through the following three ways: (1) improving the soil microbial community structure and its metabolic activity, which could directly promote Rh; (2) by changing the SWC to regulate the effectiveness of the respiratory substrate and the chance of contact between the respiratory substrate and microorganisms, which indirectly affected Rh. SWC could also control the O_2 concentration and CO_2 diffusion process in the soil voids by affecting the aeration of the soil, which in turn could affect Rh; (3) the respiration of soil microorganisms required for the participation of soil enzymes,

while soil warming generally promoted soil enzyme activity. Therefore, under normal circumstances, increasing Ts would promote Rh [27–29].

For Ra, it was mainly the root respiration of plants. Direct measurement had some technical difficulties, and indirect measurement had uncertainties, but through a large number of previous experiments by some researchers, certain rules could also be found. An increase in Ts led to a decrease in SWC. Plants would allocate more carbon to the underground root system to obtain sufficient water and nutrients; therefore, the root respiration would increase significantly. In the case of unrestricted SWC, increasing Ts could also increase the nitrogen content in root tissues and increase root respiration by promoting nutrient mineralization and nitrogen diffusion. Plant root respiration was driven by above-ground photosynthetic products, and any factors that affect plant productivity could participate in the regulation of root respiration. For example, increasing Ts could affect plant productivity and the expansion of plant roots by changing the availability of soil nutrients and SWC, thereby affecting root respiration. Within a certain temperature range, increasing Ts could promote plant root metabolism, and root respiration increases exponentially with the increase in Ts. Combined with Figures 2 and 3, the results of this experiment could also be explained. At the beginning period of the HWs, compared with the middle and late periods of the HWs, the increase in Ts was smaller, while SWC decreased, perhaps because at this stage, HWs mainly evaporated the water in the soil, resulting in a smaller increase in Ts, and then Ra decreased. While in the middle period of the HWs, the increase in Ts was within the range suitable for plant root respiration, and both Ts and Ra increased together. In the latter HWs period, because both Ts and SWC increased, Ra therefore increased, with a reduction in the magnitude of the increase. At the end period of the HWs, Ra decreased. This might be because in the late HWs period, Ts was too high, which led to the death of some plant roots, and then a reduced Ra.

4.2. Response of Rs, Rh and Ra to Mowing

The response of Rs, Rh and Ra to mowing was mainly because mowing affected the degree to which HWs changed SWC and Ts, which in turn affected Rs, Rh and Ra. Combining Figures 2 and 3 and Table 4, we could find that summer HWs would promote Rs, Rh and Ra, and this was more obvious in mowed plots. While spring HWs would inhibit Rs, Rh and Ra, this was more obvious in mowed plots. It might be that Ts changed greatly due to mowing. During the summer HWs, both the air humidity and SWC were higher than those during the spring HWs. Ts was a key factor affecting Rs, Rh and Ra. During the spring HWs, because both SWC and air humidity were low, the key factor affecting Rs, Rh and Ra was SWC. Even if the Ts was high, Rs, Rh and Ra would not increase; in fact, they would decrease instead.

4.3. Influence of HWs on the Ratio of Rh and Ra

Because HWs had varying degrees of influence on Rh and Ra in meadow grasslands, it could affect the distribution ratio of Rs. In the study of Rs components in semi-arid grasslands, Rh contributed 51% to Rs, Ra contributed 49%, and the proportion of Rh was similar to that of Ra [30]. The results of this experiment showed that during the heating period, the proportion of Rh among treatments was varied. At the same time, the results of this experiment also showed that when SWC was low, the proportion of Ra would increase, becoming even higher than that of Rh. This indicated that the plants in this drier ecosystem were more tolerant of water stress, which was similar to that of plums. The analysis of our experimental data was consistent with others [30], in that overall HWs promote Rh more strongly than Ra.

https://doi.org/10.3390/agronomy16030319

4.4. ANPP and BNPP Response to Ra

Separating the Rs from Ra and Rh was very necessary for detecting the relationships between ANPP or BNPP and Rs. For example, one previous study found that there were no evident relations between ANPP and Rs because they did not separate Ra and Rh, due to most of the components of Rs on grasslands being derived from soil microorganisms and animals, which could interfere with the comparison of Ra and NPP. We analyzed the correlation between the separated Ra and NPP and found that under the condition of spring HWs, the Ra of mowed plots had a high correlation with BNPP ($p < 0.01$). Under the summer HWs conditions, the Ra of the non-mowed plots had a high correlation with the ANPP and BNPP ($p < 0.05$). The Ra of the mowed plots had a high correlation with the BNPP ($p < 0.05$) (Table 5).

Although the results obtained in this experiment could be explained, for some reasons, interference with the experiment was certain. For example, during the HWs experiment, each time Rs, Rh and Ra were measured, the highly transparent polyvinyl chloride (PVC) plastic sheet must be opened, and the loss of heat was more or less inevitable. Analyzing all the graphs drawn from the data obtained, it could be found from the trend and changes that HWs had a considerable influence on Rs, Rh and Ra. In July, August 2018 and August 2019, Hulunbuir's rainfall was relatively sufficient [15]. Therefore, Ts was the main limiting factor during summer HWs. In July 2019, the situation was the opposite. Because there was little rain and the soil was dry, SWC during the spring HWs was the limiting factor.

5. Conclusions

An in situ spring and summer HW simulation experiment, combined with a local human disturbance (mowing), was conducted to demonstrate the effects on soil respiration, autotrophic respiration and heterotrophic respiration in a natural Eurasian meadow steppe. The three kinds of respirations were inhibited by spring HWs, but promoted by summer HWs, mostly because of significantly increased heterotrophic respiration during summer HWs, but which were insignificant during spring HWs. Our results indicated that the changing of the HWs' occurring time would cause widely divergent influences on the same ecosystem. We also found that mowing would decrease the anti-interference ability of the ecosystem, which acted as an enhancer on both the positive and negative effects of HWs.

There were few experiments on the impact of HWs on Rs, Rh and Ra. According to the prediction results of climate models, future global climate change would bring more HWs, with HWs' time of occurrence and intensity changing further. In the future, HW simulation experiments need to focus on not only the HWs' occurring time but also on HW characteristics such as changing HW intensity and last-period impacts on the ecosystem's carbon cycle, providing quantitative supports on accurate model prediction and carbon budget assessment.

Author Contributions: Performed the experiments: Y.S., Q.T. and T.G.L.; Conceived and designed the experiments: Y.S., Q.T., C.S. and X.Z.; Analyzed the data: Y.S., Q.T. and X.Z.; Contributed reagents/materials/analysis tools: Y.S., Q.T. and X.Z.; Wrote the paper: Y.S., Q.T., T.G.L., C.S. and X.Z.; Proposal writing and funding: C.S. and X.Z. All authors have read and agreed to the published version of the manuscript.

Funding: This study was supported the National Key Research and Development Program of China (2024YFE0198604), the Natural Science Foundation of China (31870466), Special Foundation for National Science and Technology Basic Research Program of China (2019FY102000).

Data Availability Statement: Data for this manuscript was collected through field sampling and observation in the field/laboratory.

Acknowledgments: During the preparation of this manuscript/study, the authors used SPSS 23.0 and SigmaPlot 12.5 for the purposes of drawing analysis. The authors have reviewed and edited the output and take full responsibility for the content of this publication.

Conflicts of Interest: The authors declare no conflicts of interest.

Abbreviations

The following abbreviations are used in this manuscript:

ANPP	Above-ground net primary production
BNPP	Below-ground net primary production
Control	No heat waves no mowing
ER	Ecosystem respiration
GEP	Gross ecosystem productivity
HWs	Heat waves
HWsp	Spring heat waves without mowing
HWsp × M	Spring heat waves plus mowing
HWsu	Summer heat waves without mowing
HWsu × M	Summer heat waves plus mowing
M	Mowing
NEE	Net ecosystem exchange
OTC	Open-top chamber
PVC	Polyvinyl chloride
Ra	Autotrophic respiration
Rh	Heterotrophic respiration
Rs	Soil respiration
SWC	Soil water content
Ts	Soil temperature

References

1. De Boeck, H.J.; Bassin, S.; Verlinden, M.; Zeiter, M.; Hiltbrunner, E. Simulated heat waves affected alpine grassland only in combination with drought. *New Phytol.* **2016**, *209*, 531–541. [CrossRef] [PubMed]
2. Li, Z.; He, L.; Zhang, H.; Urrutia-Cordero, P.; Ekvall, M.K.; Hollander, J.; Hansson, L.-A. Climate warming and heat waves affect reproductive strategies and interactions between submerged macrophytes. *Glob. Change Biol.* **2017**, *23*, 108–116. [CrossRef] [PubMed]
3. Sippel, S.; Zscheischler, J.; Reichstein, M. Ecosystem impacts of climate extremes crucially depend on the timing. *Proc. Natl. Acad. Sci. USA* **2016**, *113*, 5768–5770. [CrossRef]
4. Cremonese, E.; Filippa, G.; Galvagno, M.; Siniscalco, C.; Oddi, L.; Morra di Cella, U.; Migliavacca, M. Heat wave hinders green wave: The impact of climate extreme on the phenology of a mountain grassland. *Agric. For. Meteorol.* **2017**, *247*, 320–330. [CrossRef]
5. Frank, D.; Reichstein, M.; Bahn, M.; Thonicke, K.; Frank, D.; Mahecha, M.D.; Smith, P.; Van der Velde, M.; Vicca, S.; Babst, F.; et al. Effects of climate extremes on the terrestrial carbon cycle: Concepts, processes and potential future impacts. *Glob. Change Biol.* **2015**, *21*, 2861. [CrossRef]
6. Qu, L.; Chen, J.; Dong, G.; Shao, C. Heavy mowing enhances the effects of heat waves on grassland carbon and water fluxes. *Sci. Total Environ.* **2018**, *627*, 561–570. [CrossRef]
7. Yu, Q.; Xu, C.; Wu, H.; Ke, Y.; Zuo, X.; Luo, W.; Ren, H.; Gu, Q.; Wang, H.; Ma, W. Contrasting drought sensitivity of Eurasian and North American grasslands. *Nature* **2025**, *639*, 114–118. [CrossRef] [PubMed]
8. Christidis, N.; Jones, G.S.; Stott, P.A. Dramatically increasing chance of extremely hot summers since the 2003 European heatwave. *Nat. Clim. Change* **2015**, *5*, 46–50. [CrossRef]
9. Susan, T. Carbon respired by terrestrial ecosystems—Recent progress and challenges. *Glob. Change Biol.* **2006**, *12*, 141–153.
10. Tatarinov, F.; Rotenberg, E.; Maseyk, K.; Ogee, J.; Klein, T.; Yakir, D. Resilience to seasonal heat wave episodes in a Mediterranean pine forest. *New Phytol.* **2016**, *210*, 485–496. [CrossRef]
11. Wan, S.; Hui, D.; Wallace, L.; Luo, Y. Direct and indirect effects of experimental warming on ecosystem carbon processes in a tallgrass prairie. *Glob. Biogeochem. Cycles* **2005**, *19*, GB2014. [CrossRef]

12. Jentsch, A.; Kreyling, J.; Beierkuhnlein, C. A new generation of climate-change experiments: Events, not trends. *Front. Ecol. Environ.* **2007**, *5*, 365–374. [CrossRef]
13. Legesse, T.; Dong, G.; Dong, X.; Qu, L.; Chen, B.; Daba, N.A.; Sorecha, E.M.; Zhu, W.; Lei, T.; Shao, C. The extreme wet and large precipitation size increase carbon uptake in Eurasian meadow steppes: Evidence from natural and manipulated precipitation experiments. *Environ. Res.* **2023**, *237*, 117029. [CrossRef]
14. Wolf, S.; Keenan, T.F.; Fisher, J.B.; Baldocchi, D.D.; Desai, A.R.; Richardson, A.D.; Scott, R.L.; Law, B.E.; Litvak, M.E.; Brunsell, N.A. Warm spring reduced carbon cycle impact of the 2012 US summer drought. *Proc. Natl. Acad. Sci. USA* **2016**, *113*, 5880–5885. [CrossRef]
15. Legesse, T.G.; Qu, L.; Dong, G.; Dong, X.; Ge, T.; Daba, N.A.; Tadesse, K.A.; Sorecha, E.M.; Tong, Q.; Yan, Y.; et al. Extreme wet precipitation and mowing stimulate soil respiration in the Eurasian meadow steppe. *Sci. Total Environ.* **2022**, *851*, 158130. [CrossRef] [PubMed]
16. Reichstein, M.; Bahn, M.; Ciais, P.; Frank, D.; Mahecha, M.D.; Seneviratne, S.I.; Zscheischler, J.; Beer, C.; Buchmann, N.; Frank, D.C.; et al. Climate extremes and the carbon cycle. *Nature* **2013**, *500*, 287–295. [CrossRef]
17. Ohlert, T.; Smith, M.D.; Collins, S.L.; Knapp, A.K.; Dukes, J.S.; Sala, O.; Wilkins, K.D.; Munson, S.M.; Anderson, M.I.; Avolio, M.L. Drought intensity and duration interact to magnify losses in primary productivity. *Science* **2025**, *390*, 284–289. [CrossRef]
18. Hoover, D.L.; Knapp, A.K.; Smith, M.D. The immediate and prolonged effects of climate extremes on soil respiration in a mesic grassland. *J. Geophys. Res. Biogeosciences* **2016**, *121*, 1034–1044. [CrossRef]
19. Shao, C.; Chen, J.; Li, L.; Zhang, L. Ecosystem responses to mowing manipulations in an arid Inner Mongolia steppe: An energy perspective. *J. Arid. Environ.* **2012**, *82*, 1–10. [CrossRef]
20. Zhang, X.; Zhang, K.; Zhang, K.; Shao, C.; Zhang, A.; Chen, Y.; Hou, L. Soil fertility assessment and spatial heterogeneity of the natural grasslands in the Tibetan Plateau using a novel index. *Agronomy* **2025**, *15*, 2743. [CrossRef]
21. Wu, J.; Xu, J.; Wang, L. The physiological response of anatomical structures and physiological indexes of two potentilla species to drought stress. *Acta Agrestia Sin.* **2015**, *23*, 125–129.
22. Wang, D.; Heckathorn, S.A.; Mainali, K.; Tripathee, R. Timing effects of heat-stress on plant ecophysiological characteristics and growth. *Front. Plant Sci.* **2016**, *7*, 1629. [CrossRef] [PubMed]
23. Bauweraerts, I.; Wertin, T.M.; Ameye, M.; McGuire, M.A.; Teskey, R.O.; Steppe, K. The effect of heat waves, elevated CO_2 and low soil water availability on northern red oak (*Quercus rubra* L.) seedlings. *Glob. Change Biol.* **2013**, *19*, 517–528. [CrossRef]
24. Li, Y.; Xu, M.; Zou, X. Heterotrophic Soil Respiration in Relation to Environmental Factors and Microbial Biomass in Two Wet Tropical Forests. *Plant Soil* **2006**, *281*, 193–201. [CrossRef]
25. Tucker, C.L.; Reed, S.C. Low soil moisture during hot periods drives apparent negative temperature sensitivity of soil respiration in a dryland ecosystem: A multi-model comparison. *Biogeochemistry* **2016**, *128*, 155–169. [CrossRef]
26. Wagle, P.; Kakani, V.G. Confounding Effects of Soil Moisture on the Relationship Between Ecosystem Respiration and Soil Temperature in Switchgrass. *BioEnergy Res.* **2014**, *7*, 789–798. [CrossRef]
27. Cable, J.M.; Ogle, K.; Lucas, R.W.; Huxman, T.E.; Loik, M.E.; Smith, S.D.; Tissue, D.T.; Ewers, B.E.; Pendall, E.; Welker, J.M.; et al. The temperature responses of soil respiration in deserts: A seven desert synthesis. *Biogeochemistry* **2010**, *103*, 71–90. [CrossRef]
28. Carbone, M.S.; Still, C.J.; Ambrose, A.R.; Dawson, T.E.; Williams, A.P.; Boot, C.M.; Schaeffer, S.M.; Schimel, J.P. Seasonal and episodic moisture controls on plant and microbial contributions to soil respiration. *Oecologia* **2011**, *167*, 265–278. [CrossRef]
29. Cusack, D.F.; Ashdown, D.; Dietterich, L.H.; Neupane, A.; Ciochina, M.; Turner, B.L. Seasonal changes in soil respiration linked to soil moisture and phosphorus availability along a tropical rainfall gradient. *Biogeochemistry* **2019**, *145*, 235–254. [CrossRef]
30. Li, W.; Chen, S.; Zhang, B.; Tan, X.; Wang, S.; You, C. Partitioning of soil respiration components and evaluating the mycorrhizal contribution to soil respiration in a semiarid grassland. *Chin. J. Plant Ecol.* **2018**, *042*, 850–862. [CrossRef]

Disclaimer/Publisher's Note: The statements, opinions and data contained in all publications are solely those of the individual author(s) and contributor(s) and not of MDPI and/or the editor(s). MDPI and/or the editor(s) disclaim responsibility for any injury to people or property resulting from any ideas, methods, instructions or products referred to in the content.

agronomy

MDPI

Article

The Role of Grassland Land Use in Enhancing Soil Resilience and Climate Adaptation in Periurban Landscapes

Igor Bogunovic [1,*], Marija Galic [1], Aleksandra Percin [1], Sun Geng [2] and Paulo Pereira [3]

[1] Department of General Agronomy, University of Zagreb Faculty of Agriculture, Svetošimunska cesta 25, 10000 Zagreb, Croatia; mcacic@agr.hr (M.G.); apercin@agr.hr (A.P.)
[2] China-Croatia "Belt and Road" Joint Laboratory on Biodiversity and Ecosystem Services, Chengdu Institute of Biology, Chinese Academy of Sciences, Chengdu 610213, China; sungeng@cib.ac.cn
[3] Environmental Management Laboratory, Mykolas Romeris University, LT-08303 Vilnius, Lithuania; pereiraub@gmail.com
* Correspondence: ibogunovic@agr.hr

Abstract: Urbanisation and land-use change are among the main pressures on soil health in periurban areas, but the multifunctionality of grassland soils is still not sufficiently recognised. In this study, the physical and chemical properties of soils under grassland, forest and croplands in the periurban area of Zagreb were investigated in a two-year period. Grasslands consistently exhibited multifunctional benefits, including high organic matter content (4.68% vs. 2.24% in cropland), improved bulk density (1.14 vs. 1.24 g cm^{-3}) and an active carbon cycle indicated by increased CO_2 emissions (up to 1403 kg ha^{-1} day^{-1} in 2021). Forest soils showed the highest aggregate stability (91.4%) and infiltration (0.0006 cm s^{-1}), while croplands showed signs of structural degradation with the highest bulk density and lowest water retention (39.9%). Temporal variation showed that grassland was particularly responsive to favourable climatic conditions, with soil porosity and water content improving yearly. Principal component analysis showed that soil structure, biological activity and moisture regulation were linked, with grassland plots favourably positioned along the axes of resilience. The absence of tillage and the presence of permanent vegetation cover contributed to their high capacity for climate and water regulation and carbon sequestration. These results emphasise the importance of protecting and managing grasslands as an important component of urban green areas. Practices such as mulching, minimal disturbance and continuous cover can maximise the ecosystem services of grassland soils. In addition, the results highlight the potential risk of trace metal accumulation in cropland and grassland soils located near urban and farming infrastructure, underlining the need for regular monitoring in periurban environments. Integrating grassland functions into urban planning and policy is essential for improving the sustainability and resilience of periurban landscapes.

Keywords: urban planning; climate resilience; soil ecosystem services; land-use management; InBestSoil

1. Introduction

Soils support ecosystems and provide essential services, including carbon sequestration, water filtration, and food production [1]. However, urbanisation and land-use change can significantly impact soil properties and ecosystem services, often leading to degradation, compaction and loss of fertility [2]. Understanding these dynamics is crucial to ensure sustainable soil management and mitigate the negative impacts of urban expansion.

Like many other fast-growing cities, the Croatian capital, Zagreb, faces major challenges due to increasing urban sprawl, which affects soil health and ecosystem stability. Converting agricultural land and natural habitats into residential and industrial areas impairs soil functions such as water retention, organic matter accumulation and erosion control. Grasslands and forests provide important ecosystem services, including climate and flood regulation [3]. Previous studies confirm that agricultural land has a significantly higher degree of compaction than land with natural vegetation in arid [4] and humid conditions [5]. In an urban environment, the comparison of land use confirms a similar compaction behaviour [6–8]. In addition, the resilience of forest and grassland soils to extreme precipitation events is enormous compared to bare soils, mainly due to frequent tillage and herbicide use [9]. Bare cultivated soils significantly reduce the organic carbon content, deteriorate soil structure and increase the susceptibility of cultivated land to water erosion [10].

In addition to the deterioration of the physical properties, the chemical properties of the soil also change considerably under anthropogenic influences. Various factors are responsible for the differences in soil chemical properties between land-use types in urban and periurban areas. Agricultural soils often receive a high nutrient input through fertilisation and pesticide use, which often leads to increased phosphorus and nitrogen levels, while at the same time, the organic carbon content of the soil decreases due to frequent tillage [11,12]. In contrast, forest soils typically accumulate organic matter via natural litterfall processes, maintaining a higher carbon-to-nitrogen ratio and a slightly more acidic state due to slower decomposition rates [13]. Grasslands often retain high levels of organic matter, which supports nutrient cycling, but this level fluctuates depending on the frequency of mowing and mulching. In addition, proximity to cities poses contamination risks. Heavy metals, such as Pb, Zn and Cu, are often more prevalent in urban soils due to traffic emissions, atmospheric deposition and wastewater use, and particularly affect croplands near industrial areas [14–16]. Soil compaction and sealing in urban areas further disrupt chemical gradients by limiting the input of organic matter and altering mineralisation processes [17]. Thus, soil chemical responses in urban and periurban contexts are land-use dependent and spatially heterogeneous, reflecting both natural ecosystem functions and the intensity of human-induced pressures. Sustainable land-use planning must take these considerations into account in order to improve urban resilience and environmental sustainability.

The main objective of this study is to evaluate and compare the soil physical, chemical, and biological properties under grassland, cropland, and forest land uses in the periurban area of Zagreb over a two-year period. Special attention is given to grassland systems due to their potential role in enhancing soil resilience and providing ecosystem services. The study does not aim to propose land-use conversions (e.g., grassland to cropland), but rather to assess how different land uses contribute to climate adaptation and soil multifunctionality in urban planning contexts. By examining these land types, the main trends will be identified. The resilience of the different land-use categories will be assessed, and their contribution to ecosystem services will be evaluated. The results will inform urban planning policy and enable strategies to maintain ecological balance while adapting to urban growth.

There are several challenges to soil health in Zagreb soils: overuse [18], low biodiversity [19], structural degradation [20], low soil quality [21], soil compaction [22], low soil organic matter content [7], abandonment of land [23], risk of flooding [24] and chemical contamination [25]. Heterogeneous land-use patterns and the lack of systematic soil condition monitoring across different land types exacerbate these challenges. With its diverse land uses and types, Zagreb significantly impacts soil, environment, and ecosystem services

due to land-use change. The choice of the city of Zagreb as a study area was motivated by the coexistence of native forests, agricultural land and urbanised zones in a compact spatial framework. This mosaic-like landscape provides a unique opportunity to compare land uses with different intensities of human intervention against a shared climate and topographic background.

However, despite the obvious pressure on soil resources, there is a lack of long-term data and integrated assessments comparing the resilience of different land uses, especially grassland, in urban and periurban areas. Deforestation and cultivation have rapidly expanded around Zagreb in recent decades, but the effects on the soil's physical, chemical and biological properties remain poorly understood. This study fills this gap by conducting a two-year comparison of soil conditions in forests, grasslands and croplands in eastern Zagreb. The novelty of this study lies in the systematic and temporal assessment of soil health indicators in a periurban context, with a particular focus on grassland, a land use often overlooked in climate adaptation and flood mitigation strategies.

2. Materials and Methods

2.1. Study Area, Environmental Conditions, and Soils

Zagreb is Croatia's historical capital, consisting of densely populated urban areas and surrounding periurban regions with mixed land use. Zagreb's geographic setting includes a combination of lowland and hilly terrain, with a temperate continental (Dfb) climate [26] that influences land-use dynamics. The mean annual (1961–2023) precipitation is 887 mm, with June (95 mm) and October (90.4 mm) as the most humid and January (50.9 mm) and February (46.4 mm) as the most arid part of the year. The mean annual (1961–2023) temperature is 11.7 °C, ranging from 0.6 °C (January) to 22 °C (July) [27]. The Zagreb metropolitan area has diverse conditions. Air temperature, precipitation, and potential evapotranspiration are higher in the city centre than in the suburban part of the city [28], indicating the urban heat island effect [29]. The study area is in Zagreb's eastern part (Figure 1) (45.8527778 N; 16.1797222 E, 118 m a.s.l.). Soils are dominantly composed of silty clay, Stagnosols, and Fluvisols [30]. General soil characteristics are presented in Table 1.

Table 1. Soil physical, chemical and mechanical properties on the upper horizon of studied land uses.

Soil Properties	Forest	Cropland	Grassland
Total organic C [g/kg]	28.5	13.8	22.7
pH in KCl [w w^{-1} 1:5]	4.43	7.35	8.30
EC [dS/m]	0.050	0.071	0.151
P_2O_5 [mg/kg]	45.2	41.8	45.4
Exchangeable K [mg/kg]	43.7	88.7	118.3
N_{total} [g/kg]	2.25	1.55	2.79
Bulk density [g/cm^3]	0.92	1.32	1.14
Sand [%]	9.5	5.8	16.2
Silt [%]	80.0	81.5	72.8
Clay [%]	10.5	12.8	11.0

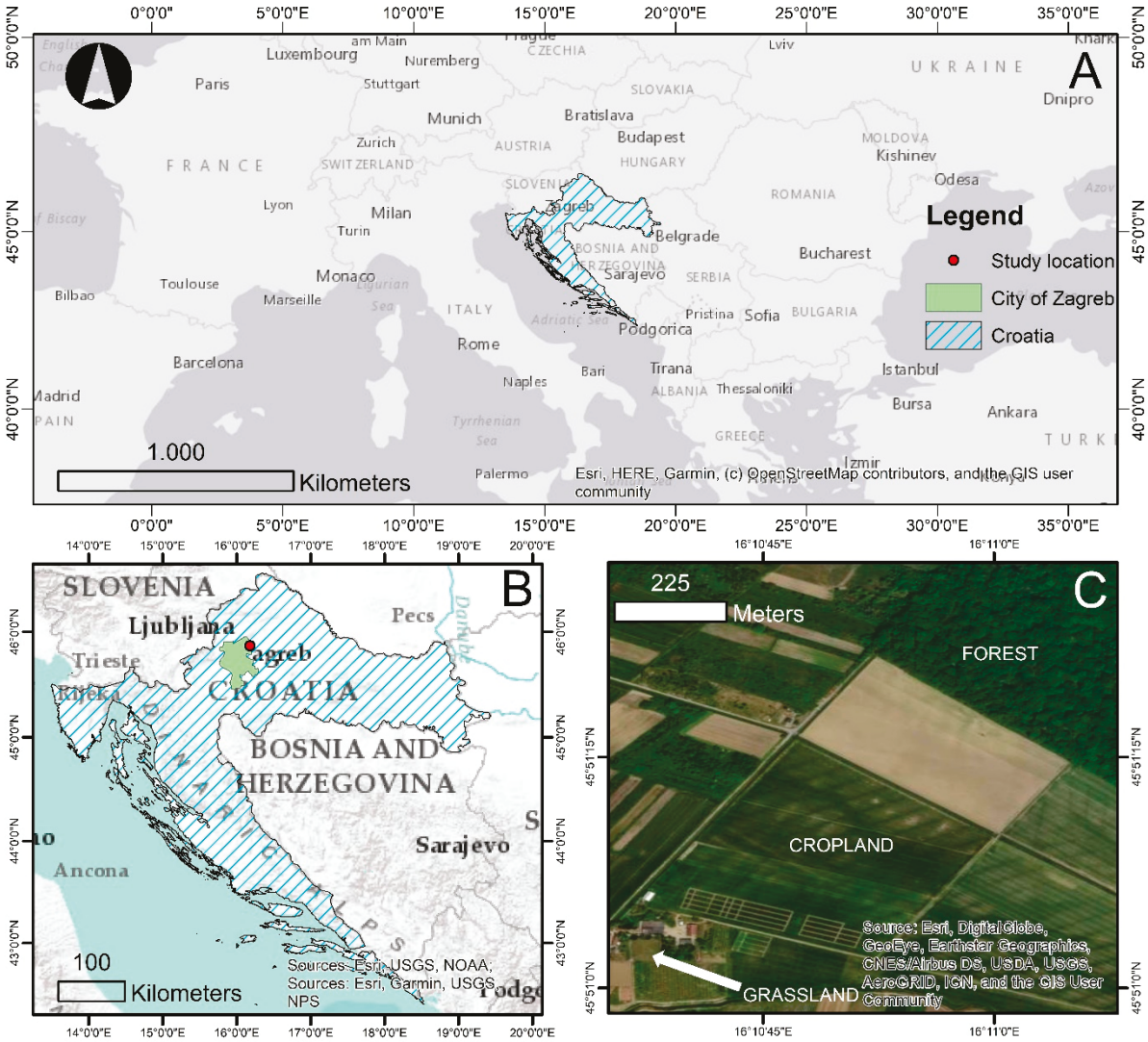


Figure 1. Study area: (**A**) location of Croatia in European comparison; (**B**) location of the study area (red dot) in the City of Zagreb; and (**C**) site photo of the study area.

2.2. Sampling Design and Laboratory Procedures

The study focuses on three primary land-use types: cropland, grassland, and forest, representing distinct ecological and management characteristics. The forest (native vegetation, dominated mainly by Quercus petraea and Robinia pseudoacacia) is >200 years old under the same land use. Sustainable management practices that permit high soil health in forest land use are the absence of soil disturbance and mineral fertilisation. At the same time, the natural decay of trees and leaves accumulates organic matter on topsoil. Grassland land use has been established since 1996, and grass–clover mixtures dominate. The annual management consists of mechanised mowing 3–4 times per year, while the mowed biomass remains as mulch and a source of nutrients. Sustainable management practices that permit high soil health in grassland land use are mulching, no soil disturbance, and permanent vegetation cover. Conversely, cropland land use is a nearby control area with low soil health, similarly conventionally managed since 2007. Management practices performed in croplands that lead to low soil health are conventional tillage (annual plowing followed by two disking and roto-harrowing before sowing), intensive mineral fertilisation, lack of organic fertilisation and the absence of cover cropping and mulching practices. The main crops grown on cropland are winter wheat, barley, oats, soybeans, and maize. Herbicides and insecticides are regularly used annually. The specific type and rate of mineral fertilisers

and herbicides applied varied depending on the crop in rotation and followed standard conventional practices typical for the region. As these inputs were not the focus of this study, they are not detailed further. All land-use types in this work are nearby and have similar topographic and geomorphological characteristics.

The sampling strategy consists of two time samples, in 2021 and 2023, to avoid possibly wrong conclusions from one-time observations, a common shortcoming in agricultural and environmental studies. Sampling points are randomly chosen in a straight direction and identified using a GPS.

Eight sampling points were selected in each land-use area (Figure 1), making 24 sampling points per measurement, for a total of 42. Water infiltration measurements were conducted near sampling points with a minidisc infiltrometer (Decagon Devices, Pullman, WA, USA). Undisturbed core samples were conducted at 0–10 soil depths using 100 cm^3 cylinders. Soil cores were wetted to measure water-holding capacity (WHC) and dried in an oven at 105 °C for 24 h to obtain the bulk density (BD) and soil water content (SWC) [31]. Near soil core sampling, undisturbed samples (8 per land-use class, 24 in total) were sampled by shovel at a 0–10 cm depth and stored in plastic boxes to preserve the aggregation. In current moisture conditions, aggregates were broken and gently manipulated by hand into small pieces before dry sieving [32]. At the same time, near sampling points, in situ measurements of soil CO_2 emissions and infiltration were carried out. Soil CO_2 emissions were measured on bare soil in a closed static chamber during 30 min of incubation using an infrared CO_2 detector (GasAlertMicro5 IR, BW Technologies Honeywell, Calgary, AB, Canada, 2011). Air temperature was measured with Testo 610 (Testo SE & Co KGaA, Lenzkirch, Germany, 2011) and air pressure with Testo 511 (Testo SE&Co KGaA, Lenzkirch, Germany, 2011). CO_2 emissions (kg ha^{-1} day^{-1}) were calculated according to Widén & Lindroth [33].

The percentage of water-stable aggregates (WSA) was determined using a wet sieving apparatus by soaking 4 g of aggregates (diameter 0.4–0.5 mm) in distilled water for 3 min [34]; sieving was continued until only the sand particles were left on the sieves after replacing cans with a dispersing solution (2 g NaOH/L). Afterwards, cans were dried at 105 °C and weighed, and the percentage of WSA was obtained with the following equation:

$$\mathrm{WSA} = \frac{Wds}{Wds + Wdw}, \quad (1)$$

WSA is the percentage of stable water aggregates, Wds is the weight of aggregates dispersed in dispersing solution (g), and Wdw is the weight of aggregates dispersed in distilled water (g). The remaining aggregate sizes were milled, sieved (2 mm mesh), and analysed to determine soil chemical properties, clay, silt, and sand content.

Soil particle size distribution was determined by the pipette method with wet sieving (sand fractions) and sedimentation (silt and clay fractions) after soil dispersion with sodium pyrophosphate. Soil pH was determined in a 1:5 soil–water suspension, using the electrometric method with a Beckman pH meter Φ72 in a 1 mol dm^{-3} KCl solution. Soil organic matter (SOM) concentration was measured using the oxidation of organic matter by a potassium dichromate–sulfuric acid mixture, followed by back titration of the excessive dichromate by ferrous ammonium sulphate solution [35]. Available phosphorus was determined using the ammonium-lactate extraction method, and exchangeable potassium was measured in the same extract by flame photometry. Finally, the Cr, Mn, Fe, Ni, Cu, and Zn contents were determined using a portable X-ray fluorescence (pXRF) spectrometer (VantaTM XRF analyser C Series) (Olympus, Waltham, MA, USA, 2019).

2.3. Statistical Analysis

Data normality and homogeneity of variances were assessed using the Shapiro–Wilk and Lilliefors tests ($p > 0.05$). Normality and homogeneity of variances were only observed in soil water content, bulk density, and infiltration data. The mean weight diameter dataset has normality requirements after the Box–Cox transformation. At the same time, the other variables did not follow the Gaussian distribution and homogeneity of variances, even after logarithm, square root, and Box–Cox transformations. A parametric two-way ANOVA was applied to the soil water content, bulk density, infiltration, and Box–Cox transformed mean weight diameter data to identify differences between sampling years and land-use treatments. A nonparametric Friedman ANOVA test was applied to observe differences between sample years in the other soil properties. The differences between land-use treatments were carried out using the nonparametric Kruskal–Wallis ANOVA test (K–W). If significant differences were observed at $p < 0.05$, Fisher's post hoc (for MWD Box–Cox, SWC, BD, and infiltration rate) and multiple comparisons rank tests were applied [36,37]. Principal component analysis (PCA) was performed, based on the correlation matrix, to identify the relationships among all soil properties. The Box–Cox transformed data were used for the PCA since it was the closest to normality when observing all datasets. All analyses were performed using Statistica 12.0 for Windows.

3. Results

3.1. Soil Physical Properties

Significant differences in physical soil properties were found between land-use types and sampling years (Table 2). In both years, the bulk density was significantly higher in croplands than in forests ($p < 0.05$), while grassland values were intermediate. In 2023, grassland BD decreased significantly compared to 2021. Soil water content (SWC) increased significantly in 2023 across croplands and grasslands compared to 2021. In 2021, cropland and forest had higher SWC than grassland ($p > 0.05$). In contrast, cropland and grassland had a significantly higher SWC than forest in 2023 ($p < 0.05$). Water-holding capacity was highest in forest and grassland soils. In 2021, the WHC in croplands was significantly lower ($p < 0.05$) than in forests. In 2023, grassland areas had a significantly higher WHC than croplands ($p < 0.05$).

Table 2. Land-use effect on soil physical properties during 2021 and 2023. Different letters indicate significant differences between sampling years (capital letters) and land use (lower-case letters). Kruskal–Wallis (K–W) tests are shown for each comparison between land uses and Friedman ANOVA between sampling years at water-stable aggregates (WSA), sand, silt, and clay content. Two-way ANOVA is shown for each land use-sampling year comparison at bulk density (BD), soil water content (SWC), water holding capacity (WHC), infiltration, and temperature.

Property	Year	Land Use	Mean		Med	Min	Max	S.D.	C.V.	SE
BD (g cm^{-3})	2021	Forest	1.164	b	1.137	1.028	1.337	0.112	9.6	0.040
		Cropland	1.245	a	1.242	1.077	1.398	0.096	7.7	0.034
		Grassland	1.236	abA	1.241	1.153	1.294	0.049	4.0	0.017
	2023	Forest	1.107	b	1.096	0.976	1.215	0.075	6.8	0.027
		Cropland	1.232	a	1.235	1.203	1.269	0.022	1.8	0.008
		Grassland	1.048	bB	1.055	0.918	1.125	0.069	6.6	0.024
SWC (%)	2021	Forest	36.1		35.6	28.2	44.4	5.97	16.5	2.11
		Cropland	36.7	B	37.7	23.9	45.0	6.26	17.1	2.21
		Grassland	30.5	B	29.7	13.3	46.1	11.72	38.5	4.14
	2023	Forest	39.1	b	36.7	30.6	54.8	7.84	20.1	2.77
		Cropland	49.0	aA	49.0	45.4	53.1	2.81	5.7	0.99
		Grassland	49.6	aA	50.9	39.0	55.3	5.06	10.2	1.79

Table 2. *Cont.*

Property	Year	Land Use	Mean		Med	Min	Max	S.D.	C.V.	SE
Temp. (°C)	2021	Forest	16.5	aB	16.4	16.2	17.5	0.41	2.5	0.14
		Cropland	14.5	abB	14.6	14.0	14.7	0.21	1.5	0.08
		Grassland	11.4	bB	11.4	11.2	11.5	0.11	1.0	0.04
	2023	Forest	23.3	bA	23.3	23.2	23.5	0.09	0.4	0.03
		Cropland	25.6	abA	25.6	24.4	26.8	0.94	3.7	0.33
		Grassland	27.9	aA	28.0	27.3	28.4	0.49	1.7	0.17
WHC (%)	2021	Forest	51.9	a	51.8	43.0	59.4	6.46	12.5	2.28
		Cropland	39.9	b	37.4	27.5	58.6	12.44	31.2	4.40
		Grassland	49.2	ab	51.2	39.0	55.6	5.85	11.9	2.07
	2023	Forest	51.7	ab	51.3	49.1	54.5	1.95	3.8	0.69
		Cropland	45.1	b	41.9	35.7	59.7	7.94	17.6	2.81
		Grassland	54.6	a	55.2	51.0	57.1	1.96	3.6	0.69
WSA (%)	2021	Forest	91.5	a	90.8	89.6	94.1	1.65	1.8	0.58
		Cropland	74.7	b	75.1	67.9	83.0	4.66	6.2	1.65
		Grassland	84.1	ab	83.2	79.3	91.1	4.29	5.1	1.52
	2023	Forest	91.2	a	91.0	88.2	94.3	1.82	2.0	0.64
		Cropland	81.0	b	81.1	72.5	88.6	4.44	5.5	1.57
		Grassland	81.3	b	81.3	63.9	90.5	8.81	10.8	3.11
Infiltration (cm/s)	2021	Forest	0.00062		0.00062	0.00044	0.00088	0.00013	21.8	0.00005
		Cropland	0.00050		0.00042	0.00034	0.00074	0.00016	32.5	0.00006
		Grassland	0.00061		0.00058	0.00029	0.00105	0.00029	47.4	0.00010
	2023	Forest	0.00057		0.00061	0.00040	0.00071	0.00011	20.0	0.00004
		Cropland	0.00067		0.00064	0.00057	0.00078	0.00008	12.1	0.00003
		Grassland	0.00056		0.00056	0.00036	0.00072	0.00012	20.6	0.00004
Sand (%)	2021	Forest	7.4	a	7.2	3.3	11.0	3.11	42.0	1.10
		Cropland	5.2	ab	3.9	2.7	10.0	3.10	59.7	1.10
		Grassland	3.8	b	3.6	2.9	4.9	0.80	21.2	0.28
	2023	Forest	7.5	a	7.2	3.5	11.2	3.09	41.1	1.09
		Cropland	5.2	ab	4.0	2.9	10.0	2.95	56.6	1.04
		Grassland	4.4	b	4.2	3.1	7.7	1.46	32.6	0.52
Silt (%)	2021	Forest	76.1		76.4	72.2	79.1	2.04	2.7	0.72
		Cropland	75.8		75.0	73.1	83.4	3.46	4.6	1.22
		Grassland	77.0		76.4	72.8	83.3	4.11	5.3	1.45
	2023	Forest	75.9		76.2	72.0	78.9	2.04	2.7	0.72
		Cropland	75.7		74.8	72.9	83.2	3.48	4.6	1.23
		Grassland	76.9		76.2	72.6	83.1	4.07	5.3	1.44
Clay (%)	2021	Forest	16.5		15.8	11.8	23.0	4.68	28.3	1.65
		Cropland	19.0		19.8	13.2	24.2	4.98	26.2	1.76
		Grassland	19.2		18.8	13.3	24.1	4.37	22.7	1.54
	2023	Forest	16.6		15.8	11.8	23.0	4.65	28.0	1.64
		Cropland	19.1		20.0	13.4	24.2	4.90	25.6	1.73
		Grassland	18.7		18.5	13.3	24.1	4.04	21.7	1.43

The WSA showed clear differences between the land uses (Table 2). Forest soils showed significantly higher WSA than cropland soils in both years ($p < 0.05$). A significant year effect was only observed for grassland, where WSA decreased in 2023 ($p < 0.05$). Infiltration rates did not show statistically significant differences among land-use types ($p > 0.05$) or between sampling years ($p > 0.05$), although slight trends indicated higher values for grassland and forests compared to croplands. Soil texture (sand, silt and clay content) showed no significant effect by year but showed slight differences between land uses. Grassland had a significantly higher sand content than croplands in both years

($p < 0.05$), while forest and cropland soils had a higher proportion of silt. Clay content did not differ significantly across land uses or years ($p > 0.05$).

3.2. Soil Chemical Properties

In 2021, CO_2 emissions were significantly higher on grassland than on cropland, while the forest had average values (Table 3). In 2023, emissions decreased in grassland and increased in forest and cropland, resulting in statistically higher CO_2 emissions than in forest and cropland land. The annual effect was significant for all land uses. Grassland had significantly higher emissions in 2021 than in 2023, while the opposite effect was observed for forest and cropland land use. Soil pH was significantly lower in forest soils than in cropland (in 2021) and grassland (in 2023) ($p < 0.05$). A significant decrease in pH was observed in forest soils in 2023 compared to 2021, while the pH of cropland and grassland soils was significantly higher in 2021 than in 2023. Soil organic matter content differed significantly between land uses in both years ($p < 0.05$). In 2021, forest soils had the highest SOM values, followed by grassland, while croplands had the lowest. In 2023, forest and grassland soils had a significantly higher SOM content than cropland soil.

Table 3. Land-use effect on soil chemical properties during 2021 and 2023. Different letters indicate significant differences between sampling years (capital letters) and land use (lower-case letters). Kruskal–Wallis (K–W) tests are shown for each comparison between land uses and Friedman ANOVA between sampling years at CO_2 emissions, pH, Cr, Fe, Ni, Cu, and Zn. Two-way ANOVA is shown for each land use-sampling year comparison at soil organic matter (SOM) and Mn.

Property	Year	Land Use	Mean		Med	Min	Max	S.D.	C.V.	SE
CO_2 (kg ha^{-1} day^{-1})	2021	Forest	66.8	abB	67.3	54.7	79.9	8.8	13.2	3.1
		Cropland	5.6	bB	5.5	4.2	8.4	1.4	26.0	0.5
		Grassland	1403.0	aA	1059.8	687.4	3492.3	940.1	67.0	332.4
	2023	Forest	122.0	bA	116.3	95.5	157.8	22.7	18.6	8.0
		Cropland	123.0	bA	116.3	70.6	232.6	47.9	38.9	16.9
		Grassland	200.9	aB	199.3	149.5	249.2	38.7	19.3	13.7
pH	2021	Forest	4.43	bA	4.04	3.69	7.45	1.25	28.2	0.44
		Cropland	7.36	aA	7.30	7.16	7.75	0.20	2.7	0.07
		Grassland	7.25	abB	7.71	3.93	7.86	1.35	18.6	0.48
	2023	Forest	3.66	bB	3.60	3.40	4.15	0.23	6.2	0.08
		Cropland	7.06	abB	7.08	6.86	7.27	0.12	1.7	0.04
		Grassland	7.36	aA	7.37	7.18	7.45	0.08	1.1	0.03
SOM (%)	2021	Forest	7.97	a	5.78	2.78	17.66	4.82	60.5	1.70
		Cropland	2.15	c	2.18	1.41	2.69	0.44	20.5	0.16
		Grassland	4.76	b	4.49	3.78	6.89	0.93	19.5	0.33
	2023	Forest	6.63	a	5.53	4.32	13.31	2.97	44.8	1.05
		Cropland	2.33	b	2.29	1.95	2.75	0.28	12.2	0.10
		Grassland	4.59	a	4.63	2.98	6.10	0.91	19.9	0.32
Cr (mg/kg)	2021	Forest	110	b	96	85	195	36	32.8	12.80
		Cropland	197	a	197	184	211	9	4.4	3.07
		Grassland	180	abB	184	128	201	23	12.9	8.16
	2023	Forest	103	b	104	70	125	19	18.3	6.65
		Cropland	203	b	198	189	228	14	6.9	4.96
		Grassland	205	aA	205	180	223	17	8.1	5.84

Table 3. *Cont.*

Property	Year	Land Use	Mean		Med	Min	Max	S.D.	C.V.	SE
Mn (mg/kg)	2021	Forest	531	b	563	256	663	141.1	26.6	49.9
		Cropland	617	b	618	545	704	50.9	8.3	18.0
		Grassland	682	a	740	360	793	139.9	20.5	49.5
	2023	Forest	536	b	553	382	684	109.1	20.4	38.6
		Cropland	677	a	683	647	701	20.8	3.1	7.3
		Grassland	686	a	681	620	748	45.7	6.7	16.2
Fe (mg/kg)	2021	Forest	30,362	b	29,589	27,986	38,176	3302	10.9	1168
		Cropland	40,216	aA	40,149	39,588	41,147	545	1.4	193
		Grassland	37,167	ab	37,826	29,419	39,884	3278	8.8	1159
	2023	Forest	29,217	b	29,833	25,490	30,953	1854	6.3	655
		Cropland	39,282	aB	39,022	38,595	40,161	601	1.5	213
		Grassland	37,775	ab	37,515	36,443	40,027	1070	2.8	378
Ni (mg/kg)	2021	Forest	41.0	b	32.0	21.0	109.0	28.0	68.4	9.9
		Cropland	102.3	a	103.5	95.0	105.0	3.3	3.2	1.2
		Grassland	97.3	ab	106.0	27.0	120.0	29.1	29.9	10.3
	2023	Forest	30.8	b	31.5	26.0	36.0	4.0	12.9	1.4
		Cropland	106.0	a	108.0	94.0	113.0	6.3	5.9	2.2
		Grassland	108.3	a	108.5	100.0	117.0	6.0	5.6	2.1
Cu (mg/kg)	2021	Forest	19.1	b	16.5	15.0	36.0	6.9	36.2	2.5
		Cropland	31.8	ab	32.0	27.0	35.0	2.5	7.9	0.9
		Grassland	34.0	a	37.5	15.0	40.0	8.3	24.5	2.9
	2023	Forest	16.3	b	17.0	12.0	19.0	2.4	14.6	0.8
		Cropland	30.4	a	29.5	28.0	34.0	2.3	7.7	0.8
		Grassland	35.3	a	36.5	29.0	40.0	4.0	11.4	1.4
Zn (mg/kg)	2021	Forest	75.1	b	73.1	67.0	95.0	9.1	12.2	3.2
		Cropland	97.3	a	97.0	88.0	105.0	4.9	5.0	1.7
		Grassland	90.3	abB	91.5	74.0	96.0	7.0	7.7	2.5
	2023	Forest	71.0	b	70.5	66.0	77.0	3.5	5.0	1.3
		Cropland	96.1	a	96.5	91.0	102.0	3.3	3.4	1.2
		Grassland	95.6	aA	96.0	88.0	101.0	4.0	4.1	1.4

All trace elements (Table 3) showed lower values in forest soils than in grassland and cropland soils. In 2021, cropland soils had significantly higher Cr concentrations than forest soils, while in 2023, the Cr concentrations in grassland soils were significantly higher than in cropland and forest soils. Temporal changes occur in grassland, where significantly higher Cr concentrations were found in 2023 than in 2021. In 2021, Mn concentrations were significantly higher in grassland, while in 2023, they were significantly lower in forest soils than in other land-use types. Fe concentrations were significantly lower in forest soils than in grassland and croplands in both years. A significant temporal decrease in Fe concentrations was observed in cropland soils. The Ni and Zn concentrations in the soil follow a similar trend. In 2021, significantly higher concentrations were measured in croplands than in forest soils, while grassland soils were in between. In 2023, forests had significantly lower Ni and Zn concentrations than grassland and croplands. In grassland soils, Zn concentrations were significantly higher in 2023 than in 2021. In addition, soil Cu concentrations were significantly lower in forest soils than in grassland soils in 2021. In 2023, soil Cu concentrations were significantly higher in cropland and grassland soils than in forest soils.

3.3. Principal Component Analysis

Factor 1 explained 40.16% of all variance, and Factors 2, 3, 4 and 5 explained 13.70%, 12.10%, 9.89% and 5.71%, respectively. Factor 1 had high positive loadings in soil pH, Cr, Mn, Fe, Ni, Cu, and Zn concentrations and high negative loadings in WSA and SOM (Table 4). Factor 2 had high positive loadings in WHC and soil temperature and high negative loadings in BD. Factor 3 had positive loading in clay and negative in silt and sand content, while factor 4 had positive loading in CO_2 emissions and negative in SWC. Factor 5 was mainly defined by infiltration rate (negative loading), representing a hydrological property gradient.

Table 4. Principal component analysis results. In bold, the eigenvalues are retained in each factor.

Property	Factor 1	Factor 2	Factor 3	Factor 4	Factor 5
Water holding capacity (%)	−0.23	**0.57**	0.41	0.17	0.29
Soil water content (%)	0.27	0.49	0.35	**−0.50**	−0.10
Bulk density (g cm^{-3})	0.27	**−0.73**	−0.25	0.14	−0.21
Water stable aggregates (%)	**−0.74**	0.18	0.10	0.21	−0.08
Infiltration rate (cm/s)	−0.16	0.11	0.19	0.06	**−0.86**
Temperature (°C)	−0.01	**0.56**	0.40	−0.55	−0.13
CO_2 (kg ha^{-1} day^{-1})	−0.06	0.36	0.19	**0.73**	−0.24
pH	**0.95**	0.11	−0.12	0.17	0.05
Soil organic matter (%)	**−0.66**	0.29	0.16	0.47	0.18
Cr (mg/kg)	**0.94**	0.15	0.05	−0.09	0.00
Mn (mg/kg)	**0.65**	0.34	−0.19	0.40	−0.13
Fe (mg/kg)	**0.95**	−0.09	−0.07	−0.10	−0.06
Ni (mg/kg)	**0.96**	0.19	−0.01	0.08	0.02
Cu (mg/kg)	**0.89**	0.20	0.00	0.25	0.07
Zn (mg/kg)	**0.94**	0.06	0.09	−0.05	0.02
Sand (%)	−0.49	0.24	**−0.54**	−0.25	−0.09
Silt (%)	0.01	0.53	**−0.73**	0.05	0.03
Clay (%)	0.25	−0.47	**0.81**	0.14	0.06

4. Discussion

4.1. Soil Properties

This study highlights the significant influence of land-use type and temporal variation on soil's physical and chemical properties in an urban environment. The results show that land-use decisions directly impact soil structure, water regulation and carbon cycling, all of which are important ecosystem services.

Bulk density was consistently higher on cropland, confirming the long-term compacting effect of conventional tillage and machine passes [4]. When ploughed regularly over the years, BD tends to increase, which was demonstrated in clay loam [38], silty clay loam [21], and silty [39] and sandy [40] soils. In addition, conventional farming methods usually involve frequent machine passes. In conventional cultivation of cereals or root crops alone, every centimetre of soil is worked 3 to 8 times with wheels [41]. The reduction in BD observed in grassland in 2023 suggests that the structure of such systems can recover over time without tillage. Similar results were reported by Franzluebbers et al. [42] and Six et al. [43]. Furthermore, these results support the protective role of herbaceous vegetation in maintaining soil porosity and infiltration.

Soil water content and WHC showed effects on land use and time course. In 2023, there was a significant increase in SWC on grassland and cropland, likely influenced by seasonal weather patterns, including higher precipitation and lower evapotranspiration. In contrast, the SWC of forest soils remained relatively stable or slightly decreased. This reduction

can be attributed to increased water uptake by the root systems of mature trees, which have a deeper and more extensive root profile than grasses or crops. Tree roots can extract water from deeper soil layers and deplete the upper soil water table, especially during the growing season. A similar trend was noted by Wang et al. [44], who observed that dense forest vegetation significantly impairs soil water dynamics through high transpiration rates and interception losses, resulting in lower near-surface soil moisture despite a higher total storage potential. In addition, Evrendilek et al. [45] found that greater biomass and a denser canopy in forest ecosystems can increase evapotranspiration, decreasing surface SWC even when deeper layers retain substantial moisture. This phenomenon emphasises the dual role of forests in water storage and the active water cycle in vegetation.

In contrast, permanent herbaceous cover in grasslands has likely enhanced infiltration and near-surface moisture retention, as Gajić [46] and Ajayi et al. [47] confirmed. These systems benefit from high porosity and dense root networks in the topsoil, which improve soil structure and facilitate water infiltration and retention. Consequently, the grasslands in our study showed an improved WHC in 2023, suggesting that extensively managed grasslands can act as a buffer against climate variability and support a stable hydrological function. Forest soils exhibited consistent WHC in both years, likely due to their stable structure, deeper root activity and higher SOM, which buffers water availability over time. A significantly higher WSA characterises forest soils as evidence of superior structural stability. This is consistent with previous findings that minimal disturbance and continuous organic inputs from litterfall promote aggregate formation and reduce susceptibility to erosion and compaction [45,48]. The high WSA values indicate a strong resistance to degradation under forest cover. In contrast, croplands showed the poorest structural integrity due to intensive tillage and lack of organic inputs [49,50]. Despite little disturbance, the decline in WSA in grasslands between 2021 and 2023 could be due to environmental stress or insufficient biomass return, warranting further monitoring.

Interestingly, infiltration rates did not show statistically significant differences between land uses, possibly due to the high variability within each land-use type. However, the observed trends support the notion that grassland and forest soils are more permeable than cropland, consistent with previous studies [5,8,47]. Soil organic matter content was significantly higher in forest and grassland soils than in cropland, highlighting the detrimental effects of intensive agriculture on carbon stocks [11]. Over-oxidation of ploughed soils increased inter- and intra-aggregate deterioration and loss of SOM [4]. The decline in SOM in forest soils between 2021 and 2023 is unexpected and likely related to environmental conditions or reduced litter input, emphasising the importance of long-term monitoring. Stable SOM concentrations in grasslands indicate high resilience and the potential for long-term carbon sequestration, especially under current mulch management.

CO_2 emissions were highest in grassland in 2021 due to increased microbial activity and carbon turnover in high organic input systems [12]. The decline in emissions in 2023 could be due to temperature, humidity, or substrate availability changes. The increasing emissions in forest and cropland soils in 2023 indicate increased microbial respiration under favourable conditions. However, despite this temporary increase, CO_2 emissions from cropland soils remained relatively low overall, likely a consequence of long-term intensive tillage, reduced organic matter input and microbial depletion. Continuous plowing accelerates the depletion of labile carbon pools at the beginning of land use, leading to a progressive decline in soil organic carbon and microbial biomass over time [43,51]. Without a regular supply of crop residues, manure or cover crops, the microbial community becomes carbon limited, reducing soil respiration [52]. In addition, the deteriorated soil structure caused by tillage restricts gas diffusion and microbial habitat, further limiting microbial activity [53].

The acidic pH observed in forest soils is a typical feature of ecosystems with high organic matter input, slow decomposition and limited base cation cycling [13]. In such systems, organic acids released during litter decomposition, combined with minimal disturbance, lead to gradual acidification. In addition, tree roots preferentially take up basic cations (e.g., Ca^{2+}, Mg^{2+}) and leave hydrogen (H^{+}) and aluminium ions (Al^{3+}) in the soil solution, which further contributes to pH reduction [54,55]. In contrast, cropland soils showed near-neutral pH values. Although nitrogen fertilisation, especially with ammonium-containing fertilisers, such as urea or ammonium sulfate, is known to acidify soils [56], regular liming and tillage can mitigate these effects. Farmers in the region occasionally apply lime ($CaCO_3$) to correct acidification, which may explain the current pH balance despite decades of synthetic fertilisation and the absence of organic amendments or cover crops. Grassland soils, on the other hand, showed an alkaline pH, which gives a more differentiated picture. One explanation could lie in the mulch residues on the soil surface. Decomposing mulch can increase the pH of the soil depending on its composition, especially if the residues come from species with a high content of base cations (e.g., Ca^{2+}, K^{+}, Mg^{2+}). Studies have shown that organic mulches and crop residues can temporarily increase soil pH by releasing base cations and buffering hydrogen ions during decomposition [57,58]. Furthermore, the grassland soils in this study were not acidified by fertiliser inputs, which could explain their higher initial pH. Interestingly, a decline in pH in forest soils between 2021 and 2023 could be due to increased decomposition rates, increased acid leaching due to higher precipitation or root activity, or decreased buffering capacity due to changes in the quality of litter input. Such changes underline the dynamic nature of forest soil chemistry and the importance of long-term monitoring.

Trace element concentrations (e.g., Cr, Ni, Cu, Zn) were higher in arable and grassland soils than in forest soils. Although these patterns are still within permissible environmental limits, they probably reflect a combination of anthropogenic influences. The spatial arrangement of land-use types, in particular, supports this interpretation. Both croplands and grassland are located close to the farm's access road and operational infrastructure, with the grassland only 20 m away from mechanisation zones, agrochemical storage areas and an intensively managed orchard (Figure 1). The arable land is also relatively close (within 100 m) to the farm and equipment zones. In contrast, the forest floor, which is located at a greater distance from anthropogenic sources, showed the lowest trace element levels. This spatial gradient suggests that localised sources of contamination, such as mechanical equipment, liquid spills, fertilizer-handling areas, and road dust, likely contribute to the elevated metal concentrations in grassland and cropland soils. Atmospheric deposition of particulate-bound metals (especially Zn and Cu from tyres and brake abrasion and Cr/Ni from fuel and machinery combustion) is a known phenomenon in soils adjacent to agricultural land [59,60]. In addition, the intensive and long-term use of phosphate-based fertilisers on croplands is another key factor, as these fertilisers often contain trace concentrations of heavy metals, such as Cd, Cr and Zn, as contaminants [61,62]. The proximity of grassland to orchards and farms could explain the comparatively high Cu concentrations. Cu-based fungicides are often used in fruit cultivation and can remain in the surrounding soils through drift or runoff [63]. These results underline the susceptibility of urban soils and soils adjacent to farms to diffuse contamination, even with low-use or near-natural land-use forms such as grassland. Therefore, they underline the need to regularly monitor trace elements on croplands and adjacent uncultivated land exposed to indirect agricultural activities.

4.2. Relation Among Soil Properties

The principal component analysis helped to clarify the underlying structure and relationships between the measured soil properties. Factor 1 showed a strong association between elevated soil pH and trace element concentrations (Cr, Mn, Fe, Ni, Cu, Zn) and a significant negative reduction in SOM and WSA. Although alkaline conditions generally reduce the solubility of trace metals, the co-occurrence observed here reflects common anthropogenic influences. Both grassland and cropland, especially near agrochemical storage areas, access roads, and intensively managed orchards, showed higher pH values due to liming or base-rich organic residues and also received long-term inputs of trace metals via fertilisers, pesticides, and atmospheric deposition [15,63]. At the same time, low SOM content has been associated with higher metal concentrations, supporting the idea that lower organic input and microbial activity limit the soil's ability to complex and immobilise trace metals [64,65]. In soils with lower SOM, metals remain in more available or weakly bound forms, which increases their environmental risk and long-term persistence. This interplay of chemical enrichment and depletion of organic matter is typical of disturbed, management-intensive systems and underlines the importance of organic inputs for buffering contamination.

Water-stable aggregates and SOM were positively associated in Factor 1, reflecting their degradation under long-term anthropogenic pressure. As an important binder, SOM promotes the formation and stability of aggregates, while the loss of SOM weakens the soil structure and makes aggregates more susceptible to degradation [48].

Factor 2, which explained 13.70% of the total variance, showed strong positive loadings for WHC and soil temperature and a strong negative loading for BD. This pattern reflects a dimension primarily related to soil porosity and its ability to retain moisture, which is strongly influenced by vegetation cover and SOM. High WHC and low BD are characteristics of soils with well-developed structure, low compaction, and sufficient organic input. In this study, these conditions will likely exist in grasslands managed with mulch residues and in forested areas where minimal disturbance and continuous litter inputs contribute to better soil aggregation and porosity [48]. The negative relationship between BD and WHC is well known; as BD decreases, soil pore space increases, improving the soil's ability to store available water [66,67]. Soils with lower BD also provide a more favourable environment for root and microbial activity, further supporting hydrological function. The positive influence of soil temperature on this factor may reflect the insulating effect of vegetation cover and surface residues that buffer diurnal and seasonal fluctuations. While soils with lower BD and higher porosity may exhibit more rapid surface heating due to lower thermal mass, especially under dry conditions, the presence of SOM and vegetation can mitigate these effects by stabilising moisture and shading the soil. Therefore, with perennial vegetation and mulch management, such soils maintain a more stable microclimate [68]. In addition, the presence of mulch and vegetation can reduce evaporative losses, contributing to a more favourable heat and moisture regime, especially in grasslands. This component represents an axis of soil physical quality, where improved structure (low BD), improved moisture retention (high WHC), and moderate thermal dynamics (soil temperature) together reflect better soil function under perennial vegetation.

Factor 4, accounting for 9.89% of the total variance, was characterised by positive loadings for CO_2 emissions and negative loadings for SWC, indicating a trade-off between soil respiration and SWC availability. At first glance, this negative correlation may seem counterintuitive, as soil respiration is generally enhanced by higher moisture, which promotes microbial activity and substrate diffusion. However, this relationship is non-linear, temperature dependent, and even more complex under field conditions. At moderate soil temperatures, such as those observed during sampling in 2023, higher SWC gener-

ally promotes CO_2 emissions by supporting microbial growth, enzymatic activity and decomposition of SOM [69]. However, when soils become excessively wet, oxygen diffusion is limited and microbial respiration shifts to anaerobic pathways, which are less efficient and result in lower CO_2 emissions [70,71]. In our study, SWC was relatively high in 2023 for all land-use types, which may have suppressed aerobic microbial activity in some plots, especially in dense vegetation or compacted conditions. Conversely, higher CO_2 emissions were recorded in 2021, when soils were drier and possibly better aerated, especially in grasslands. This likely reflects increased microbial turnover in well-drained surface layers and/or increased respiration following rewetting events, commonly called the "Birch effect" [72]. Drying and rewetting cycles stimulate microbial degradation of previously protected SOM, leading to short-term pulses of CO_2 [73,74]. This could explain the decoupling of SWC and CO_2 emissions observed in the PCA. In addition, soil temperature moderates the SWC–CO_2 relationship. Studies have shown that the effect of SWC on microbial respiration decreases at low or high-temperature extremes [75]. Under the current field conditions, where soil temperatures were in a favourable range, SWC became the dominant controlling factor, but with the caveat that very high SWC may have dampened microbial respiration due to suboptimal aeration, especially in finer textured or compacted soils. Thus, factor 4 likely represents a seasonal axis of soil biological activity, where the interplay of SWC, temperature and aeration determines microbial CO_2 emissions across all land uses.

5. Conclusions

This study demonstrates that land use significantly governs soil physical, chemical, and biological properties in periurban environments, with grasslands emerging as a high-functioning and resilient land-use type. Compared to croplands, grasslands had lower bulk density, higher water retention, organic matter content, and aggregate stability, revealing the benefits of permanent vegetation cover, minimal disturbance, and organic residue cycling. Temporal trends highlighted the ability of grassland soils to enhance water regulation and reduce compaction under favourable climatic conditions. However, observed shifts in soil structure and carbon content over time also point to the dynamic nature of grassland systems and the need for active monitoring to sustain their multifunctionality. Insights from Principal Component Analysis reinforced the central role of grasslands in maintaining soil porosity, biological activity, and structural integrity, especially when compared to degraded croplands. Grasslands show a balance between microbial CO_2 activity and water conservation, a combination critical for climate adaptation, carbon cycling, and flood mitigation in periurban zones. These findings directly contribute to understanding the multifunctionality of grassland soils. They show that well-managed grasslands deliver agronomic and ecological benefits and provide nature-based solutions for urban resilience. Promoting mulching, permanent cover, and low-intensity use can maximise the delivery of soil-based ecosystem services across grassland landscapes. Future research should prioritise long-term monitoring of grassland soil functions, especially under changing land-use intensity and climate variability. Moreover, stronger integration of grassland soil value into urban planning, agri-environmental policy, and green infrastructure investment is essential to secure their multifunctional benefits for decades.

Author Contributions: Conceptualization, I.B.; methodology, I.B. and A.P.; software, I.B.; validation, S.G., M.G. and P.P.; formal analysis, A.P.; investigation, I.B.; resources, I.B.; data curation, I.B.; writing—original draft preparation, I.B.; writing—review and editing, P.P., M.G., A.P. and S.G.; visualization, I.B.; supervision, P.P.; project administration, I.B.; funding acquisition, I.B. All authors have read and agreed to the published version of the manuscript.

Funding: This work was supported by the project "Monetary valuation of soil ecosystem services and creation of initiatives to invest in soil health: setting a framework for the inclusion of soil health in business and in the policy making process" (InBestSoil) (Horizon Europe, Grant agreement ID: 101091099).

Data Availability Statement: The raw data supporting the conclusions of this article will be made available by the authors on request.

Conflicts of Interest: The authors declare no conflicts of interest.

References

1. Evangelista, S.J.; Field, D.J.; McBratney, A.B.; Minasny, B.; Ng, W.; Padarian, J.; Dobarco, M.R.; Wadoux, A.M.C. Soil Security—Strategizing a Sustainable Future for Soil. *Adv. Agron.* **2024**, *183*, 70. [CrossRef]
2. Pereira, P.; Inácio, M.; Pinto, L.; Kalinauskas, M.; Bogdzevic, K.; Zhao, W. Mapping Ecosystem Services in Urban and Peri-Urban Areas. A Systematic Review. *Geogr. Sustain.* **2024**, *5*, 491–509. [CrossRef]
3. Ziter, C.; Turner, M.G. Current and Historical Land Use Influence Soil-Based Ecosystem Services in an Urban Landscape. *Ecol. Appl.* **2018**, *28*, 643–654. [CrossRef]
4. Haghighi, F.; Gorji, M.; Shorafa, M. A Study of the Effects of Land Use Changes on Soil Physical Properties and Organic Matter. *Land. Degrad. Dev.* **2010**, *21*, 496–502. [CrossRef]
5. Zhou, X.; Lin, H.S.; White, E.A. Surface soil hydraulic properties in four soil series under different land uses and their temporal changes. *Catena* **2008**, *73*, 180–188. [CrossRef]
6. Pouyat, R.V.; Yesilonis, I.D.; Russell-Anelli, J.; Neerchal, N.K. Soil chemical and physical properties that differentiate urban land-use and cover types. *Soil. Sci. Soc. Am. J.* **2007**, *71*, 1010–1019. [CrossRef]
7. Bogunovic, I.; Viduka, A.; Magdic, I.; Telak, L.J.; Francos, M.; Pereira, P. Agricultural and forest land-use impact on soil properties in Zagreb periurban area (Croatia). *Agronomy* **2020**, *10*, 1331. [CrossRef]
8. Francos, M.; Bogunovic, I.; Úbeda, X.; Pereira, P. Soil physico-chemical properties and Organic Carbon stocks across different land use in an urban park of Vilnius, Lithuania. *J. Cent. Eur. Agric.* **2023**, *24*, 519–530. [CrossRef]
9. Xiong, M.; Sun, R.; Chen, L. A global comparison of soil erosion associated with land use and climate type. *Geoderma* **2019**, *343*, 31–39. [CrossRef]
10. Celik, I. Land-use effects on organic matter and physical properties of soil in a southern Mediterranean highland of Turkey. *Soil. Till Res.* **2005**, *83*, 270–277. [CrossRef]
11. Lorenz, K.; Lal, R. Biogeochemical C and N cycles in urban soils. *Environ. Int.* **2009**, *35*, 1–8. [CrossRef] [PubMed]
12. Edmondson, J.L.; Davies, Z.G.; McHugh, N.; Gaston, K.J.; Leake, J.R. Organic carbon hidden in urban ecosystems. *Sci. Rep.* **2012**, *2*, 963. [CrossRef]
13. Kaye, J.P.; Groffman, P.M.; Grimm, N.B.; Baker, L.A.; Pouyat, R.V. A distinct urban biogeochemistry? *Trends Ecol. Evol.* **2006**, *21*, 192–199. [CrossRef]
14. Pouyat, R.V.; Yesilonis, I.D.; Nowak, D.J. Carbon storage by urban soils in the United States. *J. Environ. Quality* **2010**, *39*, 1566–1575. [CrossRef]
15. Zhao, K.; Liu, X.; Xu, J.; Selim, H.M. Heavy metal contaminations in a soil–rice system: Identification of spatial dependence in relation to soil properties of paddy fields. *Environ. Pollut.* **2013**, *181*, 42–51. [CrossRef]
16. Wong, C.S.C. Heavy metal pollution in urban soils and street dusts in Hong Kong. *Appl. Geochem.* **2003**, *18*, 483–494. [CrossRef]
17. Pavao-Zuckerman, M.A. The nature of urban soils and their role in ecological restoration in cities. *Restor. Ecol.* **2008**, *16*, 642–649. [CrossRef]
18. Dugan, I.; Bogunovic, I.; Pereira, P. Soil management and seasonality impact on soil properties and soil erosion in steep vineyards of north-western Croatia. *J. Hydrol. Hydromech.* **2023**, *71*, 91–99. [CrossRef]
19. Justić, M.; Jelaska, S.D. The relationship between biodiversity and the biomass of grasslands in the Zagreb area (NW Croatia). *Acta Bot. Croat.* **2022**, *81*, 221–232. [CrossRef]
20. Bogunovic, I.; Bilandzija, D.; Andabaka, Z.; Stupic, D.; Rodrigo Comino, J.; Cacic, M.; Brezinscak, L.; Maletic, E.; Pereira, P. Soil compaction under different management practices in a Croatian vineyard. *Arab. J. Geosci.* **2017**, *10*, 340. [CrossRef]
21. Brezinscak, L.; Bogunovic, I. Optimising Tillage and Straw Management for Improved Soil Physical Properties and Yield. *Land* **2025**, *14*, 376. [CrossRef]
22. Defterdarović, J.; Filipović, L.; Ondrašek, G.; Bogunović, I.; Dugan, I.; Phogat, V.; He, H.; Rashti, M.R.; Tavakkoli, E.; Baumgartl, T.; et al. Impact of Hillslope Agriculture on Soil Compaction and Seasonal Water Dynamics in a Temperate Vineyard. *Land* **2024**, *13*, 588. [CrossRef]
23. Voća, N.; Bilandžija, N.; Leto, J.; Cerovečki, L.; Krička, T. Revitalisation of Abandoned Agricultural Lands in Croatia Using the Energy Crop Miscanthus X Giganteus. *J. Process Energy Agric.* **2019**, *631*, 128. [CrossRef]

24. Nimac, I.; Cindrić Kalin, K.; Renko, T.; Vujnović, T.; Horvath, K. The analysis of summer 2020 urban flood in Zagreb (Croatia) from hydro-meteorological point of view. *Nat. Hazards* **2022**, *112*, 873–897. [CrossRef]
25. Sollitto, D.; Romic, M.; Castrignanò, A.; Romic, D.; Bakic, H. Assessing heavy metal contamination in soils of the Zagreb region (Northwest Croatia) using multivariate geostatistics. *Catena* **2010**, *80*, 182–194. [CrossRef]
26. Köppen, W. Versuch einer Klassifikation der Klimate, vorzugsweise nach ihren Beziehungen zur Pflanzenwelt. *Geogr. Z.* **1900**, *6*, 593–611.
27. Croatian Meteorological and Hydrological Service. Climatological Data. *Zagreb, Croatian Meteorological and Hydrological Service.* 2025. Available online: https://meteo.hr/klima.php?section=klima_podaci&param=k1&Grad=zagreb_gric (accessed on 1 April 2025).
28. Ugarković, D.; Matijević, M.; Tikvić, I.; Popić, K. Some features of climate and climatic elements in the area of the city of Zagreb. *Šumarski List* **2021**, *145*, 479–488. [CrossRef]
29. Seletković, A.; Kičić, M.; Ančić, M.; Kolić, J.; Pernar, R. The Urban Heat Island Analysis for the City of Zagreb in the Period 2013–2022 Utilising Landsat 8 Satellite Imagery. *Sustainability* **2023**, *15*, 3963. [CrossRef]
30. IUSS Working Group WRB. *World Reference Base for Soil Resources 2014; International Soil Classification System for Naming Soils and Creating Legends for Soil Maps, Update 2015*; World Soil Resources Reports No. 106; FAO: Rome, Italy, 2015; p. 188.
31. Blake, G.R.; Hartge, K.H. Bulk density. In *Methods of Soil Analysis: Part 1 Physical and Mineralogical Methods*; American Society of Agronomy: Madison, Wi, USA, 1986; pp. 363–375.
32. Dıaz-Zorita, M.; Perfect, E.; Grove, J.H. Disruptive methods for assessing soil structure. *Soil. Till Res.* **2002**, *64*, 3–22. [CrossRef]
33. Widén, B.; Lindroth, A. A calibration system for soil carbon dioxide-efflux measurement chambers: Description and application. *Soil. Sci. Soc. Am. J.* **2003**, *67*, 327–334. [CrossRef]
34. Kemper, W.D.; Rosenau, R.C. Aggregate stability and size distribution. In *Methods of Soil Analysis, Part 1. Physical and Mineralogical Methods*; Klute, A., Ed.; American Society of Agronomy: Madison, WI, USA, 1986; pp. 425–444.
35. Walkley, A.; Black, I.A. An examination of the Degtjareff method for determining soil organic matter, and a proposed modification of the chromic acid titration method. *Soil. Sci.* **1934**, *37*, 29–38. [CrossRef]
36. Wasserman, L. *All of Nonparametric Statistics*; Springer Science & Business Media: New York, NY, USA, 2006.
37. Sokal, R.R.; Rohlf, F.J. *Biometry the Principles and Practice of Statistics in Biological Research*, 3rd ed.; Freeman: New York, NY, USA, 1969.
38. Zhang, Y.; Wang, S.; Wang, H.; Ning, F.; Zhang, Y.; Dong, Z.; Wen, P.; Wang, R.; Wang, X.; Li, J. The effects of rotating conservation tillage with conventional tillage on soil properties and grain yields in winter wheat-spring maise rotations. *Agric. For. Meteorol.* **2018**, *263*, 107–117. [CrossRef]
39. Dekemati, I.; Simon, B.; Bogunovic, I.; Vinogradov, S.; Modiba, M.M.; Gyuricza, C.; Birkás, M. Three-year investigation of tillage management on the soil physical environment, earthworm populations and crop yields in Croatia. *Agronomy* **2021**, *11*, 825. [CrossRef]
40. Jabro, J.D.; Iversen, W.M.; Stevens, W.B.; Evans, R.G.; Mikha, M.M.; Allen, B.L. Physical and hydraulic properties of a sandy loam soil under zero, shallow and deep tillage practices. *Soil. Till Res.* **2016**, *159*, 67–72. [CrossRef]
41. Håkansson, I. *Machinery-Induced Compaction of Arable Soils*; Swedish University of Agricultural Sciences: Uppsala, Sweden, 2005.
42. Franzluebbers, A.J.; Stuedemann, J.A.; Schomberg, H.H.; Wilkinson, S.R. Soil organic C and N pools under long-term pasture management in the Southern Piedmont USA. *Soil. Biol. Biochem.* **2000**, *32*, 469–478. [CrossRef]
43. Six, J.; Conant, R.T.; Paul, E.A.; Paustian, K. Stabilisation mechanisms of soil organic matter: Implications for C-saturation of soils. *Plant Soil.* **2002**, *241*, 155–176. [CrossRef]
44. Wang, C.; Zhao, C.; Xu, Z.; Wang, Y.; Peng, H. Effect of vegetation on soil water retention and storage in a semi-arid alpine forest catchment. *J. Arid. Land.* **2013**, *5*, 207–219. [CrossRef]
45. Evrendilek, F.; Celik, I.; Kilic, S. Changes in soil organic carbon and other physical soil properties along adjacent Mediterranean forest, grassland, and cropland ecosystems in Turkey. *J. Arid. Environ.* **2004**, *59*, 743–752. [CrossRef]
46. Gajić, B. Physical properties and organic matter of Fluvisols under forest, grassland, and 100 years of conventional tillage. *Geoderma* **2013**, *200*, 114–119. [CrossRef]
47. Ajayi, A.E.; Faloye, O.T.; Reinsch, T.; Horn, R. Changes in soil structure and pore functions under long term/continuous grassland management. *Agric. Ecosyst. Environ.* **2021**, *314*, 107407. [CrossRef]
48. Bronick, C.J.; Lal, R. Soil structure and management: A review. *Geoderma* **2005**, *124*, 3–22. [CrossRef]
49. Mondal, S.; Chakraborty, D. Global meta-analysis suggests that no-tillage favourably changes soil structure and porosity. *Geoderma* **2022**, *405*, 115443. [CrossRef]
50. Sarker, T.C.; Zotti, M.; Fang, Y.; Giannino, F.; Mazzoleni, S.; Bonanomi, G.; Cai, Y.; Chang, S.X. Soil aggregation in relation to organic amendment: A synthesis. *J. Soil. Sci. Plant Nutr.* **2022**, *22*, 2481–2502. [CrossRef]
51. Poeplau, C.; Don, A. Carbon sequestration in agricultural soils via cultivation of cover crops—A meta-analysis. *Agric. Ecosyst. Environ.* **2015**, *200*, 33–41. [CrossRef]

52. Schmidt, M.W.I.; Torn, M.S.; Abiven, S.; Dittmar, T.; Guggenberger, G.; Janssens, I.A.; Klber, M.; Kögel-Knabner, I.; Lehmann, J.; Manning, D.A.C.; et al. Persistence of soil organic matter as an ecosystem property. *Nature* **2011**, *478*, 49–56. [CrossRef]
53. Luo, Z.; Wang, E.; Sun, O.J. Soil carbon change and its responses to agricultural practices in Australian agro-ecosystems: A review and synthesis. *Geoderma* **2010**, *155*, 211–223. [CrossRef]
54. Augusto, L.; Ranger, J.; Binkley, D.; Rothe, A. Impact of several common tree species of European temperate forests on soil fertility. *Ann. For. Sci.* **2002**, *59*, 233–253. [CrossRef]
55. Binkley, D.; Richter, D. Nutrient cycles and H+ budgets of forest ecosystems. *Adv. Ecol. Res.* **1987**, *16*, 1–51. [CrossRef]
56. Guo, J.H.; Liu, X.J.; Zhang, Y.; Shen, J.L.; Han, W.X.; Zhang, W.F.; Christie, P.; Goulding, K.W.T.; Vitousek, P.M.; Zhang, F.S. Significant acidification in major Chinese croplands. *Science* **2010**, *327*, 1008–1010. [CrossRef]
57. Tang, C.; Rengel, Z.; Diatloff, E.; Gazey, C. Responses of wheat and barley to liming on a sandy soil with subsoil acidity. *Field Crop Res.* **2003**, *80*, 235–244. [CrossRef]
58. Tejada, M.; García, C.; Gonzalez, J.L.; Hernandez, M.T. Use of organic amendment as a strategy for saline soil remediation: Influence on the physical, chemical and biological properties of soil. *Soil. Biol. Biochem.* **2006**, *38*, 1413–1421. [CrossRef]
59. Charlesworth, S.; Everett, M.; McCarthy, R.; Ordonez, A.; De Miguel, E. A comparative study of heavy metal concentration and distribution in deposited street dusts in a large and a small urban area: Birmingham and Coventry, West Midlands, UK. *Environ. Int.* **2003**, *29*, 563–573. [CrossRef]
60. Luo, X.S.; Yu, S.; Zhu, Y.G.; Li, X.D. Trace metal contamination in urban soils of China. *Sci. Total Environ.* **2011**, *421–422*, 17–30. [CrossRef]
61. Kabata-Pendias, A. *Trace Elements in Soils and Plants*; CRC Press: Boca Raton, FL, USA, 2000.
62. Nicholson, F.A.; Smith, S.R.; Alloway, B.J.; Carlton-Smith, C.; Chambers, B.J. An inventory of heavy metals inputs to agricultural soils in England and Wales. *Sci. Total Environ.* **2003**, *311*, 205–219. [CrossRef]
63. Komárek, M.; Čadková, E.; Chrastný, V.; Bordas, F.; Bollinger, J.C. Contamination of vineyard soils with fungicides: A review of environmental and toxicological aspects. *Environ. Int.* **2010**, *36*, 138–151. [CrossRef]
64. Park, J.H.; Lamb, D.; Paneerselvam, P.; Choppala, G.; Bolan, N.; Chung, J.W. Role of organic amendments on enhanced bioremediation of heavy metal(loid) contaminated soils. *J. Hazard. Mater.* **2011**, *185*, 549–574. [CrossRef]
65. Ducaroir, J.; Lamy, I. Evidence of trace metal association with soil organic matter using particle size fractionation after physical dispersion treatment. *Analyst* **1995**, *120*, 741–745. [CrossRef]
66. Hudson, B.D. Soil organic matter and available water capacity. *J. Soil. Water Conserv.* **1994**, *49*, 189–194. [CrossRef]
67. Hillel, D. *Introduction to Environmental Soil Physics*; Elsevier: San Diego, CA, USA, 2003.
68. Paul, K.I.; Polglase, P.J.; Smethurst, P.J.; O'Connell, A.M.; Carlyle, C.J.; Khanna, P.K. Soil temperature under forests: A simple model for predicting soil temperature under a range of forest types. *Agric. For. Meteorol.* **2004**, *121*, 167–182. [CrossRef]
69. Davidson, E.A.; Janssens, I.A.; Luo, Y. On the variability of respiration in terrestrial ecosystems: Moving beyond Q_{10}. *Glob. Chang. Biol.* **2006**, *12*, 154–164. [CrossRef]
70. Linn, D.M.; Doran, J.W. Effect of water-filled pore space on carbon dioxide and nitrous oxide production in tilled and nontilled soils. *Soil. Sci. Soc. Am. J.* **1984**, *48*, 1267–1272. [CrossRef]
71. Moyano, F.E.; Manzoni, S.; Chenu, C. Responses of soil heterotrophic respiration to moisture availability: An exploration of processes and models. *Soil. Biol. Biochem.* **2012**, *59*, 72–85. [CrossRef]
72. Birch, H.F. The effect of soil drying on humus decomposition and nitrogen availability. *Plant Soil.* **1958**, *10*, 9–31. [CrossRef]
73. Fierer, N.; Schimel, J.P. Effects of drying–rewetting frequency on soil carbon and nitrogen transformations. *Soil. Biol. Biochem.* **2002**, *34*, 777–787. [CrossRef]
74. Placella, S.A.; Brodie, E.L.; Firestone, M.K. Rainfall-induced carbon dioxide pulses result from sequential resuscitation of phylogenetically clustered microbial groups. *Proc. Natl. Acad. Sci. USA* **2012**, *109*, 10931–10936. [CrossRef]
75. Schaufler, G.; Kitzler, B.; Schindlbacher, A.; Skiba, U.; Sutton, M.A.; Zechmeister-Boltenstern, S. Greenhouse gas emissions from European soils under different land use: Effects of soil moisture and temperature. *Eur. J. Soil. Sci.* **2010**, *61*, 683–696. [CrossRef]

Disclaimer/Publisher's Note: The statements, opinions and data contained in all publications are solely those of the individual author(s) and contributor(s) and not of MDPI and/or the editor(s). MDPI and/or the editor(s) disclaim responsibility for any injury to people or property resulting from any ideas, methods, instructions or products referred to in the content.

agronomy

MDPI

Article

Soil Properties and Bacterial Community Responses to Herb Vegetation Succession Beneath Sand-Fixation Plantations in a Sandy Grassland, NE China

Cong Chen [1,2], Ying Zhang [1,2], Zhenbo Cui [1,2] and Chengyou Cao [1,2,*]

[1] College of Life and Health Sciences, Northeastern University, Shenyang 110169, China; chencong-neu@hotmail.com (C.C.); zhangying@mail.neu.edu.cn (Y.Z.); cuizhenbo@mail.neu.edu.cn (Z.C.)
[2] Liaoning Province Key Laboratory of Bioresource Research and Development, Northeastern University, Shenyang 110169, China
* Correspondence: caochengyou@mail.neu.edu.cn

Abstract

Establishing shrub plantations on mobile sand dunes is an effective strategy to combat desertification in semi-arid regions. Herbaceous communities developing beneath these plantations enhance ecosystem stability and improve revegetation outcomes. This study investigated the structural responses of soil bacterial communities, key functional genes (*nifH*, *amoA*, and *phoD*), and plant–soil–microbe interactions across a herbaceous vegetation succession gradient (initiation, early, middle, and stable stages) under *Caragana microphylla* sand-fixation plantations in the sandy Horqin Grassland. The results revealed that plant species richness, diversity, and biomass increased progressively with succession. Concurrent improvements in soil nutrients (organic matter, nitrogen, phosphorus, and potassium) and enzymatic activities (urease, protease, phosphatase, glucosidase, polyphenol oxidase, and dehydrogenase) were observed. The abundances of *nifH*, *amoA*, and *phoD* genes rose progressively with vegetation succession, contributing to enhanced soil nutrient levels. All dominant bacterial phyla and genera detected constituted shared taxa across successional stages, but their relative abundances shifted dynamically. Herbaceous succession facilitated rapid restoration of bacterial diversity, though structural recovery lagged, depending on the quantitative fluctuations of the dominant taxa. Soil pH, organic matter, electrical conductivity, total N, total P, available P, and available K all significantly influenced the soil bacterial community, with pH and organic matter being the most influential factors. These findings highlight plant–soil–microbe interactions as intrinsic drivers of vegetation succession in desertified ecosystems.

Keywords: desertification control; soil microbial diversity; vegetation succession; plant–soil–microbe interactions

1. Introduction

Desertification, a global environmental challenge, primarily occurs in arid, semi-arid, and dry sub-humid regions as a consequence of unsustainable human socioeconomic activities and global climate change. It leads to ecological degradation, resource depletion, and local impoverishment, garnering worldwide attention [1]. The Horqin Sandy Land (also known as Horqin Grassland), spanning approximately 51,750 km^2, is situated in the ecologically fragile semi-arid zone of Northeast China and serves as a significant traditional animal husbandry base. However, severe desertification has emerged since

the 1970s due to overgrazing, excessive land reclamation, and unsustainable fuelwood harvesting under an arid and windy climate. Today, it ranks among China's most severely desertified regions. Revegetation on desertified grasslands is a critical initial step for ecosystem restoration and has proven to be an effective desertification control strategy [2]. Consequently, extensive areas of tree, shrub, or semi-shrub sand-fixation vegetation have been established artificially on mobile and semi-mobile sand dunes in the Horqin Sandy Land over recent decades. These plantations play vital roles in sand stabilization, vegetation recovery, preventing windblown sand damage, and improving the local environment [3]. The ecological functions of these sand-fixation plantations vary depending on their type, age, and structure. Following establishment, greater focus should be directed towards their long-term stability and the sustainability of their protective functions.

Generally, moving sand dunes can be stabilized through plantation establishment within 3–5 years, leading to improved microenvironments. Subsequently, pioneer herbaceous species (short grasses and forbs) typically begin to colonize the area. The formation and succession of these herbaceous communities further enhance sand surface stabilization and promote water and soil conservation. Moreover, the rapid growth and turnover of herbaceous plants provide significant inputs of carbon (C), nitrogen (N), and other nutrients [3], contributing to soil property amelioration and soil microbial community recovery. However, degeneration of shrub or semi-shrub sand-fixation plantations (e.g., *Caragana microphylla* Lam., *Artemisia halodendron* Turcz., and *Salix gordejevii* Y. L. Chang et Skv.) often occurs 8–10 years after establishment. This decline is attributed to the biological and ecological limitations of the plant species under the inherently poor nutrient and arid sandy soil conditions, manifesting as growth stagnation, branch withering, and even whole-plant mortality. In such cases, if well-developed herbaceous communities have not established beneath the plantations, the previously fixed sand dunes risk becoming reactivated. Therefore, the herbaceous community plays a critical role in maintaining the long-term stability of sand-fixation plantations and restoring desertified ecosystems. Understanding the succession patterns of herbaceous communities under these plantations and their driving factors is essential for gaining deeper insights into ecological restoration processes and evaluating the effectiveness of vegetation restoration in degraded sandy land ecosystems.

Plant community succession is driven by internal forces arising from reciprocal interactions among plant populations, between plants, soil, and microbes (PSM), and among plants, animals, and microbes [4–6]. Among these, PSM interactions play a pivotal role at small scales. They influence soil physical, chemical, and microbiological properties, modulate nutrient and water availability, directly impact plant growth and development, regulate relationships among community components, and thereby drive continuous alterations in plant community structure and function, ultimately propelling succession [7,8]. Numerous PSM studies have focused on mechanisms underlying exotic species invasion, biodiversity maintenance, vegetation dynamics, and vegetation responses to global change [9–12]. Research demonstrates that both biotic (e.g., intra- and interspecific competition) and abiotic (e.g., resource availability) factors can significantly influence PSM interactions [6,13–15]. Mounting evidence underscores the fundamental role of PSM interactions in plant community assembly processes [16]. Therefore, a deeper understanding of the dynamics and underlying mechanisms of PSM interactions is essential to unravel the succession mechanisms of specific plant communities.

Soil microorganisms are considered an important driving factor for the succession of plant communities because they directly or indirectly participate in all ecological processes of soil nutrient cycles (especially C, N, P, and K) [17,18]. The composition and structure of soil microbial communities sensitively respond to environmental variations, and their

https://doi.org/10.3390/agronomy16030342

dynamics are inevitably related to soil properties and vegetation succession. Han et al. (2025) reported that during alpine grassland restoration, both bacterial and fungal communities exhibit sensitivity to changes in plant biomass and diversity, with soil nutrient availability and microenvironmental conditions playing a significant role in structuring microbial composition [19]. Regarding sand dune vegetation succession, some studies have also shown that the composition, structure, and diversity of soil bacterial and fungal communities respond in coordination with vegetation development and are significantly influenced by soil physicochemical properties and enzymatic activity [4,20,21]. Studies suggest that the response of soil microbial community to plant–soil interaction can be expressed at functional gene, species, and community levels [22,23]. Earlier studies on the succession of vegetation generally focused on the relationship between plant and soil and confirmed that plant community development alters soil nutrient pool size, which in turn shapes the plant community, while the role of soil microbial community in the interaction and feedback between plant and soil is often overlooked or underestimated. However, many recent studies in microbial ecology have been conducted to demonstrate the functions of microbial communities in plant–soil systems [22–24].

This study investigated a chronosequence of herbaceous community succession beneath *C. microphylla* sand-fixation plantations within the Horqin Sandy Land desertification control demonstration area. We assessed plant species composition, soil properties, and soil bacterial community structure across different herbaceous community succession stages. The study aimed to (1) determine structural responses of the soil bacterial community to herbaceous succession, specifically tracking changes in the abundance of ammonia-oxidizing, N-fixing, and P-transforming bacteria; (2) explore interactions between soil properties and the bacterial community during succession; and (3) identify key factors shaping the bacterial community. We hypothesize that the abundance of soil bacterial communities, particularly those involved in N and P transformation, gradually increases along the successional stages; soil nutrients significantly influence the structural shifts in bacterial communities; and vegetation succession markedly affects the relative abundance of dominant bacterial taxonomic groups.

2. Materials and Methods

2.1. Study Location and Site Description

This study was conducted within the Horqin Sandy Land Desertification Control Demonstration Area, established by the Wulanaodu Desertification Combating Ecological Station, the Institute of Applied Ecology, Chinese Academy of Sciences, beginning in 1981. The demonstration area is situated in the Wulanaodu region (43°03′ N, 119°38′ E) in the western Horqin Sandy Land, covering over 20 km^2 (Figure 1). Historically, the landscape consisted of continuous mobile and semi-mobile sand dunes interspersed with interdune bottomlands. The region experiences a temperate continental semi-arid monsoon climate. Meteorological data from the Wulanaodu Weather Station indicate a mean annual temperature of 6.3 °C, a frost-free period of 130 days, and average annual precipitation of 340.5 mm (70–80% occurring May–September). Annual pan evaporation averages approximately 2500 mm. Prevailing winds average 4.5 $m \cdot s^{-1}$ with frequent spring/winter gales (>20 $m \cdot s^{-1}$). Soils are classified as Arenosols [25]. Original vegetation comprised *Ulmus pumila*-dominant open woodlands of the Mongolian flora, largely degraded during desertification. Current sandy land vegetation includes *Caragana microphylla* Lam., *Salix microstachya* Turcz., *Artemisia halodendron* Turcz., *Agriophyllum squarrosum* (L.) Moq., *Bassia dasyphylla* O. Kuntze, *Cynachum sibiricum* L., *Lappula echinata* Gilib., *Artemisia scoparia* Waldstein et Kitaibel, *Geranium dahuricum* DC., *Cleistogens chinensis* (Maxim.) Keng, and *Setaria viridis* (L.) Beauv. Native shrubs and semi-shrubs (e.g., *C. microphylla*, *A. halodendron*,

https://doi.org/10.3390/agronomy16030342

and *Hedysarum fruticosum* Pall.) serve as pioneer species for dune stabilization. Since the 1980s, extensive sand-fixation plantations have been established using 1 m × 1 m straw checkerboard barriers followed by seeding/seedling planting. The entire demonstration area has been fenced with barbed wire post-revegetation.

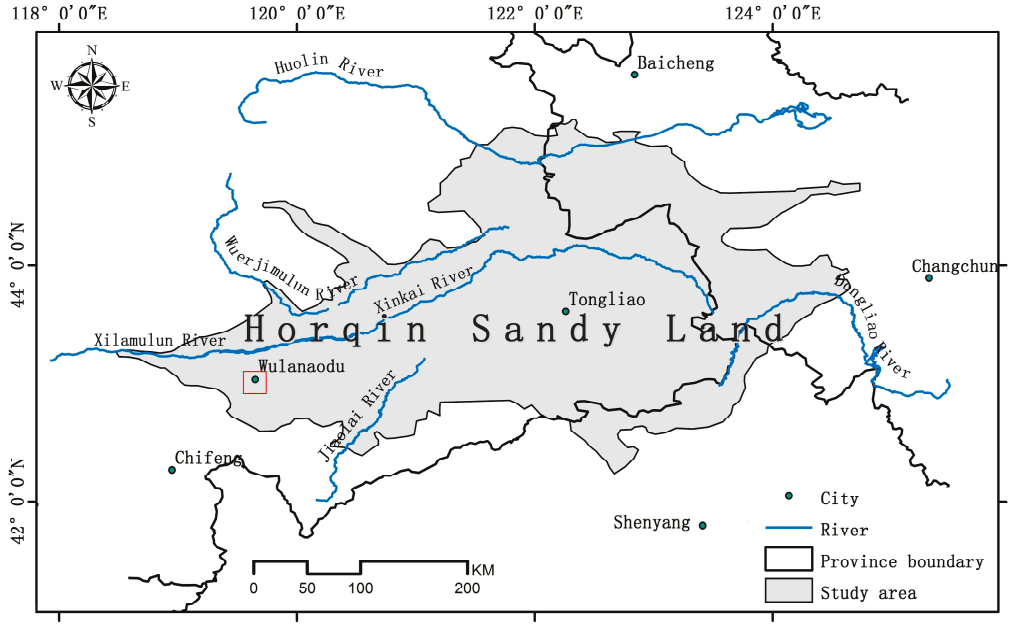


Figure 1. Study location (geographical location map was provided by Dr. Renhui Miao).

2.2. Experimental Design and Soil Sampling

A chronosequence of herbaceous community succession stages beneath sand-fixation plantations in the Wulanaodu demonstration area was selected for study. The stages comprised (1) the initiate stage (IS), an unvegetated mobile sand dune; (2) the early stage (ES), dominated by annual grasses; (3) the middle stage (MS), dominated by rhizomatous grasses; and (4) the stable stage (SS), dominated by bunchgrasses. Plant community surveys and soil sampling corresponding to these four stages were conducted in the following locations: unvegetated mobile sand dunes (IS), 10-year-old *C. microphylla* plantations (ES), 40-year-old *C. microphylla* plantations (MS), and natural *U. pumila* open forest (SS). The total vegetation coverage of IS, ES, MS, and SS was <5%, 50%, 70%, and 75%, respectively. ES and MS were all formed from revegetation via planting *C. microphylla* on similar moving sand dunes at different times, with the initial row spacing of 1 m × 1 m; SS originated from the spontaneous recovery after the enclosure of the desertified natural *C. microphylla* community in the demonstration area. Vegetation surveys and soil sample collection were conducted in August 2023, during early autumn and the most vigorous period of plant growth. Six spatially independent sitesper succession stages were established on different sand dunes as replicates. Within each site, one transect was established. Ten 1 m × 1 m quadrats spaced at 10 m intervals along the transects were used to record plant species composition, coverage, density, and above-ground biomass [26]. A total of 60 quadrats were surveyed per stage. Twenty soil subsamples (0−10 cm depth) were randomly collected within the plot using a shovel and composited into one bulk sample per site. Field-sieving through a 2 mm mesh was performed immediately after collection. Samples were placed in sterilized plastic ziplock bags. This yielded a total of 24 composite soil samples (4 stages × 6 sites). Each composite sample was split: one half was air-dried for physicochemical analysis; the other half was stored at −80 °C for DNA extraction and soil enzyme activity assays.

2.3. Soil Physicochemical Property and Enzymatic Activity Analysis

Soil moisture, pH, electrical conductivity (EC), organic matter (SOM), total N, P, and K, and available N (NH_4^+-N), P, and K were analyzed in the laboratory. Soil moisture was determined gravimetrically by oven-drying at 105 °C for 12 h. pH and EC were measured in soil–water suspensions (1:2.5 *w*/*v* for pH, 1:5 *w*/*v* for EC). SOM was quantified using the $K_2Cr_2O_7$–H_2SO_4 oxidation method. Total N was determined by the semi-micro Kjeldahl method. Total P was measured using the acid digestion molybdate colorimetric method. Available P was extracted with 0.5 M $NaHCO_3$ and measured using the molybdate ascorbic acid method. Total K and available K were determined by atomic absorption spectroscopy. Ammonium nitrogen (NH_4^+-N) was extracted from fresh soil with 1 M KCl solution and quantified using an automated discrete analyzer (CleverChem 380, Hamburg, Germany). All physicochemical analyses followed the procedures described by Lin (2004) [27].

The activities of four hydrolases (urease, alkaline phosphomonoesterase, protease, and β-glucosidase) and two oxidoreductases (polyphenol oxidase and dehydrogenase) related to soil carbon, nitrogen, and phosphorus transformation were determined. Urease activity was determined according to Kandeler & Gerber (1988) [28]. Alkaline phosphomonoesterase activity was measured following Tabatabai (1982) [29]. Protease activity was assessed using the original method of Ladd & Butler (1972) [30]. Polyphenol oxidase activity was determined as described by Perucci et al. (2000) [31]. β-glucosidase activity was measured following Xu & Zheng (1986) [32]. Dehydrogenase activity was quantified according to ISSCAS (1985) [33]. Detailed procedures for all enzyme activity assays are provided in the Supplementary Materials and Methods (File S1).

2.4. Microbial 16S rRNA Gene Sequencing and Analysis of the Composition and Diversity of the Bacterial Community

Next-generation sequencing library preparation and Illumina MiSeq sequencing were performed by GENEWIZ, Inc. (Suzhou, China). The V3–V4 hypervariable regions of bacterial 16S rRNA genes were amplified. Bioinformatic processing used the QIIME pipeline (v1.9.1). Quality-filtered sequences were clustered into operational taxonomic units (OTUs) at 97% similarity threshold using VSEARCH (v1.9.6). Representative sequences were taxonomically classified against the SILVA database using the RDP classifier. Bacterial taxonomy followed Bergey's Manual of Systematic Bacteriology. Alpha diversity metrics (Chao1 richness, observed OTUs, Shannon diversity index, and Pielou's evenness) were calculated in Mothur (v1.21.1). Beta diversity analysis employed hierarchical clustering (UPGMA) based on Bray–Curtis dissimilarity. Raw sequence data are publicly accessible in the NCBI Sequence Read Archive under BioProject PRJNA841013.

2.5. The Abundance of Soil Ammonia-Oxidizing, Nitrogen-Fixing, and Organic Phosphorus-Mineralizing Bacteria

Soil microbial DNA was extracted from IS, ES, MS, and SS sites using the FastDNA Spin Kit (Tiangen Biotech, Beijing, China). Functional gene abundances (*nifH*, *amoA*, and *phoD*) were quantified via real-time qPCR (Q5 System, Applied Biosystems, Foster City, CA, USA) to estimate the abundance of ammonia-oxidizing, nitrogen-fixing, and organic phosphorus-mineralizing bacteria, with the following primers: *nifH*: F1 (5′-TGCGAYCCSAARGCGAC-3′), R1 (5′-ATSGCCATCATYTCRCCGGA-3′) [34]; *amoA*: F2 (5′-GGGGTTTCTACTGGTGGT-3′), R2 (5′-CCCCTCKGSAAAGCCTTCTTC-3′) [35]; *phoD*: F3 (5′-TGGGAYGATCAYGARGT-3′), and R3 (5′-CTGSGCSAKSACRTTCCA-3′) [36]. Detailed protocols for sequencing, qPCR, and bioinformatics are provided in Supplementary Materials and Methods (File S1).

https://doi.org/10.3390/agronomy16030342

2.6. Data Analysis

Plant species abundance was quantified as density (number of individuals per m^2 across all quadrats), frequency (percentage occurrence across quadrats), and average coverage. For each species, an importance value (*IV*) and relative dominance value (*RDV*) were calculated [37], where $IV = RA + RC + RF$ (*RA*: relative abundance, *RC*: relative coverage, *RF*: relative frequency) and $RDV = IV/\sum IV$. Soil properties, alpha diversity indices of bacterial communities, and the abundances of *nifH*, *amoA*, and *phoD* genes across different successional stages were examined using one-way ANOVA. Post hoc comparisons were performed with the least significant difference (LSD) test in SPSS (version 18.0), with statistical significance defined at $p < 0.05$. Differentiated bacterial taxa at each succession stage were identified via LEfSe (Linear Discriminant Analysis Effect Size) analysis, applying a significance threshold of 0.05 and an LDA effect size cutoff of 4. Relationships between soil bacterial community structure and environmental factors were assessed using redundancy analysis (RDA; CANOCO v5.0).

3. Results

3.1. Dynamics of Plant Species Composition Along Plant Community Succession

Following the fixation of mobile sand dunes by *C. microphylla* planting, annual plants gradually invaded, establishing an herbaceous community beneath the plantation. Both the coverage and biomass of this herbaceous community increased with plantation development. Average coverage reached 26.1% in the early stage (ES), 39.6% in the middle stage (MS), and 75.5% in the stable stage (SS). Similarly, average dry biomass increased from 49.2 $g \cdot m^{-2}$ (ES) to 186.1 $g \cdot m^{-2}$ (MS) and 548.4 $g \cdot m^{-2}$ (SS). Species richness showed an increasing trend across succession stages, rising from 20 species in ES to 36 species in SS (Table S1). Distinct dominant species characterized each stage. ES was dominated by *Setaria viridis* (L.) Beauv. (45.9% relative importance value), *Chenopodium acuminatum* Willd. (16.1%), and *Eragrostis pilosa* (L.) P.B. (13.1%); however, their dominance declined sharply in MS and SS. In MS, perennial rhizomatous grasses invaded and became dominant, primarily *Pennisetum flaccidum* Griseb. (44.0%), *Corispermum thelegium* Kitag. (18.2%), and *Salsola collina* Pall. (11.2%). SS (climax stage) was dominated by the perennial short-rhizome grass *Agropyron cristatum* (L.) Gaertner (36.0%), followed by *P. flaccidum* (13.5%) and *S. viridis* (19.0%).

3.2. Soil Properties

Table 1 presents soil moisture, pH, electrical conductivity, organic matter, total N, P, and K, NH_4^+-N, and available P and K values for IS, ES, MS, and SS. Significant differences ($p < 0.001$) were observed in all measured soil factors, except total K, across succession stages. Most soil indicators, especially total and available nutrients in vegetation-covered sites (ES, MS, SS), were higher than in IS and exhibited increasing trends along the successional gradient. The soil organic matter, total N, total P, NH_4^+-N, available P, and available K of SS were 1.73–34.20, 3.21–11.25, 2.00–9.33, 1.25–1.860, 1.27–5.02, and 0.98–3.08 times higher than those of other successional stages (Table 1). This indicates that herbaceous vegetation development under plantations contributed significantly to soil nutrient enrichment. Activities of six soil enzymes, i.e., urease, protease, alkaline phosphomonoesterase, glucosidase, polyphenol oxidase, and dehydrogenase, are shown in Figure 2. These enzymatic activities also differed significantly among succession stages ($p < 0.001$). The activities of the six soil enzymes of SS were 1.46–12.90, 2.11–15.94, 2.81–62.90, 2.36–9.73, 9.92–33.76, and 2.64–9.69 times higher than those of other successional stages, mirroring soil nutrient trends. Values were lowest at IS and peaked at SS. The above results indicate that vegetation development is closely correlated with soil nutrients and biological activity, demonstrating

https://doi.org/10.3390/agronomy16030342

interaction and feedback mechanisms between them. Enhanced soil biological activity favors increased nutrient availability, thereby promoting plant growth and the invasion of new species. The increased complexity of plant communities and higher biomass, in turn, facilitates the accumulation of soil nutrients.

Table 1. Dynamic changes in soil physicochemical properties across different successional stages.

Item	Initiate Stage	Early Stage	Middle Stage	Stable Stage	*F*	*p*
pH	6.70 ± 0.05a	7.34 ± 0.08b	7.24 ± 0.13b	7.49 ± 0.26b	15.241	<0.001
Electrical conductivity (μs·cm^{-1})	16.0 ± 2.29a	25.9 ± 3.17a	55.2 ± 19.75b	59.9 ± 13.09b	12.922	<0.001
Soil moisture (%)	0.14 ± 0.02a	2.05 ± 0.55b	0.385 ± 0.16a	5.58 ± 0.97c	90.013	<0.001
Soil organic matter (%)	0.05 ± 0.02a	0.61 ± 0.0.08b	0.99 ± 0.32c	1.71 ± 0.34d	33.141	<0.001
Total N (%)	0.004 ± 0.002a	0.006 ± 0.001a	0.014 ± 0.007b	0.045 ± 0.007c	59.547	<0.001
Total P (%)	0.003 ± 0.001a	0.009 ± 0.002b	0.014 ± 0.004b	0.028 ± 0.005c	42.449	<0.001
Total K (%)	2.16 ± 0.12a	2.26 ± 0.05a	2.28 ± 0.05a	2.25 ± 0.04a	3.048	0.057
NH_4^+-N (mg·kg^{-1})	1.21 ± 0.61a	4.11 ± 0.60b	2.79 ± 0.72c	2.84 ± 0.20c	18.330	<0.001
Available P (mg·kg^{-1})	2.09 ± 0.55a	4.67 ± 0.83a	8.27 ± 1.92b	10.5 ± 3.03b	15.442	<0.001
Available K (mg·kg^{-1})	56.7 ± 7.07a	68.6 ± 12.77a	178.4 ± 71.9b	174.7 ± 35.3b	11.122	<0.001

Values are means ± SD. *F* and *p* values from one-way ANOVA are given. Means within a row followed by the different letters are significantly different (LSD test, $p < 0.05$).

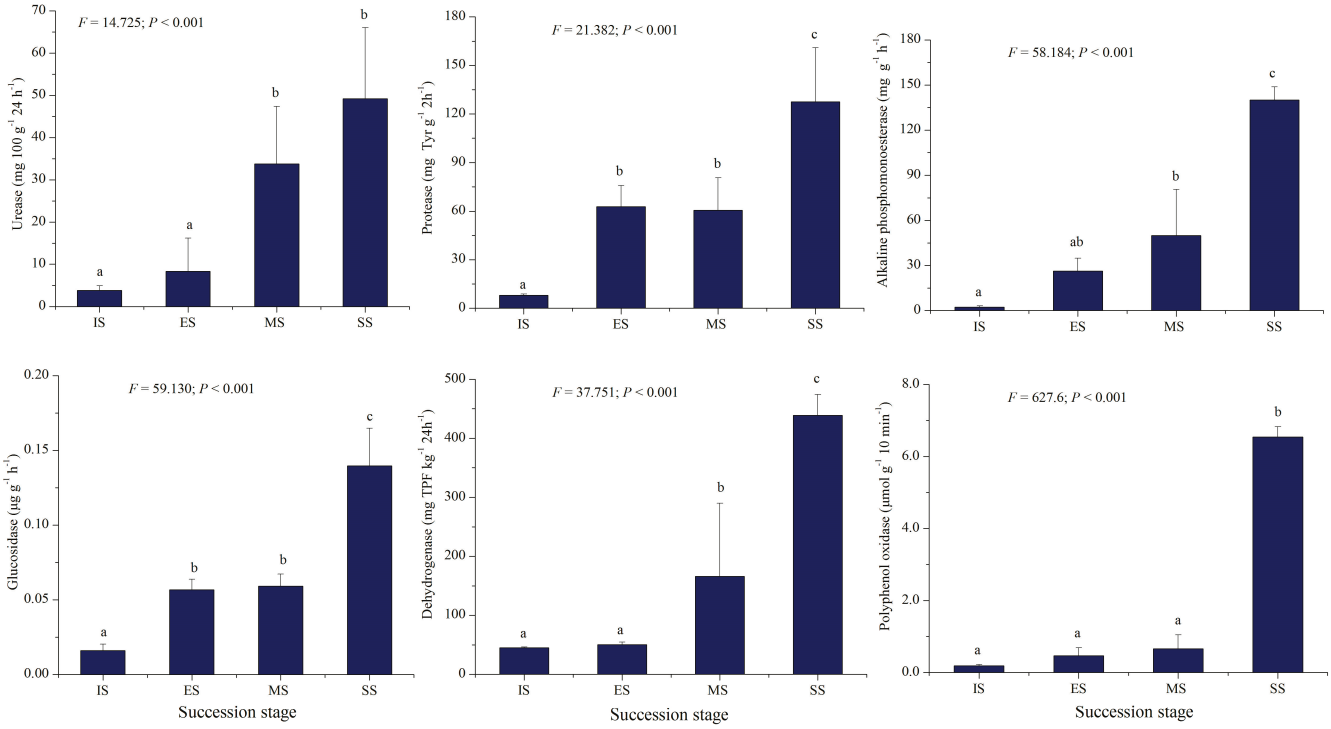


Figure 2. Soil enzymatic activities of different succession stages. IS: initiate stage, ES: early stage, MS: middle stage, SS: stable stage. Different letters indicate significant differences (LSD test, $p < 0.05$).

3.3. Composition of Soil Bacterial Communities Across Succession Stages

Soil genomic DNA was sequenced using an Illumina MiSeq high-throughput sequencing platform, yielding 1,153,233 high-quality 16S rRNA gene sequences. All rarefaction curves approached saturation at the sequencing depth (Figure S1), indicating sufficient sampling coverage to characterize bacterial community composition. Significant differences ($p < 0.001$) in α-diversity indices (Shannon–Wiener, Simpson, Chao1 richness, Pielou evenness, and observed species) were observed between IS and vegetation-covered sites (ES, MS, SS), though no significant differences emerged among ES, MS, and SS (Figure 3). All diversity indices showed significant correlations ($p < 0.05$) with soil pH, organic matter,

NH_4^+-N, electrical conductivity (except Simpson and Pielou), soil moisture (except Simpson), and total/available P (except Simpson) (Table S2). No significant correlations were found with total N, total K, or available K. Hierarchical clustering analysis based on OTUs grouped the 24 samples into four distinct clusters (Figure 4). Samples predominantly clustered by successional stage, indicating significant divergence in soil bacterial community structure along the successional gradient.

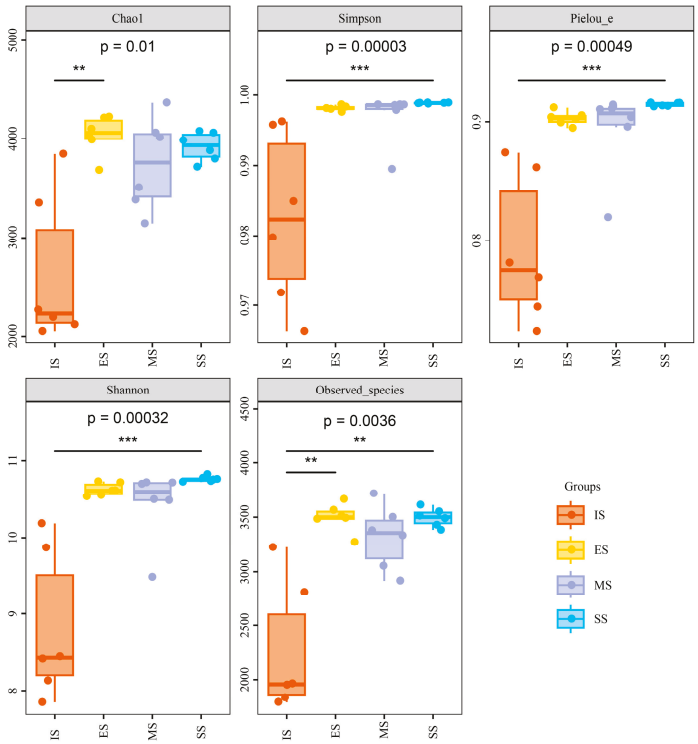


Figure 3. Alpha diversity indexes of soil bacterial communities of different succession stages. One-way ANOVA and multiple comparisons followed by LSD test are presented; **: $p \leq 0.01$; ***: $p \leq 0.001$. IS: initiate stage, ES: early stage, MS: middle stage, SS: stable stage.

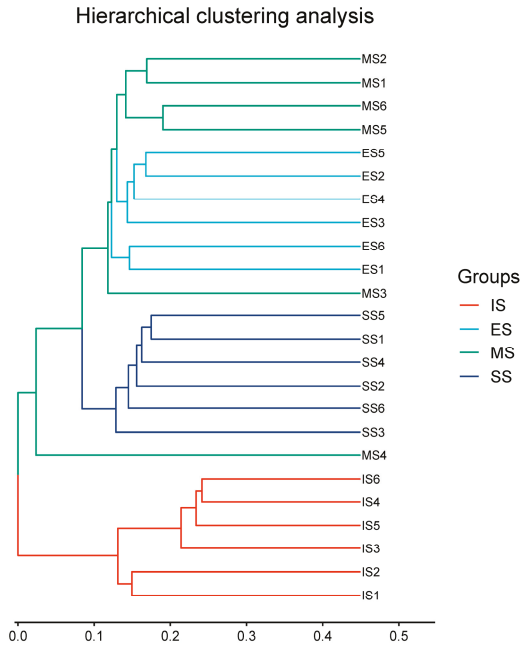


Figure 4. Hierarchical clustering analysis of different samples based on the structure of the soil bacteria community. IS: initiate stage, ES: early stage, MS: middle stage, SS: stable stage.

Actinomycetota, Pseudomonadota, Bacillota, Bacteroidota, Myxococcota, Acidobacteriota, Gemmatimonadota, and Cyanobacteriota constituted the dominant phyla (Figure 5A), with average relative abundances ranging from 29.28% to 64.20%, 18.70% to 36.63%, 6.56% to 21.41%, 1.32% to 5.55%, 0.73% to 2.30%, 0.82% to 2.15%, 0.58% to 1.38%, and 0.16% to 1.22%, respectively. Significant differences ($p < 0.05$) in the relative abundance of dominant phyla were observed across succession stages, except for Bacillota. Actinomycetota, Acidobacteriota, and Myxococcota generally increased along the successional gradient, while Pseudomonadota and Bacteroidota decreased. Figure 5B showed the relative abundances of the 30 most dominant genera. These genera comprised a shared core community across sites. However, significant differences ($p < 0.05$) in their relative abundances occurred between IS and vegetated succession stages (ES, MS, SS), except for *Rhodococcus*, *Niallia*, *Bacillus*, and *Bradyrhizobium*.

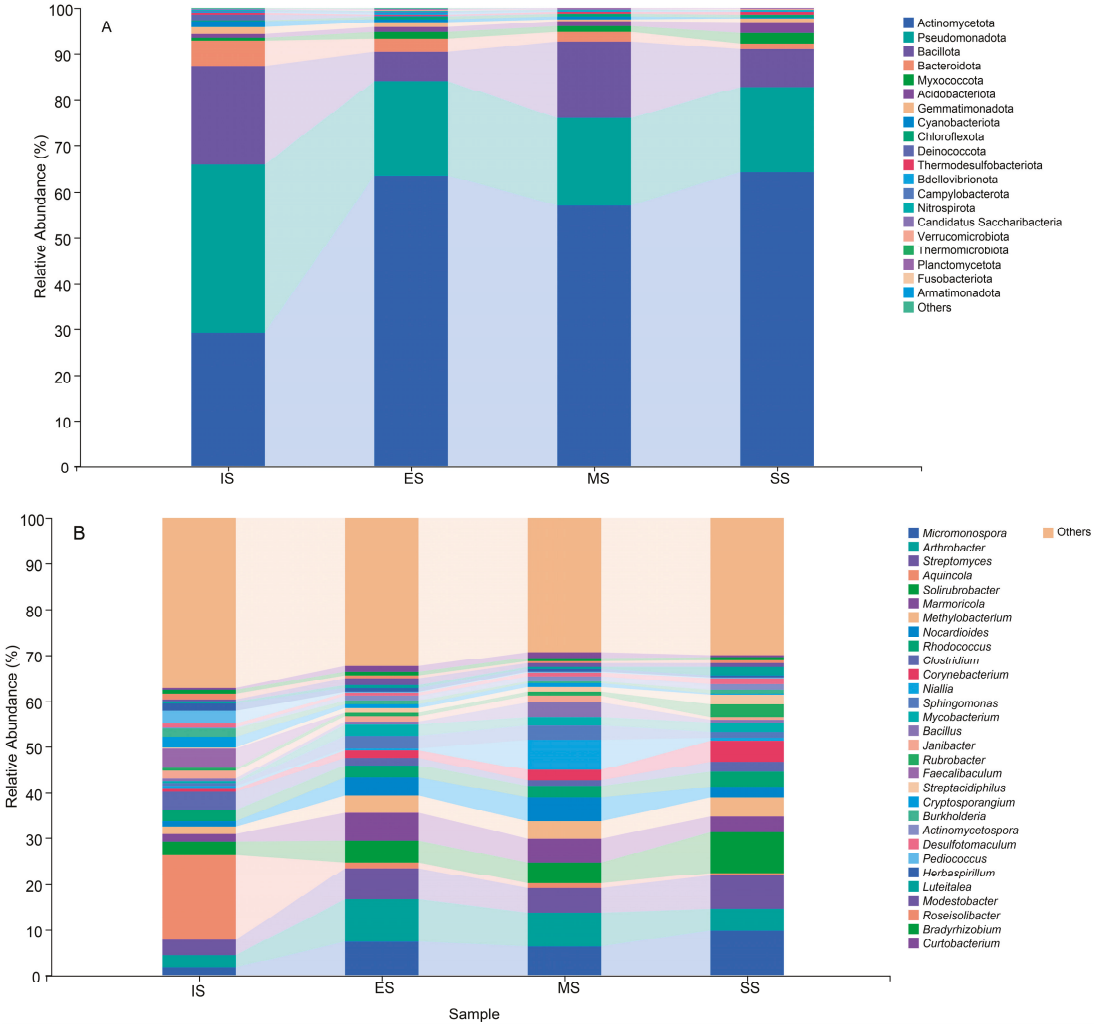


Figure 5. Relative abundances of dominant bacterial phyla (**A**) and genera (**B**) of different succession stages. IS: initiate stage, ES: early stage, MS: middle stage, SS: stable stage.

Significant abundance differences were also detected among ES, MS, and SS for 20 bacterial genera. This phenomenon indicates that soil bacterial communities rapidly respond to herbaceous plant invasion into mobile sand dunes, with bacterial succession tightly coupled to herbaceous vegetation development. In IS, *Aquincola* (18.69%), *Faecalibaculum* (4.38%), *Clostridium* (3.89%), *Pediococcus* (3.03%), *Solirubrobacter* (2.93%), and *Cryptosporangium* (2.30%) were most abundant, but their relative abundances decreased significantly in vegetation-covered sites (ES, MS, SS). Conversely, multiple genera became dominant

in vegetated sites, including *Micromonospora* (6.19–9.79%), *Arthrobacter* (4.80–9.44%), *Streptomyces* (5.28–7.15%), *Solirubrobacter* (4.49–8.83%), *Marmoricola* (3.62–6.15%), *Methylobacterium* (3.76–4.02%), *Nocardioides* (2.19–5.11%), *Corynebacterium* (1.74–4.54%), *Sphingomonas* (1.30–3.25%), *Mycobacterium* (1.74–2.38%), *Streptacidiphilus* (1.02–2.11%), and *Actinomycetospora* (1.04–1.24%). Shifts in the abundance of these genera altered soil bacterial community structure and likely contributed to herbaceous vegetation succession.

LEfSe analysis identified stage-specific bacterial taxa contributing significantly to structural variation in soil bacterial communities across herbaceous vegetation succession stages. Key biomarkers identified were (1) IS, including Cryptosporangiales (Cryptosporangiaceae and *Cryptosporangium*), Bacillota (Lactobacillales (Lactobacillaceae, and *Pediococcus*), Clostridia (Eubacteriales, Clostridiaceae, *Clostridium*, and *Hungatella*), Erysipelotrichales (Erysipelotrichaceae and *Faecalibaculum*), Bacteroidota (Bacteroidia, Bacteroidales), Pseudomonadota (Betaproteobacteria, Burkholderiales, Burkholderiaceae, Sphaerotilaceae, and *Aquincola*). (2) ES included Alphaproteobacteria, Actinomycetes, Micrococcaceae, Arthrobacter, and Marmoricola. (3) MS included Propionibacteriales (Nocardioidaceae and *Nocardioides*), Hyphomicrobiales (Methylobacteriaceae), and Sphingomonadales (Sphingomonadaceae and *Sphingomonas*). (4) SS included Actinomycetota, Kitasatosporales (Streptomycetaceae and *Streptomyces*), Micromonosporales (Micromonosporaceae and *Micromonospora*), Mycobacteriales (Corynebacteriaceae and *Corynebacterium*), Rubrobacteria (Rubrobacterales, Rubrobacteraceae, and *Rubrobacter*), Thermoleophilia (Solirubrobacterales, Solirubrobacteraceae, and *Solirubrobacter*), and *Methylobacterium*. The LEfSe results confirmed significant divergence in soil bacterial community structure across succession stages (Figure 6).

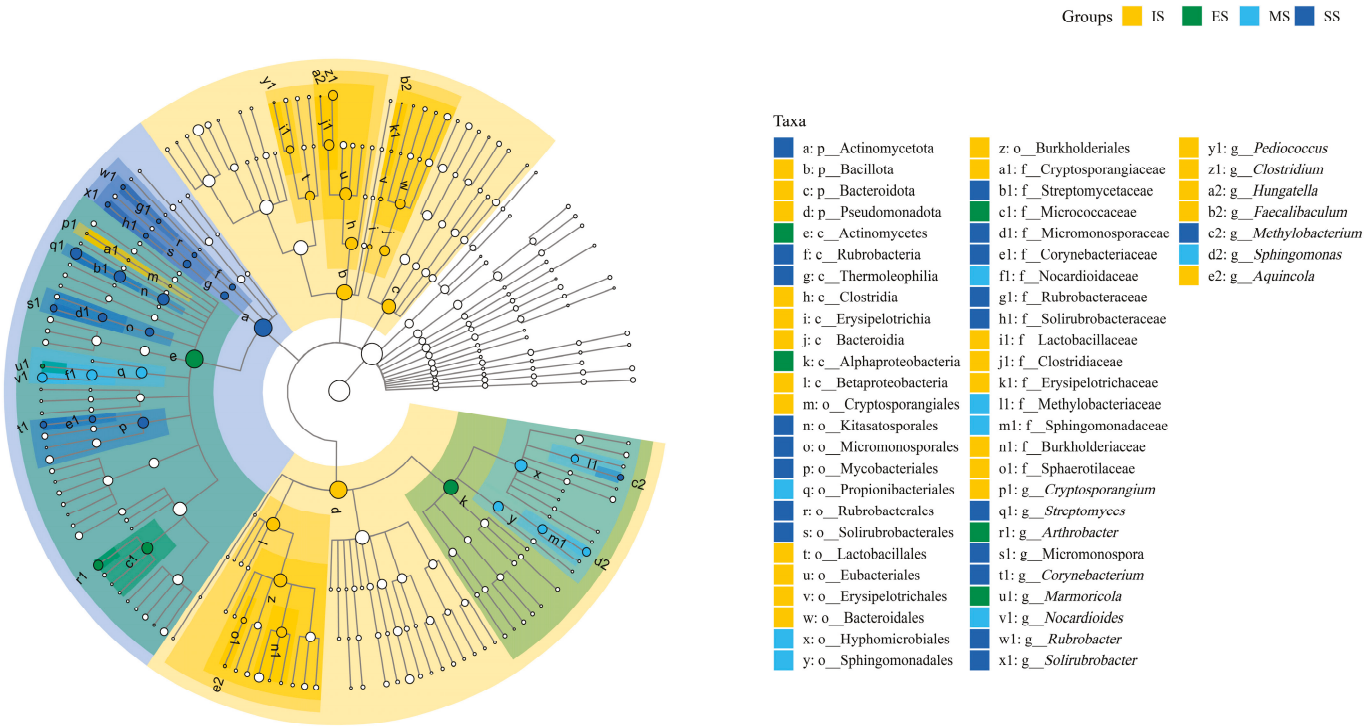


Figure 6. Significantly different taxa detected by LEfSe in different bacterial communities. A significance level of 0.05 was used for all of the biomarkers evaluated. Only taxa meeting an LDA significance threshold of >4 in soil abacterial communities are shown. IS: initiate stage, ES: early stage, MS: middle stage, SS: stable stage.

3.4. Response of nifH-, amoA-, and phoD-Harboring Microbe Abundance to Succession

Quantitative PCR determined abundances of *nifH*, *amoA*, and *phoD* genes across succession stages. All three genes exhibited increasing abundance trends along the successional gradient (Figure 7): *nifH*: 1.51 × 10^4 (IS) to 3.54 × 10^4 (SS) copies g^{-1} dry soil; *amoA*: 1.23 × 10^5 (IS) to 3.95 × 10^7 (SS) copies g^{-1} dry soil; and *phoD*: 1.08 × 10^6 (IS) to 1.91 × 10^7 (SS) copies g^{-1} dry soil. Abundances differed significantly among stages ($p < 0.001$), with herbaceous vegetation recovery driving substantial increases: *nifH*: 301.5× (ES), 1123.8× (MS), and 2337.9× (SS) higher than IS; *amoA*: 133.8× (ES), 229.4× (MS), and 321.6× (SS) higher; *phoD*: 5.6× (ES), 9.3× (MS), and 17.7× (SS) higher. These gene abundance trends mirrored those of soil properties and enzymatic activities. Correlation analysis revealed significant positive relationships ($p < 0.05$) between gene abundances and key soil parameters (pH, electrical conductivity, organic matter, total N, total P, available P, and available K (Pearson r = 0.459–0.953).

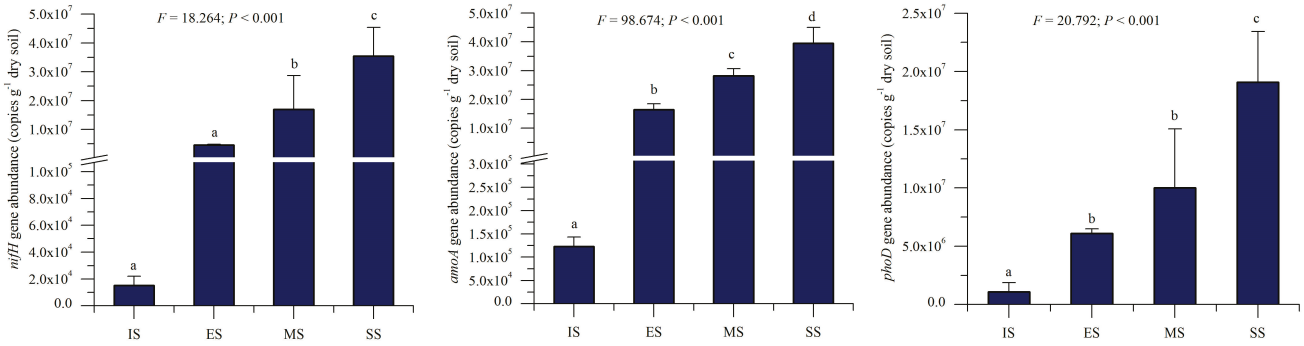


Figure 7. Abundances of soil *nifH*, *amoA*, and *phoD* genes of different succession stages. IS: initiate stage, ES: early stage, MS: middle stage, SS: stable stage. Different letters indicate significant differences (LSD test, $p < 0.05$).

3.5. Relationship Between Bacterial Community Structure and Soil Properties

Redundancy analysis (RDA) was performed to identify soil properties significantly influencing the bacterial community structure. The analyzed properties included soil moisture, pH, electrical conductivity, organic matter, total N, total P, available N, available P, and available K. The first two RDA axes collectively explained 88.3% of the variation in bacterial community structure, with the first axis accounting for 55.3% and the second axis accounting for 33.0% (Figure 8). Monte Carlo permutation tests indicated that soil pH, organic matter, electrical conductivity, total N, total P, available P, and available K all exerted significant effects on the bacterial community ($p < 0.05$). These significant variables individually explained 25%, 22%, 19%, 15%, 18%, 19%, and 18% of the variance, respectively. In the RDA ordination plot (Figure 8), samples from different succession sites were distinctly separated, primarily occupying different regions of the ordination space. Furthermore, samples from the same site tended to cluster together. This spatial distribution pattern, consistent with the results of hierarchical clustering analysis (Figure 4), clearly demonstrates the distinct shifts in soil bacterial community structure along the vegetation succession gradient.

https://doi.org/10.3390/agronomy16030342

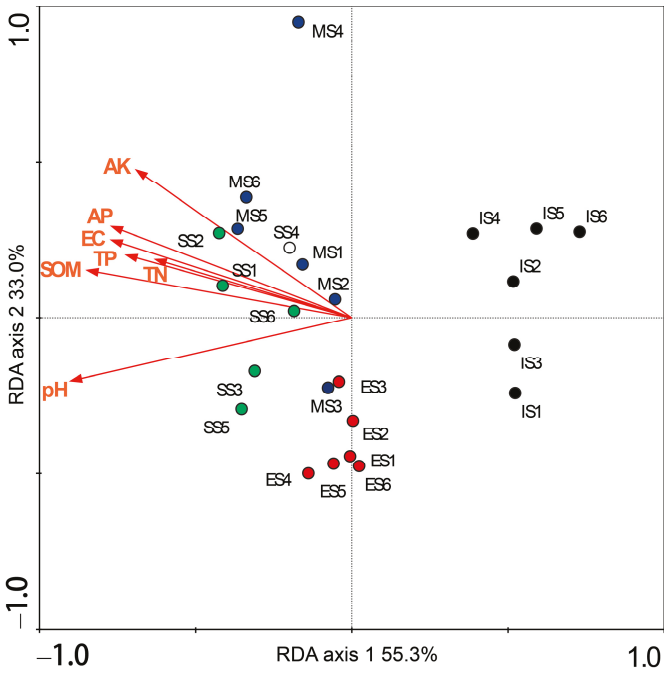


Figure 8. Redundancy analysis between the structure of bacterial communities and soil properties. SOM: organic matter, EC: electrical conductivity, TN: total nitrogen, TP: total phosphorus, AP: available phosphorus, AK: available potassium. IS: initiate stage, ES: early stage, MS: middle stage, SS: stable stage.

4. Discussion

4.1. Impact of Grassland Desertification on Vegetation and Promoting Effect of Shrub Sand-Fixation on the Succession of Herbaceous Vegetation

In this study, the moving sand land was formerly natural grassland dominated by perennial grasses (e.g., *A. cristatum* and *P. flaccidum*) and sparsely distributed elms (*U. pumila*). This sparse woodland steppe represents the native vegetation type of the Horqin Sandy Land [37]. Land desertification, primarily driven by aeolian soil erosion and deposition, led to vegetation loss and soil degradation. This degradation stemmed from physical damage to plant roots and seedlings, combined with the removal of nutrient-rich fine soil particles and litter by strong winds during spring and winter [3]. These processes progressively transformed the land into mobile sand dunes. Herbaceous plants generally struggle to colonize mobile sand dunes due to soil instability and the absence of protective native vegetation. Concurrently, severe nutrient loss, particularly organic matter and nitrogen, creates unfavorable conditions for the growth and proliferation of many soil bacterial species, thereby altering the diversity and composition of the soil bacterial community [20]. During revegetation, the establishment of *C. microphylla* sand-fixation plantations facilitates the gradual stabilization of moving sand dunes. This stabilization reduces wind velocity and surface albedo while redistributing near-surface heat and water. The improved habitat serves as an essential prerequisite for herbaceous plant invasion. However, during the early succession stage, the sandy soil remained loose, unstable, and extremely low in organic matter, creating conditions unsuitable for the survival of most native plants. Only a few nutrient-poor adaptive, drought-resistant, and sand burial-tolerant annual species, such as *Agriophyllum arenariu*m Bieb., *Setaria viridis* (L.) Beauv., *Chenopodium acuminatum* Willd, *Cynanchum sibiricum* R. BR., and *Eragrostis Pilosa* (L.) P.B., could establish and complete their life cycles (Table S1). Consequently, herbaceous community diversity, abundance, coverage, and biomass were all very low. The invasion of these pioneer species further stabilizes mobile surface soil through root systems and enhances soil properties. Their

rapid growth and mortality increase soil organic matter input [20], gradually facilitating herbaceous community reformation and succession beneath the sand-fixation plantation.

Throughout succession, diversity, coverage, abundance, and biomass exhibited continuous increases. Perennial rhizomatous and short-rhizomatous grasses sequentially invaded, eventually becoming dominant components of the herbaceous community, a pattern consistent with Zhang et al. (2005) [37]. Annual plants characterized the early succession stage, exhibiting rapid life cycles, strong resource acquisition, but low environmental resistance. In contrast, perennial herbs dominated the stable succession stage, demonstrating greater resistance and resilience to environmental disturbance. This progression reflects niche differentiation driven by interspecific competition, which progressively shapes soil nutrient acquisition strategies [38].

4.2. Coordinated Responses of Soil Physicochemical Properties and Biological Activity in the Process of Herbaceous Vegetation Succession

Herbaceous community succession progressed concurrently with improvements in soil physical, chemical, and biological properties. Soil pH, electrical conductivity, nutrient levels (organic matter, N, P, and K), and enzymatic activities all increased along the successional gradient (Table 1; Figure 2). Revegetation-induced nutrient accumulation is influenced by multiple biotic and abiotic factors. As *C. microphylla* plantations developed, expanding shrub crowns captured greater amounts of litter and nutrient-rich, fine-particle dust. Concurrently, N-fixation (by soil azotobacter or plant–microbe symbionts) and N-mineralization from litter decomposition contributed to soil N enrichment [21]. Herbaceous plant invasions generated substantial net primary productivity, while plant residues provided significant inputs of organic matter, N, P, and K [4]. Consequently, the shrub–grass association in revegetated sandy lands significantly enhanced nutrient cycling and promoted biological productivity within this sandy grassland system. Soil enzymes, being highly sensitive to environmental changes and strongly correlated with soil fertility, serve as reliable indicators for assessing the impacts of degradation, restoration, and land management on soil quality. In this study, activities of urease, protease, alkaline phosphomonoesterase, glucosidase, polyphenol oxidase, and dehydrogenase all increased throughout herbaceous succession, mirroring trends in soil nutrients (Figure 2). This rise in enzymatic activity indicates accelerated mineralization of soil organic matter and enhanced cycling of key nutrients (e.g., N and P).

Overall, herbaceous community succession beneath sand-fixation plantations is intrinsically linked to soil properties and microbial abundance. Herbaceous plants colonizing these habitats enhance soil conditions and increase microbial populations; in turn, the improved soil environment supports greater plant survival. Plants initially respond to environmental changes at physiological and biochemical levels, subsequently influencing overall growth processes. They adapt to soil heterogeneity by modifying root morphology, spatial distribution patterns, and adjusting water/nutrient uptake rates. Furthermore, soil properties and key functional microbial groups (ammonia-oxidizing, N-fixing, and organic phosphorus-mineralizing bacteria) critically influence succession by affecting individual plant growth and community biomass, establishing plant–microbe symbioses that enhance plant stress resistance, and increasing soil biological activity [39]. Thus, plant–soil–microbe interactions and feedback loops constitute the fundamental drivers of herbaceous succession. These dynamics can modulate soil attributes and water/nutrient availability, influence individual plant development, and alter intra- and interspecific relationships within plant communities, and, ultimately, propel continuous structural and functional reorganization of the plant community [6,8,40,41].

https://doi.org/10.3390/agronomy16030342

4.3. Structural Responses of Soil Bacterial Community to Herbaceous Succession

Soil microorganisms are key drivers of plant community succession, directly or indirectly participating in nearly all ecological processes, particularly nutrient cycling and energy conversion [15,42,43]. They play central roles in biogeochemical transformations of soil C, N, P, and K. Soil microbial community structure exhibits distinct spatiotemporal shifts during vegetation succession, inevitably influencing vegetation composition and soil properties [44]. This study examined structural responses of soil bacterial communities to herbaceous succession, hypothesizing differences in diversity, composition, and structure across successional stages. Despite large overlaps in shared OTUs among succession stages, seven dominant phyla (Actinomycetota, Pseudomonadota, Bacillota, Bacteroidota, Myxococcota, and Acidobacteriota) were ubiquitous. However, significant differences emerged in the relative abundances of the most dominant phyla across stages. Similarly, while dominant genera (e.g., *Micromonospora*, *Arthrobacter*, *Streptomyces*, *Solirubrobacter*, *Marmoricola*, *Methylobacterium*, *Nocardioides*, and *Corynebacterium*) were shared, their relative abundances also differed significantly across stages.

Alpha diversity indices were significantly higher in vegetation-covered sites than in mobile sand land. But, no significant differences occurred among the vegetation-covered sites themselves. This phenomenon suggests that while the core taxonomic composition of soil bacterial communities in mobile sand land can recover rapidly, restoring community structure is a slower process driven primarily by shifts in the relative abundances of dominant taxa. Bacterial communities responded quantitatively to herbaceous vegetation succession because their fundamental taxonomic composition remained largely unchanged. This observation likely indicates the presence of resilient native species that can maintain compositional stability amid environmental fluctuations. Subsequent structural reorganization is driven by asymmetric population growth responses to shifts in vegetation and soil conditions. Supporting this, Jangid et al. (2011) identified land use history, rather than contemporary vegetation or soil properties, as the primary determinant of microbial community composition [45]. They also observed that disturbed communities can gradually revert toward their original states over time. Similarly, Suleiman et al. (2013) demonstrated persistent legacy effects of historical land use on present-day microbial community structure, noting that regional climatic factors may ultimately govern core community composition [46]. Consequently, secondary succession of herbaceous vegetation and associated soil changes exerted minimal influence on dominant bacterial taxa. LEfSe analysis revealed quantitative dynamics of dominant bacterial groups across succession stages. These differentially abundant taxa, highly sensitive to vegetation and soil gradients, constituted key drivers of structural shifts in the bacterial community.

Microorganisms drive soil organic matter mineralization through extracellular enzyme secretion. Enzymatic activities are strongly dependent on microbial biomass and metabolic rates. Consequently, elevated enzyme activities and organic matter content typically correspond to higher microbial abundance. While most soil bacterial taxa contribute minimally to core ecosystem functions, key functional groups, such as N-fixing, nitrifying, and organic P-mineralizing bacteria, play critical roles. These groups directly regulate soil nutrient inputs, nutrient availability, litter decomposition rates, and plant stress tolerance. The *amoA*, *nifH*, and *phoD* genes encode essential enzymes for nutrient cycling: ammonia monooxygenase (amoA), nitrogenase (nifH), and alkaline phosphatase (phoD), respectively [47–50]. These enzymes catalyze transformations governing N/P bioavailability. This study observed increasing abundances of all three genes along the successional gradient (Figure 7), indicating the enhanced populations of N-fixing, ammonium-oxidizing, and organic P-mineralizing bacteria and the elevated potential bioavailability of soil N/P compounds. Dominant soil *amoA* carriers in the revegetation area near sampling sites

mainly belonged to *Nitrosospira* (including Cluster 3a and Cluster 6) [21]. Dominant soil *nifH*-carrying N-fixing genera included *Skermanella*, *Bradyrhizobium*, *Azospirillum*, *Azohydromonas*, and *Mesorhizobium* [51]. Dominant *phoD* carriers included Streptomycetaceae, *Bradyrhizobium*, *Kribbella*, and *Steroidobacte* [52].

4.4. Relationship Between Soil Properties and Bacterial Community During Succession

Soil constitutes the living environment for bacteria, and variations in soil properties can directly drive shifts in bacterial community structure. The RDA results in this study demonstrated that soil factors (including pH, organic matter, electrical conductivity, total N, total P, available P, and available K) significantly influenced soil bacterial community structure (Figure 8). Among these, pH and organic matter emerged as the most significant drivers, explaining 25% and 22% of the variance, respectively. Previous studies consistently report soil pH as a primary driver of bacterial community structure across geographic scales and in arable land [36,53,54]. Mendes et al. (2015) further indicated a correlation between pH and bacterial community structure during land use changes in the southeastern Amazon region [55]. The significant influence of pH likely stems from two factors: (1) its integration with other soil properties and (2) its profound effect on bacterial sensitivity to environmental change, where even slight pH variations can induce microbial stress [41,44]. Soil organic C, N, and P serve as essential nutrients for bacterial survival. Their gradual increase during vegetation succession generally promotes the growth of all bacterial groups. However, due to intra- and interspecific competition, the quantitative responses of dominant taxa to soil nutrients vary, leading to asymmetric changes in their relative abundances and, consequently, shifts in overall community structure [20]. Overall, while dominant bacterial taxa showed quantitative responses to soil improvement, the main components of the dominant soil bacterial taxa along the herbaceous plant community succession under sand-fixation plantations were only marginally affected.

5. Conclusions

This study investigated plant species composition, soil properties, and soil bacterial community structure across different stages of herbaceous community succession. Plant species richness, diversity, and biomass all increased gradually along the successional sequence. Soil nutrients (organic matter, N, P, and K) and enzymatic activities (urease, protease, alkaline phosphomonoesterase, glucosidase, polyphenol oxidase, and dehydrogenase) collectively improved. The abundances of the *amoA*, *nifH*, and *phoD* genes increased progressively throughout vegetation succession, contributing to the enhancement of soil nutrient levels. The process of herbaceous community succession was closely coupled with improvements in soil properties. All detected dominant bacterial phyla (e.g., Actinomycetota, Pseudomonadota, Bacillota, Bacteroidota, and Myxococcota) and genera (e.g., *Micromonospora*, *Arthrobacter*, *Streptomyces*, *Solirubrobacter*, *Marmoricola*, *Methylobacterium*, *Nocardioides*, and *Corynebacterium*) constituted shared taxa across successional stages, although their relative abundances varied. The invasion of annual plants into moving sand dunes significantly increased soil bacterial community diversity indices; however, these indices changed only slightly during subsequent herbaceous community succession. While the basic composition of the soil bacterial community in moving sand dunes could be readily and rapidly restored towards its original state, the restoration of its structure was a slow process, primarily dependent on quantitative shifts (increases and decreases) among dominant taxa. Soil pH, organic matter, electrical conductivity, total N and P, and available P and K all significantly influenced the soil bacterial community, with pH and organic matter being the most important factors. The interactive relationships among plants, soil,

and microbes constituted the underlying mechanisms driving herbaceous community succession within the sand-fixation plantation.

Supplementary Materials: The following supporting information can be downloaded at https://www.mdpi.com/article/10.3390/agronomy16030342/s1, File S1: Supplementary Materials and Methods [28–36,56]; Figure S1: Rarefaction curves of soil bacterial high-throughput sequencing at different successional stages; Table S1: Compositions of plant communities and their relative importance values at different succession stages. Table S2: Correlations between the indices of α-diversity of bacterial community and soil properties.

Author Contributions: C.C. (Cong Chen): writing—original draft, investigation, resources, and data curation. Y.Z.: methodology and resources. Z.C.: investigation. C.C. (Chengyou Cao): writing—review and editing, writing—original draft, conceptualization, project administration, and data curation. All authors have read and agreed to the published version of the manuscript.

Funding: This research was funded by the National Natural Science Foundation of China (42277467) and the Construction Project of Liaoning Provincial Key Laboratory, China (2022JH13/10200026).

Data Availability Statement: The original contributions presented in the study are included in the article/Supplementary Materials; further inquiries can be directed to the corresponding author.

Acknowledgments: The authors would like to express their gratitude to the Wulanaodu Desertification Combating Ecological Station, Institute of Applied Ecology, Chinese Academy of Sciences, for providing experimental and relevant support.

Conflicts of Interest: The authors declare no conflicts of interest.

References

1. Araujo, A.S.F.; de Medeiros, E.V.; da Costa, D.P.; Pereira, A.P.D.; Mendes, L.W. From desertification to restoration in the Brazilian semiarid region: Unveiling the potential of land restoration on soil microbial properties. *J. Environ. Manag.* **2024**, *351*, 119746. [CrossRef] [PubMed]
2. Miao, R.H.; Jiang, D.M.; Musa, A.; Zhou, Q.L.; Guo, M.X.; Wang, Y.C. Effectiveness of shrub planting and grazing exclusion on degraded sandy grassland restoration in Horqin sandy land in Inner Mongolia. *Ecol. Eng.* **2015**, *74*, 164–173. [CrossRef]
3. Zhao, H.L.; Zhou, R.L.; Su, Y.Z.; Zhang, H.; Zhao, L.Y.; Drake, S. Shrub facilitation of desert land restoration in the Horqin Sand Land of Inner Mongolia. *Ecol. Eng.* **2007**, *31*, 1–8. [CrossRef]
4. Hai, L.; Zhou, M.; Zhao, K.; Hong, G.; Li, Z.; Liu, L.; Gao, X.; Li, Z.; Li, F. Soil microbial communities and their relationship with soil nutrients in different density *Pinus sylvestris* var. *mongolica* plantations in the Mu Us Sandy Land. *Forests* **2025**, *16*, 547. [CrossRef]
5. Bailey, J.K.; Schweitzer, J.A. The rise of plant-soil feedback in ecology and evolution. *Funct. Ecol.* **2016**, *30*, 1030–1031. [CrossRef]
6. Dostal, P. The temporal development of plant-soil feedback is contingent on competition and nutrient availability contexts. *Oecologia* **2021**, *196*, 185–194. [CrossRef]
7. Marasco, R.; Ramond, J.B.; Van Goethem, M.W.; Rossi, F.; Daffonchio, D. Diamonds in the rough: Dryland microorganisms are ecological engineers to restore degraded land and mitigate desertification. *Microb. Biotechnol.* **2023**, *16*, 1603–1610. [CrossRef]
8. Bennett, J.A.; Klironomos, J. Mechanisms of plant-soil feedback, interactions among biotic and abiotic drivers. *New Phytol.* **2019**, *222*, 91–96. [CrossRef]
9. Chung, Y.A.; Collins, S.L.; Rudgers, J.A. Connecting plant-soil feedbacks to long-term stability in a desert grassland. *Ecology* **2019**, *100*, e02756. [CrossRef]
10. De Souza, T.A.F.; de Andrade, L.A.; Freitas, H.; Sandim, A.D. Biological invasion influences the outcome of plant-soil feedback in the invasive plant species from Brazilian semi-arid. *Microb. Ecol.* **2018**, *76*, 102–112. [CrossRef] [PubMed]
11. Gundale, M.J.; Kardol, P. Multi-dimensionality as a path forward in plant-soil feedback research. *J. Ecol.* **2021**, *109*, 3446–3465. [CrossRef]
12. Rillig, M.C.; Ryo, M.; Lehmann, A.; Aguilar-Trigueros, C.A.; Buchert, S.; Wulf, A.; Iwasaki, A.; Roy, J.; Yang, G.W. The role of multiple global change factors in driving soil functions and microbial biodiversity. *Science* **2019**, *366*, 886. [CrossRef]
13. De Long, J.R.; Fry, E.L.; Veen, G.F.; Kardol, P. Why are plant–soil feedbacks so unpredictable, and what to do about it? *Funct. Ecol.* **2019**, *33*, 118–128. [CrossRef]

14. Lekberg, Y.; Bever, J.D.; Bunn, R.A.; Callaway, R.M.; Hart, M.M.; Kivlin, S.N.; Klironomos, J.; Larkin, B.G.; Maron, J.L.; Reinhart, K.O.; et al. Relative importance of competition and plant–soil feedback, their synergy, context dependency and implications for coexistence. *Ecol. Lett.* **2018**, *21*, 1268–1281. [CrossRef] [PubMed]
15. Araujo, A.S.F.; Zhao, T.C.; Pellizzer, E.P.; de Medeiros, E.V.; da Costa, D.P.; Mendes, L.W.; Melo, V.M.M.; Pereira, A.P.D.; Salles, J.F. Restoration strategies shape ecological processes driving dominant and rare bacterial communities in soils under desertification in the Brazilian semiarid. *J. Environ. Manag.* **2026**, *397*, 128351. [CrossRef] [PubMed]
16. In 't Zand, D.; Herben, T.; van den Brink, A.; Visser, E.J.W.; de Kroon, H. Species abundance fluctuations over 31 years are associated with plant-soil feedback in a species-rich mountain meadow. *J. Ecol.* **2021**, *109*, 1511–1523. [CrossRef]
17. Yang, B.; Zhai, J.; He, M.; Ma, R.; Li, Y.; Zhang, H.; Guo, J.; Hu, Z.; Zhang, W.; Bai, J. Linking soil properties and bacterial communities with organic matter carbon during vegetation succession. *Plants* **2025**, *14*, 937. [CrossRef]
18. Araujo, A.S.F.; de Medeiros, E.V.; da Costa, D.P.; Mendes, L.W.; Cherubin, M.R.; Neto, F.D.; Beirigo, R.M.; Lambais, G.R.; Melo, V.M.M.; Nobrega, G.G.; et al. Caatinga Microbiome Initiative: Disentangling the soil microbiome across areas under desertification and restoration in the Brazilian drylands. *Restor. Ecol.* **2025**, *33*, e14298. [CrossRef]
19. Han, C.; Liang, D.; Zhou, W.; Xu, Q.; Xiang, M.; Gu, Y.; Siddique, K.H.M. Soil, plant, and microorganism interactions drive secondary succession in alpine grassland restoration. *Plants* **2024**, *13*, 780. [CrossRef]
20. Cao, C.; Zhang, Y.; Cui, Z. Successions of bacterial and fungal communities in biological soil crust under sand-fixation plantation in Horqin Sandy Land, Northeast China. *Forests* **2024**, *15*, 1631. [CrossRef]
21. Zhang, Y.; Yu, L.; Liang, C.P.; Feng, S.W.; Cao, C.Y. Effects of artificial sand-fixing plantations on ammonia-oxidizing bacterial community in Horqin Sand Land. *Chin. J. Ecol.* **2019**, *38*, 3235–3244. [CrossRef]
22. Koorem, K.; Snoek, B.L.; Bloem, J.; Geisen, S.; Kostenko, O.; Manrubia, M.; Ramirez, K.S.; Weser, C.; Wilschut, R.A.; van der Putten, W.H. Community-level interactions between plants and soil biota during range expansion. *J. Ecol.* **2020**, *108*, 1860–1873. [CrossRef] [PubMed]
23. Trivedi, C.; Delgado-Baquerizo, M.; Hamonts, K.; Lai, K.T.; Reich, P.B.; Singh, B.K. Losses in microbial functional diversity reduce the rate of key soil processes. *Soil Biol. Biochem.* **2019**, *135*, 267–274. [CrossRef]
24. Philippot, L.; Chenu, C.; Kappler, A.; Rillig, M.C.; Fierer, N. The interplay between microbial communities and soil properties. *Nat. Rev. Microbiol.* **2023**, *22*, 226–239. [CrossRef]
25. FAO; FAO/IUSS Working Group WRB. *World Reference Base for Soil Resources 2006*; World Soil Resources Reports; FAO: Rome, Italy, 2006; Volume 103.
26. Liu, Z.M.; Shou, W.K.; Qian, J.Q.; Wu, J.; Busso, C.A.; Hou, X.Z. Level of habitat fragmentation determines its non-linear relationships with plant species richness, frequency and density at desertified grasslands in Inner Mongolia, China. *J. Plant Ecol.* **2019**, *11*, 866–876. [CrossRef]
27. Lin, D.Y. *Guidance of Soil Science Experiment*; China Forestry Publishing House: Beijing, China, 2004; pp. 45–70.
28. Kandeler, E.; Gerber, H. Short-term assay of soil urease activity using colorimetric determination of ammonium. *Biol. Fertil. Soils* **1988**, *6*, 68–72. [CrossRef]
29. Tabatabai, M.A. Soil enzymes. In *Methods of Soil Analysis*; Page, A.L., Millar, E.M., Keeney, D.R., Eds.; ASA and SSSA: Madison, WI, USA, 1982; pp. 501–538.
30. Ladd, J.N.; Butler, J.H.A. Short-term assays of soil proteolytic enzyme activities using proteins and dipeptide derivatives as substrates. *Soil Biol. Biochem.* **1972**, *4*, 19–30. [CrossRef]
31. Perucci, P.; Casucc, C.; Dumontet, S. An improved method to evaluate the o-diphenol oxidase activity of soil. *Soil Biol. Biochem.* **2000**, *32*, 1927–1933. [CrossRef]
32. Xu, G.H.; Zheng, H.Y. *Manual of Analytical Methods of Soil Microorganism*; China Agriculture Press: Beijing, China, 1986; pp. 266–269.
33. Institute of Soil Science, Chinese Academy of Sciences (ISSCAS). *Methods on Soil Microorganism Study*; Science Press: Beijing, China, 1985; pp. 260–275.
34. Poly, F.; Ranjard, L.; Nazaret, S.; Gourbière, F.; Monrozier, L.J. Comparison of *nifH* gene pools in soils and soil microenvironments with contrasting properties. *Appl. Environ. Microbiol.* **2001**, *67*, 2255–2262. [CrossRef]
35. Rotthauwe, J.H.; Witzel, K.P.; Liesack, W. The ammonia monooxygenase structural gene amoA as a functional marker, Molecular fine-scale analysis of natural ammonia-oxidizing populations. *Appl. Environ. Microbiol.* **1997**, *63*, 4704–4712. [CrossRef]
36. Ragot, S.A.; Kertesz, M.A.; Bünemann, E.K. *phoD* alkaline phosphatase gene diversity in soil. *Appl. Environ. Microbiol.* **2015**, *81*, 7281–7289. [CrossRef] [PubMed]
37. Zhang, J.; Zhao, H.; Zhang, T.; Zhao, X.; Drake, S. Community succession along a chronosequence of vegetation restoration on sand dunes in Horqin Sandy Land. *J. Arid Environ.* **2005**, *62*, 555–566. [CrossRef]
38. De Long, J.R.; Heinen, R.; Jongen, R.; Hannula, S.E.; Huberty, M.; Kielak, A.M.; Steinauer, K.; Bezemer, T.M. How plant-soil feedbacks influence the next generation of plants. *Ecol. Res.* **2021**, *36*, 32–44. [CrossRef]
39. Wagg, C.; Schlaeppi, K.; Banerjee, S.; Kuramae, E.E.; van der Heijden, M.G.A. Fungal-bacterial diversity and microbiome complexity predict ecosystem functioning. *Nat. Commun.* **2019**, *10*, 4841. [CrossRef] [PubMed]

40. Aldorfová, A.; Knobová, P.; Münzbergová, Z. Plant-soil feedback contributes to predicting plant invasiveness of 68 alien plant species differing in invasive status. *Oikos* **2020**, *129*, 1257–1270. [CrossRef]
41. Zhang, J.Y.; Ai, Z.M.; Xu, H.W.; Liu, H.F.; Wang, G.L.; Deng, L.; Liu, G.B.; Xue, S. Plant-microbial feedback in secondary succession of semiarid grasslands. *Sci. Total Environ.* **2021**, *760*, 143389. [CrossRef]
42. Coleine, C.; Delgado-Baquerizo, M.; Diruggiero, J.; Guirado, E.; Harfouche, A.L.; Perez-Fernandez, C.; Singh, B.K.; Selbmann, L.; Egidi, E. Dryland microbiomes reveal community adaptations to desertification and climate change. *ISME J.* **2024**, *18*, wrae056. [CrossRef]
43. Dhawi, F. How Can we stabilize soil using microbial communities and mitigate desertification? *Sustainability* **2023**, *15*, 863. [CrossRef]
44. Cao, C.Y.; Zhang, Y.; Cui, Z.B.; Feng, S.W.; Wang, T.T.; Ren, Q. Soil bacterial community responses to revegetation of moving sand dune in semi-arid grassland. *Appl. Microbiol. Biotechnol.* **2017**, *101*, 6217–6228. [CrossRef]
45. Jangid, K.; Williams, M.A.; Franzluebbers, A.J.; Schmidt, T.M.; Coleman, D.C.; Whitman, W.B. Land-use history has a stronger impact on soil microbial community composition than aboveground vegetation and soil properties. *Soil Biol. Biochem.* **2011**, *43*, 2184–2193. [CrossRef]
46. Suleiman, A.K.A.; Manoeli, L.; Boldo, J.T.; Pereira, M.G.; Roesch, L.F.W. Shifts in soil bacterial community after eight years of land-use change. *Syst. Appl. Microbiol.* **2013**, *36*, 137–144. [CrossRef]
47. Junier, P.; Molina, V.; Dorador, C.; Hadas, O.; Kim, O.S.; Junier, T.; Witzel, K.P.; Imhoff, J.F. Phylogenetic and functional marker genes to study ammonia-oxidizing microorganisms (AOM) in the environment. *Appl. Microbiol. Biotechnol.* **2010**, *85*, 425–440. [CrossRef]
48. Ragot, S.A.; Huguenin-Elie, O.; Kertesz, M.A.; Frossard, E.; Bunemann, E.K. Total and active microbial communities and *phoD* as affected by phosphate depletion and pH in soil. *Plant Soil* **2016**, *408*, 15–30. [CrossRef]
49. Turner, B.L.; Cheesman, A.W.; Condron, L.M.; Reitzel, K.; Richardson, A.E. Introduction to the special issue, developments in soil organic phosphorus cycling in natural and agricultural ecosystems. *Geoderma* **2015**, *257*, 1–3. [CrossRef]
50. Zehr, J.P.; Jenkins, B.D.; Short, S.M.; Steward, G.F. Nitrogenase gene diversity and microbial community structure, a cross-system comparison. *Environ. Microbiol.* **2003**, *5*, 539–554. [CrossRef] [PubMed]
51. Wang, Z.Q.; Zhang, Y.; Wang, Y.; Cui, Y.N.; Cao, C.Y. Effects of revegetation on soil nitrogen-fixation and carbon-fixation microbial communities in the Horqin Sandy Land, China. *Chin. J. Appl. Ecol.* **2024**, *35*, 31–40. [CrossRef]
52. Cheng, J.; Zhang, Y.; Wang, H.N.; Cui, Z.B.; Cao, C.Y. Sand-fixation plantation type affects soil phosphorus transformation microbial community in a revegetation area of Horqin Sandy Land, Northeast China. *Ecol. Eng.* **2022**, *180*, 106644. [CrossRef]
53. Hu, Y.J.; Xia, Y.H.; Sun, Q.; Liu, K.P.; Chen, X.B.; Ge, T.D.; Zhu, B.L.; Zhu, Z.K.; Zhang, Z.H.; Su, Y.R. Effects of long-term fertilization on *phoD*-harboring bacterial community in karst soils. *Sci. Total Environ.* **2018**, *628–629*, 53–63. [CrossRef]
54. Wakelin, S.A.; Macdonald, L.M.; Rogers, S.L.; Gregg, A.L.; Bolger, T.P.; Baldock, J.A. Habitat selective factors influencing the structural composition and functional capacity of microbial communities in agricultural soils. *Soil Biol. Biochem.* **2008**, *40*, 803–813. [CrossRef]
55. Mendes, L.W.; Brossi, M.J.D.; Kuramae, E.E.; Tsai, S.M. Land-use system shapes soil bacterial communities in Southeastern Amazon region. *Appl. Soil. Ecol.* **2015**, *95*, 151–160. [CrossRef]
56. Cao, C.Y.; Jiang, D.M.; Teng, X.H.; Jiang, Y.; Liang, W.J.; Cui, Z.B. Soil chemical and microbiological properties along a chronosequence of *Caragana microphylla* Lam. plantations in the Horqin Sandy Land of Northeast China. *Appl. Soil Ecol.* **2008**, *40*, 78–85. [CrossRef]

Disclaimer/Publisher's Note: The statements, opinions and data contained in all publications are solely those of the individual author(s) and contributor(s) and not of MDPI and/or the editor(s). MDPI and/or the editor(s) disclaim responsibility for any injury to people or property resulting from any ideas, methods, instructions or products referred to in the content.

agronomy

MDPI

Article

Quantitative and Qualitative Relationships between Phospholipid Fatty Acid Analysis Biomarkers and Lignin in Soil from the Tibetan Plateau (China) under Laboratory Incubation Conditions

Degyi Yangzom [1], Shuqin Ma [2,*] and Xuyang Lu [3,*]

[1] Xizang Autonomous Region Ecological and Environmental Monitoring Center, Lhasa 851414, China; degyi_yangzom@163.com
[2] School of Economic Geography, Hunan University of Finance and Economics, Changsha 410205, China
[3] Institute of Mountain Hazards and Environment, Chinese Academy of Sciences, Chengdu 610041, China
* Correspondence: mashuqin@hufe.edu.cn (S.M.); xylu@imde.ac.cn (X.L.)

Abstract: Lignin, an organic compound with a complex structure, is formed through the polymerization of structural units linked by carbon–carbon bonds and ether bonds. The question of whether lignin is labile or resistant to biological and chemical degradation in soil, particularly in alpine ecosystems, remains unresolved. To address this knowledge gap, we analyzed the relationship between phospholipid fatty acid biomarkers and the abundance of lignin components in grassland soils from North Tibet, China. Soil samples were collected from alpine grasslands, including alpine meadows and alpine steppes. The relative abundance of lignin in these alpine grassland soils before and after a 210-day incubation period was measured. Our results indicate that the relative abundance of lignin in the alpine grassland soils decreased during the incubation period. Significant relationships were found between the phospholipid fatty acid biomarkers of bacteria, fungi, Gram-positive bacteria, and Gram-negative bacteria and the relative abundance of lignin components. This research was conducted under laboratory conditions that are optimal for the development of microorganisms but significantly different from the conditions in Tibet. Furthermore, this study contributes to the understanding of soil organic matter degradation and the dynamics of microbial communities in alpine grassland soils in the context of future global warming.

Keywords: lignin; 2-methoxy-4-vinylphenol; phospholipid fatty acid; alpine steppe; alpine meadow

1. Introduction

Lignin is the second most abundant polymer compound in nature, and it is considered the most important aromatic resource in biomass energy [1,2]. It is a type of renewable natural aromatic macromolecule polymer, containing guaiacyl, syringyl, and p-hydroxyphenyl propane monomers [3]. These monomers represent different lignin types, vegetation, and environments. Studies have shown that the syringyl propane monomer is the dominant component of lignin in forest soil and that the guaiacyl propane monomer is the main component of lignin in grassland soil [4,5]. The composition of lignin in soil reflects the degradation of plant debris, and studying the lignin in soils can help us understand the soil organic matter composition in different environments.

Lignin is considered to be resistant to biological and chemical degradation due to its complex structure [6,7]. Fungi, including brown-, white-, and soft-rot fungi, dominate the depolymerization process of lignin macromolecules in soil [8]. These fungi have unique physiological and biochemical mechanisms and strong metabolic abilities, and they mineralize lignin into carbon dioxide and water [9]. However, bacteria can also degrade lignin in the soil through the action of enzymes, such as laccase and peroxidase [10]. Therefore, lignin can be degraded by microbes in some environments, and lignin degradation and the

related microbial mechanisms need to be studied in order to obtain a better understanding of the degradation of soil organic matter.

Some studies have reported microbial mechanisms in lignin degradation in soils. These studies have indicated that more than 90% of the known wood-rotting species are white-rot fungi [11]. In the process of lignin degradation, fungi first become adsorbed on the end of lignin and then extend into the interior, where lignin-degrading enzymes are secreted, thus degrading lignin from the inside to the outside [12]. However, white-rot fungi cannot mediate lignin decomposition and transformation alone. Lignin degradation results from the combined action of various bacteria and fungi in the soil [13–15]. Lignin-degrading bacteria can be divided into three categories: actinibacteria, α-proteobacteria, and γ-proteobacteria. Among prokaryotes, one of the most commonly identified and studied lignolytic enzymes is laccase [16,17]. Phylogeny has shown that many strains with laccase genes occur in proteobacteria, actinobacteria, and firmicutes [18]. The apical and branching growth of these bacteria and the formation and development of airborne or stromal hyphae lead them to resemble fungi. Recent studies by Rashid et al. [19] showed that superoxide manganese dismutase produced by *Sphingobacterium* (bacteroides) could oxidize lignin through a hydroxyl radical mechanism. In the composting process, actinibacteria can decompose organic matter in the initial stages and decolorize refractory organic matter such as lignin in the later stages. It appears that actinibacteria can enter the interior of refractory lignin and increase its water solubility.

The Tibetan Plateau is known as the third "pole" of the world. Due to the high altitude, it is colder than anywhere else outside the polar regions. In order to adapt to such an extreme environment, the physiological structure and activity mode and microorganisms in soil may be quite unique [20–22]. The composition and transformation of soil organic matter in the alpine grassland in this area may be affected by the extreme climate [23]. However, the relationship between the soil microbial community and lignin, which is part of the chemical composition of soil organic matter, has not been reported in Northern Tibet. The lignin components in soil from alpine meadow and alpine steppe were analyzed using pyrolytic gas chromatography–mass spectrometry (Py-GC/MS). The purpose of this study was to compare the lignin content in soil organic matter in different alpine grasslands under the extreme climatic conditions in the Tibetan Plateau and to explore the relationship between lignin content and soil microorganisms.

2. Materials and Methods

2.1. Study Area

Northern Tibet is located between the Kailas Range and Nyanqentanglala in the Tibet Autonomous Region, China [24]. It covers about 446,000 km^2 and approximately one-third of the total area of the Tibet Autonomous Region, with an average elevation of more than 4500 m [25,26]. Due to the high and complex terrain, this region is characterized by cold and drought [27]. The annual average temperature is about 0 °C (the coldest month is January, and the hottest month is July), and the average annual precipitation ranges from 247.3 to 513.6 mm [28,29]. Because of the vast territory and highly divided topography, this area has different climate and vegetation belts [20,30].

Alpine grasslands are the most widely distributed ecosystems in Tibet, China. Alpine grasslands cover more than 70% of the total area of the Tibetan Plateau [31]. This ecosystem is dominated by alpine steppe and alpine meadow. Alpine meadow occupies approximately 31.3% of the total grassland area, in which the main species is *Kobresia humilis*. Alpine meadows are mainly located in Ando and Damxung in Naqu region, with cold and wet climatic conditions. Alpine steppe, which comprises approximately 38.9% of the total grassland area, is the most widely distributed alpine grassland in Tibet. Alpine steppe is mainly located in Shenza in the Naqu region, with cold and arid/semi-arid climate conditions. The main species in this grassland are *Stipa purpura* and *Carex moorcroftii* [23].

2.2. Soil Sampling

In this study, ten sampling sites were selected in eight counties—Damxung, Naqu, Nyainrong, Ando, Shenza, Baingoin, Nyima, and Gêrzê—in the Tibet Autonomous Region of China. Two alpine grasslands, i.e., alpine meadow and alpine steppe (Figure 1), were selected in this region, and five sampling sites were selected in each grassland type. The coordinates of the sampling sites are listed in Table 1. Three 1 m × 1 m quadrats were laid out at each sample site, with intervals of approximately 50 m. We removed all aboveground plants, litter, and stone on the soil surface before sampling and collected the surface (0–15 cm) soils in each quadrat. Soils from three quadrats were mixed well as a soil sample [30]. In addition, global positioning system (GPS) (Garmin MAP62CSX made in Garmin Ltd., Olathe, KS, USA) was used to measure the location and elevation of each site.



Figure 1. Photographs of the studied areas.

Table 1. Coordinates of the sampling sites.

Sample Sites	East Longitude	North Latitude
Alpine meadow site 1	91.1115°	30.7499°
Alpine meadow site 2	91.9799°	31.3774°
Alpine meadow site 3	92.0694°	31.7286°
Alpine meadow site 4	91.7296°	31.7164°
Alpine meadow site 5	88.6991°	30.9571°
Alpine steppe site 1	90.7768°	31.3887°
Alpine steppe site 2	88.6999°	31.1236°
Alpine steppe site 3	87.4833°	31.5048°
Alpine steppe site 4	86.5031°	31.9320°
Alpine steppe site 5	85.3560°	32.0315°

2.3. Incubation Experiment

Alpine meadow and alpine steppe soils (100.0 g dry-weight) were placed in 250 mL triangular flasks for 210 days, and the soil moisture was adjusted to a 40% water-holding capacity and 25 °C to activate the soil microbes. The temperature and moisture were adapted to the optimum temperature and humidity for microorganisms during incubation [32,33]. For incubation, five experimental groups were selected from five alpine meadow sites, and five soil experimental groups were selected from five alpine steppe sites, with three replicates per experimental group. When all samples were ready, the quality of each triangular flask was labeled. To reduce humidity losses while ensuring adequate gas inside, all flasks were covered with a perforated, adherent film. When the quality of the triangular flasks decreased, water was added to the soil along the flask borders every three days to maintain constant soil moisture. After 210 days of incubation, all incubation samples were harvested using the destructive method.

2.4. Pyrolysis Gas Chromatography–Mass Spectrometry

The soil samples were analyzed for lignin components using pyrolysis gas chromatography–mass spectrometry (Py-GC/MS) technology. The Py-GC/MS operational process was conducted with reference to the methods outlined in the previously published literature [5]. The soil samples were passed through a 2 mm mesh sieve and air-dried in the shade. The lignin components were identified using a pyrolyzer (CDS5200, CDS company, Oxford, PA, USA). The procedure involved placing 25 mg of soil into quartz tubes, which had a length of 2 cm and an inside diameter of 2 mm. Then, the soil samples were heated from ambient to 700 °C for 15 s at 20 °C/ms using a Mettler microbalance (Mettler–Toledo, Greifensee, Switzerland). The pyrolyzer was used with a PerkinElmer Clarus680GC-SQ8MS System (PerkinElmer, Santa Clara, CA, USA) to pyrolyze the soil samples at a high temperature in order to obtain different compounds. The operation procedure was as follows: the temperature of the gas chromatograph was maintained at 40 °C for 3 min, increased to 280 °C at a rate of 10 °C/min, and maintained for 5 min. Helium was the carrier gas. The injector temperature was 280 °C. In the electron shock mode, the temperature of the ion source of the mass spectrometry indicator was maintained at 250 °C, and it operated at an electron energy of 70 eV.

The NIST 2014 library was used to identify the pyrolysis products, as well as reports from other researchers [5,34,35]. The pyrolysis products were identified as compounds when the surface of two characteristic ion fragments of the pyrolysis products were the same as the compounds in the NIST 2014 library. The relative percentage of lignin compounds was calculated according to the proportion of the peak area of lignin pyrolysis compounds to all the peaks measured in the chromatogram. Therefore, the relative peak area of lignin compounds was calculated by normalizing results to the all the peaks measured in the chromatogram.

2.5. Phospholipid Fatty Acid Analysis

All soil samples were stored in sealed bags at 4 °C before measurement. Lipids were extracted using one-phase chloroform, water extractant, and methanol from soils. Then, using a silicic acid column, they were fractionated into neutral lipids, phospholipids, and glycolipids. The quantification of phospholipid fatty acids (PLFAs) was conducted using gas chromatography (GC Agilent 6890-Agilent Technology, Santa Clara, CA, USA) technology, coupled with an HP7673 auto-sampler, a split injector, and a flame ionization detector (FID). The carrier gas was helium. It was operated with a pressure of 35 psi and a flow rate of 0.8 mL min^{-1}. The detector temperature was 300 °C, and the injector temperature was 250 °C [36].

X: YωZ were used to designate phospholipid fatty acids. In the formula, X is the number of carbon bonds, Y is the number of unsaturated olefinic bonds, Z represents the keys or cyclopropane chain location, and ω is the end of methyl. In addition, i (iso) and a (anteriso) represent the branching chain; 10 Me represents the methyl group, which is tenth at the end of the pitch molecule carbon chain; and cy is a cyclopropyl group. The biomarkers used for each group of microorganisms were determined based on specific works in the research literature [37]. Bacterial PLFAs were estimated as the sum of i13:0, 14:0, i14:0, i15:0, a15:0, i15:1G, 16:0, i16:0, 16:1 2OH, 16:1G, 16:1ω5c, 16:1ω9c, i17:0, a17:0, cy17:0, 17:1ω8c, 18:1ω5c, 18:0, and cy19:0ω8c. In addition, 18:1ω9c and 20:1ω9c represent fungal PLFA biomarkers and 10Me17:0 and 10Me18:0 represent the actinobacteria groups. The Gram-positive bacterial PLFAs included 13:0 anteiso, 14:0, 14:0 iso, 15:0 anteiso, 15:0 iso, 15:1 iso G, 16:0 iso, 16:1 2OH, 16:1 iso G, 17:0 anteiso, and 17:0 iso. The Gram-negative bacterial PLFAs contained 16:1ω5c, 16:1ω9c, 17:0 cyclo, 17:1ω8c, 18:0, 18:1ω5c, and 19:0 cyclo ω8c. The soil microbial PLFAs are expressed as the absolute abundance of PLFA biomarkers of microorganisms in nmol/g. The microbial biomass was calculated using the sum of the absolute abundances of PLFAs. PLFAs that were present in >3 samples were selected for analysis [27].

2.6. Statistical Analysis

All statistical analyses were conducted using SPSS 20.0 (IBM, Chicago, IL, USA, 2011), and the significance level was $p < 0.05$. The differences in soil lignin and PLFA in soils from alpine meadow and alpine steppe were determined using an independent sample *t* test. The lignin relative abundance and soil microbial characteristics were subjected to a correlation analysis. All figures were developed using Sigmaplot® Version 10 software (Systat Software Inc., Chicago, IL, USA, 2007). A principal component analysis was conducted using Canoco 5.

3. Results

3.1. The Relative Abundance of Lignin in Alpine Grassland Soils

A total of 20 samples, comprising 5 alpine meadow soil samples and 5 alpine meadow soil samples before and after incubation, were analyzed using Py-GC/MS. The results showed that the relative abundance of lignin in the alpine meadow soil was significantly higher than that in the alpine steppe soil (Table 2). A comparison of the lignin before and after the experiment showed that its relative abundance decreased significantly in the alpine meadow soil, with values of 4.71% ± 1.04% and 1.32% ± 0.58%, respectively ($p < 0.05$) (Table 2). However, the relative abundance of lignin showed no significant change in the alpine steppe soil before and after the experiment ($p > 0.05$) (Table 2). The lignin components detected in the two types of alpine grassland soils are shown in Figure 2. Seven compounds with lignin as their precursor material were detected in the alpine grassland soils: 1-butanol, 2-ethyl-; 1-pentanol, 2-methyl-; 3-hexyne-2,5-diol; 3,5-hexadien-2-ol; 2-methoxy-4-vinylphenol; ethanol, 2-[2-(2-butoxyethoxy)ethoxy]-; and benzenemethanol, α-ethyl-4-methoxy- (Figure 2). The result showed that the relative abundance of 2-methoxy-4-vinylphenol increased and that the relative abundance of 1-pentanol, 2-methyl-, and benzenemethanol, α-ethyl-4-methoxy- decreased in the alpine grassland soils (Table 3; Figure 3).

Table 2. The relative abundance of lignin in alpine grassland soils before and after incubation.

Grassland Type	Alpine Meadow	Alpine Steppe
Before	4.71% ± 1.04% Aa	1.66% ± 1.39% Ba
After	1.32% ± 0.58% Ab	1.56% ± 2.42% Aa

Data are presented as the mean value and standard error of the relative abundance of lignin in soil. Different uppercase letters indicate a significant difference between alpine meadow and alpine steppe soil at $p < 0.05$. Different lowercase letters indicate a significant difference before and after the incubation of alpine grassland soil at $p < 0.05$.

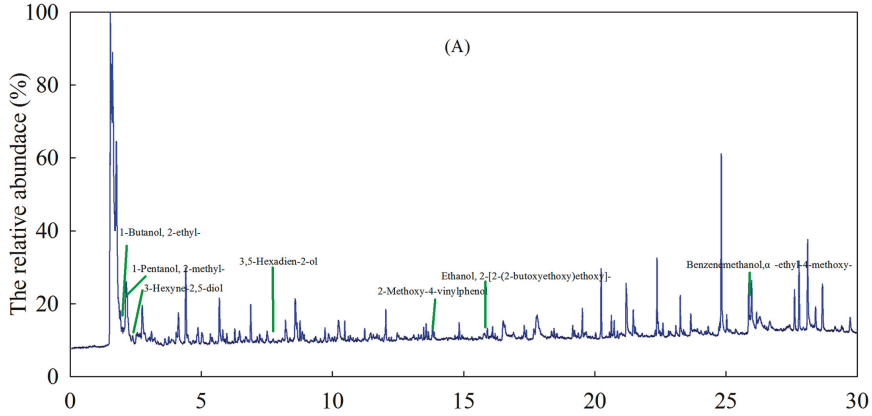


Figure 2. *Cont.*

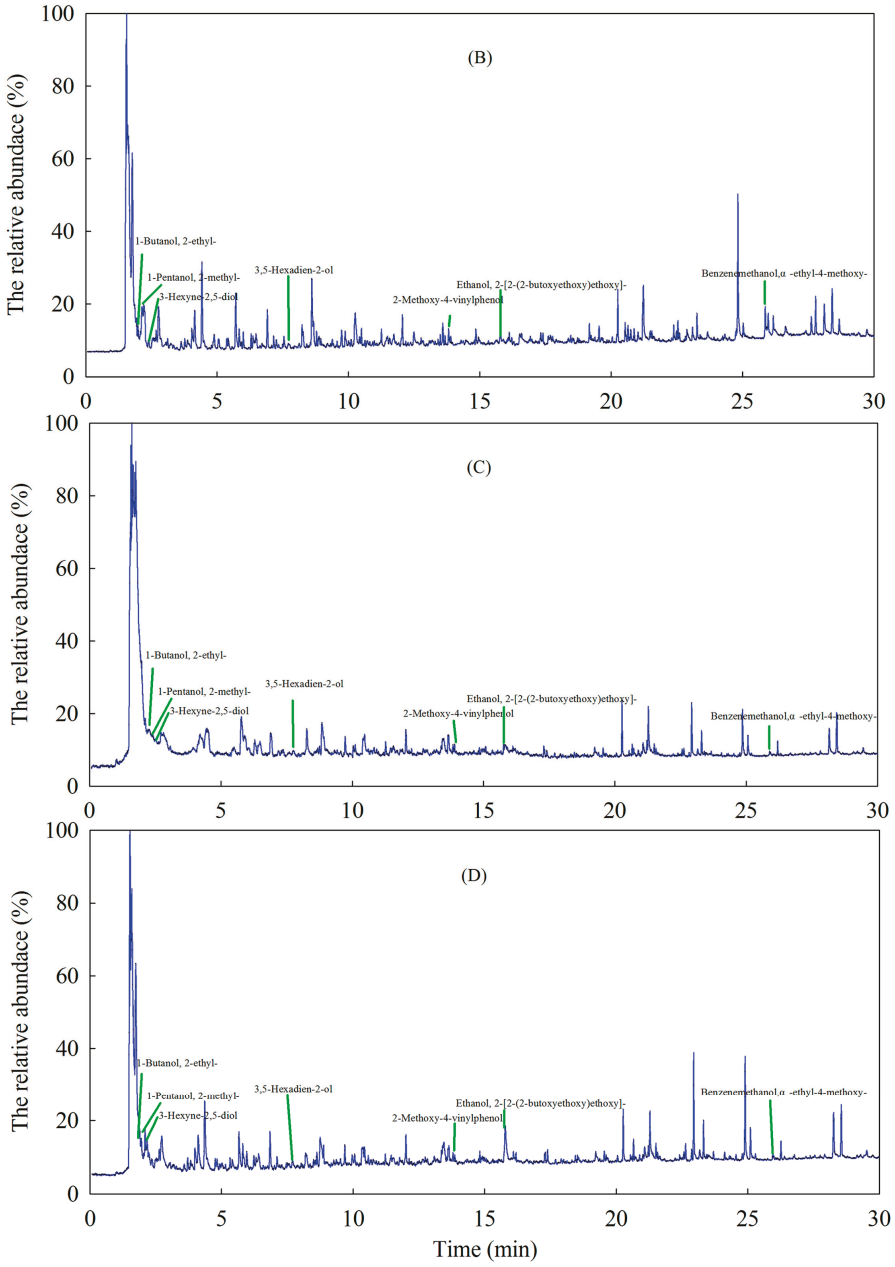


Figure 2. The dominant compositions of lignin in alpine grassland soils based on pyrolysis gas chromatography–mass spectrometry. (**A**) The alpine meadow soil before incubation; (**B**) the alpine steppe soil before incubation; (**C**) the alpine meadow soil after incubation; (**D**) the alpine steppe soil after incubation.

Table 3. Lignin components in alpine grassland soils before and after incubation.

	Component/%	Alpine Meadow					Alpine Steppe				
		AM1	AM2	AM3	AM4	AM5	AS1	AS2	AS3	AS4	AS5
Before	1-Butanol, 2-ethyl-	4.34	4.78	5.71	9.20	3.29	6.10	11.04	12.85	12.12	6.92
	1-Pentanol, 2-methyl-	40.63	29.17	30.15	33.03	24.63	24.99	19.44	18.60	18.13	4.81
	3-Hexyne-2,5-diol	0.00	22.59	26.12	27.39	28.33	26.80	18.21	18.41	19.15	16.89
	3,5-hexadien-2-ol	2.88	5.56	2.57	4.08	3.61	4.08	2.81	2.99	4.06	2.97
	2-Methoxy-4-vinylphenol	9.35	11.37	3.20	6.14	14.90	12.04	2.15	1.97	2.18	8.33
	Ethanol, 2-[2-(2-butoxyethoxy)ethoxy]-	4.56	4.33	2.70	4.45	5.12	5.44	3.29	2.47	4.63	2.80
	Benzenemethanol, α-ethyl-4-methoxy-	38.24	22.19	29.55	15.71	20.12	20.55	43.06	42.70	39.74	57.28

Table 3. *Cont.*

	Component/%	Alpine Meadow					Alpine Steppe				
		AM1	**AM2**	**AM3**	**AM4**	**AM5**	**AS1**	**AS2**	**AS3**	**AS4**	**AS5**
After	1-Butanol, 2-ethyl-	58.59	0.00	43.81	32.42	34.14	24.90	29.14	7.06	10.59	38.96
	1-Pentanol, 2-methyl-	0.00	0.00	32.28	26.18	23.29	18.79	31.50	23.45	18.52	18.19
	3-Hexyne-2,5-diol	0.00	0.00	3.46	2.66	2.85	9.12	3.62	30.59	28.59	17.49
	3,5-hexadien-2-ol	7.22	0.00	0.00	5.23	4.66	5.41	6.93	12.07	7.48	2.98
	2-Methoxy-4-vinylphenol	13.03	52.54	3.96	8.20	13.12	7.59	3.23	4.62	7.48	5.21
	Ethanol, 2-[2-(2-butoxyethoxy)ethoxy]-	14.81	47.46	11.40	20.30	15.84	28.92	20.83	15.84	23.01	6.10
	Benzenemethanol, α-ethyl-4-methoxy-	6.35	0.00	5.08	5.01	6.09	5.26	4.74	6.36	4.34	11.06

Data are presented as the percentage of each component in lignin. AM, alpine meadow; AS, alpine steppe. Numbers 1 to 5 represent the five soil samples.

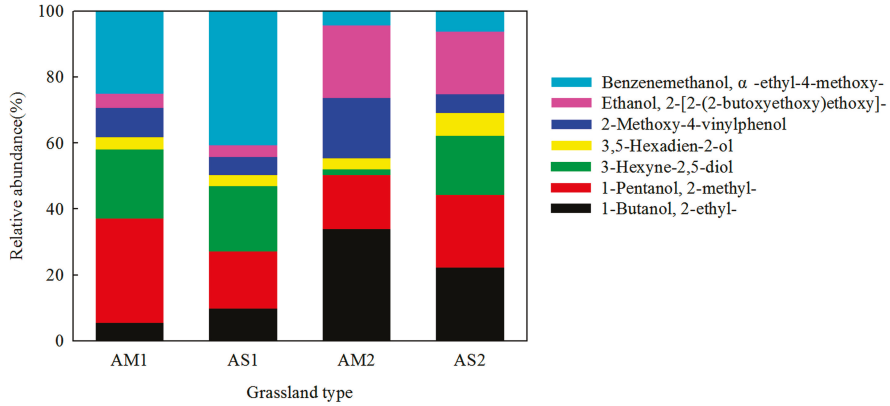


Figure 3. The compositions of lignin in alpine grassland soils before and after incubation. AM1 and AS1 are alpine meadow and alpine steppe before incubation; AM2 and AS2 are alpine meadow and alpine steppe after incubation.

3.2. Phospholipid Fatty Acid Analysis

The absolute abundance of phospholipid fatty acids (PLFAs) in the alpine grassland soils is presented in Table 4. A significant difference was observed in the microbial PLFA biomarkers in the alpine meadow soil and alpine steppe soil, as illustrated in Figure 4. The levels of PLFA biomarkers of bacteria, fungi, actinibacteria, Gram-positive bacteria, and Gram-negative bacteria were significantly higher in the alpine meadow soils than in the alpine steppe soils (Table 4). Similarly, the fungal PLFA biomarker content in the alpine meadow soils was higher than that in the alpine steppe soils (Table 4). Overall, the total PLFA content, which serves as a proxy for the total microbial biomass, was approximately twice as high in the alpine meadow soils than in the alpine steppe soils (Table 4). The alpine grassland soil PLFAs mainly contained 18:1ω9c (fungi) and 16:0 (bacteria), with a relative abundance of more than 10% in the total PLFA. Also, 19:0 and 15:0 anteiso (bacteria) were more abundant in the alpine meadow than in the alpine steppe (Figure 4).

Table 4. The phospholipid fatty acid biomarkers in alpine grassland soils.

PLFA Biomarkers/nmol g^{-1}	Grassland Type	
	Alpine Meadow	**Alpine Steppe**
Bacteria	23.64 ± 3.06 a	11.50 ± 1.51 b
Fungal	3.70 ± 0.54 a	2.03 ± 0.31 b
Actinibacteria	1.96 ± 0.27 a	1.22 ± 0.15 b
Gram-positive bacteria	10.92 ± 1.29 a	5.26 ± 0.63 b
Gram-negative bacteria	6.14 ± 0.86 a	3.14 ± 0.43 b
Total PLFAs	46.37 ± 5.16 a	23.96 ± 3.07 b

Data are presented as the mean value and standard error. Different lowercase letters indicate a significant difference between the alpine meadow and alpine steppe soils at $p < 0.05$.

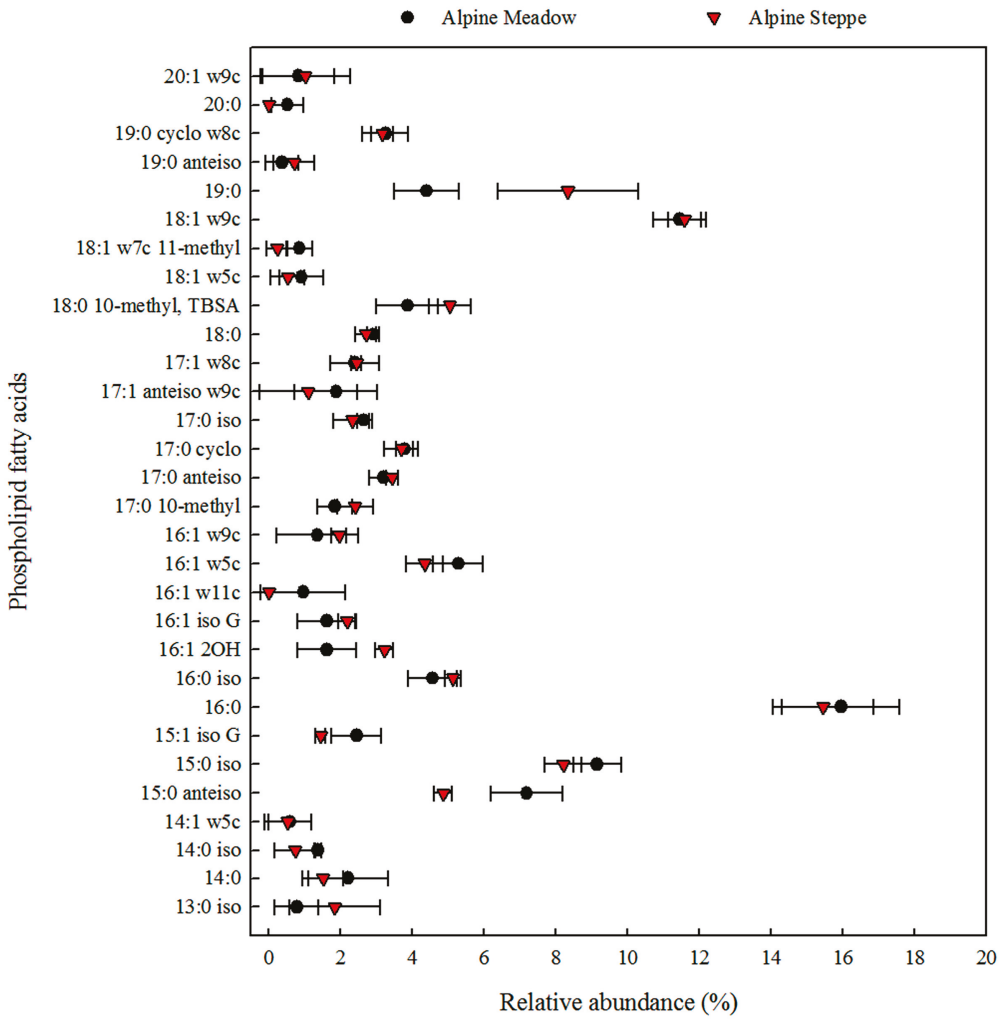


Figure 4. The relative abundance of phospholipid fatty acids in alpine grassland soils.

3.3. The Relationship between Lignin and Phospholipid Fatty Acids

The correlation analysis showed that the relative abundance of lignin components had a significant effect on the PLFA biomarkers (Figures 5 and 6). The results showed that the relative abundance of lignin was significantly correlated with the PLFA biomarkers of bacteria, fungi, Gram-positive bacteria, and Gram-negative bacteria (Figure 5). Nevertheless, the relative abundance of lignin components was not correlated with the PLFA biomarkers of actinibacteria (Figure 6). The results showed that 2-methoxy-4-vinylphenol was significantly correlated with the total PLFAs; ethanol, 2-[2-(2-butoxyethoxy)ethoxy]- and 3-hexyne-2,5-diol were significantly correlated with the PLFA biomarkers of fungi and bacteria; and 3,5-hexadien-2-ol and 1-pentanol, 2-methyl- were significantly correlated with the PLFA biomarkers of Gram-positive bacteria and Gram-negative bacteria (Figure 6).

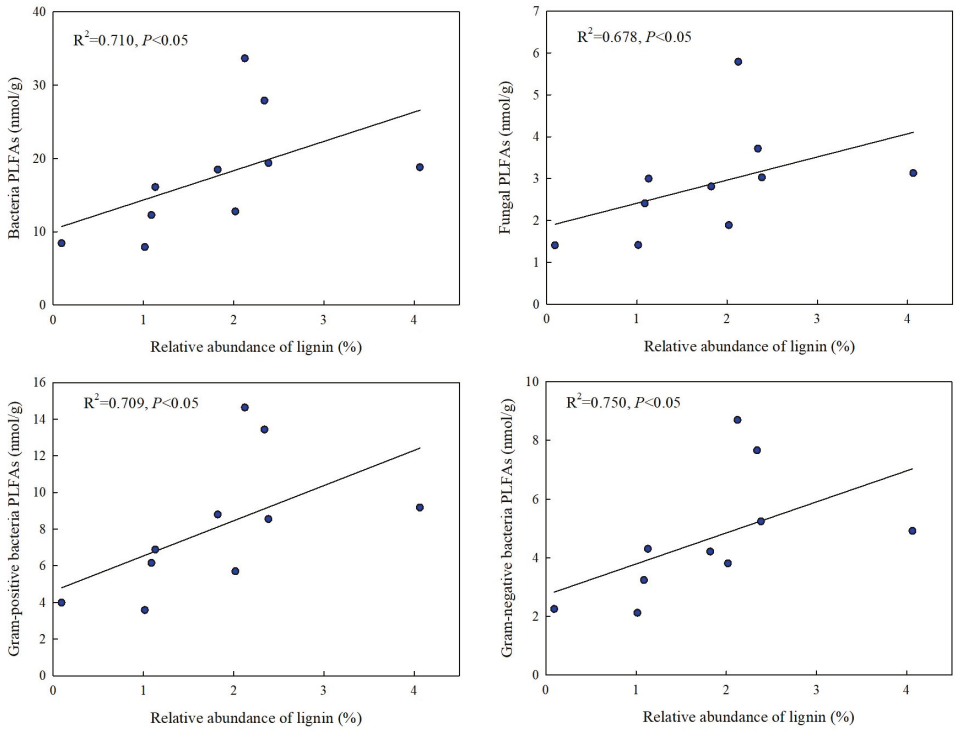


Figure 5. The correlations between lignin and soil PLFA biomarkers in alpine grassland soils.

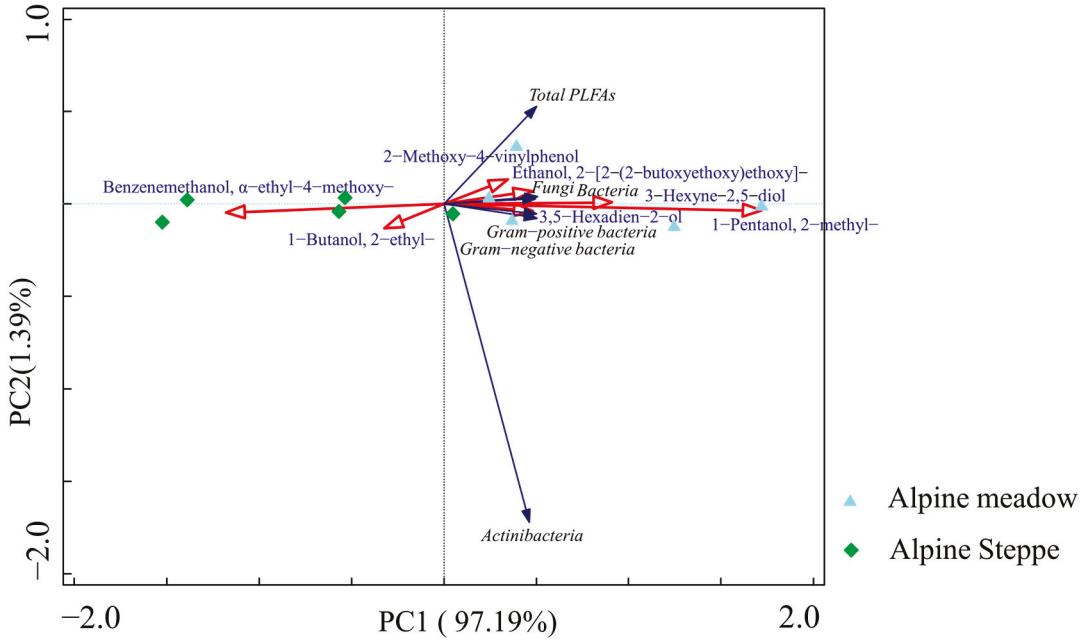


Figure 6. Principal component analysis of lignin and PLFAs in alpine grassland soils. PLFA, phospholipid fatty acid.

4. Discussion

Lignin is a major component of plants and contributes significantly to the soil organic carbon pool [38]. In addition, lignin biomarkers can reflect the vegetation type due to plant-released monomers with a vanillyl or syringyl group (depending on the lignin type), and differences between gymnosperms, angiosperms, and grasses can be detected [15,16]. Studies have indicated that the syringyl propane monomer is the dominant component of lignin in soil in forest ecosystems and that the guaiacyl propane monomer is the main component

in grassland ecosystems [5]. Vancampenhout et al. [39] provided similar evidence regarding the role of biomarkers in terms of lignin. They showed that the lignin compounds in soil under coniferous vegetation were mainly dominated by guaiacol (coniferyl-derived), while both guaiacol and syringol (sinapyl-derived) compounds were present in broadleaved forests. In this study, guaiacols, such as 2-methoxy-4-vinylphenol, were detected as lignin components, but no syringyl groups were detected (Table 3 and Figure 3). In fact, guaiacyl-type lignins have a higher resistance to biodegradation than syringyl-type lignins due to the higher degree of internal cross-linking [39]. Because of its recalcitrant nature and biomarkers, lignin is useful for studying land-use history, as reflected in the soil. Therefore, 2-methoxy-4-vinylphenol, which is a member of the guaiacol group, was preserved in the soil as a stable lignin material, and it may be an indicator of alpine grassland soil.

Scientists have found that lignin differs considerably between litters and soils, and elevation and vegetation can affect the abundance of lignin in soils [40,41]. For instance, the syringyl propane monomer is the dominant component in lignin in soil in forest ecosystems, and the guaiacyl propane monomer is the main component in lignin in soil in grassland ecosystems [35]. Lignin is dominated by guaiacol (up to 3%) in secondary succession in *Imperata* grassland soil [5]. In this study, the relative abundance of lignin was lower in the alpine steppe soils than in the alpine meadow soils. This may be due to the lower number of plant species and plant biomass in the alpine steppe [20,24]. In addition, 2-methoxy-4-vinylphenol, a type of guaiacyl propane lignin, was the dominant product in the alpine grassland soils. This finding is supported by the findings of Yassir and Buurman [5] and Nierop et al. [42]. During the incubation experiment, the relative abundance of 2-methoxy-4-vinylphenol increased in most samples (Table 3 and Figure 3). Therefore, this result suggests that 2-methoxy-4-vinylphenol can be stored in soil for a long time and is not easily broken down, thus indicating lignin in alpine grassland soils.

Lignin has been considered to be more recalcitrant than other organic matter (cellulose) in soils because it has a complex structure that includes multiple monomers connecting carbon–carbon and ether bonds [41]. However, new evidence has indicated that lignin can be degraded by microbes under some pedoclimatic conditions [43,44]. Martin and Haider [45,46] studied lignin decomposition in soils with different properties and vegetation types, and they showed that the initial amount of synthetic 14C-DHP lignin decreased by 19~60% after 13 weeks to 2 years. The degradation of lignin was also observed in field studies [6,47]. These studies indicated that the degraded lignin in litter constituted between 48% and 87% of the initial content after five years [6]. A decrease in lignin has been observed in agricultural soil. For example, lignin was more rapidly degraded than bulk soil organic matter [48,49], especially under low acidic pH conditions [39,50,51]. Kögel [52] found that lignin is significantly decreased at the transition to mineral soil in forests. Kiem and Kögel-Knabner [53] indicated that lignin is not part of the hard-to-degrade pool in temperate arable soils. A study on secondary succession in *Imperata* grassland soil also indicated that lignin underwent decomposition [5], and it showed that lignin, including 4-vinylphenol and 4-vinylguaiacol, is significantly higher in litter than in soils. These reports indicate that 4-vinylphenol can be retained in soil and is a component of plant matter. Is lignin recalcitrant or decomposed in soil? Based on this question, we incubated alpine meadow and alpine steppe soils and studied the changes in the lignin components in them. The result showed that the relative abundance of lignin decreased significantly in the alpine meadow soils (Table 2). In addition, the relative abundance of lignin components, including benzenemethanol, α-ethyl-4-methoxy-, and 1-pentanol, 2-methyl-, significantly decreased in the alpine meadow soils. However, the relative abundance of ethanol 2-[2-(2-butoxyethoxy)ethoxy]- increased during incubation (Table 3 and Figure 3). This is similar to the reports by Dao et al. [54]. They focused on lignin decomposition in the soil of the Northern Siberian tundra and discovered that the neutral sugars contained within lignin were more susceptible to degradation. Therefore, perhaps benzenemethanol, α-ethyl-4-methoxy-, and 1-pentanol, 2-methyl- are decomposed and utilized by microorganisms. They were not recalcitrant in the alpine meadow soil.

The activity of soil microbes, which produce necessary extracellular enzymes, is an important factor regulating the biological decomposition of lignin [41]. In general, white-rot fungi degrade lignin by secreting extracellular enzymes into the soil. Grandy et al. [55] found that b-1,4-N-acetyl-glucosaminidase was positively related to lignin in the light fraction in alpine and forest ecosystems, and they indicated that fungi could degrade lignin by secreting enzymes. Lignin degradation is, in fact, the result of combined fungal and bacterial activities. Some studies have shown that bacteria, including α-proteobacteria, actinibacteria, and γ-proteobacteria, can degrade lignin by secreting laccase [40]. How do the different types of bacteria, including aerobic, anaerobic, and extreme bacteria, degrade lignin? The complexity and heterogeneity of the lignin structure hinder its efficient utilization. In this study, we found that the PLFA biomarkers of bacteria, fungi, Gram-positive bacteria, and Gram-negative bacteria were significantly correlated with lignin in alpine grassland soils (Figure 5). 1-pentanol, 2-methyl decreased (Figure 3) and was significantly correlated with the PLFA biomarkers of bacteria, Gram-positive bacteria, and Gram-negative bacteria (Figure 6). This indicates that 1-pentanol, 2-methyl may have been used by bacteria in the alpine grassland soil during incubation. Researchers have found that bacteria can secrete enzymes, such as 3,4-dioxygenase, hydroxyquinol 1,2-dioxygenase, and 1,2-dioxygenase, which can reveal the lignin components [56,57]. While this study did not measure the relevant enzymes as direct evidence of the bacterial decomposition of lignin compounds, the correlation between the PLFA biomarkers of microorganisms and lignin components, as well as previous research [58], implicitly demonstrates the potential for lignin components to be utilized by microorganisms. Thus, 1-pentanol, 2-methyl could have been degraded and provided important food for microbes by secreting enzymes in the alpine meadow and alpine steppe soils. In addition, there was no correlation between the PLFA biomarkers of actinobacteria and the relative abundance of lignin components in this study (Figure 6). Although actinobacteria play an important role in soil ecosystems, they do not directly participate in the decomposition process of lignin [59]. The decomposition of lignin mainly relies on microorganisms such as bacteria, which possess specific decomposing enzymes. This finding is similar to that of Song et al. [60], Nagaraju et al. [61], and Thitinun et al. [62]. Focus should be placed on the abundance of functional bacteria and fungi, the composition of functional fungal communities, and the structure of the overall microbial community to jointly regulate the rate of lignin decomposition.

This study indicates that lignin components can be decomposed by microorganisms, as revealed by an analysis of lignin components in alpine grassland soils using Py-GC/MS. Studying the microbial degradation mechanism of lignin in the unique ecological environment of North Tibet, China, not only helps us gain a deeper understanding of soil nutrient characteristics but also provides important clues for exploring nutrient cycling patterns. Specifically, the question of whether lignin, as the second most abundant organic matter in the world [1], can be used by microorganisms has been a focus of study. However, lignin and soil organic matter degradation are highly impacted by microorganisms and environmental conditions, such as litter type, incubation temperature, and moisture [41]. We only described the factor of microorganisms in this study. Previous studies have also reported on environmental conditions. For example, on grasslands in the *Mediterranean*, it has been found that microbial communities have adapted to harsher conditions, and future climate change will affect plant biomass and enzyme activity, thereby influencing soil lignin decomposition and soil carbon storage mechanisms through temperature and humidity deviations [63]. So, what is the mechanism underlying the relationship between lignin decomposition and microorganisms in the alpine grassland in North Tibet, China? This will be the direction of our future research.

5. Conclusions

Lignin is known to be a recalcitrant compound. This study found that the relative abundance of lignin was significant and decreased in alpine grassland soils from North Tibet, China, after 210 days of incubation in a laboratory. The relative abundance of lignin

was significantly correlated with the abundance of the PLFA biomarkers of bacteria, fungi, Gram-positive bacteria, and Gram-negative bacteria. Our findings suggest that lignin can be degraded and form an important food source for microbes in alpine grassland soils.

The present study carried out preliminary research on lignin biodegradation in alpine grassland soils using incubation. However, it is difficult to determine which specific species or populations of microorganisms decompose lignin or fully understand the process of lignin degradation based on the data obtained in this study. In the future, extracellular enzyme activity around the microbes needs to be measured, and sufficient evidence of microbes degrading lignin needs to be provided. In addition, Py-GC/MS is an analytic technique that is used to calculate the relative abundance of lignin in soil organic matter. The absolute content of lignin in soil organic matter needs to be determined in combination with other methods, including an authenticated external lignin standard. Thus, quantitative analyses and the biodegradation mechanisms of lignin in the Tibetan Plateau need to be studied further.

Author Contributions: Conceptualization, D.Y. and X.L.; methodology, S.M. and X.L.; software, S.M. and X.L.; validation, D.Y., S.M. and X.L.; writing—original draft preparation, D.Y. and S.M.; writing—review and editing, D.Y., S.M. and X.L. All authors have read and agreed to the published version of the manuscript.

Funding: This research was funded by the National Natural Science Foundation of China (grant No. 41877338) and the Natural Science Foundation of the Tibet Autonomous Region.

Data Availability Statement: The original contributions presented in the study are included in the article, further inquiries can be directed to the corresponding authors.

Acknowledgments: We acknowledge the Yanting Agro-ecological Experimental Station of Purple Soil for the incubation experiments.

Conflicts of Interest: The authors declare no conflicts of interest.

References

1. Kubicek, C.; Druzhinina, I. Degradation of Plant Cell Wall Polymers by Fungi. Environmental and Microbial Relationships. *Mycota* **2007**, *4*, 325–340.
2. Jönsson, A.S. 5-Membranes for lignin and hemicellulose recovery in pulp mills. In *Membrane Technologies for Biorefining*; Alberto Figoli, A., Cassano, A., Basile, A., Eds.; Woodhead Publishing: Cambridge UK, 2016; pp. 105–133.
3. Otto, A.; Simpson, M.J. Evaluation of CuO oxidation parameters for determining the source and stage of lignin degradation in soil. *Biogeochemistry* **2006**, *80*, 121–142. [CrossRef]
4. Vancampenhout, K.; De Vos, B.; Wouters, K.; Van Calster, H.; Swennen, R.; Buurman, P.; Deckers, J. Determinants of soil organic matter chemistry in maritime temperate forest ecosystems. *Soil Biol. Biochem.* **2010**, *42*, 220–233. [CrossRef]
5. Yassir, I.; Buurman, P. Soil organic matter chemistry changes upon secondary succession in Imperata Grasslands, Indonesia: A pyrolysis–GC/MS study. *Geoderma* **2012**, *173–174*, 94–103. [CrossRef]
6. Thevenot, M.; Dignac, M.; Rumpel, C. Fate of lignins in soils: A review. *Soil Biol. Biochem.* **2010**, *42*, 1200–1211. [CrossRef]
7. He, Y.C.; Li, X.L.; Ben, H.X.; Xue, X.Y.; Yang, B. Lipid production form Dilute Alkali Corn Stover Lignin by Strains. *ACS Sustain. Chem. Eng.* **2017**, *5*, 2302–2311. [CrossRef]
8. Filley, T.R.; Cody, G.D.; Goodell, B.; Jellison, J.; Noser, C.; Ostrofsky, A. Lignin demethylation and polysaccharide decomposition in spruce sapwood degraded by brown rot fungi. *Org. Geochem.* **2002**, *33*, 111–124. [CrossRef]
9. Zhao, X.Y.; Zhao, X.Y.; Yang, J.J.; Li, S.K.; Lu, X.X.; Li, X. Research progress on lignin degradation mechanism and influencing factors during composting. *Environ. Eng.* **2021**, *39*, 128–136. (In Chinese)
10. Bugg, T.D.H.; Ahmad, M.M.; Hardiman, E.; Singh, R. The emerging role for bacteria in lignin degradation and bio-product formation. *Curr. Opin. Biotechnol.* **2011**, *22*, 394–400. [CrossRef]
11. Sánchez, C. Lignocellulosic residues: Biodegradation and bioconversion by fungi. *Biotechnol. Adv.* **2009**, *27*, 185–194. [CrossRef]
12. ten Have, R.; Teunissen, P.J.M. Oxidative mechanisms involved in lignin degradation by white-rot fungi. *Chem. Rev.* **2001**, *101*, 3397–3413. [CrossRef]
13. Masai, E.; Katayama, Y.; Fukuda, M. Genetic and biochemical investigations on bacterial catabolic pathways for ligninderived aromatic compounds. *Biosci. Biotechnol. Biochem.* **2007**, *71*, 1–15. [CrossRef] [PubMed]
14. Ahmad, M.; Taylor, C.R.; Pink, D.; Burton, K.; Eastwood, D.; Bending, G.D.; Bugg, T.D. Development of novel assays for lignin degradation: Comparative analysis of bacterial and fungal lignin degraders. *Mol. Biosyst.* **2010**, *6*, 815–821. [CrossRef]
15. Furukawa, T.; Bello, F.O.; Horsfall, L. Microbial enzyme systems for Lignin degradation and their transcriptional regulation. *Front. Biol.* **2014**, *9*, 448–471. [CrossRef]

16. Janusz, G.; Anna, P.; Justyna, S.; Urszula, W.B.; Anna, J.W.; Andrzej, P. Lignin degradation: Microorganisms, enzymes involved, genomes analysis and evolution. *FEMS Microbiol. Rev.* **2017**, *6*, 941–962. [CrossRef] [PubMed]
17. Wei, Y.; Wu, D.; Wei, D.; Zhao, Y.; Wu, J.; Xie, X.; Zhang, R.; Wei, Z. Improved lignocellulose-degrading performance during straw composting from diverse sources with actinomycetes inoculation by regulating the key enzyme activities. *Bioresour. Technol.* **2019**, *271*, 66–74. [CrossRef] [PubMed]
18. Tian, J.; Pourcher, A.; Bouchez, T.; Gelhaye, E.; Peu, P. Occurrence of lignin degradation genotypes and phenotypesamong prokaryotes. *Appl. Microbiol. Biot.* **2014**, *98*, 9527–9544. [CrossRef]
19. Rashid, G.M.; Taylor, C.R.; Liu, Y.; Zhang, X.; Rea, D.; Fülöp, V.; Bugg, T.D. Identification of manganese superoxide dismutase fromSphingobacterium sp. T2 as a novel bacterial enzyme for lignin oxidation. *ACS Chem. Biol.* **2015**, *10*, 2286–2294. [CrossRef]
20. Li, Y.; Dong, S.; Liu, S.; Zhou, H.; Gao, Q.; Cao, G.; Wang, X.; Su, X.; Zhang, Y.; Tang, L.; et al. Seasonal changes of CO2, CH4 and N2O fluxes in different types of alpine grassland in the Qinghai-Tibetan Plateau of China. *Soil Biol. Biochem.* **2015**, *80*, 306–314. [CrossRef]
21. Guo, G.; Kong, W.; Liu, J.; Zhao, J.; Du, H.; Zhang, X.; Xia, P. Diversity and distribution of autotrophic microbial community along environmental gradients in grassland soils on the Tibetan Plateau. *Appl. Microbiol. Biotechnol.* **2015**, *99*, 8765–8776. [CrossRef]
22. Pan, S.; Zhang, T.; Rong, Z.; Hu, L.; Gu, Z.; Wu, Q. Population transcriptomes reveal synergistic responses of DNA polymorphism and RNA expression to extreme environments on the Qinghai-Tibetan Plateau in a predatory bird. *Mol. Ecol.* **2017**, *26*, 2993–3010. [CrossRef] [PubMed]
23. Lu, X.Y.; Ma, S.Q.; Chen, Y.C.; Degyi, Y.Z.; Jiang, H.M. Squalene found in alpine grassland soils under a harsh environment in the Tibetan Plateau, China. *Biomolecules* **2018**, *154*, 154. [CrossRef]
24. Lu, X.Y.; Yan, Y.; Sun, J.; Zhang, X.; Chen, Y.C.; Wang, X.D. Carbon, nitrogen, and phosphorus storage in alpine grassland ecosystems of Tibet: Effects of grazing exclusion. *Ecol. Evol.* **2015**, *5*, 4492–4504. [CrossRef] [PubMed]
25. Qiu, J. China: The third pole. *Nature* **2008**, *454*, 393–396. [CrossRef] [PubMed]
26. Bibi, S.; Wang, L.; Li, X.; Zhou, J.; Chen, D.; Yao, T. Climatic and associated cryospheric, biospheric, and hydrological changes on the Tibetan Plateau: A review. *Int. J. Climatol.* **2018**, *38*, 1–17. [CrossRef]
27. Ma, S.Q.; Fan, J.H.; Chen, Y.C.; Lu, X.Y. Studying greenhouse gas emissions through interactions between phospholipid fatty acid content and soil properties of alpine grassland soil in Northern Tibet, China. *Glob. Ecol. Conserv.* **2021**, *27*, e01558. [CrossRef]
28. Lin, X.; Wang, S.; Ma, X.; Xu, G.; Luo, C.; Li, Y.; Jiang, G.; Xie, Z. Fluxes of CO_2, CH_4, and N_2O in an alpine meadow affected by yak excreta on the Qinghai-Tibetan plateau during summer grazing periods. *Soil Biol. Biochem.* **2009**, *41*, 718–725. [CrossRef]
29. Du, Z.Y.; Wang, X.D.; Liu, X.P.; Cai, J.J. Effects of rock fragments on yak dung greenhouse gas emissions on the Qinghai-Tibetan Plateau. *J. Mt. Sci.* **2016**, *13*, 2006–2014. [CrossRef]
30. Chen, Y.C.; Ma, S.Q.; Jiang, H.M.; Degyi, Y.Z.; Cheng, G.W.; Lu, X.Y. Decomposition time, chemical traits and climatic factors determine litter-mixing effects on decomposition in an alpine steppe ecosystem in Northern Tibet. *Plant Soil* **2021**, *459*, 23–34. [CrossRef]
31. Gai, J.P.; Christie, P.; Cai, X.B.; Fan, J.Q.; Zhang, J.L.; Feng, G.; Li, X.L. Occurrence and distribution of arbuscular mycorrhizal fungal species in three types of grassland community of the Tibetan Plateau. *Ecol. Res.* **2009**, *24*, 1345–1350. [CrossRef]
32. Zhang, S.W.; Gong, W.; Wan, X.; Li, J.Y.; Li, Z.G.; Chen, P.; Xing, S.; Li, Z.; Liu, Y. Influence of organic matter input and temperature change on soil aggregate-associated respiration and microbial carbon use efficiency in alpine agricultural soils. *Soil Ecol. Lett.* **2024**, *6*, 230220. [CrossRef]
33. Chen, Y.C.; Ma, S.Q.; Jiang, H.M.; Hu, Y.; Lu, X.Y. Influences of litter diversity and soil moisture on soil microbial communities in decomposing mixed litter of alpine steppe species. *Geoderma* **2020**, *377*, 114577. [CrossRef]
34. Dorado, J.; Almendros, G.; González-Vila, F.J. Response of humic acid structure to soil tillage management as revealed by analytical pyrolysis. *J. Anal. Appl. Pyrol.* **2016**, *117*, 56–63. [CrossRef]
35. Ma, S.Q.; Chen, Y.C.; Lu, X.Y.; Wang, X.D. Soil organic matter chemistry: Based on pyrolysis-gas chromatography-mass spectrometry (Py-GC/MS). *Mini-Rev. Org. Chem.* **2018**, *15*, 389–403. [CrossRef]
36. Yang, B.; Pang, X.Y.; Hu, B.; Bao, W.K.; Tian, G.L. Does thinning-induced gap size result in altered soil microbial community in pine plantaton in eastern Tibetan Plateau? *Ecol. Evol.* **2017**, *7*, 2986–2993. [CrossRef]
37. Jilkova, V.; Cajthaml, T.; Frouz, J. Relative importance of honeydew and resin for the microbial activity in wood ant nest and forest floor substrate—A laboratory study. *Soil Biol. Biochem.* **2018**, *117*, 1–4. [CrossRef]
38. Grunewald, G.; Kaiser, K.; Jahn, R.; Guggenberger, G. Organic matter stabilization in young calcareous soils as revealed by density fractionation and analysis of lignin-derived constituents. *Org. Geochem.* **2006**, *37*, 1573–1589. [CrossRef]
39. Vancampenhout, K.; De Vos, B.; Wouters, K.; Swennen, R.; Buurman, P.; Deckers, J. Organic matter of subsoil horizons under broadleaved forest: Highly processed or labile and plant-derived? *Soil Biol. Biochem.* **2012**, *50*, 40–46. [CrossRef]
40. Huang, X.F.; Santhanam, N.; Badri, D.V.; Hunter, W.J.; Manter, D.K.; Decker, S.R.; Vivanco, J.M.; Reardon, K.F. Isolation and characterization of lignin-degrading bacteria from rainforest soils. *Biotechnol. Bioeng.* **2013**, *110*, 1616–1626. [CrossRef]
41. Yang, S.; Yao, F.; Ye, J.; Fang, S.; Wang, Z.; Wang, R.; Zhang, Q.; Ma, R.; Wang, X.; Jiang, Y.; et al. Latitudinal pattern of soil lignin/cellulose content and the activity of their degrading enzeymes across a temperate forest ecosystem. *Ecol. Indic.* **2019**, *102*, 557–568. [CrossRef]
42. Nierop, K.G.J.; Pulleman, M.M.; Marinissen, J.C.Y. Management induced organic matter differentiation in grassland and arable soil: A study using pyrolysis techniques. *Soil Biol. Biochem.* **2001**, *33*, 755–764. [CrossRef]

43. Lützow, M.V.; Kögel-Knabner, I.; Ekschmitt, K.; Matzner, E.; Guggenberger, G.; Marschner, B.; Flessa, H. Stabilization of organic matter in temperate soils: Mechanisms and their relevance under different soil conditions—A review. *Eur. J. Soil Sci.* **2006**, *57*, 426–445. [CrossRef]
44. Abelenda, M.S.; Buurman, P.; Camps Arbestain, M.; Kaal, J.; Martinez-Cortizas, A.; Gartzia-Bengoetxea, N.; Macías, F. Comparing NaOH-extractable organic matter of acid forest soils that differ in their pedogenic trends: A pyrolysis-GC/MS study. *Eur. J. Soil Sci.* **2011**, *62*, 834–848. [CrossRef]
45. Martin, J.P.; Haider, K. Effect of concentration on decomposition of some 14C-labeled phenolic compounds, benzoic acid, glucose, cellulose, wheat straw, and Chlorella protein in soil. *Soil Sci. Soc. Am. J.* **1979**, *43*, 917–920. [CrossRef]
46. Martin, J.P.; Haider, K. Microbial degradation and stabilization of 14C-labeled lignins, phenols, and phenolic polymers in relation to soil humus formation. In *Lignin Biodegradation: Microbiology, Chemistry and Applications*; Kirk, T.K., Higuchi, T., Chang, H.-M., Eds.; CRC Press: Boca Raton, FL, USA, 1980; Volume I, pp. 77–100.
47. Osono, T.; Takeda, H. Effects of organic mineral chemical quality and mineral nitrogen addition on lignin and holocellulose decomposition of beech leaf litter by Xylaria sp. *Eur. J. Soil Biol.* **2001**, *37*, 17–23. [CrossRef]
48. Dignac, M.F.; Bahri, H.; Rumpel, C.; Rasse, D.P.; Bardoux, G.; Balesdent, J.; Girardin, C.; Chenu, C.; Mariotti, A. Carbon-13 natural abundance as a tool to study the dynamics of lignin monomers in soil: An appraisal at the Closeaux experimental field (France). *Geoderma* **2005**, *128*, 3–17. [CrossRef]
49. Heim, A.; Schmidt, M.W.I. Lignin turnover in arable soil and grassland analysed with two different labelling approaches. *Eur. J. Soil Sci.* **2007**, *58*, 599–608. [CrossRef]
50. Bracewell, J.M.; Robertson, G.W. Quantitative comparison of the nitrogen-containing pyrolysis products and amino acid composition of soil humic acids. *J. Anal. Appl. Pyrolysis* **1984**, *6*, 19–29. [CrossRef]
51. Buurman, P.; Roscoe, R. Different chemical compostion of free light, occluded light and extractable SOM fractions in soils of Cerrade and tilled and untilled fields, Minas Gerais Brazil, a pyrolysis-GC/MS study. *Ruropean J. Soil Sci.* **2011**, *62*, 253–266. [CrossRef]
52. Kögel, I. Estimation and decomposition pattern of the lignin component in forest humus layers. *Soil Biol. Biochem.* **1986**, *18*, 589–594. [CrossRef]
53. Kiem, R.; Kögel-Knabner, I. Contribution of lignin and polysaccharides to the refractory carbon pool in C-depleted arable soils. *Soil Biol. Biochem.* **2003**, *35*, 101–118. [CrossRef]
54. Dao, T.T.; Mikutta, R.; Sauheitl, L.; Gentsch, N.; Shibistova, O.; Wild, B.; Schnecker, J.; Bárta, J.; Čapek, P.; Gittel, A.; et al. Lignin Preservation and Microbial Carbohydrate Metabolism in Permafrost Soils. *J. Geophys. Res-Biogeo.* **2022**, *127*, e2020JG006181. [CrossRef]
55. Grandy, A.S.; Neff, J.C.; Weintraub, M.N. Carbon structure and enzyme activities in alpine and forest ecosystems. *Soil Biol. Biochem.* **2007**, *39*, 2701–2711. [CrossRef]
56. Xu, C.F.; Su, X.; Wang, J.H.; Zhang, F.Z.; Shen, G.N.; Yuan, Y.; Yan, L.; Tang, H.Z.; Song, F.Q.; Wang, W.D. Characteristics and functional bacteria in a microbial consortium for rice straw lignin-degrading. *Bioresour. Technol.* **2021**, *331*, 125066. [CrossRef]
57. Atiwesh, G.; Parrish, C.C.; Banoub, J.; Le, T.T. Lignin degradation by microorganisms: A review. *Biotechnol. Progr.* **2021**, *38*, e3226. [CrossRef] [PubMed]
58. Qian, Z.Y.; Fan, Z.; Peng, W.X.; Du, H.; Hu, P.L. Source to Sink of Lignin Phenols in a Subtropical Forest of Southwest China. *Forests* **2023**, *14*, 1701. [CrossRef]
59. Abdellatif Aya, A.M.; Gebily Doha, A.S.; Maissara, E. *Transforming Roles of Actinobacteria in Sustainable Agriculture: From Soil Health and Plant Productivity Perspective*; Sahu, P.K., Thakur, B., Kaur, S., Eds.; Springer Nature: Singapore, 2024; pp. 299–338.
60. Song, A.; Zhang, J.; Xu, D.; Wang, E.; Bi, J.; Asante-Badu, B.; Njyenawe, M.C.; Sun, M.; Xue, P.; Wang, S.; et al. Keystone microbial taxa drive the accelerated decompositions of cellulose and lignin by long-term resource enrichments. *Sci. Total Environ.* **2022**, *842*, 156814. [CrossRef]
61. Nagaraju, Y.; Mahadevaswamy; Gowder, S.B.; Triveni, S. Lignin-Degrading Microorganisms from Organic Soils. *Int. J. Plant Soil Sci.* **2021**, *33*, 78–85. [CrossRef]
62. Thitinun, S.; Esther, A.; Surang, C.; Tanaporn, P.; Wethaka, L.; Puey, O.; Phurt, H. Evaluating lignin degradation under limited oxygen conditions by bacterial isolates from forest soil. *Sci. Rep.* **2024**, *14*, 13350.
63. San-Emeterio, L.M.; Hidalgo-Galvez, M.D.; de la Rosa, J.M.; P'erez-Ramos, I.; González-Pérez, J.A. Impact of future scenarios of climate change on lignin dynamics in soil: A case study in a Mediterranean savannah. *Sci. Total Environ.* **2024**, *946*, 174317. [CrossRef]

Disclaimer/Publisher's Note: The statements, opinions and data contained in all publications are solely those of the individual author(s) and contributor(s) and not of MDPI and/or the editor(s). MDPI and/or the editor(s) disclaim responsibility for any injury to people or property resulting from any ideas, methods, instructions or products referred to in the content.

MDPI AG
Grosspeteranlage 5
4052 Basel
Switzerland
Tel.: +41 61 683 77 34

Agronomy Editorial Office
E-mail: agronomy@mdpi.com
www.mdpi.com/journal/agronomy



Disclaimer/Publisher's Note: The title and front matter of this reprint are at the discretion of the Guest Editors. The publisher is not responsible for their content or any associated concerns. The statements, opinions and data contained in all individual articles are solely those of the individual Editors and contributors and not of MDPI. MDPI disclaims responsibility for any injury to people or property resulting from any ideas, methods, instructions or products referred to in the content.





Academic Open
Access Publishing

mdpi.com

ISBN 978-3-7258-9146-7